EVOLUTIONARY GENOMICS OF *CANDIDATUS LIBERIBACTER SPP.* AND THEIR INTERACTIONS WITH PLANT AND INSECT-VECTOR HOSTS

EDITED BY: Xuefeng Wang, Changyong Zhou, Leandro Peña, Kranthi Kiran Mandadi and Mengji Cao

PUBLISHED IN: Frontiers in Microbiology and Frontiers in Plant Science

frontiers Research Topics

frontiers

ISSN 1664-8714
ISBN 978-2-83250-552-6
DOI 10.3389/978-2-83250-552-6

About Frontiers

Frontiers is more than just an open-access publisher of scholarly articles: it is a pioneering approach to the world of academia, radically improving the way scholarly research is managed. The grand vision of Frontiers is a world where all people have an equal opportunity to seek, share and generate knowledge. Frontiers provides immediate and permanent online open access to all its publications, but this alone is not enough to realize our grand goals.

Frontiers Journal Series

The Frontiers Journal Series is a multi-tier and interdisciplinary set of open-access, online journals, promising a paradigm shift from the current review, selection and dissemination processes in academic publishing. All Frontiers journals are driven by researchers for researchers; therefore, they constitute a service to the scholarly community. At the same time, the Frontiers Journal Series operates on a revolutionary invention, the tiered publishing system, initially addressing specific communities of scholars, and gradually climbing up to broader public understanding, thus serving the interests of the lay society, too.

Dedication to Quality

Each Frontiers article is a landmark of the highest quality, thanks to genuinely collaborative interactions between authors and review editors, who include some of the world's best academicians. Research must be certified by peers before entering a stream of knowledge that may eventually reach the public - and shape society; therefore, Frontiers only applies the most rigorous and unbiased reviews.
Frontiers revolutionizes research publishing by freely delivering the most outstanding research, evaluated with no bias from both the academic and social point of view. By applying the most advanced information technologies, Frontiers is catapulting scholarly publishing into a new generation.

What are Frontiers Research Topics?

Frontiers Research Topics are very popular trademarks of the Frontiers Journals Series: they are collections of at least ten articles, all centered on a particular subject. With their unique mix of varied contributions from Original Research to Review Articles, Frontiers Research Topics unify the most influential researchers, the latest key findings and historical advances in a hot research area! Find out more on how to host your own Frontiers Research Topic or contribute to one as an author by contacting the Frontiers Editorial Office: frontiersin.org/about/contact

EVOLUTIONARY GENOMICS OF *CANDIDATUS LIBERIBACTER SPP.* AND THEIR INTERACTIONS WITH PLANT AND INSECT-VECTOR HOSTS

Topic Editors:
Xuefeng Wang, Citrus Research Institute, Chinese Academy of Agricultural Sciences, China
Changyong Zhou, Southwest University, China
Leandro Peña, Polytechnic University of Valencia, Spain
Kranthi Kiran Mandadi, Texas A&M University, United States
Mengji Cao, Southwest University, China

Citation: Wang, X., Zhou, C., Peña, L., Mandadi, K. K., Cao, M., eds. (2022). Evolutionary Genomics of *Candidatus Liberibacter spp.* and Their Interactions With Plant and Insect-Vector Hosts. Lausanne: Frontiers Media SA.
doi: 10.3389/978-2-83250-552-6

Table of Contents

05 ***Editorial: Evolutionary Genomics of* Candidatus *Liberibacter spp. and Their Interactions With Plant and Insect-Vector Hosts***
Xuefeng Wang, Kranthi Mandadi, Leandro Peña, Mengji Cao and Changyong Zhou

08 **Liberibacter*, A Preemptive Bacterium: Apoptotic Response Repression in the Host Gut at the Early Infection to Facilitate Its Acquisition and Transmission***
Xiao-Tian Tang, Kelsy Fortuna, Azucena Mendoza Herrera and Cecilia Tamborindeguy

23 ***Early Population Dynamics of "*Candidatus *Liberibacter asiaticus" in Susceptible and Resistant Genotypes After Inoculation With Infected* Diaphorina citri *Feeding on Young Shoots***
Mônica Neli Alves, Juan Camilo Cifuentes-Arenas, Laudecir Lemos Raiol-Junior, Jesus Aparecido Ferro and Leandro Peña

36 ***A Significantly High Abundance of "*Candidatus *Liberibacter asiaticus" in Citrus Fruit Pith:* in planta *Transcriptome and Anatomical Analyses***
Fang Fang, Hengyu Guo, Anmin Zhao, Tao Li, Huihong Liao, Xiaoling Deng, Meirong Xu and Zheng Zheng

51 ***Bacteriomic Analyses of Asian Citrus Psyllid and Citrus Samples Infected With "*Candidatus *Liberibacter asiaticus" in Southern California and Huanglongbing Management Implications***
Jiaquan Huang, Zehan Dai, Zheng Zheng, Priscila A. da Silvia, Luci Kumagai, Qijun Xiang, Jianchi Chen and Xiaoling Deng

62 ***The Genome of "*Candidatus *Liberibacter asiaticus" Is Highly Transcribed When Infecting the Gut of* Diaphorina citri**
Josiane Cecília Darolt, Flavia de Moura Manoel Bento, Bruna Laís Merlin, Leandro Peña, Fernando Luis Cônsoli and Nelson Arno Wulff

76 ***Potato Zebra Chip: An Overview of the Disease, Control Strategies, and Prospects***
Victoria Mora, Manikandan Ramasamy, Mona B. Damaj, Sonia Irigoyen, Veronica Ancona, Freddy Ibanez, Carlos A. Avila and Kranthi K. Mandadi

83 ***Selection and Evaluation of a Thornless and HLB-Tolerant Bud-Sport of Pummelo Citrus With an Emphasis on Molecular Mechanisms***
Bo Wu, Na Li, Zhanao Deng, Feng Luo and Yongping Duan

97 ***Uncovering Symbionts Across the Psyllid Tree of Life and the Discovery of a New Liberibacter Species, "*Candidatus*" Liberibacter capsica***
Younghwan Kwak, Penglin Sun, Venkata RamaSravani Meduri, Diana M. Percy, Kerry E. Mauck and Allison K. Hansen

114 ***A Novel* Microviridae *Phage (CLasMV1) From "*Candidatus *Liberibacter asiaticus"***
Ling Zhang, Ziyi Li, Minli Bao, Tao Li, Fang Fang, Yongqin Zheng, Yaoxin Liu, Meirong Xu, Jianchi Chen, Xiaoling Deng and Zheng Zheng

126 *Overexpression of a "*Candidatus *Liberibacter Asiaticus" Effector Gene* CaLasSDE115 *Contributes to Early Colonization in* Citrus sinensis
Meixia Du, Shuai Wang, Liting Dong, Rongrong Qu, Lin Zheng, Yongrui He, Shanchun Chen and Xiuping Zou

140 *Integrated Analysis of the miRNAome and Transcriptome Reveals miRNA–mRNA Regulatory Networks in* Catharanthus roseus *Through* Cuscuta campestris*-Mediated Infection With "*Candidatus *Liberibacter asiaticus"*
Chunhua Zeng, Haodi Wu, Mengji Cao, Changyong Zhou, Xuefeng Wang and Shimin Fu

151 *An Overview of the Mechanisms Against "*Candidatus *Liberibacter asiaticus": Virulence Targets, Citrus Defenses, and Microbiome*
Chuanyu Yang and Veronica Ancona

166 *Identification and Characterization of Potato Zebra Chip Resistance Among Wild* Solanum *Species*
Victoria Mora, Manikandan Ramasamy, Mona B. Damaj, Sonia Irigoyen, Veronica Ancona, Carlos A. Avila, Maria Isabel Vales, Freddy Ibanez and Kranthi K. Mandadi

frontiers | Frontiers in Microbiology

TYPE Editorial
PUBLISHED 06 October 2022
DOI 10.3389/fmicb.2022.1025795

OPEN ACCESS

EDITED AND REVIEWED BY
Jesús Navas-Castillo,
La Mayora Experimental Station (CSIC), Spain

*CORRESPONDENCE
Xuefeng Wang
wangxuefeng@cric.cn

SPECIALTY SECTION
This article was submitted to Microbe and Virus Interactions with Plants, a section of the journal Frontiers in Microbiology

RECEIVED 23 August 2022
ACCEPTED 23 September 2022
PUBLISHED 06 October 2022

CITATION
Wang X, Mandadi K, Peña L, Cao M and Zhou C (2022) Editorial: Evolutionary genomics of *Candidatus* Liberibacter spp. and their interactions with plant and insect-vector hosts. *Front. Microbiol.* 13:1025795. doi: 10.3389/fmicb.2022.1025795

Editorial: Evolutionary genomics of *Candidatus* Liberibacter spp. and their interactions with plant and insect-vector hosts

Xuefeng Wang[1]*, Kranthi Mandadi[2,3,4], Leandro Peña[5,6], Mengji Cao[1] and Changyong Zhou[1]

[1]National Citrus Engineering Research Center, Citrus Research Institute, Southwest University, Chongqing, China, [2]Department of Plant Pathology and Microbiology, Texas A&M University, College Station, TX, United States, [3]Texas A&M AgriLife Research and Extension Center, Texas A&M University System, Weslaco, TX, United States, [4]Institute for Advancing Health Through Agriculture, Texas A&M AgriLife, College Station, TX, United States, [5]Laboratório de Biotecnologia Vegetal, Fundo de Defesa da Citricultura (Fundecitrus), Araraquara, São Paulo, Brazil, [6]Instituto de Biología Molecular y Celular de Plantas, Consejo Superior de Investigaciones Científicas (IBMCP-CSIC), Valencia, Spain

KEYWORDS

***Candidatus* Liberibacter spp., Huanglongbing, Zebra chip disease, interactions, omics, integrated pest management**

Editorial on the Research Topic
Evolutionary genomics of *Candidatus* Liberibacter spp. and their interactions with plant and insect-vector hosts

Multiple pathogenic species of "*Candidatus* Liberibacter" have been identified from plant hosts worldwide. Among these species, "*Ca.* Liberibacter asiaticus" (*C*Las) and "*Ca.* Liberibacter solanacearum" (*C*Lso) are the putative causal agents of citrus Huanglongbing (HLB) and Zebra chip disease (ZC), respectively, which are highly destructive toward the citrus and potato industries. Due to their phloem-colonized nature, the lack of pure culture, and their intracellular life in plant hosts, studies on the biology and control of "*Ca.* Liberibacter" species are facing significant challenges. Although genomic information of the "*Ca.* Liberibacter" species has been accumulated rapidly and some virulence factors have been dissected, how the three-way interactions within pathogen-insect-plant occur remains further characterization.

The purpose of the Research Topic was to publish high-quality research papers and review articles focusing on the following: (1) comparative and functional genomics of "*Ca.* Liberibacter" spp.; (2) multi-omics of plant and insect-vector hosts in response to *C*Las/*C*Lso infection; (3) characterization of effectors or other virulence traits and their interactions with plant and insect-vector hosts; (4) development of genetic and genome-editing strategies against *C*Las/*C*Lso. A total of 18 manuscripts, including original research and reviews, have been received, of which 13 were eventually accepted, comprising two reviews and 11 research papers.

Currently, *Ca*. Liberibacter is only found in Psylloidea vector hosts but not in other insect superfamilies. To discover new *Liberibacter* species and determine their phylogenetic relationship, psyllid samples from 44 species of 35 genera of five plant families, collected from 11 representative geographical locations, were used for 16S rRNA sequencing. A novel "*Ca*. Liberibacter" species, "*Ca*. Liberibacter capsica," was identified based on the phylogenomic analyses of sequencing data (Kwak et al.). Three types of phages/prophages (Type 1, Type 2, and Type 3) have been characterized in *C*Las according to the presence of circular plasmid sequences. It is generally believed that more *C*Las phages/prophages are likely to be found. A novel *Microviridae* phage, *C*LasMV1, with a small circular genome was identified in a Chinese *C*Las strain (GDHZ11) (Zhang et al.). *C*LasMV1 was frequently detected with a high copy number in a *C*Las population from southern China. Bacteriomic analyses of Asian citrus psyllids and citrus samples from California identified ten bacterial generas of endophytes, including *Bradyrhizobium*, *Buchnera*, *Burkholderia*, "*Ca*. Profftella armature," and *Mesorhizobium*. *Bradyrhizobium* and *Mesorhizobium* DNA were identified as interfering with *C*Las detection using the conventional 16S rRNA gene-based PCR due to their sequence similarity, particularly at low or zero *C*Las titer situations, likely providing false positive results (Huang et al.).

Understanding the early events of the interaction between *C*Las-plant hosts may help to develop bacterial control strategies. To better understand *C*Las dynamics and whole-plant colonization during the earliest stage of infection, Alves et al. identified the key time course of *C*Las proliferation in *Citrus sinensis* "Valencia" (susceptible host), in *Murraya paniculata* (transient host), and in *Bergera koenigii* (resistant) under similar initial inoculum pressure. Fang et al. found a high level of *C*Las population in fruit pith tissue compared with other tissues. The high-resolution *C*Las transcriptome profiles were generated using the *C*Las-abundant fruit pith samples for dual RNA-seq, suggesting that fruit pith could be an ideal host material for further studies on *C*Las–citrus interaction. The non-natural host periwinkle (*Catharanthus roseus*) infected *via* dodder (*Cuscuta campestris*) from *C*Las-infected citrus plants was subjected to the analysis of transcriptomics and small-RNA profiling. miR164-NAC1, miR828-MYB94/miR1134-HSF4, and miR827-ATG8 regulatory networks were identified as critical miRNA–mRNA regulatory channels, showing new potential connections in periwinkle–*C*Las interactions (Zeng et al.). Currently, our knowledge of the cellular function of *C*Las secretory proteins in plant or insect hosts is limited. *Ca*LasSDE115 effector was proposed as an invasion-associated locus B of *C*Las, participating in the early bacterial colonization of citrus. It could also regulate citrus resistance to HLB *via* modulating the transcriptional regulation of systemic acquired resistance (SAR)-related genes (Du et al.).

To understand the molecular interactions of *C*Las-*Diaphorina citri* during the vector acquisition process, cDNA libraries obtained from the gut of adult psyllids were sequenced on an Illumina platform. A high copy number of genes (up to 95%) were expressed in the initial step of *D. citri* gut colonization through read mapping of *C*Las genes, suggesting such genes might play critical roles in *C*Las colonizing insect organs (Darolt et al.). Tang et al. found that the expression of IAPP5.2 gene (the inhibitor of apoptosis) was significantly induced during the period that *C*Lso translocated into the gut cells. Detection of apoptosis level, *C*Lso acquisition, and transmission efficiency after silencing IAPP5.2 suggested that *C*Lso might repress the apoptotic response in the psyllid guts by upregulating IAPP5.2 at the early stages of *C*Lso infection.

Identifying novel genetic resistance and tolerance sources to *C*Las/*C*Lso can be valuable components for the integrated management of HLB/ZC. A taxonomically diverse collection of tuber-bearing *Solanum* species was screened, and a ZC-resistant accession (*Solanum berthaultii*) was identified among the 52 screened accessions. The differences in leaf trichome density and morphology of the wild accessions may play important roles in antibiosis effects. This germplasm offers a good resource for potato breeding to develop ZC resistance cultivars (Mora et al.). Wu et al. discovered and evaluated a thornless pummelo (*Citrus maxim*a var. "Mato Buntan") bud-sport that grew more vigorously and was more tolerant to HLB than the thorny wild type. Further analysis indicated that the phenotype alterations of the bud-sport were associated with significant transcriptome changes, providing useful clues and targets for genetic breeding and gene editing for citrus improvement.

Current management strategies for HLB and ZC mainly rely on chemical control and integrated pest management measures to limit the spread of the pathogen. Recent developments in potato genetic resources and solanaceous crop improvement technologies are reviewed by Mora et al. These could be further leveraged for developing new potato cultivars with genetic resistance to the psyllid and *C*Lso. Yang et al. summarize the main aspects contributing to understanding *C*Las pathogenesis, including virulence targets, citrus defenses, and interactions with the host microbiome. They discuss the possible use of antimicrobial agents, plant defense activators, and beneficial bacteria as potential strategies to combat HLB.

Final comment

In conclusion, the Research Topic articles cover a broad spectrum of *C*Las/*C*Lso-hosts interactions and may help to develop novel control strategies against HLB/ZC.

Author contributions

XW drafted and prepared the final version of the editorial. KM, LP, MC, and CZ provided feedback and edits. All authors approved the editorial.

Funding

This study was supported in part by funds from the National Key Research and Development Program of China (2021YFD1400800 and 2018YFD0201500) to XW and CZ. USDA-NIFA (2021-70029-36056), Texas A&M AgriLife Research Insect-vectored Disease Seed Grants (124185-96210), the Texas A&M AgriLife Institute for Advancing Health Through Agriculture to KM, from Fundecitrus, Grant No. 817526 from the European Union H2020 Innovation Action Program and Project PID2019-104569RB-I00 from the AEI-Spain to LP.

Acknowledgments

We thank all the authors who contributed to the Research Topic.

Conflict of interest

The authors declare that the research was conducted in the absence of any commercial or financial relationships that could be construed as a potential conflict of interest.

Publisher's note

frontiers in Microbiology

ORIGINAL RESEARCH
published: 23 December 2020
doi: 10.3389/fmicb.2020.589509

Liberibacter, A Preemptive Bacterium: Apoptotic Response Repression in the Host Gut at the Early Infection to Facilitate Its Acquisition and Transmission

*Xiao-Tian Tang, Kelsy Fortuna, Azucena Mendoza Herrera and Cecilia Tamborindeguy**

Department of Entomology, Texas A&M University, College Station, TX, United States

"*Candidatus* Liberibacter solanacearum" (Lso) is a phloem-limited Gram-negative bacterium that infects crops worldwide. In North America, two haplotypes of Lso (LsoA and LsoB) are transmitted by the potato psyllid, *Bactericera cockerelli* (Šulc), in a circulative and persistent manner. Both haplotypes cause damaging plant diseases (e.g., zebra chip in potatoes). The psyllid gut is the first organ Lso encounters and could be a barrier for its transmission. However, little is known about the psyllid gut immune responses triggered upon Lso infection. In this study, we focused on the apoptotic response in the gut of adult potato psyllids at the early stage of Lso infection. We found that there was no evidence of apoptosis induced in the gut of the adult potato psyllids upon infection with either Lso haplotype based on microscopic observations. However, the expression of the inhibitor of apoptosis IAPP5.2 gene (survivin-like) was significantly upregulated during the period that Lso translocated into the gut cells. Interestingly, silencing of IAPP5.2 gene significantly upregulated the expression of two effector caspases and induced apoptosis in the psyllid gut cells. Moreover, RNA interference (RNAi) of IAPP5.2 significantly decreased the Lso titer in the gut of adult psyllids and reduced their transmission efficiency. Taken together, these observations suggest that Lso might repress the apoptotic response in the psyllid guts by inducing the anti-apoptotic gene IAPP5.2 at an early stage of the infection, which may favor Lso acquisition in the gut cells and facilitate its transmission by potato psyllid.

Keywords: *Candidatus* Liberibacter solanacearum, *Bactericera cockerelli*, gut, apoptosis, survivin, acquisition, transmission

OPEN ACCESS

Edited by:
Xuefeng Wang,
Chinese Academy of Agricultural Sciences, China

Reviewed by:
Alex P. Arp,
United States Department of Agriculture, United States
Thawornchai Limjindaporn,
Mahidol University, Thailand

****Correspondence:***
Cecilia Tamborindeguy
ctamborindeguy@tamu.edu

Specialty section:
This article was submitted to Microbial Symbioses, a section of the journal Frontiers in Microbiology

Received: *12 October 2020*
Accepted: *04 December 2020*
Published: *23 December 2020*

Citation:
Tang X-T, Fortuna K, Mendoza Herrera A and Tamborindeguy C (2020) Liberibacter, A Preemptive Bacterium: Apoptotic Response Repression in the Host Gut at the Early Infection to Facilitate Its Acquisition and Transmission. Front. Microbiol. 11:589509. doi: 10.3389/fmicb.2020.589509

INTRODUCTION

Apoptosis, one of the programmed cell death forms, is an essential physiological process that can occur in response to intracellular or extracellular signals. It plays a critical role in a variety of biological events including development and tissue homeostasis (Zimmermann et al., 2001; Liu et al., 2008). Apoptosis is an evolutionarily conserved mechanism orchestrated by multiple proteins (Kornbluth and White, 2005). Some of the key proteins mediating

apoptosis are caspases, a family of conserved intracellular aspartate-specific cysteine proteases (Lamkanfi et al., 2002; Shi, 2004). Once an initiator caspase is activated, it processes downstream effector caspases that are responsible for apoptosis (Earnshaw et al., 1999). Apoptosis can be divided mainly into extrinsic or intrinsic pathway. In mammals, the extrinsic pathway is mediated by caspase-8, while the intrinsic pathway can be initiated through caspase-9. Both pathways trigger apoptosis through the cleavage of the downstream executioner proteins, caspases 3 and 7 (Elmore, 2007). Because apoptosis signaling mediated by caspases is an irreversible process, caspase activities must be precisely regulated in order to prevent the undesired death of the organism's cells (Goyal, 2001; Liu et al., 2008). Direct inhibition of caspase activity by inhibitor of apoptosis proteins (IAPs) is one of the most important mechanisms for apoptosis inhibition (Bergmann, 2010). To date, eight human IAPs have been identified, including NAIP, c-IAP1, c-IAP2, XIAP, Survivin, Bruce, ILP-2, and Livin (Salvesen and Duckett, 2002). However, the *Drosophila* genome encodes four IAPs: DIAP1, DIAP2, dBruce, and Deterin, the latter protein is a survivin homolog (Hay, 2000; Xu et al., 2009). IAPs are characterized by the presence of one to three baculoviral IAP repeat (BIR) domains, which are required for binding and suppression of specific cell death-inducing caspases (Silke and Meier, 2013).

Apoptosis also plays essential roles in the innate immune system, leading to the rapid destruction of cellular structures or organelles (Danial and Korsmeyer, 2004; Green, 2005). Host cells can employ apoptosis as a defense mechanism to impede the replication and spread of intracellular pathogens. However, because intracellular pathogens often rely on the host cell machinery to complete their life cycle and also require intact host cells to shield themselves from the host immune defense system, many intracellular pathogens are able to manipulate the apoptosis pathways of the host cells (Gao and Abu Kwaik, 2000). Indeed, some pathogens such as *Shigella* and *Salmonella* can hijack the immune responses of the host and take control over the fate of the host cells (Gao and Abu Kwaik, 2000). These pathogens are either directly or indirectly engaged in the host cell apoptotic pathways, and many of them target the caspase signaling to impede apoptosis of the infected host cells (Liu et al., 2008).

"*Candidatus* Liberibacter solanacearum" (Lso) is a Gram-negative, intracellular and unculturable bacterium infecting crops worldwide. Presently, several Lso haplotypes (LsoA, LsoB, LsoC, LsoD, LsoE, LsoF, and LsoU) of this pathogen exist in the world (Glynn et al., 2012; Lin et al., 2012; Nelson et al., 2013; Haapalainen et al., 2018; Grimm and Garczynski, 2019), which are transmitted by several psyllid species and result in large yield loss among different crops. Haplotypes LsoA and LsoB are mainly present in North America where they are transmitted by the potato psyllid (also known as the tomato psyllid), *Bactericera cockerelli* (Šulc; Hemiptera: Triozidae). LsoA and LsoB can infect numerous solanaceous crops and cause damaging diseases such as zebra chip in potatoes (Liefting et al., 2009; Tamborindeguy et al., 2017). Lso is transmitted by psyllids in a circulative and persistent manner (Cooper et al., 2014; Cicero et al., 2016, 2017). Despite our understanding of its transmission route within the insect body, the molecular mechanisms underlying the transmission process remain largely unknown. The psyllid gut is the first organ Lso encounters and therefore provides an essential link for understanding the biology of Lso acquisition or transmission within the potato psyllid.

Importantly, the psyllid gut could act as a barrier for Lso transmission and determine Lso transmission efficiency. Indeed, the ability of the bacteria to infect the gut depends on the insect immune responses as well as the bacterial strategies deployed to disrupt the host immunity (Vyas et al., 2015). An increasing number of studies have demonstrated that apoptosis in insect vectors can be induced by insect-borne plant pathogens. For instance, apoptosis was observed in the gut of Asian citrus psyllid (*Diaphorina citri*) adults from the "*Ca. L. asiaticus*" (*C*Las)-infected colonies, but not in the nymphal gut (Ghanim et al., 2016; Mann et al., 2018). It is probable that the apoptotic response serves to limit the acquisition or transmission efficiency of *C*Las by the Asian citrus psyllid. Indeed, *C*Las titer increased at a faster rate when the bacterium was acquired by nymphs compared to adults (Ammar et al., 2016). In contrast to *C*Las, no evidence of apoptosis was uncovered in the gut of the Lso-infected adult potato psyllids in our previous study (Tang and Tamborindeguy, 2019). However, all these studies focused on insects from infected colonies, which most likely acquired the bacteria during the nymphal stages. It is still possible that apoptosis is induced at the early stages of infection, but as the infection becomes persistent, as in the case of adults from the Lso-infected colonies, there is no evidence of apoptosis. Another possibility is that Lso could affect the gut immune response to favor its acquisition or transmission. Interestingly, while adults can efficiently transmit LsoA and LsoB if the pathogens were acquired during the nymphal stages, we have discovered that adults can acquire and transmit LsoA with lower efficiency than LsoB (Tang et al., 2020b). Therefore, it is still necessary to investigate the apoptotic response in the gut of psyllids upon Lso infection.

In the present study, we investigated the apoptotic response in the potato psyllid gut during the early stages of Lso infection. First, the accumulation of the two Lso haplotypes A and B was determined during the early infection period. Second, the occurrence of changes in nuclear morphology, actin cytoskeleton, and the integrity of the gut cell DNA were evaluated because these changes are hallmarks of apoptosis. Third, the expression of apoptosis-related genes (Tang and Tamborindeguy, 2019) was evaluated at key time points during the early infection period. Here, we showed that apoptosis is not induced in the gut of the adult potato psyllids upon infection of either Lso haplotype; however, one of the inhibitors of apoptosis, IAPP5.2 gene (survivin-like), was significantly activated. Silencing of IAPP5.2 significantly decreased the Lso titer in the gut of adult psyllids and reduced its transmission efficiency. These observations suggest that Lso could be exploiting the psyllid's cell machinery to avoid the apoptotic immune defenses by utilizing an inhibitor of apoptosis, thereby

facilitating its acquisition and transmission. This study not only provides insights into the interactions occurring between Lso and its insect vector, the potato psyllid, at the gut interface, but could also represent a stepping stone toward the development of novel control strategies to disrupt the pathogen transmission within insect vector.

MATERIALS AND METHODS

Insect Colonies and Tomato Plants

Lso-free, LsoA- and LsoB-infected psyllid colonies were maintained separately on tomato plants (Moneymaker; Victory Seed Company, Molalla, OR) in insect cages (24 × 13.5 × 13.5 cm, BioQuip®, Compton, CA) at room temperature 24 ± 1°C and photoperiod of 16: 8 h (L: D) as described in Yao et al. (2016).

To obtain Lso-infected tomato plants, 6-week-old tomato plants were infected as described in Nachappa et al. (2014) using three male psyllids harboring LsoA or LsoB, respectively. After 1 week, the psyllids were removed from the tomato plants. Around 3 weeks after Lso inoculation, the plants were tested for Lso infection using the LsoF/OI2 primers (Li et al., 2009) and the Lso haplotype in the plants was confirmed using the Lso SSR-1 primers (Lin et al., 2012).

Psyllid Exposure to Lso and Gut Dissection

Approximately 7-day-old Lso-free adult psyllids were transferred to LsoA- or LsoB-infected tomato plants. To determine the acquisition profile of LsoA and LsoB in the gut of psyllids, insects were collected after 2-, 3-, 5-, or 7-day acquisition access periods (AAPs) on LsoA- or LsoB-infected plants (**Figure 1A**). For each specified exposure time, the guts from the LsoA- or LsoB-exposed psyllids were dissected under the dissecting microscope as described in Ibanez et al. (2014) for Lso quantification and immunolocalization. DNA from pools of 50 guts was purified following the protocol of blood/tissue DNA extraction kit (Qiagen, Hilden, Germany); each pool was used as an individual template for quantitative real-time PCR (qPCR) analysis. Thus, each pool of 50 guts represented one replicate, there were three replicates for each combination of exposure time point and haplotype. Each replicate was obtained by using independent LsoA- or LsoB-infected plants as Lso inoculum.

Quantification of Lso

The Lso 16S rDNA specific primers (LsoF: 5'-CGAGCGCTTAT TTTTAATAGGAGC-3' and HLBR: 5'-GCGTTATCCCGTAG AAAAAGGTAG-3'; Li et al., 2006, 2009) were used for Lso quantification in the guts of adult psyllids, and the psyllid 28S rDNA primers (28S rDNAF: 5'-AGTTTCGTGTCGGG TGGAC -3' and 28S rDNAR: 5'-AACATCACGCCCGAAGAC-3'; Nachappa et al., 2014) were used as internal control. Quantitative PCR (qPCR) was performed using SYBR Green Supermix Kit (Bioline, Taunton, MA) according to the manufacturer's instructions. Each reaction contained 25 ng of DNA, 250 nM of each primer, and 1X of SYBR Green Master Mix; the volume was adjusted with nuclease-free water to 10 µl. The qPCR program was 95°C for 2 min followed by 40 cycles at 95°C for 5 s and 60°C for 30 s. qPCR assays were performed using a QuantStudio™ 6 Flex Real-Time PCR System (Applied Biosystems, Foster City, CA). Reactions for all samples were performed in triplicates with a negative control in each run. In order to standardize the amount of Lso in psyllid guts, data are reported as delta Ct = (Ct of Lso gene) – (Ct of psyllid 28S gene). The biological replicates were analyzed and the average delta Ct value was used to quantify the levels of Lso. A standard curve was prepared for the quantification of Lso in the psyllid guts using a plasmid containing the Lso 16S rDNA target. For the standard curve, 10-fold serial dilutions of the plasmid were performed. The procedure for the standard curve preparation and the calculations of molecules (copies) followed published methods (Levy et al., 2011). The Lso copy number in each sample was estimated by comparing the delta Ct values of each sample to the standard curve.

Immunolocalization of Lso in Psyllid Guts

Immunolocalization was used to visualize Lso in the Lso-exposed psyllid alimentary canal tissues. The psyllid guts were dissected in 1X phosphate-buffered saline (PBS; Sigma-Aldrich, St. Louis, MO) from adults, which were infected for 2, 3, 5, and 7 days, respectively (**Figure 1A**). Then the guts were fixed in 4% paraformaldehyde for 30 min at room temperature. After fixation, the guts were incubated with Sudan Black B (Sigma-Aldrich) for 20 min to quench the autofluorescence as described in Tang et al. (2019). Next, the guts were permeabilized by adding 0.1% Triton X-100 (Calbiochem/EMD Chemicals, Gibbstown, NJ) for 30 min at room temperature, and washed three times with PBS containing 0.05% Tween 20 (PBST) prior to a 1 h blocking at room temperature with blocking buffer [PBST with 1% (w/v) bovine serum albumin]. Lso immunolocalization was performed using a rabbit-derived polyclonal antibody (GenScript Corp, Piscataway, NJ) directed against Lso outer membrane protein (OMP) raised against the synthesized peptide OMP-B "VIRRELGFSEGDPIC" (Tang et al., 2019). The guts were incubated with the antibody (diluted 1: 500) overnight at 4°C. The guts were then washed three times with PBST and incubated with Alexa Fluor 594 goat anti-rabbit IgG secondary antibody (diluted 1: 2,000; Invitrogen, Carlsbad, CA) for 1 h at room temperature. The guts were washed again three times with PBST, and mounted with one drop of Vectashield mounting medium with 4',6-diamidino-2-phenylindole (DAPI; Vector Laboratories Inc., Burlingame, CA) on a microscope slide. The slide was covered with a glass coverslip and sealed with nail polish. At least 20 guts per exposure time point and haplotype were examined using an Axioimager A1 microscope (Carl Zeiss microimaging) using the rhodamine filter (594 nm, red) and the images were collected and analyzed with the Axiovision Release 4.8 software (Carl Zeiss).

TUNEL Assay

To test the integrity of the genomic DNA in gut cells after Lso exposure, the 2-, 3-, 5-, and 7-day Lso-exposed guts were

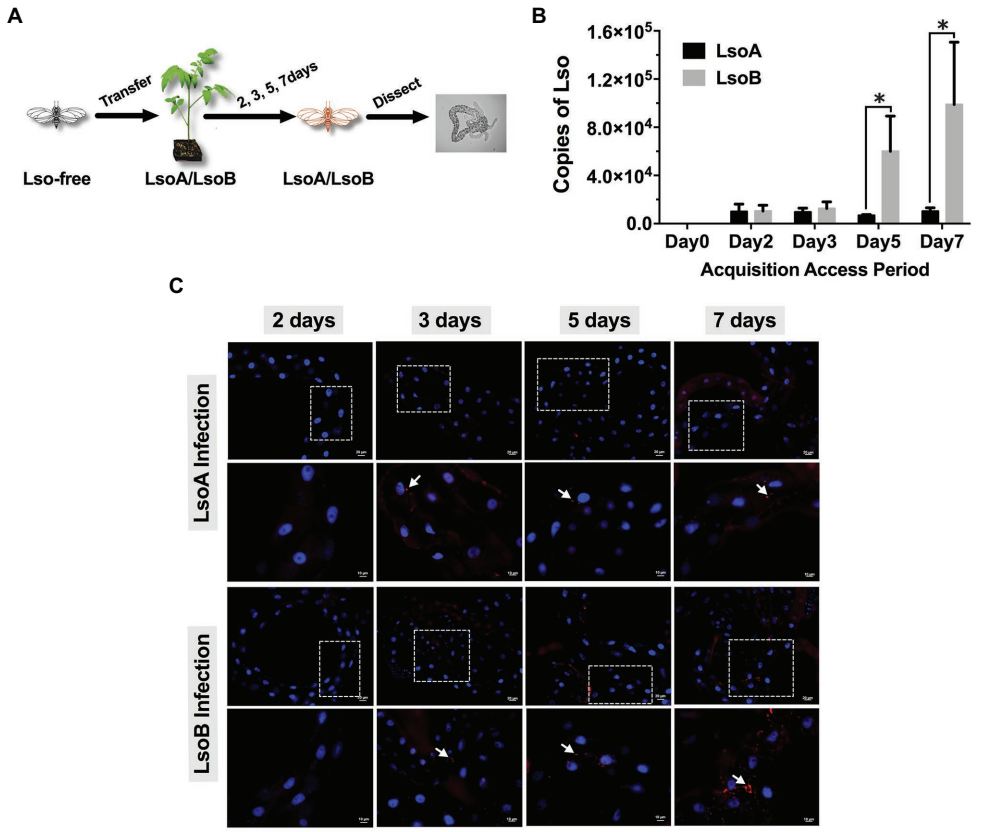

FIGURE 1 | Quantification and immunolocalization of *Candidatus* Liberibacter solanacearum (Lso) in the gut of potato psyllids following acquisition. **(A)** Adult psyllids were transferred to LsoA- or LsoB-infected tomato plants for 2-, 3-, 5-, and 7-day acquisition access periods (AAPs) and then their guts were dissected for quantification and immunolocalization as shown in the schematic representation. **(B)** Quantification analysis of Lso copies in the gut of potato psyllids following Lso acquisition. The bars represent the copies of LsoA (black) and LsoB (gray) in pools of 50 guts following a 0-, 2-, 3-, 5-, and 7-day AAP. Data represent means ± SD of three independent experiments. * indicate statistical differences at $p < 0.05$ using the Student's *t* test. **(C)** Immunolocalization of LsoA and LsoB in the gut of potato psyllids following Lso acquisition. The white dashed rectangle indicates the enlargement region of **upper panels**. White arrows indicated the Lso signals. The Lso signals can be first observed at infection day 3. The bars of **upper** and **lower panels** are 20 and 10 μm, respectively. Psyllid and tomato plant diagrams were made by Dr. Ordom Huot. The gut picture is from Tang et al. (2019).

dissected as previously described. The dissected guts were fixed in 4% paraformaldehyde for 2 h at room temperature. After that, the guts were blocked by 5% bovine serum albumin in 1X PBS with 0.1% Tween 20, then incubated with TUNEL (terminal deoxynucleotidyl transferase dUTP nick end labeling) for 6 h as described in Tang et al. (2020a) and Wang et al. (2018). TUNEL staining was performed using the *In Situ* Cell Death Detection Kit (Roche, Basel, Switzerland). After washing three times in PBS, the guts were mounted using Vectashield mounting medium with DAPI as described above. At least 20 guts per exposure time point and haplotype were observed using the FITC (488 nm, green) filter. The images were collected and analyzed with Axiovision Release 4.8 software (Carl Zeiss).

We also used the apoptosis inducer Concanavalin A (ConA) by feeding, as a positive control. Following the protocol of our colleagues (Sprawka et al., 2015; Tang et al., 2020a) with modifications, the liquid diet used for psyllid feeding bioassays was prepared with a sterilized solution of 15% (w: v) sucrose and 1X PBS (Sigma-Aldrich, St. Louis, MO). ConA (MP Biomedicals, Solon, OH) was incorporated into the diet at a concentration of 2,000 μg/ml (Sprawka et al., 2015). Young adults were placed in plastic feeding chambers (h = 2 cm, Φ = 3 cm), which were covered by two sheets of Parafilm with 100 μl of the liquid diet described above in between the two layers. Next, the guts from the ConA-treated psyllids were dissected after 72 h of feeding. The dissected guts were incubated with TUNEL as described above.

Nuclear Morphology and Actin Cytoskeleton Architecture

To investigate whether Lso impact the nuclear morphology and actin cytoskeleton architecture of the psyllid gut cells, the guts from 2-, 3-, 5-, and 7-day Lso-exposed psyllids were dissected and fixed as previously described. After fixation, the guts were first incubated with Sudan Black B to remove autofluorescence and then incubated with phalloidin (dilution 1:200; Invitrogen). The guts were washed again three times with PBST and mounted with one drop Vectashield mounting medium with DAPI as previously described. At least 20 guts per exposure time point and haplotype were examined using

Axioimager A1 microscope (Carl Zeiss microimaging) using the FITC (488 nm, green) filter. The images were collected and analyzed with Axiovision Release 4.8 software (Carl Zeiss).

Expression of Apoptosis-Related Genes

The apoptosis-related genes were identified through searching the psyllid transcriptome datasets in our previous studies (Nachappa et al., 2012a; Tang and Tamborindeguy, 2019). Three caspases and four IAPs with BIR domain(s) were selected to evaluate the gene expression in the psyllid gut upon Lso infection. The gene names and codes are listed in **Supplementary Table S1**. Of the three caspases, caspase-2 is the initiator caspase, and caspases 1 and 3 are effector caspases. Of the four IAPs, one DIAP1-like gene (IAP1), one DIAP2-like gene (IAP2), and two Deterin/Survivin-like genes (IAPP5 and IAPP5.2) were identified. About 7-day-old Lso-free female adult psyllids were transferred to LsoA- or LsoB-infected plants for 2, 3, 5, and 7 days (**Figure 1A**). The Lso-free colony was used as a control. Three replicates were conducted for each treatment, and each replicate had 200 psyllid individuals. After exposure, the psyllid guts were dissected under the stereomicroscope (Olympus) as previously described. RNA from pools of guts was purified using the RNeasy Mini Kit (Qiagen). Genomic DNA was eliminated by DNase I treatment with Turbo DNase (Ambion, Invitrogen). Then the total RNA was reverse transcribed using the Verso cDNA Synthesis kit (Thermo, Waltham, MA) and anchored-Oligo (dT) primers following the manufacturer's instructions. The expression of apoptosis-related genes in the psyllid guts upon Lso infection was evaluated by qPCR using SensiFAST SYBR Hi-ROX Kit (Bioline) according to the manufacturer's instructions. The primers for qPCR are listed in **Supplementary Table S2**. The qPCR reaction and program were performed as described above. The relative expression of the candidate genes were estimated with the delta CT method (Schmittgen and Livak, 2008), using two reference genes elongation factor-1a (GenBank KT185020) and ribosomal protein subunit 18 (GenBank KT279693; Ibanez and Tamborindeguy, 2016).

RNA Interference of IAPP5.2 and Its Effects on Lso Acquisition and Transmission

The T7 promoter was incorporated into the 5'-end of the forward and reverse IAPP5.2 primers (**Supplementary Table S2**) to enable *in vitro* transcription. The targeted region was blasted against the transcriptome of potato psyllid (Nachappa et al., 2012a) to ensure its specificity. Double-stranded RNAs (dsRNA) were synthesized *via* the MEGAscript RNA interference (RNAi) kit (Invitrogen) using PCR-generated DNA template that contained the T7 promoter sequence at both ends. The dsRNA quality was monitored by agarose gel electrophoresis. dsRNA of the *Aequorea victoria* green fluorescent protein (GFP) was used as a control. RNAi was performed by feeding assay using a liquid diet with dsRNA. Specifically, the liquid diet used for psyllid feeding bioassay was prepared with a sterilized solution of 15% (w:v) sucrose and 1X PBS (Sigma-Aldrich, St. Louis, MO). dsRNA was incorporated into the diet at a concentration of 500 ng/μl. Young female adults from the Lso-free colonies were collected and placed in plastic feeding chambers (h = 2 cm, Φ = 3 cm) for 4 days. The chambers were covered by two sheets of parafilm with 60 μl of the above liquid diet in between the two layers. The diet was refreshed every 2 days. There were three replicates with 30 psyllid individuals each. After silencing, the gene expression of apoptosis-related genes and TUNEL assays were performed as described above.

To examine the effects of silencing IAPP5.2 on the accumulation of LsoA or LsoB in the psyllid guts, 30 young psyllids were allowed to feed on LsoA- or LsoB-infected tomato plants for 2 days before a 4-day feeding on the dsRNA-containing diet. The same number of guts from the control (dsGFP) and dsIAPP5.2 RNAi treatments were dissected for Lso quantification. Three replicates were conducted for the Lso accumulation assays.

To examine the effects of silencing IAPP5.2 on the transmission of LsoA or LsoB by potato psyllid, young Lso-free adult psyllids were exposed to LsoA- or LsoB-infected plants for a 2-day AAP as described above. Then, the Lso-infected psyllids were fed with the dsRNA-containing diet for 4 days. Groups of four treated psyllids were transferred to 10 4-week-old non-infected recipient tomato plants for an 11-day inoculation access period according to the latent period of Lso (Tang et al., 2020b). Then every 4 days, the same batch of LsoA- or LsoB-exposed psyllids was continuously transferred to a new set of 10 non-infected recipient tomato plants. The sequential transmissions were stopped at day 25 because of psyllid mortality. In total, three rounds of transfer were conducted. Around 4 weeks after the end of the inoculation access period, the plants were tested for Lso infection as described above. The transmission assays were performed three times.

Data Analysis

All data were analyzed with JMP Version 12 (SAS Institute Inc., Cary, NC, United States). For gene expression results upon Lso infection, different letters indicate statistical differences at $p < 0.05$ using one-way ANOVA with Tukey's *post hoc* test. For RNAi assays, gene expression and quantification of Lso were determined with Student's *t*-tests. For transmission assays, the percentage of infected plants from the three replicated experiments of each time point and treatment were determined using a logistic regression model, which was fit to evaluate the effects of two factors (RNAi treatments and the days post acquisition) on the probability that a plant would become infected. The log-odds model is given by:

$$\log\left[\frac{p}{(1-p)}\right] = b0 + b1\,\text{RNAi treatments} + b2\,\text{Days} + b3\,\text{RNAi treatments} * \text{Days} + e$$

where p = probability plant becomes infected after being exposed to the Lso a given number of days after the potato psyllid was exposed to the Lso and dsRNA, and p/(1-p) is the odds of an exposed plant becoming infected.

RESULTS

Accumulation of LsoA and LsoB in the Gut of Adult Potato Psyllids

Lso was quantified in the gut of psyllids following different AAPs (2-, 3-, 5-, and 7-day). The results showed that both LsoA and LsoB were detectable with ~10,285 copies in pools of 50 guts of adult potato psyllids at the beginning of infection (2-day AAP; **Figure 1B**). Similar Lso titers were measured after a 3-day AAP. However, after 3 days, LsoB titer increased rapidly with on average ~60,031 copies after a 5-day AAP, and reached a high level of ~98,896 copies after a 7-day AAP. In contrast, the titer of LsoA did not increase over time. In addition, LsoB titer was significantly higher than LsoA titer after 5 days of AAP ($p < 0.05$).

Comparable results were obtained by immunolocalization of Lso in the psyllid guts. No obvious LsoA or LsoB signal could be observed after a 2-day AAP (**Figure 1C**). However, LsoA- or LsoB-derived signal could first be observed after the 3 days of AAP. In accordance with the quantification analysis by qPCR, LsoA signal remained low after the 5-day and 7-day AAPs; however, increasing LsoB signal was observed after the 5-day AAP. In particular, the LsoB-derived signal was strong and more widespread after 7 days of AAP (**Figure 1C**).

Lack of Evidence of Apoptosis in the Lso-Exposed Gut of Adult Potato Psyllids

As indicated above, Lso was detectable in the guts of adult potato psyllids from the beginning of infection (2-day AAP), then the DNA fragmentation of the psyllid gut cells was tested following the 2-, 3-, 5-, and 7-day based on TUNEL assay. However, no signal of DNA fragmentation was detected in the newly Lso-infected guts (**Figure 2** shows he results following the 7-day AAP). In contrast, several cell nuclei from the ConA-treated psyllid guts (positive control) exhibited signals of DNA fragmentation (**Figure 2**). Also, the nuclear morphology and actin cytoskeleton architecture of the psyllid gut cells were observed following 2-, 3-, 5-, and 7-day acquisition of LsoA or LsoB based on DAPI and phalloidin staining, respectively. The results showed that both LsoA- or LsoB-exposed gut nuclei appeared regularly dispersed in the cells and were of uniform round shape and size based on DAPI staining (blue, **Figure 3**). The actin filaments in those guts appeared organized as well (green, **Figure 3**).

IAPP5.2 Was Induced During the Period That Lso Translocated Into the Gut Cells

To test apoptotic responses upon Lso infection at the molecular level, three caspases and four IAPs with BIR domain(s) were selected to evaluate the gene expression in the psyllid gut at the early stage of Lso infection.

In response to LsoA acquisition, two inhibitors IAP1 and IAPP5 were upregulated at day 3 compared to days 2, 5, and 7. IAPP5.2 was significantly upregulated at days 3 and 5 compared to non-infected guts as well as after a 2- and 7-day AAP. Caspase-3 was significantly upregulated at day 7 compared to the uninfected guts and guts following the 3- and 5-day AAP.

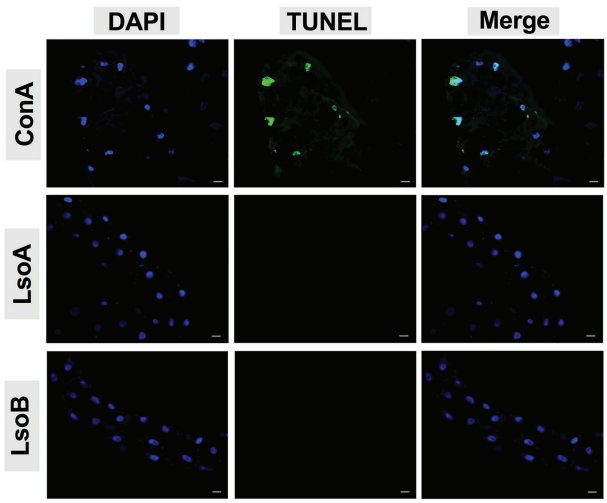

FIGURE 2 | Detection of apoptosis in Lso-exposed potato psyllid gut using TUNEL. The newly Lso-exposed guts were stained using TUNEL to detect the apoptotic signals (green) and counterstained with 4',6-diamidino-2-phenylindole (DAPI) to show the nuclei (blue) of the gut cells. The ConA treatment was used as a positive control. Only 7-day LsoA- or LsoB-exposed guts are shown, similar results were found for the other AAPs. Scale bar is 20 μm.

Furthermore, caspase-3 had the opposite expression profile than IAPP5.2. No significant regulation of IAP2 and the other two caspases was observed in response to LsoA acquisition (**Figure 4**).

In response to LsoB acquisition, the inhibitor IAP1 was upregulated at day 2 compared to days 3 and 5. IAP2 was significantly upregulated at day 7 compared to day 2. In addition, IAPP5 was significantly upregulated at day 2 compared to day 3. Similar to LsoA infection, IAPP5.2 was upregulated at day 3 compared to day 7, and at day 5 compared to the uninfected gut as well as to the 2- and 7-day AAP. Of the three caspase genes, caspase-1 was upregulated at day 2 compared to day 5 and caspase-2 was upregulated at day 3 compared to day 7 infection, however, in both cases the changes in gene expression were relatively minor. On the other hand, caspase-3 was upregulated in response to LsoB acquisition at day 7, and it had the opposite expression profile as IAPP5.2 (**Figure 5**).

In summary, IAPP5.2 was significantly upregulated in response to both LsoA and LsoB between the 3- and 5-day AAP, which is the period that Lso translocated into the gut cells as indicated by immunolocalization of Lso in the psyllid guts.

Silencing of IAPP5.2 Induces Apoptosis in the Gut of Adult Potato Psyllids

Because IAPP5.2 had the opposite expression profile as the effector caspase-3 in response to both LsoA and LsoB, we hypothesized that IAPP5.2 could be the key inhibitor for caspase activity inhibition in the apoptosis pathway of potato psyllid. Then we silenced IAPP5.2 gene expression by RNAi and evaluated the expression of caspases. The oral delivery of dsRNA resulted in 55% decrease of the expression of IAPP5.2 in the gut (**Figure 6A**), and in the upregulation of the transcriptional

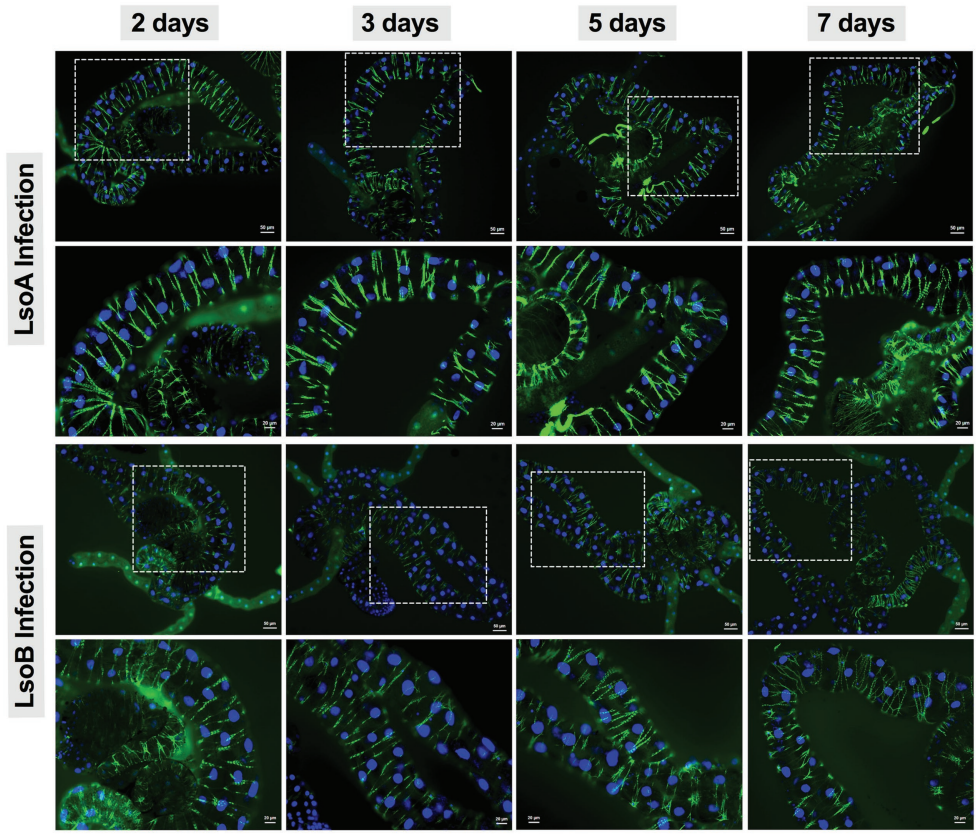

FIGURE 3 | Nuclear morphology and actin cytoskeleton organization in gut cells following Lso exposure. All the guts showed uniform and round shape of cell nuclei (blue) and organized structure of the actin filaments (green). The white dashed rectangle indicates the enlargement region of **upper panels**. The bars of **upper** and **lower panels** are 50 and 20 μm, respectively.

expression of the two effector caspases, caspase-1 and caspase-3. However, it had no impact on the initiator caspase, caspase-2 (**Figure 6A**). Therefore, IAPP5.2 could bind and interact specifically with the two effector caspases with its BIR domain (**Figure 6B**; **Supplementary Figure S1**). Importantly, the upregulation of two effector caspases was accompanied by DNA fragmentation in the IAPP5.2-silenced guts based on TUNEL assay (**Figure 6C**).

Silencing of IAPP5.2 Decreases Lso Acquisition and Transmission Efficiency

Because IAPP5.2 (survivin-like) gene was significantly upregulated during the period Lso translocated into the gut cells, we hypothesized that IAPP5.2 could be involved in the acquisition or even transmission process of Lso. We first silenced IAPP5.2 gene by RNAi and quantified Lso in psyllid gut. Interestingly, silencing of IAPP5.2 significantly decreased both LsoA and LsoB titers in the guts of adult psyllids after 6 days with a 2-day AAP (**Figure 6D**). Therefore, we further hypothesized that the transmission efficiency of Lso by potato psyllid were also affected by dsIAPP5.2-induced apoptosis in psyllid gut. Then we silenced the IAPP5.2 gene and performed sequential inoculation of tomato plants following a 2-day AAP. The results showed that all the recipient tomato plants were tested LsoB-negative at day 17 post acquisition, and similar LsoB transmission rates (23.3–33.3%) were observed at day 21 post acquisition between silencing of GFP (control) and IAPP5.2. However, the LsoB transmission rates were significantly decreased after silencing of IAPP5.2 (average rates = 40%) compared to the control (average rates = 76.7%), at 25 days post acquisition (**Figure 7**). Based on the logistic regression model, there was significance of the effects of two factors (RNAi treatments and the days post acquisition) on the probability that a plant would become infected ($p < 0.01$). However, no significance of the RNAi treatments by days interaction was observed ($p = 0.586$). Importantly, by silencing of IAPP5.2, the plants also had significantly lower odds (probability of infection) of infection at 25 days post acquisition relative to the control (silencing of GFP). For transmission assay of LsoA, none of the plants were infected by LsoA at 17, 21, or 25 days post acquisition, although the inoculated insects were tested positive.

DISCUSSION

A variety of pathogenic organisms can infect insects, including bacteria, viruses, and other organisms. Understanding the

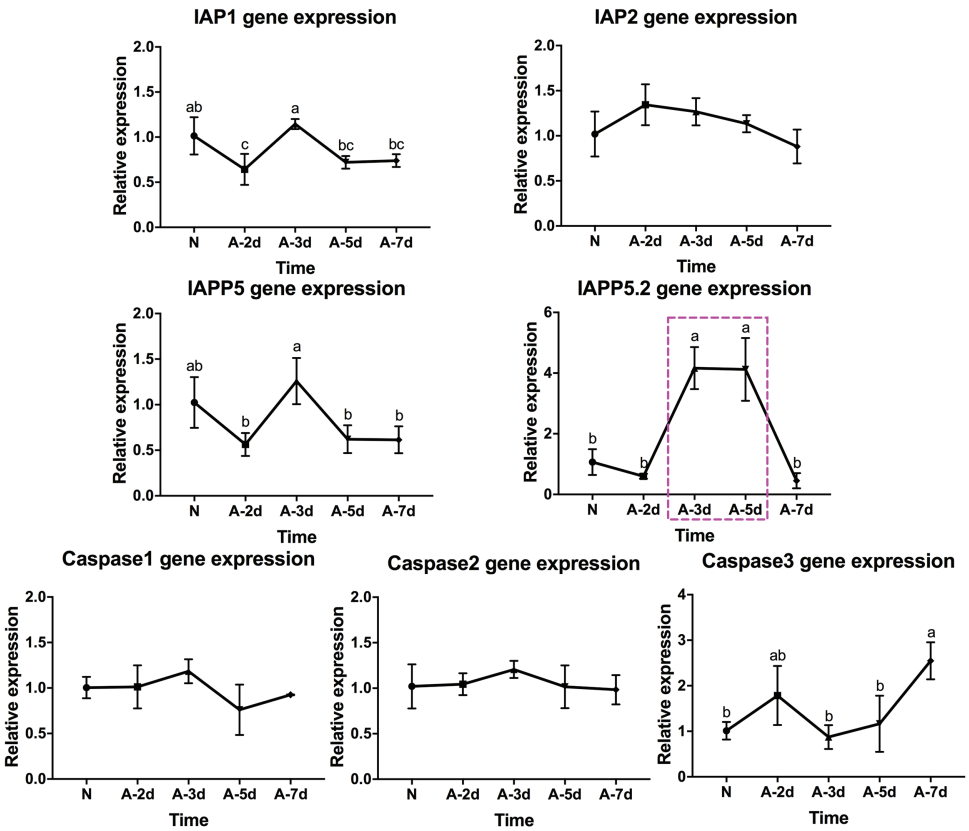

FIGURE 4 | Regulation of apoptosis-related genes in the psyllid gut upon LsoA infection. Data represent means ± SD of three independent experiments. Different letters indicate statistical differences at $p < 0.05$ using one-way ANOVA with Tukey's *post hoc* test. N: Lso-free colonies; A-2d, A-3d, A-5d, and A-7d indicate the psyllids were infected by LsoA for 2, 3, 5, and 7 days, respectively. The pink dashed rectangle indicates the significant upregulation profile of IAPP5.2 gene. The IAPP5.2 gene also had the opposite regulation profile with the effector caspase-3.

characteristics of pathogens and the transmission mechanisms by insect vectors will greatly contribute to create new approaches for controlling diseases caused by insect-borne plant pathogens. The innate immunity plays a critical part in the outcome of pathogens infection of insects (Kingsolver et al., 2013; Cao et al., 2015; Hillyer, 2016). Meanwhile, pathogens can exploit their host's cell machinery and avoid the host's immune defenses for successful replication and transmission (Vyas et al., 2015).

Apoptosis, as an important part of the innate immunity, plays a crucial role in defending against pathogens and limiting the spread of infections. In turn, many intracellular pathogens target caspase signaling as a means to impede apoptosis of the infected host cells. Different strategies are utilized by pathogens to repress the host apoptotic response *via* caspase signaling. For instance, the malaria parasite, *Plasmodium falciparum* alters the cell death pathway of the invaded mosquito midgut cells by disrupting c-Jun N-terminal kinase (JNK) signaling, which regulates the activation of the effector caspase-S2 (Ramphul et al., 2015). Another example is the baculovirus caspase inhibitors, which block apoptosis downstream of effector caspase DrICE in *Drosophila* cells (Lannan et al., 2007). In fact, inhibitors of apoptosis were discovered in baculoviruses and the BIR domain present in the IAP proteins stands for Baculovirus IAP Repeat (Crook et al., 1993). Apart from parasites and viruses, bacteria also have evolved a variety of strategies to block apoptosis at different stages within the apoptotic pathways. For example, *Chlamydia* presumably secretes proteins that result in blocking the release of cytochrome c from the mitochondria and in the inhibition of the activation of effector caspase-3 (Fan et al., 1998).

Numerous studies have focused on the immune responses of host plants to pathogens or the manipulation of plant immunity by pathogens (Dodds and Rathjen, 2010; Weiberg et al., 2013; Asai and Shirasu, 2015; Hacquard et al., 2017). Recently, several studies investigated the immune interactions between insect vectors and plant pathogens, and they found that plant pathogens, in particular plant viruses can induce programmed cell death in their vectors. The induced cell death may fill different roles: it could be a defensive mechanism to protect the insect against the invasion of the pathogens (Wang et al., 2016), or could help the pathogens be acquired or escape specific tissues (Huang et al., 2015; Chen et al., 2017). In both scenarios, these cell death responses can affect the pathogen

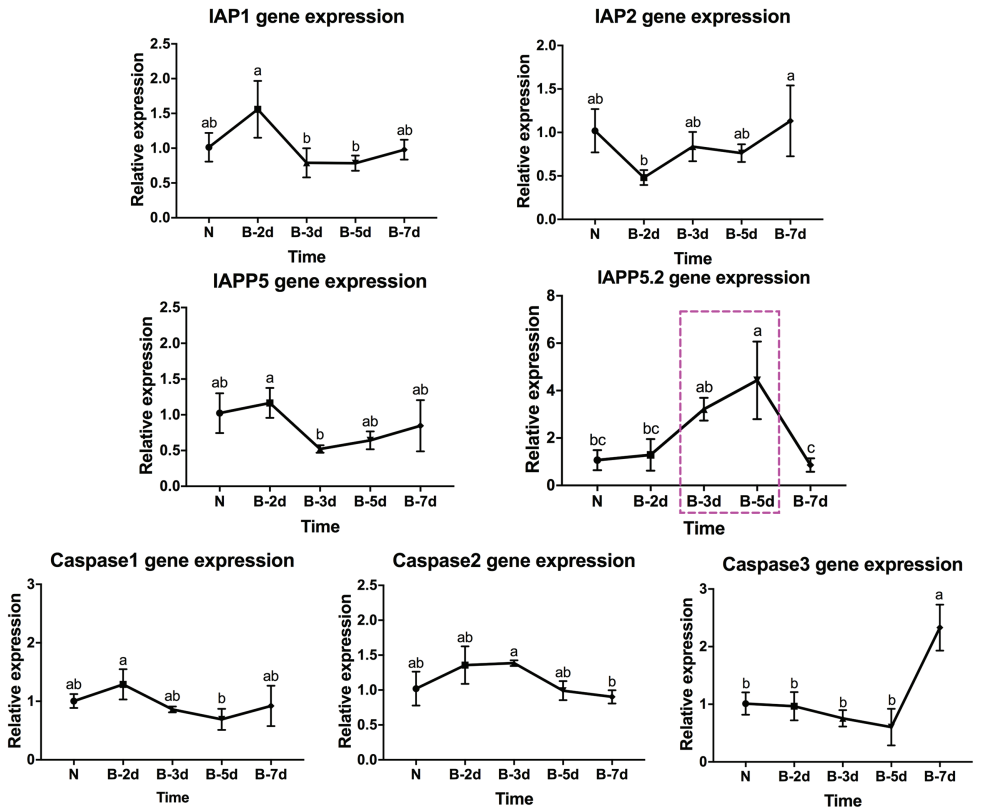

FIGURE 5 | Regulation of apoptosis-related genes in the psyllid gut upon LsoB infection. Data represent means ± SD of three independent experiments. Different letters indicate statistical differences at $p < 0.05$ using one-way ANOVA with Tukey's *post hoc* test. N: Lso-free colonies; B-2d, B-3d, B-5d, and B-7d indicate the psyllids were infected by LsoB for 2, 3, 5, and 7 days, respectively. The pink dashed rectangle indicates the significant upregulation profile of IAPP5.2 gene. The IAPP5.2 gene also had the opposite regulation profiles with the effector caspase-3.

acquisition or transmission. However, our understanding of apoptosis induction or inhibition by vector-borne plant pathogenic bacteria remains largely limited.

In our previous study, no evidence of apoptosis was observed in the gut of adult potato psyllids in response to either Lso haplotype in the case of a persistent infection (Tang and Tamborindeguy, 2019). In the present study, we focused on the potential role of apoptosis as a response in the gut of adult potato psyllids at the early stage of Lso infection. We evaluated if an apoptotic immune response in the psyllid gut occurred between the 2- and 7-day Lso AAP. However, the fluorescent imaging of the TUNEL assay, the nuclear morphology and the actin cytoskeleton architecture also indicated no evidence of Lso-induced abnormalities in newly Lso-exposed guts. Because pathogens can manipulate the apoptotic response of their host, we further evaluated the expression of apoptosis-related genes during this infection period. Interestingly, IAP1 and IAPP5 had similar expression profiles in response to LsoA or LsoB, and therefore these two inhibitors might be co-regulated in the psyllid gut. Furthermore, analysis of the expression of apoptosis-related genes revealed that the inhibitor of apoptosis IAPP5.2 (survivin-like) was significantly upregulated in response to both LsoA and LsoB after a 3- and 5-day AAP. We also noted that the effector caspase-3 had the opposite regulation profiles with IAPP5.2 in response to both LsoA and LsoB. It is possible that LsoA and LsoB suppress caspase activation and further repress the apoptotic response during early infection *via* the upregulation of IAPP5.2 (survivin-like). Indeed, survivin has been shown to prevent the host cellular apoptosis in other infection models. For instance, viral pathogens such as hepatitis B virus (HBV) and human neurotropic virus JC virus have been shown to suppress host caspase activation and apoptosis in a survivin-dependent manner (Marusawa et al., 2003; Pina-Oviedo et al., 2007). In addition to viruses, during the infection by the intracellular parasite *Cryptosporidium parvum* mRNA levels of survivin increases between 12 and 48 h post infection in gut cells. Moreover, siRNA depletion of survivin significantly increases the effector caspase-3/7 activity and further reduces the parasite growth (Liu et al., 2008). siRNA depletion also suggested the role of survivin in blocking apoptosis especially more critical after 24 h of *C. parvum* infection. In the present study, we also found that silencing of IAPP5.2 significantly upregulated the transcriptional expression of the effector caspases 1 and 3 and resulted in the occurrence of TUNEL-positive cells. Therefore, IAPP5.2 could inhibit these caspases and the apoptotic response in the psyllid gut cells. This study represents the first report

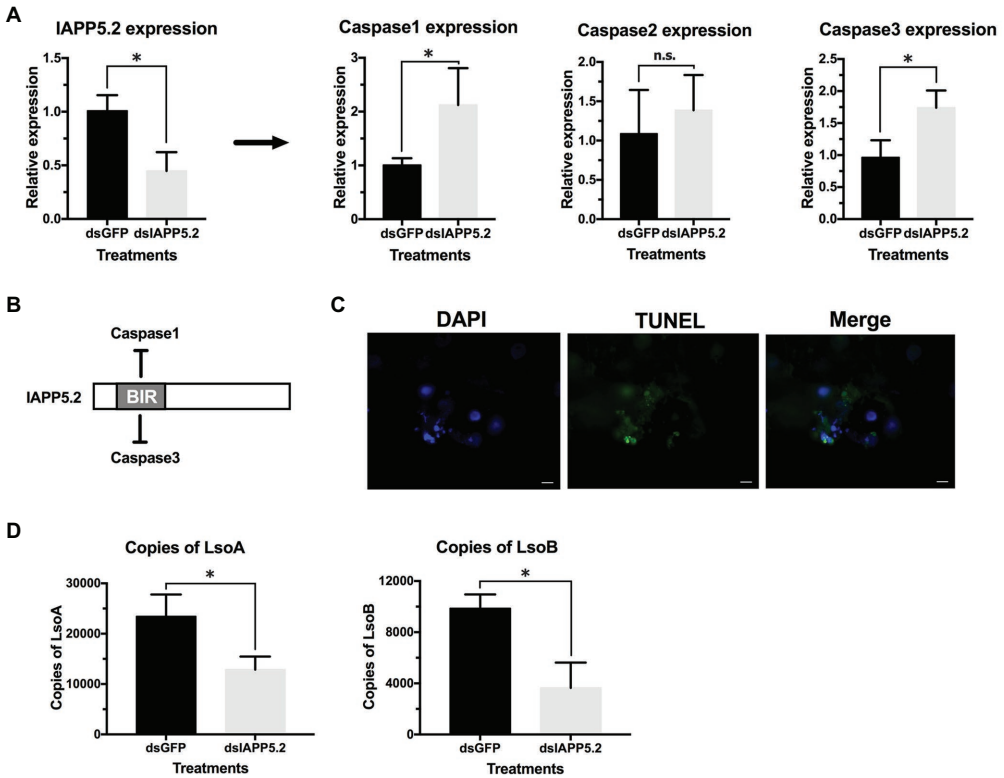

FIGURE 6 | Silencing of IAPP5.2 and its effect on Lso acquisition in psyllid gut. **(A)** Relative gene expression of IAPP5.2, caspases-1, 2, and 3 in psyllid gut following RNA interference (RNAi) silencing of IAPP5.2. **(B)** IAPP5.2 probably binds and interacts with caspases 1 and 3 *via* the baculoviral IAP repeat (BIR) domain. **(C)** DNA fragmentation of guts could be observed based on TUNEL assays after silencing of IAPP5.2. **(D)** Quantification of LsoA and LsoB in the potato psyllid gut after silencing of IAPP5.2. Silencing of IAPP5.2 in the guts of psyllids resulted in reduced LsoA and LsoB accumulation. * indicates $p < 0.05$.

showing that bacterial pathogen might repress host caspase activation and apoptosis in a survivin-dependent manner.

In humans, the apoptosis inhibitors XIAP, c-IAP1, and c-IAP2 are able to directly inhibit caspase-3, -7, and -9, while survivin binds specifically to the effector caspase-3 and -7 rather than the initiator caspases (Shin et al., 2001; Liu et al., 2008). Very little is known about apoptosis in phloem-feeding insects or the role of different proteins involved in this process. Based on our phylogenetic study, caspase-2 is the initiator caspase, while caspases 1 and 3 are effector caspases (Tang and Tamborindeguy, 2019). Thus, in psyllids also, the survivin-like gene could regulate the effector caspases rather than initiator caspase. We noted that at 7-day infection, the caspase-3 gene was upregulated; however, we could not observe apoptosis in the psyllid gut. This may reflect the existence of a potato psyllid response to Lso since Lso, in particular LsoB, is detrimental to the vector fitness (Nachappa et al., 2012b; Yao et al., 2016; Frias et al., 2020). Although caspase-3 was upregulated at day 7 of the infection, it might not have reached or exceeded the threshold to trigger an intracellular apoptotic immune reaction (Maiuri et al., 2007). Another possibility is that apoptosis induction in potato psyllid is regulated by the two effector caspases (caspases 1 and 3). The fact is that Lso still successfully crosses the gut cells, therefore, Lso seems to be preemptive, and has evolved to repress or reduce the apoptotic response in the psyllid gut. This mechanism may help Lso successfully translocate and colonize into the gut cells, and further affect its transmission efficiency.

Indeed, the depletion of IAPP5.2 significantly decreased LsoA and LsoB accumulation in the psyllid gut. Lso ingestion occurred before dsRNA ingestion, therefore any change in Lso accumulation was not linked to a potential behavioral change due to silencing or induced apoptosis, such as a reduction in feeding which could affect Lso ingestion. Therefore, these results indicate that the accumulation of Lso in the psyllid gut could require survivin expression within the infected host cells. Unexpectedly, LsoA titer was higher in the control and silenced insects than LsoB, which is contrary to the results obtained in the accumulation assays. This difference could arise from the use of different donor plants, even if the titer in those plants was within the range commonly measured in LsoA-infected plants (Herrera et al., 2018). The only difference in the experimental set-up between these two experiments is that insects were allowed to feed on the dsRNA solution after exposure to the infected plants. Whether this could affect Lso titer in the gut needs to be investigated. In addition, we demonstrated that the LsoB transmission rates by adult potato psyllid were significantly decreased after silencing of

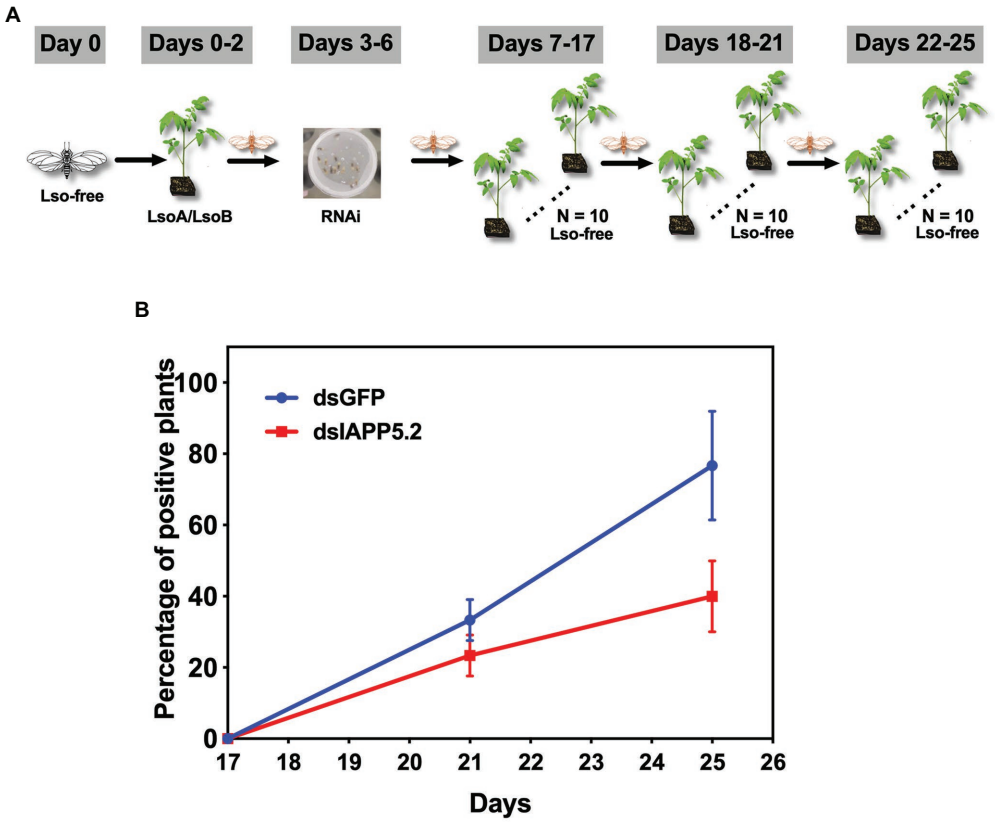

FIGURE 7 | The effect of silencing of IAPP5.2 on LsoB transmission by potato psyllid. **(A)** Adult psyllids were given a 2-day AAP on Lso infected tomato plants and fed with the double-stranded RNAs (dsRNA)-containing diet for 4 days. Then, groups of five adult psyllids were transferred to 10 recipient non-infected tomato plants for an 11-day inoculation access period, and each group was sequentially transferred to a new uninfected recipient plant every 4 days as shown in the schematic representation. The days showed in the figure indicate the days post acquisition. Day 0 is the initial day Lso-free psyllids were exposed to Lso-infected plants. **(B)** Silencing of IAPP5.2 decreases LsoB transmission efficiency. Data represent means ± SD of three independent experiments.

IAPP5.2 at 25 days post acquisition. As summarized in **Figure 8**, it seems that psyllids start to feed plant phloem within 2 days, and around day 3, Lso enter the gut cells and are replicating. Indeed, Lso-derived signal could be observed after the 3 days of AAP. However, Lso meet the immune response of the host gut cells. Lso seem to be preemptive and could induce the inhibitor of apoptosis IAPP5.2 at the early stage of infection. The resulting attenuation of the apoptotic response in the psyllid gut favors Lso, which can replicate safely in the gut cells. This is probably one of the strategies Lso utilizes to successfully colonize and further facilitate its transmission within the potato psyllid at the gut interface. But how does Lso regulate the expression of IAPP5.2 is still unknown, however, bacterial effector proteins could be involved (Levy et al., 2019).

Both the studies on the Asian citrus psyllid-CLas system and the present study suggested that apoptosis could affect the bacterial pathogen acquisition and transmission by insect vectors. As indicated above, the citrus Huanglongbing pathogen, CLas, was reported to induce apoptosis in the gut of the adult vector of the Asian citrus psyllid while there was no evidence of apoptosis in the nymphal gut (Ghanim et al., 2016; Mann et al., 2018) and it was suggested that this apoptotic response in adults might contribute to their reduced efficiency to acquire and transmit CLas compared to nymphs (Inoue et al., 2009; Ghanim et al., 2016). In addition, no evidence of apoptosis was observed in the gut of adult potato psyllids in response to either Lso haplotype in the case of a persistent infection (Tang and Tamborindeguy, 2019) or upon infection in this study, which is also consistent with the efficient transmission of each Lso haplotype by adults that acquired the pathogen during the nymphal stage. Therefore, an apoptotic immune response seems to be a key factor in *Liberibacter* bacteria transmission by psyllids. In fact, psyllids and another hemipteran pest such as aphids have "odd" immune systems likely lacking common immune pathways and antimicrobial effectors (Gerardo et al., 2010; Arp et al., 2016). For instance, the genome of pea aphid *Acyrthosiphon pisum* has been shown to lack genes in the immune deficiency (IMD) pathway (Gerardo et al., 2010), and the IMD pathway gene transcripts were also not found in the transcriptome of the Asian citrus psyllid and potato psyllid (Nachappa et al., 2012a; Kruse et al., 2017).

Quantification of each Lso haplotype following early exposure times to infected plants revealed that LsoA and LsoB population increased with different rates in the psyllid guts. LsoB density

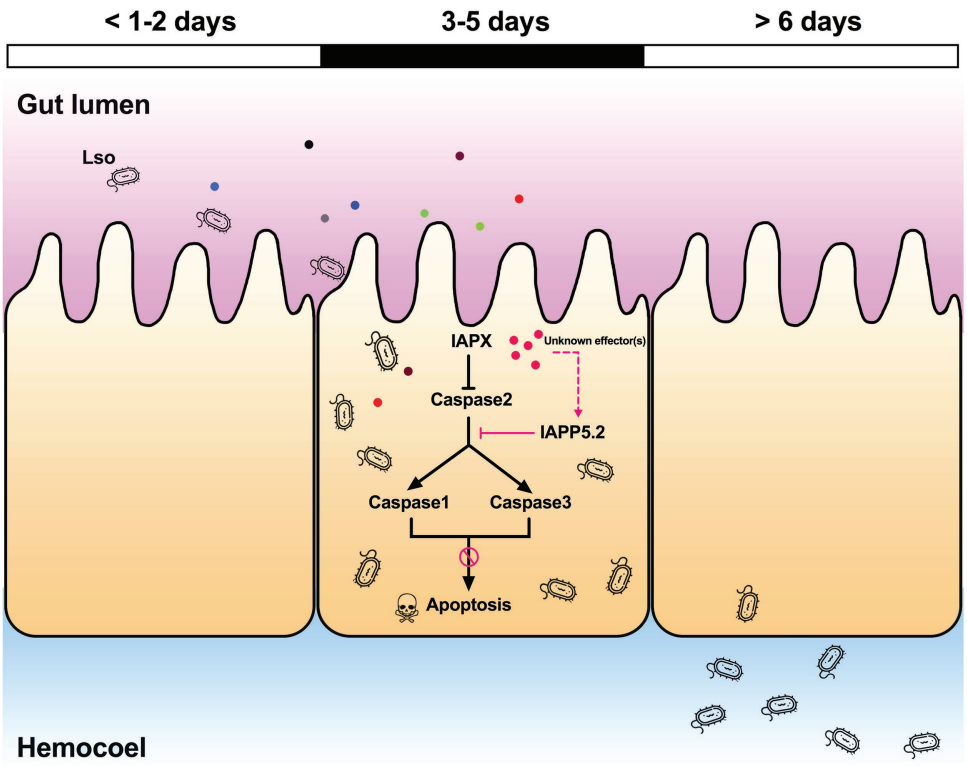

FIGURE 8 | Model of the Lso-repressed apoptotic response in the psyllid gut during early infection. At days 3 and 5 of the infection when Lso first translocate into gut cells, Lso attenuate the psyllid immune responses by upregulating the inhibitor of apoptosis IAPP5.2 gene *via* unknown bacterial effectors (pink dots). The upregulation of IAPP5.2 specifically blocks the activation of effector caspases 1 and 3, which further inhibits the apoptotic response in potato psyllid gut. Other colored dots represent different Lso effectors.

increased rapidly after 3 days, while the increase in LsoA copy number was much slower. During the period of early infection, LsoB has probably entered the gut cells and is replicating, however, LsoA is not actively replicating yet. Our previous studies determined that this delay in LsoA accumulation in the psyllid gut is accompanied by a significant decrease in Lso transmission (Tang et al., 2020b). This probably could explain why none of the plants tested positive for LsoA infection in the transmission assays. In addition, the differences of LsoA and LsoB titer in the gut of adult psyllids could be the result of differences of bacterial pathogenicity or the elicited psyllid immune responses. Indeed, differences in virulence between these two haplotypes were determined in association with their host plants and insect vector: in both cases, LsoB was found to be more pathogenic (Yao et al., 2016; Herrera et al., 2018; Harrison et al., 2019). Similarly, the vector immune response could be one factor explaining the different Lso accumulation profiles. It appears that similar to LsoB, LsoA might stop the apoptotic response in the psyllid gut, as showed in this study; however, other immune responses might be differentially elicited in response to each Lso haplotype. It is therefore possible that LsoB is able to better defend itself against the psyllid immunity. As a consequence, LsoB could be acquired with higher efficiency than LsoA.

In summary, our study demonstrates for the first time that the regulation of apoptosis and the suppression of caspase activation observed in the Lso-exposed cells were due to the upregulation of survivin and was probably mediated by the effector caspases 1 and 3 with unknown bacterial effector (s). This is not only the first study showing that bacterial pathogen represses the host caspase activation and apoptosis in a survivin-dependent manner, but it is the first report indicating that a plant bacterial pathogen can impede the immunity in its insect vector.

DATA AVAILABILITY STATEMENT

The original contributions presented in the study are included in the article/**Supplementary Material**, further inquiries can be directed to the corresponding author.

AUTHOR CONTRIBUTIONS

CT and X-TT designed the study, performed the data analyses, and wrote the manuscript. X-TT, KF, and AM were responsible for performing the experiment. All authors contributed to the article and approved the submitted version.

FUNDING

This research was funded by Texas A&M University and Texas A&M AgriLife Research (Controlling Exotic and Invasive Insect-Transmitted Pathogens) and Hatch project TEX0-1-9381.

ACKNOWLEDGMENTS

KF is an undergraduate student at Texas A&M University. X-TT received the Herb Dean'40 Endowed Scholarship from the Department of Entomology at Texas A&M University. We are grateful to Courtney Adams and Barbara Gastel from Texas A&M University for editorial assistance with an earlier version of our manuscript.

SUPPLEMENTARY MATERIAL

The Supplementary Material for this article can be found online at: https://www.frontiersin.org/articles/10.3389/fmicb.2020.589509/full#supplementary-material

REFERENCES

Ammar, E. -D., Ramos, J. E., Hall, D. G., Dawson, W. O., and Shatters, R. G. Jr. (2016). Acquisition, replication and inoculation of *Candidatus* Liberibacter asiaticus following various acquisition periods on huanglongbing-infected citrus by nymphs and adults of the Asian citrus psyllid. *PLoS One* 11:e0159594. doi: 10.1371/journal.pone.0159594

Arp, A. P., Hunter, W. B., and Pelz-Stelinski, K. S. (2016). Annotation of the Asian citrus psyllid genome reveals a reduced innate immune system. *Front. Physiol.* 7:570. doi: 10.3389/fphys.2016.00570

Asai, S., and Shirasu, K. (2015). Plant cells under siege: plant immune system versus pathogen effectors. *Curr. Opin. Plant Biol.* 28, 1–8. doi: 10.1016/j.pbi.2015.08.008

Bergmann, A. (2010). The role of ubiquitylation for the control of cell death in *Drosophila*. *Cell Death Differ.* 17, 61–67. doi: 10.1038/cdd.2009.70

Cao, X., He, Y., Hu, Y., Wang, Y., Chen, Y. R., Bryant, B., et al. (2015). The immune signaling pathways of *Manduca sexta*. *Insect Biochem. Mol. Biol.* 62, 64–74. doi: 10.1016/j.ibmb.2015.03.006

Chen, Y., Chen, Q., Li, M., Mao, Q., Chen, H., Wu, W., et al. (2017). Autophagy pathway induced by a plant virus facilitates viral spread and transmission by its insect vector. *PLoS Pathog.* 13:e1006727. doi: 10.1371/journal.ppat.1006727

Cicero, J. M., Fisher, T. W., and Brown, J. K. (2016). Localization of '*Candidatus* Liberibacter solanacearum' and evidence for surface appendages in the potato psyllid vector. *Phytopathology* 106, 142–154. doi: 10.1094/PHYTO-04-15-0088-R

Cicero, J. M., Fisher, T. W., Qureshi, J. A., Stansly, P. A., and Brown, J. K. (2017). Colonization and intrusive invasion of potato psyllid by '*Candidatus* Liberibacter solanacearum.' *Phytopathology* 107, 36–49. doi: 10.1094/PHYTO-03-16-0149-R

Cooper, W. R., Sengoda, V. G., and Munyaneza, J. E. (2014). Localization of '*Candidatus* Liberibacter solanacearum'(Rhizobiales: Rhizobiaceae) in *Bactericera cockerelli* (Hemiptera: Triozidae). *Ann. Entomol. Soc. Am.* 107, 204–210. doi: 10.1603/AN13087

Crook, N. E., Clem, R. J., and Miller, L. K. (1993). An apoptosis-inhibiting baculovirus gene with a zinc finger-like motif. *J. Virol.* 67, 2168–2174. doi: 10.1128/JVI.67.4.2168-2174.1993

Danial, N. N., and Korsmeyer, S. J. (2004). Cell death: critical control points. *Cell* 116, 205–219. doi: 10.1016/S0092-8674(04)00046-7

Dodds, P. N., and Rathjen, J. P. (2010). Plant immunity: towards an integrated view of plant-pathogen interactions. *Nat. Rev. Genet.* 11, 539–548. doi: 10.1038/nrg2812

Earnshaw, W. C., Martins, L. M., and Kaufmann, S. H. (1999). Mammalian caspases: structure, activation, substrates, and functions during apoptosis. *Annu. Rev. Biochem.* 68, 383–424. doi: 10.1146/annurev.biochem.68.1.383

Elmore, S. (2007). Apoptosis: a review of programmed cell death. *Toxicol. Pathol.* 35, 495–516. doi: 10.1080/01926230701320337

Fan, T., Lu, H., Hu, H., Shi, L., Mcclarty, G. A., Nance, D. M., et al. (1998). Inhibition of apoptosis in chlamydia-infected cells: blockade of mitochondrial cytochrome c release and caspase activation. *J. Exp. Med.* 187, 487–496. doi: 10.1084/jem.187.4.487

Frias, A. A. T., Ibanez, F., Mendoza, A., De Carvalho Nunes, W. M., and Tamborindeguy, C. (2020). Effects of "*Candidatus* Liberibacter solanacearum" (haplotype B) on Bactericera cockerelli fitness and vitellogenesis. *Insect Sci.* 27, 58–68. doi: 10.1111/1744-7917.12599

Gao, L. -Y., and Abu Kwaik, Y. (2000). Hijacking of apoptotic pathways by bacterial pathogens. *Microbes Infect.* 2, 1705–1719. doi: 10.1016/S1286-4579(00)01326-5

Gerardo, N. M., Altincicek, B., Anselme, C., Atamian, H., Barribeau, S. M., De Vos, M., et al. (2010). Immunity and other defenses in pea aphids, *Acyrthosiphon pisum*. *Genome Biol.* 11:R21. doi: 10.1186/gb-2010-11-2-r21

Ghanim, M., Fattah-Hosseini, S., Levy, A., and Cilia, M. (2016). Morphological abnormalities and cell death in the Asian citrus psyllid (*Diaphorina citri*) midgut associated with *Candidatus* Liberibacter asiaticus. *Sci. Rep.* 6:33418. doi: 10.1038/srep33418

Glynn, J. M., Islam, M., Bai, Y., Lan, S., Wen, A., Gudmestad, N. C., et al. (2012). Multilocus sequence typing of '*Candidatus* Liberibacter solanacearum' isolates from North America and New Zealand. *J. Plant Pathol.* 94, 223–228. doi: 10.4454/jpp.fa.2012.007

Goyal, L. (2001). Cell death inhibition: keeping caspases in check. *Cell* 104, 805–808. doi: 10.1016/S0092-8674(01)00276-8

Green, D. R. (2005). Apoptotic pathways: ten minutes to dead. *Cell* 121, 671–674. doi: 10.1016/j.cell.2005.05.019

Grimm, K. D. S., and Garczynski, S. F. (2019). Identification of a new haplotype of '*Candidatus* Liberibacter solanacearum' in *Solanum tuberosum*. *Plant Dis.* 103, 468–474. doi: 10.1094/PDIS-06-18-0937-RE

Haapalainen, M. L., Wang, J., Latvala, S., Lehtonen, M. T., Pirhonen, M., and Nissinen, A. I. (2018). Genetic variation of '*Candidatus* Liberibacter solanacearum'haplotype C and identification of a novel haplotype from *Trioza urticae* and stinging nettle. *Phytopathology* 108, 925–934. doi: 10.1094/PHYTO-12-17-0410-R

Hacquard, S., Spaepen, S., Garrido-Oter, R., and Schulze-Lefert, P. (2017). Interplay between innate immunity and the plant microbiota. *Annu. Rev. Phytopathol.* 55, 565–589. doi: 10.1146/annurev-phyto-080516-035623

Harrison, K., Tamborindeguy, C., Scheuring, D. C., Herrera, A. M., Silva, A., Badillo-Vargas, I. E., et al. (2019). Differences in zebra chip severity between '*Candidatus* Liberibacter solanacearum' haplotypes in Texas. *Am. J. Potato Res.* 96, 86–93. doi: 10.1007/s12230-018-9692-7

Hay, B. A. (2000). Understanding IAP function and regulation: a view from *Drosophila*. *Cell Death Differ.* 7, 1045–1056. doi: 10.1038/sj.cdd.4400765

Herrera, A. M., Levy, J., Harrison, K., Yao, J., Ibanez, F., and Tamborindeguy, C. (2018). Infection by *Candidatus* Liberibacter solanacearum'haplotypes A and B in Solanum lycopersicum'Moneymaker'. *Plant Dis.* 102, 2009–2015. doi: 10.1094/PDIS-12-17-1982-RE

Hillyer, J. F. (2016). Insect immunology and hematopoiesis. *Dev. Comp. Immunol.* 58, 102–118. doi: 10.1016/j.dci.2015.12.006

Huang, H. -J., Bao, Y. -Y., Lao, S. -H., Huang, X. -H., Ye, Y. -Z., Wu, J. -X., et al. (2015). Rice ragged stunt virus-induced apoptosis affects virus transmission from its insect vector, the brown planthopper to the rice plant. *Sci. Rep.* 5, 102–118. doi: 10.1016/j.dci.2015.12.006

Ibanez, F., Hancock, J., and Tamborindeguy, C. (2014). Identification and expression analysis of aquaporins in the potato psyllid, *Bactericera cockerelli*. *PLoS One* 9:e111745. doi: 10.1371/journal.pone.0111745

Ibanez, F., and Tamborindeguy, C. (2016). Selection of reference genes for expression analysis in the potato psyllid, *Bactericera cockerelli*. *Insect Mol. Biol.* 25, 227–238. doi: 10.1111/imb.12219

Inoue, H., Ohnishi, J., Ito, T., Tomimura, K., Miyata, S., Iwanami, T., et al. (2009). Enhanced proliferation and efficient transmission of *Candidatus* Liberibacter

asiaticus by adult *Diaphorina citri* after acquisition feeding in the nymphal stage. *Ann. Appl. Biol.* 155, 29–36. doi: 10.1111/j.1744-7348.2009.00317.x

Kingsolver, M. B., Huang, Z., and Hardy, R. W. (2013). Insect antiviral innate immunity: pathways, effectors, and connections. *J. Mol. Biol.* 425, 4921–4936. doi: 10.1016/j.jmb.2013.10.006

Kornbluth, S., and White, K. (2005). Apoptosis in *Drosophila*: neither fish nor fowl (nor man, nor worm). *J. Cell Sci.* 118, 1779–1787. doi: 10.1242/jcs.02377

Kruse, A., Fattah-Hosseini, S., Saha, S., Johnson, R., Warwick, E., Sturgeon, K., et al. (2017). Combining'omics and microscopy to visualize interactions between the Asian citrus psyllid vector and the huanglongbing pathogen *Candidatus* Liberibacter asiaticus in the insect gut. *PLoS One* 12:e0179531. doi: 10.1371/journal.pone.0179531

Lamkanfi, M., Declercq, W., Kalai, M., Saelens, X., and Vandenabeele, P. (2002). Alice in caspase land. A phylogenetic analysis of caspases from worm to man. *Cell Death Differ.* 9, 358–361. doi: 10.1038/sj.cdd.4400989

Lannan, E., Vandergaast, R., and Friesen, P. D. (2007). Baculovirus caspase inhibitors P49 and P35 block virus-induced apoptosis downstream of effector caspase DrICE activation in *Drosophila melanogaster* cells. *J. Virol.* 81, 9319–9330. doi: 10.1128/JVI.00247-07

Levy, J. G., Gross, R., Herrera, M. A. M., Tang, X., Babilonia, K., Shan, L., et al. (2019). Lso-HPE1, an effector of '*Candidatus* Liberibacter solanacearum' can repress plant immune response. *Phytopathology* 110, 648–655. doi: 10.1094/PHYTO-07-19-0252-R

Levy, J., Ravindran, A., Gross, D., Tamborindeguy, C., and Pierson, E. (2011). Translocation of '*Candidatus* Liberibacter solanacearum', the zebra chip pathogen, in potato and tomato. *Phytopathology* 101, 1285–1291. doi: 10.1094/PHYTO-04-11-0121

Li, W., Abad, J. A., French-Monar, R. D., Rascoe, J., Wen, A., Gudmestad, N. C., et al. (2009). Multiplex real-time PCR for detection, identification and quantification of '*Candidatus* Liberibacter solanacearum' in potato plants with zebra chip. *J. Microbiol. Methods* 78, 59–65. doi: 10.1016/j.mimet.2009.04.009

Li, W., Hartung, J. S., and Levy, L. (2006). Quantitative real-time PCR for detection and identification of *Candidatus* Liberibacter species associated with citrus huanglongbing. *J. Microbiol. Methods* 66, 104–115. doi: 10.1016/j.mimet.2005.10.018

Liefting, L. W., Southerland, P. W., Ward, L. I., Paice, K. L., Weir, B. S., and Clover, G. R. G. (2009). A new "*Candidatus* Liberibacter" species associated with diseases of solanaceous crops. *Plant Dis.* 93, 208–214. doi: 10.1094/PDIS-93-3-0208

Lin, H., Islam, M. S., Bai, Y., Wen, A., Lan, S., Gudmestad, N. C., et al. (2012). Genetic diversity of '*Candidatus* Liberibacter solanacearum' strains in the United States and Mexico revealed by simple sequence repeat markers. *Eur. J. Plant Pathol.* 132, 297–308. doi: 10.1007/s10658-011-9874-3

Liu, J., Enomoto, S., Lancto, C. A., Abrahamsen, M. S., and Rutherford, M. S. (2008). Inhibition of apoptosis in *Cryptosporidium parvum*-infected intestinal epithelial cells is dependent on survivin. *Infect. Immun.* 76, 3784–3792. doi: 10.1128/IAI.00308-08

Maiuri, M. C., Zalckvar, E., Kimchi, A., and Kroemer, G. (2007). Self-eating and self-killing: crosstalk between autophagy and apoptosis. *Nat. Rev. Mol. Cell Biol.* 8, 741–752. doi: 10.1038/nrm2239

Mann, M., Fattah-Hosseini, S., Ammar, E. -D., Stange, R., Warrick, E., Sturgeon, K., et al. (2018). *Diaphorina citri* nymphs are resistant to morphological changes induced by "*Candidatus* Liberibacter asiaticus" in midgut epithelial cells. *Infect. Immun.* 86, e00889–e00897. doi: 10.1128/IAI.00889-17

Marusawa, H., Matsuzawa, S., Welsh, K., Zou, H., Armstrong, R., Tamm, I., et al. (2003). HBXIP functions as a cofactor of survivin in apoptosis suppression. *EMBO J.* 22, 2729–2740. doi: 10.1093/emboj/cdg263

Nachappa, P., Levy, J., Pierson, E., and Tamborindeguy, C. (2014). Correlation between "*Candidatus* Liberibacter solanacearum" infection levels and fecundity in its psyllid vector. *J. Invertebr. Pathol.* 115, 55–61. doi: 10.1016/j.jip.2013.10.008

Nachappa, P., Levy, J., and Tamborindeguy, C. (2012a). Transcriptome analyses of *Bactericera cockerelli* adults in response to "*Candidatus* Liberibacter solanacearum" infection. *Mol. Genet. Genomics* 287, 803–817. doi: 10.1007/s00438-012-0713-9

Nachappa, P., Shapiro, A. A., and Tamborindeguy, C. (2012b). Effect of '*Candidatus* Liberibacter solanacearum' on fitness of its insect vector, *Bactericera cockerelli* (Hemiptera: Triozidae), on tomato. *Phytopathology* 102, 41–46. doi: 10.1094/PHYTO-03-11-0084

Nelson, W. R., Sengoda, V. G., Alfaro-Fernandez, A. O., Font, M. I., Crosslin, J. M., and Munyaneza, J. E. (2013). A new haplotype of "*Candidatus* Liberibacter solanacearum" identified in the Mediterranean region. *Eur. J. Plant Pathol.* 135, 633–639. doi: 10.1007/s10658-012-0121-3

Pina-Oviedo, S., Urbanska, K., Radhakrishnan, S., Sweet, T., Reiss, K., Khalili, K., et al. (2007). Effects of JC virus infection on anti-apoptotic protein survivin in progressive multifocal leukoencephalopathy. *Am. J. Pathol.* 170, 1291–1304. doi: 10.2353/ajpath.2007.060689

Ramphul, U. N., Garver, L. S., Molina-Cruz, A., Canepa, G. E., and Barillas-Mury, C. (2015). *Plasmodium falciparum* evades mosquito immunity by disrupting JNK-mediated apoptosis of invaded midgut cells. *Proc. Natl. Acad. Sci. U. S. A.* 112, 1273–1280. doi: 10.1073/pnas.1423586112

Salvesen, G. S., and Duckett, C. S. (2002). IAP proteins: blocking the road to death's door. *Nat. Rev. Mol. Cell Biol.* 3, 401–410. doi: 10.1038/nrm830

Schmittgen, T. D., and Livak, K. J. (2008). Analyzing real-time PCR data by the comparative CT method. *Nat. Protoc.* 3, 1101–1108. doi: 10.1038/nprot.2008.73

Shi, Y. (2004). Caspase activation: revisiting the induced proximity model. *Cell* 117, 855–858. doi: 10.1016/j.cell.2004.06.007

Shin, S., Sung, B. -J., Cho, Y. -S., Kim, H. -J., Ha, N. -C., Hwang, J. -I., et al. (2001). An anti-apoptotic protein human survivin is a direct inhibitor of caspase-3 and-7. *Biochemistry* 40, 1117–1123. doi: 10.1021/bi001603q

Silke, J., and Meier, P. (2013). Inhibitor of apoptosis (IAP) proteins-modulators of cell death and inflammation. *Cold Spring Harb. Perspect. Biol.* 5:a008730. doi: 10.1101/cshperspect.a008730

Sprawka, I., Goławska, S., Parzych, T., Sytykiewicz, H., and Czerniewicz, P. (2015). Apoptosis induction by concanavalin A in gut cells of grain aphid. *Arthropod Plant Interact.* 9, 133–140. doi: 10.1007/s11829-015-9356-1

Tamborindeguy, C., Huot, O. B., Ibanez, F., and Levy, J. (2017). The influence of bacteria on multitrophic interactions among plants, psyllids, and pathogen. *Insect Sci.* 24, 961–974. doi: 10.1111/1744-7917.12474

Tang, X. T., Ibanez, F., and Tamborindeguy, C. (2019). Quenching autofluorescence in the alimentary canal tissues of *Bactericera cockerelli* (Hemiptera: Triozidae) for immunofluorescence labeling. *Insect Sci.* 27, 475–486. doi: 10.1111/1744-7917.12660

Tang, X. -T., Ibanez, F., and Tamborindeguy, C. (2020a). Concanavalin a toxicity towards potato psyllid and apoptosis induction in midgut cells. *Insects* 11:243. doi: 10.3390/insects11040243

Tang, X. -T., Longnecker, M., and Tamborindeguy, C. (2020b). Acquisition and transmission of two '*Candidatus* Liberibacter solanacearum' haplotypes by the tomato psyllid *Bactericera cockerelli*. *Sci. Rep.* 10:14000. doi: 10.1038/s41598-020-70795-4

Tang, X. T., and Tamborindeguy, C. (2019). No evidence of apoptotic response of the potato psyllid, *Bactericera cockerelli*, to "*Candidatus* Liberibacter solanacearum" at the gut interface. *Infect. Immun.* 88, e00242–e00319. doi: 10.1128/IAI.00242-19

Vyas, M., Fisher, T. W., He, R., Nelson, W., Yin, G., Cicero, J. M., et al. (2015). Asian citrus psyllid expression profiles suggest *Candidatus* Liberibacter asiaticus-mediated alteration of adult nutrition and metabolism, and of nymphal development and immunity. *PLoS One* 10:e0130328. doi: 10.1371/journal.pone.0130328

Wang, X. R., Wang, C., Wang, X. W., Qian, L. X., Chi, Y., Liu, S. S., et al. (2018). The functions of caspase in whitefly *Bemisia tabaci* apoptosis in response to ultraviolet irradiation. *Insect Mol. Biol.* 27, 739–751. doi: 10.1111/imb.12515

Wang, L. -L., Wang, X. -R., Wei, X. -M., Huang, H., Wu, J. -X., Chen, X. -X., et al. (2016). The autophagy pathway participates in resistance to tomato yellow leaf curl virus infection in whiteflies. *Autophagy* 12, 1560–1574. doi: 10.1080/15548627.2016.1192749

Weiberg, A., Wang, M., Lin, F. -M., Zhao, H., Zhang, Z., Kaloshian, I., et al. (2013). Fungal small RNAs suppress plant immunity by hijacking host RNA interference pathways. *Science* 342, 118–123. doi: 10.1126/science.1239705

Xu, D., Woodfield, S. E., Lee, T. V., Fan, Y., Antonio, C., and Bergmann, A. (2009). Genetic control of programmed cell death (apoptosis) in *Drosophila*. *Fly* 3, 78–90. doi: 10.4161/fly.3.1.7800

Yao, J., Saenkham, P., Levy, J., Ibanez, F., Noroy, C., Mendoza, A., et al. (2016). Interactions '*Candidatus* Liberibacter solanacearum'—*Bactericera cockerelli*: haplotype effect on vector fitness and gene expression analyses. *Front. Cell. Infect. Microbiol.* 6:62. doi: 10.3389/fcimb.2016.00062

Zimmermann, K. C., Bonzon, C., and Green, D. R. (2001). The machinery of programmed cell death. *Pharmacol. Ther.* 92, 57–70. doi: 10.1016/s0163-7258(01)00159-0

Conflict of Interest: The authors declare that the research was conducted in the absence of any commercial or financial relationships that could be construed as a potential conflict of interest.

frontiers in Microbiology

ORIGINAL RESEARCH
published: 09 June 2021
doi: 10.3389/fmicb.2021.683923

Early Population Dynamics of "*Candidatus* Liberibacter asiaticus" in Susceptible and Resistant Genotypes After Inoculation With Infected *Diaphorina citri* Feeding on Young Shoots

*Mônica Neli Alves[1,2], Juan Camilo Cifuentes-Arenas[2], Laudecir Lemos Raiol-Junior[3], Jesus Aparecido Ferro[1] and Leandro Peña[2,4]**

[1] Faculdade de Ciências Agrárias e Veterinárias (FCAV), Universidade Estadual Paulista (UNESP), Jaboticabal, Brazil, [2] Fundo de Defesa da Citricultura (Fundecitrus), Araraquara, Brazil, [3] Empresa Brasileira de Pesquisa Agropecuária (Embrapa), Cruz das Almas, Brazil, [4] Instituto de Biología Molecular y Celular de Plantas (IBMCP), Consejo Superior de Investigaciones Científicas (CSIC), Universidad Politécnica de Valencia (UPV), Valencia, Spain

OPEN ACCESS

Edited by:
Lukasz Lech Stelinski, University of Florida, United States

Reviewed by:
Greg McCollum, Horticultural Research Laboratory (USDA-ARS), United States

***Correspondence:**
Leandro Peña
lpenya@fundecitrus.com.br

Specialty section:
This article was submitted to Microbe and Virus Interactions with Plants, a section of the journal Frontiers in Microbiology

Received: *22 March 2021*
Accepted: *29 April 2021*
Published: *09 June 2021*

Citation:
Alves MN, Cifuentes-Arenas JC, Raiol-Junior LL, Ferro JA and Peña L (2021) Early Population Dynamics of "Candidatus Liberibacter asiaticus" in Susceptible and Resistant Genotypes After Inoculation With Infected Diaphorina citri Feeding on Young Shoots. Front. Microbiol. 12:683923. doi: 10.3389/fmicb.2021.683923

Huanglongbing is a highly destructive citrus disease associated with "*Candidatus* Liberibacter asiaticus" (Las), a phloem–limited and non-culturable bacterium, naturally transmitted by the psyllid *Diaphorina citri.* Although diverse approaches have been used to understand the molecular mechanisms involved in the pathogen–host interaction, such approaches have focused on already infected and/or symptomatic plants, missing early events in the initial days post-inoculation. This study aimed to identify the time course of Las multiplication and whole-plant colonization immediately following inoculation by infected psyllids feeding for 2 days. Thus, the experimental approach was to track Las titers after psyllid inoculation in new shoots (NS) of *Citrus* × *sinensis* (susceptible), *Murraya paniculata* (partially resistant), and *Bergera koenigii* (fully resistant). Soon after psyllid removal, Las titers dropped until the 10–12th days in all three species. Following this, Las titers increased exponentially only in *C.* × *sinensis* and *M. paniculata*, indicating active bacterial multiplication. In *C.* × *sinensis*, Las reached a stationary phase at ∼5 log Las cells/g of tissue from the 40th day onward, while in *M. paniculata*, Las increased at a lower rate of up to ∼3 log Las cells/g of tissue between the 40th and 60th days, decreasing gradually thereafter and becoming undetectable from the 160th day onward. In *B. koenigii*, Las titers decreased from the start and remained undetectable. In *C.* × *sinensis*, an average of 2.6 log of Las cells/g of tissue was necessary for Las to move out of 50% of the NS in 23.6 days and to colonize the rest of the plant, causing a successful infection. Conversely, the probability of Las moving out of the NS remained below 50% in *M. paniculata* and zero in *B. koenigii*. To our knowledge, this is the first study on Las dynamics and whole-plant

colonization during the earliest stages of infection. Identification of critical time-points for either successful multiplication or Las resistance may help to elucidate initial events of Las–host interactions that may be missed due to longer sampling intervals and at later stages of infection.

Keywords: HLB, Las multiplication, *Citrus* spp., *Murraya paniculata, Bergera koenigii,* bacterial growth, qPCR

INTRODUCTION

Huanglongbing (HLB) is the most severe citrus disease worldwide (Bové, 2006). In Asia and America, the unculturable α-proteobacteria, phloem-limited "*Candidatus* Liberibacter asiaticus" (Las) is associated with HLB (Gottwald, 2010). It is transmitted in the field by the Asian citrus psyllid *Diaphorina citri* (Kuwayama) (Sternorrhyncha: Liviidae) (Capoor et al., 1967). As there is no known cure for this disease, HLB control in Brazil is based on the use of healthy plants from certified nurseries, elimination of symptomatic plants in the groves, and inspection and rigorous control of the insect vector (Bassanezi et al., 2020). However, these strategies may be economically and environmentally unsustainable and inefficient for the management of HLB, whose incidence continues to increase, and it is currently estimated to be present in more than 20% of symptomatic trees in the citrus belt of São Paulo and Minas Gerais (Fundecitrus, 2020). In Florida, United States, the citrus industry relies on the production of more than 80% of the orchards that are Las-infected (Singerman and Useche, 2016). Leaves from affected trees show typical HLB symptoms such as asymmetrical chlorosis called blotchy mottle, enlarged veins, and intense canopy defoliation (Bové, 2006). The evolution of symptoms in Las-positive plants is rapid once they appear, and as the disease severity increases, the yield and fruit quality decrease (Gottwald, 2010). HLB-affected fruits are smaller, lighter, and highly acidic and have a reduced Brix ratio (Bassanezi et al., 2009).

Diaphorina citri acquires Las when they feed on the phloem sap from infected trees by inserting their stylets into the sieve elements. Las infects psyllids in a propagative and circulative manner (Inoue et al., 2009; Ammar et al., 2016; Canale et al., 2017). After a minimum latent period of 2–3 weeks, infected psyllids can transmit the bacterium to healthy plants by releasing it directly into the phloem when feeding (Canale et al., 2017). Electrical penetration graph (EPG) experiments have shown that 8 h is usually sufficient for the psyllid to come in contact with the phloem (Bonani et al., 2010; Wu et al., 2016; Carmo-Souza et al., 2020), but the efficiency of Las transmission is strongly dependent on the developmental stage of the plant tissue in which the insect settles as well as the environmental conditions (Raiol-Junior et al., 2017; Lopes and Cifuentes-Arenas, 2021; Pandey et al., 2021). The nature of insect saliva effectors capable of counteracting host defenses, similar to those shown for other phloem-feeding insects (Hogenhout and Bos, 2011), is largely unknown for *D. citri*. Since Las is released into the phloem, it is notable that symptoms appear in infected plants after the bacterium has already reached high titers, in a time period ranging from 4 to 8 months after inoculation under experimental conditions (Lopes et al., 2009) and to more than a year under field conditions (Gottwald, 2010). However, little is known about citrus host–Las interactions before the onset of symptoms, especially during the initial days and weeks after psyllid inoculation. Pandey and Wang (2019) detected Las as early as 2 days after *D. citri* fed on new shoots (NS), but the subsequent population growth was not monitored. It has been reported that Las moves through the phloem pores in an elongated form and adheres to the plasma membrane in sieve plates through unknown extracellular dark materials (Achor et al., 2020). Las preferentially invades new tissues during development (Raiol-Junior et al., 2021a) and irregularly colonizes different parts of the plant (Tatineni et al., 2008; Li et al., 2009), which makes the selection of the tissue used for study and/or diagnostics very important (Tatineni et al., 2008; Johnson et al., 2014; Raiol-Junior et al., 2021a). Moreover, losses in the root system caused by Las occur before the appearance of symptoms in the canopy (Johnson et al., 2014). Therefore, the first steps of the vector–plant–pathogen interaction are challenging to study. In addition, most previous studies were conducted using only susceptible *Citrus* species.

Although susceptibility to Las varies among *Citrus* species and varieties (Folimonova et al., 2009), full resistance has already been described in species that are sexually and/or graft-compatible with *Citrus* (Alves et al., 2021) as well as in species that are phylogenetically more distant within the family Rutaceae, subfamily Aurantioideae (Ramadugu et al., 2016; Beloti et al., 2018; Cifuentes-Arenas et al., 2019). *Murraya paniculata* (L.) Jack and *Bergera koenigii* L. plants, known as orange jasmine and curry leaf, respectively, are commonly used as ornamental plants in tropical and subtropical regions of the world (Swingle and Reece, 1967). Both these species are good hosts for *D. citri* (Damsteegt et al., 2010; Teck et al., 2011; Westbrook et al., 2011), being much more attractive to psyllid females as compared to sweet orange under laboratory and field conditions (Beloti et al., 2017; Tomaseto et al., 2019). However, low suitability and immunity to Las have been reported in *M. paniculata* and *B. koenigii*, respectively (Damsteegt et al., 2010; Beloti et al., 2018; Cifuentes-Arenas et al., 2019). The role of *D. citri* as a Las vector and the first stages of Las infection in the phloem of the two plant species remain unexplored.

We studied the time course of Las multiplication in the susceptible host *Citrus* × *sinensis* 'Valencia', in the transient host *M. paniculata*, and in the fully resistant *B. koenigii* to better understand the initial bacterial dynamics between the delivery of Las into the phloem by adults psyllids, bacterial multiplication at the first stages post-inoculation, and the time taken for Las to get out from the NS and spread through the rest of the plant. The use of a well-controlled challenge-inoculation system using infective psyllids allowed us to replicate experiments with consistent

results, leading to the establishment of the earliest events of Las infection and whole-plant colonization. Understanding Las progression and defense responses triggered by resistant species may help to develop bacterial control strategies.

MATERIALS AND METHODS

Plant Material and Growth Conditions

One-year-old plantlets of *Citrus* × *sinensis* (L.) Osbeck 'Valencia' sweet orange grafted on 'Rangpur' lime (*Citrus* × *limonia* Osbeck) rootstock and 1-year-old seedlings of *M. paniculata* (orange jasmine) and *B. koenigii* (curry leaf) were used. All plants were grown in 300-ml conical tubes (6.5 × 5.9 cm, upper × lower diameter; 16 cm, height), filled with coconut fiber, and irrigated twice a week. Prior to the experimental use, the *C.* × *sinensis* plantlets were 20 to 30 cm above the substrate level, and *M. paniculata* and *B. koenigii* were 20–40 cm above the substrate level. Rearing of Las-infected *Diaphorina citri* and studies on the time course of Las multiplication were carried out inside a controlled environmental room (CER) using shelves where the light source was 20 to 30 cm above the plants. The daily temperature varied from 24°C to 27°C, relative humidity ranged between 55% and 78%, and photoperiod was set to 12 h of light at 300 μmol m^{-2} s^{-1} of photosynthetically active radiation and 12 h of darkness. At the end of the longest sampling time (see below) for up to 12 months, plants were transferred from CER to a greenhouse in which the mean daily air temperature varied between 18.5°C and 34.4°C, and illumination was natural.

Rearing of Las-Infective Psyllids and Inoculation Procedure

A methodology adapted from Lopes and Cifuentes-Arenas (2021) was used for insect rearing and inoculation purposes. Las-positive, fully symptomatic, and 2-year-old plants of *C.* × *sinensis* grafted on 'Swingle' citrumelo (*Citrus* × *paradisi* Macfad. × *Poncirus trifoliata* L. Raf.) growing in 4.7-l pots were used for rearing Las-infective *D. citri* insects. The Ct value of Las in these source plants was 20.7 ± 0.33 (equivalent to ca. 6.2 ± 0.1 log of Las cells/g of tissue). Las infection in *C.* × *sinensis* plants was confirmed by qPCR (Li et al., 2006). Plants were lightly pruned to stimulate the growth of NS, and when they reached the V2 stage of development (Cifuentes-Arenas et al., 2018), four Las-negative 10- to 20-day-old psyllids were confined per shoot for oviposition for 7 days. The Las-negative mixed sex psyllids were obtained from a colony kept at Fundecitrus, reared on healthy *M. paniculata*, adapting the methodology proposed by Skelley and Hoy (2004). The adult psyllids were then removed from the plants, and the plants remained inside the CER to allow for the eggs to hatch and nymphs to develop into first-generation adults (F1). Once F1 adults began to emerge, a random sample of three insects per source plant was taken at 5 days postemergence to confirm Las presence by qPCR, and the rest were maintained in the same plants up to 10–15 days before being used (**Figure 1**).

The *C.* × *sinensis* plantlets and the *M. paniculata* and *B. koenigii* seedlings were pruned at ∼15 cm above the substrate level to force NS growth until they reached stage V3 of development 18 to 23 days post-pruning (Cifuentes-Arenas et al., 2018). In *M. paniculata* and *B. koenigii*, V3 shoots were characterized by the presence of one partially unfurled and one or more tender expanding leaflets (**Figure 2**).

Five 10–15-day-old Las-exposed adults were confined to a single V3 NS per plant for 48 h of inoculation access period (IAP). The adults were then removed and stored at −20°C. Subsequently, random-stratified samplings were performed, where one of the five adult insects from each of three randomly selected plants per NS detaching time (see below) for qPCR analysis was selected. The plants were then sprayed with insecticide (Abamectin EC 7.2 g of active ingredient per 1 l of water) to eliminate any psyllid eggs or nymphs present. This experiment was repeated twice with 70, 100, and 41 individuals of *C.* × *sinensis*, *M. paniculata*, and *B. koenigii*, respectively, in the first replication, and 95, 106, and 70 individuals in the second replication. As a control group, 8–10 plants of each species in both experimental replicates were exposed to Las-negative adults of similar age and conditions as described above.

Time Course of Las Multiplication and Whole Plant Colonization

To determine the population dynamics of Las multiplication after psyllid feeding, 5–10 plants per genotype were randomly selected at each time point, and the NS on which the Las-positive adults fed was detached from time 0 (day of psyllid removal) and at variable times post-IAP. Each plant was used at a single time point. For *C.* × *sinensis*, sampling was performed at 0, 5, 10, 15, 25, 40, 55, and 70 days and 0, 5, 10, 15, 18, 20, 30, 40, 65, and 95 days post-IAP in the first and second experiment replicates, respectively. For *M. paniculata*, sampling was performed at 0, 5, 10, 15, 25, 40, 55, 70, 95, 110, and 180 days and 0, 5, 10, 15, 20, 25, 30, 40, 65, 95, and 170 days post-IAP in the first and second experiment replicates, respectively. For *B. koenigii*, sampling was performed at 0, 5, 10, 15, 30, 60, and 95 days and 0, 5, 10, 15, 20, 34, and 55 days post-IAP in the first and second experiment replicates, respectively. NS was analyzed to verify the presence of Las by qPCR. In the first sampling intervals, the whole NS on which the Las-positive adults fed was used for processing, but as they grew, only a proportion of the tissue was necessary; it was ensured that tissue pieces were randomly sampled from all parts (tip to base) of the NS on which the Las-positive adults fed. At the end of the longest sampling time (180 days), the plants were transferred from the CER to a greenhouse to complete up to 12 months post-IAP. Then, these plants were sampled again, selecting four to five leaves randomly distributed in the whole canopy. The entire leaves were processed to detect Las presence using qPCR; thus, the successful establishment of the infection was verified.

DNA Extraction and qPCR

Tissue samples (0.3 g) were processed as described by Teixeira et al. (2005) using a TissueLyser II system (Qiagen, Valencia, CA, United States) at 45 Hz for 30 s in a 2.0-ml microtube containing 5-mm steel beads. For psyllid DNA extraction, one insect and a 3-mm steel bead were used in a 1.5-ml microtube.

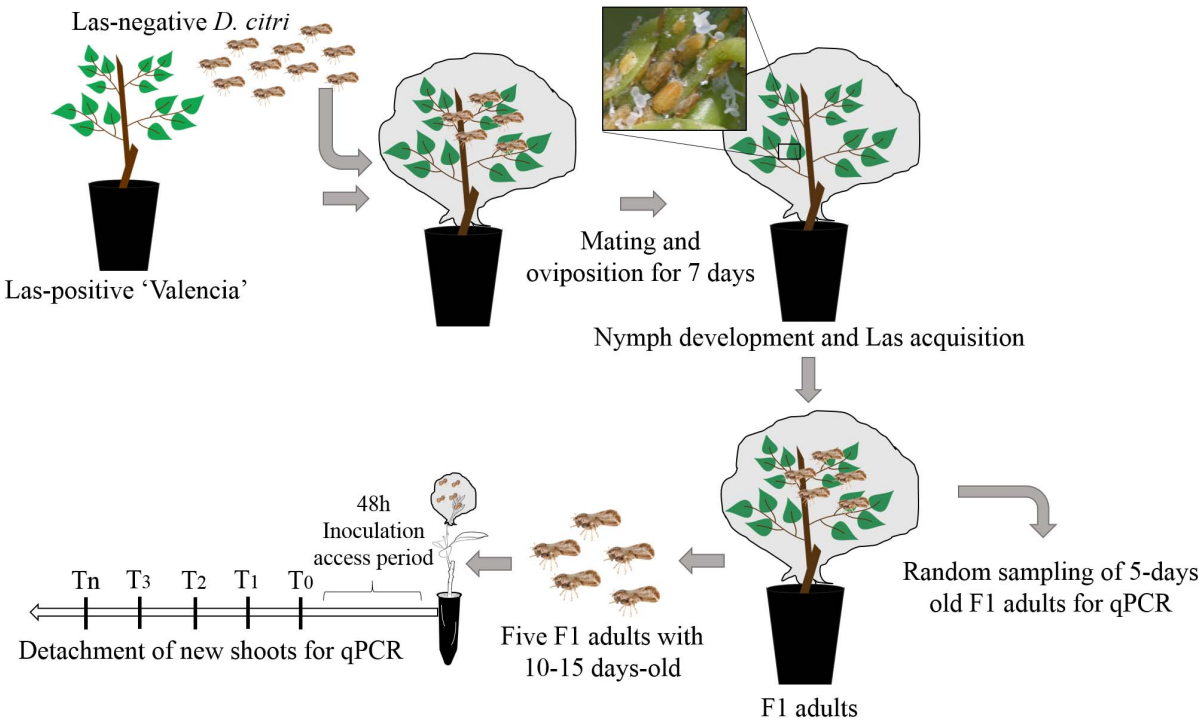

FIGURE 1 | Experimental procedures for "*Candidatus* Liberibacter asiaticus" transmission by *Diaphorina citri*.

Total DNA was extracted using the cetyltrimethylammonium bromide (CTAB) extraction buffer as mentioned in Murray and Thompson (1980), with adaptations. Briefly, for *C.* × *sinensis*, *M. paniculata*, and *D. citri* DNA extraction, 1.5 ml of CTAB buffer was used (2% CTAB; 1.4 M NaCl; 2% PVP 10000; 0.5 M EDTA pH 8; 1 M Tris–HCl pH 8; 0.2% β-mercaptoethanol), incubated at 65°C for 30 min, and then centrifuged for 10 min at 12000 × *g*. The supernatant was transferred to a new 1.5-ml microtube, followed by extraction with chloroform/isoamyl alcohol (24:1). For *B. koenigii*, to avoid oxidation of phenolic compounds after sampling, 0.3 g of the tissue was immediately cooled with liquid nitrogen and stored at −80°C until DNA extraction. The tissue trituration was done with 350 μl of a modified CTAB buffer (2% CTAB; 1.4 M NaCl; 2% PVP 10000; 0.5 M EDTA pH 8; 1 M Tris–HCl pH 8; 5% β-mercaptoethanol) and then 1.15 ml of this buffer was added, incubated at 60°C for 20 min, and centrifuged for 10 min at 12000 × *g*. The supernatant was transferred to a new 1.5-ml microtube, followed by two extractions with phenol/chloroform/isoamyl alcohol (25:24:1) and one with chloroform/isoamyl alcohol (24:1). In both extractions, DNA precipitation was performed with 0.6 V isopropanol, washed twice with 70% ethanol, and resuspended in 50 μl of Milli-Q® water. DNA quality was checked using a NanoDrop (Thermo Fisher Scientific, Massachusetts, EUA) (Desjardins and Conklin, 2010).

For real-time polymerase chain reactions (qPCR) and the identification of the 16S rRNA of Las, 1.0 μl of total DNA (100 ng/μl), TaqMan® PCR Master Mix (1×) (Invitrogen, Carlsbad, CA, United States), and HLBas primer/probe (0.5 μM/0.2 μM) were used in a StepOnePlus thermocycler (Applied Biosystems, California, USA) as described by Li et al. (2006). To estimate Las multiplication in time-course experiments, qPCR analysis was performed in triplicate, and for Las colonization and Las detection in the whole plant, qPCR analyses were performed only once. The mitochondrial gene *cytochrome oxidase* (*COX*) and an insect *wingless* (*Wg*) gene region were used in all samples as internal controls for the quality of plants and psyllid DNA, respectively (Li et al., 2006; Manjunath et al., 2008). In addition, negative and positive citrus leaf and psyllid samples were included during DNA extraction and qPCR assays. Las was quantified based on the linear relationship between Ct and the 16S rRNA log, according to Lopes et al. (2013). As Ct values higher than 34.0 (below 0.9 log Las cells/g of tissue) produce variable results (Lopes et al., 2013), samples were considered Las-positive when the qPCR cycle threshold (Ct) was lower than 34.0, suspected to be positive when Ct values were between 34.0 and 36.0, and negative when Ct > 36 and/or when undetermined.

Data Analysis

Data on adult survival at the time of psyllid removal were analyzed using a chi-square test by adjusting a binomial generalized linear model (GLM). To determine if there were significant differences in Las titers between the groups of psyllids used to inoculate the three plant species (in each repetition of the experiment and between time points within each species), a two-way ANOVA with interactions was first performed considering the species and the repetition of the experiment as a factor with three and two levels, respectively. Subsequently, the possible

differences between the time points within each species were analyzed by performing a one-way ANOVA, considering each shoot detachment time point as a treatment. These analyses were performed by adjusting a Gaussian GLM. Similarly, to compare the initial bacterial load in NS between species at the time of psyllid removal, a two-way ANOVA (plant species × experiment repetition) was carried out. When significant differences were found, the means were separated using Tukey's post hoc test.

To analyze the time course of Las population multiplication in NS after psyllid removal, data on Las titer were submitted to nonlinear regressions to compare several growth models. The best model was selected based on the overall model significance and R^2. For this, data consisted of log values estimated over the Ct values (including those above 34) according to Lopes et al. (2013). An arbitrary value of 39.9999 was assigned to the qPCR results that gave "undetermined" outputs.

Data on new shoot growth were subjected to nonlinear regression to adjust the Gompertz growth model (Tjørve and Tjørve, 2017). To analyze the probability of successful infection after 48 h of psyllid IAP and subsequent detachment of NS at different time intervals, data on Las-positive leaf samples (Ct < 34.0) taken 1 year after the start of the experiments were subjected to a logistic regression by adjusting a binomial GLM (Peng et al., 2002).

RESULTS

Adult survival after 48 h of IAP was not significantly different between plant species [$\chi^2_{(2,2403)}$ = 466.81; p > 0.05]. On an average, psyllid survival after the confinement period was 99.1%, 99.6%, and 96.6% in the first experiment and 95.8, 97.4, and 99.4% in the second experiment replicates on *C.* × *sinensis* 'Valencia', *M. paniculata*, and *B. koenigii*, respectively (**Supplementary Table 1**). Las titers in psyllids did not differ between plant species on which they were confined [$F_{(2,158)}$ = 1.4863; $p > 0.05$] or between replicates [$F_{(1,158)}$ = 0.1535; $p > 0.05$], and there was no significant interaction [$F_{(2,158)}$ = 2.6445; $p > 0.05$] between these two factors (**Supplementary Table 2**). At different time points after NS detachment, there was no difference in Las titers in psyllids used in *C.* × *sinensis* [$F_{(12,53)}$ = 0.9967; $p > 0.05$], *M. paniculata* [$F_{(14,64)}$ = 1.7563; $p > 0.05$], and *B. koenigii* [$F_{(10,38)}$ = 1.7061; $p > 0.05$]. The averages of Las titers varied from 5.33 to 5.98 log (min. = 1.94; max. = 6.94; **Figure 3**). The amount of initial bacterial load injected by the adult psyllids after 48 h of IAP was not influenced by the plant species [$F_{(2,50)}$ = 0.003; $p > 0.05$] or by the repetition of the experiment [$F_{(1,50)}$ = 1.542; $p > 0.05$]. The interaction between the two factors was not significant [$F_{(2,50)}$ = 3.220; $p = 0.05$]. Details on Ct and log values of each plant and time of evaluation are shown in **Supplementary Tables 3**, **4**.

The data on Las titers in *C.* × *sinensis* and *M. paniculata* adjusted well to the Lorentzian growth model (**Table 1** and **Supplementary Figure 1**). This model describes two contrasting situations for both species in both replicates (**Figure 4**). At time 0 (the day of psyllid removal after 48 h of IAP), 10/10 and 7/10 *C.* × *sinensis* plants had Ct values lower than 34.0, in the first and second replicates, respectively. The average Las titer in NS at time 0 was 2.91 ± 0.16 log cell/g of tissue. After this, there was an initial decrease in Las titers soon after psyllid removal until the 10–12th days, up to ∼2.0 log cell/g of tissue. Subsequently, Las multiplied exponentially, reaching ∼90% of its final population after ∼40 days (**Figure 4**). A stationary phase was then observed, and the bacterial titer remained stable (∼4.5–5 log cell/g of tissue) until the last evaluation (70 and 95 days post-IAP in experiment replicates 1 and 2, respectively) with 80%–100% Las-positive plants.

Moreover, 9/10 and 10/10 *M. paniculata* plants were Las-positive at time 0 in the first and second experiment replicates, with an average titer of 2.90 ± 0.10 log cell/g of tissue. The initial decrease in Las titer up to the 10–12th days was less severe than that in *C.* × *sinensis*, with an average titer of ∼2.5 log cell/g of tissue. The subsequent exponential increase was also less pronounced, and Las reached a maximum titer between the 40th and 60th days, with a population similar to that of the day of psyllid removal (∼3 log cell/g of tissue). After reaching this maximum, Las titer decreased slowly until it reached undetectable levels from the ∼180th and 170th days onward in the first and second experiment replicates, respectively (**Figure 4**).

In *B. koenigii*, the best model describing Las population progress was the negative exponential model (**Table 1** and **Supplementary Figure 1**). At time 0, 6/8 and 6/10 *B. koenigii* plants showed Ct values lower than 34.0, in the first and second replicates, respectively. The average of the Las titer in NS at time 0 was 2.93 ± 0.15 log cells/g of tissue, but after this, a fast reduction in Las titer following psyllid removal was observed, reaching undetectable levels from the 30th and 10th days onward in the first and second replicates, respectively (**Figure 4**).

For the three species, the Gompertz model described sufficiently well the growth of NS (**Table 2**), with very active growth from 15 to approximately 45 days after pruning. The maximum rate of NS growth was found in *C.* × *sinensis* at days 25–30 in both experimental replicates, followed by *B. koenigii* at days 33–35 also in both experimental replicates. *M. paniculata* presented the lowest growth rate, reaching the maximum rate at days 20 and 23 in replicates 1 and 2, respectively (**Figure 5** and **Supplementary Table 5**).

In *C.* × *sinensis*, the time after 48 h of IAP in which NS was detached significantly affected the probability of a successful infection in the whole plant, evaluated by qPCR 1 year after the initial insect confinement (**Table 3**), indicating that Las was restricted to the NS during the first weeks post-inoculation. In *C.* × *sinensis*, the mean time for the NS to begin to serve as source of Las for the rest of the plant and thus to establish a successful infection was 21.8 days (∼15 to 30 days) in the first experiment replicate and 25.3 (∼18 to 33 days) in the second replicate. For *M. paniculata*, the results indicated that Las was almost unable to achieve whole-plant stable infections in the host (**Figure 6**), as only 18 out of 100 and 10 out of 106 seedlings in the first and second experiment replicates, respectively, were infected out of the NS at 12 months after psyllid inoculation, and such Las-positive plants were distributed randomly along the time

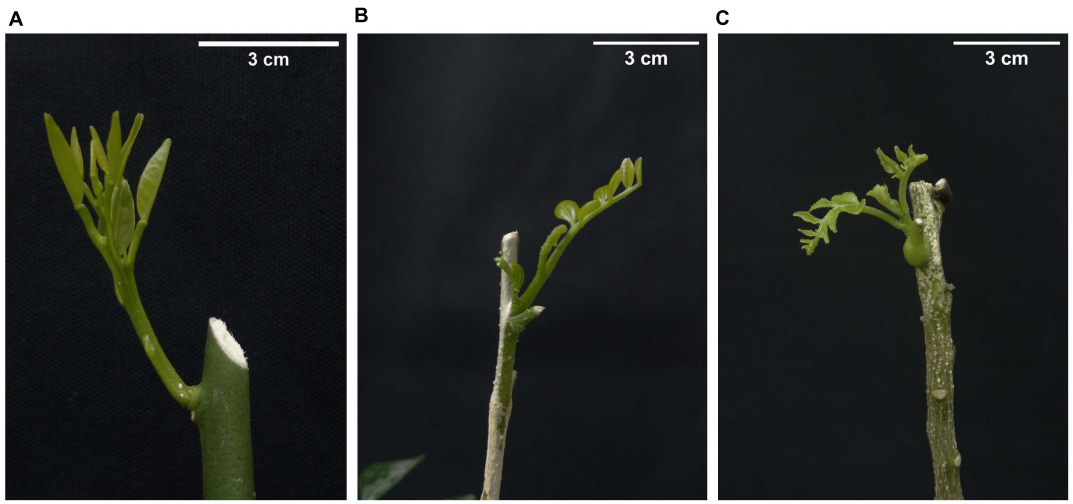

FIGURE 2 | Aspect of new shoots in **(A)** *Citrus* × *sinensis*, **(B)** *Murraya paniculata*, and **(C)** *Bergera koenigii.* Such shoot stages were used for "*Candidatus* Liberibacter asiaticus" challenge *Diaphorina citri*-mediated inoculation experiments.

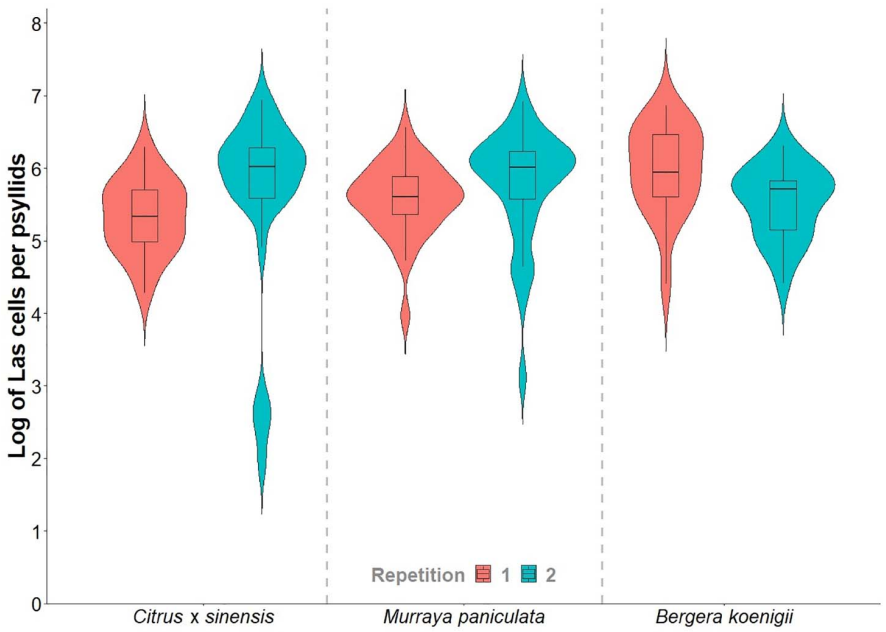

FIGURE 3 | Violin plots of the "*Candidatus* Liberibacter asiaticus" titer in a subsample of 15- to 20-day-old *Diaphorina citri* adults reared on Las-positive *Citrus* × *sinensis* plants and confined during 48 h of inoculation access period (IAP) in new shoots of healthy *Citrus* × *sinensis*, *M. paniculata*, and *B. koenigii*.

points evaluated in both replicates (**Supplementary Table 4**). In *B. koenigii*, Las could not establish successful infections regardless of the NS detachment time.

DISCUSSION

In this study, we investigated the earliest steps of *D. citri*–Las–host interactions, which resulted in the establishment of either bacterial infection in the susceptible *C.* × *sinensis* 'Valencia' host or in resistance to Las in *M. paniculata* and *B. koenigii*. These two latter species were considered among the most suitable *D. citri* hosts among the Rutaceae, because volatile and visual cues made them more attractive than *Citrus* (Beloti et al., 2017; Tomaseto et al., 2019). The number of adult psyllids settled on the seedlings, number of eggs laid, and nymphs developed were also higher in *M. paniculata* and *B. koenigii* than in *Citrus* in host choice assays (Teck et al., 2011). However, we did not find differences among these three host plants in the ability of infected psyllids to inoculate Las into them, because Las showed similar titers at

TABLE 1 | Nonlinear regression models describing the time course of "*Candidatus* Liberibacter asiaticus" population dynamics in new shoots after 48 h of Las-exposed *Diaphorina citri* confinement at 25°C ± 2°C.

	Model parameters				Model statistics		
	$\beta_0 \pm$ SE	$\beta_1 \pm$ SE	$\beta_2 \pm$ SE	$\beta_3 \pm$ SE	$F_{(df)}$	$P(>F)$	R^2
Replicate 1							
C. × *sinensis*[a]	5.356 ± 0.333	13.343 ± 1.730	29.682 ± 7.507	−176.41 ± 47.940	$24.85_{(3,9)}$	0.002	0.8994
M. paniculata[a]	1.389 ± 0.418	64.819 ± 12.341	130.6 ± 57.449	339.349 ± 201.587	$4.92_{(3,11)}$	0.0381	0.5403
B. koenigii[b]	3.424 ± 0.445	−0.211 ± 0.051	–	–	$105.73_{(2,6)}$	< 0.001	0.7627
Replicate 2							
C. × *sinensis*[a]	5.172 ± 0.220	12.798 ± 1.044	32.917 ± 5.326	−206.907 ± 34.916	$69.42_{(3,11)}$	< 0.001	0.9535
M. paniculata[a]	1.118 ± 0.388	45.641 ± 6.797	84.272 ± 32.31	277.056 ± 125.897	$6.66_{(3,12)}$	0.0126	0.6207
B. koenigii[b]	3.285 ± 0.488	−0.405 ± 0.073	–	–	$76.80_{(2,7)}$	< 0.001	0.8018

[a] *The final model selected was* $Las = \beta_0 + \frac{2\beta_3}{\pi} \frac{\beta_2}{4(x-\beta_1)^2+(\beta_2)^2}$, *were* β_0 *is the baseline offset,* β_1 *is the center of the peak,* β_2 *is the full width of the peak at half height, and* β_3 *is the total area of the curve from the baseline.*

[b] *The final model selected was Las* $\beta_0 x^{\beta_1}$, *were* β_0 *is the coefficient and* β_1 *is power.*

time 0 in NS of the three plant species, after the infected insects fed on them for 48 h. Although it has been reported that Las infection negatively affects *D. citri* performance (Ghanim et al., 2016) and induces important transcriptome reprogramming in the insect midgut (Yu et al., 2020), most infected *D. citri* individuals used in our experiments remained alive after 48 h of IAP and were efficient in transmitting Las to the three hosts. Morphological, developmental, and chemical differences among the three Rutaceae species (Beloti et al., 2018; Cifuentes-Arenas et al., 2019; Tomaseto et al., 2019) did not influence the ability of psyllids to overcome physical barriers and access sieve elements through their stylets to release the bacterium at relatively high titers. However, it is possible that Las acquisition by the psyllids may differ between these three host plants, whether due to the above differences or for other reasons including different Las titers in these hosts.

Once released into the phloem, bacterial titers decreased during the first 10–12 days after inoculation, reaching very low concentrations in the three species investigated. Such bacterial titer decline may be attributed, at least in part, to a dilution effect due to active NS growth a few days after pruning at the V2–V3 developmental stages in *C.* × *sinensis*, according to Cifuentes-Arenas et al. (2018). However, there was a clear lag between Las titer fall and NS enlargement, which occurred from 15 to 45 days after pruning. Moreover, Las decline was similar in the three species and quite comparable in the two replicates, while NS development followed slightly differing patterns in the two replicates, especially for *C.* × *sinensis* and *B. koenigii* (**Figures 4**, **5**). Las has a reduced genome size and lacks genes involved in type 3 and most part of type 2 and 4 secretion systems, as well as those required for life *in vitro* (Duan et al., 2009). Indeed, it is only able to metabolize some sugars, which makes it dependent on phloem sap as a carbon source (Fagen et al., 2014), as it occurs in many other phloem-restricted bacteria (Huang et al., 2020). It is possible that Las needs some time to adapt to the new phloem environment to sequester metabolites from the host required to live and multiply. On the other hand, such initial bacterial titer decline does not occur when *Liberibacter crescens* strain BT-1, the only cultured wild-type strain of the *Liberibacter* genus, is grown *in vitro* under optimal nutritional and environmental conditions (Sena-Vélez et al., 2019). This suggests that the phloem does not provide the necessary metabolites to Las so fast and/or they need to be transformed for use by bacterial cells, as it occurs with sugars for spiroplasmas (André et al., 2005). Killiny (2016) proposed that the *M. paniculata* and *B. koenigii* phloem sap has poor nutrient qualities, which may be associated with the limited or lack of Las multiplication in these two species observed in later time-course phases, but not during the first 12 days after inoculation, because the bacterial titer decrease was similar in *C.* × *sinensis*, an excellent Las host.

Alternatively, bacterial titer decrease may be caused as a consequence of defense responses induced by plant cells to either psyllid damage through herbivore-associated molecular patterns or to Las through microbe-associated molecular patterns (Huang et al., 2020). Although it is unclear whether the latter occurs in phloem sieve elements (Jiang et al., 2019), it has been recently found that Las can attach and move into nucleated cells associated with the phloem, at least in seed coat phloem tissue (Achor et al., 2020), which would likely activate immune cell responses. Moreover, such a drastic and consistent decline in bacterial titers in different plant species at a few days post-inoculation may explain, at least in part, the relatively low efficiency of Las inoculation and the frequent failures in attempts to inoculate Las into citrus plants through psyllids under controlled conditions (Pelz-Selinski et al., 2010; Ammar et al., 2016; Canale et al., 2017). Therefore, Las should be able to overcome such a lag, probably caused by the presence of physical and chemical obstacles, to remain alive and proceed with the infection process. It is known that the Las genome encodes a functional salicylic acid hydroxylase capable of degrading salicylic acid to neutralize plant defenses (Li et al., 2017). Moreover, the Las prophage gene SC2-gp095 encodes a ROS-scavenging peroxidase, which may assist Las in evading plant defense responses (Jain et al., 2015).

After the decrease phase, the Las concentration increased exponentially until it reached a titer of approximately 5 log Las cells/g of NS tissue at 45 days, which was maintained stationary in the susceptible *C.* × *sinensis* host. Other studies conducted

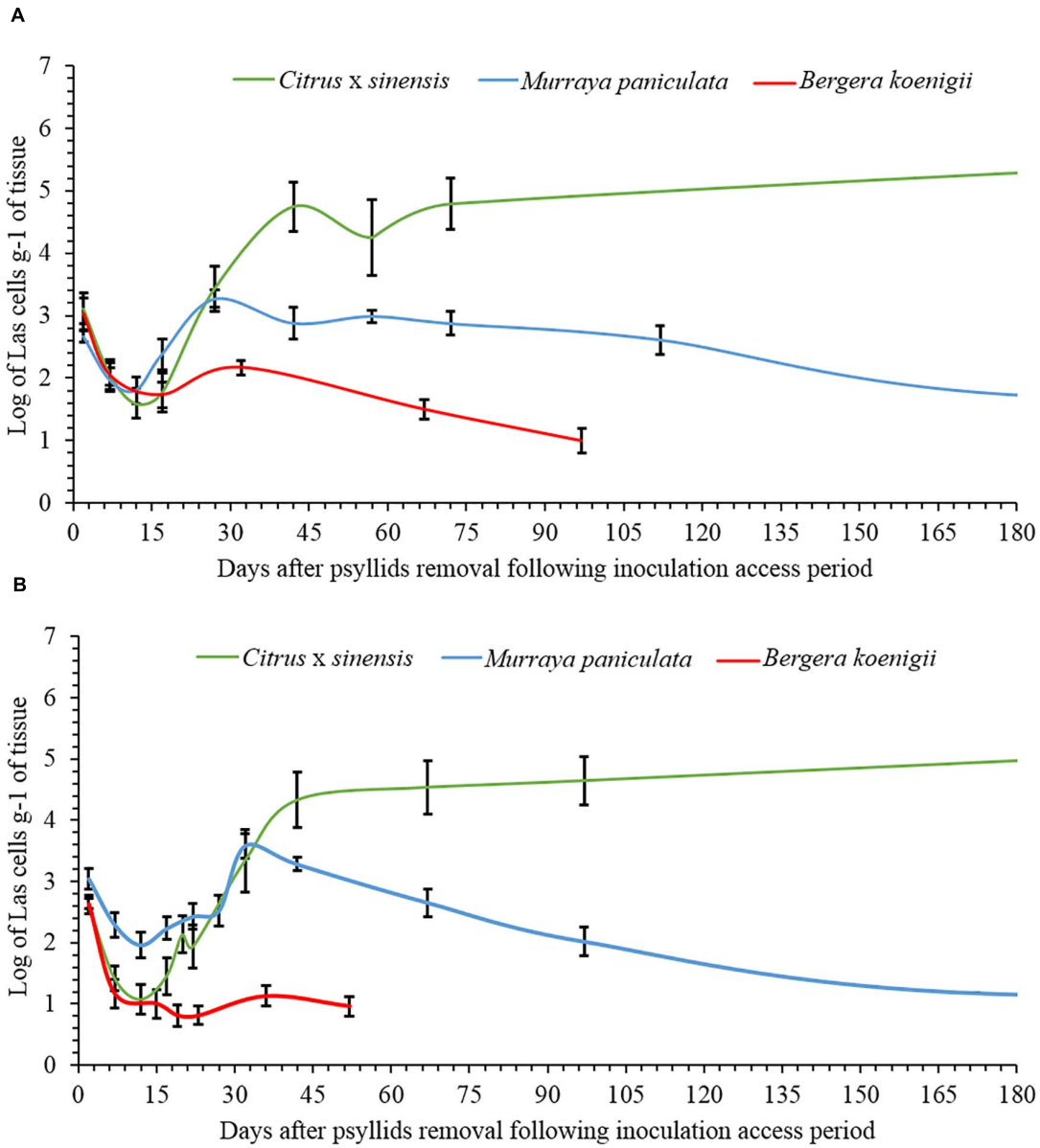

FIGURE 4 | Evolution of the population dynamics of "*Candidatus* Liberibacter asiaticus" over time in new shoots of *Citrus* × *sinensis*, *Murraya paniculata*, and *Bergera koenigii*, following a 48-h period of Las-exposed *Diaphorina citri* confinement in experiment replicates 1 **(A)** and 2 **(B)**.

with already Las-infected plants, inoculated by grafting, obtained similar results in terms of stationary phase titers in susceptible citrus genotypes (Hilf and Luo, 2018; Raiol-Junior et al., 2021a). However, in our study, there was a lag of approximately 15–30 days for Las to reach a plateau of 5 log Las cells/g of tissue compared to the previous studies, which may be due to differences in the initial inoculum titers (budwoods vs. psyllids), a dose–effect already reported (Raiol-Junior et al., 2017), which seems to lose relevance once Las is established (Cifuentes-Arenas et al., 2019). An average of 23.6 (16.5–31.5) days of post-IAP was required for Las to move out of 50% of the NS and colonize the rest of the plant, causing a successful infection, that is, for the initially infected shoot to serve as a source of Las for the rest of the *C.* × *sinensis* plant. This occurred several months before Las-secreted proteins may be suitable for interaction with host cell enzymes to induce disease symptoms (Clark et al., 2018; Pang et al., 2020), including conspicuous callose deposition on sieve plates and consequent leaf mottling in infected *C.* × *sinensis* plants (Kim et al., 2009; Achor et al., 2010). Other phloem responses arising just after Las phloem translocation from infected tissues, but much earlier than the expression of symptoms, remain poorly understood.

In *M. paniculata*, Las population dynamics were similar to those of *C.* × *sinensis* up to the 30th day. Las reached a

TABLE 2 | Parameters of the Gompertz growth model of new shoots of *Citrus* × *sinensis*, *Murraya paniculata*, and *Bergera koenigii*.

	Model parameters			Model statistics		
	$\beta_0 \pm$ SE	$\beta_1 \pm$ SE	$\beta_2 \pm$ SE	$F_{(df)}$	$P(> F)$	R^2
Replicate 1						
C. × *sinensis*[a]	15,586 ± 0,872	25,027 ± 0,99	0,255 ± 0,082	$157.18_{(3,77)}$	< 0.001	0.5711
M. paniculata[a]	6,52 ± 0,214	20,53 ± 2,068	0,123 ± 0,037	$483.95_{(3,107)}$	< 0.001	0.6226
B. koenigii[a]	17,103 ± 0,814	33,345 ± 1,268	0,153 ± 0,034	$221.61_{(3,41)}$	< 0.001	0.8922
Replicate 2						
C. × *sinensis* [a]	10,579 ± 0,447	24,697 ± 0,922	0,249 ± 0,074	$271.25_{(3,102)}$	< 0.001	0.5606
M. paniculata[a]	4,139 ± 0,221	23,431 ± 2,57	0,062 ± 0,015	$316.01_{(3,113)}$	< 0.001	0.5615
B. koenigii[a]	22,132 ± 1,599	32,672 ± 1,434	0,11 ± 0,024	$179.62_{(2,77)}$	< 0.001	0.6964

[a] *The final model selected was* $Shootsize = \beta_0 * e^{\left(-e^{(-\beta_2 * (time - \beta_1))}\right)}$, *where* β_0 *is maximum shoot size (cm),* β_1 *is the center of the curve (days), and* β_2 *is the growth rate (cm day*$^{-1}$*).*

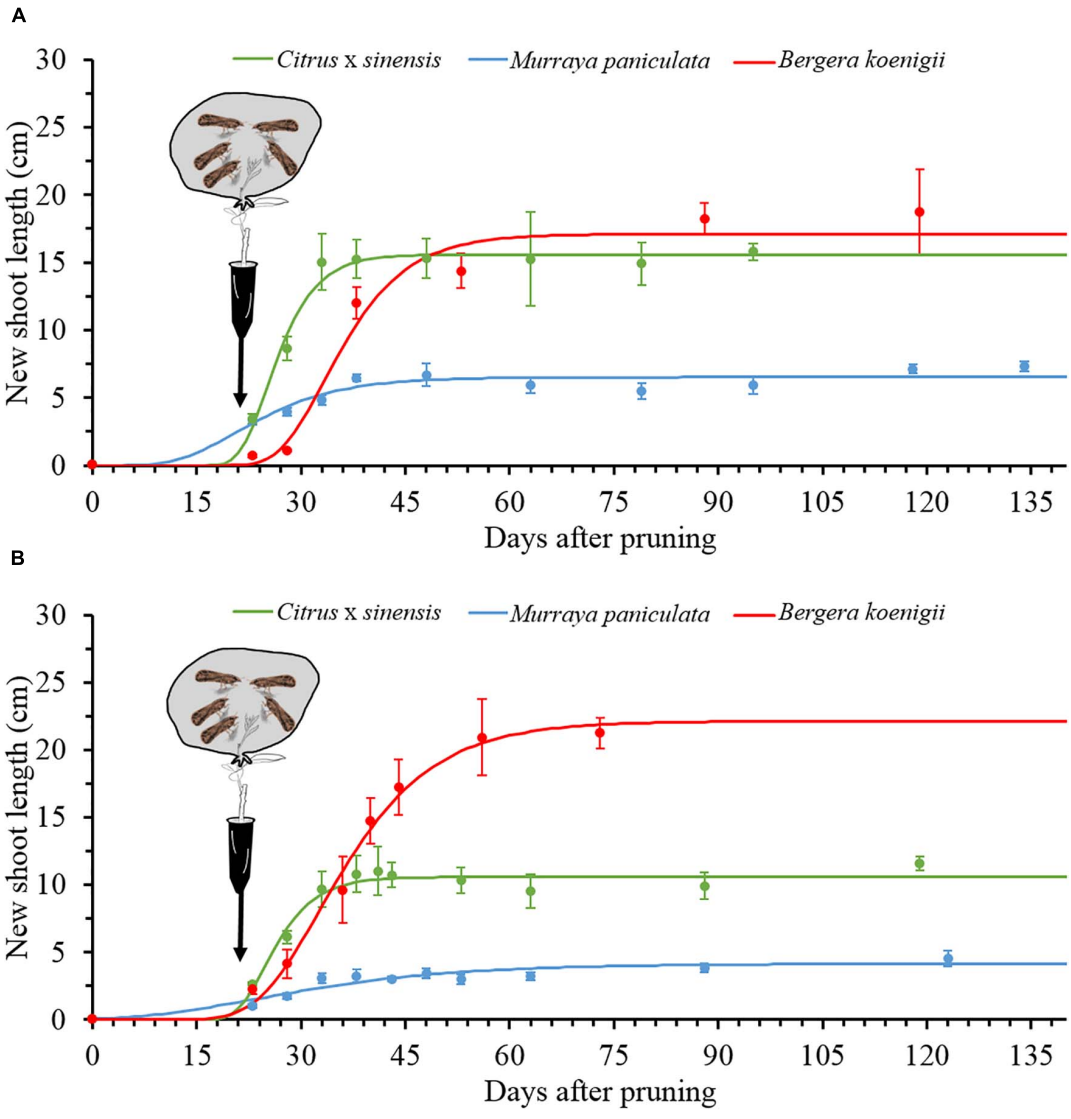

FIGURE 5 | The Gompertz models for new shoot growth of *Citrus* × *sinensis*, *M. paniculata*, and *B. koenigii* in an acclimatized room at 25°C (black arrows indicate the day of psyllid confinement for a 48-h inoculation access period (IAP), (see section "Materials and Methods" for details), in experiment replicates 1 **(A)** and 2 **(B)**.

TABLE 3 | Logistic models for the probability of a successful infection after 48 h of Las-positive inoculation by *Diaphorina citri* adults onto new shoots.

	Model parameters[a]		Model statistics		
Species	**$\beta_0 \pm$ SE**	**$\beta 1 \pm$ SE**	**$X^2_{(df)}$**	**$P(>X^2)$**	**pseudo-R^2**
Replicate 1					
C. × *sinensis*	**−1.917 ± 0.494**	**0.088 ± 0.022**	$67.25_{(1,68)}$	5.40×10^{-8}	0.3054
M. paniculata	**−1.920 ± 0.391**	0.008 ± 0.005	$92.01_{(1,98)}$	0.1322	0.0240
Replicate 2					
C. × *sinensis*	**−2.305 ± 0.503**	**0.091 ± 0.021**	$88.06_{1,88)}$	4.21×10^{-9}	0.2816
M. paniculata	**−2.110 ± 0.438**	0.004 ± 0.008	$65.97_{(1,104)}$	0.6058	0.0040

[a]*SE, standard error of the parameter; bold values are significant ($p < 0.05$).*

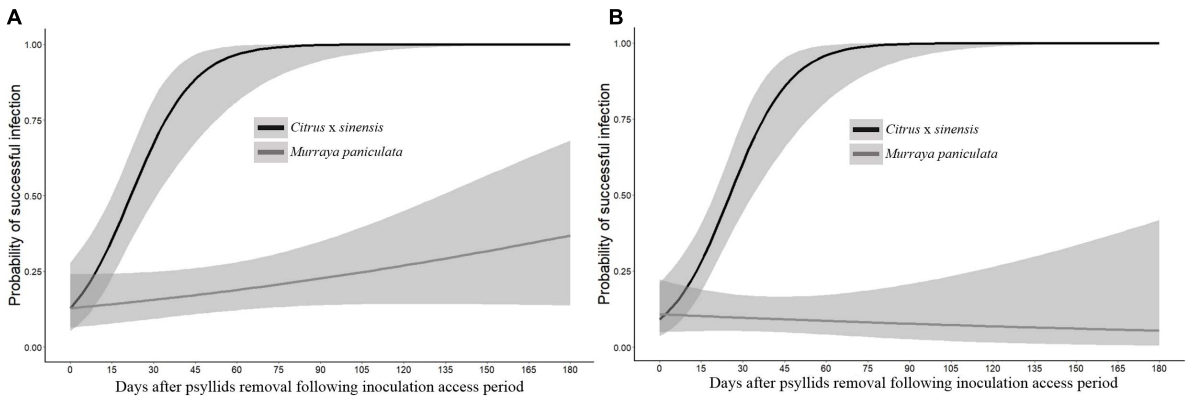

FIGURE 6 | Probability of occurrence of a successful infection of the whole plant of *Citrus* × *sinensis* and *M. paniculata* after an initial 48 h of Las-exposed psyllid confinement and subsequent removal of new shoots at different time intervals in experiment replicates 1 **(A)** and 2 **(B)**.

semi-stationary phase for about 15–30 days, and then bacterial titers declined progressively to become undetectable at 180 days onward. Moreover, Las translocation from the NS to the rest of the plant was rare and uneven. In previous controlled experiments with *M. paniculata*, the earliest samplings were taken from the second to fourth months post-IAP (Damsteegt et al., 2010; Cifuentes-Arenas et al., 2019). However, the continuous decrease in Las titers to undetectable levels confirms previous consideration of *M. paniculata* as a transient host for Las (Damsteegt et al., 2010; Cifuentes-Arenas et al., 2019). Even at low titers, the transitory presence of Las in *M. paniculata* (Damsteegt et al., 2010; Walter et al., 2012; Cifuentes-Arenas et al., 2019) suggests that this species may be a suitable host for Las spread. However, Las transmission from *M. paniculata* to *C.* × *sinensis* by *D. citri* was observed at very low frequencies (less than 1%) in controlled experiments and only when environmental and plant developmental conditions were highly favorable for Las infection (Cifuentes-Arenas et al., 2019). Indeed, both the transient nature of Las infection and its low titers when the bacterium remains detectable in this host explain the 43% reduction in HLB incidence in a sweet orange orchard when *M. paniculata* was used as a trap crop fence to efficiently attract and control the *D. citri* population and its spread (Tomaseto et al., 2019).

In contrast, Las could not be established in NS of *B. koenigii*, as shown previously by Beloti et al. (2018). However, we were able to detect Las multiplication in *B. koenigii* NS in one of the experiment replicates, indicating that under specific, highly suitable conditions, the bacterium could attain low but clearly detectable concentrations in the inoculated shoots, although only occasionally. Moreover, the probability of Las moving out of the NS was null in the *B. koenigii*. Whether *M. paniculata* and *B. koenigii* phloem sap are unsuitable for Las survival (Killiny, 2016) and/or their cells activate efficient defense responses to hold bacterial infections remains to be further investigated. Nevertheless, *B. koenigii* is more efficient than *M. paniculata* in limiting Las. Considering the different responses of Las infection between *Murraya paniculata* and *Bergera koenigii*, their close phylogenetic relationships, and the wide diversity of *Murraya* and *Bergera* species found in Asia (Nguyen et al., 2019), the interactions of the two genera with Las is worth investigating, as they seem to represent hosts at the frontier between resistance and susceptibility to the bacterium.

This is the first study to investigate the early population dynamics of Las in three species with contrasting susceptibility/resistance responses to this bacterium, by simulating the natural Las inoculation system using infective *D. citri* and evaluating the presence of Las in NS by qPCR at different short time intervals post-IAP. Using this controlled and reproducible system, we were able to expose all the plants to similar initial inoculum pressure, as they received the same initial bacterial load injected into the phloem by

psyllids and the environmental conditions were adequate to maximize the chances of successful infection occurrence (Raiol-Junior et al., 2021b). Our results allowed us to identify the key time points of Las growth in plant genotypes with different responses to Las infection. This information could be essential to investigating whether or when plant cell defense responses are activated after wounding and bacterial release into the phloem by *D. citri*, as well as how Las is able to evade such responses in *C.* × *sinensis* but not in *B. koenigii* and only partially in *M. paniculata*. It may also help to identify suitable targets to be knocked out or overexpressed biotechnologically with the aim of creating HLB-resistant varieties.

DATA AVAILABILITY STATEMENT

The original contributions presented in the study are included in the article/**Supplementary Material**, further inquiries can be directed to the corresponding author.

AUTHOR CONTRIBUTIONS

MA, LP, and JF conceptualized the work. MA, LP, JF, and J-CA designed the work. MA, J-CA, and LR-J collected the data. J-CA performed the statistical analysis. MA, J-CA, LR-J, JF, and LP contributed to interpretation, drafting the article, and critical revision of the manuscript. All authors contributed to the article and approved the submitted version.

FUNDING

This study was financed in part by Fundecitrus, grant no. 817526 from the European Union H2020 Innovation Action Program and Project PID2019-104569RB-I00 from the AEI-Spain, the Coordenação de Aperfeiçoamento de Pessoal de Nível Superior - Brazil (CAPES) - Finance Code 001. MA is recipient of a Ph.D. fellowship from CAPES. JF is recipient of a fellowship grant (#312089/2019-8) from Conselho Nacional de Desenvolvimento Científico e Tecnológico – Brazil (CNPq).

ACKNOWLEDGMENTS

We thank André Luís Sanches from Fundecitrus for his help with grafting for propagation and plant maintenance, as well as Berta Alquézar and Jose Gadea from the Universidad Politécnica de Valencia and Nelson A. Wulff and Silvio A. Lopes from Fundecitrus for their invaluable comments during the design of this work. We also thank Fernanda Benedito and Priscila Alves from Fundecitrus for their assistance with DNA extraction and qPCR analysis.

SUPPLEMENTARY MATERIAL

The Supplementary Material for this article can be found online at: https://www.frontiersin.org/articles/10.3389/fmicb.2021.683923/full#supplementary-material

REFERENCES

Achor, D. S., Etxeberria, E., Wang, N., Folimonova, S. Y., Chung, K. R., and Albrigo, L. G. (2010). Sequence of anatomical symptom observations in Citrus affected with Huanglongbing disease. *Plant Pathol. J.* 9, 56–64. doi: 10.3923/ppj.2010.56.64

Achor, D. S., Welker, S., Ben-Mahmoud, S., Wang, C., Folimonova, S. Y., Dutt, M., et al. (2020). Dynamics of *Candidatus* Liberibacter asiaticus movement and sieve-pore plugging in Citrus sink cells. *Plant Physiol.* 188, 882–891. doi: 10.1104/pp.19.01391

Alves, M. N., Lopes, S. A., Raiol-Junior, L. L., Wulff, N. A., Girardi, E. A., Ollitrault, P., et al. (2021). Resistance to '*Candidatus* Liberibacter asiaticus,' the Huanglongbing associated bacterium, in sexually and/or graft-compatible *Citrus* relatives. *Front. Plant Sci.* 11:617664. doi: 10.3389/fpls.2020.617664

Ammar, E.-D., Ramos, J. E., Hall, D. G., Dawson, W. O., and Shatters, R. G. Jr. (2016). Acquisition, replication and inoculation of *Candidatus* Liberibacter asiaticus following various acquisition periods on Huanglongbing-infected *Citrus* by nymphs and adults of the Asian Citrus Psyllid. *PLoS ONE* 11:e0159594. doi: 10.1371/journal.pone.0159594

André, A., Maucourt, M., Moing, A., Rolin, D., and Renaudin, J. (2005). Sugar import and phytopathogenicity of *Spiroplasma citri*: Glucose and fructose play distinct roles. *MPMI* 18, 33–42. doi: 10.1094/MPMI-18-0033

Bassanezi, R. B., Lopes, S. A., Miranda, M. P., Wulff, N. A., Volpe, H. X. L., and Ayres, A. J. (2020). Overview of citrus huanglongbing spread and management strategies in Brazil. *Trop. Plant Pathol.* 45, 251–264. doi: 10.1007/s40858-020-00343-y

Bassanezi, R. B., Montesino, L. H., and Stuchi, E. S. (2009). Effects of huanglongbing on fruit quality of sweet orange cultivars in Brazil. *Eur. J. Plant Pathol.* 125, 565–572. doi: 10.1007/s10658-009-9506-3

Beloti, V. H., Alves, G. R., Coletta-Filho, H. D., and Yamamoto, P. T. (2018). The Asian Citrus psyllid host *Murraya koenigii* is immune to *Citrus* huanglongbing pathogen '*Candidatus* Liberibacter asiaticus'. *Phytopathology* 108, 1089–1094. doi: 10.1094/PHYTO-01-18-0012-R

Beloti, V. H., Santo, F., Alves, G. R., Bento, J. M. S., and Yamamoto, P. T. (2017). Curry leaf smells better than citrus to females of *Diaphorina citri* (Hemiptera: Liviidae). *Arthropod-Plant Interact.* 11, 709–716. doi: 10.1007/s11829-017-9524-6

Bonani, J. P., Fereres, A., Garzo, E., Miranda, M. P., Appezato-Da-Gloria, B., and Lopes, J. R. S. (2010). Characterization of electrical penetration graphs of the Asian citrus psyllid, *Diaphorina citri*, in sweet orange seedlings. *Entomol. Exp. Appl.* 134, 35–49. doi: 10.1111/j.1570-7458.2009.00937.x

Bové, J. M. (2006). Huanglongbing: a destructive, newly-emerging, century-old disease of citrus. *J. Plant Pathol.* 88, 7–37. doi: 10.4454/jpp.v88i1.828

Canale, M. C., Tomaseto, A. F., Haddad, M. L., Coletta-Filho, H. D., and Lopes, J. R. S. (2017). Latency and persistence of '*Candidatus* Liberibacter asiaticus' in its psyllid vector, *Diaphorina citri* (Hemiptera: Liviidae). *Phytopathology* 107, 264–272. doi: 10.1094/PHYTO-02-16-0088-R

Capoor, S., Rao, D., and Viswanath, S. (1967). *Diaphorina citri* Kuway., a vector of the greening disease of citrus in India. *Indian J. Agric. Sci.* 37, 572–579.

Carmo-Souza, M., Garcia, R. B., Wulff, N. A., Fereres, A., and Miranda, M. P. (2020). Drench application of systemic insecticides disrupts probing behavior of *Diaphorina citri* (Hemiptera: Liviidae) and inoculation of *Candidatus* Liberibacter asiaticus. *Insects* 11, 314–325. doi: 10.3390/insects11050314

Cifuentes-Arenas, J. C., Beattie, G. A. C., Peña, L., and Lopes, S. A. (2019). *Murraya paniculata* and *Swinglea glutinosa* as short-term transient hosts of '*Candidatus* Liberibacter asiaticus' and implications for the spread of huanglongbing. *Phytopathology* 109, 2064–2073. doi: 10.1094/PHYTO-06-19-0216-R

Cifuentes-Arenas, J. C., de Goes, A., de Miranda, M. P., Beattie, G. A. C., and Lopes, S. A. (2018). Citrus flush shoot ontogeny modulates biotic potential of *Diaphorina citri*. *PLoS One* 13:e0190563. doi: 10.1371/journal.pone.0190563

Clark, K., Franco, J. Y., Schwizer, S., Pang, Z., Hawara, E., Liebrand, T. W. H., et al. (2018). An effector from the Huanglongbing-associated pathogen targets citrus proteases. *Nature communications* 9, 1718. doi: 10.1038/s41467-018-04140-9

Damsteegt, V. D., Postnikova, E. N., and Stone, A. L. (2010). *Murraya paniculata* and related species as potential hosts and inoculum reservoirs of '*Candidatus* Liberibacter asiaticus', causal agent of Huanglongbing. *Plant Dis*. 94, 528–533. doi: 10.1094/PDIS-94-5-0528

Desjardins, P., and Conklin, D. (2010). NanoDrop microvolume quantitation of nucleic Acids. *J. Vis. Exp*. 45, e2565. doi: 10.3791/2565

Duan, Y., Zhou, L., Hall, D. G., Li, W., Doddapaneni, H., Lin, H., et al. (2009). Complete genome sequence of Citrus Huanglongbing bacterium, '*Candidatus* Liberibacter asiaticus' obtained through metagenomics. *MPMI* 22, 1011–1020.

Fagen, J. R., Leonard, M. T., Coyle, J. F., McCullough, C. M., Davis-Richardson, A. G., Davis, M. J., et al. (2014). Liberibacter crescens gen. nov., sp. nov., the first cultured member of the genus *Liberibacter*. *Int. J. Syst. Evol. Microbiol.* 64, 2461–2466. doi: 10.1099/ijs.0.063255-0

Folimonova, S. Y., Robertson, C. J., Gamsey, S. M., and Dawson, W. O. (2009). Examination of the responses of different genotypes of citrus to huanglongbing (citrus greening) under different conditions. *Phytopathology* 23, 1346–1354. doi: 10.1094/PHYTO-99-12-1346

Fundecitrus. (2020). *Doenças: Greening/HLB*. Available online at: https://www.fundecitrus.com.br/levantamentos/greening (accessed March 21, 2020).

Ghanim, M., Fattah-Hosseini, S., Levy, A., and Cilia, M. (2016). Morphological abnormalities and cell death in the Asian citrus psyllid (*Diaphorina citri*) midgut associated with *Candidatus* Liberibacter asiaticus. *Sci. Rep.* 6, 33418. doi: 10.1038/srep33418

Gottwald, T. R. (2010). Current epidemiological understanding of citrus Huanglongbing. *Annu. Rev. Phytopathol* 48, 119–139. doi: 10.1146/annurev-phyto-073009-114418

Hilf, M. E., and Luo, W. (2018). Dynamics of '*Candidatus* Liberibacter asiaticus' colonization of new growth of citrus. *Phytopathology* 108, 1165–1171. doi: 10.1094/PHYTO-12-17-0408-R

Hogenhout, S. A., and Bos, J. I. (2011). Effector proteins that modulate plant–insect interactions. *Curr. Opin. Plant Biol.* 14, 422–428. doi: 10.1016/j.pbi.2011.05.003

Huang, W., Reyes-Caldas, P., Mann, M., Seifbarghi, S., Kahn, A., Almeida, R. P. P., et al. (2020). Bacterial vector-borne plant diseases: unanswered questions and future directions. *Mol. Plant.* 13, 1379–1393. doi: 10.1016/j.molp.2020.08.010

Inoue, H., Ohnish, J., Ito, T., Tomimur, K., Miyata, S., and Ashihara, W. (2009). Enhanced proliferation and efficient transmission of *Candidatus* Liberibacter asiaticus by adult *Diaphorina citri* after acquisition feeding in the nymphal stage. *Ann. Appl. Biol.* 155, 29–36. doi: 10.1111/j.1744-7348.2009.00317.x

Jain, M., Fleites, L. A., and Gabriel, D. W. (2015). Prophage-encoded peroxidase in '*Candidatus* Liberibacter asiaticus' is a secreted effector that suppresses plant defenses. *Mol. Plant Microbe Interact*. 12, 1330–1337. doi: 10.1094/MPMI-07-15-0145-R

Jiang, Y., Zhang, C.-X., Chen, R., and He, S. Y. (2019). Challenging battles of plants with phloem-feeding insects and prokaryotic pathogens. *PNAS.* 116, 23390–23397. doi: 10.1073/pnas.1915396116

Johnson, E. G., Wu, J., Bright, D. B., and Graham, J. H. (2014). Association of '*Candidatus* Liberibacter asiaticus' root infection, but not phloem plugging with root loss on huanglongbing-affected trees prior to appearance of foliar symptoms. *Plant Pathol.* 63, 290–298. doi: 10.1111/ppa.12109

Killiny, N. (2016). Metabolomic comparative analysis of the phloem sap of curry leaf tree (*Bergera koenegii*), orange jasmine (*Murraya paniculata*), and Valencia sweet orange (*Citrus sinensis*) supports their differential responses to Huanglongbing. *Plant signal. behav.* 11, e1249080. doi: 10.1080/15592324.2016.1249080

Kim, J.-S., Sagaram, U. S., Burns, J. K., Li, J.-L., and Wang, N. (2009). Response of sweet orange (*Citrus sinensis*) to '*Candidatus* Liberibacter asiaticus' Infection: Microscopy and Microarray Analyses. *Phytopathology* 99, 50–57. doi: 10.1094/PHYTO-99-1-0050

Li, J., Pang, Z., Trivedi, P., Zhou, X., Ying, X., Jia, H., et al. (2017). *'Candidatus* Liberibacter asiaticus' encodes a functional salicylic acid (SA) hydroxylase that degrades SA to suppress plant defenses. *MPMI* 30, 620–630. doi: 10.1094/MPMI-12-16-0257-R

Li, W., Hartung, J. S., and Levy, L. (2006). Quantitative real-time PCR for detection and identification of *Candidatus* Liberibacter species associated with citrus huanglongbing. *J. Microbiol. Methods* 66, 104–115. doi: 10.1016/j.mimet.2005.10.018

Li, W., Levy, L., and Hartung, J. S. (2009). Quantitative distribution of "*Candidatus* Liberibacter asiaticus" in citrus plants with citrus huanglongbing. *Phytopathology* 99, 139–144. doi: 10.1094/PHYTO-99-2-0139

Lopes, S. A., and Cifuentes-Arenas, J. C. (2021). A protocol for successful transmission of '*Candidatus* Liberibacter asiaticus' from citrus to citrus using *Diaphorina citri*. *Phytopathology* doi: 10.1094/PHYTO-02-21-0076-R [Epub ahead of print].

Lopes, S. A., Frare, G. F., Bertolni, E., Cambra, M., Fernandes, N. G., Ayres, A. J., et al. (2009). Liberibacters associated with citrus huanglongbing in Brazil: '*Candidatus* Liberibacter asiaticus' is heat tolerant, '*Ca*. L. americanus' is heat sensitive. *Plant Dis*. 3, 257–262. doi: 10.1094/PDIS-93-3-0257

Lopes, S. A., Luiz, F. Q. B. Q., Martins, E. C., Fassini, C. G., Barbosa, J. C., and Beattie, G. A. C. (2013). *Candidatus* Liberibacter asiaticus titers in citrus and acquisition rates by *Diaphorina citri* are decreased by higher temperature. *Plant Dis*. 97, 1563–1570. doi: 10.1094/PDIS-11-12-1031-RE

Manjunath, K. L., Halbert, S. E., Ramadugu, C., Weeb, S., and Lee, R. F. (2008). Detection of '*Candidatus* Liberibacter asiaticus' in *Diaphorina citri* and its importance in the management of Citrus Huanglongbing in Florida. *Phytopathology* 98, 387–396. doi: 10.1094/PHYTO-98-4-0387

Murray, M. G., and Thompson, W. F. (1980). Rapid isolation of high molecular weight plant DNA. *Nucleic Acids Res*. 8, 4321–4325. doi: 10.1093/nar/8.19.4321

Nguyen, C. H., Beattie, A. C., Haigh, A. M., Astuti, I. P., Mabberley, D. J., Weston, P. H., et al. (2019). Molecular differentiation of the *Murraya paniculata* Complex (Rutaceae: Aurantioideae: Aurantieae). *BMC Evol. Biol.* 19:236. doi: 10.1186/s12862-019-1555-4

Pandey, S. S., Vasconcelos, F. N. C., and Wang, N. (2021). Spatiotemporal dynamics of *Candidatus* Liberibacter asiaticus colonization inside citrus plant and Huanglongbing disease development. *Phytopathology* doi: 10.1094/PHYTO-09-20-0407-R [Epub ahead of print].

Pandey, S. S., and Wang, N. (2019). Targeted early detection of *Citrus* Huanglongbing causal agent '*Candidatus* Liberibacter asiaticus' before symptom expression. *Phytopathology* 109, 952–959. doi: 10.1094/PHYTO-11-18-0432-R

Pang, Z., Zhang, L., Coaker, G. L., Ma, W., He, S. Y., and Wang, N. (2020). Citrus CsACD2 is a target of *Candidatus* Liberibacter asiaticus in Huanglongbing disease. *Plant Physiol.* 184, 792–805. doi: 10.1104/pp.20.00348

Pelz-Selinski, K. S., Brlansky, R. H., Ebert, T. A., and Rogers, M. E. (2010). Transmission parameters for *Candidatus* Liberibacter asiaticus by Asian Citrus Psyllid (Hemiptera: Psyllidae). *J. Econ. Entomol*. 103, 1531Ð1541. doi: 10.1603/EC10123

Peng, C.-Y. J., Le, K. L., and Ingersoll, G. M. (2002). An introduction to Logistic regression analysis and reporting. *J. Educ. Res*. 96, 3–14. doi: 10.1080/00220670209598786

Raiol-Junior, L. L., Baia, A. D. B., Luiz, F. Q. B. F., Fassini, C. G., Marques, V. V., and Lopes, S. A. (2017). Improvement in the excised citrus leaf assay to investigate inoculation of '*Candidatus* Liberibacter asiaticus' by the Asian Citrus Psyllid *Diaphorina citri*. *Plant Dis* 101, 409–413. doi: 10.1094/PDIS-08-16-1093-RE

Raiol-Junior, L. L., Cifuentes-Arenas, J. C., Carvalho, E. V., Girardi, E. A., and Lopes, S. A. (2021a). Evidence that '*Candidatus* Liberibacter asiaticus' moves predominantly towards new tissue growth in citrus plants. *Plant Dis.* 105, 34–42. doi: 10.1094/PDIS-01-20-0158-RE

Raiol-Junior, L. L., Cifuentes-Arenas, J. C., Cunniffe, N. J., Turgeon, R., and Lopes, S. A. (2021b). Modelling '*Candidatus* Liberibacter asiaticus' movement within citrus plants. *Phytopathology* doi: 10.1094/PHYTO-12-20-0559-R [Epub ahead of print].

Ramadugu, C., Keremane, M. L., Halbert, S. E., Duan, Y. P., Roose, M. L., Stover, E., et al. (2016). Long-term field evaluation reveals huanglongbing resistance in *Citrus* relatives. *Plant Dis.* 9, 1858–1869. doi: 10.1094/PDIS-03-16-0271-RE

Sena-Vélez, M., Holland, S. D., Aggarwal, M., Cogan, N. G., Jain, M., Gabriel, D. W., et al. (2019). Growth dynamics and survival of *Liberibacter crescens* BT-1, an important model organism for the citrus Huanglongbing pathogen "*Candidatus* Liberibacter asiaticus.". *Appl. Environ. Microbiol.* 85, e1656–e1619. doi: 10.1128/AEM.01656-19

Singerman, A., and Useche, P. (2016). *Impact of Citrus* greening on *Citrus* operations in Florida. Available online at: https://edis.ifas.ufl.edu/fe983#:~{}:text=Summary,an%20increased%20cost%20of%20production (accessed March 09, 2021).

Skelley, L. H., and Hoy, M. A. (2004). A synchronous rearing method for the asian citrus psyllid and its parasitoids in quarantine. *Biol. Control.* 29, 14–23. doi: 10.1016/S1049-9644(03)00129-4

Swingle, W. T., and Reece, C. (1967). "The botany of *Citrus* and its wild relatives," in *The Citrus Industry*, eds W. Reuther, H. J. Webber, and L. D. Batchelor (Berkeley, CA: University of California Press), 191–430.

Tatineni, S., Sagaram, U. S., Gowda, S., Robertson, C. J., Dawson, W. O., Iwanami, T., et al. (2008). In planta distribution of '*Candidatus* Liberibacter asiaticus' as revealed by polymerase chain reaction (PCR) and real-time PCR. *Phytopathology* 98, 592–599. doi: 10.1094/PHYTO-98-5-0592

Teck, S. L. X., Fatimah, A., Beattie, A., Heng, R. K. J., and King, W. S. (2011). Influence of host plant species and flush growth stage on the Asian Citrus Psyllid, *Diaphorina citri* Kuwayama. *Am. J. Agric. Biol. Sci.* 6, 536–543. doi: 10.3844/ajabssp.2011.536.543

Teixeira, D. C., Danet, J. L., Eveillard, S., Martins, E. C., Junior, W. C. J., Yamamoto, P. T., et al. (2005). Citrus huanglongbing in São Paulo State, Brazil: PCR detection of the '*Candidatus*' Liberibacter species associated with the disease. *Mol. Cell. Probes* 19, 173–179. doi: 10.1016/j.mcp.2004.11.002

Tjørve, K. M. C., and Tjørve, E. (2017). The use of Gompertz models in growth analyses, and new Gompertz-model approach: An addition to the unified-richards family. *PLoS One* 12:e0178691. doi: 10.1371/journal.pone.0178691

Tomaseto, A. F., Marques, R. N., Fereres, A., Zanardi, O. A., Volpe, H. X. L., Alquézar, B., et al. (2019). Orange jasmine as a trap crop to control *Diaphorina citri*. *Sci. Rep.* 9, 2070. doi: 10.1038/s41598-019-38597-5

Walter, A. J., Duan, Y. P., and Hall, D. G. (2012). Titers of '*Ca*. Liberibacter asiaticus' in *Murraya paniculata* and *Murraya*-reared *Diaphorina citri* are much lower than in *Citrus* and *Citrus*-reared psyllids. *Hortscience* 47, 1449–1452. doi: 10.21273/HORTSCI.47.10.1449

Westbrook, C. J., Hall, D. G., Stover, E., Duan, Y. P., and Lee, R. F. (2011). Colonization of *Citrus* and *Citrus*-related germplasm by *Diaphorina citri* (Hemiptera: Psyllidae). *Hortscience* 46, 997–1005. doi: 10.21273/HORTSCI.46.7.997

Wu, T., Lou, X., Xu, C., Wu, F., Qureshil, W. A., and Cen, Y. (2016). Feeding behavior of *Diaphorina citri* and its transmission of '*Candidatus* Liberibacter asiaticus' to citrus. *Entomol. Exp. Appl* 161, 104–111. doi: 10.1111/eea.12496

Yu, H.-Z., Li, N.-Y., Zeng, X.-D., Song, J.-C., Yu, X.-D., Su, H.-N., et al. (2020). Transcriptome Analyses of *Diaphorina citri* Midgut Responses to *Candidatus* Liberibacter asiaticus infection. *Insects* 11, 171–187. doi: 10.3390/insects11030171

Conflict of Interest: The authors declare that the research was conducted in the absence of any commercial or financial relationships that could be construed as a potential conflict of interest.

frontiers in Microbiology

ORIGINAL RESEARCH
published: 11 June 2021
doi: 10.3389/fmicb.2021.681251

A Significantly High Abundance of "*Candidatus* Liberibacter asiaticus" in Citrus Fruit Pith: *in planta* Transcriptome and Anatomical Analyses

Fang Fang[1†], Hengyu Guo[1†], Anmin Zhao[1], Tao Li[1], Huihong Liao[2], Xiaoling Deng[1], Meirong Xu[1] and Zheng Zheng[1]**

[1] Guangdong Province Key Laboratory of Microbial Signals and Disease Control, South China Agricultural University, Guangzhou, China, [2] Horticulture Research Institute, Guangxi Academy of Agricultural Sciences, Nanning, China

OPEN ACCESS

Edited by:
Xuefeng Wang,
Chinese Academy of Agricultural Sciences, China

Reviewed by:
Yongping Duan,
United States Department of Agriculture (USDA), United States
Fang Ding,
Huazhong Agricultural University, China

***Correspondence:**
Meirong Xu
meirongxu@scau.edu.cn
Zheng Zheng
zzheng@scau.edu.cn

[†] These authors have contributed equally to this work and share first authorship

Specialty section:
This article was submitted to Microbe and Virus Interactions with Plants, a section of the journal Frontiers in Microbiology

Received: 16 March 2021
Accepted: 10 May 2021
Published: 11 June 2021

Citation:
Fang F, Guo H, Zhao A, Li T, Liao H, Deng X, Xu M and Zheng Z (2021) A Significantly High Abundance of "Candidatus Liberibacter asiaticus" in Citrus Fruit Pith: in planta Transcriptome and Anatomical Analyses. Front. Microbiol. 12:681251. doi: 10.3389/fmicb.2021.681251

Huanglongbing, a highly destructive disease of citrus, is associated with the non-culturable phloem-limited α-proteobacterium "*Candidatus* Liberibacter asiaticus" (CLas). The distribution patterns of CLas in infected plant are variable and not consistent, which make the CLas detection and characterization more challenging. Here, we performed a systemic analysis of CLas distribution in citrus branches and fruits of 14 cultivars. A significantly high concentration of CLas was detected in fruit pith (dorsal vascular bundle) of 14 citrus cultivars collected at fruit maturity season. A 2-year monitoring assay of CLas population in citrus branches of "Shatangju" mandarin (*Citrus reticulata* Blanco "Shatangju") revealed that CLas population already exhibited a high level even before the appearance of visual symptoms in the fruit rind. Quantitative analyses of CLas in serial 1.5-cm segments of fruit piths showed the CLas was unevenly distributed within fruit pith and tended to colonize in the middle or distal (stylar end) regions of pith. The use of CLas-abundant fruit pith for dual RNA-seq generated higher-resolution CLas transcriptome data compared with the leaf samples. CLas genes involved in transport system, flagellar assembly, lipopolysaccharide biosynthesis, virulence, stress response, and cell surface structure, as well as host genes involved in biosynthesis of antimicrobial-associated secondary metabolites, was up-regulated in leaf midribs compared with fruit pith. In addition, CLas infection caused the severe collapse in phloem and callose deposition in the plasmodesmata of fruit pith. The ability of fruit pith to support multiplication of CLas to high levels makes it an ideal host tissue for morphological studies and *in planta* transcriptome analyses of CLas–host interactions.

Keywords: citrus huanglongbing, *Candidatus* Liberibacter asiaticus, high abundance, fruit pith, *in planta* transcriptome, anatomical analyses

INTRODUCTION

Huanglongbing (HLB, also called yellow shoot disease) is a highly destructive disease currently threatening citrus production worldwide. It is associated with three unculturable phloem-limited α-proteobacterium, *Candidatus* Liberibacter asiaticus (CLas), "*Ca.* L. africanus," and "*Ca.* L. americanus" (Jagoueix et al., 1994; Teixeira et al., 2005). The most severe form of the disease is

associated with CLas, which is most commonly transmitted by Asian citrus psyllid (*Diaphorina citri* Kuwayama). In China, HLB was first observed in Chaoshan region of Guangdong province over a century ago (Lin, 1956). Literature records indicated the HLB was initially endemic in the coastal region of southern China and spread to other citrus-growing province after the 1970s (Lin, 1956; Zheng et al., 2018). The association of CLas to HLB in China was established in 1996 (Deng and Tang, 1996; Tian et al., 1996). Because of the current inability to culture CLas *in vitro*, the identification of CLas was usually performed with total plant DNA by polymerase chain reaction (PCR) or real-time PCR targeting the specific and conserved genomic loci of CLas genome, mostly in the 16S rRNA gene (Li et al., 2006; Bao et al., 2020) or recently identified ribonucleotide reductase genes (Zheng et al., 2016).

The destructive impact of HLB on cultivation of citrus stems from the impact of the disease on the lifespan of trees, yields, and fruit quality (Bové, 2006; Zheng et al., 2018). Most commercial cultivars are susceptible to severe impacts of the disease (Bové, 2006). Although citrus trees can be affected by HLB at any age, symptoms caused by disease are variable, with differences related to host cultivar and age, time of infection, and season and types of tissues in which symptoms are expressed (Lin, 1956; Zheng et al., 2018). The most characteristic symptoms of HLB included the yellowing of leaves, initially on one or branches among many, asymmetrical blotchy mottling of leaves, unseasonal flowering, small asymmetrical fruit with aborted seeds, uneven initial coloring of fruit, and premature fruit drop (Lin, 1956; Zheng et al., 2018). As the extent of infection increases, leaves on new growth may be atypically small and exhibit symptoms of zinc or manganese deficiency symptoms. Diseased fruits that color unevenly are referred to as "red-nose" fruit, with color changing from green to yellow occurring initially from the calyx (stem) end instead of stylar end, with the stylar end, in most situations, remaining green as fruit mature. Occurrence of "red-nose" fruit was reported as a characteristic HLB symptom observed in "Shatangju" mandarin (*Citrus reticulata* Blanco "Shatangju") (Zhang et al., 2011).

Although HLB is a systemic disease, CLas is generally unevenly distributed within infected plants (Tatineni et al., 2008; Li et al., 2009; Hartung et al., 2010; Kunta et al., 2014; Ding et al., 2015; Louzada et al., 2016; Fu et al., 2019). It is more frequently found in symptomatic leaves than the asymptomatic leaves from infected trees (Ding et al., 2015; Louzada et al., 2016). Even within the individual symptomatic leaves, the CLas tends to colonize the underside of petioles in preference to the upside of petiole (Ding et al., 2015). An *in planta* distribution analysis of CLas in different tissues from diseased trees has shown that CLas cells were most abundant in the fruit peduncles than in other tissues but absent in the endosperm and embryos of infected seeds (Tatineni et al., 2008). Highest CLas titers have been recorded in fruit peduncles of CLas-infected grapefruit and sweet orange in contrast to low titers in young shoots (Kunta et al., 2014). However, another investigation based on different tissues of six citrus species/hybrids revealed that the CLas population levels in the fruit tissues were significantly less (∼1,000-fold) than those in the midribs, leaf blades, barks, and roots (Li et al., 2009). The pattern of CLas distribution within infected citrus trees could be different according to citrus species/hybrids and disease severity (Li et al., 2009).

Currently, the CLas has not been cultured *in vitro* yet. The characterization of CLas was mainly relied on the analyses of CLas-infected host tissue. However, the uneven distribution of CLas and the highly variable bacterial titers in infected plant makes the CLas research more challenging. A reliable CLas characterization requires that host tissue contains a stable high CLas concentration. In this study, the distribution of CLas was thoroughly analyzed in citrus branches and fruits of 14 commercial cultivars collected in southern China. Significantly high levels of CLas population were detected in fruit pith tissue compared with other tissues of the 14 cultivars. A 2-year monitoring assay confirmed the high stable abundance of CLas in fruit pith before the external symptoms were expressed in the fruit rind. We also found the CLas was unevenly distributed within individual fruit pith and tended to colonize in the middle or distal region. In addition, the genome-wide transcriptome profiling of CLas in fruit pith, as well as the anatomical changes of fruit pith caused by CLas infection and the morphology characterization of CLas in fruit pith tissue, was also analyzed. The ability to support multiplication of CLas to high levels by fruit pith makes it an ideal host tissue for morphological studies and *in planta* bacterial transcriptome analyses of CLas–host interaction.

MATERIALS AND METHODS

Plant Materials and DNA Extraction

For the spatial distribution analysis of CLas, the HLB-affected citrus branches of 14 commercial citrus cultivars were collected at fruit maturity season in three provinces (Guangdong, Guangxi, and Zhejiang) in China during November 2018 to January 2019 (**Table 1** and **Supplementary Figures 1**, **2**). They were "Pink" grapefruit (*Citrus* × *paradisi* "Pink"), "Eureka" lemon (*C. limon* "Eureka"), "Hu" pomelo (*C. maxima* L. "Changshanhu Yu"), "Shatian" pomelo ("Shatian Yu"), "Liu" sweet orange (*C. sinensis* cv. "Liu Cheng"), "Hongjiang" sweet orange ("Gailiang Cheng"), "Suanju" mandarin (*C. reticulata* Blanco "Suanju"), "Wenzhou" mandarin ("Wenzhou"), "Shatangju" mandarin ("Shatangju"), "Huangyan" mandarin ("Subcompress"), "Nanfeng" mandarin ("Kinokuni"), "Wokan" mandarin ("Wokan"), "Jiaokan" mandarin ("Tankan"), and "Gongkan" mandarin ("Gongkan"). Each citrus branch contained at least one fruit and one new flush (**Supplementary Figure 1**). For each citrus cultivar, 8–12 symptomatic branches were collected from CLas-infected trees. Samples used for analyses of CLas distribution in the individual citrus branch were collected from three parts, i.e., the new flush, fruit part, and mature leaf (**Supplementary Figure 3**). For new flush and mature leaves, the leaf midribs were collected for DNA extraction. For branches of "Pink" grapefruit and "Hu" pomelo (**Supplementary Figure 1**), the mature leaf was not commonly found in HLB-affected branches, and stem bark tissue was collected accordingly. For fruit, three types of subsamples were collected, including the fruit pith, peduncle,

and central axis (**Supplementary Figure 3**). In addition, leaves adjacent to the fruit were also collected for CLas quantification (**Supplementary Figure 3**).

For the temporal dynamics analysis of CLas, 10 HLB-affected 4-year-old "Shatangju" mandarin trees from a commercial citrus orchard located in Huizhou city of Guangdong province were selected. For each tree, one citrus branch, with at least one new shoot and one fruit, was collected monthly (from 2017 to 2019). Six different types of tissues (**Supplementary Figure 3**) were collected from each diseased citrus branch. To obtain adequate samples of fruit for sampling of fruit pith, sampling commenced in August and continued until the end of January (the harvest month) of the next year.

For all samples, 100 mg of flesh tissue was cut into sections of approximately 1 mm wide and ground with an MP FastPrep® −24 Grinder (MP Biomedicals LLC, Santa Ana, CA, United States) under speed of 4 M/S for 1 min. Total DNA was extracted using an E.Z.N.A. HP Plant DNA Kit (OMEGA Bio-Tek Co., Guangdong, China) according to the manufacturer's manual. The concentration of all extracted DNA samples was determined using Qubit 2.0 (Thermo Fisher Scientific Inc., Waltham, MA, United States).

Sampling of Fruit Piths

The CLas-infected fruits of three citrus varieties ("Pink" grapefruit, "Wenzhou" mandarin, and "Eureka" lemon), which had relatively large fruits for sampling of long fruit piths, were selected for analyzing the distribution of CLas in fruit pith. For each variety, a total of 10 diseased fruits from different HLB-affected trees were collected. Individual fruit piths were carefully removed intact from HLB-affected fruits. For each fruit, three to five fruit piths were initially pulled out with tweezers, and the longest one (≥6 cm) was selected for further quantification of CLas. Each fruit pith was oriented from calyx-end to stylar-end and cut into four (6 cm ≤ total length < 7 cm) or five (7.5 cm ≤ total length < 8 cm) 1.5-cm segments. Each segment was separately ground with MP FastPrep® −24 Grinder (MP Biomedicals LLC) and used for DNA extraction and CLas quantification analysis.

Quantification of *Candidatus* Liberibacter asiaticus

The quantitative real-time PCR assays for CLas were performed with primer set (CLas4G/HLBr) and probe (HLBp) according to a previous study (Bao et al., 2020). The standard equation ($y = -2.883x + 38.32$) ($R^2 = 0.9995$) for quantification of CLas was developed. Briefly, a recombinant plasmid contained the CLas-4G/HLBr primer region was used for construction of the standard equation. The concentration of recombinant plasmid and all DNA extracts were determined using Qubit 2.0 (Thermo Fisher Scientific Inc.). The copy number of plasmid was calculated according to the following formula: the number of copies = (amount in nanograms × Avogadro number)/(length in base pairs × 1 × 10^9 × 650). The quantification of CLas for each sample was presented as CLas cells per nanograms of total DNA. All TaqMan quantitative real-time PCR was performed in CFX Connect Real-Time System (Bio-Rad, Hercules, CA, United States). The 20 μL of PCR mixture contained 1 μL of DNA template (∼25 ng), 10 μL of Bestar qPCR Master Mix (DBI Bioscience, Shanghai, China), 0.2 μL of PCR Probe (10 μM), 0.4 μL of each forward and reverse primer (10 μM), and 8 μL of ddH_2O. All PCR was performed under the following procedure: 95°C for 2 min, followed by 40 cycles at 95°C for 10 s and 58°C for 30 s, with fluorescence signal capture at the end of each 58°C step. The data were analyzed using Bio-Rad CFX Manager 2.1 software with automated baseline settings and threshold. The concentration of CLas among different types of tissues from the same cultivar was analyzed by independent-sample *t* test under the SPSS statistical package (v19.0, IBM, Armonk, NY, United States).

Dual RNA-Seq and Transcriptome Analyses

The high levels of CLas population in fruit pith provided an opportunity to analyze the genome-wide transcriptome profiling of CLas by dual RNA-seq. Therefore, the *in planta* transcriptome analyses of CLas genes in fruit pith and leaf midribs samples were analyzed and compared. The HLB symptomatic leaf samples and fruit pith tissues of the "red-nose" fruit from the same HLB-affected "Shatangju" mandarin branch were collected in December 2018 and then immediately put into the liquid nitrogen before being taken to the laboratory for RNA extraction. Three biological replicates of leaf midribs samples (average Ct value ≈ 22 by primer set of CLas4G/HLBr) and fruit piths samples (average Ct value ≈ 19 by primer set CLas4G/HLBr) were collected. Total RNA was extracted using E.Z.N.A. Total RNA Kit I (OMEGA Bio-Tek Co.) following the manufacturer's manual. The quality of total RNA sample was tested by Qubit 2.0 (Thermo Fisher Scientific Inc.) and Agilent 2100 (Agilent Technologies Inc., Santa Clara, CA, United States). Library preparation for dual RNA-seq was performed with a TruSeq RNA library Prep Kit (Illumina, San Diego, CA, United States) by removing rRNA from total RNA. High-throughput sequencing was carried out on an Illumina HiSeq 3000 system with 150-bp paired-end reads by a commercial sequencing company.

For CLas transcriptome analysis, all clean HiSeq data from leaf midribs and fruit piths samples were mapped to CLas strain A4 genome (CP010804.2) by CLC Genomic Workbench v9.5 (Qiagen Bioinformatics, Aarhus, Denmark) (length faction = 0.95; similarity fraction = 0.95). Reads mapped to each CLas gene were then summarized into count tables of "Total Gene Reads." The normalization of RNA-seq was referenced to the transcripts per kilobase million (TPM) method, i.e., $TPM = A \times 10^6 \times 1/\Sigma(A)$, where A = total reads mapped to gene × 10^3/gene length in bp. Differentially expressed genes (DEGs) between leaf midribs HiSeq data and fruit pith HiSeq data were performed with GFOLD V1.1.4 (Feng et al., 2012). Log2 fold change ≥ | 1 | was set as cutoff values. All identified DEGs were further submitted for functional annotation and

TABLE 1 | Quantification of "*Candidatus Liberibacter asiaticus*" (CLas) from six different parts of huanglongbing-affected citrus branches from 14 citrus cultivars.

No.	Cultivar	Location	Age of host trees (years)	No. of citrus branch	CLas cells/ng of total DNA[1]					
					Leaf midrib (new flush)	Pith (fruit)	Peduncle (fruit)	Central axis (fruit)	Leaf midrib (adjacent to fruit)	Leaf midrib (mature leaves) or stem bark[2]
1	*Citrus* × *paradisi* "Pink"	Zhejiang	Seven	10	484 ± 78 b	10,772 ± 2,770 a	218 ± 30 b	7,517 ± 1,331 a	804 ± 429 b	160 ± 47 b
2	*C. limon* "Eureka"	Zhejiang	Five	8	592 ± 116 b	7,690 ± 1,724 a	265 ± 41 b	1,853 ± 610 b	477 ± 92 b	350 ± 115 b
3	*C. maxima* "Changshanhu Yu"	Zhejiang	Eight	10	116 ± 41 b	77,584 ± 17,698 a	2,120 ± 448 b	58,805 ± 13,245 a	972 ± 257 b	160 ± 44 b
4	*C. maxima* "Shatian Yu"	Guangxi	Five	10	610 ± 215 b	12,934 ± 3,688 a	629 ± 135 b	7,123 ± 3,405 a	227 ± 36 b	180 ± 131 b
5	*C. sinensis* "Liu Cheng"	Guangdong	Ten	10	900 ± 300 b	31,026 ± 16,361 a	391 ± 148 b	2,872 ± 856 b	355 ± 169 b	285 ± 258 b
6	*C. sinensis* "Gailiang Cheng"	Guangdong	Six	10	675 ± 354 c	47,537 ± 35,484 a	543 ± 188 c	6,650 ± 2,155 b	492 ± 160 c	85 ± 25 c
7	*C. reticulata Blanco* "Suanju"	Zhejiang	Six	12	1,361 ± 326 c	27,424 ± 3,780 a	756 ± 195 c	8,218 ± 1,562 b	1,963 ± 325 c	509 ± 79 c
8	*C. reticulata Blanco* "Wenzhou"	Zhejiang	Six	12	94 ± 60 b	68,361 ± 20,863 a	172 ± 37 b	10,708 ± 3,802 b	106 ± 51 b	52 ± 24 b
9	*C. reticulata Blanco* "Shatangju"	Guangdong	Seven	10	127 ± 65 b	20,460 ± 4,731 a	2,239 ± 1,281 b	1,813 ± 518 b	194 ± 60 b	195 ± 63 b
10	*C. reticulata Blanco* "Subcompress"	Zhejiang	Five	8	199 ± 95 b	8,143 ± 3,810 a	204 ± 58 b	1,269 ± 579 b	83 ± 56 b	33 ± 11 b
11	*C. reticulata Blanco* "Kinokuni"	Zhejiang	Six	10	93 ± 35 b	9,544 ± 1,599 a	367 ± 103 b	415 ± 143 b	54 ± 33 b	7 ± 2 b
12	*C. reticulata Blanco* "Wokan"	Guangxi	Four	10	85 ± 33 b	20,646 ± 6,424 a	120 ± 55 b	3,369 ± 872 b	62 ± 23 b	35 ± 9 b
13	*C. reticulata Blanco* "Tankan"	Guangdong	Five	10	595 ± 84 c	5,701 ± 1,098 a	463 ± 76 c	2,256 ± 643 b	519 ± 83 c	62 ± 20 c
14	*C. reticulata Blanco* "Gongkan"	Guangdong	Five	8	418 ± 295 b	9,331 ± 4,637 a	109 ± 46 b	1,625 ± 880 b	353 ± 253 b	221 ± 113 b
		Location		138	465 ± 60 c	27,157 ± 4,084 a	633 ± 115 c	8,613 ± 1,622 b	507 ± 69 c	168 ± 27 c

[1] Single-factor analysis of variance (Duncan multiple-range test) at 95% (P = 0.05) confidence interval was used to determine statistical significance. The same line with different letters represents significant difference of CLas density in different parts of citrus branches from individual cultivars.

[2] For "Pink" grapefruit (Citrus × paradisi "Pink") and "Hu" pomelo (C. maxima "Changshanhu Yu"), no mature leaf was found in the branch, and the stem bark tissue was sampled as alternative.

ortholog assignment with eggNOG mapper (Huerta-Cepas et al., 2017). The top 20 most highly expressed genes evaluated by TPM value from leaf midribs data and fruit pith data were manually retrieved. Heatmap for comparison of CLas gene expression (by TPM value) between leaf midribs and fruit pith was generated in TBtools software (Chen et al., 2020).

For host transcriptome analyses, all clean HiSeq data from leaf midribs and fruit piths samples were mapped to *Citrus clementina* v1.0 reference genome (Wu et al., 2014) by using Tophat2 with the mismatch penalty of no more than two nucleotides (Kim et al., 2013). DEGs between leaf midribs and fruit pith were identified with DEGseq (Wang et al., 2010). Log2 fold change $\geq | 1 |$ and $q < 0.005$ were set as cutoff values. DEGs were assigned into GO (Gene Ontology) categories with GOseq (Young et al., 2010). Kyoto Encyclopedia of Genes and Genomes (KEGG) pathway enrichment analysis of DEGs was conducted using KOBAS 2.0 software (Xie et al., 2011).

Light Microscopy and Transmission Electron Microscopy

Leaf midribs and fruit pith tissues from both HLB-affected and healthy "Gongkan" and "Shatangju" mandarin trees were used for light microscopy assessments. All tissues were initially cut into approximately 3-mm segments and further fixed with 3% glutaraldehyde in 0.1 M potassium phosphate buffer (pH 7.2) at 4°C overnight. The fixed tissues were then washed in the same buffer and postfixed in 2% osmium tetroxide for 4 h at room temperature, dehydrated in an acetone series, and embedded in Spurr resin. One micrometer of sections was cut with glass knives and stained with safranin O and fast green solution. The stained tissues were dehydrated and cleared with 95% ethyl alcohol, absolute alcohol, and xylene using two changes each (2 min each). Light micrographs were taken on a Nikon Eclipse Ni microscope (Nikon Instruments Inc., Melville, NY, United States) with a Nikon DS-Ri2 camera. The fruit pith tissues with high abundance of CLas were used for transmission electron microscopy (TEM) analyses. For TEM, 100-nm sections of CLas-infected fruit pith tissues were cut with a diamond knife, stained with 2% aq. uranyl acetate, and poststained with lead citrate. TEM micrographs were taken by an AMT (Advanced Microscopy Techniques Corp., Danvers, MA, United States) digital camera on a Morgagni 268 (FEI Company, Hillsboro, OR, United States) transmission electron microscope.

RESULTS

Distribution of CLas in Citrus Branches and Fruits of 14 Citrus Cultivars

Quantification analyses showed CLas was most abundant in the fruit pith (27,157 cells/ng of total DNA), followed by central axis (8,613 cells/ng of total DNA), peduncle (633 cells/ng of total DNA), midribs of leaf adjacent to fruit (507 cells/ng of total DNA), leaf midribs of new flush (465 cells/ng of total DNA), and midribs of mature leaf (168 cells/ng of total DNA). Statistical analysis revealed that the concentration of CLas was significantly higher in fruit pith (11 citrus cultivars) or in both fruit pith and central axis than in other tissues collected from the same citrus branch ($P < 0.05$) (**Table 1**). The concentration of CLas in fruit pith varied among 14 citrus varieties, ranging from 5,701 cells/ng of total DNA ("Tankan" mandarin) to 77,584 cells/ng of total DNA ("Shatian" pomelo) (**Table 1**). In addition, the lowest concentrations of CLas were mainly recorded in the midribs of mature leaf than other tissues in 14 citrus varieties (**Table 1**).

Temporal Dynamics of CLas Population in HLB-Affected "Shatangju" Mandarin Branches

The temporal dynamics analyses of CLas population showed that CLas concentration in fruit pith was consistently higher than other parts in "Shatangju" branches collected monthly from August to January ($P < 0.05$) (**Figure 1B**). The CLas populations peaked in September and then decreased slightly as fruit ripened (in December and January) (**Figure 1B**). However, although the highest concentrations of CLas were detected in fruit pith collected in September, "red-nose" symptom was not observed in HLB-affected "Shatangju" fruits in September (**Figure 1A**). In contrast, typical "red-nose" symptom was observed in diseased fruits collected at January, when CLas concentrations in fruit pith were at a lowest level recorded over 6 months (**Figure 1B**). Concentrations of CLas in the other tissues sampled also declined gradually from peaks in August to January when the lowest concentrations were recorded (**Figure 1B**).

Quantification and Distribution of CLas in Fruit Pith of Three Citrus Cultivars

Overall, the average population of CLas in 1.5-cm segment of "Eureka" lemon pith (209,916 $\pm$ 42,937) was significantly lower than in those from "Pink" grapefruit (1,418,281 $\pm$ 241,315) and "Wenzhou" mandarin (1,261,757.66 $\pm$ 334,300) ($P < 0.05$) (**Figure 2**). CLas population ranged from 8.6×10^3 to 1.3×10^7, 2.0×10^3 to 9.1×10^6, and 5.8×10^3 to 1.1×10^6 cells for each of the 1.5-cm pith segment from "Wenzhou" mandarin, "Pink" grapefruit, and "Eureka" lemon, respectively (**Figure 2**). Fresh 1.5-cm segment of pith weighted, on average, approximately 8 mg. Therefore, CLas populations ranged from 1.0×10^6 to 1.6×10^9, 2.5×10^5 to 1.1×10^9, and 7.3×10^5 to 1.4×10^8 cells per gram of fresh fruit pith from "Wenzhou" mandarin, "Pink" grapefruit, and "Eureka" lemon, respectively.

Quantitative analyses revealed CLas was unevenly distributed in fruit pith (**Figure 2**). In "Eureka" lemon fruit, the population of CLas was significantly higher in the 1.5-cm segments of pith sampled from 3.0 to 4.5 cm in the middle region than those from stylar and calyx region (from 0 to 3.0 cm and 4.5 to 7.5 cm) (**Figure 2**). In fruit of "Pink" grapefruit and "Wenzhou" mandarin, the significantly higher CLas population was observed in the 1.5-cm segments of pith sampled from the stylar region (from 4.5 to 7.5 cm of "Pink" grapefruit and from 3.0 to 4.5 cm "Wenzhou" Mandarin) than in the 1.5-cm segments of calyx region (from 0 to 3.0 cm of "Pink" grapefruit and "Wenzhou" mandarin) (**Figure 2**).

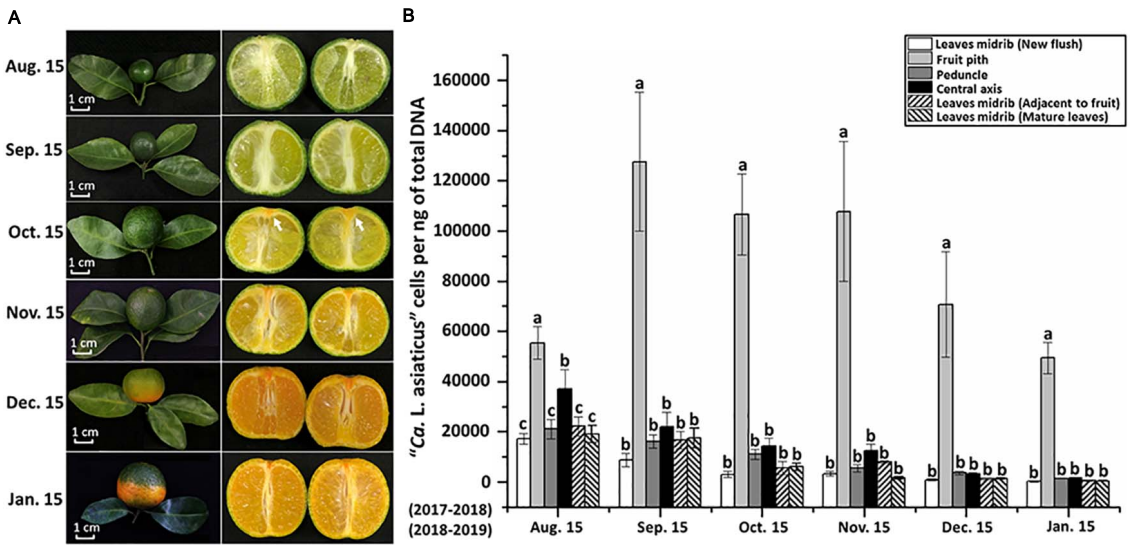

FIGURE 1 | Quantitative distribution off "*Candidatus*f Liberibacter asiaticus" (CLas) in citrus branches and fruits. **(A)** Symptom development of HLB-affected "Shatangju" mandarin (*Citrus reticulata* Blanco "Shatangju") fruits. **(B)** Temporal dynamics of CLas population in different parts of HLB-affected "Shatangju" branches. Ten citrus branches were monthly collected from HLB-affected citrus trees during August 15, 2017, to January 15, 2018, and August 15, 2018 to January 15, 2019. Note the vascular columella (white arrow) under the peduncle of diseased fruit started to turn into orange in October.

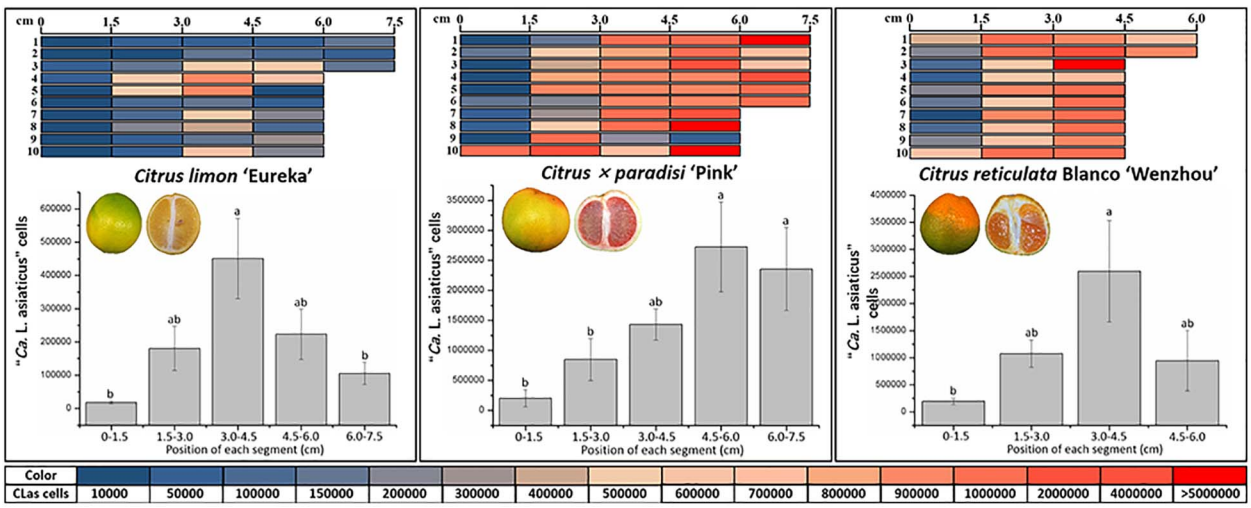

FIGURE 2 | Quantitative distribution of "*Candidatus* Liberibacter asiaticus" (CLas) in fruit piths of three citrus varieties. Graphic denoted 1.5-cm segment of fruit piths. Color scale indicates the CLas cell number in each 1.5-cm segment following quantitative real-time PCR. The average number of CLas cells in each 1.5-cm segment of fruit piths from individual citrus variety is indicated as bar graph. The different letters at the top of the bar represent significant difference by single-factor analysis of variance (Duncan multiple-range test) at 95% ($P < 0.05$) confidence interval.

Genome-Wide Gene Expression Profiling of CLas in Leaf Midribs and Fruit Piths

Approximately 100 and 147 million HiSeq reads were obtained from CLas-infected citrus leaf midribs and fruit piths RNA samples, respectively. Mapping to CLas A4 genome (CP010804.2) identified a total of 3,423 reads (average coverage of 0.4 × of mapped consensus) from leaf midribs RNA-seq data and 109,191 reads (average coverage of ∼13 × to the mapped consensus) from fruit piths RNA-seq data. Differential expression analyses revealed 151 DEGs of CLas between leaf midribs and fruit piths. Of 151 DEGs, 147 were significantly up-regulated (log2 fold change ≥ | 1 |) in leaf midribs compared with fruit piths, whereas only four CLas genes were significantly up-regulated in fruit piths compared with leaf midribs (**Supplementary Table 1**). Functional classification showed 151 DEGs were categorized into 19 diverse function groups plus one group of genes not classified in the COG database (**Figure 3A**). Large numbers of genes involved in replication, recombination,

repair, transcription, translation, transport/metabolism, and cell wall/membrane/envelope biogenesis were up-regulated in leaf midribs compared with fruit pith tissue (**Figure 3A**).

It was found that 10 genes involved in active transport system were up-regulated in leaf midribs compared with fruit pith (**Supplementary Table 1**), including five ABC transporter genes (CD16_RS00210, CD16_RS00215, CD16_RS02450, CD16_RS03160, and CD16_RS04765), one glycine betaine transporter gene (CD16_RS01075), and four genes involved in the efflux pumps system (CD16_RS00510, CD16_RS03560, CD16_RS04390, and CD16_RS05425) (**Supplementary Table 1**). The expression of genes involved in flagellar assembly, including *flaF* (CD16_RS03425), *flgH* (CD16_RS01235), *flgA* (CD16_RS01250), *flgK* (CD16_RS03415), and *fliK* (CD16_RS03400), and the CD16_RS02435 involved in pilus assembly, were also up-regulated in leaf midribs (**Supplementary Table 1**). It should be noted that genes involved in virulence/toxicity were overexpressed in leaf midribs tissue and included three genes involved in lipid A or lipopolysaccharide (LPS) biosynthesis (CD16_RS01575, CD16_RS02310, CD16_RS03055, and CD16_RS05315) and CD16_RS01040 involved in toxin biosynthetic process (**Supplementary Table 1**). In addition, *gndA* (CD16_RS02465) and *gshB* (CD16_RS02570), encoding enzymes involved in the metabolism of glutathione, were also up-regulated in the leaf midribs. However, four CLas genes that up-regulated in fruit pith were not assigned with any COG function categories (**Supplementary Table 1**).

The top 20 highest expressed CLas genes in leaf midribs and fruit pith were compared (**Figure 3B**). Three genes involved in bacterial cell surface structure, including two porin family genes (CD16_RS03055 and CD16_RS00940) and a collagen-like protein gene (CD16_RS05425), were highly expressed in both leaf midribs and fruit pith tissue (**Figure 3B**). A Bax inhibitor-1/YCCA family gene (CD16_RS01625), encoded putative plant cell death suppressor, was also highly expressed in leaf midribs and fruit pith tissue (**Figure 3B**). Three known stress-related genes, *DnaK* (CD16_RS02830), *GroES* (CD16_RS03695), and *GroEL* (CD16_RS03700), and a heat shock protein (CD16_RS02920) were found to express in a high level in leaf midrib and fruit pith (**Figure 3B**). In addition, the high expression level of a peroxiredoxin gene (CD16_RS00915) was also detected in leaf midrib and fruit pith tissue.

Transcriptome Profiling of Leaf Midribs and Fruit Pith Response to CLas Infection

Approximately 92.67% of leaf midribs HiSeq reads and 97.42% of fruit pith HiSeq reads were successfully mapped to *C. clementina* genome. A total of 2,517 DEGs were identified between CLas-infected leaf midribs and fruit pith. There were 2,256 DEGs up-regulated in CLas-infected leaf midrib, whereas 261 DEGs were up-regulated in CLas-infected fruit pith (**Figure 4**). GO enrichment analysis showed that the up-regulated DEGs in CLas-infected leaf midribs were mainly enriched in biological process, metabolic process, catalytic activity, single-organism metabolic process, oxidation–reduction process and oxidoreductase activity, whereas the up-regulated DEGs in CLas-infected fruit pith were mainly involved in biological process (**Figure 5**). Among genes enriched in biological process, a gene-encoded leucine-rich repeat receptor-like protein kinase (Ciclev10024853m.v1.0) was strongly up-regulated in CLas-infected leaf midribs compared with CLas-infected fruit pith (log2 fold change = 8.21) (**Supplementary Table 2**). In addition, the result of KEGG pathway analysis revealed that the large numbers of up-regulated DEGs in CLas-infected leaf midribs were mainly enriched in metabolic pathway and biosynthesis of secondary metabolites (**Figure 6**). The pathway of biosynthesis of secondary metabolites mainly contained genes involved in the synthesis of secondary metabolites, which have functions such as antimicrobial activities, including acridone, germanicol, chalcone, cinnamyl alcohol, neomenthol, caffeic acid, flavonol, β-amyrin, and chitinase (**Supplementary Table 3**). In contrast, genes involved in protein processing in endoplasmic reticulum, carotenoid biosynthesis, amino, and nucleotide sugar metabolism were up-regulated in CLas-infected fruit pith.

Anatomical Changes in the Phloem of Leaf Midribs and Fruit Piths Caused by CLas Infection

Although the CLas cells were abundant in fruit pith tissues, the microscopic manifestations of fruit pith caused by CLas infection were unclear. Compared with the healthy citrus, the phloem of CLas-infected fruit pith was severely collapsed with cell wall distortion (**Figure 7**, black arrow), especially the sieve elements that appeared irregular with jagged boundaries (**Figure 7**, black arrow). The thickened and disrupted cell walls of the sieve element and companion cells were also commonly found in the phloem of CLas-infected fruit piths (**Figure 7**). Compared with the CLas-infected leaf midribs tissue, a higher level of phloem collapse was observed in CLas-infected fruit pith (**Figure 7**). In contrast, a relatively higher concentration of starch granule accumulation was observed in parenchyma cells of CLas-infected leaf midribs, whereas no starch accumulation was observed in CLas-infected fruit pith (**Figure 7**).

The severe collapse with heavy callose deposition around the plasmodesmata pore of sieve element in phloem of CLas-infected fruit pith was also confirmed by the TEM analysis (**Figure 8A**). Two possible forms of CLas cells, the elongated and round forms, were present at a high abundance in phloem cells of CLas-infected fruit pith (**Figures 8B,C**). A high magnification electron of TEM micrographs revealed the unknown filamentous materials were commonly found around CLas cells and connected between CLas cells (**Figure 8C**).

DISCUSSION

The current inability to culture CLas *in vitro* leads to the characterization of CLas need to rely on the analysis of CLas-abundant host tissue. In this study, we found a stable high abundance of CLas in fruit pith of 14 citrus cultivars. Previous

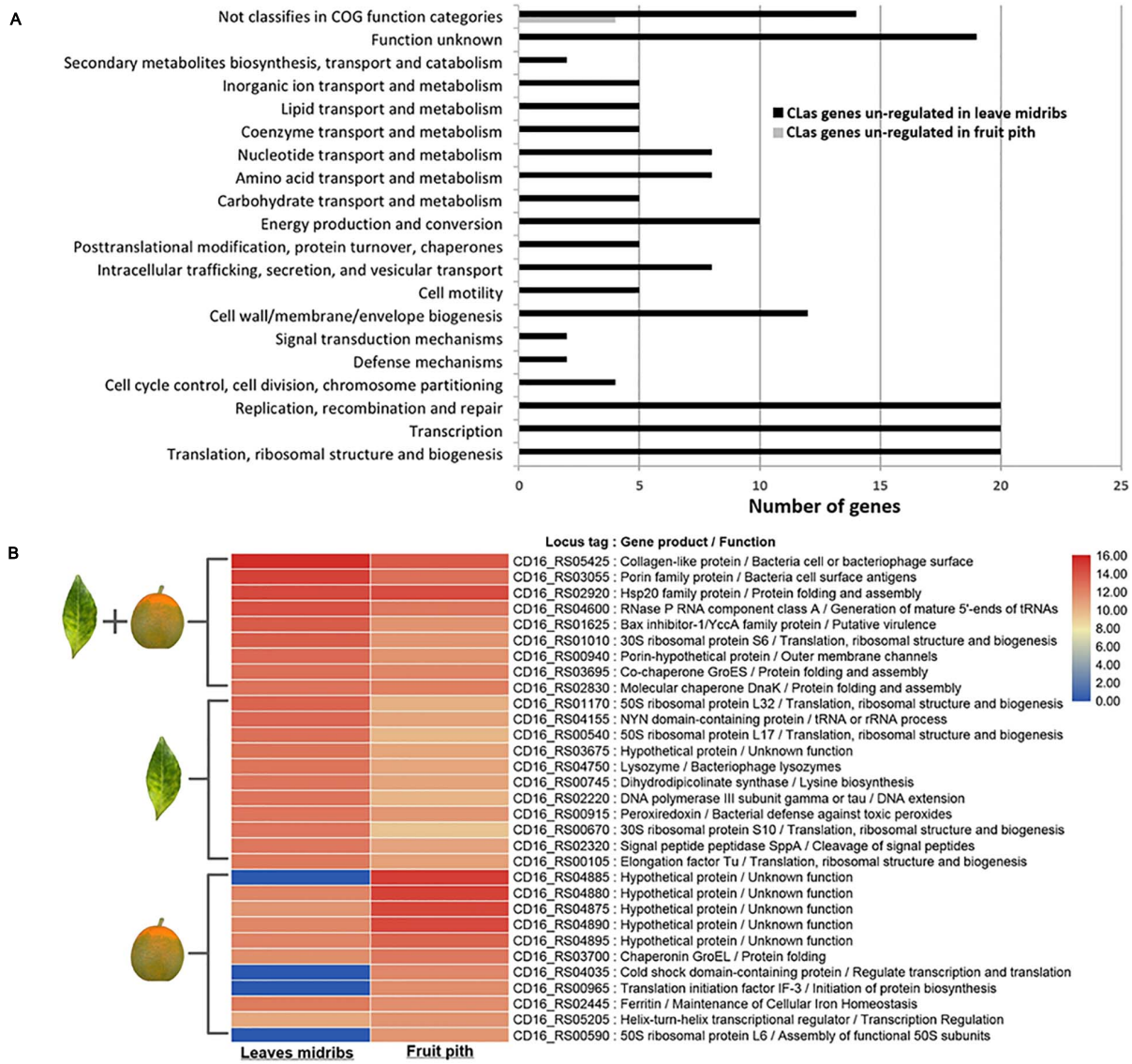

FIGURE 3 | Functional classification of differentially expressed genes **(A)** and top 20 highly expressed gene **(B)** of "*Candidatus* Liberibacter asiaticus" (CLas) in fruit pith and leaf midribs. The differentially expression genes (DEGs) are identified with GFOLD v1.1.4 software by setting log2 fold change $\geq$ | 1 |. Classification of DEGs is performed with EggNOG v5.0 by using Clusters of Orthologous Groups database. Black bar represents genes up-regulated in fruit pith compared with leaf midribs. Gray bar represents genes up-regulated in leaf midribs compared with fruit pith. Heatmap shows the log2 of normalized TPM values for the top 20 most highly expressed CLas genes in leaf midribs tissue and fruit pith tissue. Genes that belong to the list of the top 20 most highly expressed genes in leaf midribs or fruit piths are labeled with leaf or fruit symbol in the left.

studies have reported relatively high concentrations of CLas in fruit tissue, for instance, in the peduncles (Tatineni et al., 2008) and locular membranes/septa (Li et al., 2009). As phloem-limited bacteria, CLas could be able to move with phloem flow from source tissues (e.g., mature leaves) to sink tissues (e.g., fruit) and accumulated in higher numbers in the sink tissue (Tatineni et al., 2008; Achor et al., 2020). The pith of citrus fruit used in this study mainly comprises the scattered dorsal vascular bundles (**Supplementary Figure 3**), which transport nutrients for fruit developing. Therefore, the high level of CLas population in fruit pith tissue was mainly because it can be acted as the nutritional sink for CLas accumulation and contained the abundance of nutrients for CLas multiplication. This also implies that fruit pith tissue can be used as ideal host material for CLas multiplication. Further analyses of nutrients composition and microenvironment in the fruit pith can help to identify fastidious requirements for *in vitro* culturing of CLas. Nonetheless, the density of CLas populations in the fruit pith tissue from different citrus cultivars varied, ranging from 5,701 to 77,584 cells/ng of total DNA (**Table 1**). The different nutritional contents, metabolites, or even resistance substances in the phloem sap of different citrus cultivars could have influence

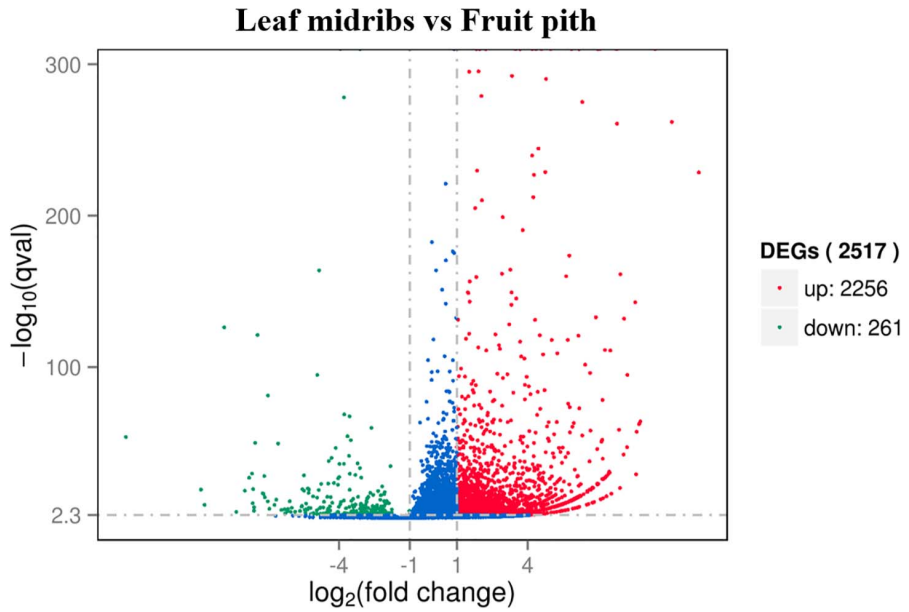

FIGURE 4 | Volcano plot representation of differential expression analysis of host genes in "*Candidatus* Liberibacter asiaticus" (CLas)–infected leaf midribs and CLas-infected fruit pith. Red and green points mark the genes with significantly increased or decreased expression, respectively, in leaf midribs compared with fruit pith samples (FDR < 0.01). The blue points mark the genes with no significantly different expression. The *x*-axis represents log2 fold changes in expression, and the *y*-axis represents statistically significant difference in gene expression.

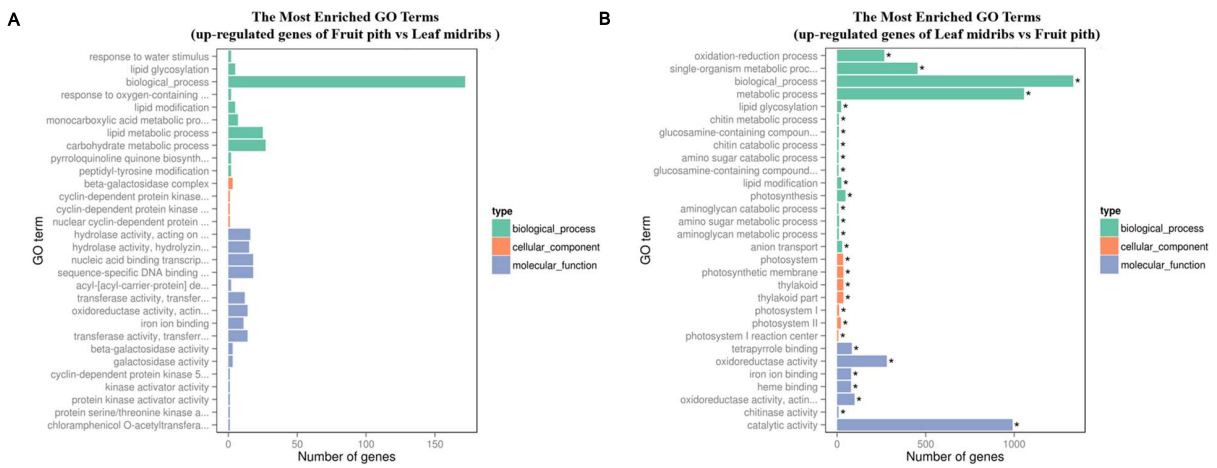

FIGURE 5 | GO term enrichment analyses of the up-regulated genes in "*Candidatus* Liberibacter asiaticus" (CLas)–infected fruit pith **(A)** and CLas-infected leaf midribs **(B)**. The vertical coordinates represent enriched GO terms, and the horizontal coordinates represent the numbers of up-regulated genes in these GO terms. Green columns: biological process GO terms; purple columns: cellular component GO terms; orange columns: molecular function GO terms. *Significantly enriched GO term.

on CLas populations in fruit piths among different cultivars. Therefore, further comparison of phloem sap composition of fruit pith from different citrus cultivars should help to identify substances responsible for tolerance/susceptibility to CLas, as well as the essential requirements for culturing CLas *in vitro*.

Quantification analyses of CLas populations in consecutive 1.5-cm length of fruit pith between the calyx (proximal) and stylar (distal) regions of mature fruit of three citrus cultivars showed that CLas cells were unevenly distributed in fruit pith, with populations in central and stylar region higher than in the calyx region (**Figure 2**). The fruit pith collected in this study mainly comprised dorsal vascular bundles, which was part of the vascular system of citrus fruit. The vascular system of citrus fruit forms a broadly branched network of main vascular bundles and subsidiary traces, including the axial, dorsal, septal, and marginal bundles (Tadeo et al., 2020). In citrus fruit, the central axial bundle extends down to the stylar end, diverges into the septa to become the marginal bundles, then merges with the

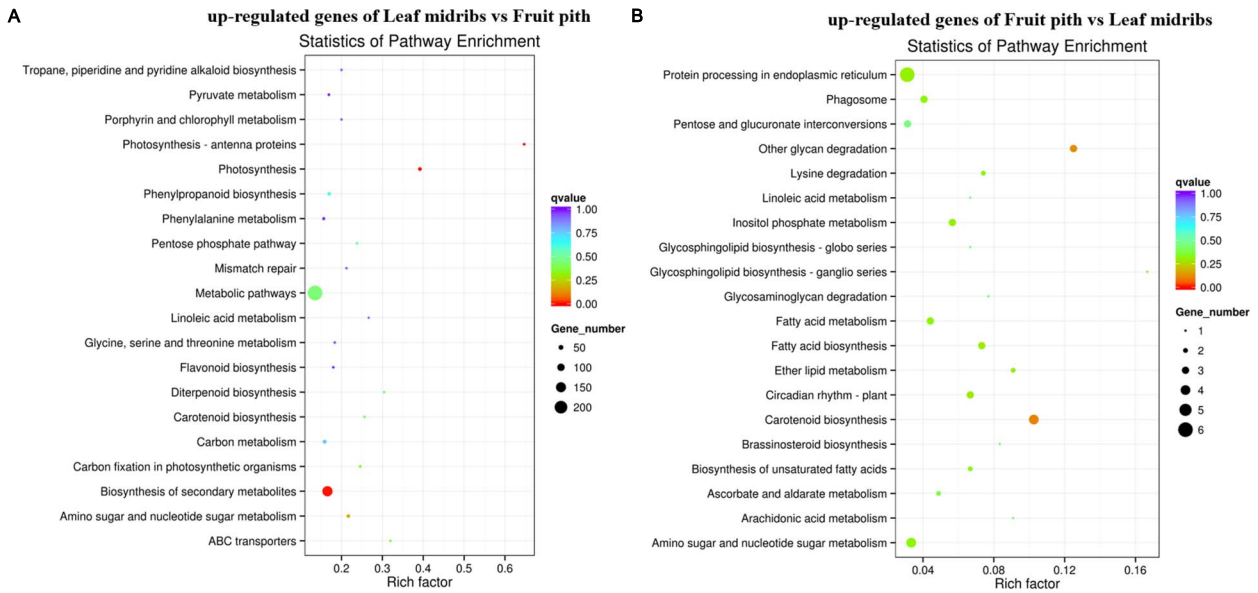

FIGURE 6 | KEGG enrichment analyses of the up-regulated genes in "*Candidatus* Liberibacter asiaticus" (CLas)–infected leaf midribs **(A)** and CLas-infected fruit pith **(B)**. The vertical coordinates represent the enriched pathways, and the horizontal coordinates represent the rich factors. The size of each point represents the number of up-regulated genes in the pathway, and the color of the point represents the *q* value.

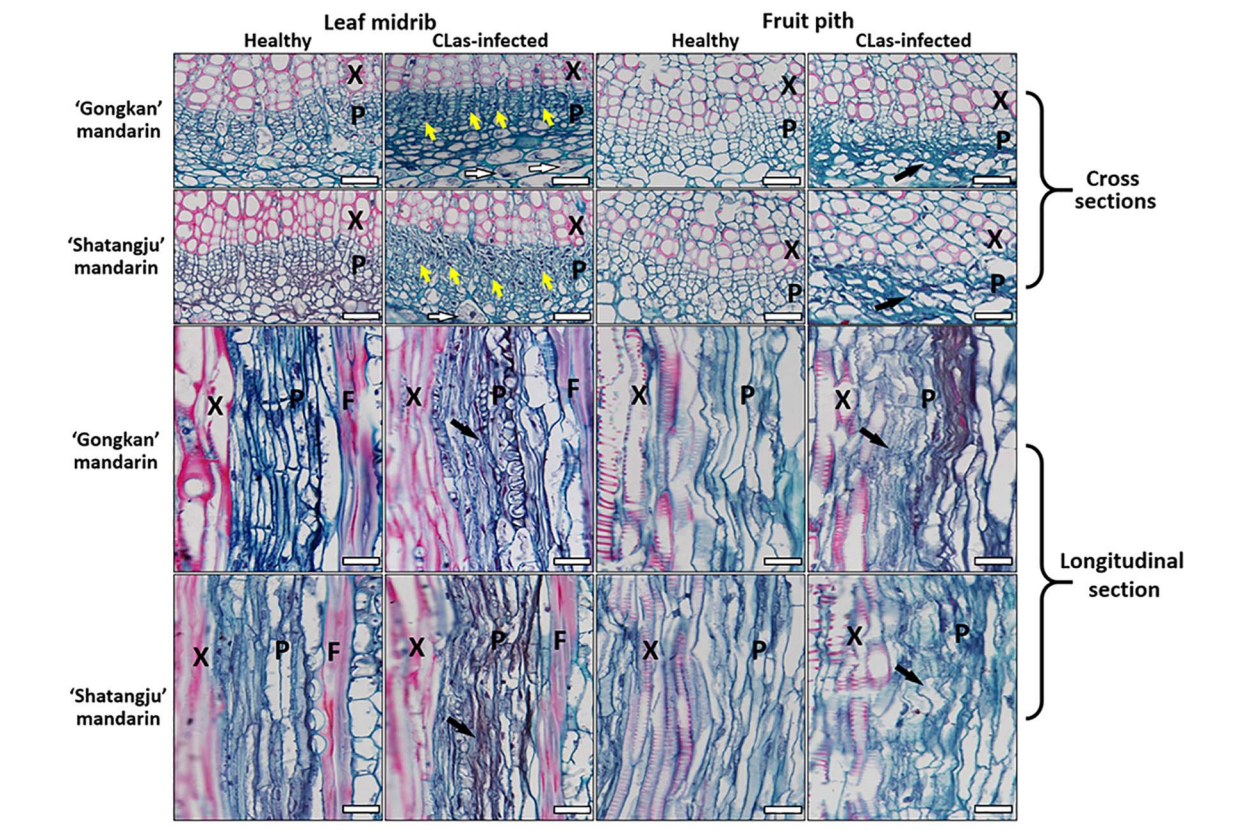

FIGURE 7 | Light micrographs of leaf midribs and fruit pith from "*Candidatus* Liberibacter asiaticus"–infected and healthy "Gongkan" and "Shatangju" mandarin. X, xylem; F, fiber; P, phloem. The callose plugs (yellow arrow), collapsed phloem (black arrow), and starch granule accumulation (white arrow) are commonly observed in CLas-infected lead midrib. Bar = 30 μm.

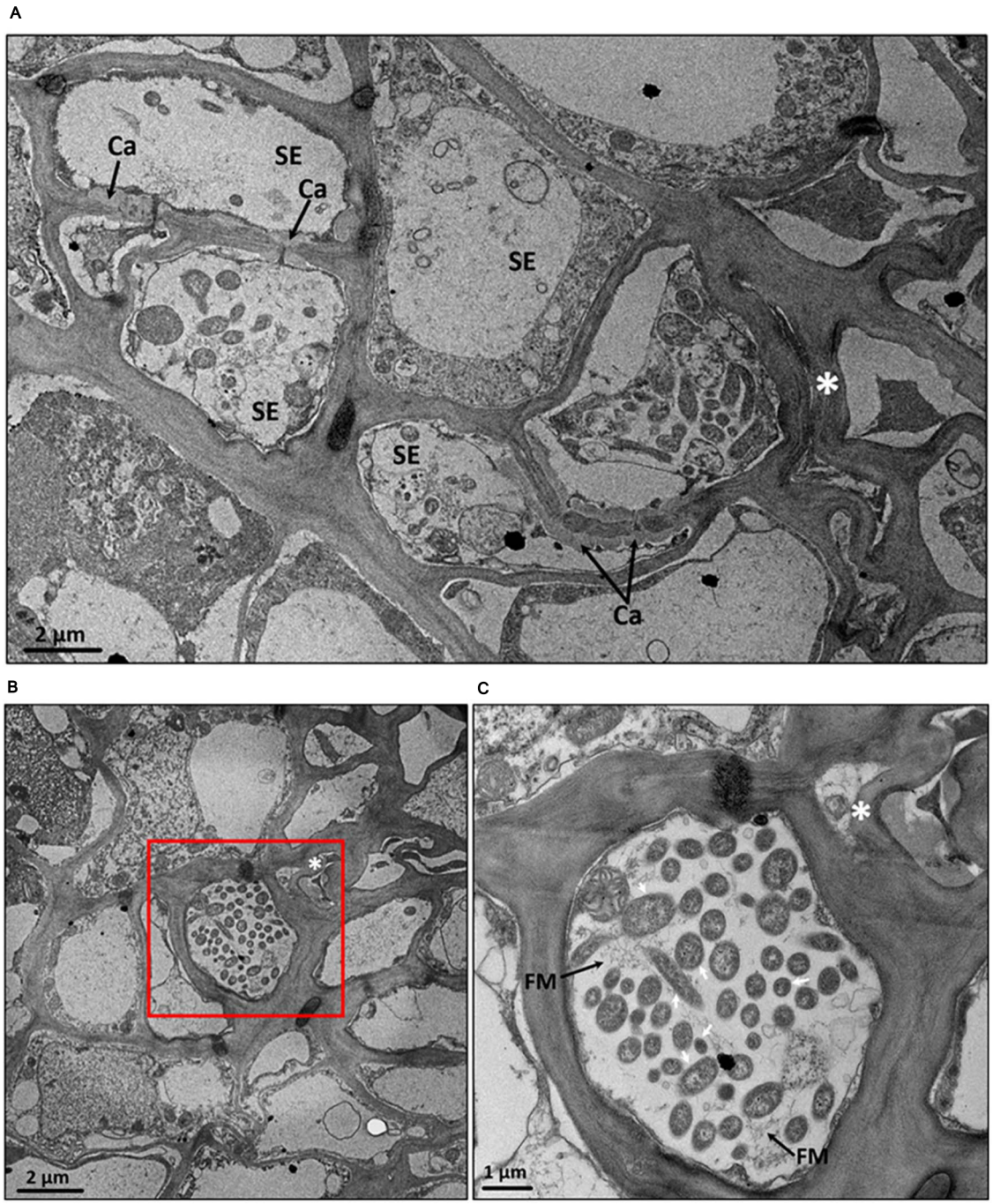

FIGURE 8 | Transmission electron micrographs of cross section of fruit pith tissues from "*Candidatus* Liberibacter asiaticus"–infected "Shatangju" mandarin. **(A)** Collapsed phloem cells and callose deposition in the plasmodesmata pore between sieve elements of CLas-infected fruit pith. **(B)** A high abundance of CLas cells with elongated and round forms in the phloem cell. **(C)** The close-up of red region in panel **(B)**. SE, sieve element; Ca, callose; FM, filamentous material found around CLas cells. *Phloem cells collapse. Note double cell walls (white arrows) characteristic of Gram-negative bacterium, which is presumed to be CLas cells.

dorsal and septal bundles at the stylar end, and finally closes the vascular circuit at this region (Ladanyia, 2010; Tadeo et al., 2020). Consequently, the distribution of photosynthates and sugars is higher in the stylar region than the calyx/stem region (Ladanyia, 2010). Therefore, the higher populations of CLas cells in the middle and stylar region than in the calyx region could be attributed to the distribution of nutrients.

Details on genome-wide transcriptome profile of CLas in infected citrus trees have not been described yet mainly due to the low abundance of CLas RNA compared with host

citrus RNA in total RNA samples. Compared with the leaf midrib sample, the use of CLas-abundant fruit pith samples for dual RNA-seq generated a higher depth (>10×) of CLas genome and allowed more genes to be quantified, indicating a higher resolution of transcriptome profile for CLas revealed by using CLas-infected fruit pith. It was found that four CLas genes highly expressed in fruit pith were not detectable in leaf midribs by HiSeq data (**Figure 3B**). However, annotation showed three of four genes (CD16_RS04035, CD16_RS00965, and CD16_RS00590) were involved in the essential function of transcription and translation process of CLas (**Figure 3B**), indicating the undetectable expression of these constitutive genes could be due to the shallow sequencing depth of CLas genes in RNA-seq of leaf midribs sample.

Differential gene expression analyses still identified a total of 151 DEGs, with most (147 DEGs) of them up-regulated in leaf midrib compared with fruit pith. The higher number of up-regulated CLas genes in leaf midribs implied the CLas–host interaction could be much stronger in leaf midribs than in fruit pith. In addition, nearly a third of CLas DEGs that were mainly involved in the replication, transcription, translation, ribosomal structure, and biogenesis process were up-regulated in leaf midribs compared with fruit pith (**Figure 3A**). This suggested that CLas population could be still under the growth phase in the leaf midribs in December. By contrast, the inactive CLas gene expression and the starting decline of CLas population in December (**Figure 1B**) suggested the CLas population could be in a decline/death phase in the fruit pith collected in December.

Genes involved in active transport system of CLas were up-regulated in leaf midrib compared with fruit pith. ABC transporters are known to be involved in bacteria virulence associated with the uptake of nutrients (Boyer et al., 2002). The overexpression of five genes involved in ABC transporters in leaf midribs suggested they could be involved in virulence of CLas in leaf. Four genes associated with the efflux pumps system were also up-regulated in leaf midribs (**Supplementary Table 1**). The bacterial efflux pumps were able to extrude a wide range of toxic compounds out of cells, such as antibiotic, heavy metals, organic pollutants, plant-produced compounds, quorum sensing signals, or bacterial mechanism (Blanco et al., 2016). In addition, genes (*gndA* and *gshB*) involved in the metabolism of glutathione were also found to be up-regulated in leaf midrib (**Supplementary Table 1**). The bacterial glutathione peroxidase was known as a common antioxidant in protecting bacterial cells against oxidative stress (Arenas et al., 2011). The up-regulation of efflux pump genes and stress resistance–related genes in leaf is believed to protect CLas from harmful plant environments in leaf, which also indicated that CLas could be under a higher plant toxins or defense responses in leaf midrib compared with fruit pith.

The up-regulated CLas LPS genes in leaf midribs may play a critical role in CLas–host interaction. In this study, four CLas LPS genes were up-regulated in leaf midribs (**Supplementary Table 1**). The up-regulation of LPS genes could be important for CLas to survive in leaf, as LPS is the major component of the outer membrane in Gram-negative bacteria and can be served as a physical barrier to protect bacterial cells from the unfavorable host plant environments (Rosenfeld and Shai, 2006). In addition, the bacterial LPS was known to play an important role in eliciting plant basal defense-related response by acting as a pathogen-associated molecular pattern (PAMP) (Parker, 2003). The bacterial PAMP can be recognized by host innate immunity system during the infection (Parker, 2003). This was consistent with our observation that the gene (Ciclev10024853m.v1.0) that encoded the leucine-rich repeat receptor-like protein, a critical gene in plant innate immunity, was strongly up-regulated in leaf midribs compared with fruit pith (**Supplementary Table 2**).

Genes involved in CLas cell surface structure, stress response, and virulence was highly expressed in both leaf midribs and fruit pith. A large number of collagen-like proteins have been identified in bacteria and play a critical role in extracellular matrix structural properties and cell signaling. In *Bacillus*, the glycosylated collagen-like proteins have been shown to be present in thin hair-like surface filaments of bacteria cells (Yu et al., 2014). The high expression level of CLas collagen-like gene (CD16_RS05425) in fruit pith tissue was consistent with the observation of filamentous material around CLas cells (**Figure 8C**), although its function remains to be determined. The BAX inhibitor was known as an ancient conserved cell death suppressor in mammals and plants with prokaryotic relatives (Hückelhoven, 2004). In addition, peroxiredoxin was found to play an important role in bacterial defense against oxidative stress and toxic peroxides (Dubbs and Mongkolsuk, 2007). The high expression of the BAX inhibitor-1/YCCA family gene and peroxiredoxin gene in leaf midribs and fruit pith indicated they might contribute to the compatible interaction between the pathogen and host plant by suppressing of the host cell death and defensing against the oxidative stress and toxic chemicals produced by host, respectively.

The secondary metabolites may play an important role in plant defense against CLas in leaf midribs. We observed that large numbers of genes involved in the synthesis of antimicrobial secondary metabolites were up-regulated in leaf midribs (**Figure 6** and **Supplementary Table 3**). Especially, an acridone synthase gene (Ciclev10025807m.v1.0), germanicol synthase gene (Ciclev10033766m.v1.0), and a chalcone synthase gene (Ciclev10032697m.v1.0) were strongly up-regulated in leaf midribs compared with fruit pith (log2 fold change > 4). The acridone and its derivatives were commonly found in plant and exhibited the antibacterial activity (Wainwright, 2001). Germanicol was found as one of the main constituents in essential oil of the *Pistacia lentiscus* leaves, which showed strong activity against *Klebsiella pneumoniae* (Mharti et al., 2011). Chalcones is one of the important compound groups of flavonoids and exhibited a wide spectrum of biological activities, such as antimicrobial activity (Xu et al., 2019). Therefore, the up-regulated genes involved in secondary metabolites against microbe/bacteria in leaf midribs compared with fruit pith revealed a lower concentration of antimicrobial compound produced by host in fruit pith than in leaf midrib, which could also explain why the fruit pith could be a more suitable host tissue for CLas reproducing.

Anatomical changes in phloem caused by CLas infection mainly included the phloem collapse with jagged and thickened

cell walls, hypertrophic parenchyma cells, callose plugging, and massive starch accumulation (Schneider, 1968; Etxeberria et al., 2009; Kim et al., 2009; Achor et al., 2010; Folimonova and Achor, 2010; Koh et al., 2012; Brodersen et al., 2014). Callose deposition induced by CLas infection blocks transport of photoassimilate in phloem. This leads to starch accumulation in phloem (Schneider, 1968; Koh et al., 2012). Phloem collapse and plugging led to the starch packing in chloroplasts of host cells, manifested as chlorosis associated with HLB (Achor et al., 2010). Based on our observation, starch accumulation was not observed in the CLas-infected fruit pith tissue but was common in CLas-infected leaf midribs (**Figure 7**). Starch grain accumulation in infected citrus was usually observed in the parenchyma tissue, as well as in phloem cells, but they were often concealed by the collapsed phloem cells in phloem tissue (Etxeberria et al., 2009).

Severe collapse of phloem cells and cell wall distortion in CLas-infected fruit pith were more apparent than in leaf midribs (**Figure 7**). This may have been related to higher abundance of CLas population in fruit pith. Previous studies have indicated that phloem collapse caused by CLas infection is primarily due to hyperactive differentiation of vascular cambium and hyperplasia of parenchyma cells surrounding the necrotic phloem pocket (Kim et al., 2009). Moreover, the significant swelling of middle lamella between cell walls surrounding sieve elements occurred at an early stage of CLas infection, also potentially leading to phloem collapse and necrosis in infected leaves (Folimonova and Achor, 2010). However, although the phloem collapse was identified as an intrinsic characteristic caused by CLas infection, the mechanism of how CLas causes the damage on phloem and the host response in fruit pith tissues was still unclear. It is possible that the CLas might secrete the virulence factors into the phloem, trigger the plant defense, and cause the phloem collapse.

In addition to phloem collapse and starch accumulation, callose deposition in the sieve pores and plasmodesmata is another characteristic ultrastructure change in the CLas-infected lead midrib (Kim et al., 2009; Achor et al., 2010). In this study, we observed that a heavy callose accumulates around the phloem plasmodesmata pore of sieve elements in CLas-infected fruit pith (**Figure 8A**). The callose plugging in plasmodesmata was also known to be a plant defense response to diverse biotic and abiotic stresses, such as insect/pathogen attack (Nishimura et al., 2003; Rinne and Schoot, 2003; Roberts, 2003), wounding (Radford et al., 1998), and cellular plasmolysis (Drake et al., 1978). A previous study also suggested that the CLas infection triggered production of reactive oxygen species, which in turn promoted callose synthesis at plasmodesmata (Koh et al., 2012).

Based on the high-magnification electron of TEM, we observed two possible forms of CLas cells, elongated and round forms, in phloem cell of fruit pith (**Figures 8B,C**). Although it was not certain whether both elongated and round forms of cells were CLas, the similar types (both elongated and round shapes) of CLas cells have been observed and confirmed in early studies (Hilf et al., 2013; Achor et al., 2020). Especially, a recent study showed the CLas was able to change its morphology from round form to elongated form, which enables the CLas movement through host phloem pores (Achor et al., 2020). A further immuneolabeling or fluorescence *in situ* hybridization analysis of CLas cell is required. In addition, the filamentous-like material was commonly found around CLas cells and connected between CLas cells (**Figure 8C**). The filamentous material around CLas cells was thought to be utilized by CLas for attachment of bacterial cells to the host cell membrane adjacent to the phloem pores (Achor et al., 2020). However, no adhesion protein of CLas has been described. Interestingly, a bacterial (or bacteriophage) cell surface–associated gene (CD16_RS05425) that encoded a collagen-like protein was found to be highly expressed in both CLas-infected citrus leaf midribs and fruit piths (**Figure 3B**). This suggested that this gene may be involved in the CLas–host interaction.

In conclusion, based on the distribution analyses of CLas in citrus branches of 14 citrus cultivars, we found that a significantly high abundance of CLas cells was consistently detected in fruit pith of all citrus cultivars. Highest densities of CLas in fruit pith occurred before visual symptoms of HLB developed in infected fruits. CLas was unevenly distributed within fruit pith and tended to colonize in the middle or stylar region of fruit pith. The use of CLas-abundant fruit pith sample for dual RNA-seq provided the reliable and high-resolution of CLas transcriptome profile compared by using CLas-infected leaf midribs. CLas infection caused the severe phloem collapse and the heavy callose deposition in the plasmodesmata of sieve elements in fruit pith. The highly simplified anatomy of fruit pith and its ability to support multiplication of CLas to high abundance make it as an ideal host material for further studies on the morphology and transcriptomic analyses of CLas–host interaction.

DATA AVAILABILITY STATEMENT

RNA-seq data from CLas-infected leaf midribs and fruit pith samples supporting the findings of this study are available at the National Center for Biotechnology Information under SRA accession PRJNA660208.

AUTHOR CONTRIBUTIONS

FF, HG, MX, XD, and ZZ conceived and designed the experiments. FF, HG, AZ, TL, ZZ, and HL performed the experiments. FF and ZZ contributed to bioinformatics and statistical analysis. FF, HG, and ZZ prepared figures/table and wrote the draft manuscript. MX, XD, and ZZ reviewed the manuscript. All authors contributed to the article and approved the submitted version.

FUNDING

This work was supported by Special fund for the National Key Research and Development Program of China (2018YFD0201500), National Natural Science Foundation of China (31901844), the cultivating key project of international cooperation in science and technology (2019SCAUGH04), and China Agriculture Research System of MOF and MARA.

ACKNOWLEDGMENTS

We would like to thank Andrew Beattie (University of Western Sydney) for linguistic assistance during the preparation of this manuscript.

SUPPLEMENTARY MATERIAL

The Supplementary Material for this article can be found online at: https://www.frontiersin.org/articles/10.3389/fmicb.2021.681251/full#supplementary-material

REFERENCES

Achor, D., Welker, S., Ben-Mahmoud, S., Wang, C., Folimonova, S. Y., Dutt, M., et al. (2020). Dynamics of *Candidatus Liberibacter asiaticus* movement and sieve-pore plugging in citrus sink cells. *Plant Physiol.* 182, 882–891. doi: 10.1104/pp.19.01391

Achor, D. S., Etxeberria, E., Wang, N., Folimonova, S. Y., Chung, K. R., and Albrigo, L. G. (2010). Sequence of anatomical symptom observations in citrus affected with huanglongbing disease. *Plant Pathol. J.* 9, 56–64. doi: 10.3923/ppj.2010.56.64

Arenas, F. A., Covarrubias, P. C., Sandoval, J. M., Perez-Donoso, J. M., Imlay, J. A., and Vasquez, C. C. (2011). The *Escherichia coli* BtuE protein functions as a resistance determinant against reactive oxygen species. *PLoS One* 6:e15979. doi: 10.1371/journal.pone.0015979

Bao, M., Zheng, Z., Sun, X., Chen, J., and Deng, X. (2020). Enhancing PCR capacity to detect 'Candidatus Liberibacter asiaticus' utilizing whole genome sequence information. *Plant Dis.* 104, 527–532. doi: 10.1094/PDIS-05-19-0931-RE

Blanco, P., Hernando-Amado, S., Reales-Calderon, J. A., Corona, F., Lira, F., Alcalde-Rico, M., et al. (2016). Bacterial multidrug efflux pumps: much more than antibiotic resistance determinants. *Microorganisms* 4:14. doi: 10.3390/microorganisms4010014

Bové, J. M. (2006). Huanglongbing: a destructive, newly-emerging, century-old disease of citrus. *J. Plant Pathol.* 88, 7–37. doi: 10.4454/jpp.v88i1.828

Boyer, E., Bergevin, I., Malo, D., Gros, P., and Cellier, M. F. M. (2002). Acquisition of Mn (II) in addition to Fe (II) is required for full virulence of *Salmonella enterica* serovar Typhimurium. *Infect. Immun.* 70, 6032–6042. doi: 10.1128/IAI.70.11.6032-6042.2002

Brodersen, C., Narciso, C., Reed, M., and Etxeberria, E. (2014). Phloem production in Huanglongbing-affected citrus trees. *HortScience* 49, 59–64. doi: 10.21273/HORTSCI.49.1.59

Chen, C., Chen, H., Zhang, Y., Thomas, H. R., Frank, M. H., He, Y., et al. (2020). TBtools: an integrative toolkit developed for interactive analyses of big biological data. *Mol. Plant.* 13, 1194–1202. doi: 10.1016/j.molp.2020.06.009

Deng, X. L., and Tang, W. W. (1996). The studies on detection of citrus Huanglongbing pathogen by polymerase chain reaction. *J. South China Agric. Univ.* 17, 119–120.

Ding, F., Duan, Y., Paul, C., Brlansky, R. H., and Hartung, J. S. (2015). Localization and distribution of '*Candidatus Liberibacter asiaticus*' in citrus and periwinkle by direct tissue blot immuno assay with an Anti-OmpA polyclonal antibody. *PLoS One* 10:e0123939. doi: 10.1371/journal.pone.0123939

Drake, G. A., Carr, D. J., and Anderson, W. P. (1978). Plasmolysis, plasmodesmata, and the electrical coupling of oat coleoptile cells. *J. Exp. Bot.* 29, 1205–1214. doi: 10.1093/jxb/29.5.1205

Dubbs, J. M., and Mongkolsuk, S. (2007). Peroxiredoxins in bacterial antioxidant defense. *Peroxiredoxin Syst.* 44, 143–193. doi: 10.1007/978-1-4020-6051-9_7

Etxeberria, E., Gonzalez, P., Achor, D., and Albrigo, G. (2009). Anatomical distribution of abnormally high levels of starch in HLB-affected Valencia orange trees. *Physiol. Mol. Plant Pathol.* 74, 76–83. doi: 10.1016/j.pmpp.2009.09.004

Feng, J., Meyer, C. A., Wang, Q., Liu, J. S., Shirley Liu, X., and Zhang, Y. (2012). GFOLD: a generalized fold change for ranking differentially expressed genes from RNA-seq data. *Bioinformatics* 28, 2782–2788. doi: 10.1093/bioinformatics/bts515

Folimonova, S. Y., and Achor, D. S. (2010). Early events of citrus greening (Huanglongbing) disease development at the ultrastructural level. *Phytopathology* 100, 949–958. doi: 10.1094/PHYTO-100-9-0949

Fu, S. M., Liu, H. W., Liu, Q. H., Zhou, C. Y., and Hartung, J. S. (2019). Detection of '*Candidatus Liberibacter asiaticus*' in citrus by concurrent tissue print-based qPCR and immunoassay. *Plant Pathol.* 68, 796–803. doi: 10.1111/ppa.12998

Hartung, J. S., Paul, C., Achor, D., and Brlansky, R. H. (2010). Colonization of dodder, *Cuscuta indecora*, by '*Candidatus Liberibacter asiaticus*' and '*Ca. L. americanus*'. *Phytopathology* 100, 756–762. doi: 10.1094/PHYTO-100-8-0756

Hilf, M. E., Sims, K. R., Folimonova, S. Y., and Achor, D. S. (2013). Visualization of 'Candidatus Liberibacter asiaticus' cells in the vascular bundle of citrus seed coats with fluorescence in situ hybridization and transmission electron microscopy. *Phytopathology* 103, 545–554. doi: 10.1094/PHYTO-09-12-0226-R

Hückelhoven, R. (2004). BAX Inhibitor-1, an ancient cell death suppressor in animals and plants with prokaryotic relatives. *Apoptosis* 9, 299–307. doi: 10.1023/b:appt.0000025806.71000.1c

Huerta-Cepas, J., Forslund, K., Coelho, L. P., Szklarczyk, D., Jensen, L. J., Von Mering, C., et al. (2017). Fast genome-wide functional annotation through orthology assignment by eggNOG-mapper. *Mol. Biol. Evol.* 34, 2115–2122. doi: 10.1093/molbev/msx148

Jagoueix, S., Bové, J. M., and Garnier, M. (1994). The phloem-limited bacterium of greening disease of citrus is a member of the alpha subdivision of the *Proteobacteria*. *Int. J. Syst. Bacteriol.* 44, 379–386. doi: 10.1099/00207713-44-3-379

Kim, D., Pertea, G., Trapnell, C., Pimentel, H., Kelley, R., and Salzberg, S. L. (2013). TopHat2: accurate alignment of transcriptomes in the presence of insertions, deletions and gene fusions. *Genome Biol.* 14, 1–13. doi: 10.1186/gb-2013-14-4-r36

Kim, J. S., Sagaram, U. S., Burns, J. K., Li, J. L., and Wang, N. (2009). Response of sweet orange (*Citrus sinensis*) to '*Candidatus Liberibacter asiaticus*' infection: microscopy and microarray analyses. *Phytopathology* 99, 50–57. doi: 10.1094/PHYTO-99-1-0050

Koh, E. J., Zhou, L., Williams, D. S., Park, J., Ding, N., Duan, Y. P., et al. (2012). Callose deposition in the phloem plasmodesmata and inhibition of phloem transport in citrus leaves infected with "*Candidatus Liberibacter asiaticus*". *Protoplasma* 249, 687–697. doi: 10.1007/s00709-011-0312-3

Kunta, M., da Graça, J. V., Malik, N. S., Louzada, E. S., and Sétamou, M. (2014). Quantitative distribution of *Candidatus Liberibacter asiaticus* in the aerial parts of the huanglongbing-infected citrus trees in Texas. *HortScience* 49, 65–68. doi: 10.21273/HORTSCI.49.1.65

Ladanyia, M. (2010). *Citrus Fruit: Biology, Technology and Evaluation*. Cambridge, MA: Academic Press.

Li, W., Hartung, J. S., and Levy, L. (2006). Quantitative real-time PCR for detection and identification of *Candidatus Liberibacter* species associated with citrus huanglongbing. *J. Microbiol. Methods* 66, 104–115. doi: 10.1016/j.mimet.2005.10.018

Li, W., Levy, L., and Hartung, J. S. (2009). Quantitative distribution of 'Candidatus Liberibacter asiaticus' in citrus plants with citrus huanglongbing. *Phytopathology* 99, 139–144. doi: 10.1094/PHYTO-99-2-0139

Lin, K. H. (1956). Observations on yellow shoot of citrus. *Acta Phytopathol. Sin.* 2, 1–11.

Louzada, E. S., Vazquez, O. E., Braswell, W. E., Yanev, G., Devanaboina, M., and Kunta, M. (2016). Distribution of '*Candidatus Liberibacter asiaticus*' above and below ground in *Texas citrus*. *Phytopathology* 106, 702–709. doi: 10.1094/PHYTO-01-16-0004-R

Mharti, F. Z., Lyoussi, B., and Abdellaoui, A. (2011). Antibacterial activity of the essential oils of *Pistacia lentiscus* used in Moroccan folkloric medicine. *Nat. Product Commun.* 6:1934578X1100601024. doi: 10.1177/1934578X1100601024

Nishimura, M. T., Stein, M., Hou, B. H., Vogel, J. P., Edwards, H., and Somerville, S. C. (2003). Loss of a callose synthase results in salicylic acid-dependent disease resistance. *Science* 301, 969–972. doi: 10.1126/science.1086716

Parker, J. E. (2003). Plant recognition of microbial patterns. *Trends Plant Sci.* 8, 245–247. doi: 10.1016/S1360-1385(03)00105-5

Radford, J. E., Vesk, M., and Overall, R. L. (1998). Callose deposition at plasmodesmata. *Protoplasma* 201, 30–37. doi: 10.1007/BF01280708

Rinne, P. L., and Schoot, C. V. D. (2003). Plasmodesmata at the crossroads between development, dormancy, and defense. *Can. J. Bot.* 81, 1182–1197. doi: 10.1139/b03-123

Roberts, A. (2003). Plasmodesmata, and the control of symplastic transport. *Plant Cell Environ.* 26, 103–124. doi: 10.1046/j.1365-3040.2003.00950.x

Rosenfeld, Y., and Shai, Y. (2006). Lipopolysaccharide (Endotoxin)-host defense antibacterial peptides interactions: role in bacterial resistance and prevention of sepsis. *Biochim. Biophys. Acta Biomembr.* 1758, 1513–1522. doi: 10.1016/j.bbamem.2006.05.017

Schneider, H. (1968). Anatomy of greening-diseased sweet orange shoots. *Phytopathology* 58, 1555–1160.

Tadeo, F. R., Terol, J., Rodrigo, M. J., Licciardello, C., and Sadka, A. (2020). "Fruit growth and development," in *The Genus Citrus*, eds M. Talon, M. Caruso, F. G. Gmitter (Sawston: Woodhead Publishing), 245–269.

Tatineni, S., Sagaram, U. S., Gowda, S., Robertson, C. J., Dawson, W. O., Iwanami, T., et al. (2008). In planta distribution of 'Candidatus Liberibacter asiaticus' as revealed by polymerase chain reaction (PCR) and real-time PCR. *Phytopathology* 98, 592–599. doi: 10.1094/PHYTO-98-5-0592

Teixeira, D., Saillard, C., Eveillard, S., Danet, J. L., da Costa, P. I., Ayres, A. J., et al. (2005). '*Candidatus Liberibacter americanus*', associated with citrus huanglongbing (greening disease) in São Paulo State. *Int. J. Syst. Evol. Microbiol.* 55, 1857–1862. doi: 10.1099/ijs.0.63677-0

Tian, Y. N., Ke, S., and Ke, C. (1996). Detection and quantitation of citrus huanglongbing pathogen by polymerase chain reaction. *Acta Phytopathol. Sin.* 26, 243–250.

Wainwright, M. (2001). Acridine–a neglected antibacterial chromophore. *J. Antimicrob. Chemother.* 47, 1–13. doi: 10.1093/jac/47.1.1

Wang, L., Feng, Z., Wang, X., Wang, X., and Zhang, X. (2010). DEGseq: an R package for identifying differentially expressed genes from RNA-seq data. *Bioinformatics* 26, 136–138. doi: 10.1093/bioinformatics/btp612

Wu, G. A., Prochnik, S., Jenkins, J., Salse, J., Hellsten, U., Murat, F., et al. (2014). Sequencing of diverse mandarin, pummelo and orange genomes reveals complex history of admixture during citrus domestication. *Nat. Biotechnol.* 32, 656–662. doi: 10.1038/nbt.2906

Xie, C., Mao, X., Huang, J., Ding, Y., Wu, J., Dong, S., et al. (2011). KOBAS 2.0: a web server for annotation and identification of enriched pathways and diseases. *Nucleic Acids Res.* 39(Suppl._2), W316–W322. doi: 10.1093/nar/gkr483

Xu, M., Wu, P., Shen, F., Ji, J., and Rakesh, K. P. (2019). Chalcone derivatives and their antibacterial activities: current development. *Bioorg. Chem.* 91:103133. doi: 10.1016/j.bioorg.2019.103133

Young, M. D., Wakefield, M. J., Smyth, G. K., and Oshlack, A. (2010). Gene ontology analysis for RNA-seq: accounting for selection bias. *Genome Biol.* 11, 1–12. doi: 10.1186/gb-2010-11-2-r14

Yu, Z., An, B., Ramshaw, J. A., and Brodsky, B. (2014). Bacterial collagen-like proteins that form triple-helical structures. *J. Struct. Biol.* 186, 451–461.

Zhang, P., Guan, L., Liu, R., Pu, X., and Deng, X. (2011). Relationship between the "red nose" fruit of Shatangju tangerine with "*Candidatus Liberibacter asiaticus*". *Chin. J. Trop. Crop.* 32, 738–742.

Zheng, Z., Chen, J., and Deng, X. (2018). Historical perspectives, management, and current research of citrus HLB in Guangdong province of China, where the disease has been endemic for over a hundred years. *Phytopathology* 108, 1224–1236. doi: 10.1094/PHYTO-07-18-0255-IA

Zheng, Z., Xu, M., Bao, M., Wu, F., Chen, J., and Deng, X. (2016). Unusual five copies and dual forms of nrdB in "*Candidatus Liberibacter asiaticus*": biological implications and PCR detection application. *Sci. Rep.* 6:39020. doi: 10.1038/srep39020

Conflict of Interest: The authors declare that the research was conducted in the absence of any commercial or financial relationships that could be construed as a potential conflict of interest.

frontiers in Microbiology

ORIGINAL RESEARCH
published: 02 July 2021
doi: 10.3389/fmicb.2021.683481

Bacteriomic Analyses of Asian Citrus Psyllid and Citrus Samples Infected With "*Candidatus* Liberibacter asiaticus" in Southern California and Huanglongbing Management Implications

Jiaquan Huang[1,2], Zehan Dai[1], Zheng Zheng[1], Priscila A. da Silvia[3], Luci Kumagai[4], Qijun Xiang[5], Jianchi Chen[2] and Xiaoling Deng[1]**

[1] Laboratory of Citrus Huanglongbing Research, College of Plant Protection, South China Agricultural University, Guangzhou, China, [2] San Joaquin Valley Agricultural Sciences Center, Agricultural Research Service, United States Department of Agriculture, Parlier, CA, United States, [3] Fundo de Defesa da Citricultura–Fundecitrus, Araraquara, Brazil, [4] Plant Pest Diagnostic Center, California Department of Food and Agriculture, Sacramento, CA, United States, [5] Jerry Dimitman Laboratory, Riverside, CA, United States

OPEN ACCESS

Edited by:
Kranthi Kiran Mandadi, Texas A&M University, United States

Reviewed by:
Monica Rosenblueth, National Autonomous University of Mexico, Mexico
Madhurababu Kunta, Texas A&M University Kingsville, United States

***Correspondence:**
Jianchi Chen
Jianchi.chen@usda.gov
Xiaoling Deng
xldeng@scau.edu.cn

Specialty section:
This article was submitted to Microbe and Virus Interactions with Plants, a section of the journal Frontiers in Microbiology

Received: 21 March 2021
Accepted: 17 May 2021
Published: 02 July 2021

Citation:
Huang J, Dai Z, Zheng Z, da Silvia PA, Kumagai L, Xiang Q, Chen J and Deng X (2021) Bacteriomic Analyses of Asian Citrus Psyllid and Citrus Samples Infected With "Candidatus Liberibacter asiaticus" in Southern California and Huanglongbing Management Implications. Front. Microbiol. 12:683481. doi: 10.3389/fmicb.2021.683481

Citrus Huanglongbing (HLB; yellow shoot disease) is associated with an unculturable α-proteobacterium "*Candidatus* Liberibacter asiaticus" (CLas). HLB was found in southern California in 2012, and the current management strategy is based on suppression of the Asian citrus psyllid (*Diaphorina citri*) that transmits CLas and removal of confirmed CLas-positive trees. Little is known about Asian citrus psyllid-associated bacteria and citrus-associated bacteria in the HLB system. Such information is important in HLB management, particularly for accurate detection of CLas. Recent advancements in next-generation sequencing technology provide new opportunities to study HLB through genomic DNA sequence analyses (metagenomics). In this study, HLB-related bacteria in Asian citrus psyllid and citrus (represented by leaf midrib tissues) samples from southern California were analyzed. A metagenomic pipeline was developed to serve as a prototype for future bacteriomic research. This pipeline included steps of next-generation sequencing in Illumina platform, *de novo* assembly of Illumina reads, sequence classification using the Kaiju tool, acquisition of bacterial draft genome sequences, and taxonomic validation and diversity evaluation using average nucleotide identity. The identified bacteria in Asian citrus psyllids and citrus together included *Bradyrhizobium*, *Buchnera*, *Burkholderia*, "*Candidatus* Profftella armature," "*Candidatus* Carsonella ruddii," CLas, *Mesorhizobium*, *Paraburkholderia*, *Pseudomonas*, and *Wolbachia*. The whole genome of a CLas strain recently found in San Bernardino County was sequenced and classified into prophage typing group

1 (PTG-1), one of the five known CLas groups in California. Based on sequence similarity, *Bradyrhizobium* and *Mesorhizobium* were identified as possible source that could interfere with CLas detection using the 16S rRNA gene-based PCR commonly used for HLB diagnosis, particularly at low or zero CLas titer situation.

Keywords: "*Candidatus* Liberibacter asiaticus", *Diaphorina citri*, metagenomic, bacteriomic, bacteriobiomic, HLB management, endosymbionts, endophytes

INTRODUCTION

Citrus Huanglongbing (HLB; yellow shoot disease) is a highly destructive disease associated with a non-culturable α-proteobacterium, "*Candidatus* Liberibacter asiaticus" (CLas) (Jagoueix et al., 1994). Under field condition, CLas is transmitted by Asian citrus psyllid (ACP; *Diaphorina citri*) (Bové, 2006). In California, CLas was first detected in both ACP and citrus plants in 2012 in a residential area of the city of Hacienda Heights (Kumagai et al., 2013). Since then, CLas has been found in multiple residential areas, but not in citrus production fields despite active detection efforts, in southern California. As of the start of this project, the most recent CLas detection in both ACP and citrus was from San Bernardino county. To facilitate HLB research, selected genomes of CLas strains from California have been sequenced (Zheng et al., 2014a; Wu et al., 2015b; Dai et al., 2019). A prophage typing group (PTG) system that differentiates CLas strains in California has been established (Zheng et al., 2017; Dai et al., 2019).

Like other insects and plants, ACP and citrus also host microorganisms (microbiome, or bacteriome/bacteriobiome when bacteria are the focus). Examples of well-known ACP-associated bacteria (AABacts) are symbiotic "*Candidatus* Carsonella ruddii" and "*Candidatus* Profftella armature." Both provide critical amino acids for ACP growth and development. Whole-genome sequences of these two symbionts have been published (Nakabachi et al., 2013; Wu et al., 2015a). Similarly, citrus-associated bacteria (CABacts) were also reported (Blaustein et al., 2017; Ginnan et al., 2018). CABacts identified after surface sterilization are referred to as endophytes, e.g., *Pantoea*, *Bacillus*, and *Curtobacterium* (Blacutt et al., 2020). The biological roles of most endophytic bacteria vary from beneficial to detrimental (Lodewyckx et al., 2002).

Recently, there has been increasing interests in research related on bacteriomes/microbiomes of plant diseases that could provide useful information for disease management. For example, grape Pierce's disease (PD), caused by *Xylella fastidiosa* in California, was found to be effectively controlled by the inoculation of a bacterial endophyte, *Paraburkholderia phytofirmans* (Baccari et al., 2019). Strains of *Burkholderia* in citrus roots could trigger expression of disease-resistant genes (Zhang et al., 2017). CABacts were suspected to interfere with reliable detection of CLas with the commonly used TaqMan PCR protocol (HLBaspr-PCR, Li et al., 2006), particularly when samples contain a low titer of CLas (Ct value > 30) or no CLas (Shin et al., 2018; Bao et al., 2020).

Traditionally, plant bacteriome research utilized *in vitro* cultivation methodology. The use of next-generation sequencing (NGS) technology has extended the research to unculturable or not-yet-culturable bacteria. Studies on the microbiome associated with disease tissue begin with DNA extraction from pathogen-infected samples. The DNA is sequenced through an NGS platform such as Illumina to generate millions of short reads of 50–350 bp. Bacterial operational taxonomic units (OTUs) are created and tentatively named according to GenBank taxonomy. Typically, metagenomic programs such as Kaiju (Menzel et al., 2016), Kraken 2 (Wood et al., 2019), and MetaWRAP (Uritskiy et al., 2018) are used to assist the classification process.

It is also noted that mitochondria and chloroplasts are of prokaryotic origins and occur in high abundance (high copy number). Both mitochondria and chloroplasts have their own DNA genomes and could serve as sequence analysis controls in metagenomic experiments. Chloroplast DNA had a strong influence on CLas whole-genome assembly using Illumina MiSeq data (Zheng et al., 2014b). A metagenomic study of grape PD leaf samples revealed that chloroplast DNA was commonly found in putative bacterial reads (Van Horn et al., 2019). Filtering potential interfering sequences in an NGS data set before metagenomic analysis would improve the accuracy of sequence taxonomic classifications (Zhang et al., 2017).

This study explored the use of metagenomic technology to characterize the bacteriomes of HLB-associated ACP and citrus leaf samples collected from southern California. The objectives were as follows: (1) to establish a metagenomic pipeline to identify AABacts and CABacts and extract their draft genome sequences without chloroplast and/or mitochondrial sequence contamination, and the draft genome sequences were further cross-checked using GenBank bacterial whole-genome sequence database; (2) to evaluate the taxonomy status and diversity of AABacts and CABacts among the California samples collected from residential areas in southern California using average nucleotide identity (ANI) values, the current standard for bacterial species definition utilizing whole-genome sequences; and (3) to search for genome sequence evidence in AABacts and CABacts that could impact HLBaspr-PCR detection of CLas.

MATERIALS AND METHODS

Asian Citrus Psyllid and Citrus DNA Samples

Asian citrus psyllid and citrus plant samples were collected from three geographically adjacent counties in southern California (**Table 1**). Collecting sites were in residential areas. Samples were collected by the California Department of Food and Agriculture

or the California Citrus Research Board. DNA was extracted from individual ACP adults or citrus leaf midribs using the Qiagen MagAttract 96 DNA plant kit (QIAGEN Inc., Valencia, CA, United States) as described previously (Kumagai et al., 2013). The presence or absence of CLas in each sample was confirmed by HLBaspr-PCR targeting 16S rRNA gene (Li et al., 2006) and the PCR protocol targeting *nrdB* gene (Zheng et al., 2016), designated as RNRf-PCR.

As shown in **Table 1**, samples 1, 2, and 3 were from San Bernardino County, the most recent location where CLas was confirmed at the time this research started. Sample 1 (A-SBCA19) was used as the ACP model for metagenomic pipeline development. Similarly, sample 2 (C-SBCA19) was used as a citrus model. Both samples 1 and 2 were from the same citrus tree. Sample 3, 4, and 5 had high HLBaspr-PCR Ct values (>28); and sample 5 (A-TECA18) was confirmed to be CLas negative by RNR-PCR; samples 6 and 7 were sequenced previously (Dai et al., 2019) but were used in this study as an ACP–citrus pair (Orange county) for comparison; another ACP–citrus pair was samples 1 and 2 from a different location (San Bernardino county).

Development of Metagenomic Pipeline

Sample Preparation and Next-Generation Sequencing

Illumina sequencing (Illumina, Inc., San Diego, CA, United States) required > 1 μg of DNA. To meet this standard, 2–4 μl of sample DNA (mixture of bacteria + ACP or citrus hosts) was enlarged (i.e., increased all DNA simultaneously) with GenomiPhi^{TM} V2 DNA Amplification kit (GE Healthcare, Sigma-Aldrich Corp., St. Louis, MO, United States) following manufacturer's instructions. The enlarged DNAs were sequenced by Illumina NextSeq or HiSeq formats (**Table 1**) through commercial sources. Only sequence reads with Q score > 30 were collected.

Acquiring Mitochondrial Genome (Mitogenome) and Chloroplast Genome Sequences

Illumina short reads were assembled into contigs (longer sequences) by MEGAHIT software version 1.1.2, a *de novo* assembler for metagenomics data (Li et al., 2016), with the default setting (–*k*-min = 21, –*k*-max = 99, –min-count = 2, –merge-level = 20, 0.98). MEGAHIT contigs of ACP mitogenome and citrus mitogenome and chloroplast genome were first identified by BLASTn (Camacho et al., 2009) search (identity > 95% and *e*-value > 1E-64) referenced to DQ864733.1 (citrus chloroplast genome, Bausher et al., 2006), NC_037463.1 (citrus mitogenome, Yu et al., 2018), and KY426014.1 (ACP mitogenome, Wu et al., 2017). Sample mitogenome and chloroplast genome sequences were then collected using the criteria of >99% identity and >200 bp in alignment length.

Filtering Sequences of Host Mitochondria, Chloroplasts, and Chromosomes

Illumina short reads of each ACP or citrus samples were filtered using Bowtie 2 software (Langmead and Salzberg, 2012) to remove sequences of host mitochondria, chloroplasts, and chromosomes. For mitochondrial and chloroplast DNA filtering, the corresponding sequences acquired as mentioned above were used as references. For host chromosomal DNA filtering, the ACP whole genome (Diaci V3 with the removal of No. 9 chromosomal scaffold containing bacterial symbiont sequences, available in https://citrusgreening.org/, Hosmani et al., 2019), *Citrus sinensis* genome (AJPS00000000.1, Xu et al., 2013), and *Citrus clementine* genome (AMZM00000000.1, Wu et al., 2014) were used as references. The filtered reads of each ACP and citrus samples were assembled in contigs by MEGAHIT software version 1.1.2, with the default setting mentioned above.

Acquisition of Asian Citrus Psyllid-Associated Bacteria and Citrus-Associated Bacteria Draft Genome Sequences

The filtered MEGAHIT contigs of each sample were classified by the Kaiju program using greedy mode (-a greedy -e 2 -m 20 -E 1E-5) against the bacterial RefSeq database (version 94). The classified contigs were collected according to the proposed OTUs at the genus level. The sequences were considered as the draft genome sequence version 1. The final version was generated after validation and removal of redundant sequences using CD-HITest at identity cutoff of 95% and coverage threshold of 0.0 (Huang et al., 2010).

Draft Genome Sequence Evaluation

The bacterial nature of each contig in a draft genome version 1 was evaluated through standalone BLASTn search against the genome sequences of the corresponding bacterial genus in GenBank RefSeq database (version 99) with the following parameters: word size = 28, *e*-value = 1E-64, and cover length > 200 bp, with identity > 80%. For the non-BLASTn matched contigs, BLASTx search was further used since protein sequences were evolutionally more conserved. The BLASTx parameters were as follows: word size = 3, *e*-value = 1E-64, cover length > 30 amino acid, and similarity > 40%. All BLASTn and BLASTx confirmed contigs were collected as the final version of the draft genome sequences. Assessment metrics of draft genome sequences were obtained using QUAST version 16 (Gurevich et al., 2013).

Bacterial Taxonomy Evaluation

The Kaiju taxonomy assignments of each OTU were evaluated by calculating ANI (Konstantinidis and Tiedje, 2005) using program pyani version 0.1.3.2 (Pritchard et al., 2016) with fragment size of 500 bp. From each OTU (at genus level), the corresponding whole-genome sequences in GenBank RefSeq database were used for pairwise ANI calculations. Bacterial genome ANIs were also calculated among the seven ACP/citrus samples for inter-strain/inter-sample diversity evaluations. To estimate average nucleotide coverage (ANC), Illumina reads from each sample were mapped to the draft genome using BBMAP program[1].

Characterization of "*Candidatus* Liberibacter asiaticus" Strains

The draft genome sequences of all CLas strains were characterized following the outline of Dai et al. (2019), which

[1]http://sourceforge.net/projects/bbmap

TABLE 1 | General information and selected metrics of next-generation sequencing data of Asian citrus psyllid (ACP) and citrus leaf DNA samples from southern California, United States.

No.	Sample	County	Host	Year of collection	Sequencing format	Read length (bp)	Total reads/total length (bp)	CLas Ct value[a]	References
1	A-SBCA19	San Bernardino	ACP	2019	NextSeq 500 1 × 75	35–85	507,362,298/ 43,125,795,330	23.39	This study
2	C-SBCA19	San Bernardino	Citrus	2019	NextSeq 500 1 × 75	35–85	468,054,578/ 39,784,639,130	26.78	This study
3	A-SBCA18	San Bernardino	ACP	2018	HiSeq 3000 2 × 100	101	482,412,866/ 48,723,699,466	28.62	This study
4	A-RSCA17	Riverside	ACP	2017	HiSeq 3000 2 × 100	101	471,308,572/ 47,602,165,772	29.80	This study
5	A-TECA18	Riverside	ACP	2018	HiSeq 3000 2 × 100	101	366,175,592/ 36,983,734,792	36.81	This study
6	A-AHCA17	Orange	ACP	2017	HiSeq 3000 2 × 150	150	611,118,478/ 91,667,771,700	23.31	Dai et al. (2019)
7	C-AHCA17	Orange	Citrus	2017	HiSeq 3000 2 × 100	101	593,133,332/ 59,906,466,532	27.52	Dai et al. (2019)

Note Ct was obtained according to HLBaspr-PCR (Li et al., 2006).
[a]*CLas, "Candidatus Liberibacter asiaticus."*

included prophage typing, and descriptions of loci *terL* (phage DNA terminase large subunit, Deng et al., 2014), *trn* (tandem repeat number at open reading frame CLIBASIA_01645, Chen et al., 2010), and miniature inverted-repeat transposable elements (MITEs; Wang et al., 2013). To detect the circularity of prophage sequence, the method of Zheng et al. (2018) involving identification of related *de novo* contigs and read walking (Shih et al., 2019) was used.

CLas strain A-SBCA19 was further used to acquire a more complete whole-genome sequence on top of the draft genome sequence from the Kaiju collection of MEGAHIT contigs. The process primarily combined the assemblies of reference-mapping and *de novo* assembly of both NextSeq data (**Table 1**) and the data from an additional Illumina sequencing (HiSeq 2000, a total of 20 Gbp) as reported previously (Wu et al., 2015b; Zheng et al., 2017). The improved A-SBCA19 genome sequence was annotated using RAST webserver (Aziz et al., 2008).

In Silico Investigation of Asian Citrus Psyllid-Associated Bacteria and Citrus-Associated Bacteria Sequences Related to HLBaspr-PCR

Because *Bradyrhizobium* and *Mesorhizobium* were detected in all ACP samples by Kaiju analysis, which by design focused on protein coding sequences, rRNA gene sequences might not be included in the draft genome. As a correction effort, the 16S rRNA gene sequences of *Mesorhizobium terrae* str. NIBRBAC000500504 (NZ_CP044218.1) and *Bradyrhizobium* SK17 (NZ_CP025113.1) that had the highest ANI values in A-SBCA19 sample were downloaded from GenBank database and used as references for bowtie 2 mapping with sensitive parameter (-D 15 -R 2 -N 0 -L 22 -i S,1,1.15) using Illumina short reads of each sample. Reads similar to HLBas/HLBp/HLBr region were identified, assembled, and aligned with manual justifications.

TaqMan PCR Procedures

TaqMan PCR was performed on an Applied Biosystems Step One Plus Real-Time PCR System. PCR was performed in 20-μl volume reactions consisting of the following reagent: 10 μl of Fast Universal PCR Master Mix (2×) (Applied Biosystems, Foster City, CA, United States), 1 μl of DNA template (25 ng), 0.2 μl of TaqMan probe (5 μM), and 0.4 μl of each forward and reverse primer (10 μM). The primer/probe sets were HLBas/HLBp/HLBr (Li et al., 2006) and RNR1f/RNRp/RNR1r (Zheng et al., 2016). The standard amplification procedure started at 95°C for 20 s, following by 40 cycles at 95°C for 10 s and 60°C for 20 s. The fluorescence signal was captured at the end of each 60°C step. The data were analyzed in Step One plus software (version 2.3, Applied Biosystems).

RESULTS

A total of seven sets of Illumina sequencing data ranging from 36 to 91 Gbp were collected (**Table 1**). Each data set was considered as a pro-metagenome for further analyses to generate a set of bacterial draft genome sequences (bacteriome). With the NextSeq data from sample A-SBCA19 (representing ACP) and the NextSeq data from C-SBCA19 (representing citrus), a pipeline from DNA preparation to acquisition of draft bacterial genome sequences was presented in **Table 2**. The pipeline was used to acquire bacterial draft genome sequences from the other five data sets/pro-metagenomes, i.e., A-SBCA18, A-RSCA17, A-TECA18, A-AHCA17, and C-AHCA17.

Ten bacterial genera were selected based on the contigs abundance from Kaiju classification results to describe the seven bacteriomes (i.e., seven samples) (**Figure 1**). These were *Bradyrhizobium*, *Buchnera*, *Burkholderia*, "*Ca*. Carsonella ruddii," CLas, "*Ca*. Profftella armature," *Mesorhizobium*, *Paraburkholderia*, *Pseudomonas*, and *Wolbachia*. The five ACP bacteriomes had all 10 bacteria. The two citrus bacteriomes had

TABLE 2 | A pipeline to acquire draft genome sequences of ACP-associated bacteria (AABacts; represented by sample A-SBCA19) and citrus-associated bacteria (CABacts; represented by sample C-SBCA19).

Step	Action	Results
1	Extraction of ACP/citrus midrib DNA and MDA amplification	DNA preparation
2	High throughput sequencing (Illumina HiSeq, NextSeq)	Short reads
3	Filtering short reads using Bowtie 2 with (1) ACP mitogenome and whole-genome sequences (2) Citrus chloroplast genome, mitogenome, whole-genome sequences	Presumably AABacts or CABacts enriched short reads
4	*De novo* assembly using MEGAHIT software	Presumably AABacts or CABacts long contigs (MEGAHIT contigs)
5	Kaiju taxonomic classification of MEGAHIT contigs referenced to GenBank Refseq database	Operational taxonomic units (OTUs) with GenBank taxonomy to genus level
6	Extraction of Kaiju contigs from each OTU	Version 1 of draft bacterial genome sequences
7	Validation of sequences in draft genome sequence version 1 using BLASTn and BLASTx against corresponding bacterial whole-genome sequences in GenBank RefSeq database	Final version of draft bacterial genome sequences
8.	Calculation of average nucleotide identity (ANI) between the final version of draft genome sequences and the whole-genome sequences of the corresponding bacterial genus in GenBank RefSeq database	Taxonomic conclusion of AABacts and CABacts

Note Computer scripts are available at request.

only four bacteria: CLas, *Burkholderia*, *Bradyrhizobium*, and *Pseudomonas* (**Figure 2**).

The final versions of draft genome sequences of all AABacts and CABacts are shown in **Supplementary Table 1**. The mitogenome and chloroplast genome sequences are shown in **Supplementary Table 2**. **Figure 2** graphically summarizes the data in **Supplementary Tables 1**, **2**. Each draft genome was described by five metrics: draft genome size (DGS), RC% (percentage of DGS/Reference genome size), Total contig in number, N50 in bp, and ANC. RC% provided an estimate of a genome completeness related to the arbitrarily selected reference genome. Noted that no CLas sequences was detected in A-TECA18 (Ct = 36.81). *Buchnera* was found only in A-SBCA19.

Pairwise ANI comparisons of mitogenomes and chloroplast genomes are shown in **Figure 3A**. ANIs of all ACP mitogenomes were >99.00. Similarly, the two citrus samples showed a high degree of relatedness in their mitogenomes and chloroplast genomes (ANI > 99.00). ANIs of CLas and ACP endosymbionts are shown in **Figure 3B**. The ANIs were all >99.00, confirming the species status of these bacteria from different samples. The genome sequences of ACP endosymbionts have been deposited in the National Center for Biotechnology Information (NCBI) with GenBank accession numbers listed in **Supplementary Table 1**.

In contrast, pairwise ANI values of the five AABacts and CABacts revealed significant inter-strain/inter-sample variations (**Figure 4**). For all the five bacteria genera from different samples, many ANIs were below the species threshold of 95, suggesting the presence of different species, or even different genera. An ANI of 0.00 represented that the draft genomes are too small to compare or ANI < 70, the program threshold. For the convenience of discussion, these bacteria were named only by the genus names, i.e., *Bradyrhizobium*, *Burkholderia*, *Mesorhizobium*, *Paraburkholderia*, and *Pseudomonas*. The draft genome sequences of these bacteria and the single sample *Buchnera* have been deposited in NCBI and identified by contig numbers under a common GenBank accession number for each bacteriome (**Supplementary Table 1**).

Table 3 summarizes the analyses on prophage typing and variations of CLas strains at the selected loci (*terL*, MITE, and *trn*). The final draft genome of CLas strain A-SBCA19 was 1,186,882 bp (81 contigs) with a Type 1 prophage that had no detected circular plasmid form. This recent CLas strain from San Bernardino County belonged to PTG-1, one of the five reported CLas groups in California (Dai et al., 2019). The genome sequence of CLas strain A-SBCA19 has been deposited in the NCBI under the GenBank accession number JADBIB000000000.1.

As shown in **Table 3**, Type 1 prophages were also detected in the other CLas strains. However, circular plasmid forms of the prophages were only detected in strain C-SBCA19 (38,221 bp) and A-AHCA17 (38,730 bp). In strain C-SBCA19, the CLas chromosomal sequence was partial (98,097 bp, RC% = 7.99), whereas in strain A-AHCA17, CLas chromosomal sequence was complete (1,222,637 bp, RC% = 99.10).

Sequences homologous to HLBas/HLBp/HLBr (primers/probe sequences) were detected in *Mesorhizobium* and *Bradyrhizobium*, in both selected reference genomes and draft genomes of AABacts (**Table 4**). Sequence comparisons showed that there existed nucleotide mismatches in HLBas and HLBr regions but none in HLBp region. Although not experimentally tested, it was believed that these *Mesorhizobium* and *Bradyrhizobium* sequences were similar enough to generate some level of DNA amplification in the HLBaspr-PCR, particularly in the absence of CLas and when the titers of *Mesorhizobium* and *Bradyrhizobium* were high.

DISCUSSION

We developed a metagenomic pipeline (**Table 2**) and used it to identify and characterize 10 AABacts/CABacts at the draft whole-genome sequence level (**Figure 2**). This research is unique and an extension of the HLB metagenomic research based on a single *rrn* locus (Zhang et al., 2013; Kolora et al., 2015; Blaustein et al., 2017; Ginnan et al., 2018; Meng et al., 2019; Song et al., 2019). As anticipated, the metagenomic pipeline successfully assembled the sequences of ACP and citrus mitogenome, and citrus chloroplast genome (**Supplementary Table 2**). Similarly, genome sequences

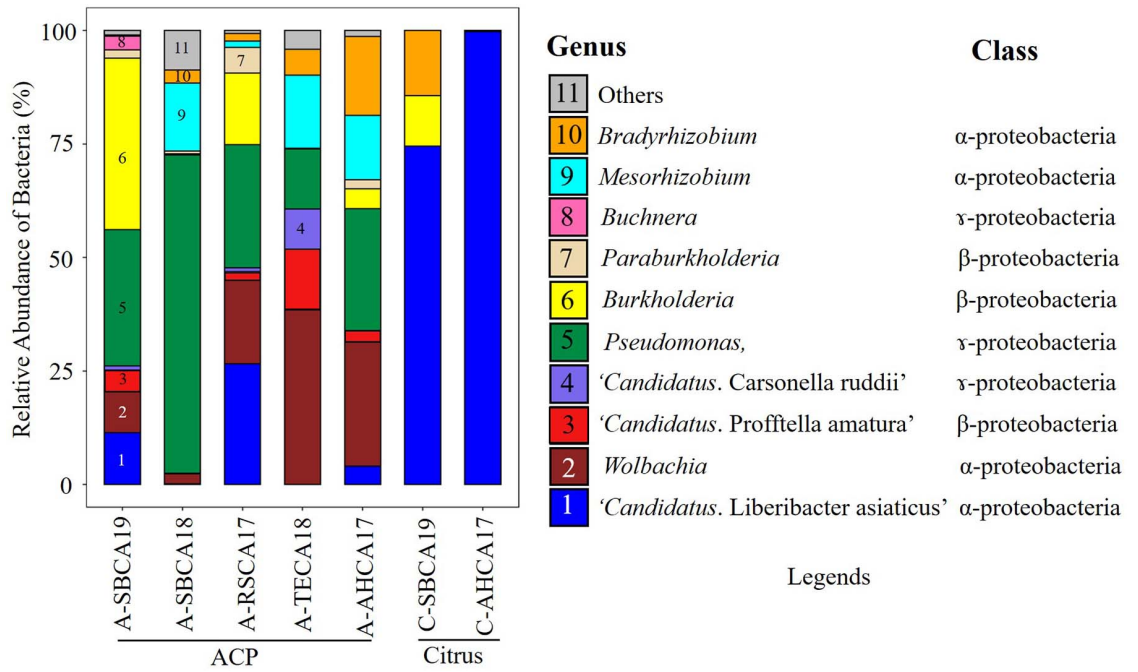

FIGURE 1 | Relative abundance of bacteria (%) in Asian citrus psyllid (ACP)/citrus samples from southern California. The relative abundance was calculated based on the Kaiju classification of top 10 ranked genera from *de novo* assembled (MEGAHIT) contigs filtered by mitogenome, chloroplast genome (citrus only), and host genome. Bacterial names were coded with colors and numbers along with their class and shown in legends.

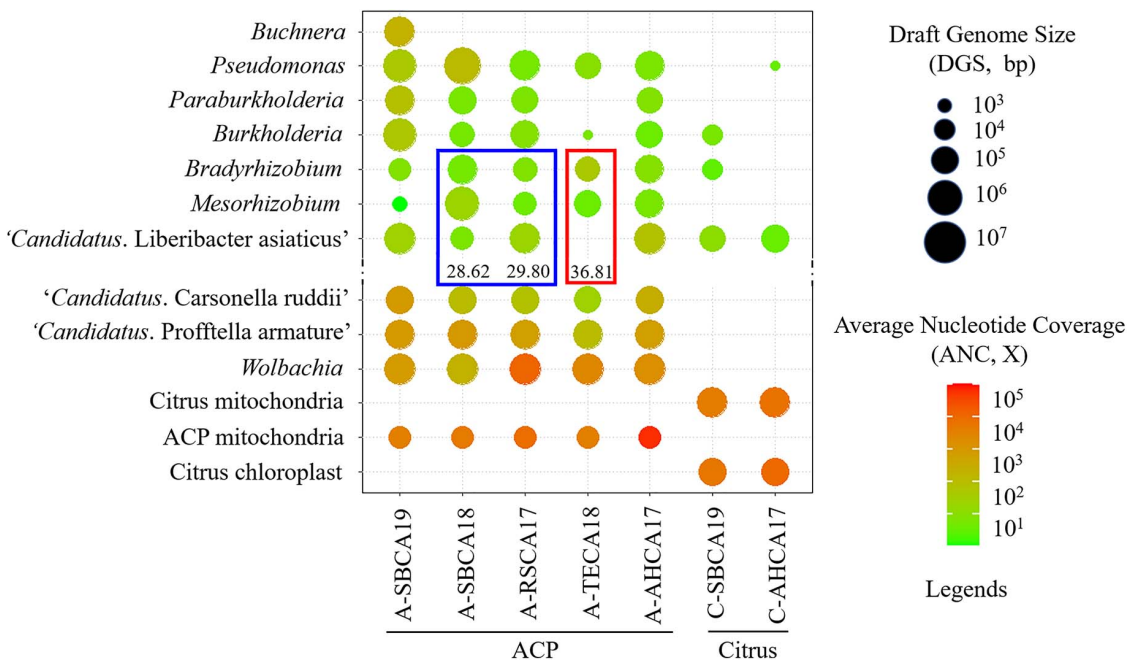

FIGURE 2 | Graphical representation of draft genomes of ACP-associated bacteria (AABacts) and citrus-associated bacteria (CABacts) as listed in **Supplementary Tables 1**, **2**. Draft genome size (DGS) is coded by circle sizes; average nucleotide coverage (ANC) is coded by colors. The blue box highlights the comparison of three bacteria in two samples with "*Candidatus* Liberibacter asiaticus" (CLas) in TaqMan HLBaspr-PCR Ct values near 30. The red box highlights the comparison of three bacteria in a single sample where CLas was not detected but shows TaqMan HLBaspr-PCR Ct values.

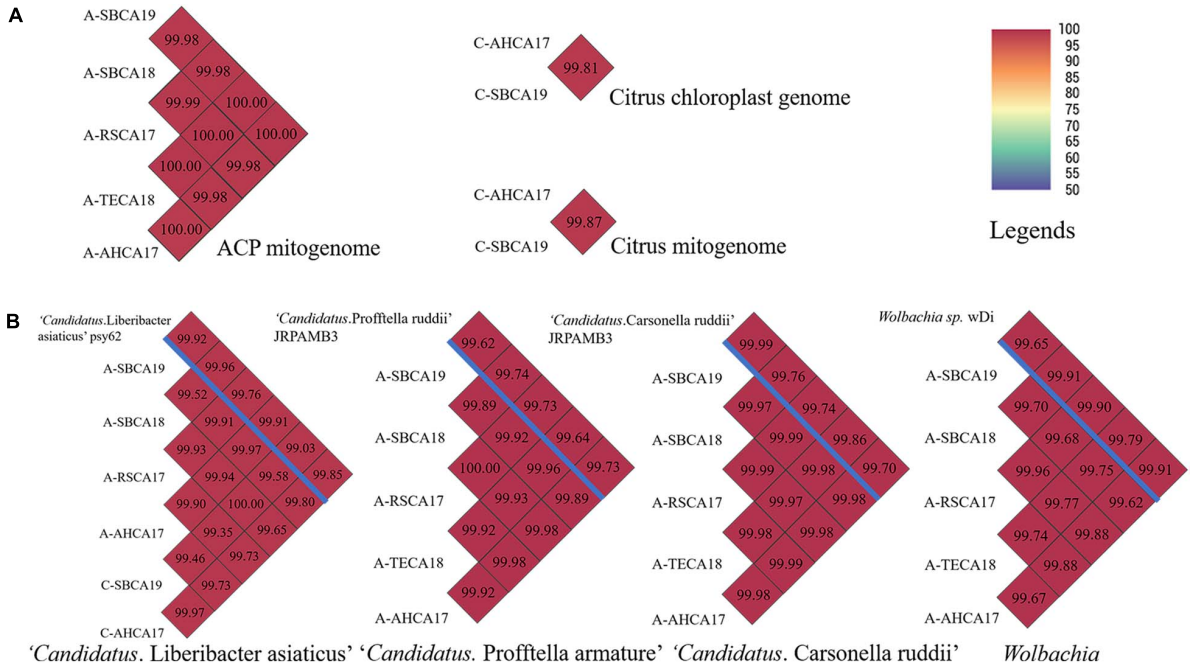

FIGURE 3 | Pairwise average nucleotide identity (ANI) comparisons of **(A)** mitogenomes of ACP samples and mitogenome and chloroplast genome of citrus samples and **(B)** draft genomes of "*Candidatus* Liberibacter asiaticus," "*Candidatus* Profftella armature," "*Candidatus* Carsonella ruddii," and *Wolbachia*, from ACP and citrus samples from southern California. Draft genome sizes were listed in **Supplementary Tables 1**, **2**. **(B)** Reference genomes were listed above the blue bar. ANI values were also coded in color as explained in the legends. ANI was calculated based on fragment size of 500 bp.

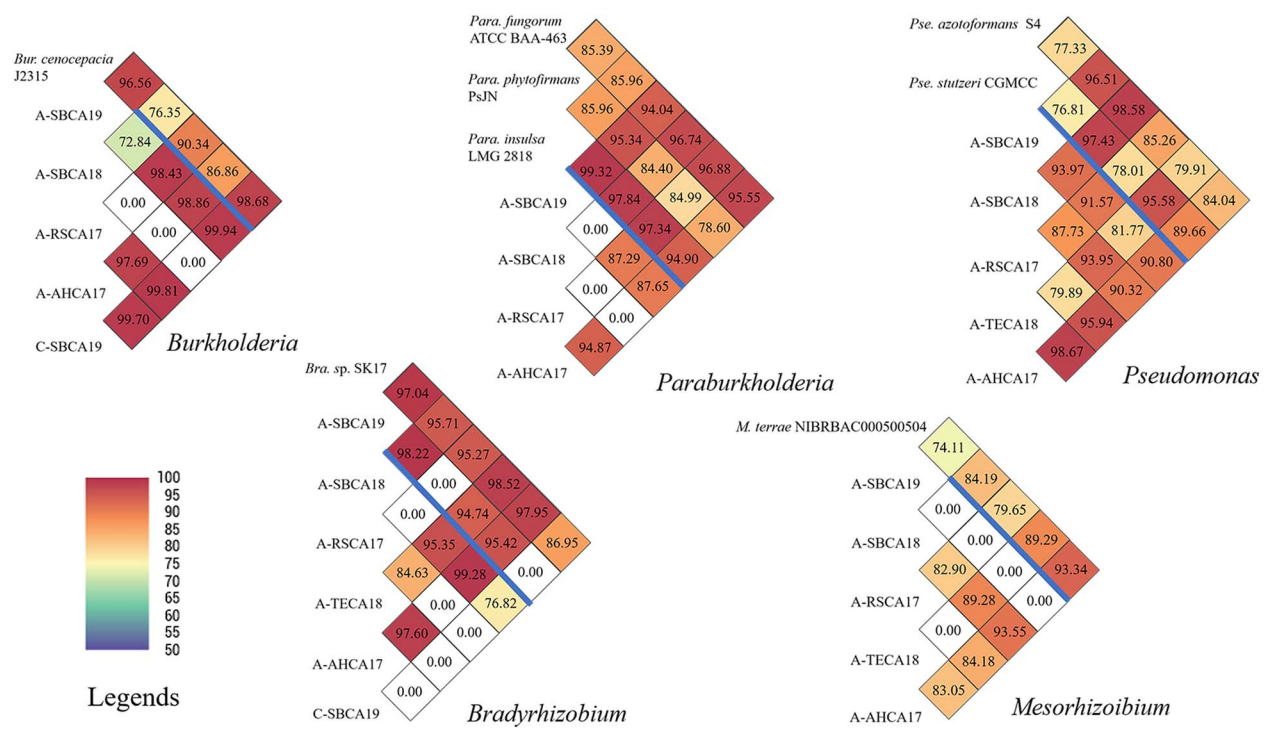

FIGURE 4 | Pairwise ANI comparisons of draft genomes of *Burkholderia*, *Paraburkholderia*, *Pseudomonas*, *Bradyrhizobium*, and *Mesorhizobium* strains from ACP and citrus leaf samples from southern California. Draft genome sizes are listed in **Supplementary Table 2**. Reference genomes are listed above the blue bar. ANI values are also coded in color as explained in the legends. ANI was calculated based on fragment size of 500 bp.

TABLE 3 | Genomic characterization and comparisons of "*Candidatus* Liberibacter asiaticus" (CLas) strains from ACP or citrus samples collected from three counties in southern California.

CLas strain	CLas draft genome size (bp)/contigs/N50	PTG (prophage type group)/prophage sequence (bp)/circularity	*terL* group	MITE type	*trn* type (repeat number)	References
San Bernardino county						
A-SBCA19	1,186,882/81/27,492	1/33,553/no	Asiatic	B1	<10 (6)	This study
C-SBCA19	349,326/959/338	1/38, 221/yes	Asiatic	A, B2	Not found	This study
A-SBCA18	173,412/1,229/106	1/6,886/no	Asiatic	Not found	Not found	This study
Riverside county						
A-RSCA17	964,918/705/5,117	1/37,300/no	Asiatic	A, B2	<10 (8)	This study
A-TECA18	CLas not detected	Not applied	Not applied	Not applied	Not applied	This study
Orange county						
A-AHCA17	1,229,739/1/1,229,739	1/38,730/yes	Asiatic	B1	<10 (7)	Dai et al. (2019)
C-AHCA17	925,768/3,696/286	1/22,589/no	Asiatic	B1	<10 (8)	Dai et al. (2019)

TABLE 4 | Nucleotide sequence comparisons of HLBas/HLBp/HLBr locus among CLas strain A4, *Bradyrhizobium* and *Mesorhizobium* strains shown in **Figure 2**, and representative strains of *Mesorhizobium terrae* str. NIBRBAC000500504 and *Bradyrhizobium* sp. SK17.

Bacterial strain/ GenBank accession[a]	Contig/start position	Sequence alignments[b]		
		HLBas	HLBp	HLBr
		TCGAGCGCGTATGC-AATACG	AGACGGGTGAGTAACGCG	CTACCTTTTTCTACGGGATAACGC
CLas strain A4, NZ_CP010804.2	1/780,114	**TCGAGCGCGTATGCGAATACG** AGCGG**C** **AGACGGGTGAGTAACGCG** TAGGAAT **CTACCTTTTTCTACGGGATAACGC**		
Mesorhizobium:				
***M. terrae* NIB RBAC000500504 NZ_CP044218.1**	1/2,495,405	**TCGAGCGCCC-CGC-AAGGGG** AGCGGC **AGACGGGTGAGTAACGCG** TGGGAAT **CTACCCATCACTACGGAACAACTC**		
A-SBCA19	SBCA19_ k103_233/32	**TCGAGCGCCC-CGC-AAGGGG** AGCGGC **AGACGGGTGAGTAACGCG** TGGGAAT **CTAC**– – – – – – – – – – – – – – – – – –		
A-SBCA18	SBCA18_ k119_600859/ 366	**TCGAGCGCCC-CGC-AAGGGG** AGCGGC **AGACGGGTGAGTAACGCG** TGGGAAT **CTACCCATCACTACGGAACAACTC**		
A-RSCA17		Not found		
A-TECA18	TECA18_ k141_392/63	**TCGAGCGCCC-CGC-AAGGGG** AGCGGC **AGACGGGTGAGTAA** –		
A-AHCA17	AHCA17_ k141_180833/ 630	**TCGAGCGCCC-CGC-AAGGGG** AGCGGC **AGACGGGTGAGTAACGCG** TGGGAAT **CTACCCATCACTACGGAACAACTC**		
Bradyrhizobium:				
***Bra. sp.* SK17 NZ_CP025113.1**	1/2,489,490	**TCGAGCGGGCATAGCAATATG** TCAGCGGC **AGACGGGTGAGTAACGCG** TGGGAAC **GTACCTTTTGGTTCGGAACAACTG**		
A-SBCA19		Not found		
A-SBCA18	SBCA18_ k119_230/39	**TCGAGCGGGCATAGCAATATG** TCAGCGGC **AGACGGGTGAGTAACGCG** TGGGAAC **GTACCTTTT** – – – – – – – – – – – –		
A-RSCA17		Not found		
A-TECA18	TECA18_ k141_390/1	– **GACGGGTGAGTAACGCG** TGGGAAC **GTACCTTTTGGTTCGGAACAACTG**		
A-AHCA17		Not found		
C-SBCA19		Not found		

[a] *Gray shading highlights the reference strains.*
[b] *Yellow highlights are regions aligned with HLBas, HLBp, and HLBr. Red letters indicate mismatched nucleotides.*

of ACP endosymbionts were effectively acquired with RC% mostly over 90 and the lowest at 55 (**Supplementary Table 2**). All these indicate the reliable performance of the metagenomic pipeline (**Table 2**).

Draft genome sequence analyses provided new information that facilitates our understanding of HLB biology and management. However, research challenges remain, particularly for the AABacts and CABacts that could only be named at the genus level (**Figure 2**), along with their significant sequence variations to reference genomes and among different samples (**Figure 4**).

Burkholderia

To our knowledge, *Burkholderia* has not been identified in ACP. The biological role of this bacterium is not clear. The bacterium has been reported in citrus root samples (Trivedi et al., 2010; Zhang et al., 2017), and it may not be surprising to find them in leaves. The ACP strain (A-SBCA19) and the citrus strain (C-SBCA19), both from San Bernardino county, were highly similar (ANI = 99.94), suggesting that they were the same species or even the same strain. This implies that ACP might have acquired *Burkholderia* from the infected citrus tree in San Bernardino county.

Paraburkholderia

Similar to *Burkholderia*, *Paraburkholderia* has not been identified in ACP. Unlike the case of *Burkholderia*, *Paraburkholderia* was not detected in citrus sample C-SBCA19 or in C-AHCA17 (**Figure 2**). However, we could not exclude the possibility that the bacterial titer was too low to be detected by the technique used. The same explanation could be applied to the absence of *Paraburkholderia* in the ACP sample A-TECA18 (**Figure 2**). It is interesting that *Paraburkholderia* strain A-SBCA19 was highly similar to *Pa. phytofirmans* strain PsJN (ANI = 95.34, **Figure 4**). Strain PsJN showed its biocontrol capacity grape PD (Baccari et al., 2019).

Pseudomonas

All ACP samples had *Pseudomonas* bacteria in relatively high abundance (**Figure 2**). A 16S rRNA gene-based study identified *Pseudomonas* from an egg through all nymph stages of ACP in China (Meng et al., 2019). In this study, *Pseudomonas* was also detected in at least one citrus sample (C-AHCA17, **Figure 2**). An interesting observation was that, in ACP, an *in vitro* culture method detected *Pseudomonas putida*, yet the 16S rRNA gene-based 454 pyrosequencing approach did not reveal the presence of *Pseudomonas* (Kolora et al., 2015). It is noted that ACP sample A-SBCA18 had a very large DGS (>30 Mbp, **Figure 2** and **Supplementary Table 1**). This suggests that the sample could contain a mixture of significantly different *Pseudomonas* species. As shown in **Figure 4**, DGS of the A-SBCA18 *Pseudomonas* is highly similar to that of *Pseudomonas azotoformans* S4 (ANI = 98.58) and that of *Pseudomonas stutzeri* CGMCC (ANI = 97.43). However, *Pse. azotoformans* S4 and *Pse. stutzeri* CGMCC are significantly different (ANI = 77.33). The exact taxonomy details of these pseudomonads remain to be studied in the future.

The HLBaspr-PCR (Li et al., 2006) has widely been used in HLB diagnosis. It has long been suspected that some AABacts and CABacts could contribute to the high Ct values of the PCR results (Bao et al., 2020). Shin et al. (2018) isolated *Bradyrhizobium* from citrus roots and demonstrated that the bacterium interfered with HLBaspr-PCR. The detection of *Bradyrhizobium* and the closely related *Mesorhizobium* prompted us to investigate the nucleotide sequence evidence of HLBaspr-PCR interference.

Bradyrhizobium/Mesorhizobium

The roles of *Bradyrhizobium* and *Mesorhizobium* bacteria in ACP are not known. Current knowledge about these bacteria is mostly limited to their nitrogen-fixing capacity in plant roots (Sawada et al., 2003). Differences between CLas and *Bradyrhizobium*/*Mesorhizobium* at the HLBas/HLBp/HLBr locus are mainly nucleotide mismatches and deletions, eight in HLBas and seven in HLBr (**Table 4**). This level of mismatches would make *Bradyrhizobium*/*Mesorhizobium* DNA not as competitive as CLas DNA to serve as template for HLBaspr-PCR. Therefore, at high CLas titer sample, the influence on *Bradyrhizobium*/*Mesorhizobium* is minimal. However, in the absence of CLas (sample A-TECA18, red box in **Figure 2**), high Ct values (36.81) could be generated, which might be interpreted as false positives.

Another situation in which *Bradyrhizobium* and *Mesorhizobium* bacteria could impact HLBaspr-PCR is the reduction of Ct values when CLas titers are low. As shown in the blue box in **Figure 2** and **Supplementary Table 1**, A-SBCA18 had a lower Ct value (28.62) but smaller CLas DGS (19,674 bp), whereas, A-RSCA17 had a higher Ct value (29.80) but larger CLas DGS (799,019 bp). This could be explained by the higher level of *Mesorhizobium* DGS (5,990,225 bp) and *Bradyrhizobium* DGS (464,062 bp) in the A-SBCA18 sample than that in the A-RSCA17 sample (21,714 and 26,967 bp, respectively). Therefore, at low CLas titers (Ct values around 30 in this study), high titers of *Mesorhizobium* and *Bradyrhizobium* could inflate the true CLas titer using HLBaspr-PCR. Note that partial CLas genome assembly is associated with low CLas titer in a sample based on our past CLas genome sequencing experience.

Buchnera

Buchnera has never been reported in ACP. It was a surprise that the bacterium was detected and only detected in sample A-SBCA19. Among the 63 *Buchnera* whole-genome sequences in GenBank Refseq database (version 99), the highest ANI was 86.49 with *Buchnera aphidicola* str. Afa-UT1. The 16S rRNA gene sequence of A-SBCA19 *Buchnera* is 98.24% similar to that of *Bu. aphidicola* str. Afa-UT1 (**Supplementary Table 3**). Put together, the exact biological nature and even the origin of the A-SBCA19 *Buchnera* are not clear and deserve further investigation. Based on 16S rRNA gene sequence, Morrow et al. (2020) reported *Buchnera* in *Diaphorina communis*, as well as in other *Cacopsylla* species and *Cornopsylla rotundiconis*.

"Candidatus Liberibacter asiaticus"

All three San Bernardino county CLas strains from both citrus and ACP were in the PGT-1 group (Dai et al., 2019) (**Table 3**), suggesting that the San Bernardino strains were still part of the California/Asiatic CLas group. Of particular interest is citrus sample C-SBCA19, which had high plasmid titer (ANC = 20.00) but only partial CLas genome. Considering the lytic nature of Type 1 prophage (Zhang et al., 2011), it is assumed that sample C-SBCA19 could have been collected during the phage induced lytic stage of CLas, i.e., degraded CLas chromosomes and high number of phage particles (containing circular DNA molecules/plasmids).

In summary, a metagenomic pipeline was established for bacteriomic analysis of HLB related ACP and citrus samples from southern California. Ten bacteria including six previously unknown or little known AABacts/CABacts were identified based on draft whole-genome sequences. The whole genome of a CLas strain recently found in San Bernardino County was sequenced. Based on sequence similarity, presence of *Bradyrhizobium* and *Mesorhizobium* could be the source of interference in CLas detection using TaqMan HLBaspr-PCR, particularly at low or zero CLas titer situation.

DATA AVAILABILITY STATEMENT

The data presented in this study are deposited in the NCBI GenBank repository with Bioproject No. PRJNA704462 and No. PRJNA706130. Genome sequence accession numbers can be found in the article/ **Supplementary Material**.

AUTHOR CONTRIBUTIONS

JC, XD, and JH designed the project, conducted the data analysis, and wrote the manuscript. ZD, ZZ, and PS assisted in data analyses. LK and QX performed the samples collection and DNA preparation. All the authors contributed to the manuscript revision and read and approved the submitted version.

FUNDING

This work was supported in part by California Citrus Research Board (5300-188), the National Key Research and Development Program of China (2018YFD0201500), and Key-Area Research and Development Program of Guangdong Province (2019B020217003).

ACKNOWLEDGMENTS

We thank Y. Chavez for technical assistance. Any mention of trade names or commercial products in this publication is solely for the purpose of providing specific information and does not imply recommendation or endorsement by the US Department of Agriculture (USDA). USDA is an equal-opportunity employer. We thank USDA Forest Service International Programs for their administrative assistance.

SUPPLEMENTARY MATERIAL

The Supplementary Material for this article can be found online at: https://www.frontiersin.org/articles/10.3389/fmicb.2021.683481/full#supplementary-material

REFERENCES

Aziz, R. K., Bartels, D., Best, A. A., DeJongh, M., Disz, T., Edwards, R. A., et al. (2008). The RAST server: rapid annotations using subsystems technology. *BMC Genomics* 9:75. doi: 10.1186/1471-2164-9-75

Baccari, C., Antonova, E., and Lindow, S. (2019). Biological control of Pierce's disease of grape by an endophytic bacterium. *Phytopathology* 109, 248–256. doi: 10.1094/PHYTO-07-18-0245-FI

Bao, M., Zheng, Z., Sun, X., Chen, J., and Deng, X. (2020). Enhancing PCR capacity to detect '*Candidatus Liberibacter asiaticus*' utilizing whole genome sequence information. *Plant Dis.* 104, 527–532. doi: 10.1094/PDIS-05-19-0931-RE

Bausher, M. G., Singh, N. D., Lee, S. B., Jansen, R. K., and Daniell, H. (2006). The complete chloroplast genome sequence of *Citrus sinensis* (L.) Osbeck var 'Ridge Pineapple': organization and phylogenetic relationships to other angiosperms. *BMC Plant Biol.* 6:21. doi: 10.1186/1471-2229-6-21

Blacutt, A., Ginnan, N., Dang, T., Bodaghi, S., Vidalakis, G., Ruegger, P., et al. (2020). An in vitro pipeline for screening and selection of citrus-associated microbiota with potential anti - "*Candidatus Liberibacter asiaticus*" properties. *Appl. Environ. Microbiol.* 86:e02883. doi: 10.1128/AEM.02883-19

Blaustein, R. A., Lorca, G. L., Meyer, J. L., Gonzalez, C. F., and Teplitski, M. (2017). Defining the core citrus leaf-and root-associated microbiota: factors associated with community structure and implications for managing huanglongbing (citrus greening) disease. *Appl. Environ. Microbiol.* 83, e210–e217. doi: 10.1128/AEM.00210-17

Bové, J. M. (2006). *Huanglongbing*: a destructive, newly-emerging, century-old disease of citrus. *J. Plant Pathol.* 88, 7–37. doi: 10.4454/jpp.v88i1.828

Camacho, C., Coulouris, G., Avagyan, V., Ma, N., Papadopoulos, J., Bealer, K., et al. (2009). BLAST+: architecture and applications. *BMC Bioinf.* 10:421. doi: 10.1186/1471-2105-10-421

Chen, J., Deng, X., Sun, X., Jones, D., Irey, M., and Civerolo, E. (2010). Guangdong and florida populations of '*Candidatus Liberibacter asiaticus*' distinguished by a genomic locus with short tandem repeats. *Phytopathology* 100, 567–572. doi: 10.1094/PHYTO-100-6-0567

Dai, Z., Wu, F., Zheng, Z., Yokomi, R., Kumagai, L., Cai, W., et al. (2019). Prophage diversity of '*Candidatus Liberibacter asiaticus*' strains in California. *Phytopathology* 109, 551–559. doi: 10.1094/PHYTO-06-18-0185-R

Deng, X., Lopes, S., Wang, X., Sun, X., Jones, D., Irey, M., et al. (2014). Characterization of "*Candidatus Liberibacter asiaticus*" populations by double-locus analyses. *Curr. Microbiol.* 69, 554–560. doi: 10.1007/s00284-014-0621-9

Ginnan, N. A., Dang, T., Bodaghi, S., Ruegger, P. M., Peacock, B. B., McCollum, G., et al. (2018). Bacterial and fungal next generation sequencing datasets and metadata from citrus infected with '*Candidatus Liberibacter asiaticus*'. *Phytobiomes* 2, 64–70. doi: 10.1094/PBIOMES-08-17-0032-A

Gurevich, A., Saveliev, V., Vyahhi, N., and Tesler, G. (2013). QUAST: quality assessment tool for genome assemblies. *Bioinformatics* 29, 1072–1075. doi: 10.1093/bioinformatics/btt086

Hosmani, P. S., Flores-Gonzalez, M., Shippy, T., Vosburg, C., Massimino, C., Tank, W., et al. (2019). Chromosomal length reference assembly for *Diaphorina citri* using single-molecule sequencing and Hi-C proximity ligation with manually curated genes in developmental, structural and immune pathways. *Biorxiv* [Preprint] doi: 10.1101/869685 bioRxiv: 869685,

Huang, Y., Niu, B., Gao, Y., Fu, L., and Li, W. (2010). CD-HIT suite: a web server for clustering and comparing biological sequences. *Bioinformatics* 26, 680–682. doi: 10.1093/bioinformatics/btq003

Jagoueix, S., Bové, J. M., and Garnier, M. (1994). The phloem-limited bacterium of greening disease of citrus is a member of the alpha subdivision of the *Proteobacteria*. *Int. J. Syst. Bacteriol.* 44, 379–386. doi: 10.1099/00207713-44-3-379

Kolora, L. D., Powell, C. M., Hunter, W., Bextine, B., and Lauzon, C. R. (2015). Internal extracellular bacteria of *Diaphorina citri* Kuwayama (Hemiptera: Psyllidae), the Asian citrus psyllid. *Curr. Microbiol.* 70, 710–715. doi: 10.1007/s00284-015-0774-1

Konstantinidis, K. T., and Tiedje, J. M. (2005). Genomic insights that advance the species definition for prokaryotes. *Proc. Natl. Acad. Sci.* U.S.A. 102, 2567–2572.

Kumagai, L. B., LeVesque, C. S., Blomquist, C. L., Madishetty, K., Guo, Y., Woods, P. W., et al. (2013). First report of *Candidatus Liberibacter asiaticus* associated with citrus huanglongbing in California. *Plant Dis.* 97, 283–283. doi: 10.1094/PDIS-09-12-0845-PDN

Langmead, B., and Salzberg, S. L. (2012). Fast gapped-read alignment with bowtie 2. *Nat. Methods* 9:357. doi: 10.1038/nmeth.1923

Li, D., Luo, R., Liu, C., Leung, C., Ting, H., Sadakane, K., et al. (2016). MEGAHIT v1. 0: a fast and scalable metagenome assembler driven by advanced methodologies and community practices. *Methods* 102, 3–11. doi: 10.1016/j.ymeth.2016.02.020

Li, W., Hartung, J. S., and Levy, L. (2006). Quantitative real-time PCR for detection and identification of *Candidatus* Liberibacter species associated with citrus huanglongbing. *J. Microbiol. Methods* 66, 104–115. doi: 10.1016/j.mimet.2005.10.018

Lodewyckx, C., Vangronsveld, J., Porteous, F., Moore, E. R., Taghavi, S., Mezgeay, M., et al. (2002). Endophytic bacteria and their potential applications. *Crit. Rev. Plant Sci.* 21, 583–606. doi: 10.1080/0735-260291044377

Meng, L., Cheng, X., and Zhang, H. (2019). 16S rRNA gene sequencing reveals a shift in the microbiota of *Diaphorina citri* during the psyllid life cycle. *Front. Microbiol.* 10:1948. doi: 10.3389/fmicb.2019.01948

Menzel, P., Ng, K. L., and Krogh, A. (2016). Fast and sensitive taxonomic classification for metagenomics with Kaiju. *Nat. Commun.* 7:11257. doi: 10.1038/ncomms11257

Morrow, J. L., Om, N., Beattie, G. A., Chambers, G. A., Donovan, N. J., Liefting, L. W., et al. (2020). Characterization of the bacterial communities of psyllids associated with Rutaceae in Bhutan by high throughput sequencing. *BMC Microbiol.* 20:215. doi: 10.1186/s12866-020-01895-4

Nakabachi, A., Ueoka, R., Oshima, K., Teta, R., Mangoni, A., Gurgui, M., et al. (2013). Defensive bacteriome symbiont with a drastically reduced genome. *Curr. Biol.* 23, 1478–1484. doi: 10.1016/j.cub.2013.06.027

Pritchard, L., Glover, R. H., Humphris, S., Elphinstone, J. G., and Toth, I. K. (2016). Genomics and taxonomy in diagnostics for food security: soft-rotting enterobacterial plant pathogens. *Anal. Methods* 8, 12–24. doi: 10.1039/C5AY02550H

Sawada, H., Kuykendall, L. D., and Young, J. M. (2003). Changing concepts in the systematics of bacterial nitrogen-fixing legume symbionts. *J. Gen. Appl. Microbiol.* 49, 155–179. doi: 10.2323/jgam.49.155

Shih, H. T., Su, C. C., Chang, C. J., Vargas, S., Dai, Z., and Chen, J. (2019). Draft genome sequence of "*Candidatus* Sulcia muelleri" strain KPTW1 from Kolla paulula, a vector of *Xylella fastidiosa* causing Pierce's disease of grapevine in Taiwan. *Microbiol. Resour. Announc.* 8:e01347. doi: 10.1128/MRA.01347-18

Shin, K., and van Bruggen, A. H. (2018). *Bradyrhizobium* isolated from huanglongbing (HLB) affected citrus trees reacts positively with primers for '*Candidatus Liberibacter asiaticus*'. *Eur. J. Plant Pathol.* 151, 291–306.

Song, X. B., Peng, A. T., Ling, J. F., Cui, Y. P., Cheng, B. P., and Zhang, L. H. (2019). Composition and change in the microbiome of *Diaphorina citri* infected with *Candidatus Liberibacter asiaticus* in China. *Int. J. Trop. Insect Sci.* 39, 283–290. doi: 10.1007/s42690-019-00036-3

Trivedi, P., Duan, Y., and Wang, N. (2010). Huanglongbing, a systemic disease, restructures the bacterial community associated with citrus roots. *Appl. Environ. Microbiol.* 76, 3427–3436. doi: 10.1128/AEM.02901-09

Uritskiy, G. V., DiRuggiero, J., and Taylor, J. (2018). MetaWRAP—a flexible pipeline for genome-resolved metagenomic data analysis. *Microbiome* 6:158. doi: 10.1186/s40168-018-0541-1

Van Horn, C., Dai, Z., Sisterson, M., and Chen, J. (2019). Microbiomes of *Xylella fastidiosa* infected grapevine in California. *Am. Phytopathol. Soc. Abstr.* 109:S2.

Wang, X., Tan, J., Bai, Z., Su, H., Deng, X., Li, Z., et al. (2013). Detection and characterization of miniature inverted-repeat transposable elements in "*Candidatus Liberibacter asiaticus*". *J. Bacteriol.* 195, 3979–3986. doi: 10.1128/JB.00413-13

Wood, D. E., Lu, J., and Langmead, B. (2019). Improved metagenomic analysis with Kraken 2. *Genome Biol.* 20:257. doi: 10.1186/s13059-019-1891-0

Wu, F., Deng, X., Liang, G., Huang, J., Cen, Y., and Chen, J. (2015a). Whole-genome sequence of "*Candidatus* Profftella armatura" from *Diaphorina citri* in Guangdong, China. *Genome Announc.* 3:e1282. doi: 10.1128/genomeA.01282-15

Wu, F., Kumagai, L., Cen, Y., Chen, J., Wallis, C. M., Polek, M., et al. (2017). Analyses of mitogenome sequences revealed that Asian citrus psyllids (*Diaphorina citri*) from California were related to those from Florida. *Sci. Rep.* 7:10154. doi: 10.1038/s41598-017-10713-3

Wu, F., Kumagai, L., Liang, G., Deng, X., Zheng, Z., Keremane, M., et al. (2015b). Draft genome sequence of "*Candidatus Liberibacter asiaticus*" from a citrus tree in San Gabriel, California. *Genome Announc.* 3:e1508–e1515. doi: 10.1128/genomeA.01508-15

Wu, G. A., Prochnik, S., Jenkins, J., Salse, J., Hellsten, U., Murat, F., et al. (2014). Sequencing of diverse mandarin, pummelo and orange genomes reveals complex history of admixture during citrus domestication. *Nat. Biotechnol.* 32, 656–662. doi: 10.1038/nbt.2906

Xu, Q., Chen, L., Ruan, X., Chen, D., Zhu, A., Chen, C., et al. (2013). The draft genome of sweet orange (*Citrus sinensis*). *Nat. Genet.* 45:59. doi: 10.1038/ng.2472

Yu, F., Bi, C., Wang, X., Qian, X., and Ye, N. (2018). The complete mitochondrial genome of Citrus sinensis. *Mitochondrial DNA B Resour.* 3, 592–593. doi: 10.1080/23802359.2018

Zhang, M., Powell, C. A., Guo, Y., Benyon, L., and Duan, Y. (2013). Characterization of the microbial community structure in '*Candidatus Liberibacter asiaticus*'-infected citrus plants treated with antibiotics in the field. *BMC Microbiol.* 13:112. doi: 10.1186/1471-2180-13-112

Zhang, S., Flores-Cruz, Z., Zhou, L., Kang, B. H., Fleites, L. A., Gooch, M. D., et al. (2011). 'Ca. Liberibacter asiaticus' carries an excision plasmid prophage and a chromosomally integrated prophage that becomes lytic in plant infections. *Mol. Plant-Microbe Interact.* 24, 458–468. doi: 10.1094/MPMI-11-10-0256

Zhang, Y., Xu, J., Riera, N., Jin, T., Li, J., and Wang, N. (2017). Huanglongbing impairs the rhizosphere-to-rhizoplane enrichment process of the citrus root-associated microbiome. *Microbiome* 5:97. doi: 10.1186/s40168-017-0304-4

Zheng, Z., Bao, M., Wu, F., Van Horn, C., Chen, J., and Deng, X. (2018). A type 3 prophage of '*Candidatus Liberibacter asiaticus*' carrying a restriction-modification system. *Phytopathology* 108, 454–461. doi: 10.1094/PHYTO-08-17-0282-R

Zheng, Z., Deng, X., and Chen, J. (2014b). Whole-genome sequence of "*Candidatus Liberibacter asiaticus*" from Guangdong, China. *Genome Announc.* 2:e00273. doi: 10.1128/genomeA.00273-14

Zheng, Z., Deng, X., and Chen, J. (2014a). Draft genome sequence of "*Candidatus Liberibacter asiaticus*" from California. *Genome Announc.* 2:e00999. doi: 10.1128/genomeA.00999-1

Zheng, Z., Wu, F., Kumagai, L. Á, Polek, M., Deng, X., and Chen, J. (2017). Two '*Candidatus Liberibacter asiaticus*' strains recently found in California harbor different prophages. *Phytopathology* 107, 662–668. doi: 10.1094/PHYTO-10-16-0385-R

Zheng, Z., Xu, M., Bao, M., Wu, F., Chen, J., and Deng, X. (2016). Unusual five copies and dual forms of *nrdB* in "*Candidatus Liberibacter asiaticus*": Biological implications and PCR detection application. *Sci. Rep.* 6:39020. doi: 10.1038/srep39020

Conflict of Interest: The authors declare that the research was conducted in the absence of any commercial or financial relationships that could be construed as a potential conflict of interest.

frontiers in Microbiology

ORIGINAL RESEARCH
published: 12 July 2021
doi: 10.3389/fmicb.2021.687725

OPEN ACCESS

Edited by:
Elvira Fiallo-Olivé, Institute of Subtropical and Mediterranean Horticulture La Mayora, Spain

Reviewed by:
Cecilia Tamborindeguy, Texas A&M University, United States
Bryce Falk, University of California, Davis, CA, United States
Murad Ghanim, Agricultural Research Organization (ARO), Israel

***Correspondence:**
Nelson Arno Wulff
nelson.wulff@fundecitrus.com.br

†ORCID:
Josiane Cecília Darolt
orcid.org/0000-0003-3091-8747
Flavia de Moura Manoel Bento
orcid.org/0000-0003-1034-8943
Bruna Laís Merlin
orcid.org/0000-0003-4444-3906
Leandro Peña
orcid.org/0000-0002-9853-366X
Fernando Luis Cônsoli
orcid.org/0000-0002-2287-0782
Nelson Arno Wulff
orcid.org/0000-0002-4557-2075

Specialty section:
This article was submitted to Microbe and Virus Interactions with Plants, a section of the journal Frontiers in Microbiology

Received: *30 March 2021*
Accepted: *04 June 2021*
Published: *12 July 2021*

Citation:
Darolt JC, Bento FMM, Merlin BL, Peña L, Cônsoli FL and Wulff NA (2021) The Genome of "Candidatus Liberibacter asiaticus" Is Highly Transcribed When Infecting the Gut of Diaphorina citri. Front. Microbiol. 12:687725. doi: 10.3389/fmicb.2021.687725

The Genome of "*Candidatus* Liberibacter asiaticus" Is Highly Transcribed When Infecting the Gut of *Diaphorina citri*

Josiane Cecília Darolt[1,2†], Flavia de Moura Manoel Bento[3†], Bruna Laís Merlin[3†], Leandro Peña[2,4†], Fernando Luis Cônsoli[3†] and Nelson Arno Wulff[1,2*†]

[1] Instituto de Química, Universidade Estadual Paulista "Julio de Mesquita Filho" – UNESP, Araraquara, Brazil, [2] Departamento de Pesquisa & Desenvolvimento, Fundo de Defesa da Citricultura – Fundecitrus, Araraquara, Brazil, [3] Laboratório de Interações em Insetos, Departamento de Entomologia e Acarologia, Escola Superior de Agricultura Luiz de Queiroz, Universidade de São Paulo, Piracicaba, Brazil, [4] Instituto de Biologia Molecular y Celular de Plantas – Consejo Superior de Investigaciones Científicas, Universidade Politécnica de Valencia, Valencia, Spain

The Asian citrus psyllid, *Diaphorina citri*, is the vector of the bacterium "*Candidatus* Liberibacter asiaticus" (Las), associated with the devastating, worldwide citrus disease huanglongbing. In order to explore the molecular interactions of this bacterium with *D. citri* during the vector acquisition process, cDNA libraries were sequenced on an Illumina platform, obtained from the gut of adult psyllids confined in healthy (H) and in Las-infected young shoots (Las) for different periods of times (I = 1/2 days, II = 3/4 days, and III = 5/6 days). In each sampling time, three biological replicates were collected, containing 100 guts each, totaling 18 libraries depleted in ribosomal RNA. Reads were quality-filtered and mapped against the Chinese JXGC Las strain and the Floridian strain UF506 for the analysis of the activity of Las genome and SC1, SC2, and type 3 (P-JXGC-3) prophages of the studied Las strain. Gene activity was considered only if reads of at least two replicates for each acquisition access period mapped against the selected genomes, which resulted in coverages of 44.4, 79.9, and 94.5% of the JXGC predicted coding sequences in Las I, Las II, and Las III, respectively. These genes indicate an active metabolism and increased expression according to the feeding time in the following functional categories: energy production, amino acid metabolism, signal translation, cell wall, and replication and repair of genetic material. Pilins were among the most highly expressed genes regardless of the acquisition time, while only a few genes from cluster I of flagella were not expressed. Furthermore, the prophage region had a greater coverage of reads for SC1 and P-JXGC-3 prophages and low coverage in SC2 and no indication of activity for the lysis cycle. This research presents the first descriptive analysis of Las transcriptome in the initial steps of the *D. citri* gut colonization, where 95% of Las genes were active.

Keywords: greening, HLB, prophage, psyllid, Las, ACP, metatranscriptomics

INTRODUCTION

"*Candidatus* Liberibacter asiaticus" (Las), a Gram-negative bacterium belonging to the α-proteobacteria group (Garnier et al., 1984; Jagoueix et al., 1994), is the main agent associated with huanglongbing (HLB) (Bassanezi et al., 2020). The Las vector insect is the Asian citrus psyllid (ACP) *Diaphorina citri* Kuwayama (Hemiptera: Psyllidae) (Capoor et al., 1967; Canale et al., 2017) that frequently acquires Las in areas surrounding healthy commercial groves, with the consequent psyllid dispersion causing primary infections (Bergamin Filho et al., 2016) resulting in economic loss due to impacted production (Bassanezi et al., 2020). Owing to the importance of the disease and because there are no curative methods to control HLB, the bacterium and the psyllid are considered to be the main pests in citriculture worldwide (Miranda and Ayres, 2020).

The psyllid may acquire Las from symptomatic plants (Hung et al., 2004; Pelz-Stelinski et al., 2010; Canale et al., 2017; Lopes and Cifuentes-Arenas, 2021) as well as from asymptomatic citrus plants (Lee et al., 2015). Las transmission by psyllids requires a latent period of 16 to 18 days (Canale et al., 2017) and its relationship with the psyllid is persistent and propagative (Hung et al., 2004; Inoue et al., 2009; Ammar et al., 2011a; Canale et al., 2017). The acquisition of bacteria by the psyllid has direct implication on its transmission efficiency and consequently on its dissemination (Inoue et al., 2009; Pelz-Stelinski et al., 2010; Canale et al., 2017). The gut represents the first cell barrier that the Liberibacter needs to cross inside the psyllid before accessing the hemolymph to migrate and infect salivary glands, from where it will be inoculated into plants. Gene expression studies showed a pattern of response in the gut and salivary glands of *D. citri* to Las infection (Kruse et al., 2017; Liu et al., 2020). There are exploratory studies that report transcriptional modifications in plants due to the presence of Las in *Catharanthus roseus* (Liu et al., 2019) and in leaves (Fu et al., 2016; Hu et al., 2017) and fruits of *Citrus* spp. (Martinelli et al., 2012).

The transcriptional analysis of Las is more commonly assessed *via* RT-qPCR in psyllids and in citrus, with modifications in the expression of genes related to the regulation of transcription, transport, secretion, flagellar assembly, metabolic pathways, and resistance to stress, by the assessment of a group of selected genes (Yan et al., 2013; Prasad et al., 2016; Thapa et al., 2020) or associated with functional studies (Fleites et al., 2014; Jain et al., 2015; Li et al., 2017). Sequencing of cDNA libraries *via* RNA-Seq has been an important tool in studies of transcriptional modification in bacteria (Croucher and Thomson, 2010; Haas et al., 2012; Creecy and Conway, 2015). Transcriptome analysis of Las genome in citrus and dodder has shown a high correlation in gene expression in both hosts, expected since dodder was parasitizing citrus, and in both hosts, Las encounters similar nutrients and micro-environmental conditions (Li et al., 2021). A predicted model of metabolite usage was created for *Liberibacter crescens* growing in culture media and for Las in plant and psyllid hosts, using RNA-seq data (Zuñiga et al., 2020). A transcriptome analysis of *Bactericera cockerelli* indicated a high percentage of "*Ca.* L. solanacearum" (Lso) expressed genes, particularly of putative genes involved in translation and in post-translation modification, protein turnover, and chaperone functions (Ibanez et al., 2014). Here, "*Ca.* L. asiaticus" had 95% of genes mapped with reads in the *D. citri* gut, with pilins, flagella, translation, and cell wall biogenesis genes with marked expression. The Las prophage genes, with their high diversity in Las populations, were mapped mostly to SC1 and type 3 prophages, in both late and early genes, without indication of an active lytic cycle. The transcriptional mapping analysis of Las genes in the gut of *D. citri* that fed in Las-infected citrus was performed in this study, evidencing the expression of almost all genes of Las as a manner to generate knowledge in the initial phase of the Las infection in the psyllid.

MATERIALS AND METHODS

Obtention of Samples

The stock colony of Las-free *D. citri* was maintained in cages in *Murraya paniculata* L. (Jack) plants, as described by Carmo-Souza et al. (2020). Adults from 7 to 10 days were selected for the Las acquisition step.

Nursery plants of sweet orange [*Citrus* × *sinensis* (L.) Osbeck grafted on "Rangpur" lime (*C.* × *limonia* Osbeck)] were maintained in 4-L bags in a greenhouse and grown in decomposed pine bark substrate (Plantmax citrus, Eucatex, Paulínia, SP, Brazil). Las infection was confirmed by qPCR (Li et al., 2006), and plants presented symptoms of blotchy mottle. Healthy plants of the same age and under similar growing conditions were used as negative control. The Las isolate employed in this study had a profile of SSR markers and prophages identical to Las 9PA isolate (Silva et al., 2019, 2021).

Plants underwent drastic pruning and were maintained under controlled conditions of temperature of 26°C ± 2°C, relative humidity of 70%, and photoperiod of 14/10 h of light/dark for shoot development and experimentation. Adult psyllids were confined and kept on citrus shoots at the vegetative stage V2/V3 of both healthy and Las-infected sweet orange plants (Cifuentes-Arenas et al., 2018; Lopes and Cifuentes-Arenas, 2021). Prior to the confinement of the insects, shoots were sampled to confirm the presence of Las (Li et al., 2006).

Dissection of psyllids for gut sampling was carried out after different acquisition access periods of 24, 48, 72, 96, 120, and 144 h, equivalent to 1- to 6-day intervals of acquisition. Psyllids from each period were removed from plants and dissected in 70% ethanol with 1% diethyl pyrocarbonate (DEPC) with the aid of a needle under stereoscopic microscope. Three repetitions were performed for each acquisition period in healthy or infected plants, each comprising 100 guts. Guts were immediately transferred to 100 μl of RNA Later (Invitrogen/ThermoFisher Scientific, Waltham, MA, United States, EUA) in ice and then immediately stored at −80°C.

Extraction of Total RNA From Psyllid Gut Samples, Detection of the Presence of "*Candidatus* Liberibacter asiaticus," and Treatment With DNase

Extraction of total RNA from dissected psyllid gut samples was performed using the SV RNA Isolation System (Promega, Madison, WI, United States) kit. Samples were resuspended in 30 μl of nuclease-free water and were assessed by spectrophotometry in NanoDrop V 3.8.1 (ThermoFisher Scientific) in relation to total RNA concentration.

The detection of the presence of Las was carried out prior to treating RNA samples with DNase by qPCR (Li et al., 2006), monitoring the presence of Las 16S rDNA (**Table 1**) and of the *wingless* gene (**Table 1**) for *D. citri* DNA (Manjunath et al., 2008) using hydrolysis probes (PathID qPCR Master Mix, Ambion/ThermoFisher Scientific; Primers and probes by Macrogen, Seoul, South Korea). The target sequence threshold was manually adjusted in the StepOnePlus software version 2.3 (ThermoFisher Scientific). The qPCR was carried out in duplicate and samples were considered positive for the presence of Las when Ct values were equal to or lower than 35.0 and negative when greater than that value. The presence of *D. citri* DNA produces Ct values equal to or lower than 36.0. Psyllid DNA samples with and without Las were used as positive and negative controls, respectively, besides water control (non-template control).

Selected total RNA samples were treated with Turbo^{TM} DNase (2 U/μl) (Ambion/ThermoFisher Scientific). The confirmation of the DNase action to cleave residual DNA was validated by qPCR with the *wingless* gene for *D. citri* (Manjunath et al., 2008).

Enrichment of mRNA in Samples and Quality Assessment for Sequencing

At this step, samples were grouped into pools: H = Healthy citrus or Las = Las-infected citrus sources. H I and Las I = 1 and 2 days of feeding on citrus; H II and Las II = 3 and 4 days; H III and Las III = 5 and 6 days. Each period and source had three biological repetitions. Next, samples were subjected to mRNA enrichment with the Ribo-Zero Gold rRNA Removal Kit (Illumina, San Diego, CA, United States). Two microliters of each sample was used to determine mRNA concentration and quality in the Synergy Multi-Detection reader (Biotec Synergy Winooski, EUA; software Gen5). Samples with total mRNA concentrations between 80 and 200 ng were used for metatranscriptome sequencing.

cDNA Sequencing *via* Illumina Platform

Samples enriched in mRNA were subjected to the cDNA library preparation protocol TruSeq RNA Library Prep Kit (Illumina), according to the paired-end (2 × 100 bp) strategy that consists in fragmenting the mRNA-enriched RNA into sequences of 200 nucleotides, followed by binding with random primers for reverse transcription and building of cDNA libraries. The cDNA was synthesized and purified through magnetic beads and washings with ethanol. Next, ends were repaired and adenosines were added to the 3′ ends of each fragment. Then, adaptors were connected and samples were subjected to PCR amplification. Sequencing of cDNA libraries was carried out on the Illumina HiScanSQ platform (Illumina), at the Centro Multiusuário de Biotecnologia Agrícola of the Departamento de Zootecnia at ESALQ/USP (Piracicaba, SP, Brazil). Readings were obtained from triplicates of the six treatments, for periods I, II, and III for healthy and Las-infected adults, totaling 18 libraries.

Sequencing Analysis and Transcriptome Assembly

Readings obtained from sequencing cDNA libraries were analyzed with the FastQC software (Andrews, 2010) for quality assurance. Remaining adaptors were removed and sequences were trimmed according to the SLIDINGWINDOW 4:22 parameter for the start (LEADING:3) and end (LEADING:3) of readings, which determined the minimum quality score (22) for each group of four nucleotides analyzed in the Trimmomatic 0.36 software (Bolger et al., 2014). Sequences below 25 nucleotides were excluded.

The analysis of Las transcripts abundance in the ACP gut was carried out by counting the number of fragments per kilobase million (FPKM) through the calculation of log2(FPKM) of the reads present in at least two out of the three sequenced libraries for each of the acquisition access periods (Las I, Las II, and Las III). Las strain JXGC (NZ_CP019958; Zheng et al., 2018) was the reference for mapping and counting of reads in Las genome and consequently for determining the transcribed genes. The draft genome of Las strain 9PA from Brazil was not used due to the presence of several gaps in the genome assembly (Silva et al., 2021). Reads mapped to ribosomal RNA, pseudogenes, and tRNAs were disregarded, the latter due to their size. Additionally, in the analysis of SC1 and SC2 prophages, the sequence of the

TABLE 1 | Primers and probes to detect 16SrDNA from "*Candidatus* Liberibacter asiaticus" and *wingless* gene from *Diaphorina citri* using qPCR.

Primer/Probe name	Nucleotide sequences (5′ to 3′) and modifications (probes)	References
HLBas	TCGAGCGCGTATGCAATACG	Li et al., 2006
HLBr	GCGTTATCCCGTAGAAAAAGGTAG	
HLBp	FAM-AGACGGGTGAGTAACGCG-BHQ1	
DCF	TGGTGTAGATGGTTGTGATCTGATGTG	Manjunath et al., 2008
DCR	ACCGTTCCACGACGGTGA	
DCP	HEX-TGTGGGCGAGGCTACAGAAC-BHQ1	

strain Las UF506 (HQ377374.1; Zhang et al., 2011) and that of prophage type 3 (P-JXGC-3) of Las JXGC (KY661963) were used. Those analyses employed the following parameters: mismatches cost: 2; insertion cost: 3; deletion cost: 3; length fraction: 0.8; similarity fraction: 0.8; strand specific: both; maximum number of hits for a read: 2, and were carried out in the CLC Genomics v. 21.0 software (Qiagen, Hilden, Germany).

The functional annotation of transcripts (Cluster of Orthologous Groups of proteins—COGs), generated through mapping genes of Las, was carried out (Tatusov et al., 2000). Three reference genomes were used, of which two were α-proteobacteria: "*Ca.* L. solanacearum" (strain CLso-ZC1), *Rhizobium leguminosarum* bv. viciae (strain 3841), and *Escherichia coli* (O157:H7 strain Sakai). Graphs were plotted with GraphPad Prism version 8.0.0 (Windows GraphPad Software, San Diego, CA, United States) and the Venn diagram was plotted using "*Draw Venn Diagram*"[1].

RESULTS

Presence of "*Candidatus* Liberibacter asiaticus" in Gut Samples of Psyllid *D. citri*

The qPCR analysis of citrus shoots used as food by psyllids confirmed the presence of Las exclusively in infected plants, with an average cycle threshold (Ct) of 20.7 (standard error ± 3.4). The presence of the psyllid DNA was detected in all gut RNA samples, with an average Ct for the *D. citri wingless* gene of 30.7 (**Table 2**), corroborating the need for treatment with DNase before cDNA synthesis. The DNA presence, however, enabled the monitoring of the Las DNA presence by qPCR as a way to validate the presence of the bacterium in the dissected guts of *D. citri* before transcriptome analysis. The presence of Las was detected only in RNA samples from guts of insects that fed on shoots of Las-infected plants (**Table 2**). In the Las I and Las II libraries, the mean Ct-value for the Las gene 16S rRNA was 30.6 and 30.8, respectively, whereas in Las III libraries, the Ct-value was 27.3. For gut samples of psyllids confined in healthy plants (libraries H I, II, and III), Las DNA was not detected.

TABLE 2 | Spectrophotometrically measured RNA concentration (ng/μl) and quality (260/280) and detection of *Diaphorina citri* (DC) and "*Candidatus* Liberibacter asiaticus" (Las) (HLBaspr) DNA by qPCR in RNA samples prepared from *D. citri* gut, prior to DNase treatment and library setup.

AAP	Sample	RNA		qPCR Ct [a]	
		ng/μl	260/280	DC [b]	HLBaspr [c]
I = 1/2 days	H I_1	59.06	2.06	31.11 ± 0.77	nd
	H I_2	68.86	2.16	29.91 ± 0.20	nd
	H I_3	46.59	2.07	30.44 ± 0.79	nd
	Las I_1	56.20	2.03	30.25 ± 0.15	32.18 ± 2.72
	Las I_2	56.85	2.10	30.77 ± 0.43	30.68 ± 0.54
	Las I_3	65.10	2.05	29.20 ± 0.12	28.99 ± 0.87
II = 3/4 days	H II_1	69.69	2.12	31.91 ± 1.27	nd
	H II_2	58.69	2.12	29.39 ± 1.87	nd
	H II_3	57.89	2.13	29.46 ± 1.20	nd
	Las II_1	74.56	2.04	30.52 ± 1.49	29.69 ± 1.53
	Las II_2	48.18	2.08	31.17 ± 0.21	32.24 ± 2.08
	Las II_3	65.88	2.13	33.71 ± 0.04	30.45 ± 0.68
III = 5/6 days	H III_1	68.21	2.01	30.09 ± 0.16	nd
	H III_2	58.44	2.07	30.90 ± 0.11	nd
	H III_3	46.42	2.07	32.50 ± 1.71	nd
	Las III_1	51.26	2.14	28.96 ± 0.85	26.18 ± 2.10
	Las III_2	45.92	2.02	30.10 ± 0.80	26.48 ± 0.02
	Las III_3	51.08	2.04	31.86 ± 0.77	29.40 ± 0.69

Diaphorina citri gut samples dissected from psyllids reared in either healthy (H) or Las-infected citrus plants (Las) for increasing (I, II, and III) acquisition access periods (AAP) of time.
[a]Ct, Cycle threshold, mean from duplicate value ± standard error; nd, not detected.
[b]DC = qPCR for D. citri wingless gene detection (Manjunath et al., 2008).
[c]HLBaspr = qPCR for "Ca. L. asiaticus" 16S rDNA detection (Li et al., 2006).

Mapping of Reads of "*Candidatus* Liberibacter asiaticus"

The average percentage of mapped reads in the "*Ca.* L. asiaticus" genome in healthy samples (H I, II, and III) was 0.01, 0.00, and 0.02, respectively, whereas that percentage in libraries set up from guts of psyllids that fed on Las, Las I, II, and III-infected plants was 0.07, 0.16, and 0.53, respectively (**Table 3**).

Reads in Las I libraries mapped against 432 genes of the Las JXGC reference genome, whereas reads in Las II and Las III libraries mapped against 777 and 967 genes, respectively (**Figure 1**). Out of the genes predicted in the Las JXGC isolate (Zheng et al., 2018), 972 had reads mapped in at least one of the three acquisition access periods (Las I, II, or III) in the gut of psyllids that fed on shoots of Las-infected plants. The transcriptome of all libraries in the three periods assessed corresponds to mapping of 95% of the genes predicted in Las. Out of that total, 406 or 41.8% of mapped genes were shared among libraries from all acquisition periods, whereas 367 genes were mapped only to reads in the Las II and Las III libraries (**Figure 1**). Reads in the Las I library were the only ones to map against the gene B2I23_RS05235 that codes a YdaU family protein (unknown function with domain DUF1376), showing the specific expression of this gene at the initial stage of the acquisition process. Four other genes (B2I23_RS00005, a prophage helicase; B2I23_RS00270; B2I23_RS02880; and B2I23_RS05570, coding three hypothetical proteins) were mapped only to reads in the Las II library. In the libraries Las III, 169 genes were mapped exclusively in this stage, with COG distribution equivalent to the whole library set. Into that group were 57 hypothetical protein coding genes, two of the three full-length β-subunits of ribonucleotide reductase (RNR) (B2I23_RS03685 and B2I23_RS04305), and 12 genes from the flagellar clusters (**Supplementary Table 1**). Only 51 of the genes predicted in the Las strain JXGC had no mapped reads in the transcriptome of the gut of infected adult psyllids, showing that these genes are not expressed in the vector gut during the infection process. These comprise two genes coding for the short forms of the β-subunit of RNR B2I23_RS00035 and B2I23_RS04515, one containing

[1]http://bioinformatics.psb.ugent.be/webtools/Venn/

TABLE 3 | Transcript read mapping against "*Candidatus* Liberibacter asiaticus" (Las) JXGC strain (NZ_CP019958.1) from sequenced libraries prepared with enriched mRNA from *Diaphorina citri* gut samples, reared either in healthy (H) or in Las infected-citrus shoots (Las), for increasing (I, II, and III) acquisition access periods (AAP).

AAP	Library	Input reads	Mapped paired pairs (%)
I = 1/2 days	H I_1	14,662,250	0.00
	H I_2	17,002,637	0.01
	H I_3	16,119,271	0.01
	Mean	15,928,053	0.01
	Las I_1	16,809,192	0.06
	Las I_2	16,066,925	0.19
	Las I_3	14,342,296	0.09
	Mean	15,739,471	0.07
II = 3/4 days	H II_1	15,288,196	0.00
	H II_2	17,110,015	0.01
	H II_3	17,831,678	0.00
	Mean	16,743,296	0.00
	Las II_1	15,083,210	0.09
	Las II_2	16,125,467	0.03
	Las II_3	14,389,488	0.36
	Mean	15,199,388	0.16
III = 5/6 days	HIII_1	16,064,435	0.01
	HIII_2	15,614,261	0.04
	HIII_3	15,142,440	0.01
	Mean	15,607,045	0.02
	Las III_1	17,908,705	0.40
	Las III_2	16,163,569	0.86
	Las III_3	16,311,141	0.33
	Mean	16,794,472	0.53

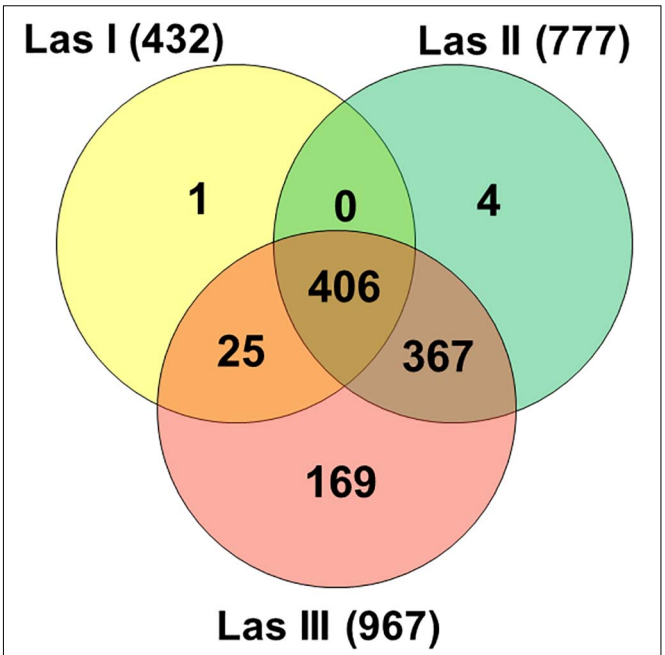

FIGURE 1 | Venn diagram of "*Candidatus* Liberibacter asiaticus" genes with mapped reads (strain JXGC, NZ_CP019958.1) in *Diaphorina citri* gut samples after acquisition access periods of 1/2 days (Las I), 3/4 days (Las II), or 5/6 days (Las III).

the VRR-NUC (B2I23_RS05600) domain, two containing the DUF59 domain (B2I23_RS01860 and B2I23_RS03885), one containing the DUF2815 domain (B2I23_RS05410), one ATPase (B2I23_RS02840), one nuclease (B2I23_RS05420), one primase (B2I23_RS05400), and 35 genes that code hypothetical proteins (**Supplementary Table 2**).

In the analysis of read abundance for each library and its distribution along the JXGC reference genome, an average of 42.2% of the genes predicted in the genome was obtained for Las I (**Figure 2**), and in the Las II and Las III libraries, coverage was 76 and 94.5%, respectively (**Figure 2**). Although the number of genes with mapped reads increased considerably according to the period of time the psyllid remained feeding on the Las-infected plant (Las III > Las II > Las I), the average log2(FPKM) value was slightly reduced from 9.38 in Las I to 8.84 and 8.41 in Las II and Las III, respectively (**Figure 2**). Only in the Las III library is there a greater number of mapped genes with values higher than the average.

When the top 10 genes with a greater number of reads in each period are analyzed, three are annotated as coding hypothetical proteins: B2I23_RS05520, B2I23_RS05120, and B2I23_RS04020 mapped in all periods (**Figure 2**).

The transcription of genes *flp1* (B2I23_RS02385), *flp4* (B2I23_RS02400), and *flp5* (B2I23_RS02405) annotated as "*Flp family type IVb pilin*" was significant in the Las I, II, and III libraries. Besides these three genes, *flp2*, *flp3*, and *flp7* were also mapped (B2I23_RS02390; RS02395 and RS02410). Reads for B2I23_RS03065, whose annotation is for a membrane protein ("*porin family protein*"), were also expressive.

Reads for the gene B2I23_RS03735 ("*NADH-quinone oxidoreductase subunit C*") were present among the 10 genes with greater representativeness in the Las I and Las II libraries. B2I23_RS04070 (*rfb*C) that codes the dTDP-4-dehydrorhamnose 3,5-epimerase involved in the synthesis of rhamnose-containing polysaccharides, such as lipopolysaccharides, is highly expressed in Las I. An ATP-dependent Clp protease ATP-binding subunit, *clpX* (B2I23_RS00740), was mapped in Las I as one of the most expressed genes (**Figure 2**). Additionally, all genes coding for components of the protease Clp family were expressed in Las III: *clpA* (B2I23_RS00185), *clpS* (B2I23_RS00190), endopeptidase La (B2I23_RS00735), *clpP* (B2I23_RS00745), *hslU* (B2I23_RS01895), *hslV* (B2I23_RS01900), lon peptidase (B2I23_RS02370), and *clpB* (B2I23_RS03845) (**Supplementary Table 3**).

The other genes mapped with a representative number of reads are involved in ribosome metabolism, such as the transfer-messenger RNA–*ssrA* (B2I23_RS04260), *rnpB*–RNAse P (B2I23_RS04605), and ribosomal proteins *rpmJ* (B2I23_RS00165) and *rpsT* (B2I23_RS02910) genes. The chaperone gene for the "*cold shock domain-containing protein*" (B2I23_RS04040) is among the most expressed in Las III.

The classification of genes mapped in the COGs (Tatusov et al., 2000) identified a greater number of genes mapped in the COGs translation (J), replication and repair (L), cell wall/membrane

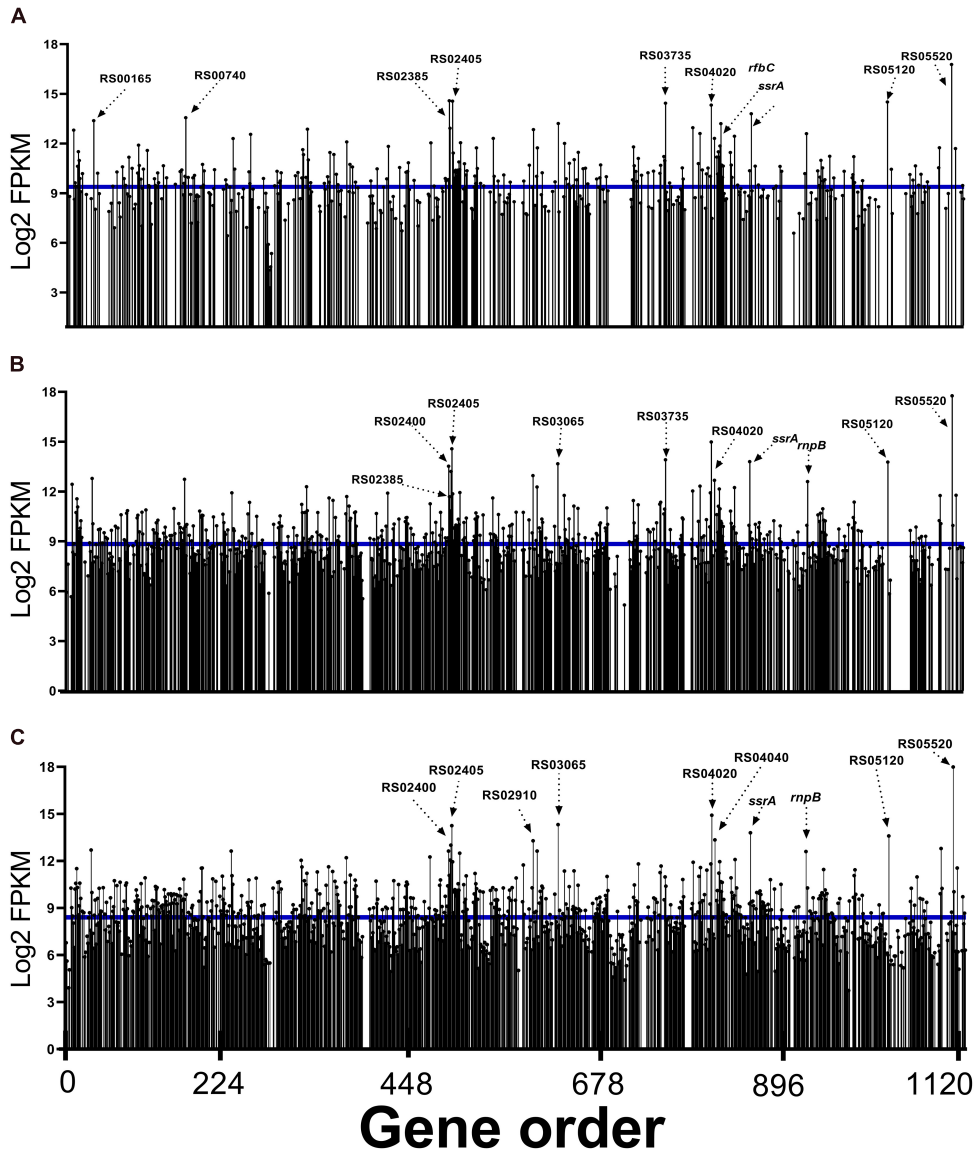

FIGURE 2 | Read abundance mapped to "*Candidatus* Liberibacter asiaticus" genes (reference strain JXGC, NZ_CP019958.1) expressed in gut samples from *Diaphorina citri* after acquisition access periods of 1/2 days (Las I) **(A)**, 3/4 days (Las II) **(B)**, or 5/6 days (Las III) **(C)**, mean log2FPKM.

biogenesis (M), energy production (C), and amino acid transport and metabolism (E) (**Figure 3**).

When only Las III libraries were analyzed, Clusters I, II, and III that code flagellar proteins (COG N) with average values of log2(FPKM) of 5.53, 6.27, and 6.11, respectively (**Figure 4**), stand out. The genes *motE*, *flgA*, *fliE*, *flgB*, and *flgC* were not mapped (**Supplementary Table 1**). The sequences predicted for *pilins* (COG: U) present average values of log2(FPKM) of 12.49, above the average value of Las III. A region with genes for proteins involved in the lipopolysaccharide synthesis (COG: M) presented values of log2(FPKM) of 10.8, also above the average in Las III. The region that includes 21 out of the 54 ribosomal proteins annotated in the Las genome, located in the region 128 kbp to 137 kbp, and others where 14 subunits of NADH-quinone oxidoreductases are annotated in the region 816 kbp to 829 kbp (**Figure 4**), presented average log2(FPKM) values of 9.0 and 8.4, respectively. The list with FPKM and log2(FPKM) values for all mapped genes from the Las JXGC strain in each library is available as **Supplementary Table 3**.

Mapping of Las Prophages SC1, SC2, and P-JXGC-3 in the Gut of *D. citri*

Reads from Las-infected libraries mapped against the genomes of prophages SC1 (UF506) and type 3 (P-JXGC-3) (**Figure 5**). In the widely conserved region shared between both prophages, known as early genes and also shared with SC2, the high similarity of gene sequences does not allow for differentiation as to the presence of reads between prophages, except in divergent

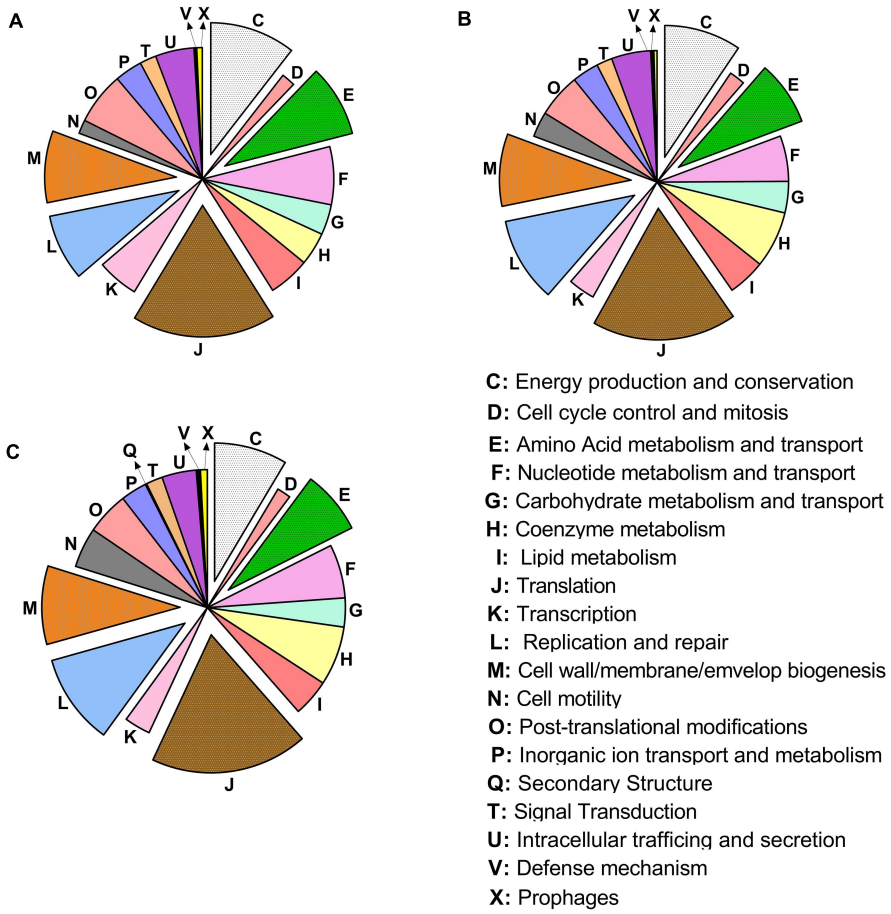

FIGURE 3 | Distribution of the cluster of ortholog groups in "*Candidatus* Liberibacter asiaticus" (reference strain JXGC, NZ_CP019958.1), measured as mapped reads in *Diaphorina citri* gut after acquisition access periods of 1/2 days (Las I) **(A)**, 3/4 days (Las II) **(B)** or 5/6 days (Las III) **(C)**.

regions. There were no reads mapped in the SC1/type 3 genes: SC1_gp175/PJXGC_gp25 and SC1_gp185/PJXGC_gp26, both coding hypothetical proteins, and in SC1_gp215/PJXGC_gp32, an endonuclease (VVR-NUC). The other shared genes were mapped, while a few divergent genes were not mapped (**Figure 5**). The highest number of mapped reads among all libraries was for the hypothetical protein PJXGC_gp17 gene (B2I23_RS05520)/SC1_gp135 (**Figure 2**).

In prophage late region, read coverage was 68.75% in the SC1 genes and 60% in P-JXGC-3 (**Figure 5**). In the prophage SC1, the following genes had reads mapped (genes without indication are hypothetical proteins): SC1_gp005, SC1_gp010, SC1_gp015, SC1_gp025 (tail fiber protein), SC1_gp030, SC1_gp035 (endolysin), SC1_gp045, SC1_gp050, SC1_gp060 (colicin IA), SC1_gp080, and SC1_gp085 (major tail subunit). The following genes were not mapped: SC1_gp090 (major capsid protein), SC1_gp095, SC1_gp100, SC1_gp105 (head-to-tail joining protein), and SC1_gp110 (holin). In P-JXGC-3, only the genes PJXGC_gp01, PJXGC_gp02, and PJXGC_gp07 to PJXGC_gp10 that code subunits R and S of the deoxyribonuclease type I site-specific (HsdR) and two subunits of the SAM-dependent DNA methyltransferase, respectively, were mapped. From the SC2 prophage, only SC2_gp020 was exclusively mapped.

DISCUSSION

Diaphorina citri acquires Las during feeding on infected plants (Hung et al., 2004; Inoue et al., 2009; Pelz-Stelinski et al., 2010), while transovarial transmission of Las to vector offspring is reported as low or absent (Hung et al., 2004; Pelz-Stelinski et al., 2010). The obtention of *D. citri* gut samples with Las requires manipulation of individuals to dissect them while keeping not only the integrity of the organ but also the quality and amount of mRNA necessary, in particular from the bacterium, to reveal genes whose transcription does occur in the psyllid gut. *D. citri* feeding on young citrus flushes infected by Las, under proper environmental conditions as those used in this study, generates high rates of infective psyllids, also able to transmit Las at high rates as a consequence of the high bacterial titer in the psyllid (Lopes and Cifuentes-Arenas, 2021). Psyllids that fed on Las-infected citrus shoots for a period of 5 to 6 days had 10 times more Las in their guts than those that fed for shorter periods of

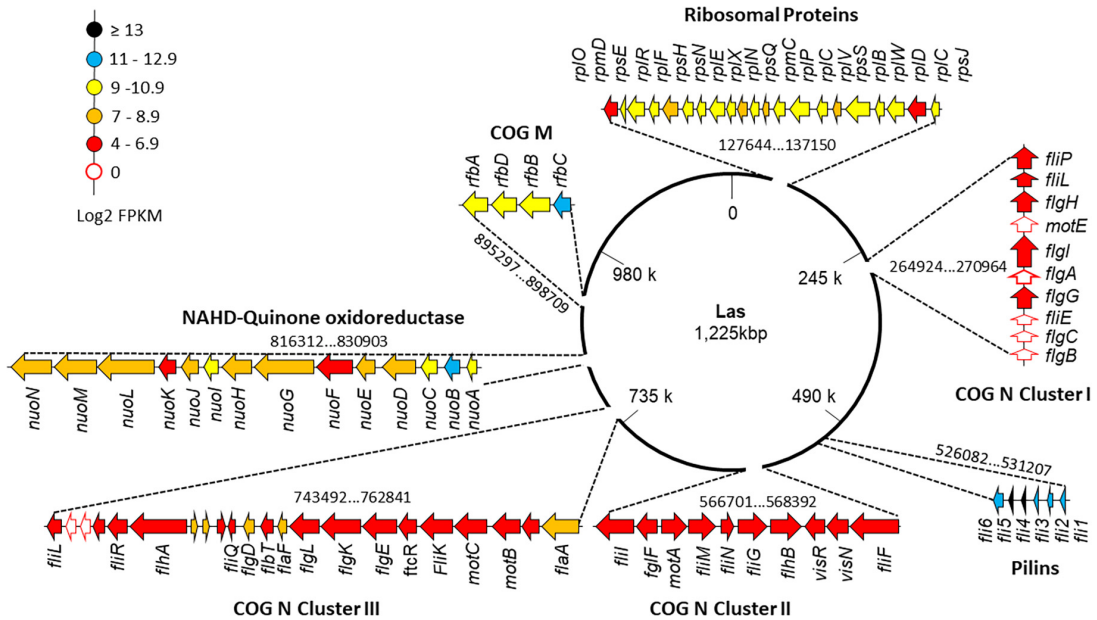

FIGURE 4 | Gene expression level along "*Candidatus* Liberibacter asiaticus" chromosome of selected clusters of genes. Flagellar clusters (COG N: Clusters I, II, and III), "Flp family type IVb pilins" (COG U), transferases (COG M), ribosomal proteins, and NADH-quinones genes are individually shown and their position in the chromosome is indicated. Read abundance (log2FPKM) taken from *Diaphorina citri* gut library from the acquisition time 5/6 days (Las III) mapped in strain JXGC (NZ_CP019958.1).

up to 4 days. The employed methodology enabled us to assess the Las transcriptome in the gut lumen and in association with gut epithelium from *D. citri*. Meanwhile, lower Ct-values for Las 16SrDNA were observed for the longer feeding time and higher Las read mapping was found in those libraries (Las III > Las II > Las I). For the longer feeding time (Las III, of 5 and 6 days) assessed in Las-infected plants, 0.53% of total reads mapped against Las reference genome JXGC. This value falls in the range observed by other authors, such as the mapping of 0.50% of transcriptome reads of the whole body of *B. cockerelli* against the Lso genome (Ibanez et al., 2014). Transcriptome analysis of Las was comparatively carried out in citrus and in dodder, with read mapping ranging from 0.11% to 1.44%, respectively (Li et al., 2021), while in adventitious citrus roots in culture media and in alimentary canals of *D. citri*, 0.28% to 2.51% of reads mapped to Las genome (Zuñiga et al., 2020). In contrast, only 0.01% of reads obtained from infected grapevine mapped against the flavescence dorée phytoplasma (Abbà et al., 2014). Las DNA detection in relation to host DNA is higher in psyllids than in citrus (Selvaraj et al., 2018), and this favors the obtention of Las nucleic acid from psyllids for metagenomic (Duan et al., 2009; Lin et al., 2013) and metatranscriptomic (Zuñiga et al., 2020) analysis.

The gut represents the first cell barrier that Las has to cross to systemically infect the psyllid body (Ammar et al., 2011a) and Las achieves high titer in this organ (Ammar et al., 2011a,b; Ghanim et al., 2017), though most of psyllid organs become infected (Ammar et al., 2011a,b). The transmission efficiency of Las by psyllids is related to the ability of the bacteria to multiply in the psyllid body (Ukuda-Hosokawa et al., 2015), as well as their ability to cross internal barriers in the ACP body, particularly the psyllid gut, hemolymph, and salivary glands (Ammar et al., 2011a,b; Ammar et al., 2016; Cicero et al., 2017; Ghanim et al., 2017). In this regard, the transcriptional status of Las in the gut is critical for psyllid infection and colonization. Reads from psyllids fed on healthy citrus plants (H I, II, and III) have, in addition to hits of psyllids sequences, reads with sequences similar to Las from endosymbiont bacteria, such as in the conserved regions from bacterial ribosomal genes. Depletion of ribosomal RNA prior to library construction allowed mRNA enrichment with the concomitant obtention of a representative number of reads (0.53%) with a Las gene expression coverage of 95%. While part of the reads still mapped to ribosomal genes, as observed in the RNA-Seq of Lso (Ibanez et al., 2014), depletion of such abundant sequences is essential to transcriptomic studies of eukaryote-associated bacteria (Kumar et al., 2015). *D. citri* has a rich microbial flora, composed of primary syncytium endosymbionts, "*Ca*. Carsonella ruddi" and "*Ca*. Profftella armature" (Nakabachi et al., 2013), secondary intracellular symbionts (Subandiyah et al., 2000; Guidolin and Cônsoli, 2013), and a range of extracellular bacteria (Kolora et al., 2015). The gene *lys*E from Las (B2I23_RS04390) codes for a protein whose function is predicted in amino acid transport and metabolism. That gene was acquired from "*Ca*. P. armatura" (Nakabachi et al., 2013a,b), indicating not only horizontal gene transference but also similarity between gene sequences from endosymbiotic bacteria with Las in the psyllids. Besides primary endosymbionts, *D. citri* populations in particular from Brazil have fixed infections by *Wolbachia* (Guidolin and Cônsoli, 2013; Dossi et al., 2014). Average incidence of Las in *D. citri* was

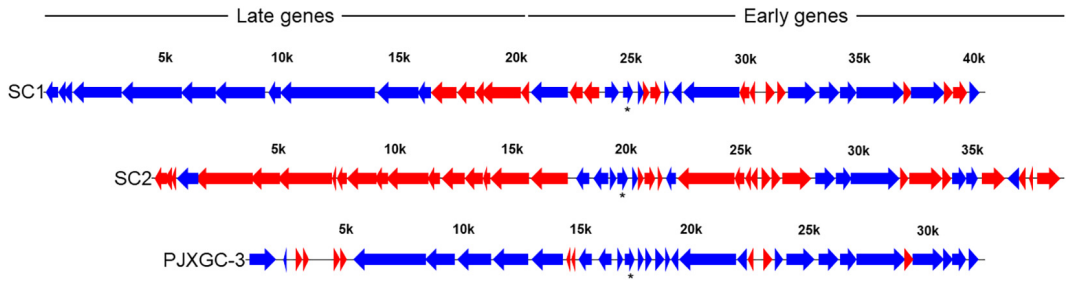

FIGURE 5 | Read mapping against "*Candidatus* Liberibacter asiaticus" (Las) SC1 (type 1) and SC2 (type 2) prophages from Las UF506 (HQ377374) and P-JXGC-3 (type 3) prophage from Las JXGC (KY661963). Blue arrows indicate genes mapped in at least two libraries while red arrows had no reads mapped. Asterisk is the Las genes with the highest number of mapped reads. Expression level taken from *Diaphorina citri* gut library from the acquisition time 5/6 days of rearing in Las-infected citrus (Las III).

65% in São Paulo State/West Minas Gerais State in Brazil (Wulff et al., 2020).

Plant pathogenic Liberibacters infect a range of hosts of economic importance (Garnier et al., 1984; Teixeira et al., 2008; Bové, 2006; Liefting et al., 2008; Munyaneza et al., 2009; Thapa et al., 2020), share features that render their study cumbersome, such as growth restricted to the phloem of infected plants, and are well-adapted to psyllid vectors. The majority of bacteria with reduced genome sizes, as is the case of Liberibacters (Duan et al., 2009; Lin et al., 2011; Wulff et al., 2014; Lin et al., 2015), have lost genes underlying the biosynthesis of compounds readily available from the host, as well as regulatory elements such as sigma factors (Konstantinidis and Tiedje, 2004). *Ca*. Liberibacter americanus (Lam) is also associated with HLB symptoms and have *D. citri* as vector, although currently is rare to find in the field (Teixeira et al., 2008; Bassanezi et al., 2020). Genes absent in Lam (Wulff et al., 2014) but found in Las were expressed in the psyllid gut. A relation that can be seen in reduced genomes with adaptive pressure and evolutive process is the loss of redundant and non-functional gene sequences (Mira et al., 2001; Sällsträm and Andersson, 2005), a factor that certainly renders these Liberibacters highly host-dependent for growth. *L. crescens* is the only Liberibacter available in axenic culture, which makes it suitable to functional studies and growth assays (Leonard et al., 2012; Jain et al., 2015; Jain et al., 2017b; Cruz-Munoz et al., 2019; Zuñiga et al., 2020). In Las strains and other Liberibacters that have their genomes sequenced, type II secretion system, avr and hrp genes, plant cell wall degrading enzymes, and several known virulence determinants also found in other plant pathogenic bacteria are absent (Duan et al., 2009; Lin et al., 2011; Wulff et al., 2014; Lin et al., 2015) but potential Las effectors (Thapa et al., 2020) were expressed in the psyllid gut in our analysis, except for CLIBASIA_04530.

The greater resolution power provided by the transcriptome analysis as compared to RT-qPCR might be used to link diverse cellular processes to gain understanding in active metabolic pathways for Las (Zuñiga et al., 2020). The process of host invasion and colonization by pathogens, leading to multiplication and increased titer, requires gene expression for the synthesis of proteins from housekeeping functions and energy production. A high number of reads mapped to genes coding for ribosomal proteins, NADH-quinone oxidoreductases, and genes for lipopolysaccharides synthesis, collectively indicating metabolic activity of Las during gut infection in *D. citri*. B2I23_RS03735 codes for subunit C of NADH-quinone oxidoreductase (NuoC). Subunits NuoA to NuoN form the core enzyme of complex I for the bacterial respiratory chain (Spero et al., 2015). The *nuo*C gene was mapped as one of the most expressed in Las I and Las II, and the 14 genes of the complex I subunits were expressed in Las II and Las III. In most bacterial clades, *nuo*A to *nuo*N are expressed as a polycistronic operon (Spero et al., 2015). Yan et al. (2013) assessed the expression of *nuo*A from this operon and found higher expression in psyllids than in plants. The expression of genes from the complex I by Las during gut colonization indicates that NADH reoxidation maintains the redox state of the cell (Spero et al., 2015).

Overall, 35 genes coding for hypothetical proteins were not mapped in Las in the psyllid gut, whereas 44 genes were not expressed in Lso in the *B. cockerelli* body (Ibanez et al., 2014). A gene coding for a protein with a VRR-NUC domain was not expressed in either Liberibacter (CKC_RS01050 or B2I23_RS05600). Lack of expression of four out of the five genes preceding the insertion point of the type 3 prophage was observed in Las. Twenty-one of the genes not expressed in psyllid gut were also not expressed in citrus, while only three were not expressed in dodder (Li et al., 2021).

The Clp protease complex degrades unfolded proteins, transcription factors, and phage proteins, besides being involved in regulatory processes (Porankiewicz et al., 1999). The high read mapping to B2I23_RS00740 together with the expression of other genes from the protease complex indicates coordinated expression for proteolysis. B2I23_RS04070 codes for a dTDP-4-dehydrorhamnose 3,5-epimerase (RfbC) that together with RfbABD (Graninger et al., 1999) produces rhamnose containing-polysaccharide, such as those found in *Rhizobium* spp. (Ghosh and Maiti, 2016). All four genes (rfbABCD, B2I23_RS04070 to B2I23_RS04085) were highly expressed in all time periods, and additional genes for the lipopolysaccharide biosynthesis were gradually expressed from Las I to Las II, with all genes being expressed in Las III, indicating active synthesis of cell envelope components.

Chaperonins such as the cold shock domain-containing protein (B2I23_RS04040) and the hsp20 family protein (B2I23_RS02935) were highly mapped in Las genome in the *D. citri* gut. Lso in *B. cockerelli* also had high expression of the gene coding for a cold shock protein (CKC_03300), whose regulation is correlated with pathogenicity factors and adaptation to new environments (Ibanez et al., 2014; Mohamed et al., 2020). GroEL/GroES were expressed in all libraries. Not only the same cold shock domain gene but also chaperonins groEL/groES were among the 20 most expressed genes from Las in citrus (Li et al., 2021).

Six *flp* family type IVb pilin genes from Las were mapped in the gut libraries. Type IV pili is a virulence factor (Wairuri et al., 2012), and pilins exert a role during interaction with surfaces, notably during superficial adhesion, potentially being involved in biofilm formation. Las *flp3* is upregulated in whole psyllid bodies, while *visN* and *visR*, two LuxR-type transcriptional regulators, are downregulated (Andrade and Wang, 2019). In contrast to the expression profile observed in whole *D. citri* bodies, all six pilin genes were highly mapped in the gut, with *flp1*, *flp4*, and *flp5* among the most mapped genes. Las express four pilins in citrus (Li et al., 2021) and *flp1* has the highest number of mapped reads in contrast to that observed in psyllids (Andrade and Wang, 2019). Oppositely, *flp4* and *flp5* were not expressed in citrus (Li et al., 2021), but were in the psyllid gut. Both *visN* and *visR* were mapped in citrus, while in the psyllid gut, the expression of both regulators was only observed in the library Las III. Regulation of *flp3* by VisNR might allow Las to switch between forming biofilm and circulative status inside the psyllid hemocoel (Andrade and Wang, 2019). Lso establishes biofilm during gut infection of *B. cockerelli* (Cicero et al., 2016), and *L. crescens* forms biofilm *in vitro* (Naranjo et al., 2019). Whether Las also form biofilm during gut infection is expected but not shown yet.

Las genome codes for three flagellar clusters, even though flagella formation in Las is an open question (Andrade et al., 2019). While at clusters II and III all genes were expressed in Las III, cluster I had five genes not mapped, which might account for the absence of flagella in Las (Andrade et al., 2019), since *fliE*, *flgB*, and *flgC* are not expressed and form the proximal rod together with *flgF*, which, in turn, was expressed in Las III libraries. Flagella-like structures were found in *L. crescens* (Andrade et al., 2019) and superficial appendages were found in Lso (Cicero et al., 2016). Andrade et al. (2019) have shown a higher expression level of flagella genes in psyllids than in plants, which is in sharp contrast to what had been observed previously (Yan et al., 2013). The genes *motE* and *flgC* were not mapped in citrus also, in addition to *fliQ*, while *flg*A, *flg*B, and *fli*E had a low expression level (Li et al., 2021), also in agreement with Andrade et al. (2019) and the mapping analysis shown here.

Among the top 10 genes with higher reads mapped, three codes for hypothetical proteins (B2I23_RS04020, B2I23_RS05120, and B2I23_RS05520). In the first genome sequenced from Las, strain psy62, 26% of the coding sequences were annotated as hypothetical proteins (Duan et al., 2009). In the strain Las JXGC, the annotation of hypothetical proteins was reduced to 14% (Zheng et al., 2018), and from this, 72% were located in the genome from 687 kbp to 1219 kbp, a region where the above three hypothetical protein coding genes are located. Also, the P-JXGC-3 prophage is located in that region, whose 64% of genes code for hypothetical proteins, including the most mapped gene B2I23_RS05520. The presence and abundance of reads in genes from the prophage highlight the need to perform functional studies with such genes, as already carried out for some of the Las prophage genes (Fleites et al., 2014; Jain et al., 2015). Prophage presence stood as a hallmark of variation between Las genomes, and indeed the average nucleotide identity for Las isolates is between 99% to 100% (Thapa et al., 2020) except that larger differences among Las strains are located in prophage sequences (Duan et al., 2009; Zhang et al., 2011; Katoh et al., 2014; Zheng et al., 2018), mainly due to the presence or absence of either one of the prophages or parts of them. The lack or the presence of prophages can account for a large fraction of the variation among individuals within a bacterial species (Casjeans, 2003). Prophages in Las were first characterized as SC1 and SC2 (Zhang et al., 2011) and later a third prophage was described (Zheng et al., 2018). There are potential advantages to the prophage-harboring strains during host colonization. Prophages contribute to "*Ca.* Liberibacter spp." diversity (Tomimura et al., 2009; Wulff et al., 2014; Jain et al., 2017a), while there is a small proportion of Las strains without prophages (Silva et al., 2019; Zheng et al., 2018, 2021). A higher read mapping was observed in genes from SC1 and P-JXGC-3 prophages and a few mapped to SC2. There are several genes potentially involved in lysogenic conversion in SC2 (Zhang et al., 2011), as well as in plant defense suppression, such as peroxidases coded by SC2_gp095 and SC2_gp100 (Jain et al., 2015). The absence of reads mapping to SC2, at least in the late region that is phage specific, in the current study is in accordance with the absence of a "standard" SC2 in Las strains from Brazil (Silva et al., 2019; Silva et al., 2021), as well as in the Las strain CoFLP1 from Colombia that is a strain from South America with a completely sequenced genome (Wang et al., 2021). Coding sequences for B2I23_RS05520 and B2I23_RS05445 are phage located and among the most mapped genes in Las in the gut of *D. citri*. While B2I23_RS05445 is exclusive from type 3 prophage, there might be a bias in read mapping for B2I23_RS05520, since this gene has identical copies in SC1 and type 3 prophages, both belonging to the early gene region of high similarity among Las prophages. Both genes were also highly mapped in Las transcriptome from citrus (Li et al., 2021). Genes whose products are involved in phage activity were expressed, such as SC1_gp115 (terminase), SC1_gp195 (exonuclease), SC1_gp210 DNA (polymerase A), and SC1_gp220 (helicase). The absence of reads mapped to SC1_gp090 (major capsid protein) and SC1_gp110 (holin) from Las while in the psyllid gut indicates no production of viral particles. Nevertheless, there is low similarity in the genomic sequence between SC1_gp090 (UF506) and Las strain 9PA (Silva et al., 2021) or the isolate CoFLP (Wang et al., 2021), and even though the Las strain from Brazil is not completely sequenced, the absence of the major capsid protein gene in the strain used is more likely, since neighboring genes are present as is the case of SC1_gp110 (holin) in that strain. The orthologous gene CD16_RS05495 that codes for a major capsid protein from Las

strain A4 was expressed in citrus and dodder (Li et al., 2021), in agreement with phage particles being found in periwinkle (Zhang et al., 2011). Read mapping to SC2_gp020 would not be expected if the SC2 prophage is absent in the studied Las strain, but reads were mapped to this exclusive gene. Nonetheless, the presence of only SC2_gp020 from the late region from SC2 might indicate rearrangement among 3′ and 5′ of the SC2 prophage, as observed for the Las strain 9PA, and besides that, genes exclusive to the 5′ of SC2 are also present in Las Brazilian strains (Silva et al., 2019, 2021). The expression of the SC1 prophage late genes was outstanding but not all genes were expressed, indicating specific transcription inhibition in the psyllid, as observed for SC1_gp110 (holin) (Jain et al., 2017a) and adjacent genes.

Read mapping of Las genes indicates a high number of genes being expressed in the initial step of *D. citri* gut colonization. Such genes should be essential for Las to colonize insect organs, since higher read coverage was observed after longer feeding periods in Las-affected plants. The low percentage of non-expressed genes indicates that the reduced genome of Las is highly active in transcription. Transcriptome studies should help define targets to better understand the interaction of Liberibacter with its hosts and to design strategies to better cope with HLB in the near future.

DATA AVAILABILITY STATEMENT

The data presented in the study is available in the Sequence Read Archive under the accession PRJNA722422 and accession number for each library is provided in **Supplementary Table 4**.

AUTHOR CONTRIBUTIONS

FC and NW designed the experiments. JD prepared plants, insects, and samples. BM, FB, and JD processed and analyzed sequencing data. JD and NW interpreted the data and drafted the manuscript. All authors commented on the initial draft and approved the final version of this manuscript. FC, NW, and LP secured the funds.

FUNDING

Financial support from FAPESP (2015/07011-3) and post-doctoral fellowship to FB (FAPESP 2018/24234-4). Doctorate scholarship to JD from CNPq (141042/2017-6).

ACKNOWLEDGMENTS

The authors would like to thank Renato de Freitas, Rômulo Y. Carvalho, Abner A. L. Pegoraro, and Odimar Z. Zanardi for providing psyllids and Juan C. Arena-Cifuentes and Sidnei F. Alkimin for their exceptional assistance.

SUPPLEMENTARY MATERIAL

The Supplementary Material for this article can be found online at: https://www.frontiersin.org/articles/10.3389/fmicb.2021.687725/full#supplementary-material

Supplementary Table 1 | The list of exclusive coding sequences mapped only in Las III.

Supplementary Table 2 | The list of genes without mapped reads.

Supplementary Table 3 | The list of coding sequences for each Las library mapped against Las JXGC genome with FPKM values, average and log2FPKM used for analysis.

Supplementary Table 4 | Accession number for each library.

REFERENCES

Abbà, S., Galetto, L., Carle, P., Carrère, S., Delledonne, M., Foissac, X., et al. (2014). RNA-Seq profile of flavescence dorée phytoplasma in grapevine. *BMC Genom.* 15:1088. doi: 10.1186/1471-2164-15-1088

Ammar, E. D., Ramos, J. E., Hall, D. G., Dawson, W. O., and Shatters, R. G. Jr. (2016). Acquisition, Replication and Inoculation of *Candidatus* Liberibacter asiaticus following various acquisition periods on huanglongbing infected citrus by nymphs and adults of the asian citrus psyllid. *PLoS One* 11:e0159594. doi: 10.1371/journal.pone.0159594.t006

Ammar, E. D., Robert, G., Shatters, R. G. Jr., Lynch, C., and Hall, D. G. (2011a). Detection and relative titer of *Candidatus* Liberibacter asiaticus in the salivary glands and alimentary canal of *Diaphorina citri* (Hemiptera: Psyllidae) vector of citrus Huanglongbing disease. *Ann. Entomol. Soc. A.* 104, 526–533. doi: 10.1603/AN10134

Ammar, E. D., Shatters, R. G. Jr., and Hall, D. G. (2011b). Localization of *Candidatus* Liberibacter asiaticus, associated with citrus Huanglongbing disease, in its psyllid vector using fluorescence in situ hybridization. *J. Phytopathol.* 159, 726–734. doi: 10.1111/j.1439-0434.2011.01836.x

Andrade, M., and Wang, N. (2019). The Tad Pilus apparatus of '*Candidatus* Liberibacter asiaticus' and its regulation by VisNR. *Mol. Plant Microbe. Interact.* 32, 1175–1187. doi: 10.1094/MPMI-02-19-0052-R

Andrade, M. O., Pang, Z., Achor, D. S., Wang, H., Yao, T., Singer, B. H., et al. (2019). The flagella of '*Candidatus* Liberibacter asiaticus' and its movement in planta. *Mol. Plant Pathol.* 21, 109–123. doi: 10.1111/mpp.12884

Andrews, S. (2010). *FastQC: a Quality Control Tool for High Throughput Sequence Data*. Available online at: http://www.bioinformatics.babraham.ac.uk/projects/fastqc (accessed December 16, 2020).

Bassanezi, R. B., Lopes, S. A., Miranda, M. P., Wulff, N. A., Volpe, H. X. L., and Ayres, A. J. (2020). Overview of citrus huanglongbing spread and management strategies in Brazil. *Trop Plant Pathol.* 45, 251–264. doi: 10.1007/s40858-020-00343-y

Bergamin Filho, A., Inoue-Nagata, A. K., Bassanezi, R. B., Belasque, J. Jr., Amorim, L., Macedo, M. A., et al. (2016). The importance of primary inoculum and area-wide disease management to crop health and food security. *Food Sec.* 8, 221–238. doi: 10.1007/s12571-015-0544-8

Bolger, A. M., Lohse, M., and Usadel, B. (2014). Trimmomatic: a flexible trimmer for Illumina sequence data. *Bioinformatics* 30, 2114–2120. doi: 10.1093/bioinformatics/btu170

Bové, J. M. (2006). Huanglongbing: a destructive, newly emerging, century-old disease of citrus. *J. Plant Pathol.* 88, 7–37. doi: 10.4454/jpp.v88i1.828

Canale, M. C., Tomaseto, A. F., Haddad, M. L., Coletta-Filho, H. D., and Lopes, J. R. S. (2017). Latency and Persistence of '*Candidatus* Liberibacter asiaticus' in

Its Psyllid Vector, *Diaphorina citri (Hemiptera: Liviidae*). *Phytopathology* 107, 264–272. doi: 10.1094/PHYTO-02-16-0088-R

Capoor, S. P., Rao, D. G., and Viswanath, S. M. (1967). *Diaphorina citri*: a vector of the greening disease of citrus in India. *Indian J. Agricult. Sci.* 37, 572–576.

Carmo-Souza, M., Garcia, R. B., Wulff, N. A., Fereres, A., and Miranda, M. P. (2020). Drench application of systemic insecticides disrupts probing behavior of *Diaphorina citri* (*Hemiptera: Liviidae*) and inoculation of *Candidatus* Liberibacter asiaticus. *Insects* 11:314. doi: 10.3390/insects11050314

Casjeans, S. (2003). Prophages and bacterial genomics: what have we learned so far? *Mol. Microb.* 49, 277–300.

Cicero, J. M., Fisher, T. W., and Brown, J. K. (2016). Localization of '*Candidatus* Liberibacter solanacearum' and evidence for surface appendages in potato psyllid vector. *Phytopathology* 106, 142–154. doi: 10.1094/PHYTO-04-15-0088-R

Cicero, J. M., Fisher, T. W., Qureshi, J. A., Stansly, P. A., and Brown, J. K. (2017). Colonization and intrusive invasion of potato psyllid by '*Candidatus* Liberibacter solanacearum'. *Phytopathology* 107, 36–49. doi: 10.1094/PHYTO-03-16-0149-R

Cifuentes-Arenas, J. C., Goes, A., Miranda, M. P., Beattie, G. A. C., and Lopes, S. A. (2018). Citrus flush shoot ontogeny modulates biotic potential of *Diaphorina citri*. *PLoS One* 13:e0190563. doi: 10.1371/journal.pone.0190563

Creecy, J. P., and Conway, T. (2015). Quantitative bacterial transcriptomics with RNA-seq. *Curr. Opin. Microbiol.* 23, 133–140. doi: 10.1016/j.mib.2014.11.011

Croucher, N. J., and Thomson, N. R. (2010). Studing bacterial trancriptomes using RNA-seq. *Curr. Opin. Microbiol.* 13, 619–624. doi: 10.1016/j.mib.2010.09.009

Cruz-Munoz, M., Munoz-Beristain, A., Petrone, J. R., Robinson, A. M., and Triplett, E. W. (2019). Growth parameters of *Liberibacter crescens* suggest ammonium and phosphate as essential molecules in the Liberibacter-plant host interface. *BMC Microbiol.* 19:222. doi: 10.1186/s12866-019-1599-z

Dossi, F. C. A., Silva, E. P., and Cônsoli, F. L. (2014). Population dynamics and growth rates of endosymbionts during *Diaphorina citri* (*Hemiptera. Liviidae*) ontogeny. *Microbiol. Ecol.* 68, 881–889. doi: 10.1007/s00248-014-0463-9

Duan, Y., Zhou, L., Hall, D. G., Li, W., Doddapaneni, H., Lin, H., et al. (2009). Complete genome sequence of Citrus Huanglongbing bacterium, '*Candidatus* Liberibacter asiaticus' obtained through metagenomics. *Mol. Plant Microbe. Interact.* 22, 1011–20. doi: 10.1094/MPMI-22-8-1011

Fleites, L., Jain, M., Zhang, S., and Gabriel, D. W. (2014). "*Candidatus* Liberibacter asiaticus" prophage late genes may limit host range and culturability. *Appl. Environ. Microbiol.* 80, 6023–6030.

Fu, S., Shao, J., Zhou, C., and Hartung, J. S. (2016). Transcriptome analysis of sweet orange trees infected with '*Candidatus* Liberibacter asiaticus' and two strains of Citrus Tristeza Virus. *BMC Genomics* 17:349. doi: 10.1186/s12864-016-2663-9

Garnier, M., Danel, N., and Bové, J. M. (1984). *The Greening Organism is a Gran Negative Bacterium*. United States: University of California.

Ghanim, M., Achor, D., Ghosh, S., Kontsedalov, S., Lebedev, G., and Levy, G. (2017). '*Candidatus* Liberibacter asiaticus' accumulates inside endoplasmic reticulum associated vacuoles in the gut cells of *Diaphorina citri*. *Sci. Rep.* 7:16945. doi: 10.1038/s41598-017-16095-w

Ghosh, P. K., and Maiti, T. K. (2016). Structure of extracellular polysaccharides (EPS) produced by Rhizobia and their functions in legume-bacteria symbiosis: a review. *Achiev. Life Sci.* 10, 136–143. doi: 10.1016/j.als.2016.11.003

Graninger, M., Nidetzky, B., Heinrichs, D. E., Whitfield, C., and Messner, P. (1999). Characterization of dTDP-4-dehydrorhamnose 3,5-epimerase and dTDP-4-dehydrorhamnose reductase, required for dTDP-L-rhamnose biosynthesis in *Salmonella enterica* serovar typhimurium LT2. *J. Biol. Chem.* 274, 25069–25077.

Guidolin, A. S., and Cônsoli, F. L. (2013). Molecular characterization of *Wolbachia* strains associated with the invasive asian citrus psyllid *Diaphorina citri* in Brazil. *Microb. Ecol.* 65, 475–486. doi: 10.1007/s00248-012-0150-7

Haas, B. J., Chin, M., Nusbaum, C., Birren, B. W., and Livny, J. (2012). How deep is deep enough for RNA-Seq profiling of bacterial transcriptomes? *BCM Genom.* 13:734. doi: 10.1186/1471-2164-13-734

Hu, Y., Zhong, X., Liu, X., Lou, B., Zhou, C., and Wang, X. (2017). Comparative transcriptome analysis unveils the tolerance mechanisms of *Citrus hystrix* in response to '*Candidatus* Liberibacter asiaticus' infection. *PLoS One* 12:e0189229. doi: 10.1371/journal.pone.0189229

Hung, T. H., Hung, S. C., Chen, C. N., Hsu, M. H., and Su, H. J. (2004). Detection by PCR of *Candidatus* Liberibacter asiaticus, the bacterium causing citrus Huanglongbing in vector psyllids: application to the study of vector-pathogen relationships. *Plant Pathol.* 53, 96–102. doi: 10.1111/j.1365-3059.2004.00948.x

Ibanez, F., Levy, J., and Tamborindeguy, C. (2014). Transcriptome analysis of "*Candidatus* Liberibacter solanacearum" in its Psyllid Vector, *Bactericera cockerelli*. *PLoS One* 9:e100955. doi: 10.1371/journal.pone.0100955

Inoue, H., Ohnish, I. J., Ito, T., Tomimura, K., Miyata, S., Iwanami, T., et al. (2009). Enhanced proliferation and efficient transmission of *Candidatus* Liberibacter asiaticus by adult *Diaphorina citri* after acquisition feeding in the nymphal stage. *Ann. Appl. Biol.* 155, 29–36. doi: 10.1111/j.1744-7348.2009.00317.x

Jagoueix, S., Bové, J. M., and Garnier, M. (1994). The phloem-limited bacterium of greening disease of citrus is a member of the alpha subdivision of the *Proteobacteria. Int. J. Syst. Bacteriol.* 44, 379–386. doi: 10.1099/00207713-44-3-379

Jain, M., Fleites, L. A., and Gabriel, D. W. (2015). Prophage-encoded peroxidase in '*Candidatus* Liberibacter asiaticus' is a secreted effector that suppresses plant defenses. *Mol. Plant Microbe. Interact.* 28, 1330–1337. doi: 10.1094/MPMI-07-15-0145-R

Jain, M., Fleites, L. A., and Gabriel, D. W. (2017a). A small *Wolbachia* protein directly represses phage lytic cycle genes in "*Candidatus* Liberibacter asiaticus" within psyllids. *mSphere* 2, e00171–17. doi: 10.1128/mSphere.00227-17

Jain, M., Munoz-Bodnar, A., and Gabriel, D. W. (2017b). Concomitant loss of the glyoxalase system and glycolysis makes the uncultured pathogen "*Candidatus* Liberibacter asiaticus" an energy scavenger. *Appl. Environ. Microbiol.* 83, e01670–17. doi: 10.1128/AEM.01670-17

Katoh, H., Miyata, S., Inoue, H., and Iwanami, T. (2014). Unique features of a japanese '*Candidatus* Liberibacter asiaticus' strain revealed by whole genome sequencing. *PLoS One* 9:e106109. doi: 10.1371/journal.pone.0106109

Kolora, L. D., Powell, C. M., Hunter, W., Bextine, B., and Lauzon, C. R. (2015). Internal extracellular bacteria of *Diaphorina citri* Kuwayama (*Hemiptera: Psyllidae*), the asian citrus psyllid. *Curr. Microb.* 70, 710–715. doi: 10.1007/s00284-015-0774-1

Konstantinidis, K. T., and Tiedje, J. M. (2004). Trends between gene content and genome size in prokaryotic species with larger genomes. *Proc. Nat. Acad. Sci. U. S. A.* 101, 3160–3165. doi: 10.1073/pnas.0308653100

Kruse, A., Fattah-Hosseini, S., Saha, S., Johnson, R., Warwick, E. R., Sturgeon, K., et al. (2017). Combining 'omics and microscopy to visualize interactions between the asian citrus psyllid vector and the huanglongbing pathogen *Candidatus* Liberibacter asiaticus in the insect gut. *PLoS One* 12:e0179531. doi: 10.1371/journal.pone.0179531

Kumar, N., Lin, M., Zhao, X., Ott, S., Santana-Cruz, I., Daugherty, S., et al. (2015). Efficient enrichment of bacterial mRNA from host-bacteria total RNA samples. *Sci. Rep.* 6:34850. doi: 10.1038/srep34850

Lee, J. A., Halbert, S. E., Dawson, W. O., Robertson, C. J., Keesling, J. E., and Singer, B. H. (2015). Asymptomatic spread of huanglongbing and implications for disease control. *Proc. Nat. Acad. Sci. U. S. A.* 112, 7605–7610. doi: 10.1073/pnas.1508253112

Leonard, M. T., Fagen, J. R., Davis-Richardson, A. G., Davis, M. J., and Triplett, E. W. (2012). Complete genome sequence of *Liberibacter crescens* BT-1. *Stand. Genomic. Sci.* 7, 271–283. doi: 10.4056/sigs.3326772

Li, J., Pang, Z., Trivedi, P., Zhou, X., Ying, X., Jia, H., et al. (2017). "*Candidatus* Liberibacter asiaticus" encodes a functional salicylic acid (SA) hydroxylase that degrades SA to suppress plant defence. *Mol. Plant Microbe. Interact.* 8, 620–630. doi: 10.1094/MPMI-12-16-0257-R

Li, T., Zhang, L., Deng, Y., Deng, X., and Zheng, Z. (2021). Establishment of a *Cuscuta campestris*-mediated enrichment system for genomic and transcriptomic analysis of '*Candidatus* Liberibacter asiaticus'. *Microbial. Biotec.* 2021, 737–751. doi: 10.1111/1751-7915.13773

Li, W. B., Hartung, J. S., and Levy, L. (2006). Quantitative real-time PCR for detection and identification of *Candidatus* Liberibacter species associated with citrus Huanglongbing. *J. Microbiol. Methods* 66, 104–115. doi: 10.1016/j.mimet.2005.10.018

Liefting, L. W., Perez-Egusquiza, Z. C., Clover, G. R. G., and Anderson, J. A. D. (2008). A new '*Candidatus* Liberibacter' species in *Solanum tuberosum* in New Zealand. *Plant Dis.* 92:1474. doi: 10.1094/PDIS-92-10-1474A

Lin, H., Han, C. S., Liu, B., Lou, B., Bai, X., Deng, C., et al. (2013). Complete genome sequence of a chinese strain of '*Candidatus* Liberibacter asiaticus'. *Genome Announc.* 1, e00184–13. doi: 10.1128/genomeA.00184-13

Lin, H., Lou, B., Glynn, J. M., Doddapaneni, H., Civerolo, E. L., Chen, C., et al. (2011). The complete genome sequence of '*Candidatus* Liberibacter solanacearum', the bacterium associated with potato zebra chip disease. *PLoS One* 6:e19135. doi: 10.1371/journal.pone.0019135

Lin, H., Pietersen, G., Han, C., Read, D. A., Lou, B., Gupta, G., et al. (2015). Complete genome sequence of "*Candidatus* Liberibacter africanus," a bacterium associated with citrus Huanglongbing. *Genome Announc.* 3, e00733–15. doi: 10.1128/genomeA.00733-15

Liu, X., Zheng, Y., Wang-Pruski, G., Gan, Y., Zhang, B., Hu, Q., et al. (2019). Transcriptome profiling of periwinkle infected with Huanglongbing ('*Candidatus* Liberibacter asiaticus'). *Eur. J. Plant Pathol.* 153, 891–906. doi: 10.1007/s10658-018-01607-9

Liu, X.-Q., Jiang, H.-B., Liu, T.-Y., Yang, L., Fan, J.-Y., Xiong, Y., et al. (2020). A Transcriptomic and Proteomic analysis of the *Diaphorina citri* salivary glands reveals genes responding to *Candidatus* Liberibacter asiaticus. *Front. Physiol.* 11:582505. doi: 10.3389/fphys.2020.582505

Lopes, S. A., and Cifuentes-Arenas, J. C. (2021). A protocol for successful transmission of '*Candidatus* Liberibacter asiaticus' from citrus to citrus using *Diaphorina citri*. *Phytopathology* doi: 10.1094/PHYTO-02-21-0076-R [Epub ahead of print].

Manjunath, K. L., Halbert, S. E., Ramadugu, C., Webb, S., and Lee, R. F. (2008). Detection of *Candidatus* Liberibacter asiaticus" in *Diaphorina citri* and its importance in the management of Citrus Huanglongbing in Florida. *Phytopathology* 98, 387–396. doi: 10.1094/PHYTO-98-4-0387

Martinelli, A. F., Uratsu, S. L., Albrecht, U., Reagan, R. L., Phu, M. P., Britton, M., et al. (2012). Transcriptome profiling of citrus fruit response to huanglongbing disease. *PLoS One* 7:e38039. doi: 10.1371/journal.pone.0038039

Mira, A., Ochman, H., and Moran, N. A. (2001). Deletional bias and the evolution of bacterial genomes. *Trends Genet.* 17, 589–596. doi: 10.1016/S0168-9525(01)02447-7

Miranda, M. P., and Ayres, A. J. (2020). "Asian citrus psyllid management in São Paulo, Brazil" in *Asian Citrus Psyllid: biology, Ecology and Management of Huanglongbing Vector*. eds Qureshi J., Stansly P.A. (Wallingford: CABI).

Mohamed, A. R., Chan, C. X., Ragan, M. A., Zhang, J., Cooke, I., Ball, E. E., et al. (2020). Comparative transcriptomic analyses of *Chromera* and Symbiodiniaceae. *Environ. Microbiol. Rep.* 12, 435–443. doi: 10.1111/1758-2229.12859

Munyaneza, J. E., Sengoda, V. G., Crosslin, J. M., Garzón-Tiznado, J. A., and Cardenas-Valenzuela, O. G. (2009). First report of "*Candidatus* Liberibacter solanacearum" in tomato plants in Mexico. *Plant Dis.* 93:552. doi: 10.1094/PDIS-93-10-1076A

Nakabachi, A., Nikoh, N., Oshima, K., Inoue, H., Ohkuma, M., Hongoh, Y., et al. (2013a). Horizontal gene acquisition of Liberibacter plant pathogens from a bacteriome-confined endosymbiont of their psyllid vector. *PloS One* 8:e82612. doi: 10.1371/journal.pone.0082612

Nakabachi, A., Ueoka, R., Oshima, K., Teta, R., Mangoni, A., Gurgui, M., et al. (2013b). Defensive bacteriome symbiont with a drastically reduced genome. *Curr. Biol.* 23, 1478–1484. doi: 10.1016/j.cub.2013.06.027

Naranjo, E., Merfa, M. V., Ferreira, V., Jain, M., Davis, M. J., Bahar, O., et al. (2019). *Liberibacter crescens* biofilm formation *in vitro*: establishment of a model system for pathogenic '*Candidatus* Liberibacter spp.'. *Sci. Rep.* 9:5150. doi: 10.1038/s41598-019-41495-5

Pelz-Stelinski, K. S., Brlansky, R. H., Ebert, T. A., and Rogers, M. E. (2010). Transmission parameters for *Candidatus* Liberibacter asiaticus by asian citrus psyllid (*Hemiptera: Psyllidae*). *J. Econ. Entomol.* 103, 1531–41. doi: 10.1603/EC10123

Porankiewicz, J., Wang, J., and Clarke, A. K. (1999). New insights into the ATP-dependent Clp protease: *escherichia coli* and beyond. *Mol. Microb.* 32, 449–458. doi: 10.1046/j.1365-2958.1999.01357.x

Prasad, S., Xu, J., Zhang, Y., and Wang, N. (2016). SEC-translocon dependent extracytoplasmic proteins of *Candidatus* Liberibacter asiaticus. *Front. Microbiol.* 7:1989. doi: 10.3389/fmicb.2016.01989

Sällsträm, B., and Andersson, G. E. (2005). Genome reduction in the α-*Proteobacteria*. *Curr. Opin. Microbiol.* 8, 579–585. doi: 10.1016/j.mib.2005.08.002

Selvaraj, V., Maheshwari, Y., Hareji, S., Chen, J., McCollum, T. G., and Yokomi, R. (2018). Development of a duplex droplet digital PCR assay for absolute quantitative detection of '*Candidatus* Liberibacter asiaticus'. *PLoS One* 13:e0197184. doi: 10.1371/journal.pone.0197184

Silva, P. A., Fassini, C. G., Sampaio, L. S., Dequigiovanni, G., Zucchi, M. A., and Wulff, N. A. (2019). Genetic diversity of *Candidatus* Liberibacter asiaticus revealed by short tandem repeats and prophages typing indicates population homogeneity in Brazil. *Phytophathology* 109, 960–971. doi: 10.1094/PHYTO-08-18-0295-R

Silva, P. A., Huang, J., Wulff, N. A., Zheng, Z., Krugner, R., and Chen, J. (2021). Genome sequence resource of '*Candidatus* Liberibacter asiaticus' strain 9PA from Brazil. *Plant Dis.* 105, 199–201. doi: 10.1094/PDIS-05-20-1018-A

Spero, M. A., Aylward, F. O., Currie, C. R., and Donohue, T. J. (2015). Phylogenomic analysis and predicted physiological role of the proton-translocating NADH:quinone oxidoreductase (Complex I) across bacteria. *mBio* 6, 389–315. doi: 10.1128/mBio.00389-15

Subandiyah, S., Nikoh, N., Tsuyumu, S., Somowiyarjo, S., and Fukatsu, T. (2000). Complex endosymbiotic microbiota of the citrus psyllid *Diaphorina citri* (*Homoptera: Psylloidea*). *Zool. Sci.* 17, 983–989. doi: 10.2108/zsj.17.983

Tatusov, R. M., Gasperim, M. Y., Natale, D. A., and Koonin, E. V. (2000). The COG database: a tool for genome-scale analysis of protein functions and evolution. *Nucl. Acid Res.* 28:1. doi: 10.1093/nar/28.1.33

Teixeira, D. C., Colette, S., Carole, C., Martins, E. C., Wulff, N. A., Jagoueix, S. E., et al. (2008). Distribution and quantification of *Candidatus* Liberibacter americanus, agent of Huanglongbing disease of citrus in São Paulo State, Brasil, in leaves of an affected sweet orange tree as determined by PCR. *Mol. Cell. Probes* 22, 139–150. doi: 10.1016/j.mcp.2007.12.006

Thapa, S. P., De Francesco, A., Trinh, J., Gurung, F. B., Pang, Z., Vidalakis, G., et al. (2020). Genome-wide analyses of Liberibacter species provides insights into evolution, phylogenetic relationships, and virulence factors. *Mol. Plant Pathol.* 21, 716–731. doi: 10.1111/mpp.12925

Tomimura, K., Miyata, S., Furuya, N., Kubota, K., Okud, A. M., Subandiyah, S., et al. (2009). Evaluation of genetic diversity among '*Candidatus* Liberibacter asiaticus' isolates collected in Southeast Asia. *Phytopathogy* 99, 1062–9. doi: 10.1094/PHYTO-99-9-1062

Ukuda-Hosokawa, R., Sodayama, Y., Kishaba, M., Kuriwada, T., Anbutsu, H., and Fukatsu, T. (2015). Infection density dynamics of the citrus greening bacterium "*Candidatus* Liberibacter asiaticus" in field populations of the psyllid *Diaphorina citri* and its relevance to the efficiency of pathogen transmission to citrus plants. *Appl. Environ. Microbiol.* 81, 3728–3736. doi: 10.1128/AEM.00707-15

Wairuri, C. K., Van der Waals, J. E., Van Schalkwyk, A., and Theron, J. (2012). *Ralstonia solanacearum* needs Flp Pili for virulence on potato. *Mol. Plant Microbe Interact.* 25, 546–556. doi: 10.1094/MPMI-06-11-0166

Wang, Y., Kondo, T., He, Y., Zhou, Z., and Lu, J. (2021). Genome sequence resource of '*Candidatus* Liberibacter asiaticus' from *Diaphorina citr*i Kuwayama (*Hemiptera: Liviidae*) in Colombia. *Plant Dis.* 105, 193–195. doi: 10.1094/PDIS-06-20-1249-A

Wulff, N. A., Daniel, B., Sassi, R. S., Moreira, A. S., Bassanezi, R. B., Sala, I., et al. (2020). Incidence of *Diaphorina citri* carrying *Candidatus* Liberibacter asiaticus in Brazil's citrus belt. *Insects* 11:672. doi: 10.3390/insects11100672

Wulff, N. A., Zhang, S., Setubal, J., Almeida, N. F., Martins, E. C., Harakava, R., et al. (2014). The complete genome sequence of *Candidatus* Liberibacter americanus, associated with citrus huanglongbing. *Mol. Plant Microbe Interact.* 27, 163–176. doi: 10.1094/MPMI-09-13-0292-R

Yan, Q., Sreedharan, A., Wei, S., Wang, J., Pelz-Stelinski, K., Folimonova, S., et al. (2013). Global gene expression changes in *Candidatus* Liberibacter asiaticus during the transmission in distinct host between plant and insects. *Mol. Plant Pathol.* 14, 391–404. doi: 10.1111/mpp.12015

Zhang, S., Flores-Cruz, Z., Zhou, L., Kang, B. H., Fleites, L. A., Gooch, M. D., et al. (2011). Ca. Liberibacter asiaticus' carries an excision plasmid prophage and a chromosomally integrated prophage that becomes lytic in plant infections. *Mol. Plant Microbe Interact.* 24, 458–468. doi: 10.1094/MPMI-11-10-0256

Zheng, Y., Huang, H., Huang, Z., Deng, X., Zheng, Z., and Xu, M. (2021). Prophage region and short tandem repeats of "*Candidatus* Liberibacter asiaticus" reveal significant population structure in China. *Plant Pathol.* 70, 959–969 doi: 10.1111/ppa.13332

Zheng, Z., Bao, M., Wu, F., Van Horn, C., Chen, J., and Deng, X. (2018). A type 3 prophage of '*Candidatus* Liberibacter asiaticus' carring a restricition-modification system. *Phytopathology* 108, 454–461. doi: 10.1094/PHYTO-08-17-0282-R

Zuñiga, C., Peacock, B., Liang, B., McCollum, G., Irigoyen, S. C., Tec-Campos, D., et al. (2020). Linking metabolic phenotypes to pathogenic traits among "*Candidatus* Liberibacter asiaticus" and its hosts. *Syst. Biol. Appl.* 6:24. doi: 10.1038/s41540-020-00142-w

Conflict of Interest: The authors declare that the research was conducted in the absence of any commercial or financial relationships that could be construed as a potential conflict of interest.

frontiers in Microbiology

MINI REVIEW
published: 22 July 2021
doi: 10.3389/fmicb.2021.700663

Potato Zebra Chip: An Overview of the Disease, Control Strategies, and Prospects

*Victoria Mora[1], Manikandan Ramasamy[1], Mona B. Damaj[1], Sonia Irigoyen[1], Veronica Ancona[2], Freddy Ibanez[1,3], Carlos A. Avila[1,4] and Kranthi K. Mandadi[1,5]**

[1] Texas A&M AgriLife Research and Extension Center, Weslaco, TX, United States, [2] Department of Agriculture, Agribusiness, and Environmental Sciences, Citrus Center, Texas A&M University-Kingsville, Weslaco, TX, United States, [3] Department of Entomology, Minnie Bell Heep Center, Texas A&M University, College Station, TX, United States, [4] Department of Horticultural Sciences, Texas A&M University, College Station, TX, United States, [5] Department of Plant Pathology and Microbiology, Texas A&M University, College Station, TX, United States

Potato (*Solanum tuberosum* L.) is an important food crop worldwide. As the demand for fresh and processed potato products is increasing globally, there is a need to manage and control devastating diseases such as zebra chip (ZC). ZC disease causes major yield losses in many potato-growing regions and is associated with the fastidious, phloem-limited bacterium *Candidatus* Liberibacter solanacearum (*C*Lso) that is vectored by the potato-tomato psyllid (*Bactericera cockerelli* Šulc). Current management measures for ZC disease mainly focus on chemical control and integrated pest management strategies of the psyllid vector to limit the spread of *C*Lso, however, they add to the costs of potato production. Identification and deployment of *C*Lso and/or the psyllid resistant cultivars, in combination with integrated pest management, may provide a sustainable long-term strategy to control ZC. In this review, we provide a brief overview of the ZC disease, epidemiology, current management strategies, and potential new approaches to manage ZC disease in the future.

Keywords: Fastidious bacteria, zebra chip, psyllids, *Candidatus* Liberibacter solanacearum, *Solanaceae*, Resistant varieties, crop improvement

OPEN ACCESS

Edited by:
Milko Alberto Jorquera, University of La Frontera, Chile

Reviewed by:
Gary Secor, North Dakota State University, United States
Jessica Vereijssen, The New Zealand Institute for Plant and Food Research Ltd, New Zealand
Karin Cruzado, University of Idaho, United States

***Correspondence:**
Kranthi K. Mandadi
kkmandadi@tamu.edu

Specialty section:
This article was submitted to Microbe and Virus Interactions with Plants, a section of the journal Frontiers in Microbiology

Received: *26 April 2021*
Accepted: *30 June 2021*
Published: *22 July 2021*

Citation:
Mora V, Ramasamy M, Damaj MB, Irigoyen S, Ancona V, Ibanez F, Avila CA and Mandadi KK (2021) Potato Zebra Chip: An Overview of the Disease, Control Strategies, and Prospects. Front. Microbiol. 12:700663. doi: 10.3389/fmicb.2021.700663

INTRODUCTION

Potatoes (*Solanum tuberosum* L.) constitute a centuries-old world dietary staple, with total world production estimated at 368.2 million tons in 2018 (Faostat, 2020). The United States is the fifth largest potato producer, after China, India, Russia, and Ukraine (Faostat, 2020), with an industry valued at ∼3.5 billion (USDA, 2019; Faostat, 2020). About one-third of United States grown potatoes are for processing, of which 63–83% are for frying, chipping and other packaged products, and the rest for fresh market, fodder, or used as seed (USDA, 2019). Potato domestication resulted in cultivars with reduced glycoalkaloid tuber content, making them more palatable and leading to increased tuber size and improved carbon fixation and transport (Spooner et al., 2014; Machida-Hirano, 2015). Few hardy wild potatoes were also crossed with their cultivated relatives to improve disease resistance, yield and quality for almost a century (Jansky et al., 2013). This yielded highly marketable improvements, like enhanced processing quality for chipping and frying, and resistance to some viruses and nematodes (Douches et al., 1996; Hirsch et al., 2013; Bethke et al., 2017). However, their low genetic diversity led to vulnerability to pests and diseases, and acute inbreeding depression.

EARLY REPORTS OF ZEBRA CHIP DISEASE

Zebra chip (ZC) disease was first reported in 1994 in Saltillo, Mexico, and later in South Texas, United States in 2000 (Munyaneza et al., 2007, 2009), The fastidious phloem-limited bacterium, *Candidatus* Liberibacter solanacearum (*C*Lso), was identified as a putative causal agent. *C*Lso is transmitted to plants by the potato-tomato psyllid *Bactericera cockerelli* Šulc (Munyaneza et al., 2007; Hansen et al., 2008; Liefting et al., 2009). Vegetative symptoms of ZC disease on plants include leaf chlorosis, discoloration, curling or upward rolling, aerial tubers, axillary bud proliferation, stunted growth, and eventually premature plant death (**Figure 1**). *C*Lso-infected potato tubers are often deformed and of poor quality, exhibiting collapsed stolons, vascular ring browning and brown flecks. When fried for chipping, the brown discoloration becomes darker, making chips bitter to taste, and unmarketable (**Figure 1D**; Secor and Rivera-Varas, 2004). Beyond North America, ZC disease is also documented in South America, New Zealand, and Australia (Hansen et al., 2008; Liefting et al., 2008a, 2009; Teulon et al., 2009; Crosslin et al., 2012; Munyaneza, 2012; Vereijssen et al., 2018).

Despite the relatively recent origins of ZC, potato psyllid infestation was first documented in peppers in Colorado, United States and was described as a potential pest in 1909 by Šulc (1909). The detrimental effects of psyllids were not fully noticed until 1927, when vast outbreaks of what was then described as psyllid yellows (PY) disease led to reduction of potato yields in Utah to the Rocky Mountain states of the United States (Linford, 1928; Richards, 1928). The description of the PY foliar symptoms (Arslan et al., 1985) was very similar to the foliar symptoms of ZC (Pitman et al., 2011; **Figure 1**). Although initially PY was thought to be associated with toxins released by psyllid feeding, so far, no other pathogens nor toxins have been associated with PY. Hence it led to a hypothesis that PY could be a mild case of ZC, wherein *C*Lso was present at low, undetectable levels in the affected plants (Richards and Blood, 1933; Carter, 1939; Arslan et al., 1985; Munyaneza et al., 2011; Monger and Jeffries, 2018).

Nevertheless today, the potato psyllid is considered an A1 quarantine pest by the EPPO (European and Mediterranean Plant Protection Organization), and as a primary vector for *C*Lso, together cause significant economic losses (PM, 2017).

*C*Lso-POTATO PSYLLID HOST RANGE, TRANSMISSION, AND DIAGNOSTICS

In addition to causing ZC disease on potatoes, *C*Lso can be transmitted to and infect other solanaceous crops such as tomato (*S. lycopersicum*), tomatillo (*Physalis* spp.), eggplant (*S. melongena*), pepper (*Capsicum* spp.), tobacco (*Nicotiana tabacum*), and tamarillo (*Solanum betaceum*; Hansen et al., 2008; Liefting et al., 2008b, 2009; Munyaneza et al., 2009, 2013, 2014; Aguilar et al., 2013). *B. cockerelli* is the main *C*Lso vector to infect these solanaceous crops in Mexico, United States, Central America (Guatemala, Honduras, and Nicaragua), Ecuador, Canada, New Zealand, and Australia (Liefting et al., 2008a; Munyaneza et al., 2009; Bextine et al., 2013; Thomas et al., 2018; Carrillo et al., 2019; Henrickson et al., 2019). Few wild solanaceous species can serve as a reservoir for both *B. cockerelli* and *C*Lso (Henne et al., 2010; Murphy et al., 2014; Vereijssen et al., 2015). Studies have found certain psyllid haplotypes (Northwestern Haplotype) can overwinter on natural vegetations such as bittersweet nightshade (*Solanum dulcamara* L.; Murphy et al., 2013, 2014; Horton et al., 2015) and can remerge in the Summer to infect agronomic crops. Similarly, in New Zealand, both *C*Lso and *B. cockerelli* were found on bittersweet nightshade and thorn-apple (*Datura stramonium*; Vereijssen et al., 2015). Further studies to determine specific *C*Lso haplotypes prevalent in the wild species and weedy plants will provide new insights into the significance of reservoir hosts in *C*Lso and ZC epidemiology (Bradshaw and Ramsay, 2005).

Feeding on infected plants is the main mode of *C*Lso acquisition by adult psyllids and nymphs (Buchman et al., 2011). After acquisition, there is a 2-week latent period before the infected psyllid is able to transmit the bacterium into new plant tissues (Sengoda et al., 2013). Upon feeding on a plant, it takes as little as 1 h for *C*Lso to be transmitted into plant tissues (Buchman et al., 2011). Subsequently, depending on the host plant, it can take approximately 3 weeks for the onset of ZC symptoms (Charkowski et al., 2020). Within an infected plant, *C*Lso is not evenly distributed and as such is present in low levels (Charkowski et al., 2020). Polymerase chain reaction (PCR) and/or quantitative PCR is the most widely used diagnostic approach for detecting *C*Lso in both the host plants and the psyllids, and can be used to distinguish the different haplotypes (Hansen et al., 2008; Secor et al., 2009; Swisher et al., 2012; Ananthakrishnan et al., 2013; Beard and Scott, 2013; Beard et al., 2013; Contreras-Rendón et al., 2020). Other emerging technologies such as Raman Spectroscopy are also being explored to detect ZC disease, that allows for rapid, non-invasive and in-field diagnostics (Farber et al., 2021).

*C*Lso HAPLOTYPES AND DIVERSITY

Twelve different *C*Lso haplotypes have been reported so far [A, B, C, D, F, G, H, H (Con), U, Cras1 and Cras2] (Wen et al., 2009; Munyaneza et al., 2010; Nelson et al., 2011, 2013; Teresani et al., 2014; Haapalainen et al., 2018, 2020; Mauck et al., 2019; Swisher Grimm and Garczynski, 2019; Contreras-Rendón et al., 2020; Sumner-Kalkun et al., 2020). In addition to *B. cockerelli,* other relatives in the Triozidae family (Hemiptera) transmit certain *C*Lso haplotypes. For example, haplotype C found in carrots is vectored by *Trioza apicalis* Förster (Munyaneza et al., 2010). Haplotypes D and E are transmitted by the carrot psyllid vector, *Bactericera trigonica* Hodkinson (Nelson et al., 2011; Swisher et al., 2014; Borges et al., 2017; Charkowski et al., 2020). While, *C*Lso haplotype U identified in northern Europe, is associated to *Trioza urticae* psyllid (Haapalainen et al., 2018). In the Americas, ZC disease is primarily associated with the haplotypes A, B, and F. *C*Lso A and B are transmitted by *B. cockerelli*, while the vector of haplotype F is still unknown

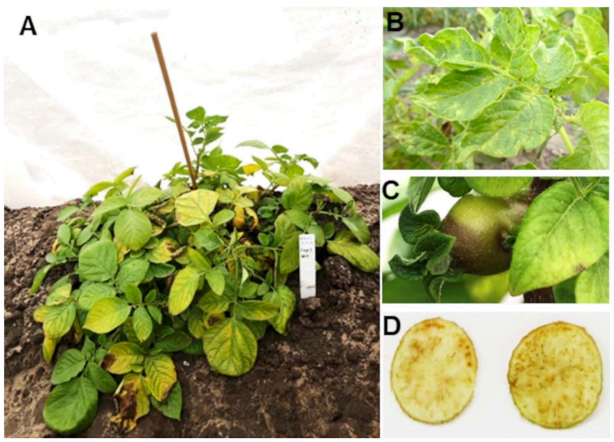

FIGURE 1 | Characteristic symptoms of zebra chip (ZC) disease. Infection of *Candidatus* Liberibacter solanacearum (CLso) often results in **(A,B)** chlorosis and upward curling/rolling of leaves, stunted plants, **(C)** aerial tuber growth, and **(D)** necrotic flecking/browning of tubers/chips and overall reduction of marketable yield.

(Hansen et al., 2008; Wen et al., 2009; Nelson et al., 2011; Swisher Grimm and Garczynski, 2019). In New Zealand and Norfolk Island (Australia) the *C*Lso haplotype A vectored by *B. cockerelli* interaction is considered the predominant haplotype causing ZC disease (Liefting et al., 2008a; Nelson et al., 2011; Thomas et al., 2018). Taken together, *C*Lso haplotypes A and B appear to be the most predominant across the world, in the Americas, New Zealand, and Australia, and associated with the ZC disease in potatoes (Rosson et al., 2006; Liefting et al., 2008a; Nelson et al., 2011; Thomas et al., 2018; Savary et al., 2019; Delgado et al., 2020).

Studies with *C*Lso haplotypes A and B showed that both haplotypes can infect plants either individually, or as co-infections (Harrison et al., 2019). Haplotype distribution and resulting effects on disease severity in single or co-infections were also studied in tomatoes and potatoes (Mendoza-Herrera et al., 2018; Harrison et al., 2019). For instance, infection of haplotype B is detrimental to tomato plants, as they usually die before fruit development, whereas plants can remain alive with symptoms when infected with haplotype A (Mendoza-Herrera et al., 2018). In potatoes, haplotype B induces greater ZC symptoms in tubers than haplotype A (Grimm et al., 2018), and dual-haplotype AB infections usually result in greater severe symptoms than infections with only haplotype B (Hernández-Deheza et al., 2018; Harrison et al., 2019). Interestingly, haplotype B seems to lower psyllid nymph survival rate, compared to those carrying haplotype A (Yao et al., 2016).

ZC CONTROL: PSYLLID MONITORING, CHEMICAL, BIOLOGICAL AND INTEGRATED PEST MANAGEMENT

Currently, a primary approach to manage ZC is by controlling the psyllid vector populations. Components of integrated pest management (IPM) such as chemical, cultural, and biocontrol strategies have been implemented worldwide (Vereijssen et al., 2018). Extensive monitoring and detection of psyllid population are also being used to determine psyllid movements (Butler and Trumble, 2012). Data gathered from monitoring psyllids on sweep nets are correlated with psyllid-vectored diseases in tomato fields (Pletsch, 1947; Cranshaw, 1994). Generally, psyllid infestations start along the perimeter of a field, moving toward the center as their population increases (Wallis, 1955; Cranshaw, 1994). Evidence of psyllid infestation can also be obtained by leaf examination, though tedious and time consuming (Pletsch, 1947; Goolsby et al., 2007). While, other studies have found sticky traps to be useful for monitoring psyllid populations, even at low densities (Goolsby et al., 2007).

For psyllid control, pesticide use has been the main course of action in several regions. Typical pest management guidelines for potato psyllids include the application of neonicotinoids like imidacloprid and thiamethoxam at planting as a seed treatment, with a subsequent foliar application to control adults and nymphs (Prager et al., 2013; Vereijssen et al., 2015; Nuñez et al., 2019). Unfortunately, excessive use of pesticides led to incidences of neonicotinoid resistance in Southwestern United States, South Texas, and Northern Mexico (Prager et al., 2013; Chávez et al., 2015; Szczepaniec et al., 2019). As such pesticide reliance is both economically and environmentally unsustainable.

Some cultural methods for the control of psyllids have also been tested. Such as by using certified clean seed, and planting non-host plants in crop rotations to maintain disease free planting areas (Vereijssen et al., 2018). In warmer climates such as in Southern United States, planting dates could be altered to delay exposure to potato psyllids (Guenthner et al., 2012). Few organic farmers have also found some success using physical barriers such as mesh covers to lower psyllid infestations (Merfield et al., 2015).

Lastly, biocontrol strategies have also been employed. Natural enemies of the psyllid, such as ectoparasitoids, coccinellids, and entomopathogenic fungi have shown promising effects against psyllids, by parasitizing them at multiple life stages, in greenhouse and laboratory studies (Al-Jabr, 1999; MacDonald et al., 2010; Lacey et al., 2011; Walker et al., 2011; Mauchline and Stannard, 2013; Rojas et al., 2015). Deployment of such natural enemies as biocontrol agents in greenhouse production systems (e.g., tomato) or in the field-scale (e.g., potato) could allow growing an earlier crop and reduce reliance on insecticides.

HOST PLANT RESISTANCE AND BREEDING STRATEGIES FOR ZC RESISTANCE

Efforts were made to study host plant resistance toward developing ZC resistant potato cultivars. Plants employ different mechanisms to protect themselves against pathogens and insects. Some host-plant resistance mechanisms are constitutive, such as physical or pre-formed structural barriers and release of chemicals that disrupt pathogen transmission, insect feeding, and oviposition. Other plant defenses, such as volatile compounds emission or upregulation of resistance genes can also be triggered

in response to a pest or pathogen (Dicke and Van Poecke, 2002; War et al., 2012). The host resistance mechanisms to pests can also be categorized as antixenosis and antibiosis. Generally, antixenosis refers to a deterring effect that plants can have on insect behavior, where antibiosis affects their lifecycle and reproduction (Painter, 1951; Kogan and Ortman, 1978; Smith, 2005).

In the case of ZC, several varieties of potato and potato hybrids were identified to possess some degree of tolerance to ZC disease. In some varieties, tolerance was attributed to the antixenotic effects of glandular trichomes (Butler et al., 2011; Diaz-Montano et al., 2014; Rubio-Covarrubias et al., 2017). While few varieties appear to have a genetic basis for tolerance to *C*Lso in addition to having effects on the psyllid behavior (Rashidi et al., 2017; Fife et al., 2020). Recently, few wild-relatives of tomato, *S. pennelli*, and *S. corneliomulleri* were identified to possess resistance to *B. cockerelli* (Avila et al., 2019), with several quantitative trait loci (QTL) associated with insect mortality and lower fecundity in *S. habrochaites*. Such QTL in wild species could be a valuable source for breeding resistance to cultivars, however, their complex inheritance, modes of action, and pathogen-vector-host interactions require further characterization.

FUTURE PROSPECTS AND STRATEGIES FOR ZC RESISTANCE

In the past, lack of advanced genomic tools, combined with the cost effectiveness of chemical control strategies led to heavy reliance on pesticides, rather than prioritizing the development of new resistance varieties to pests/pathogens (Rowe, 1992; Spooner and Bamberg, 1994). However, recent advances in genomics and genetics resources (Varshney et al., 2005; Broekgaarden et al., 2011) including those for potato[1], should help in identifying desirable traits, alleles, and marker development to develop new ZC resistance cultivars. For instance, the availability of the potato reference genome sequence, the discovery of SNPs in elite North American potato germplasm and the development of the Infinium 8,303 potato array have helped in identification of genes linked to improved agronomic traits (Hamilton et al., 2011; Massa et al., 2011; Felcher et al., 2012). The resources also enabled marker-assisted selection (MAS), which helps identify markers tightly linked to a target locus, instead of relying on phenotypic selection alone in making selections for crosses. Thus, MAS can be used to accelerate introgression of desirable ZC tolerance traits from various potato breeding clones or wild species into cultivar development. Several studies showed the potential of improving potato traits by increasing heterozygosity and genetic diversity of parental clones (Mendoza and Haynes, 1974; Bradshaw and Ramsay, 2005; Jansky and Peloquin, 2006). Thus, more focus will need to be given for identification and introgression of alleles from a diverse pool of genetic resources, including wild species, landraces, and cultivated potatoes (Bethke et al., 2019).

Introgression of desirable traits from related or distant species to cultivated potatoes using genetic engineering (GE) can be a viable alternative to speed cultivar development and reduce introgression of undesirable genetic material or traits (Halterman et al., 2016). Few example, GE potatoes that received United States regulatory approval include the "NewLeaf" Bt potatoes for resistance against Colorado beetle (*Leptinotarsa decemlineata*), "Innate^{TM}" potatoes with resistance to fungal disease (late blight) and acrylamide formation[2] (Halterman et al., 2016). Despite the significant advantages of GE crops, the costs associated with R&D and regulatory approval is tremendous and necessitates private sector investments, or public-private partnership. Furthermore, the GE products face marketing hurdles due to public skepticism (Halterman et al., 2016).

Selected traits can also be modified/introduced by genome editing technologies such as TALEN or CRISPR-Cas9 without introducing new foreign DNA (Wolt et al., 2016; Hameed et al., 2018). Derived plant products potentially face less regulatory scrutiny and approval burden. For instance, the United States regulatory body (USDA APHIS) determined that several transgene-free, genome-edited potato plants with disease resistance and other superior agronomic traits, would not be considered regulated under 7 CFR part 340 (Wolt et al., 2016). Although this does not preclude regulation by other agencies world-wide, it is nevertheless a significant advantage when it comes to commercialization.

CONCLUSION

Since its first report in 1994, ZC disease is now established in several potato producing regions worldwide. The putative causal agent, *C*Lso, can also infect other economically significant *Solanaceae* crops, thus posing an even more threat to the agricultural industry. IPM strategies (chemical, cultural, and biological control) have been implemented to manage psyllid vector population and limit ZC disease. However, we still need long-term solutions. Recent developments in potato genetic resources and crop improvement technologies could be further leveraged for developing new potato cultivars with genetic resistance to the psyllid and/or *C*Lso. In combination with IPM practices, the ZC resistant or tolerant cultivars could be deployed in the future to effectively manage ZC disease.

AUTHOR CONTRIBUTIONS

KM supervised the study. All others contributed to the preparation and editing of the review.

FUNDING

This study was supported by funds from Texas A&M AgriLife Research Insect-Vectored Disease Seed Grant (124190-96210), USDA-NIFA-AFRI (2018-70016-28198; HATCH 1023984), and Foundation for Food and Agricultural Research New Innovator Award (534299) to KM.

[1]http://solcap.msu.edu/; https://www.polyploids.org/

[2]https://apnews.com/article/1d3c790ad18f4e828598ccf44ec047bf

REFERENCES

Aguilar, E., Sengoda, V., Bextine, B., Mccue, K., and Munyaneza, J. (2013). First report of "*Candidatus* Liberibacter solanacearum" on tobacco in Honduras. *Plant Dis.* 97, 1376–1376. doi: 10.1094/pdis-04-13-0453-pdn

Al-Jabr, A. M. (1999). *Integrated Pest Management of Tomato/Potato Psyllid, Paratrioza Cockerelli (Sulc)(Homoptera: Psyllidae) with Emphasis on its Importance in Greenhouse Grown Tomatoes*. United States: Colorado State University.

Ananthakrishnan, G., Choudhary, N., Roy, A., Sengoda, V., Postnikova, E., Hartung, J., et al. (2013). Development of primers and probes for genus and species specific detection of '*Candidatus* Liberibacter species' by real-time PCR. *Plant Dis.* 97, 1235–1243. doi: 10.1094/pdis-12-12-1174-re

Arslan, A., Bessey, P. M., Matsuda, K., and Oebker, N. F. (1985). Physiological effects of psyllid (*Paratrioza cockerelli*) on potato. *Am. Potato J.* 62, 9–22. doi: 10.1007/bf02871295

Avila, C. A., Marconi, T. G., Viloria, Z., Kurpis, J., and Del Rio, S. Y. (2019). *Bactericera cockerelli* resistance in the wild tomato *Solanum habrochaites* is polygenic and influenced by the presence of *Candidatus* Liberibacter solanacearum. *Sci. Rep.* 9, 1–11.

Beard, S. S., Pitman, A. R., Kraberger, S., and Scott, I. A. W. (2013). SYBR Green real-time quantitative PCR for the specific detection and quantification of '*Candidatus* Liberibacter solanacearum' in field samples from New Zealand. *Eur. J. Plant Pathol.* 136, 203–215. doi: 10.1007/s10658-012-0156-5

Beard, S. S., and Scott, I. A. (2013). A rapid method for the detection and quantification of the vector-borne bacterium '*Candidatus* Liberibacter solanacearum'in the tomato potato psyllid, *Bactericera cockerelli*. *Entomol. Exp. Appl.* 147, 196–200. doi: 10.1111/eea.12056

Bethke, P. C., Halterman, D. A., and Jansky, S. (2017). Are we getting better at using wild potato species in light of new tools? *Crop Sci.* 57, 1241–1258. doi: 10.2135/cropsci2016.10.0889

Bethke, P. C., Halterman, D. A., and Jansky, S. H. (2019). Potato germplasm enhancement enters the genomics era. *Agron. J.* 9:575. doi: 10.3390/agronomy9100575

Bextine, B., Aguilar, E., Rueda, A., Caceres, O., Sengoda, V., Mccue, K., et al. (2013). First report of "*Candidatus* Liberibacter solanacearum" on tomato in El Salvador. *Plant Dis.* 97, 1245–1245. doi: 10.1094/pdis-03-13-0248-pdn

Borges, K. M., Cooper, W. R., Garczynski, S. F., Thinakaran, J., Jensen, A. S., Horton, D. R., et al. (2017). "*Candidatus* Liberibacter solanacearum" associated with the psyllid, *Bactericera maculipennis* (Hemiptera: Triozidae). *Environ. Entomol.* 46, 210–216.

Bradshaw, J. E., and Ramsay, G. (2005). Utilisation of the commonwealth potato collection in potato breeding. *Euphytica* 146, 9–19. doi: 10.1007/s10681-005-3881-4

Broekgaarden, C., Snoeren, T. A., Dicke, M., and Vosman, B. (2011). Exploiting natural variation to identify insect-resistance genes. *Plant Biotechnol. J.* 9, 819–825. doi: 10.1111/j.1467-7652.2011.00635.x

Buchman, J. L., Heilman, B. E., and Munyaneza, J. E. (2011). Effects of liberibacter-infective *Bactericera cockerelli* (*Hemiptera: Triozidae*) density on zebra chip potato disease incidence, potato yield, and tuber processing quality. *J. Econ. Entomol.* 104, 1783–1792. doi: 10.1603/ec11146

Butler, C. D., Gonzalez, B., Manjunath, K. L., Lee, R. F., Novy, R. G., Miller, J. C., et al. (2011). Behavioral responses of adult potato psyllid, *Bactericera cockerelli* (Hemiptera: Triozidae), to potato germplasm and transmission of Candidatus Liberibacter psyllaurous. *J. Crop Prot.* 30, 1233–1238. doi: 10.1016/j.cropro.2011.05.006

Butler, C. D., and Trumble, J. T. (2012). The potato psyllid, *Bactericera cockerelli* (Sulc)(Hemiptera: Triozidae): life history, relationship to plant diseases, and management strategies. *Terr. Arthropod. Rev.* 5, 87–111. doi: 10.1163/187498312x634266

Carrillo, C. C., Fu, Z., and Burckhardt, D. (2019). First record of the tomato potato psyllid *Bactericera cockerelli* from South America. *Bull. Insectol.* 72, 85–91.

Carter, W. (1939). Injuries to plants caused by insect toxins. *Bot. Rev.* 5:273. doi: 10.1007/bf02878504

Charkowski, A., Sharma, K., Parker, M. L., Secor, G. A., and Elphinstone, J. (2020). "Bacterial diseases of potato" in *The Potato Crop*. eds H. Campos, O. Ortiz. (Germany: Springer). 351–388. doi: 10.1007/978-3-030-28683-5_10

Chávez, E. C., Bautista, O. H., Flores, J. L., Uribe, L. A., and Fuentes, Y. M. O. (2015). Insecticide-resistance ratios of three populations of *Bactericera cockerelli* (*Hemiptera*: *Psylloidea*: *Triozidae*) in regions of northern Mexico. *Fla. Entomol.* 98, 950–953. doi: 10.1653/024.098.0322

Contreras-Rendón, A., Sánchez-Pale, J. R., Fuentes-Aragón, D., Alanís-Martínez, I., and Silva-Rojas, H. V. (2020). Conventional and qPCR reveals the presence of '*Candidatus* Liberibacter solanacearum'haplotypes A, and B in *Physalis philadelphica* plant, seed, and B*actericera cockerelli* psyllids, with the assignment of a new haplotype H in Convolvulaceae. *Antonie Van Leeuwenhoek* 113, 533–551. doi: 10.1007/s10482-019-01362-9

Cranshaw, W. (1994). "The potato (tomato) psyllid, Paratrioza cockerelli (Sulc), as a pest of potatoes" in *Advances in Potato Pest Biology and Management*. eds G.W. Zehnder, M.L. Powelson, R.K. Hansson, and K.V. Raman. (St. Paul, MN: APS Press). 83–95.

Crosslin, J., Hamm, P., Eggers, J., Rondon, S., Sengoda, V., and Munyaneza, J. (2012). First report of zebra chip disease and "*Candidatus Liberibacter solanacearum*" on potatoes in Oregon and Washington State. *Plant Dis.* 96, 452. doi: 10.1094/pdis-10-11-0894

Delgado, L., Schuster, M., and Torero, M. (2020). Quantity and quality food losses across the value chain: a comparative analysis. *Food Policy* 98:101958. doi: 10.1016/j.foodpol.2020.101958

Diaz-Montano, J., Vindiola, B. G., Drew, N., Novy, R. G., Miller, J. C., and Trumble, J. T. (2014). Resistance of selected potato genotypes to the potato psyllid (*Hemiptera*: *Triozidae*). *Am. J. Pot. Res.* 91, 363–367. doi: 10.1007/s12230-013-9356-6

Dicke, M., and Van Poecke, R. M. (2002). Signalling in plant-insect interactions: signal transduction in direct and indirect plant defence. *J. Signal Transduct.* 289:316.

Douches, D., Maas, D., Jastrzebski, K., and Chase, R. (1996). Assessment of potato breeding progress in the USA over the last century. *Crop Sci.* 36, 1544–1552. doi: 10.2135/cropsci1996.0011183x003600060024x

Faostat, F. (2020). *FAOSTAT*. Available online at: http://www.fao.org/faostat/en/#data/QC [Accessed May 04, 2020]

Farber, C., Sanchez, L., Pant, S., Scheuring, D., Vales, I., Mandadi, K., et al. (2021). Potential of spatially offset Raman Spectroscopy for detection of Zebra Chip and Potato Virus Y diseases of potatoes (*Solanum tuberosum*). *ACS Agric. Sci. Technol.* 1, 211–221. doi: 10.1021/acsagscitech.1c00024

Felcher, K. J., Coombs, J. J., Massa, A. N., Hansey, C. N., Hamilton, J. P., Veilleux, R. E., et al. (2012). Integration of two diploid potato linkage maps with the potato genome sequence. *PLoS One* 7:e36347. doi: 10.1371/journal.pone.0036347

Fife, A. N., Cruzado, K., Rashed, A., Novy, R. G., and Wenninger, E. J. (2020). Potato Psyllid (*Hemiptera*: *Triozidae*) Behavior on Three Potato Genotypes With Tolerance to '*Candidatus* Liberibacter solanacearum'. *J. Insect Sci.* 20:15.

Goolsby, J. A., Adamczyk, J., Bextine, B., Lin, D., Munyaneza, J. E., and Bester, G. (2007). Development of an IPM program for management of the potato psyllid to reduce incidence of zebra chip disorder in potatoes. *Subtrop. Plant Sci.* 59, 85–94.

Grimm, K. D. S., Mustafa, T., Cooper, W. R., and Munyaneza, J. E. (2018). Role of '*Candidatus* Liberibacter solanacearum'and *Bactericera cockerelli* haplotypes in zebra chip incidence and symptom severity. *Am. J. Potato Res.* 95, 709–719. doi: 10.1007/s12230-018-9678-5

Guenthner, J., Goolsby, J., and Greenway, G. (2012). Use and cost of insecticides to control potato psyllids and zebra chip on potatoes. *Southwest. Entomol.* 37, 263–268. doi: 10.3958/059.037.0302

Haapalainen, M., Latvala, S., Wickström, A., Wang, J., Pirhonen, M., and Nissinen, A. I. (2020). A novel haplotype of '*Candidatus* Liberibacter solanacearum'found in Apiaceae and Polygonaceae family plants. *Eur. J. Plant Pathol.* 156, 413–423. doi: 10.1007/s10658-019-01890-0

Haapalainen, M., Wang, J., Latvala, S., Lehtonen, M. T., Pirhonen, M., and Nissinen, A. (2018). Genetic variation of '*Candidatus* Liberibacter solanacearum'haplotype C and identification of a novel haplotype from *Trioza urticae* and stinging nettle. *Phytopathology* 108, 925–934. doi: 10.1094/phyto-12-17-0410-r

Halterman, D., Guenthner, J., Collinge, S., Butler, N., and Douches, D. (2016). Biotech potatoes in the 21st century: 20 years since the first biotech potato. *Am. J. Pot. Res.* 93, 1–20. doi: 10.1007/s12230-015-9485-1

Hameed, A., Zaidi, S. S.-E.-A., Shakir, S., and Mansoor, S. (2018). Applications of new breeding technologies for potato improvement. *Front. Plant Sci.* 9:925. doi: 10.3389/fpls.2018.00925

Hamilton, J. P., Hansey, C. N., Whitty, B. R., Stoffel, K., Massa, A. N., Van Deynze, A., et al. (2011). Single nucleotide polymorphism discovery in elite North American potato germplasm. *BMC Genom.* 12:302. doi: 10.1186/1471-2164-12-302

Hansen, A. K., Trumble, J., Stouthamer, R., and Paine, T. (2008). A new huanglongbing species,"*Candidatus* Liberibacter psyllaurous," found to infect tomato and potato, is vectored by the psyllid *Bactericera cockerelli* (Sulc). *Appl. Environ. Microbiol.* 74, 5862–5865. doi: 10.1128/aem.01268-08

Harrison, K., Tamborindeguy, C., Scheuring, D. C., Herrera, A. M., Silva, A., Badillo-Vargas, I. E., et al. (2019). Differences in Zebra Chip severity between '*Candidatus* Liberibacter solanacearum'haplotypes in Texas. *Am. J. Potato Res.* 96, 86–93. doi: 10.1007/s12230-018-9692-7

Henne, D., Paetzold, L., Workneh, F., and Rush, C. (2010). "Evaluation of potato psyllid cold tolerance, overwintering survival, sticky trap sampling, and effects of Liberibacter on potato psyllid alternate host plants" in *Proceedings 10th Annual Zebra Chip Reporting Session*. (Dallas: Hyatt DFW Airport).

Henrickson, A., Kalischuk, M., Lynn, J., Meers, S., Johnson, D., and Kawchuk, L. (2019). First report of zebra chip on potato in Canada. *Plant Dis.* 103, 1016–1016. doi: 10.1094/pdis-09-18-1576-pdn

Hernández-Deheza, M. G., Rojas-Martínez, R. I., Rivera-Peña, A., Zavaleta-Mejía, E., Ochoa-Martínez, D. L., and Carrillo-Salazar, A. (2018). Resistance in potato to two haplotypes of '*Candidatus* Liberibacter solanacearum'. *Plant Pathol. J.* 100, 191–196. doi: 10.1007/s42161-018-0046-6

Hirsch, C. N., Hirsch, C. D., Felcher, K., Coombs, J., Zarka, D., Van Deynze, A., et al. (2013). Retrospective view of North American potato (*Solanum tuberosum* L.) breeding in the 20th and 21st centuries. *G3* 3, 1003–13. doi: 10.1534/g3.113.005595

Horton, D. R., Cooper, W. R., Munyaneza, J. E., Swisher, K. D., Echegaray, E. R., Murphy, A. F., et al. (2015). A new problem and old questions: potato psyllid in the Pacific Northwest. *Am. Entomol.* 61, 234–244. doi: 10.1093/ae/tmv047

Jansky, S., Dempewolf, H., Camadro, E. L., Simon, R., Zimnoch-Guzowska, E., Bisognin, D., et al. (2013). A case for crop wild relative preservation and use in potato. *Crop Sci.* 53, 746–754. doi: 10.2135/cropsci2012.11.0627

Jansky, S. H., and Peloquin, S. J. (2006). Advantages of wild diploid *Solanum species* over cultivated diploid relatives in potato breeding programs. *Genet. Resour. Crop Evol.* 53, 669–674. doi: 10.1007/s10722-004-2949-7

Kogan, M., and Ortman, E. F. (1978). Antixenosis–a new term proposed to define Painter's "nonpreference" modality of resistance. *Bull. Ecol. Soc. Am.* 24, 175–176. doi: 10.1093/besa/24.2.175

Lacey, L., Liu, T.-X., Buchman, J., Munyaneza, J., Goolsby, J., and Horton, D. (2011). Entomopathogenic fungi (Hypocreales) for control of potato psyllid, *Bactericera cockerelli* (Šulc)(*Hemiptera*: *Triozidae*) in an area endemic for zebra chip disease of potato. *Biol. Control* 56, 271–278. doi: 10.1016/j.biocontrol.2010.11.012

Liefting, L., Perez-Egusquiza, Z., Clover, G., and Anderson, J. (2008a). A new '*Candidatus* Liberibacter'species in *Solanum tuberosum* in New Zealand. *Plant Dis.* 92, 1474–1474. doi: 10.1094/pdis-92-10-1474a

Liefting, L., Ward, L., Shiller, J., and Clover, G. (2008b). A new '*Candidatus* Liberibacter'species in *Solanum betaceum* (tamarillo) and *Physalis peruviana* (cape gooseberry) in New Zealand. *Plant Dis.* 92, 1588–1588. doi: 10.1094/pdis-92-11-1588b

Liefting, L. W., Sutherland, P. W., Ward, L. I., Paice, K. L., Weir, B. S., and Clover, G. R. (2009). A new '*Candidatus* Liberibacter'species associated with diseases of solanaceous crops. *Plant Dis.* 93, 208–214. doi: 10.1094/pdis-93-3-0208

Linford, M. (1928). Psyllid-yellows (cause undetermined). *Plant Dis. Rep. Suppl.* 59, 95–99.

MacDonald, F., Walker, G., Larsen, N., and Wallace, A. (2010). Naturally occurring predators of *Bactericera cockerelli* in potatoes. *N. Z. Plant Prot.* 63, 275–275. doi: 10.30843/nzpp.2010.63.6583

Machida-Hirano, R. (2015). Diversity of potato genetic resources. *Breed. sci.* 65, 26–40. doi: 10.1270/jsbbs.65.26

Massa, A. N., Childs, K. L., Lin, H., Bryan, G. J., Giuliano, G., and Buell, C. R. (2011). The transcriptome of the reference potato genome *Solanum tuberosum* Group Phureja clone DM1-3 516R44. *PLoS One* 6:e26801. doi: 10.1371/journal.pone.0026801

Mauchline, N., and Stannard, K. (2013). Evaluation of selected entomopathogenic fungi and bioinsecticides against *Bactericera cockerelli* (Hemiptera). *N. Z. Plant Prot.* 66, 324–332. doi: 10.30843/nzpp.2013.66.5707

Mauck, K. E., Sun, P., Meduri, V. R., and Hansen, A. K. (2019). New Ca. Liberibacter psyllaurous haplotype resurrected from a 49-year-old specimen of *Solanum umbelliferum*: a native host of the psyllid vector. *Sci. Rep.* 9, 1–13.

Mendoza, H., and Haynes, F. (1974). Genetic basis of heterosis for yield in the autotetraploid potato. *Theor. Appl. Genet.* 45, 21–25. doi: 10.1007/bf00281169

Mendoza-Herrera, A., Levy, J., Harrison, K., Yao, J., Ibanez, F., and Tamborindeguy, C. (2018). Infection by *Candidatus* Liberibacter solanacearum'haplotypes A and B in *Solanum lycopersicum* 'Moneymaker'. *Plant Dis.* 102, 2009–2015. doi: 10.1094/pdis-12-17-1982-re

Merfield, C., Geary, I., Hale, R., and Hodge, S. (2015). Field evaluation of the effectiveness of mesh crop covers for the protection of potatoes from tomato potato psyllid. *N. Z. J. Crop Hortic. Sci.* 43, 123–133. doi: 10.1080/01140671.2015.1015576

Monger, W. A., and Jeffries, C. J. (2018). A survey of '*Candidatus* Liberibacter solanacearum'in historical seed from collections of carrot and related *Apiaceae* species. *Eur. J. Plant Pathol.* 150, 803–815. doi: 10.1007/s10658-017-1322-6

Munyaneza, J., Buchman, J., Heilman, B., Sengoda, V., and Henne, D. (2011). "Effects of zebra chip and potato psyllid on potato seed quality" in *11th Annual Zebra Chip Reporting Session*. (TX: San Antonio)6–9.

Munyaneza, J., Crosslin, J., and Upton, J. (2007). Association of *Bactericera cockerelli* (*Homoptera*: *Psyllidae*) with "zebra chip," a new potato disease in southwestern United States and Mexico. *J. Econ. Entomol.* 100, 656–663. doi: 10.1093/jee/100.3.656

Munyaneza, J., Fisher, T., Sengoda, V., Garczynski, S., Nissinen, A., and Lemmetty, A. (2010). First report of" *Candidatus* Liberibacter solanacearum" associated with psyllid-affected carrots in Europe. *Plant Dis.* 94:639. doi: 10.1094/pdis-94-5-0639a

Munyaneza, J., Sengoda, V., Aguilar, E., Bextine, B., and Mccue, K. (2013). First report of '*Candidatus* Liberibacter solanacearum' infecting eggplant in Honduras. *Plant Dis.* 97, 1654–1654. doi: 10.1094/pdis-06-13-0641-pdn

Munyaneza, J., Sengoda, V., Aguilar, E., Bextine, B., and Mccue, K. (2014). First report of 'Candidatus Liberibacter solanacearum'on pepper in Honduras. *Plant Dis.* 98, 154–154. doi: 10.1094/pdis-06-13-0598-pdn

Munyaneza, J., Sengoda, V., Crosslin, J., Garzon-Tiznado, J., and Cardenas-Valenzuela, O. (2009). First report of "*Candidatus* Liberibacter solanacearum" in tomato plants in Mexico. *Plant Dis.* 93, 1076–1076. doi: 10.1094/pdis-93-10-1076a

Munyaneza, J. E. (2012). Zebra chip disease of potato: biology, epidemiology, and management. *Am. J. Pot. Res.* 89, 329–350. doi: 10.1007/s12230-012-9262-3

Murphy, A., Cating, R., Goyer, A., Hamm, P., and Rondon, S. (2014). First report of natural infection by '*Candidatus* Liberibacter solanacearum'in bittersweet nightshade (*Solanum dulcamara*) in the Columbia Basin of Eastern Oregon. *Plant Dis.* 98, 1425–1425. doi: 10.1094/pdis-05-14-0497-pdn

Murphy, A. F., Rondon, S. I., and Jensen, A. S. (2013). First report of potato psyllids, *Bactericera cockerelli*, overwintering in the Pacific Northwest. *Am. J. Pot. Res.* 90, 294–296. doi: 10.1007/s12230-012-9281-0

Nelson, W. R., Fisher, T. W., and Munyaneza, J. E. (2011). Haplotypes of "*Candidatus* Liberibacter solanacearum" suggest long-standing separation. *Eur. J. Plant Pathol.* 130, 5–12. doi: 10.1007/s10658-010-9737-3

Nelson, W. R., Sengoda, V. G., Alfaro-Fernandez, A. O., Font, M. I., Crosslin, J. M., and Munyaneza, J. E. (2013). A new haplotype of "*Candidatus* Liberibacter solanacearum" identified in the Mediterranean region. *Eur. J. Plant Pathol.* 135, 633–639. doi: 10.1007/s10658-012-0121-3

Nuñez, J. H. D., Aegerter, B. J., Baldwin, R. A., Westerdahl, B. B., Trumble, J. T., and Wilson, R. G. (2019). *UC IPM Pest Management Guidelines: Potato*. United States: University of California.

Painter, R. H. (1951). *Insect Resistance in Crop Plants*. United States: LWW.

Pitman, A. R., Drayton, G. M., Kraberger, S. J., Genet, R. A., and Scott, I. A. (2011). Tuber transmission of '*Candidatus* Liberibacter solanacearum' and its association with zebra chip on potato in New Zealand. *Euro. J. Plant Patho.* 129, 389–398. doi: 10.1007/s10658-010-9702-1

Pletsch, D. J. (1947). The potato psyllid, *Paratrioza cockerelli* (Sulc), its biology and control. *Bull. Mont. agric. Exp. Stn.* 446:95.

PM. (2017). 9/25 (1) *Bactericera cockerelli* and '*Candidatus* Liberibacter solanacearum'. *EPPO Bull.* 47, 513–523. doi: 10.1111/epp.12442

Prager, S. M., Vindiola, B., Kund, G. S., Byrne, F. J., and Trumble, J. T. (2013). Considerations for the use of neonicotinoid pesticides in management of *Bactericera cockerelli* (Šulk)(*Hemiptera*: *Triozidae*). *J. Crop Prot.* 54, 84–91. doi: 10.1016/j.cropro.2013.08.001

Rashidi, M., Novy, R. G., Wallis, C. M., and Rashed, A. (2017). Characterization of host plant resistance to zebra chip disease from species-derived potato genotypes and the identification of new sources of zebra chip resistance. *PLoS One*:12:e0183283. doi: 10.1371/journal.pone.0183283

Richards, B. (1928). A new and destructive disease of the potato in Utah and its relation to the potato psylla. *Phytopathology* 18, 140–141.

Richards, B., and Blood, H. (1933). Psyllid yellows of the potato. *J. Agric. Res.* 46, 189–216.

Rojas, P., Rodríguez-Leyva, E., Lomeli-Flores, J. R., and Liu, T.-X. (2015). Biology and life history of *Tamarixia triozae*, a parasitoid of the potato psyllid *Bactericera cockerelli*. *Biol. Control* 60, 27–35. doi: 10.1007/s10526-014-9625-4

Rosson, P., Niemeyer, M., Palma, M., and Ribera, L. (2006). *Economic Impacts of Zebra Chips on the Texas Potato Industry center for North American Studies*. United States: Texas A&M University.

Rowe, R. C. (1992). Future challenges in managing potato health. *Am. Potato J.* 69, 769–775. doi: 10.1007/bf02853818

Rubio-Covarrubias, O., Cadena-Hinojosa, M., Prager, S., Wallis, C., and Trumble, J. (2017). Characterization of the tolerance against zebra chip disease in tubers of advanced potato lines from Mexico. *Am. J. Pot. Res.* 94, 342–356. doi: 10.1007/s12230-017-9570-8

Savary, S., Willocquet, L., Pethybridge, S. J., Esker, P., Mcroberts, N., and Nelson, A. (2019). The global burden of pathogens and pests on major food crops. *Nat. Ecol. Evol.* 3, 430–439. doi: 10.1038/s41559-018-0793-y

Secor, G., Rivera, V., Abad, J., Lee, I.-M., Clover, G., Liefting, L., et al. (2009). Association of '*Candidatus* Liberibacter solanacearum'with zebra chip disease of potato established by graft and psyllid transmission, electron microscopy, and PCR. *Plant Dis.* 93, 574–583. doi: 10.1094/pdis-93-6-0574

Secor, G. A., and Rivera-Varas, V. V. (2004). Emerging diseases of cultivated potato and their impact on Latin America. *Rev. Latinoamericana Papa* 1, 1–8.

Sengoda, V. G., Buchman, J. L., Henne, D. C., Pappu, H. R., and Munyaneza, J. E. (2013). "*Candidatus* Liberibacter solanacearum" titer over time in *Bactericera cockerelli* (*Hemiptera*: *Triozidae*) after acquisition from infected potato and tomato plants. *J. Econ. Entomol.* 106, 1964–1972. doi: 10.1603/ec13129

Smith, C. M. (2005). *Plant Resistance to Arthropods: Molecular and Conventional Approaches*. Netherlands: Springer.

Spooner, D. M., and Bamberg, J. B. (1994). Potato genetic resources: sources of resistance and systematics. *Am. J. Bot.* 71, 325–337. doi: 10.1007/bf02849059

Spooner, D. M., Ghislain, M., Simon, R., Jansky, S. H., and Gavrilenko, T. (2014). Systematics, diversity, genetics, and evolution of wild and cultivated potatoes. *Bot. Rev.* 80, 283–383. doi: 10.1007/s12229-014-9146-y

Šulc, K. (1909). *Trioza cockerelli*, a novelty from North America, being also of economic importance. *Acta Soc. Entomol. Bohem.* 6, 102–108.

Sumner-Kalkun, J. C., Highet, F., Arnsdorf, Y. M., Back, E., Carnegie, M., Madden, S., et al. (2020). '*Candidatus* Liberibacter solanacearum'distribution and diversity in Scotland and the characterisation of novel haplotypes from *Craspedolepta* spp.(*Psyllidae*: *Aphalaridae*). *Sci. Rep.* 10, 1–11. doi: 10.1007/978-3-319-23534-9_1

Swisher, K. D., Munyaneza, J. E., and Crosslin, J. M. (2012). High resolution melting analysis of the cytochrome oxidase I gene identifies three haplotypes of the potato psyllid in the United States. *Environ. Entomol.* 41, 1019–1028. doi: 10.1603/en12066

Swisher, K. D., Sengoda, V. G., Dixon, J., Munyaneza, J. E., Murphy, A. F., Rondon, S. I., et al. (2014). Assessing potato psyllid haplotypes in potato crops in the Pacific Northwestern United States. *Am. J. Potato Res.* 91, 485–491. doi: 10.1007/s12230-014-9378-8

Swisher Grimm, K., and Garczynski, S. (2019). Identification of a new haplotype of '*Candidatus* Liberibacter solanacearum'in *Solanum tuberosum*. *Plant Dis.* 103, 468–474.

Szczepaniec, A., Varela, K. A., Kiani, M., Paetzold, L., and Rush, C. M. (2019). Incidence of resistance to neonicotinoid insecticides in *Bactericera cockerelli* across Southwest US. *J. Crop Prot.* 116, 188–195. doi: 10.1016/j.cropro.2018.11.001

Teresani, G. R., Bertolini, E., Alfaro-Fernández, A., Martínez, C., Tanaka, F. A. O., Kitajima, E. W., et al. (2014). Association of '*Candidatus* Liberibacter solanacearum'with a vegetative disorder of celery in Spain and development of a real-time PCR method for its detection. *Phytopathology* 104, 804–811. doi: 10.1094/phyto-07-13-0182-r

Teulon, D., Workman, P., Thomas, K., and Nielsen, M. (2009). *Bactericera cockerelli* incursion dispersal and current distribution on vegetable crops in New Zealand. *N. Z. Plant Prot.* 62, 136–144. doi: 10.30843/nzpp.2009.62.4783

Thomas, J., Geering, A., and Maynard, G. (2018). Detection of "*Candidatus* Liberibacter solanacearum" in tomato on Norfolk Island. Australia. *Australas. Plant Dis. Notes* 13:7.

USDA, N. (2019). *Potatoes 2018 Summary*. United States: USDA.

Varshney, R. K., Graner, A., and Sorrells, M. E. (2005). Genomics-assisted breeding for crop improvement. *Trends Plant Sci.* 10, 621–630. doi: 10.1016/j.tplants.2005.10.004

Vereijssen, J., Smith, G. R., and Weintraub, P. G. (2018). *Bactericera cockerelli* (*Hemiptera*: *Triozidae*) and *Candidatus* Liberibacter solanacearum in potatoes in New Zealand: biology, transmission, and implications for management. *J. Integr. Pest Manag.* 9:13.

Vereijssen, J., Taylor, N., Barnes, A., Thompson, S., Logan, D., Butler, R., et al. (2015). First report of '*Candidatus* Liberibacter solanacearum'in Jerusalem cherry (*Solanum pseudocapsicum*) and thorn-apple (*Datura stramonium*) in New Zealand. *New Dis. Rep.* 32:5197.

Walker, G., Macdonald, F., Larsen, N., and Wallace, A. (2011). Monitoring *Bactericera cockerelli* and associated insect populations in potatoes in South Auckland. *N. Z. Plant Prot.* 64, 269–275. doi: 10.30843/nzpp.2011.64.6009

Wallis, R. L. (1955). *Ecological Studies on the Potato Psyllid as a Pest of Potatoes*. Washington: D.C.

War, A. R., Paulraj, M. G., Ahmad, T., Buhroo, A. A., Hussain, B., Ignacimuthu, S., et al. (2012). Mechanisms of plant defense against insect herbivores. *Plant Signal. Behav.* 7, 1306–1320. doi: 10.4161/psb.21663

Wen, A., Mallik, I., Alvarado, V., Pasche, J., Wang, X., Li, W., et al. (2009). Detection, distribution, and genetic variability of '*Candidatus* Liberibacter'species associated with zebra complex disease of potato in North America. *Plant Dis.* 93, 1102–1115. doi: 10.1094/pdis-93-11-1102

Wolt, J. D., Wang, K., and Yang, B. (2016). The regulatory status of genome-edited crops. *Plant Biotech. J.* 14, 510–518. doi: 10.1111/pbi.12444

Yao, J., Saenkham, P., Levy, J., Ibanez, F., Noroy, C., Mendoza, A., et al. (2016). Interactions "*Candidatus Liberibacter solanacearum*"—*Bactericera cockerelli*: haplotype effect on vector fitness and gene expression analyses. *Front. Cell. Infect. Microbiol.* 6:62. doi: 10.3389/fcimb.2016.00062

Conflict of Interest: The authors declare that the research was conducted in the absence of any commercial or financial relationships that could be construed as a potential conflict of interest.

frontiers in Plant Science

ORIGINAL RESEARCH
published: 31 August 2021
doi: 10.3389/fpls.2021.739108

Selection and Evaluation of a Thornless and HLB-Tolerant Bud-Sport of Pummelo Citrus With an Emphasis on Molecular Mechanisms

Bo Wu[1†], Na Li[2,3†], Zhanao Deng[4], Feng Luo[1] and Yongping Duan[2*]*

[1] School of Computing, Clemson University, Clemson, SC, United States, [2] United States Department of Agriculture-Agriculture Research Service-United States Horticultural Research Laboratory, Fort Pierce, FL, United States, [3] College of Horticulture, Hunan Agricultural University, Changsha, China, [4] Department of Environmental Horticulture, Gulf Coast Research and Education Center, IFAS, University of Florida, Wimauma, FL, United States

OPEN ACCESS

Edited by:
Xuefeng Wang, Citrus Research Institute, Chinese Academy of Agricultural Sciences, China

Reviewed by:
Xiuping Zou, Citrus Research Institute, Chinese Academy of Agricultural Sciences, China
Qiang Xu, Huazhong Agricultural University, China

***Correspondence:**
Feng Luo
luofeng@clemson.edu
Yongping Duan
Yongping.Duan@ars.usda.gov

[†] These authors have contributed equally to this work

Specialty section:
This article was submitted to Plant Pathogen Interactions, a section of the journal Frontiers in Plant Science

Received: *10 July 2021*
Accepted: *04 August 2021*
Published: *31 August 2021*

Citation:
Wu B, Li N, Deng Z, Luo F and Duan Y (2021) Selection and Evaluation of a Thornless and HLB-Tolerant Bud-Sport of Pummelo Citrus With an Emphasis on Molecular Mechanisms. Front. Plant Sci. 12:739108. doi: 10.3389/fpls.2021.739108

The selection of elite bud-sports is an important breeding approach in horticulture. We discovered and evaluated a thornless pummelo bud-sport (TL) that grew more vigorously and was more tolerant to Huanglongbing (HLB) than the thorny wild type (W). To reveal the underlying molecular mechanisms, we carried out whole-genome sequencing of W, and transcriptome comparisons of W, TL, and partially recovered thorny "mutants" (T). The results showed W, TL, and T varied in gene expression, allelic expression, and alternative splicing. Most genes/pathways with significantly altered expression in TL compared to W remained similarly altered in T. Pathway and gene ontology enrichment analysis revealed that the expression of multiple pathways, including photosynthesis and cell wall biosynthesis, was altered among the three genotypes. Remarkably, two polar auxin transporter genes, PIN7 and LAX3, were expressed at a significantly lower level in TL than in both W and T, implying alternation of polar auxin transport in TL may be responsible for the vigorous growth and thornless phenotype. Furthermore, 131 and 68 plant defense-related genes were significantly upregulated and downregulated, respectively, in TL and T compared with W. These genes may be involved in enhanced salicylic acid (SA) dependent defense and repression of defense inducing callose deposition and programmed cell death. Overall, these results indicated that the phenotype changes of the TL bud-sport were associated with tremendous transcriptome alterations, providing new clues and targets for breeding and gene editing for citrus improvement.

Keywords: pummelo, bud sport, transcriptome, thornless, huanglongbing, alternative splicing, allelic expression difference

INTRODUCTION

A bud-sport is a phenotypically distinct part of a plant, frequently observed in woody perennials (Foster and Aranzana, 2018). Bud-sports usually harbor a limited number of mutations based on the original plants and retain most of the original traits, making them an excellent resource for breeding new cultivars. Many bud-sports have been developed into new cultivars in

several important horticultural plants such as citrus (Usman and Fatima, 2018), apple (Li et al., 2018), and grape (Xu et al., 2019). In *Citrus*, which has a relatively long juvenile period, the selection of bud-sports has been widely applied in breeding. The most notable instance is the sweet orange [*Citrus sinensis* (L.) Osbeck], in which more than one hundred cultivars have been selected from bud-sports. Many cultivars in another economically important cultivar group, grapefruit (*Citrus* × *paradise* Macfayden), were also derived from bud-sport selections (Uzun et al., 2010).

Bud-sports are a valuable source of new cultivars and critical materials for studying molecular mechanisms underlying essential traits. A study on Sicilian blood oranges (*C. sinensis*) revealed that the translocation of a retrotransposon affected the expression of an anthocyanin production activator-encoding gene, *Ruby*, and caused the accumulation of anthocyanin in the fruit (Butelli et al., 2012). Transcriptome profiling has been widely used to identify the differentially expressed genes (DEGs) between citrus bud sports and their corresponding wild types. Studies on late-ripening mutants from sweet orange, clementine (*Citrus* × *clementina* Hort. ex Tan.), and "Wuzishatangju" (*C. reticulata* L.) identified tens to hundreds of DEGs at different developing stages, respectively (Wu J. et al., 2014; Wang J. et al., 2017; Wang L. et al., 2017; Terol et al., 2019). Similar studies have also been conducted on an orange-pericarp pummelo mutant (Guo et al., 2015), a wax deficient sweet orange mutant (He et al., 2018), a sweet orange mutant with impaired carotenoid biosynthesis (Romero et al., 2019), two red flesh sweet orange mutants (Pan et al., 2012; Yu et al., 2012), and two sweet orange mutants different in citrate content (Lu et al., 2016).

Pummelo [*C. maxima* (J. Burman) Merrill] is one of the economically important species in *Citrus*. Like most *Citrus* species, pummelo has thorny branches during the juvenile stage, which are believed to protect them from herbivores. In contrast, new branches grown from mature trees usually have no or much fewer and shorter thorns. Different early flowering transgenic plants could be thorny or thornless (Peña et al., 2001; Velázquez et al., 2016), indicating the pathways controlling the thorn development and the juvenile period in citrus are only partially overlapped. We also observed that some 4-year-old seedlings of sour orange (*Citrus aurantium* L.) bearing fruits remained thorny. In contrast, its thornless mutant and other thorny sibling plants remained in the juvenile state. Thorns are supposed to be modified lateral branches or axillary buds (Singh, 2019), whose development is related to the crosstalk between cytokinin and auxin (Schaller et al., 2015) and other plant hormones. Through silencing two TCP transcription factor genes, TI1 and TI2, citrus thorns were successfully transformed into branches (Zhang et al., 2020). In this study, the thorns were repressed rather than converted on thornless bud-sport (TL) branches.

When compared to the original plant (W), TL and its partially recovered mutants with short thorns (T) showed enhanced tolerance to Huanglongbing (HLB), a devastating disease of citrus worldwide. HLB has a relatively short-recorded history of fewer than 200 years (Killiny et al., 2018), and so far, no HLB-resistant citrus cultivar is commercially available. However, some citrus species/varieties did display different degrees of tolerance (Manjunath et al., 2008; da Graça et al., 2016) and higher expression levels of basal defense-related genes (Wang et al., 2016), and typical plant defense responses, such as callose deposition, were observed in Las-infected citrus leaves (da Graça et al., 2016; Wang N. et al., 2017). Many efforts have been carried out to breed HLB resistant/tolerant citrus cultivars both by the citrus industry and scientific communities (Wang, 2019), and the selection of HLB tolerant citrus is considered an important approach. Moreover, a comparison of bud-sports with enhanced HLB tolerance/resistance with their maternal lines will unravel the molecular mechanisms of HLB tolerance/resistance in citrus.

In this study, to unravel the underlying molecular mechanisms of the phenotypical differences among the three pummelo genotypes (W, TL, and T), we compared their gene/pathway expression, alternative splicing, and allelic expression through transcriptome profiling and genotyping by genome sequencing. Several genes putatively underlying the thornless mutation were identified, and their expression was quantified in similar bud-sports from two other *Citrus* species, grapefruit and sour orange.

MATERIALS AND METHODS

Plant Materials

A relatively tolerant seedling of *C. maxima* (J. Burman) var. "Mato Buntan" (accession no. PI 5359398) was selected via inoculation by hot psyllid that carried high titers of *Candidatus* Liberibacter asiaticus (Las) in the USHRL greenhouse, Fort Pierce, FL. The infected plant displayed asymptomatic to very mild symptoms though it carried high Las titers with Ct = 24.5. Branches from the HLB tolerant seedling (wild type, W) were grafted on sour orange rootstocks after treatment with ampicillin and streptomycin, as described by Zhang et al. (2012). The plants were maintained in the greenhouse, and a thornless bud-sport was observed 18 months after grafting. The thornless bud-sport was further propagated using bud-grafting, from which both thornless plants (TL) and partial thorn-recovery plants (T) were obtained. We also selected two thornless bud-sports from a 3-year-old Duncan grapefruit (*Citrus* × *paradisi* Macfad. var. Duncan) seedling and a common sour orange (*Citrus* × *aurantium* L. var. Amara Engl.) seedling with relatively higher HLB tolerance than their mother plants. The seedlings of these two mutants were surveyed for gene expression confirmation via qRT-PCR.

Evaluation of HLB Resistance/Tolerance

Clones of W, T, and TL were evaluated for HLB resistance/tolerance via graft inoculation using an aggressive Las isolate in an insect-proof greenhouse. The Las titer was quantified with qPCR using the 16S rDNA primer and probe (Li et al., 2006). Las quantification by qPCR was performed in triplicate for each propagated plant and repeated every 6 months since inoculation.

RNA Extraction and Transcriptome Sequencing

Newly expanded leaves from 3 W, 3 TL, and 4 T clonal plants were subjected to RNA extraction and RNA-seq. Another two transcriptomes (WT and TT) were sequenced using RNA extracted from thorns of W, and T. Total RNA was extracted from the leaves or thorn barks using the RNeasy Plant Mini Kit (Qiagen Inc., Valencia, CA) following the manual. The RNA concentration and quality were assessed by NanoDrop ND-1000 spectrophotometer, and concentration $\geq$ 250 ng/μL, OD260/OD280 = 1.8∼2.2, and OD260/OD230 $\geq$ 2.0 were required. More than 20 μg RNA of each sample was sent to BGI (Beijing Genomics Institute) Genomics (Shenzhen, China), which carried out poly-A selection of mRNA, pair-end library construction, and high-throughput sequencing on HiSeq2000 (Illumina, San Diego, CA) sequencing machine. More than 5 Gb sequencing reads were obtained for each sample.

Differential Expression Analysis on the Transcript and Gene Levels

The quality of sequencing reads was examined by FastQC v0.11.8,[1] after which Trimmomatic v0.38 was applied in read cleaning (Bolger et al., 2014). Adapters and low-quality read ends (average base quality < 15) were trimmed from reads. Sequencing reads including $\geq$ 5% ambiguous bases (N) were discarded.

A strategy based on both assembly and mapping (Pertea et al., 2016) was used to enhance the gene structure annotation of the pummelo reference genome (Wang X. et al., 2017). The reads from the 12 transcriptomes were mapped to the same haploid pummelo genome used in the variant analysis by HISAT2 v2.1.0 (Kim et al., 2015). The obtained RNA-seq alignments were further assembled into potential transcripts using StringTie v1.3.4 (Pertea et al., 2015), and gene structures were inferred from all the 10 assemblies, which were merged with the gene structure annotation of the pummelo reference (Wang X. et al., 2017) by StringTie v1.3.4 to generate one merged gene structure annotation. Statistics on novel genes and transcripts were carried out by comparing the merged gene structure annotation with the reference gene structure annotation using gffcompare in StringTie v1.3.4. The longest transcripts of the novel genes were further aligned to the transcript sequences annotated in the *Citrus sinensis* (Xu et al., 2013) and *Citrus clementina* (Wu G. A. et al., 2014) reference genomes via blastn. Genes or transcripts with targets sharing $\geq$ 95% nucleotide similarity, $\geq$ 50% alignment coverage of the queries, and *E*-value $\leq$ 1E-3 were recognized as annotated in the reference genomes.

Based on the merged annotation, the transcriptomes were compared pairwise among W, TL, and T at the gene and transcript (gene isoform) levels. The expression of transcripts was estimated by StringTie v1.3.4 using the acquired RNA-seq alignments. Data normalization and statistical analysis on transcript levels were processed by R package ballgown v3 (Frazee et al., 2015). For gene-level analysis, the raw read counts per gene were calculated using Salmon v0.11.3 (Patro et al., 2017) and Tximport v1.12.1 (Soneson et al., 2015). Gene read count was normalized using the median of ratios method (Love et al., 2014). The Wald test for the generalized linear model (GLM) coefficients was applied in the differential expression test using DESeq2 v1.28.0 (Love et al., 2014).

Gene expression correlation analysis, principal component analysis (PCA), and hierarchical clustering were carried out among the 12 transcriptomes using Pivot v1.0.0 (Zhu et al., 2018). In hierarchical clustering, Euclidean distance was calculated based on log10 (Normalized gene read counts), and the Ward.D2 method was applied in agglomeration.

Allelic Expression Difference (AED) Analysis

Long-read sequencing of whole-genome DNA was applied to detect exonic heterozygous variants in W. The genomic DNAs were extracted from the leaves of W using the DNeasy Plant Mini Kit (Qiagen Inc., Valencia, CA). The quality of the DNAs was measured using NanoDrop ND-1000 spectrophotometer (Thermo Fisher Scientific, Waltham, MA) and agarose gel electrophoresis. Library construction and sequencing on the PacBio RS II system (Pacific Biosciences, Menlo Park, CA) was carried out by Yale Center for Genome Analysis (YCGA, CT, United States).

Two different methods were applied to identify SNVs (Single nucleotide variants) based on the sequencing reads. The published haploid pummelo genome was used as a reference in both methods. We first used the Resequencing Application implemented in SMRT Analysis v6.0.0 (Pacific Biosciences, Menlo Park, CA) for variation identification. Pbalign v0.4.1 was used for mapping the reads to the reference genome, and then arrow v2.3.3 was applied to call both heterozygous and homozygous variants with the option "diploid." In the second method, the subreads were transformed into fastq by SMRT Analysis v6.0.0 and mapped to the reference by Minimap2 v2.17 using Pacbio read mode (Li, 2018). Variant calling was performed by the UnifiedGenotyper algorithm in GATK v3.8 (McKenna et al., 2010), using the parameters suggested by Carneiro et al. (2012). Then, variants detected by both methods were identified as high-quality variants for further analysis. Based on the acquired gene structure annotation, heterozygous exonic SNVs were output by Bedtools 2.28 (Quinlan and Hall, 2010) and applied in allelic expression analysis.

Based on the BAM files from mapping RNA-seq reads to the reference in the previous step, allelic read counts were output on all exonic SNVs using the ASEReadCounter command in GATK 4.1.2.0 (McKenna et al., 2010). The reference allelic expression ratio was calculated by dividing the reference allelic count on an SNV by the total local read count (the sum of reference and alternative allele read counts). Repeated *G*-tests of Goodness-of-Fit test[2] were carried out to check the alleles on each SNV were expressed at the same ratios within each group and among different groups (W, TL, and T). When both pooled *G*-test *p*-value and total *G*-test *p*-value were $\leq$ 0.001, the allelic expression was considered significantly different.

[1] http://www.bioinformatics.babraham.ac.uk/projects/fastqc/

[2] https://rcompanion.org/rcompanion/b_09.html

Enrichment Analysis of Differentially Expressed Genes on Metabolic Pathways and Functional Categories

Gene Ontology annotation of all the expressed genes was carried out by Blast2GO v5.2.1 (Götz et al., 2008). Fisher's exact test was applied to test for significantly (FDR < 0.05) enriched GO terms in biological process, molecular function, and cellular component. The general enriched GO terms were removed using Blast2GO v5.2.1 if a more specific term existed.

Gene set enrichment analysis (GSEA) was carried out using GSEA v4.0.3 (Subramanian et al., 2007). We obtained the gene sets from KEGG pathways, the WikiPathway database, and the PMN database (Schläpfer et al., 2017). The orthologs of all pummelo genes were identified in *Arabidopsis thaliana* proteins (Lamesch et al., 2012) and *Citrus clementina* genes (Wu G. A. et al., 2014) through searching for the best hit using blastx or blastn, and ≥ 50% alignment coverage and ≤ 1E-3 *E*-value were required.

Corresponding protein sequences of all plant disease resistance genes (R genes) were downloaded from PRGdb 3.0 database (Osuna-Cruz et al., 2018). All pummelo genes were searched against the database using blastx, and any gene that had a blastx hit with E-value ≤ 1E-3 and ≥ 50% coverage of the target was considered as a putative R gene. The putative R genes in our gene set were output in FASTA format and submitted to Drago 2 server (Osuna-Cruz et al., 2018), which searched the leucine-rich region, kinase domain, nucleotide-binding region, Toll-interleukin region, coiled-coil, and transmembrane domain with HMM modules. Based on the results, the R genes were classified according to the domain combinations (Osuna-Cruz et al., 2018). Other plant defense response genes were obtained through their GO annotation.

RT-qPCR Quantification of Gene Expression

cDNA synthesis was performed with oligo (dT) primers using the M-MLV reverse transcriptase system (Promega Corporation, Madison, United States) according to the manufacture's instructions. A 20 μL reaction was applied in qPCR, including 10 μL of 2 × FAST SYBR Green Master Mix (Quanta Bio) reagent and 2 μL of DNA template. The following standard thermal profile was used for all amplifications: 95°C for 5 min, followed by 40 cycles of 95°C for 3 s and 60°C for 30 s. Primer sequences are listed in **Supplementary Table 1**, and ACT2 and GAPDH primers from the study of Mafra et al. (2012) were used as reference genes. Reactions were performed in triplicate, and the $2^{-\Delta\Delta Ct}$ method was used to calculate relative expression as described by Pitino et al. (2015).

RESULTS

Phenotype Difference Among the Analyzed Pummelo Genotypes

Among the three analyzed genotypes, the thornless genotype (TL) was obtained from a bud mutation of the original seedling (wild type, W) in **Figure 1A**. The partially recovered thorny genotype (T) was derived from the bud propagations of TL with a ∼50% ratio (14 of 30). The difference in phenotype was mainly found in two aspects among W, T, and TL (**Figures 1B,C**). The first is the thorn length. W and T branches are thorny, while the TL plants are thornless. However, there was a significant difference in the thorn length between W and T. The latter had a 65% reduction compared with the wild type. The second difference is in the growing vigor of the bud-sport. As shown in **Figure 1B**, T and TL grew more vigorously than W. All the three genotypes have shown high HLB tolerance in our tests compared with the other original pummelo sibling seedlings. In our HLB tolerance/resistance tests, at 6 months after inoculation with a highly virulent Las isolate, no typical HLB symptom but only slight growth retardation was observed on TL and T (**Figure 1D**). However, on the tested non-tolerant grapefruit and W seedlings, severe symptoms (yellow shoots) and mild symptoms were observed, respectively. The RT-PCR results showed that the titers of Las bacteria were not significantly different between W and T or TL, but were significantly lower ($p < 0.05$ by *t*-test) than those in grapefruit.

Novel Transcript and Gene Discovery From RNA-Seq Data

We carried out RNA-seq on 10 leaf samples from 3 W, 3 TL, and 4 T clonal plants and two thorn samples (WT and TT) from W and T. An assembly-based strategy was applied to discover novel genes and transcripts absent in the reference annotation. 4,165 putative novel gene loci and 38,825 putative novel transcripts were identified from the 12 transcriptomes (**Supplementary Table 2**), which increased the number of analyzed genes and transcripts by 14.1 and 89.2% compared to the pummelo reference (Wang X. et al., 2017) gene models. Of the 4,165 putative novel gene loci, 1,133 were present in the gene annotation of *Citrus sinensis* (Xu et al., 2013) or *Citrus clementina* (Wu G. A. et al., 2014). Among the rest 3,032 loci, 1,303 had homologous proteins in the NCBI nr database, while the remaining 1,729 could be genes specific in *Citrus* (*maxima*) or non-coding RNAs. On average, each expressed gene had 1.14 novel transcripts detected in this study. Among the novel transcripts, 33,423 belonged to genes annotated in the reference genome, and the rest 4,830 belonged to the 4,165 novel gene loci.

Transcriptome Profiling and Clustering

Gene expression correlation analysis showed that intra-group transcriptomes generally had a higher Pearson correlation coefficient than inter-group transcriptomes, except for the T leaf transcriptomes. As shown in **Supplementary Figure 1**, T3 and T4 had higher correlation coefficients with most TL transcriptomes than T1 and T2. The W and TL leaf transcriptomes were clustered into separate clades by hierarchical clustering (**Figure 2A**), and the two thorn transcriptomes (TT and WT) were clustered together. The four T leaf transcriptomes clustered with the TL clade, and both T3 and T4 were closer to TL leaf transcriptomes than T1 and T2 (**Figure 2A**).

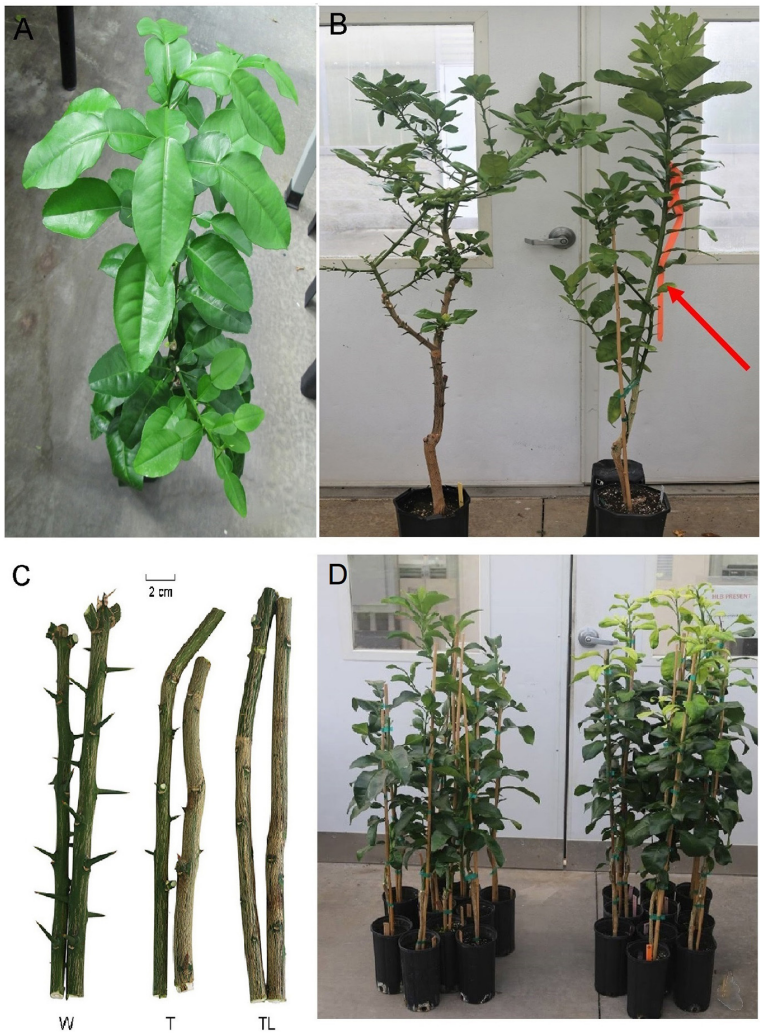

FIGURE 1 | Pummelo thornless bud-sport selection and evaluation. **(A)** Asymptomatic HLB-tolerant Mato Buntan seedling (wild type W) with CT = 24.5 1 year after Las inoculation. **(B)** Comparison of the growth of W (left) and thornless bud-sport (red arrow). **(C)** The branches of W, T, and TL. **(D)** The HLB-tolerant mutants (TL and T) in the left show growth retardation, while the susceptible grapefruit plants on the right showed typical yellow shoot symptoms 12 months after inoculation with an aggressive Las isolate.

In PCA, 11 principal components (PC) explain ∼100% total variability of the transcriptomes (**Supplementary Figure 2**). The first two components PC1 and PC2 accounted for 51.9% of the total variance. On PC1 (28.3% of total variance), the distribution of leaf transcriptomes was mainly explained by the origin relationship among W, TL, and T (**Figure 2B**). PC2 (23.6%) could mainly be explained by the thorn-related phenotype difference. Since the two thorn transcriptomes, WT and TT, lay below all the leaf transcriptomes, and W1-3 and T1-4 lay below TL1-3 (**Figure 2B**).

Differentially Expressed Pathways in the Bud Sports

Among pairwise comparisons, 3,496 and 4,057 differentially expressed genes (DEG) were identified between W and TL and between TL and T, respectively (**Supplementary Figure 3**). Interestingly, the most DEGs (6,378) were detected between W and T. A majority of DEGs between TL and W (2290/3496) remained significantly upregulated or downregulated in T compared with W (**Supplementary Figure 3**).

Gene ontology (GO) and pathway enrichment analysis revealed multiple pathways with significant expression alteration in W to TL transition. Compared with W, 204 GOs/12 pathways and 43 GOs/2 pathways were significantly (FDR < 0.05) over-represented for genes upregulated (1,995) and down-regulated (1,519) in TL, respectively (**Supplementary Table 3**). Multiple upregulated pathways were related to photosynthesis (**Figure 3A**, **Supplementary Figure 4**, and **Supplementary Table 3**). The down-regulated pathways included the cell wall biogenesis and several other pathways (**Supplementary Figure 5A** and **Supplementary Table 3**).

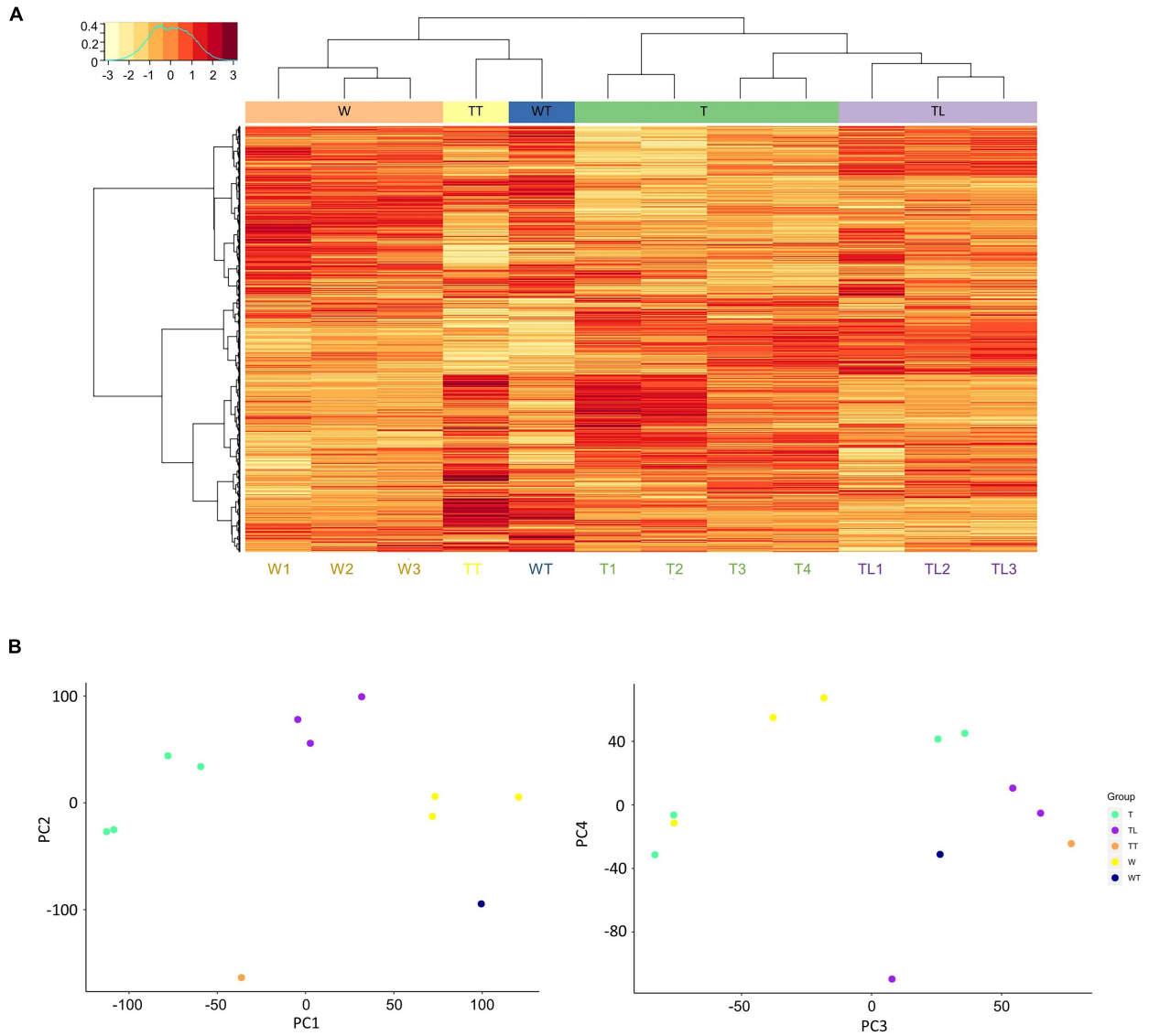

FIGURE 2 | Clustering of the transcriptomes. **(A)** Hierarchical clustering and gene expression heatmap. In the heat map, each row represents a gene, and each column represents a transcriptome. The clustering trees based on transcriptomes and genes are shown on the top and to the left of the heat map. In the left top legend, the horizontal axis denotes the normalized expression values of genes, and the vertical axis shows the normalized frequency of genes at the different expression levels. **(B)** Distribution of samples along PC1 to 4 from the principal component analysis.

Compared to TL, 84 GOs/9 pathways, and 15 GOs/6 pathways were significantly over-represented for the upregulated and downregulated genes in T, respectively. Genes involved in cytokinin signaling, response to auxin, salicylic acid (SA) metabolic process regulation, anatomical structure development, cell cycle regulation, and several cell wall metabolism-related pathways were enriched in upregulated genes in T (**Supplementary Table 3**). Several processes down-regulated in TL (compared with W) were upregulated in T (compared with TL), including secondary cell wall biosynthesis, xyloglucan biosynthesis, carbohydrate biosynthetic process, lipid metabolism, and lignin metabolism (**Figure 3B** and **Supplementary Figure 6**). A few GO terms and pathways were also down-regulated in T compared with TL (**Supplementary Figure 5B** and **Supplementary Table 3**).

DEGs and Pathways Putatively Responsible for the Thornless Mutation

Because both W and T are thorny while TL is thornless, common DEGs between TL and both W and T may be responsible for the thornless mutation. Accordingly, we identified 293 upregulated and 397 down-regulated DEGs in TL compared to W and T (**Supplementary Table 4**). The upregulated and downregulated genes were distributed in multiple functional categories (**Supplementary Figure 7**), and

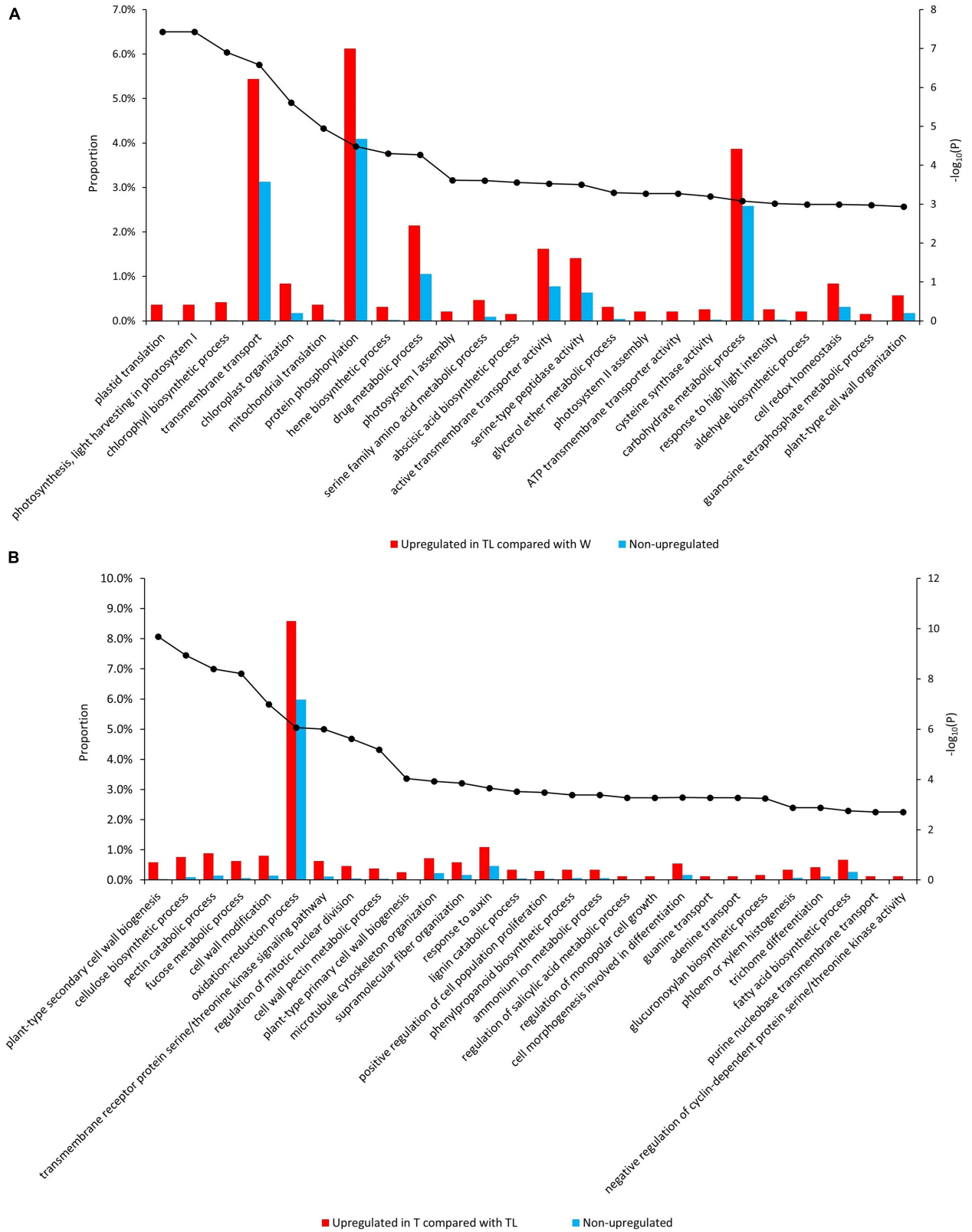

FIGURE 3 | Enriched GO terms from the comparative transcriptomic analysis. Significantly enriched GOs in genes upregulated in TL compared with W **(A)** and those upregulated in T compared with TL **(B)**. The bars denote the proportion of genes (the left vertical axis) with each GO in the tested gene sets, and the black dots indicate the –log10 (*p*-value of enrichment test) (the right vertical axis) of each GO.

both included a response to stimulus, including phytohormones and transcription factors. The transcription factors differentially expressed in TL mainly were related to phytohormone or involved in secondary cell wall biogenesis (**Supplementary Table 4**). The expression levels of the genes mentioned in this section below have been shown in **Supplementary Figure 8**.

We identified 1 upregulated and 7 down-regulated auxin-related DEGs in TL compared to W and T (**Supplementary Table 4**). PIN5 (auxin efflux carrier component 5, Cs6g02450) was upregulated in TL, while two other auxin transporter genes, LAX3 (auxin transporter-like protein 3, Cg3g016080) and PIN7 (auxin efflux carrier component 7, Cs1g26700), were significantly down-regulated. The rest down-regulated genes included PTL (trihelix transcription factor, Cg2g035410), IAA16 (auxin-responsive IAA16, Cs4g17050), YUC2 (Indole-3-pyruvate monooxygenase YUC2, Cs4g15810), PLC2 (phosphoinositide phospholipase C 2, Cs7g31080), and SAUR78 (small auxin upregulated RNA 78, Cs5g15740). Five cytokinin-related genes were differentially expressed in TL compared to both W and T. Among them, CYP735A1 (cytokinin hydroxylase, Cg6g019610) was significantly upregulated in TL. LOG5 (cytokinin riboside 5′-monophosphate phosphoribohydrolase, Cs3g27020), ZOG1 (zeatin-O-glucosyltransferase, Cs7g32210), CYCD3 (Cyclin-D3-1, Cg3g020940), and AHK2 (Histidine kinase 2, Cs4g02460) were significantly down-regulated in TL.

Eleven secondary cell wall biogenesis-related genes were significantly down-regulated in TL compared with both W and T. Moreover, all the 11 genes were expressed at lower levels in leaf transcriptomes than in the thorn transcriptomes. Five of them were transcription factors, including four NAC domain-containing transcription factor genes, SND1 (secondary wall-associated NAC domain protein 1, Cs5g01350), SND2 (secondary wall-associated NAC domain protein 2, Cs2g16190), NST1 (NAC secondary wall thickening promoting factor 1, orange1.1t00561), and VND1 (vascular-related NAC-domain, Cs1g25100), and MYB42 (MYB domain-containing transcription factor 42, Cg5g008830). The remaining six genes include two fasciclin-like arabinogalactan protein-encoding genes FLA11 (Cg6g002120) and FLA12 (Cg8g020560), two UDP-glucuronate: xylan alpha-glucuronosyltransferase encoding genes GUX1 (Cs1g05500) and GUX2 (Cs3g23600), IRX9 (beta-1,4-xylosyltransferase, Cg6g002620), and CTL2 (chitinase-like protein 2 gene, Cg9g001540).

Differentially Expressed Plant Defense Genes Among the Genotypes

A total of 3,110 plant defense-related genes, including 1,594 putative R genes, were identified in the pummelo genome through bioinformatic analysis. Since no difference in HLB tolerance was observed between TL and T and both were more tolerant than W, common DEGs in TL and T compared to W may contribute to the higher HLB tolerance. Among the defense-related genes, 221 and 365 were significantly upregulated in TL and T compared with W, respectively, and 131 were upregulated in both of them (**Supplementary Table 5**). Besides, 125 and 295 plant defense-related genes were down-regulated in TL and T, respectively, and 68 down-regulated in both of them compared with W (**Supplementary Table 5**). The expressions of the genes mentioned below in this section have been shown in **Supplementary Figure 9**.

Four positive regulators of SA-dependent defense were significantly upregulated in both TL and T (Yang et al., 2008; Birkenbihl et al., 2017), including WRKY70 (Cs7g29570), CDR1 (constitutive disease resistance 1, Cg6g008170), and two citrus orthologs (Cs1g23170 and Cs7g27540) of the Arabidopsis methylesterase 1 gene (MES1). Two negative regulators of SA -dependent plant defense (von Saint Paul et al., 2011; Liu et al., 2015), UGT76B (UDP-Glycosyltransferase superfamily protein UGT76B1, Cg7g000350) and WRKY33 (Cg6g009940), were significantly down-regulated in both TL and T.

There were several DEGs related to the pathogen-associated molecular pattern (PAMP)-triggered immunity (PTI) and (or) effector-triggered immunity (ETI). Ten receptor-like kinases of PTI, including six cysteine-rich receptor-like protein genes (CRKs) and four L-type lectin-domain containing receptor kinase genes (LECRKs), were significantly upregulated in both TL and T (**Supplementary Table 5**). Eight resistance (R) genes involved in ETI were upregulated in both TL and T (**Supplementary Table 5**). Several genes involved in PTI or ETI were significantly down-regulated in TL and T, including ACS6 (Cg5g002190), OST1 (Cs5g07700), and SPL6 (Cs5g12260).

Defense induced callose deposition and cell-death were most likely suppressed in TL and T. MLO (MLO-like protein gene, Cs7g27330), a suppressor of callose deposition and second oxidative burst of cell-death in plant defense response (Kusch et al., 2019), had 46.4- and 29.8-fold expression abundance of W in TL and T, respectively, and was the most highly upregulated. Several genes putatively involved in defense-induced callose deposition and programmed cell death (Takahashi et al., 2003; Shindo et al., 2012; D'Ambrosio et al., 2017; Liu et al., 2017) were significantly down-regulated in TL and T, including PLC2 (Cg8g024170), HSP90-1 (Cg5g002260), two orthologs of EP3 (Cg5g026680 and Cg5g026650), and RD21A (Cs3g23180).

qPCR Quantification of DEGs in Other Thornless Citrus Genotypes

We also identified two thornless mutants with relatively higher HLB tolerance in another two Citrus species, grapefruit (*C.* × *paradisi* var. "Duncan") and sour orange (*C.* × *aurantium* L.) (**Supplementary Figure 10**). qPCR quantification was executed on 15 candidate DEGs between W and TL in all the selected lineages. As shown in **Figure 4A**, 12 of the 15 genes showed consistent upregulated and downregulated patterns between RNA-seq and qPCR analyses for TL. The gene expression changes in thornless Duncan grapefruit (DC) were highly similar and significantly correlated with those in TL, while sour orange (SO) was more different (**Figure 4**).

Genes with similar expression alterations in different thornless mutants were probably related to thorn development or higher HLB tolerance. Two genes, SEP2 (Developmental protein SEPALLATA 2, Cg7g016020) and EXPA1 (expansin-A1,

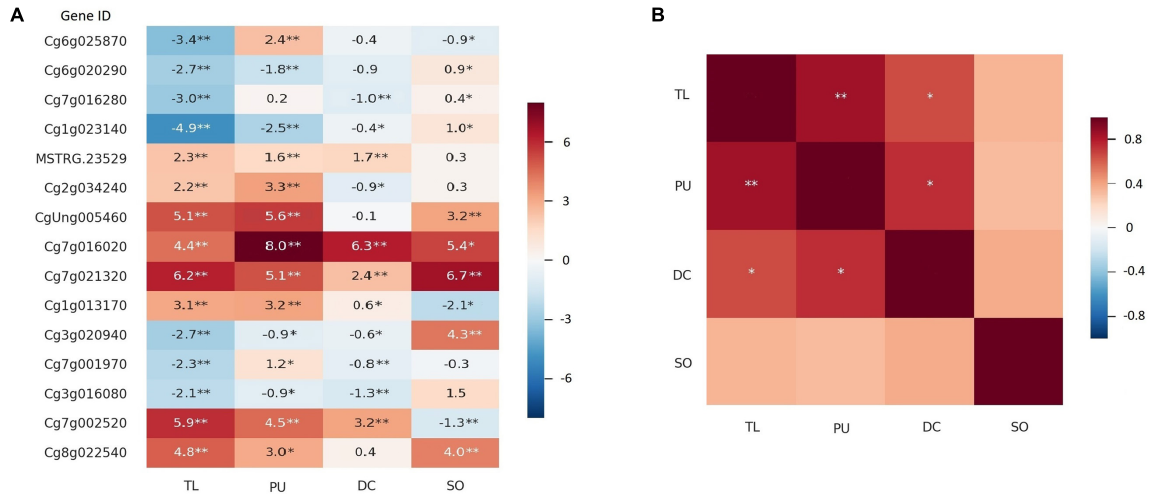

FIGURE 4 | Expression of DEGs in more Citrus thornless bud-sports. The RNA-seq and qPCR results for the thornless pummelo bud-sport were shown as TL and PU, respectively. The qPCR results for Duncan grapefruit (DC) and sour orange (SO) were shown in the graphs. Single and double asterisk(s) indicate statistical significance at $p < 0.05$ and $p < 0.001$ levels, respectively. **(A)** Expression of 15 genes in bud-sports compared with their corresponding original types. The values in the cells were log2(expression value in bud-sport/expression value in original type) for RNA-seq and $-\Delta\Delta$Ct for qPCR. **(B)** Correlation of gene expression on the 15 genes among the citrus genotypes.

Cg7g021320), were significantly upregulated in all three thornless genotypes. PYR1 (abscisic acid receptor PYR1, MSTRG.23529) and SAG21 (senescence-associated gene 21, Cg1g013170) were significantly upregulated in TL, PU, and DC, while LAX3 (auxin transporter-like protein 3, Cg3g016080) and CYCD3 (CYCLIN D3, Cg3g020940) were significantly down-regulated in them. A SAUR-like auxin-responsive protein family gene (CgUng005460) and EXPA4 (expansin A4, Cg8g022540) were both upregulated in TL, PU (qPCR results for TL), and SO.

Change in Alternative Splicing in Bud-Sports

Gene alternative splicing was widely observed in the transcriptomes. At least two transcripts were detected on 48.1–49.2% of the expressed genes in the transcriptomes (**Supplementary Figure 11**). The proportions of genes with different numbers of transcripts detected were highly similar among the transcriptomes.

G-test of independence was performed to test the hypothesis if the transcript expression ratio was consistent within each group. The null hypothesis was rejected ($p < 0.001$) for 85.2—87.5% of transcripts within each of the three leaf-transcriptome groups, TL, W, and T (**Supplementary Figure 11**). The test was also carried out between the two thorn transcriptomes, WT and TT, and the null hypothesis was rejected for the majority (67.0%) tested transcripts. These results suggested that the expression ratios of most transcripts were distributed in a specific range rather than at a fixed ratio.

We carried out a pairwise comparison on transcript expression ratio among W, TL, and T. The results showed that the expression ratio of the transcript was significantly different ($p < 0.001$) for 77 (belonging to 64 genes), 70 (58), and 178 (146) transcripts between W and TL, T and TL, and T and W, respectively (**Supplementary Table 6**). For instance, on ARF6 (auxin response factor 6, Cs2g09440.1), the 4th transcript had a higher expression ratio (p= 0.077) in W than TL, while the 3rd transcript was expressed significantly higher (p = 3.6e-7) in T than in W (**Figure 5**). The 2nd transcript of BAT1 (bidirectional amino acid transporter 1, Cs2g24220) was expressed at a significantly ($p < 0.001$) lower ratio in TL than in T, W, WT, and TT (**Supplementary Figure 12**).

Allelic Expression Difference (AED) Among the Transcriptomes

Based on whole-genome sequencing of W, a total of 1,749,437 high-quality SNVs were detected, of which 1,007,731 were heterozygous, and 738,319 were homozygous. In allelic expression difference (AED) analysis, 287,115 heterozygous exonic SNVs were applied.

The overall distribution of the reference allelic expression ratios was highly similar among the different transcriptomes (**Figure 6A**). The null hypotheses that both alleles were expressed at the same level were rejected ($p < 0.001$) only for a small percentage ($\leq$ 3.2%) of the tested SNPs, suggesting that the allelic expression ratios for most SNPs were stable within each transcriptome group. Pairwise tests among the three leaf-transcriptome groups were implemented to detect inter-group AEDs. As shown in **Figure 6B**, AEDs ($p < 0.001$) were identified between W and TL, W and T, and TL and T for 1067, 1263, and 782 SNVs, respectively, located in 602, 647, and 433 genes. The 433 genes on which AED was observed on at least two SNVs between at least two genotypes were listed in **Supplementary Table 7**. For 25 genes, significant AED was observed on at least 2 SNVs between TL and both W and T (**Figure 6C**), and

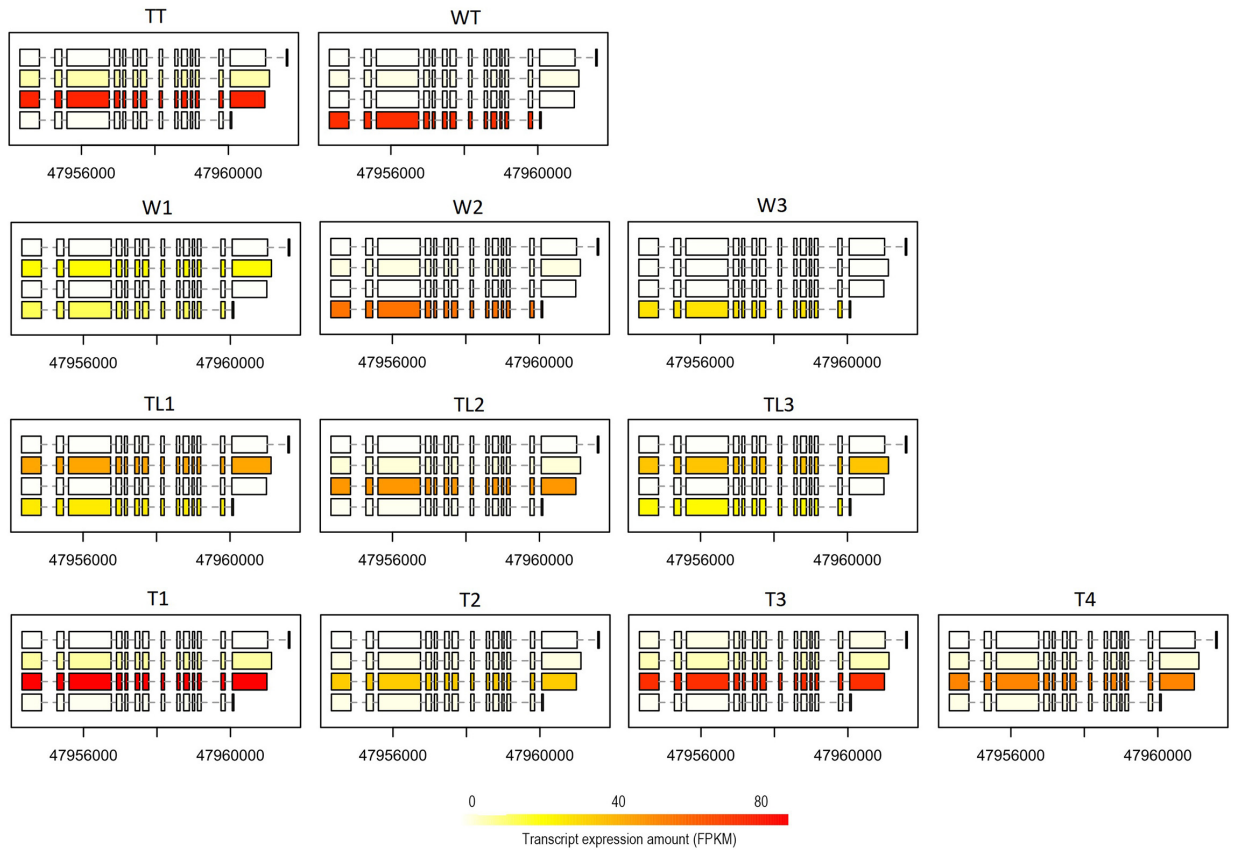

FIGURE 5 | Expression of ARF6 at the transcript level in the 12 transcriptomes. For each transcriptome, the expression quantities of the four different transcript forms have been indicated by the color depth of the rectangles (exons) connected by dashed lines (introns) in the box.

on 66 genes, it was observed between W and both TL and T (**Supplementary Table 7**).

DISCUSSION

Pummelo seedlings are derived from mono-embryonic seeds. In this study, we first identified an HLB tolerant pummelo seedling and then discovered a thornless bud sport from the grafted clonal plants of the seedling. We also found similar thornless bud sports from HLB tolerant Duncan grapefruit and sour orange seedlings, respectively, at the middle of their juvenile stage (**Supplementary Figure 10**). The correlation between HLB tolerance and thornless mutation may provide new clues for future selection and evaluation of a bud sport aimed at citrus improvement, including HLB tolerance/resistance. Therefore, we further conducted a comprehensive transcriptome comparison and unraveled the potential molecular mechanisms conferring the phenotypical changes of the bud sports, TL and T.

The changes in the transcriptomes of TL and T occurred in multiple aspects. This study showed that there were thousands of DEGs, hundreds of genes with differential allelic expression, and tens of genes with different alternative splicing among W, TL, and T. Allelic expression patterns have long been known to be important in the development and associated with phenotypes in parent-of-origin effects in both animals and plants (Lawson et al., 2013). They also are correlated with environmental variables and associated with some human diseases (McKean et al., 2016; Knowles et al., 2017). Alternative splicing plays an essential role in protein function/interaction and eukaryote development (Yang X. et al., 2016). This study has confirmed their wide existence between bud-sports and the original plants. Though the impact of AEDs and alternative splicing have not been revealed in citrus, they could have played essential roles in its phenotypic diversity.

Genes with full or partial recovered expression in T were the most likely responsible for the TL-specific thornless phenotype. Thorns are modified lateral branches on citrus shoots that grow from lateral buds (Zhang et al., 2020). Crosstalk between auxin and cytokinin, especially polar auxin transport, has been known to play a determinant role in lateral bud activation (Müller and Leyser, 2011), a precondition for thorn development. In this study, a few auxin- and cytokinin-related DEGs were identified between TL and both W and T, including three polar auxin transporters, PIN5, PIN7, and LAX3. PIN5 has been reported to be located at the endoplasmic reticulum and involved in intracellular auxin transport in Arabidopsis (Mravec et al., 2009). PIN7 mediates cell to cell auxin transport in Arabidopsis and is involved in auxin export during shoot branching

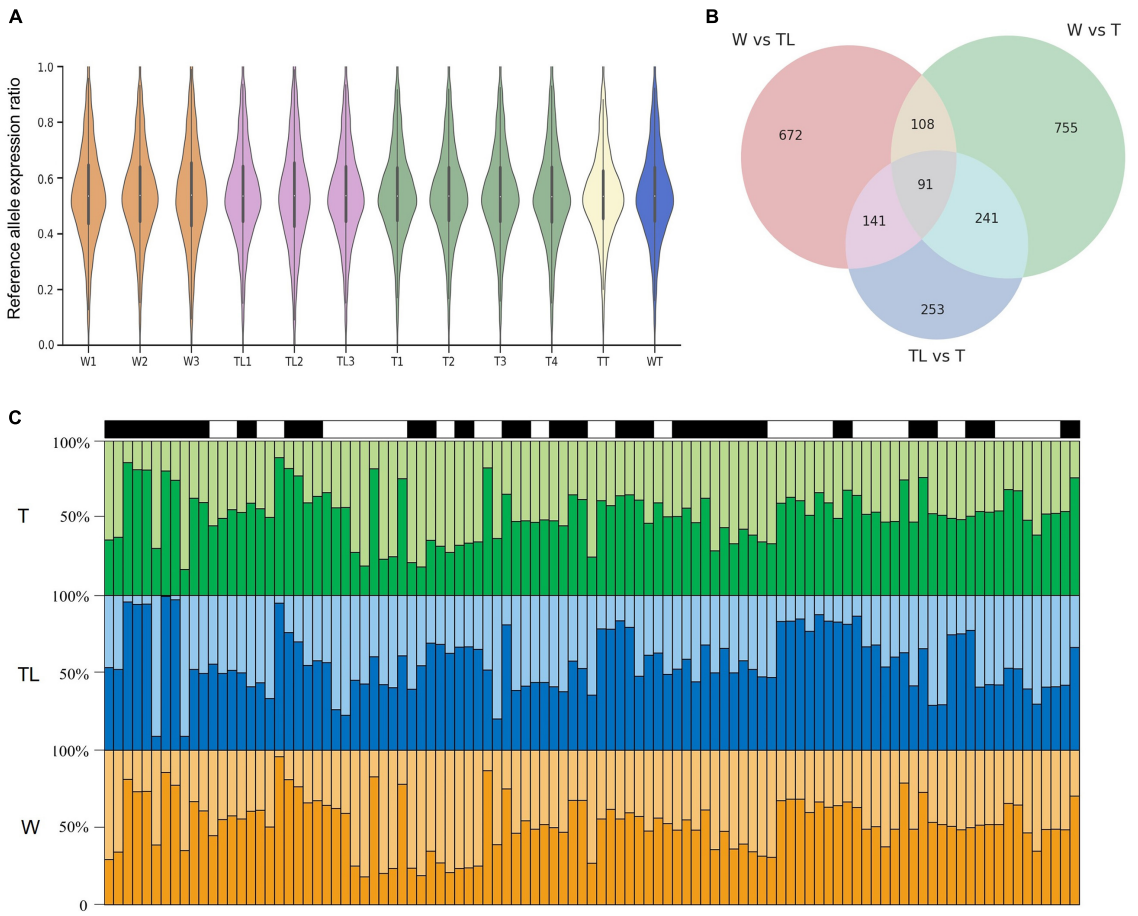

FIGURE 6 | Allelic expression difference (AED) in the pummelo genotypes. **(A)** Reference allelic expression ratio distribution on heterozygous exonic SNVs in the 12 transcriptomes. **(B)** Number of SNVs with significant AED in W, TL, and T and their overlapping relationship. **(C)** Allelic expression ratio on 25 genes in which significant AED was observed between TL and both W and T. Each of the black and white rectangle represents a gene on top of the three panels, and each bin in the bar graphs represents an SNV. The vertical axis denotes the allelic expression ratio. Reference allelic expression and alternative allelic expression are represented by dark and light colors in the three panels.

(van Rongen et al., 2019). LAX3, which is necessary for lateral root primordia origin in Arabidopsis through regulating cell wall remodeling (Porco et al., 2016), was significantly downregulated in TL compared with leaf and thorn transcriptomes from W and T, and it was also significantly downregulated in the thornless Duncan grapefruit. Cell wall remodeling is an important regulator of meristem morphogenesis and is involved in initiating different plant organs (Yang W. et al., 2016). In this study, cell wall biogenesis and modification-related genes/pathways were generally downregulated in TL. These results suggested the thorn bud activation on TL branches could have been disturbed by altered auxin transport and cell wall metabolism.

The high HLB tolerance in TL and T could be partially derived from the enhanced SA-dependent defense response. In citrus, SA-dependent defense is positively correlated with HLB tolerance (Oliveira et al., 2019; Zou et al., 2019), and SA-dependent systematic acquired resistance (SAR) has been suggested to improve HLB tolerance in citrus germplasms (Manjunath et al., 2008; Hu et al., 2018). Several positive regulators of SA-dependent defense have been reported to be significantly upregulated in HLB tolerant citrus accessions, including PtCDR2, PtCDR8 (Rawat et al., 2017), and CDR1 (Albrecht and Bowman, 2012). In TL and T, four positive regulators of SA-dependent defense response, including CDR1 were significantly upregulated, and two negative regulators were significantly down-regulated compared with W, implying the SA-dependent defense was enhanced.

Repression of callose deposition in the phloem could have enhanced HLB tolerance in TL and T. Though callose deposition is an important defense response in plants, it has not worked efficiently to block Las due to the slow response. Callose deposition caused by Las infection has been hypothesized to induce sieve pore blockage and starch accumulation in the leaves, and unplugging the phloem has been proposed to relieve HLB symptoms (Achor et al., 2020). Anatomical comparison between HLB susceptible and tolerant citrus accessions showed

that cellulose deposition, phloem cell collapse, and starch accumulation were observed in HLB susceptible citrus, but not in an HLB-tolerant rough lemon (Fan et al., 2012). In this study, a repressor (MLO) of programmed cell death and callose deposition was significantly upregulated in both TL and T. In contrast, several genes positively related to programmed cell death and callose deposition were significantly down-regulated as shown in the results section, indicating repression of callose deposition could have contributed to their high HLB tolerance.

CONCLUSION

In conclusion, we identified thornless bud-sports from pummelo, grapefruit, and sour orange seedlings in the middle of their juvenile stage. These individuals were selected as they were more HLB-tolerant in the psyllid- or graft-based evaluation. The transcriptome analyses of these thornless mutations revealed many differences in gene expression, allelic expression, and alternative splicing, though these bud-sports were derived from asexual propagation. Furthermore, the identification of thornless and HLB-tolerance-related genes may provide new clues and targets for breeding and gene editing for citrus improvement.

DATA AVAILABILITY STATEMENT

The original contributions presented in the study are publicly available. This data can be found here: National Center for Biotechnology Information (NCBI) BioProject database under accession number PRJNA557834.

AUTHOR CONTRIBUTIONS

YD, FL, and ZD designed the research. BW and NL drafted the manuscript. NL carried out all the lab experiments. BW carried out the bioinformatical analysis. YD selected the bud sports. All authors participated in the manuscript writing and have agreed to the published version of the manuscript.

FUNDING

This work was supported in part by the U.S. National Institute of Food and Agriculture (NIFA; Grant Number 2017-70016-26051). Mention of trade names or commercial products in this publication is solely for the purpose of providing specific information and does not imply recommendation or endorsement by the U.S. Department of Agriculture. USDA is an equal opportunity employer.

SUPPLEMENTARY MATERIAL

The Supplementary Material for this article can be found online at: https://www.frontiersin.org/articles/10.3389/fpls.2021.739108/full#supplementary-material

REFERENCES

Achor, D., Welker, S., Ben-Mahmoud, S., Wang, C., Folimonova, S. Y., Dutt, M., et al. (2020). Dynamics of candidatus *Liberibacter* asiaticus movement and sieve-pore plugging in *Citrus* sink cells. *Plant Physiol.* 182, 882–891. doi: 10.1104/pp.19.01391

Albrecht, U., and Bowman, K. D. (2012). Transcriptional response of susceptible and tolerant citrus to infection with candidatus *Liberibacter* asiaticus. *Plant Sci.* 185, 118–130. doi: 10.1016/j.plantsci.2011.09.008

Birkenbihl, R. P., Liu, S., and Somssich, I. E. (2017). Transcriptional events defining plant immune responses. *Curr. Opin. Plant Biol.* 38, 1–9. doi: 10.1016/j.pbi.2017.04.004

Bolger, A. M., Lohse, M., and Usadel, B. (2014). Trimmomatic: a flexible trimmer for Illumina sequence data. *Bioinformatics* 30, 2114–2120. doi: 10.1093/bioinformatics/btu170

Butelli, E., Licciardello, C., Zhang, Y., Liu, J., Mackay, S., Bailey, P., et al. (2012). Retrotransposons control fruit-specific, cold-dependent accumulation of anthocyanins in blood oranges. *Plant Cell* 24, 1242–1255. doi: 10.1105/tpc.111.095232

Carneiro, M. O., Russ, C., Ross, M. G., Gabriel, S. B., Nusbaum, C., and DePristo, M. A. (2012). Pacific biosciences sequencing technology for genotyping and variation discovery in human data. *BMC Genomics* 13:375. doi: 10.1186/1471-2164-13-375

D'Ambrosio, J. M., Couto, D., Fabro, G., Scuffi, D., Lamattina, L., Munnik, T., et al. (2017). Phospholipase C2 affects MAMP-triggered immunity by modulating ROS production. *Plant Physiol.* 175, 970–981. doi: 10.1104/pp.17.00173

da Graça, J. V., Douhan, G. W., Halbert, S. E., Keremane, M. L., Lee, R. F., Vidalakis, G., et al. (2016). Huanglongbing: an overview of a complex pathosystem ravaging the world's citrus. *J. Integr. Plant Biol.* 58, 373–387. doi: 10.1111/jipb.12437

Fan, J., Chen, C., Yu, Q., Khalaf, A., Achor, D. S., Brlansky, R. H., et al. (2012). Comparative transcriptional and anatomical analyses of tolerant rough lemon and susceptible sweet orange in response to 'Candidatus *Liberibacter* asiaticus' infection. *Mol. Plant Microbe Interact.* 25, 1396–1407. doi: 10.1094/MPMI-06-12-0150-R

Foster, T. M., and Aranzana, M. J. (2018). Attention sports fans! The far-reaching contributions of bud sport mutants to horticulture and plant biology. *Hortic. Res.* 5:44. doi: 10.1038/s41438-018-0062-x

Frazee, A. C., Pertea, G., Jaffe, A. E., Langmead, B., Salzberg, S. L., and Leek, J. T. (2015). Ballgown bridges the gap between transcriptome assembly and expression analysis. *Nat. Biotechnol.* 33, 243–246. doi: 10.1038/nbt.3172

Götz, S., García-Gómez, J. M., Terol, J., Williams, T. D., Nagaraj, S. H., Nueda, M. J., et al. (2008). High-throughput functional annotation and data mining with the Blast2GO suite. *Nucleic Acids Res.* 36, 3420–3435. doi: 10.1093/nar/gkn176

Guo, F., Yu, H., Xu, Q., and Deng, X. (2015). Transcriptomic analysis of differentially expressed genes in an orange-pericarp mutant and wild type in pummelo (*Citrus grandis*). *BMC Plant Biol.* 15:44. doi: 10.1186/s12870-015-0435-3

He, Y., Han, J., Liu, R., Ding, Y., Wang, J., Sun, L., et al. (2018). Integrated transcriptomic and metabolomic analyses of a wax deficient citrus mutant exhibiting jasmonic acid-mediated defense against fungal pathogens. *Hortic. Res.* 5:43. doi: 10.1038/s41438-018-0051-0

Hu, J., Jiang, J., and Wang, N. (2018). Control of citrus Huanglongbing via trunk injection of plant defense activators and antibiotics. *Phytopathology* 108, 186–195. doi: 10.1094/PHYTO-05-17-0175-R

Killiny, N., Jones, S. E., Nehela, Y., Hijaz, F., Dutt, M., Gmitter, F. G., et al. (2018). All roads lead to Rome: towards understanding different avenues of tolerance to Huanglongbing in citrus cultivars. *Plant Physiol. Biochem.* 129, 1–10. doi: 10.1016/j.plaphy.2018.05.005

Kim, D., Langmead, B., and Salzberg, S. L. (2015). HISAT: a fast spliced aligner with low memory requirements. *Nat. Methods* 12, 357–360. doi: 10.1038/nmeth.3317

Knowles, D. A., Davis, J. R., Edgington, H., Raj, A., Favé, M. J., Zhu, X., et al. (2017). Allele-specific expression reveals interactions between genetic variation and environment. *Nat. Methods* 14, 699–702. doi: 10.1038/nmeth.4298

Kusch, S., Thiery, S., Reinstädler, A., Gruner, K., Zienkiewicz, K., Feussner, I., et al. (2019). Arabidopsis mlo3 mutant plants exhibit spontaneous callose deposition and signs of early leaf senescence. *Plant Mol. Biol.* 101, 21–40. doi: 10.1007/s11103-019-00877-z

Lamesch, P., Berardini, T. Z., Li, D., Swarbreck, D., Wilks, C., Sasidharan, R., et al. (2012). The *Arabidopsis* information resource (TAIR): improved gene annotation and new tools. *Nucleic Acids Res.* 40, D1202–D1210. doi: 10.1093/nar/gkr1090

Lawson, H. A., Cheverud, J. M., and Wolf, J. B. (2013). Genomic imprinting and parent-of-origin effects on complex traits. *Nat. Rev. Genet.* 14, 609–617. doi: 10.1038/nrg3543

Li, H. (2018). Minimap2: pairwise alignment for nucleotide sequences. *Bioinformatics* 34, 3094–3100. doi: 10.1093/bioinformatics/bty191

Li, W., Hartung, J. S., and Levy, L. (2006). Quantitative real-time PCR for detection and identification of Candidatus *Liberibacter* species associated with citrus Huanglongbing. *J. Microbiol. Methods* 66, 104–115. doi: 10.1016/j.mimet.2005.10.018

Li, W., Mao, J., Yang, S. J., Guo, Z. G., Ma, Z. H., Dawuda, M. M., et al. (2018). Anthocyanin accumulation correlates with hormones in the fruit skin of 'Red Delicious' and its four-generation bud sport mutants. *BMC Plant Biol.* 18:363. doi: 10.1186/s12870-018-1595-8

Liu, S., Kracher, B., Ziegler, J., Birkenbihl, R. P., and Somssich, I. E. (2015). Negative regulation of ABA signaling by WRKY33 is critical for *Arabidopsis* immunity towards *Botrytis cinerea* 2100. *eLife* 4:e07295. doi: 10.7554/eLife.07295

Liu, Z., Shi, L., Yang, S., Lin, Y., Weng, Y., Li, X., et al. (2017). Functional and promoter analysis of ChiIV3, a chitinase of pepper plant, in response to *Phytophthora capsici* Infection. *Int. J. Mol. Sci.* 18:1661. doi: 10.3390/ijms18081661

Love, M. I., Huber, W., and Anders, S. (2014). Moderated estimation of fold change and dispersion for RNA-seq data with DESeq2. *Genome Biol.* 15:550. doi: 10.1186/s13059-014-0550-8

Lu, X., Cao, X., Li, F., Li, J., Xiong, J., Long, G., et al. (2016). Comparative transcriptome analysis reveals a global insight into molecular processes regulating citrate accumulation in sweet orange (*Citrus sinensis*). *Physiol. Plant* 158, 463–482. doi: 10.1111/ppl.12484

Mafra, V., Kubo, K. S., Alves-Ferreira, M., Ribeiro-Alves, M., Stuart, R. M., Boava, L. P., et al. (2012). Reference genes for accurate transcript normalization in citrus genotypes under different experimental conditions. *PLoS One* 7:e31263. doi: 10.1371/journal.pone.0031263

Manjunath, K. L., Halbert, S. E., Ramadugu, C., Webb, S., and Lee, R. F. (2008). Detection of 'candidatus *Liberibacter* asiaticus' in *Diaphorina citri* and its importance in the management of citrus Huanglongbing in Florida. *Phytopathology* 98, 387–396. doi: 10.1094/PHYTO-98-4-0387

McKean, D. M., Homsy, J., Wakimoto, H., Patel, N., Gorham, J., DePalma, S. R., et al. (2016). Loss of RNA expression and allele-specific expression associated with congenital heart disease. *Nat. Commun.* 7:12824. doi: 10.1038/ncomms12824

McKenna, A., Hanna, M., Banks, E., Sivachenko, A., Cibulskis, K., Kernytsky, A., et al. (2010). The Genome analysis toolkit: a mapreduce framework for analyzing next-generation DNA sequencing data. *Genome Res.* 20, 1297–1303. doi: 10.1101/gr.107524.110

Mravec, J., Skůpa, P., Bailly, A., Hoyerová, K., Křeček, P., Bielach, A., et al. (2009). Subcellular homeostasis of phytohormone auxin is mediated by the ER-localized PIN5 transporter. *Nature* 459, 1136–1140. doi: 10.1038/nature08066

Müller, D., and Leyser, O. (2011). Auxin, cytokinin and the control of shoot branching. *Ann. Bot.* 107, 1203–1212. doi: 10.1093/aob/mcr069

Oliveira, T. S., Granato, L. M., Galdeano, D. M., Marques, J. P. R., Coerini, L. F., Freitas-Astúa, J., et al. (2019). Genetic analysis of salicylic acid-mediated defenses responses and histopathology in the Huanglongbing pathosystem. *Citrus Res. Technol.* 40:1049. doi: 10.4322/crt.18419

Osuna-Cruz, C. M., Paytuvi-Gallart, A., Di Donato, A., Sundesha, V., Andolfo, G., Aiese Cigliano, R., et al. (2018). PRGdb 3.0: a comprehensive platform for prediction and analysis of plant disease resistance genes. *Nucleic Acids Res.* 46, D1197–D1201. doi: 10.1093/nar/gkx1119

Pan, Z., Zeng, Y., An, J., Ye, J., Xu, Q., and Deng, X. (2012). An integrative analysis of transcriptome and proteome provides new insights into carotenoid biosynthesis and regulation in sweet orange fruits. *J. Proteomics* 75, 2670–2684. doi: 10.1016/j.jprot.2012.03.016

Patro, R., Duggal, G., Love, M. I., Irizarry, R. A., and Kingsford, C. (2017). Salmon provides fast and bias-aware quantification of transcript expression. *Nat. Methods* 14, 417–419. doi: 10.1038/nmeth.4197

Peña, L., Martín-Trillo, M., Juárez, J., Pina, J. A., Navarro, L., and Martínez-Zapater, J. M. (2001). Constitutive expression of *Arabidopsis* LEAFY or APETALA1 genes in citrus reduces their generation time. *Nat. Biotechnol.* 19, 263–267. doi: 10.1038/85719

Pertea, M., Kim, D., Pertea, G. M., Leek, J. T., and Salzberg, S. L. (2016). Transcript-level expression analysis of RNA-seq experiments with HISAT, StringTie and Ballgown. *Nat. Protoc.* 11, 1650–1667. doi: 10.1038/nprot.2016.095

Pertea, M., Pertea, G. M., Antonescu, C. M., Chang, T. C., Mendell, J. T., and Salzberg, S. L. (2015). StringTie enables improved reconstruction of a transcriptome from RNA-seq reads. *Nat. Biotechnol.* 33, 290–295. doi: 10.1038/nbt.3122

Pitino, M., Armstrong, C. M., and Duan, Y. (2015). Rapid screening for citrus canker resistance employing pathogen-associated molecular pattern-triggered immunity responses. *Hortic. Res.* 2:15042. doi: 10.1038/hortres.2015.42

Porco, S., Larrieu, A., Du, Y., Gaudinier, A., Goh, T., Swarup, K., et al. (2016). Lateral root emergence in *Arabidopsis* is dependent on transcription factor LBD29 regulation of auxin influx carrier LAX3. *Development* 143, 3340–3349. doi: 10.1242/dev.136283

Quinlan, A. R., and Hall, I. M. (2010). BEDTools: a flexible suite of utilities for comparing genomic features. *Bioinformatics* 26, 841–842. doi: 10.1093/bioinformatics/btq033

Rawat, N., Kumar, B., Albrecht, U., Du, D., Huang, M., Yu, Q., et al. (2017). Genome resequencing and transcriptome profiling reveal structural diversity and expression patterns of constitutive disease resistance genes in Huanglongbing-tolerant *Poncirus trifoliata* and its hybrids. *Hortic. Res.* 4:17064. doi: 10.1038/hortres.2017.64

Romero, P., Lafuente, M. T., and Rodrigo, M. J. (2019). A sweet orange mutant impaired in carotenoid biosynthesis and reduced ABA levels results in altered molecular responses along peel ripening. *Sci. Rep.* 9:9813. doi: 10.1038/s41598-019-46365-8

Schaller, G. E., Bishopp, A., and Kieber, J. J. (2015). The yin-yang of hormones: cytokinin and auxin interactions in plant development. *Plant Cell* 27, 44–63. doi: 10.1105/tpc.114.133595

Schläpfer, P., Zhang, P., Wang, C., Kim, T., Banf, M., Chae, L., et al. (2017). Genome-wide prediction of metabolic enzymes, pathways, and gene clusters in plants. *Plant Physiol.* 173, 2041–2059. doi: 10.1104/pp.16.01942

Shindo, T., Misas-Villamil, J. C., Hörger, A. C., Song, J., and van der Hoorn, R. A. L. (2012). A role in immunity for *Arabidopsis* cysteine protease RD21, the ortholog of the tomato immune protease C14. *PLoS One* 7:e29317. doi: 10.1371/journal.pone.0029317

Singh, G. (2019). *Plant Systematics: An Integrated Approach*. Boca Raton, FL: CRC Press.

Soneson, C., Love, M. I., and Robinson, M. D. (2015). Differential analyses for RNA-seq: transcript-level estimates improve gene-level inferences. *F1000Research* 4:1521. doi: 10.12688/f1000research.7563.2

Subramanian, A., Kuehn, H., Gould, J., Tamayo, P., and Mesirov, J. P. (2007). GSEA-P: a desktop application for gene set enrichment analysis. *Bioinformatics* 23, 3251–3253. doi: 10.1093/bioinformatics/btm369

Takahashi, A., Casais, C., Ichimura, K., and Shirasu, K. (2003). HSP90 interacts with RAR1 and SGT1 and is essential for RPS2-mediated disease resistance in *Arabidopsis*. *Proc. Natl. Acad. Sci. U.S.A.* 100, 11777–11782. doi: 10.1073/pnas.2033934100

Terol, J., Nueda, M. J., Ventimilla, D., Tadeo, F., and Talon, M. (2019). Transcriptomic analysis of *Citrus clementina* mandarin fruits maturation reveals a MADS-box transcription factor that might be involved in the regulation of earliness. *BMC Plant Biol.* 19:47. doi: 10.1186/s12870-019-1651-z

Usman, M., and Fatima, B. (2018). "Mandarin (Citrus reticulata Blanco) breeding," in *Advances in Plant Breeding Strategies: Fruits*, eds J. M. Al-Khayri, S. M. Jain, and D. V. Johnson (Berlin: Springer), 465–533.

Uzun, A., Gulsen, O., Yesiloglu, T., Aka-Kacar, Y., and Tuzcu, O. (2010). Distinguishing grapefruit and pummelo accessions using ISSR markers. *Czech J. Genet. Plant Breed.* 46, 170–177. doi: 10.17221/89/2010-CJGPB

van Rongen, M., Bennett, T., Ticchiarelli, F., and Leyser, O. (2019). Connective auxin transport contributes to strigolactone-mediated shoot branching control independent of the transcription factor BRC1. *PLoS Genet.* 15:e1008023. doi: 10.1371/journal.pgen.1008023

Velázquez, K., Agüero, J., Vives, M. C., Aleza, P., Pina, J. A., Moreno, P., et al. (2016). Precocious flowering of juvenile citrus induced by a viral vector based on *Citrus* leaf blotch virus: a new tool for genetics and breeding. *Plant Biotechnol. J.* 14, 1976–1985. doi: 10.1111/pbi.12555

von Saint Paul, V., Zhang, W., Kanawati, B., Geist, B., Faus-Keßler, T., Schmitt-Kopplin, P., et al. (2011). The *Arabidopsis* glucosyltransferase UGT76B1 conjugates isoleucic acid and modulates plant defense and senescence. *Plant Cell* 23, 4124–4145. doi: 10.1105/tpc.111.088443

Wang, J., Liu, J., Chen, K., Li, H., He, J., Guan, B., et al. (2017). Comparative transcriptome and proteome profiling of two *Citrus sinensis* cultivars during fruit development and ripening. *BMC Genomics* 18:984. doi: 10.1186/s12864-017-4366-2

Wang, L., Hua, Q., Ma, Y., Hu, G., and Qin, Y. (2017). Comparative transcriptome analyses of a late-maturing mandarin mutant and its original cultivar reveals gene expression profiling associated with citrus fruit maturation. *PeerJ* 5:e3343. doi: 10.7717/peerj.3343

Wang, N. (2019). The citrus Huanglongbing crisis and potential solutions. *Mol. Plant* 12, 607–609. doi: 10.1016/j.molp.2019.03.008

Wang, N., Pierson, E. A., Setubal, J. C., Xu, J., Levy, J. G., Zhang, Y., et al. (2017). The Candidatus *Liberibacter*-host interface: insights into pathogenesis mechanisms and disease control. *Annu. Rev. Phytopathol.* 55, 451–482. doi: 10.1146/annurev-phyto-080516-035513

Wang, X., Xu, Y., Zhang, S., Cao, L., Huang, Y., Cheng, J., et al. (2017). Genomic analyses of primitive, wild and cultivated citrus provide insights into asexual reproduction. *Nat. Genet.* 49, 765–772. doi: 10.1038/ng.3839

Wang, Y., Zhou, L., Yu, X., Stover, E., Luo, F., and Duan, Y. (2016). Transcriptome profiling of Huanglongbing (HLB) tolerant and susceptible citrus plants reveals the role of basal resistance in HLB tolerance. *Front. Plant Sci.* 7:933. doi: 10.3389/fpls.2016.00933

Wu, G. A., Prochnik, S., Jenkins, J., Salse, J., Hellsten, U., Murat, F., et al. (2014). Sequencing of diverse mandarin, pummelo and orange genomes reveals complex history of admixture during citrus domestication. *Nat. Biotechnol.* 32, 656–662. doi: 10.1038/nbt.2906

Wu, J., Xu, Z., Zhang, Y., Chai, L., Yi, H., and Deng, X. (2014). An integrative analysis of the transcriptome and proteome of the pulp of a spontaneous late-ripening sweet orange mutant and its wild type improves our understanding of fruit ripening in citrus. *J. Exp. Bot.* 65, 1651–1671. doi: 10.1093/jxb/eru044

Xu, Q., Chen, L. L., Ruan, X., Chen, D., Zhu, A., Chen, C., et al. (2013). The draft genome of sweet orange (*Citrus sinensis*). *Nat. Genet.* 45, 59–66. doi: 10.1038/ng.2472

Xu, Y., Zheng, H., Wang, Q., Khalil-Ur-Rehman, M., Meng, L., and Tao, J. (2019). Comparison among 'Benitaka' grape, ABA-treated 'Benitaka', and its deeper-colored bud mutation revealed the coloring mechanisms on grapes. *J. Plant Interact.* 14, 102–109. doi: 10.1080/17429145.2018.1547843

Yang, W., Schuster, C., Beahan, C. T., Charoensawan, V., Peaucelle, A., Bacic, A., et al. (2016). Regulation of meristem morphogenesis by cell wall synthases in *Arabidopsis*. *Curr. Biol.* 26, 1404–1415. doi: 10.1016/j.cub.2016.04.026

Yang, X., Coulombe-Huntington, J., Kang, S., Sheynkman, G. M., Hao, T., Richardson, A., et al. (2016). Widespread expansion of protein interaction capabilities by alternative splicing. *Cell* 164, 805–817. doi: 10.1016/j.cell.2016.01.029

Yang, Y., Xu, R., Ma, C. J., Vlot, A. C., Klessig, D. F., and Pichersky, E. (2008). Inactive methyl indole-3-acetic acid ester can be hydrolyzed and activated by several esterases belonging to the AtMES esterase family of *Arabidopsis*. *Plant Physiol.* 147, 1034–1045. doi: 10.1104/pp.108.118224

Yu, K., Xu, Q., Da, X., Guo, F., Ding, Y., and Deng, X. (2012). Transcriptome changes during fruit development and ripening of sweet orange (*Citrus sinensis*). *BMC Genomics* 13:10. doi: 10.1186/1471-2164-13-10

Zhang, F., Rossignol, P., Huang, T., Wang, Y., May, A., Dupont, C., et al. (2020). Reprogramming of stem cell activity to convert thorns into branches. *Curr. Biol.* 30, 2951–2961.e5. doi: 10.1016/j.cub.2020.05.068

Zhang, M., Powell, C. A., Guo, Y., Doud, M. S., and Duan, Y. (2012). A graft-based chemotherapy method for screening effective molecules and rescuing huanglongbing-affected citrus plants. *Phytopathology* 102, 567–574. doi: 10.1094/PHYTO-09-11-0265

Zhu, Q., Fisher, S. A., Dueck, H., Middleton, S., Khaladkar, M., and Kim, J. (2018). PIVOT: platform for interactive analysis and visualization of transcriptomics data. *BMC Bioinformatics* 19:6. doi: 10.1186/s12859-017-1994-0

Zou, X., Bai, X., Wen, Q., Xie, Z., Wu, L., Peng, A., et al. (2019). Comparative analysis of tolerant and susceptible Citrus reveals the role of methyl salicylate signaling in the response to Huanglongbing. *J. Plant Growth Regul.* 38, 1516–1528. doi: 10.1007/s00344-019-09953-6

Conflict of Interest: The authors declare that the research was conducted in the absence of any commercial or financial relationships that could be construed as a potential conflict of interest.

Publisher's Note: All claims expressed in this article are solely those of the authors and do not necessarily represent those of their affiliated organizations, or those of the publisher, the editors and the reviewers. Any product that may be evaluated in this article, or claim that may be made by its manufacturer, is not guaranteed or endorsed by the publisher.

frontiers in Microbiology

ORIGINAL RESEARCH
published: 29 September 2021
doi: 10.3389/fmicb.2021.739763

Uncovering Symbionts Across the Psyllid Tree of Life and the Discovery of a New Liberibacter Species, "*Candidatus*" Liberibacter capsica

*Younghwan Kwak[1], Penglin Sun[1], Venkata RamaSravani Meduri[1], Diana M. Percy[2], Kerry E. Mauck[1] and Allison K. Hansen[1]**

[1] Department of Entomology, University of California, Riverside, Riverside, CA, United States, [2] Department of Botany, University of British Columbia, Vancouver, BC, Canada

OPEN ACCESS

Edited by:
Changyong Zhou,
Southwest University, China

Reviewed by:
Raymond Yokomi,
Agricultural Research Service, United States Department of Agriculture, United States
Yunzeng Zhang,
Yangzhou University, China
Carol Dean Von Dohlen,
Utah State University, United States
Joel Brown,
Cornell University, United States

***Correspondence:**
Allison K. Hansen
allison.hansen@ucr.edu

Specialty section:
This article was submitted to Microbial Symbioses, a section of the journal Frontiers in Microbiology

Received: 11 July 2021
Accepted: 10 September 2021
Published: 29 September 2021

Citation:
Kwak Y, Sun P, Meduri VR, Percy DM, Mauck KE and Hansen AK (2021) Uncovering Symbionts Across the Psyllid Tree of Life and the Discovery of a New Liberibacter Species, "Candidatus" Liberibacter capsica. Front. Microbiol. 12:739763. doi: 10.3389/fmicb.2021.739763

Sap-feeding insects in the order Hemiptera associate with obligate endosymbionts that are required for survival and facultative endosymbionts that can potentially modify resistance to stress, enemies, development, and reproduction. In the superfamily Psylloidea, the jumping plant lice (psyllids), less is known about the diversity and prevalence of their endosymbionts compared to other sap-feeding pests such as aphids (Aphididae). To address this knowledge gap, using 16S rRNA sequencing we identify symbionts across divergent psyllid host lineages from around the world. Taking advantage of a new comprehensive phylogenomic analyses of Psylloidea, we included psyllid samples from 44 species of 35 genera of five families, collected from 11 international locations for this study. Across psyllid lineages, a total of 91 OTUs were recovered, predominantly of the *Enterobacteriaceae* (68%). The diversity of endosymbionts harbored by each psyllid species was low with an average of approximately 3 OTUs. Two clades of endosymbionts (clade 1 and 2), belonging to *Enterobacteriaceae*, were identified that appear to be long term endosymbionts of the psyllid families Triozidae and Psyllidae, respectively. We also conducted high throughput metagenomic sequencing on three *Ca*. Liberibacter infected psyllid species (*Russelliana capsici*, *Trichochermes walkeri*, and *Macrohomotoma gladiata*), initially identified from 16S rRNA sequencing, to obtain more genomic information on these putative Liberibacter plant pathogens. The phylogenomic analyses from these data identified a new *Ca*. Liberibacter species, *Candidatus* Liberibacter capsica, that is a potential pathogen of solanaceous crops. This new species shares a distant ancestor with *Ca*. L. americanus, which occurs in the same range as *R. capsici* in South America. We also detected the first association between a psyllid specializing on woody hosts and the Liberibacter species *Ca*. L. psyllaurous, which is a globally distributed pathogen of herbaceous crop hosts in the Solanaceae. Finally, we detected a potential association between a psyllid pest of figs (*M. gladiata*) and a *Ca*. Liberibacter related to *Ca*. L.

asiaticus, which causes severe disease in citrus. Our findings reveal a wider diversity of associations between facultative symbionts and psyllids than previously reported and suggest numerous avenues for future work to clarify novel associations of ecological, evolutionary, and pathogenic interest.

Keywords: microbiome, *Candidatus* Liberibacter capsica, *Candidatus* Liberibacter psyllaurous, *Candidatus* Liberibacter asiaticus, endosymbiont, psyllid, endosymbiont evolution, long-term endosymbiont

INTRODUCTION

The widespread application of genomic approaches has brought new insights to our understanding of the evolution of microbial symbioses with animals, especially for bacterial symbionts that are not culturable and have small genomes (Moran and Bennett, 2014). Many of these symbionts live inside the bodies or cells of herbivorous insects as symbionts and are involved in synthesizing nutrients, digesting and detoxifying plant materials and pesticides, and/or conferring defense toward natural enemies (Buchner, 1965; Moran, 2007; Hansen and Moran, 2014). These diverse insect-microbe associations, including some plant pathogens, enable insect herbivores to exploit different ecological niches and plant parts (Douglas, 2009; Feldhaar, 2011; Casteel and Hansen, 2014; Hansen and Moran, 2014; Sudakaran et al., 2017). These heritable symbiotic associations range from obligate mutualists and long-term endosymbiont associates that are generally present in all insect individuals of a species, to beneficial, commensal, and antagonistic facultative endosymbionts that are present in only some insect individuals of a population or species. Among plant sap-feeding herbivore groups with endosymbiotic associations, the pea aphids (Aphididae) and their endosymbionts are one of the most comprehensively studied (Oliver et al., 2010). Endosymbiont associations, however, are widespread in other pest sap-feeding insect systems as well. The relationships between these insect-symbiont systems are not as well-known, regardless of their putative impacts on insect phenotype and insect-plant interactions (Oliver et al., 2010; Feldhaar, 2011; Hansen and Moran, 2014; Sudakaran et al., 2017).

One group of sap-feeding herbivores, the psyllids in the superfamily Psylloidea, suborder Sternorrhyncha (Burckhardt et al., 2021) are known to harbor a diversity of heritable endosymbionts, which include obligate and facultative associations (Thao et al., 2000a; Hall et al., 2016; Morrow et al., 2017). Psyllids are also considered to be alternative hosts rather than passive carriers of the plant pathogen "*Candidatus* (*Ca.*) Liberibacter" (Nadarasah and Stavrinides, 2011); in turn *Ca.* Liberibacter is also regarded as a psyllid endosymbiont (Hansen et al., 2008; Casteel and Hansen, 2014; Hansen and Moran, 2014). Interestingly, *Ca.* Liberibacter only specializes in Psylloidea hosts and is not generally present in other insect superfamilies (Raddadi et al., 2011; Wang et al., 2017; Mauck et al., 2019). In consequence, new *Ca.* Liberibacter species such as "*Ca.* Liberibacter psyllaurous, *Ca.* L. europaeus, *Ca.* L. brunswickensis," and "*Ca.* L. ctenaryainae" have been discovered in the past by screening psyllid species for microbes (Hansen et al., 2008; Raddadi et al., 2011; Morris et al., 2017; Thompson et al., 2017). This screening approach in psyllids not only adds to our understanding of endosymbiont associations that may impact psyllid fitness, but also identifies new *Ca.* Liberibacter species that may threaten our agriculture now, without our knowledge, or in the near future.

One of the first studies to reveal that psyllid species harbor a diversity of bacterial endosymbionts, in addition to its obligate nutritional endosymbiont "*Candidatus* Carsonella ruddii," hereafter referred to as *Carsonella* (Baumann, 2005), was published by Thao et al. (2000a). Thao et al. (2000a) discovered that a large diversity of psyllid species harbor bacterial endosymbionts that belong to a wide diversity of taxonomic associations. Recently, Hall et al. (2016) and Morrow et al. (2017) investigated the diversity and composition of facultative endosymbionts by using conventional PCR and high-throughput 16S rRNA sequencing in a diversity of psyllid taxa from divergent families of Psylloidea, however, these studies primarily focused on native psyllid species from Australia. Thao et al. (2000a) and Morrow et al. (2017) found that most psyllid species harbor only one dominant facultative endosymbiont representative, in addition to *Carsonella*, suggesting that psyllids have a minimal core bacterial community. Moreover, in contrast to *Carsonella*, several studies have suggested that many of these psyllid endosymbionts were recently horizontally transmitted in psyllid taxa (Thao et al., 2000a; Spaulding and von Dohlen, 2001; Hall et al., 2016; Morrow et al., 2017). Currently, more studies are needed that examine a broader diversity of psyllid taxa from more geographic regions around the world to more fully understand the diversity, prevalence and codivergence patterns of psyllid endosymbionts among divergent psyllid lineages.

In addition to horizontally transmitted facultative endosymbionts, genomic studies on psyllid endosymbionts have revealed that some endosymbionts can have long-term evolutionary relationships with their psyllid host lineages (Sloan and Moran, 2012). In these cases, the long-term endosymbiont appears to be transitioning into an obligate endosymbiont role and is generally present in all individuals of that psyllid species (hereafter referred to as long-term endosymbiont). For example, these symbionts in transition display genomic signatures of long-term host associations, such as an increase in A + T richness of genomic sequences and genome reduction, while retaining genes that have a potential obligate role for their insect host (Sloan and Moran, 2012). Based on genome sequencing data, long-term endosymbionts in two psyllid species were identified with biosynthetic pathways for essential amino acid biosynthesis that complement pathways that are absent in *Carsonella* (Sloan and Moran, 2012). In another psyllid

species, Nakabachi et al. (2013) identified *Ca*. Profftella armatura (hereafter referred as *Profftella*) in *Diaphorina citri* and revealed multiple roles of *Profftella* in providing defensive toxins, vitamins and carotenoids for the psyllid host. *Profftella* is also harbored in psyllid species that are closely related to *D. citri* (Nakabachi et al., 2020a,b). These results collectively suggest that some psyllid endosymbionts have a longer evolutionary association with certain psyllid lineages compared to more recent facultative endosymbiont associations.

To address multiple knowledge gaps regarding evolutionary associations among psyllids and their symbionts, we performed high-throughput 16S rRNA sequencing across 44 divergent psyllid species from 35 genera that reside in five of the seven families of Psylloidea, as classified by Burckhardt et al. (2021). These psyllids were collected from 11 different geographic regions around the world. This wide sampling approach, both taxonomically and geographically, allows us for the first time to (1) identify endosymbiont associations, including novel *Ca*. Liberibacter species, for 44 divergent psyllid taxa, and (2) detect hallmark signatures of long-term endosymbiont evolution to identify putative long-term endosymbiont taxa in psyllids. In addition, we (3) determine the phylogenetic relationship of all new *Ca.* Liberibacter taxa identified in psyllid microbiomes using gene content from metagenomic sequencing.

MATERIALS AND METHODS

Psyllid Collection and DNA Extractions

For 16S rRNA amplicon sequencing (detailed below), a total of 45 psyllid samples were analyzed, and included 44 different psyllid species. Two of the psyllid samples were the same psyllid species, *Trioza urticae*, however, the samples were collected from two different locations and time points (**Supplementary Table 1**). The 44 psyllid species represent 35 genera from five families within Psylloidea. Psyllid species were collected from 11 international geographic locations for this study and are detailed in **Supplementary Table 1**. Each psyllid sample consisted of an average of two psyllid adults pooled for DNA extractions, because most psyllid species are extremely small and not enough DNA can be obtained from just one individual per sample given our extraction protocol, which preserves voucher specimens for species identification of each sample (see below). Only the *Trichochermes walkeri* (P1–28) sample consisted of pooled nymphs (**Supplementary Table 1**). Psyllid DNAs were extracted following a nondestructive DNA extraction protocol (Percy et al., 2018) in order to correctly identify psyllid species with high confidence using both a molecular and morphological diagnostic approach as described in Percy et al. (2018). Briefly, collections were made by sweep net and aspirating directly from the plant, specimens were placed into 95–100% ethanol in the field and stored at −20°C thereafter. Field collected specimens were sorted and identified by DP and are maintained in DP's personal collection; individuals selected for DNA extraction were then placed (whole or bisected) in the tissue lysate buffer with proteinase K [as per the Qiagen (Germantown, Maryland) protocol] and incubated for 12–15 h at 56°C. After incubation the specimen was retained and preserved in 70–95% ethanol as a DNA voucher. Genomic DNAs was obtained using a Qiagen DNeasy Blood and Tissue Kit and eluted in 200 μl of the elution buffer.

High Throughput Sequencing and Data Analysis of 16S rRNA Amplicons

For library preparation of 16S rRNA libraries, custom 16S rRNA primers were synthesized by Integrated DNA Technologies, Inc. (San Diego, CA, United States) using a dual barcode design with 25 primer pairs based on the primer constructs used by the Earth Microbiome Project (EMP[1]) similar to Walters et al. (2016) and Caporaso et al. (2012). Our aim was to amplify the 16S rRNA gene region of endosymbionts from psyllids including putative plant pathogens such as *Ca*. Liberibacter species. In turn, these barcode primers contained the primer sequences (341F and 805R) that target the 16S rRNA region. The primer sequences (341F and 805R) were designed previously by Morrow et al. (2017), because these primers successfully amplified psyllid endosymbionts in addition to plant pathogens such as *Ca*. Liberibacter species; the forward primer, 16S-341F = 5′-CCTACGGGNGGCWGCAG-3′, and the reverse primer, 16S-805R = 5′-GACTACHVGGGTATCTAATCC-3′. These latter primers span the V3–V4 region of the 16S rRNA gene resulting in a 464 bp amplicon. This primer set was selected, based on results from Morrow et al. (2017), because it did not preferentially amplify the most abundant obligate endosymbiont of psyllids, *Carsonella*. *Carsonella* is present in all psyllids at very high titers (Thao et al., 2000b). Moreover, these primers did not preferentially amplify plant plastid 16S rRNA genes from psyllid DNA (Morrow et al., 2017), which can abundantly amplify from psyllid DNA when targeting other variable regions of the 16S rRNA gene (Nachappa et al., 2011).

Amplicon PCR using the above primer set consisted of 4 μl of template DNA, 0.9 μl of each 10 μM primer, and 20 μl of Phusion master mix (ThermoFisher Scientific) per each reaction. The 16S rRNA amplicons were then purified using PureLink™ PCR Purification Kit (Invitrogen). Using the cleaned PCR product as template, a second PCR was performed with HPLC-cleaned primers (5′-TATGGTAATTGTCCTACGGGNGGCWGCAG-3′ and 5′-AGTCAGCCAGCCGACTACHVGGGTATCTAATCC-3′) to complete the Illumina sequencing construct as described in McFrederick and Rehan (2016). Second PCR reactions consisted of 1 μl of template DNA, 0.5 μl of each forward and reverse primer, and 23 μl of Phusion master mix (ThermoFisher Scientific). For all PCR conditions, we followed PCR protocols as described in McFrederick and Rehan (2016). A total of 18 μl of PCR product from each reaction was normalized using SequalPrep™ Normalization Plate Kit (Invitrogen). We pooled 4 μl of each of the normalized samples, and performed additional bead clean up. The quality of the libraries was then assessed using a 2100 Bioanalyzer.

All 16S rRNA amplicons from psyllid samples were multiplexed in a single lane for dual index sequencing on the Illumina MiSeq PE300 at the DNA Technologies and Expression

[1]http://www.earthmicrobiome.org/protocols-and-standards/16s/

Analysis Core Laboratory at the University of California, Davis. The mothur v.1.41.3 pipeline was used to process raw read data following the protocol described in the MiSeq Standard Operating Procedure to process high-quality contigs from overlapping paired-end reads (Schloss et al., 2009; Kozich et al., 2013). To trim off adaptors and control against sequencing errors, low-quality reads were trimmed and removed using the following parameters: the maximum ambiguous base = 0, the maximum sequence length = 440 bp. Chimera vsearch was then used to remove chimeric sequences. To assign taxonomy, the SILVA database (release 132) was used. Operational taxonomic units (OTUs) were clustered at the level of ≥ 97% nucleotide sequence similarity (Stackebrandt and Goebel, 1994).

Morrow et al. (2017) suspected a high amount of OTU splitting when using the primers 341F and 805R (see above) because several OTUs were highly similar in SILVA taxonomy affiliation within a single psyllid sample. These related OTUs potentially can be real and represent different co-occurring strains within a sample, however, they can also represent amplification and/or sequencing error (during library preparation and/or Illumina sequencing), or different 16S rRNA copies from a single bacterium. To help control further against amplification and sequencing errors, in addition to the read quality control filtering steps mentioned above, OTUs with low read abundance per sample were removed from the dataset during the OTU picking step if the total counts of contigs for a particular OTU were equal to and/or less than five. Moreover, to control against environmental or aerosolized contaminates during library preparation five control samples that consisted of water instead of the DNA template were also included during the construction of the 16S rRNA libraries to detect if library contamination occurred. After taxonomy assignments using SILVA (above) we used BLASTn searches against the NCBI non redundant nucleotide database to further annotate 16S rRNA contigs. Furthermore, the aim of this study was to identify common and abundant endosymbionts and plant pathogens within psyllid bodies, therefore, OTUs of mitochondria, chloroplasts, and *Carsonella* were removed prior to analysis.

A + T Richness Analyses of Operational Taxonomic Unit 16S rRNA Gene Sequences

The 16S rRNA gene sequences of known free-living bacterial relatives or endosymbionts belonging to three host association categories such as obligate, long-term symbionts that co-occur with obligate endosymbionts, and facultative endosymbionts were obtained from NCBI GenBank to compare AT/GC content with the same 16S rRNA region of sequences in this study (**Supplementary Table 2**). All NCBI sequences were aligned with the 16S sequences here to obtain the same 16S rRNA gene region using NCBI BLASTn. The percent GC nucleotide composition was calculated for each of these aligned 16S rRNA sequence regions using BBMap (Bushnell, 2014) and Genomics % G–C Content Calculator (Science Buddies 2021). The box and whisker plot were generated based on GC content data using the package "ggplot" (Wickham, 2016) in R v.4.0.2 integrated in Rstudio v.1.3.959 (R Core Team, 2021).

Metagenomic Sequencing and Data Analysis of *Ca*. Liberibacter Infected Samples

Psyllid samples where *Ca*. Liberibacter was identified, using 16S rRNA sequencing (above), were further examined using a metagenomic approach. The goal of metagenomic sequencing was to generate more sequence data for *Ca*. Liberibacter loci, to further determine the evolutionary relationships of newly identified *Ca*. Liberibacter taxa. Psyllid samples that were positive for *Ca*. Liberibacter, based on 16S rRNA sequencing, include *Macrohomotoma gladiata* (P1–9), *Russelliana capsici* (P1–16), and *Trichochermes walkeri* (P1–28). A preserved herbarium specimen of *Solanum umbelliferum* (HS9) collected in 2011 that was infected with the *Ca*. L. psyllaurous haplotype G, based on our previous study Mauck et al. (2019), was also sequenced. Prior to library preparation, each sample was subjected to whole genome amplification using the Repli-G whole genome amplification kit (Qiagen) according to the manufacturer's instructions. Illumina library preparation and sequencing were conducted by Vincent J. Coates Genomics Sequencing Laboratory at the University of California, Berkeley. To increase the number of reads per sample, each *Ca*. Liberibacter-infected psyllid/plant library was sequenced twice as paired-end, 150 bp reads on two lanes of Illumina NovaSeq SP. The quality of raw reads for each sample run was verified with FASTQC v.0.11.3 (Andrews, 2010), and low-quality reads and adapter sequences were removed using Trimmomatic v.0.36 (Bolger et al., 2014). For each independent sample run, the trimmed sequences were assembled using MEGAHIT v.1.2.8 (Li et al., 2015), and the resulting contigs were categorized into either unassigned taxonomy or *Ca*. Liberibacter based on best BLASTn hits against nucleotide databases. To assess the overall quality of *Ca*. Liberibacter metagenomes, read coverage statistics of putative *Ca*. Liberibacter associated contigs were calculated using BBMap (Bushnell, 2014). To improve the binning of *Ca*. Liberibacter specific contigs, contigs from assembly outputs of each independent sample run were analyzed following the Anvi'o metagenomic workflow (Eren et al., 2015). Putative *Ca*. Liberibacter contigs were selected from both Anvi'o and best BLAST hit results from NCBI BLASTn with the following constraints, *E*-value = 1e-4 and sequence similarity >70%. Resulting putative *Ca*. Liberibacter contigs from independent sample runs were merged for each sample using MEGAHIT v.1.2.8. (Li et al., 2015). The genome assemblies were annotated using Prokka v1.14.5 (Seemann, 2014), and BLASTp searches of output files were conducted against non-redundant NCBI databases.

Phylogenetic Analyses

To determine the evolutionary relationships of putative novel *Ca*. Liberibacter species, orthologous proteins were obtained from metagenomes generated in this study and

those available on NCBI Genbank (below) using Orthofinder (Emms and Kelly, 2015). For phylogenetic analyses, we included a total of four draft *Ca.* Liberibacter genomes from this study and seven complete *Ca*. Liberibacter reference genomes from NCBI of *Ca*. L. africanus (NZ_CP004021.1), *Ca*. L. americanus (NC_022793.1), *Ca*. L. asiaticus (NC_012985.3), *Ca*. L. europaeus (GCA_003045065.1), *Ca*. L. psyllaurous (NC_014774.1), and *L. crescens* (NC_019907.1) in phylogenetic analyses. Due to low read coverage of *Ca*. Liberibacter in one of the *Ca*. Liberibacter positive psyllid samples (*M. gladiata*, P1–9) a low number of shared orthologs were identified. In consequence, phylogenetic analyses were conducted only with samples obtained from the psyllids *R. capsici* (P1–16) and *T. walkeri* (P1–28), in addition to the herbarium sample, *S. umbelliferum* (HS9), which shared 102 orthologs with the six fully sequenced *Ca*. Liberibacter reference genomes (above; **Supplementary Table 3**).

For the ortholog phylogenetic analysis, 102 orthologous sequences from three draft genomes along with the reference sequences (see above) were aligned using MAFFT v7.407 (Katoh and Standley, 2013). Trimming was performed using trimAL v1.2 (Capella-Gutiérrez et al., 2009) with two parameters, gap threshold "gt" and minimum coverage: "cons" in the trimmed alignment. In this case the gt and cons were considered as 0.9 and 20, respectively. All the alignments were visualized using the graphical user interface, and the PHYLIP file was generated from Mesquite v3.51 (Maddison and Maddison, 2018) and further used for phylogenetic tree construction. RAxML version 8.2.12 (Stamatakis, 2014) was used to obtain phylogenetic inferences. The MPI version was executed to run the program parallelly over many connected machines on the cluster. The "PROTGAMMAAUTO" model along with option (-f a) was used to perform rapid bootstrap analysis and to find the best scoring Maximum Likelihood (ML) tree. 100 searches from the parsimony start tree were performed. The Bipartitions tree generated from RAxML was visualized using FigTree v1.4.4 (Rambaut, 2018). The generated tree was then exported to Adobe Illustrator v 25.1 (Adobe Systems Incorporated, United States) for further editing.

For the 16S rRNA and endosymbiont phylogenetic analyses, similar to above, *Ca*. Liberibacter and endosymbiont sequences from 16S rRNA gene amplicon sequencing and NCBI GenBank were aligned using MAFFT v7.407 (Katoh and Standley, 2013) and trimmed manually. Mesquite v3.51 (Maddison and Maddison, 2018) was then used to generate the PHYLIP file. To generate the ML tree, the file was submitted to the CIPRES web server to run the RAxML-HPC BlackBox with "GTRGAMMA" model. For the *Ca*. Liberibacter, *Enterobacteriaceae*, or *Wolbachia* phylogeny the outgroup was set as *L. crescens*, *Escherichia coli* strain U 5/41, and *Wolbachia* endosymbiont of *Cimex lectularius*, respectively, and other settings were kept as default. Visualization and further editing of the bipartitions tree was performed using FigTree v1.4.4 (Rambaut, 2018) and Adobe Illustrator v 25.1 (Adobe Systems Incorporated, United States). The Psylloidea cladogram of 44 psyllid species, that was modified from Burckhardt et al. (2021), was redrawn using the package "ape" (Paradis et al., 2004) in R v.4.0.2 integrated in Rstudio v.1.3.959 (R Core Team, 2021).

DNA–DNA Hybridization and Average Nucleotide Identity Analyses

If phylogenetic analyses and BLAST identify a potentially new *Ca*. Liberibacter species DNA–DNA hybridization (DDH) and the average nucleotide identity (ANI) values will be computed pairwise with the new *Ca*. Liberibacter species and the reference *Ca*. Liberibacter genomes used above for phylogenetic analyses. DDH values were calculated using the Genome-to-Genome Distance Calculator 3.0 (GGDC[2])(Meier-Kolthoff et al., 2013). Briefly, according to Meier-Kolthoff et al. (2013) genome distances were calculated with BLAST+ local alignments and by calculating genomic distance as identities/HSP length (Formula 2). Distance values were then converted to estimated DDH values and their associated confidence intervals using a generalized linear model. The ANI of common genes and the percentage of conserved DNA among the *Ca*. Liberibacter genomes were calculated using the ANI calculator[3] (Rodriguez and Konstantinidis, 2016).

Further Screening for *Ca*. Liberibacter Taxa in Additional Psyllid Specimens

We obtained additional psyllid specimens from species that were identified as *Ca*. Liberibacter positive from our 16S rRNA amplicon sequencing to determine how prevalent *Ca*. Liberibacter infection is in these species. We were able to obtain additional psyllid specimens from two of the three *Ca*. Liberibacter positive species, which includes *Trichochermes walkeri* (N = 9 samples) and *Macrohomotoma gladiata* (N = 2 samples) (**Supplementary Table 4**). We also obtained three additional psyllid species to screen that feed on the same host plant genus (*Rhamnus* sp.) as one of our *Ca.* Liberibacter infected species here, *T. walkeri*, to determine if these psyllid species were infected with *Ca.* Liberibacter as well; these psyllid species include *Trioza rhamni* (N = 4 samples), *Cacopsylla alaterni* (N = 6 samples), and *Cacopsylla rhamnicola* (N = 7 samples) (**Supplementary Table 4**). Depending on specimen availability, for each psyllid sample a single adult individual and/or 2–3 nymphs were pooled for each DNA extraction (**Supplementary Table 4**).

DNA was extracted from whole psyllids using the Quick-DNA^{TM} Microprep Kit (Zymo Research). DNA quality and yield was assessed by gel electrophoresis and the SpectraMax QuickDrop Micro-Volume Spectrophotometer (Molecular Devices). Based on *Ca*. Liberibacter phylogenetic analyses here of 16S rRNA amplicon samples (see above), *T. walkeri* and *M. gladiata* were infected with *Ca*. Liberibacter taxa that were closely related to *Ca*. L. asiaticus and *Ca*. L. psyllaurous, respectively, in consequence, modified universal *Ca*. Liberibacter primers, LG774F/LG1436R (Morris et al., 2017), were used for screening additional psyllid specimens. This primer pair is expected to amplify a 684 bp fragment from the 16S rRNA gene region of *Ca*. L. asiaticus, *Ca*. L. psyllaurous, and *Ca*. L. europaeus. PCR was performed in 25 μl reactions consisting of 2 μl of DNA

[2]http://ggdc.dsmz.de/ggdc.php#

[3]http://enve-omics.ce.gatech.edu/ani/index

template, 2.5 μl of 10X Thermopol buffer (NEB), 0.5 μl of dNTP mix (2 mM each), 0.5 μl of each 10 μM primer, and 0.125 μl of Taq DNA polymerase (NEB). The Bio-Rad C1000 Touch^{TM} Thermal Cycler was used with the following protocol: 95°C for 30 s, followed by 30 cycles of 95°C for 30 s, 58°C for 1 min, and 72°C for 1 min, then 72°C for 5 mins. Only *T. walkeri* samples ($N = 9$ samples) were positive for *Ca*. Liberibacter based on PCR screening with universal *Ca*. Liberibacter primers (above). In turn, amplicons from *T. walkeri* were purified with QIAquick Gel Extraction Kit (Qiagen) and cloned into the pGEM T-easy vector (Promega) following the manufacturer's instruction. Sanger sequencing was conducted by the Genomics Core facility at the University of California, Riverside.

RESULTS

16S rRNA Amplicon Sequencing of Psyllid Microbiomes

Amplicon sequencing of the bacterial 16S rRNA gene region from 45 psyllid samples, which includes 44 psyllid species (**Supplementary Table 1**), generated a total of 7,516,747 contigs. Following quality control and criteria filtration, 198,560 high-quality contigs (305,128 reads) were retained. The total number of contig counts per psyllid sample ranged from 17 to 4,531 with an average of 798. These contigs were clustered into 91 OTUs, and each psyllid sample possessed an average of 2–3 OTUs, (min = 1, max = 7, and SD = 1; **Supplementary Table 5**). Non-target OTUs, such as mitochondria, chloroplasts, and *Carsonella*, only represented 7% of the total reads for high-quality contigs. Seven OTUs were present in two out of the five control samples. Specifically, three OTUs were unique to one control sample (P2–96) and four OTUs were unique to the second control sample (P3–96) (**Supplementary Table 6**). None of the OTUs in the control samples were present in any of the psyllid samples. The contig counts for control samples were relatively low with an average of 21 contigs per OTU (min = 7, max = 80, and SD = 27) (**Supplementary Table 6**). In turn, sequences present in control samples may have been airborne contaminants that were present at low abundance during the library preparation process.

Low Diversity of Putative Psyllid Endosymbiont Operational Taxonomic Units Within 44 Divergent Psyllid Species From 45 Psyllid Samples

From 16S rRNA amplicon sequencing, OTUs that belong to four bacterial phyla (Proteobacteria, Bacteroidetes, Firmicutes, and Fusobacteria) were identified from 45 psyllid microbiomes (**Figure 1**). The majority of OTUs, among all psyllid samples examined, reside within Proteobacteria (83 OTUs out of 92 OTUs) (**Supplementary Table 5**), and all psyllid samples possess Proteobacteria OTUs (**Supplementary Table 5**). Within Proteobacteria, OTUs reside from two classes, Alphaproteobacteria (13 OTUs) and Gammaproteobacteria (70 OTUs), and were found in 24 and 36 psyllid samples, respectively (**Supplementary Table 5**).

The majority of OTUs (77%) from psyllid samples belong to the class Gammaproteobacteria, and primarily reside within the bacterial Class *Enterobacteriaceae* (68% of OTUs) (**Figure 1**). These *Enterobacteriaceae* OTUs were unique to their psyllid species, except for OTUs 8, 33, 72, 76, and 162, which occur in more than one psyllid sample (**Supplementary Table 5** and **Supplementary Figure 1**). Approximately 55% of *Enterobacteriaceae* OTUs were not identified to the genus level, however, ∼8, 1, 1, and 2% were identified as *Arsenophous*, *Sodalis*, *Pantoea*, and Enteric bacteria, respectively (**Figure 1** and **Supplementary Table 5**).

Within the class Alphaproteobacteria, five *Wolbachia* (*Anaplasmataceae*) OTUs were present in 19 out of 45 psyllid samples (∼42% of all psyllid samples). *Wolbachia* OTU1 was present in 19 psyllid samples/species (**Supplementary Figure 1** and **Supplementary Table 5**), and the other four *Wolbachia* OTUs co-occur with *Wolbachia* OTU1 in three psyllid samples, *Cornegenapsylla allophyli*, *Cacopsylla pruni*, and *Trioza vitiensis* (**Supplementary Table 5**). Other alphaproteobacterial OTUs include the genus *Sphingomonas* and *Rickettsia* (**Figure 1**). The genus *Spingomonas* was detected in four psyllid samples (∼9% of all psyllid samples) with two different OTUs; OTU1799 was detected in *Pachypsylla celtidismamma*, while OTU72 was present in *Livia junci*, *Triozoida limbata*, and *Arytaina devia* ssp. *insularis* (**Supplementary Table 5** and **Supplementary Figure 1**). The psyllid sample, *C. pruni*, was infected with two different *Rickettsia* OTUs, OTU127 and OTU367, and *Heterotrioza chenopodii* was detected with *Rickettsia* OTU183 (**Supplementary Table 5**).

BLAST results from psyllid microbiome 16S rRNA sequences reveal that the vast majority (80%) of sequences had best BLAST hits to insect endosymbionts on NCBI GenBank and displayed an average of >∼96% nucleotide sequence similarity to known insect-associated endosymbionts (**Supplementary Table 5**). The remaining sequences were primarily found to be plant (2%) or environmental associated microbiomes (10%) (**Supplementary Table 5**). Sequences that are related to known plant pathogens were ∼5%, including the three *Ca*. Liberibacter OTUs and a Xylella related OTU (OTU155) (**Supplementary Table 5**). Only two OTUs (OTUs 618 and 1,355) (2%) in two samples had best BLAST hits to human associated microbes, and therefore these latter OTUs may be contamination from psyllid collection or extraction (**Supplementary Table 5**).

Identification of Putative Long-Term Endosymbionts in Psyllid Species

The obligate endosymbiont of aphids (*Buchnera*), in addition to other obligate host-restricted endosymbiont species in insects, possess 16S rRNA gene sequences that are significantly higher in AT richness compared to their free-living relatives (Lambert and Moran, 1998; Nováková et al., 2009). Therefore, we analyzed GC content of the 16S rRNA gene region sequenced for OTUs in this study (**Supplementary Table 2**) and compared them to free-living relatives and known obligate, long-term, and facultative endosymbionts of insects. These free-living relatives and known insect

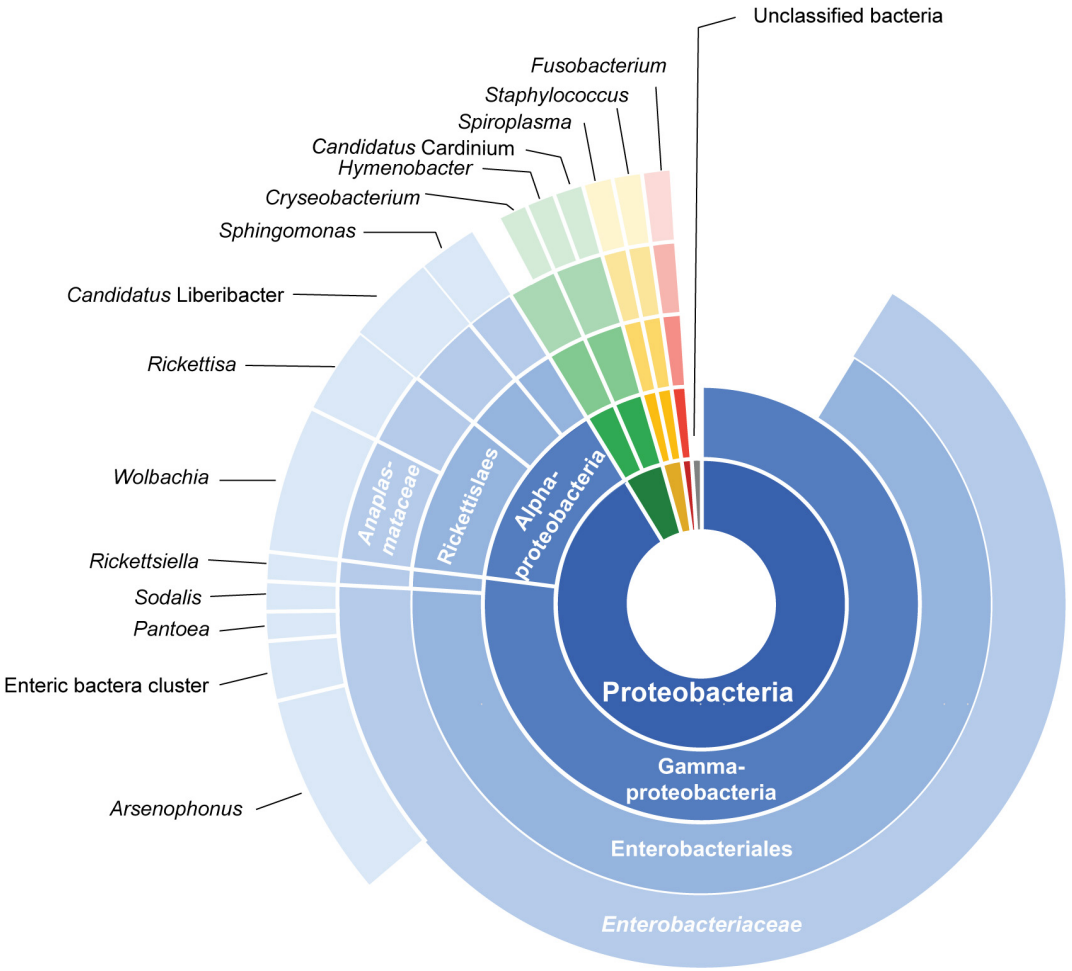

Phylum	Class	Order	Family	Genus
Unclassified Bacteria (1.1 %)				
Fusobacteria (1.1 %)	Fusobacteria (1.1 %)	Fusobacteriales (1.1 %)	*Fusobacteriaceae* (1.1 %)	*Fusobacterium* (1.1 %)
Firmicutes (2.2 %)	Bacilli (1.1 %)	Bacillales (1.1 %)	*Staphylococcaceae* (1.1 %)	*Staphylococcus* (1.1 %)
	Mollicutes (1.1 %)	Entomoplasmatales (1.1 %)	*Spiroplasmataceae* (1.1 %)	*Spiroplasma* (1.1 %)
Bacteriodetes (4.4 %)	Sphingobacteria (2.2 %)	Sphingobacteriales (2.2 %)	*Flammeovirgaceae* (2.2 %)	*Candidatus* Cardinium (1.1 %)
				Hymenobacter (1.1 %)
	Flavobacteria (2.2 %)	Flavobacteriales (2.2 %)	*Flavobacteriaceae* (2.2 %)	*Chryseobacterium* (1.1 %)
				Unclassified *Flavobacteriaceae* (1.1 %)
Proteobacteria (91.2 %)	Alphaproteobacteria (14 %)	Sphingomonadales (2.2 %)	*Sphingomonadaceae* (2.2 %)	*Sphingomonas* (2.2 %)
		Rizobiales (3.3 %)	*Rizobiaceae* (3.3 %)	*Candidatus* Liberibacter (3.3 %)
		Rickettislaes (9 %)	*Rickettsiaceae* (3.3 %)	*Rickettisa* (3.3 %)
			Anaplasmataceae (5.5 %)	*Wolbachia* (5.5 %)
	Gammaproteobacteria (76.9 %)	Legionellaes (1.1 %)	*Coxiellaceae* (1.1 %)	*Rickettsiella* (1.1 %)
		Enterobacteriales (67 %)	*Enterobacteriaceae* (67 %)	*Sodalis* (1.1 %)
				Pantoea (1.1 %)
				Enteric bacteria cluster (2.2 %)
				Arsenophonus (7.7 %)
				Unclassified *Enterobacteriaceae* (54.9 %)
		Unclassified Gammaproteobacteria (8.8%)		

FIGURE 1 | The sunburst diagram above represents the percentage of 91 operational taxonomic units (OTUs) from 44 psyllid species (from 45 psyllid samples) that belong to a particular taxonomic group. The ring positions of the diagram represents taxonomic hierarchy: (inner to outer) Phylum/Class/Order/Family/Genus.

endosymbionts were chosen because they belong to the same bacterial classes that the majority of OTUs from our study were classified as based on Silva, as average GC content can vary with taxonomy (**Supplementary Table 2**). Specifically, we analyzed: (1) the percentage of GC content from 16S rRNA sequences and (2) the phylogenetic patterns of 16S

rRNA sequences that were in the average GC percent range of known primary and long-term insect endosymbionts of insects (**Figure 2**).

We found that *Carsonella*, the obligate endosymbiont of psyllids, displays the lowest average GC content (∼35% GC and SD = 0.9) compared to all sequences analyzed in this analysis for the same 402-nt 16S rRNA gene region (**Supplementary Table 2** and **Figure 2**). In contrast, the obligate endosymbiont of aphids, *Buchnera*, which also belongs to Gammaproteobacteria, shows an average of ∼47% GC (SD = 0.3) content (**Figure 2**), which was very similar to *Profftella*, the Gammaproteobacterial long-term symbiont that is harbored within the psyllid genus Diaphorina (**Figure 2** and **Supplementary Table 2**). Other Gammaproteobacterial long-term endosymbionts identified in the psyllids *Ctenarytaina eucalypti* and *Heteropsylla cubana* displayed an average of ∼52% GC content (**Figure 2** and **Supplementary Table 2**). Obligate and long-term symbionts that belong to Alphaproteobacteria and Gammaproteobacteria such as *Wolbachia* and *Arsenophonus*, respectively, displayed an average of ∼48% (SD = 0 and 0.9, respectively) GC content for this 16S rRNA gene region (**Figure 2** and **Supplementary Table 2**). Interestingly, facultative *Wolbachia* endosymbionts display very similar average GC content (∼ 47% GC, SD = 0.4) compared to the average of obligate *Wolbachia* endosymbionts. In contrast, facultative *Arsenophonus* symbionts displayed an average of ∼52% GC (SD = 1.6) content (**Figure 2** and **Supplementary Table 2**). The free-living relatives of these latter endosymbionts and sequences from this study display an average of ∼53% GC (SD = 1.4), which is in the range of several facultative endosymbionts analyzed in this study (**Figure 2** and **Supplementary Table 2**). Overall, we found that the average percentage of GC content of obligate and long-term endosymbionts ranged from ∼41 to 49% GC (**Figure 2** and **Supplementary Table 2**).

A second signature of long-term endosymbiont evolution is congruent phylogenetic patterns between endosymbiont insect taxa and their insect hosts. For this analysis we only constructed phylogenies of endosymbiont sequences if their 16S rRNA sequence's percent GC content was between the average range of obligate and long-term endosymbionts (∼41–49%) (above). We found 34 sequences that fell within this range and they either belonged to *Enterobacteriaceae* or *Wolbachia*. In turn we constructed two separate phylogenies for these two distinct classes of bacteria (**Figure 3** and **Supplementary Figure 2**). Compared to the psyllid host phylogeny, *Wolbachia* sequences appear to be recently diverged, largely sharing the same OTU (OTU1) and are horizontally transmitted across all psyllid families examined (**Supplementary Figure 2**). For the *Enterobacteriaceae* phylogeny four distinct bacterial lineages were supported with bootstrap values of 87% and higher. However, only two clades (hereafter named clade 1 and 2) appear to have congruent phylogenies with the psyllid host phylogeny at the family level for Triozidae and Psyllidae (**Figure 3**). More sequence information for both bacterial and psyllid phylogenies are required, however, to provide robust bootstrap support at a finer resolution.

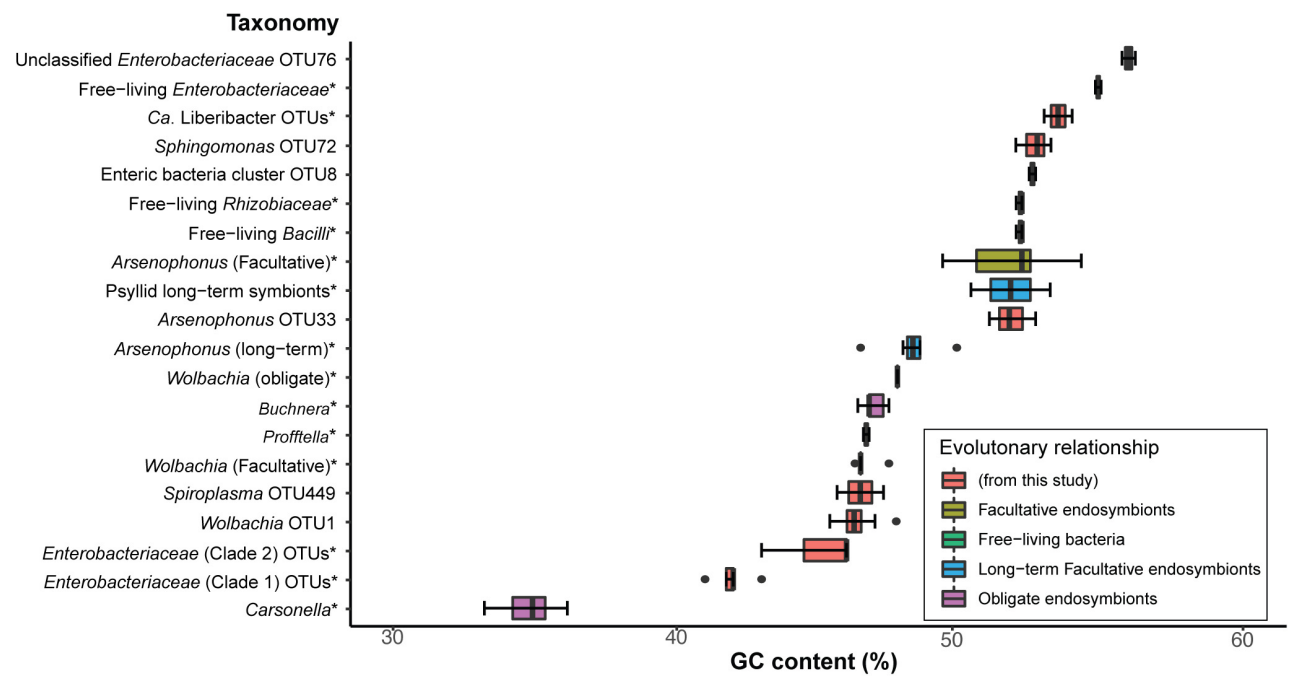

FIGURE 2 | Comparison of GC contents from a 429-nt 16S rRNA gene region obtained from endosymbiont taxa of known insect host associations (obligate, long-term, and facultative), free-living bacterial relatives, and a selection of OTUs from this study. * indicates that detailed OTU and NCBI sequence and species information is available in **Supplementary Table 2**. Percent GC content for all 16S rRNA sequence data are also presented in **Supplementary Table 2**. Box and whisker plots represent average percent GC content and the standard deviation.

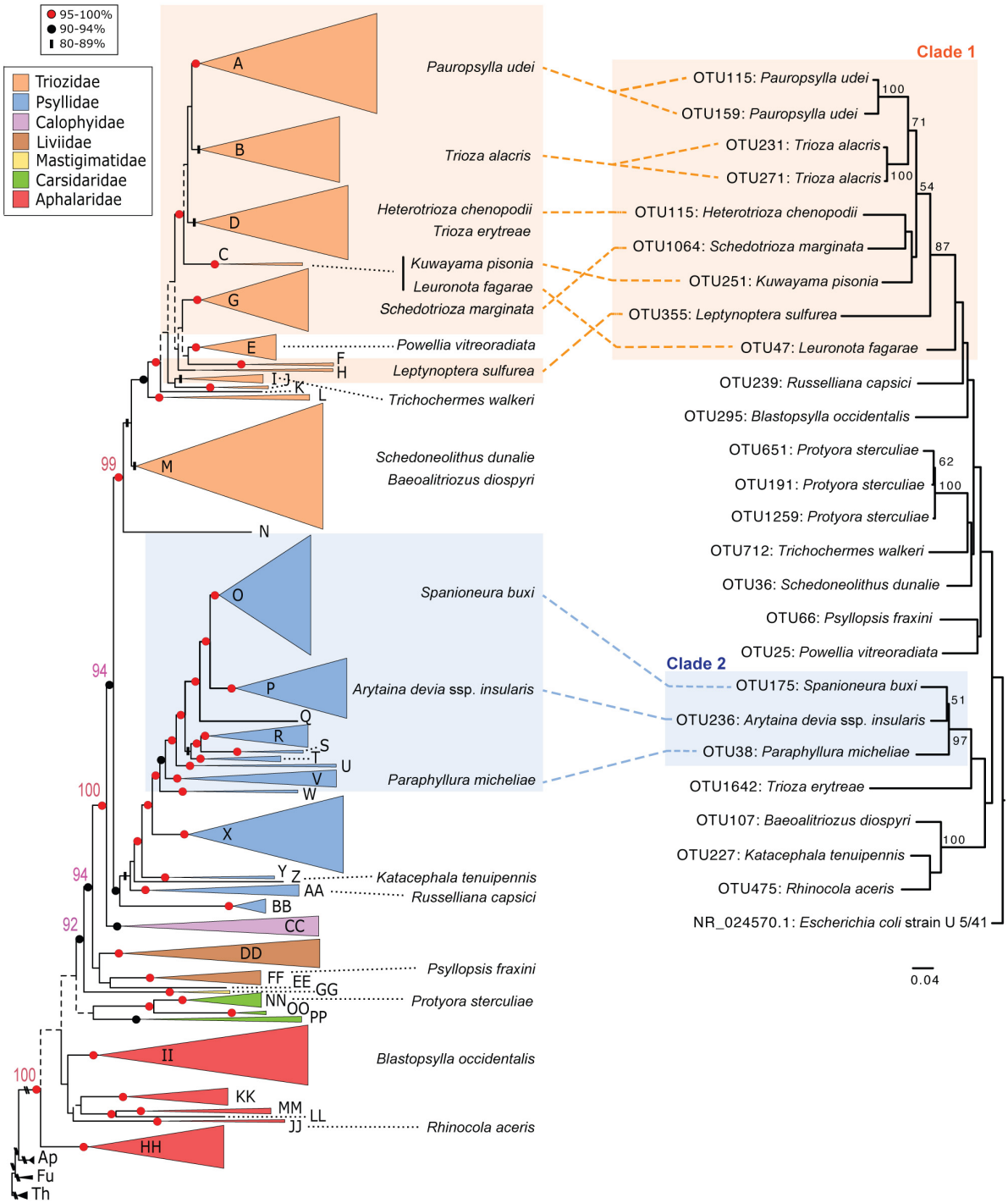

FIGURE 3 | Comparison of phylogenies from both psyllid hosts and their endosymbiont *Enterobacteriaceae*. Maximum likelihood tree of Psylloidea (*left*) redrawn from Percy et al. (2018) with updated classification according to Burckhardt et al. (2021). For the psyllid phylogeny node support is indicated by shape and color of node symbols, and nodes with <50% bootstrap support are indicated by dotted lines. Capital letters in the psyllid phylogeny represent generic groups presented in Percy et al. (2018) and are detailed in **Supplementary Table 1**. Psyllid species names from samples in this study that harbor *Enterobacteriaceae* with 16S rRNA sequences that have a GC content in the range of ~41–49% are indicated on both the psyllid and *Enterobacteriaceae* phylogenies. For the *Enterobacteriaceae* 16S rRNA phylogeny (429-nt) using RAxML with 100 bootstraps only branch support at 50% or above is shown. The scale bar indicates nucleotide changes per site. The tree was rooted with the outgroup *Escherichia coli* strain U 5/41 (NR_024570.1).

Candidatus Liberibacter Taxa Identified From 16S rRNA Amplicon Sequencing in Three Psyllid Species

Three *Ca*. Liberibacter OTUs (OTU526, OTU841, and OTU443) were identified in three different psyllid species, *Macrohomotoma gladiata* (P1–9), *Russelliana capsici* (P1–16), and *Trichochermes walkeri* (P1–28). In *M. gladiata*, OTU526 has the best BLAST hit to *Ca*. L. asiaticus with 98% nucleotide sequence similarity (**Supplementary Table 5**). The OTU841 in *R. capsici* has the best BLAST hit to *Ca*. L. americanus with 96.8% nucleotide sequence similarity (**Supplementary Table 5**). The OTU443 from the psyllid sample *T. walkeri*, displayed the best BLAST hit to "unclassified *Ca*. Liberibacter" with 98.3% nucleotide sequence similarity (**Supplementary Table 5**). To further determine the identity and evolutionary relationships of these latter *Ca*. Liberibacter taxa psyllid DNA samples that were positive for *Ca*. Liberibacter were subject to metagenomic sequencing for downstream phylogenetic analyses.

Four *Ca*. Liberibacter Draft Genomes Were Obtained From Metagenomic Sequencing

To further analyze *Ca*. Liberibacter taxa identified from 16S rRNA amplicon sequencing, we performed metagenomic sequencing on the three *Ca*. Liberibacter positive psyllid samples (*M. gladiata*, *R. capsici*, and *T. walkeri*) and one herbarium specimen infected with *Ca*. L. psyllaurous haplotype G from a previous study (Mauck et al., 2019). An average of 66,126,618 high quality reads were generated for each independent psyllid/plant sample run (SD = 5,675,882; **Supplementary Table 7**). Metagenomic assemblies for the four samples yielded an average of ∼0.9 Mb (SD = 0.3 Mb) of *Ca*. Liberibacter specific sequences per sample with approximately 322–1,637 contigs per sample (**Table 1**). The *Ca*. Liberibacter assembly from *M. gladiata* had very low sequence coverage and a low N50 value (**Table 1**) and therefore was not included in downstream phylogenetic analyses. The remaining three *Ca*. Liberibacter assemblies had variable levels of read coverage per contig because DNA samples were of low concentration and obtained from Repli-G whole genome amplification (**Supplementary Table 8**), however, a total of 102 shared orthologous *Ca*. Liberibacter genes (**Supplementary Table 3**) were still obtained and used for subsequent phylogenetic analyses.

TABLE 1 | Statistics of mapping and assembly of *Ca*. Liberibacter sequences from psyllids and plant DNA.

Samples	*M. gladiata*	*R. capsici*	*T. walkeri*	*S. umbelliferum*
Total sequence length (bp)	606681	1212287	922660	803932
The number of contigs	1,063	1,637	322	407
N50 (bp)	583	1,530	4,943	3,031
Average (bp)	570	740	2,865	1,975
Min (bp)	200	200	301	301
Max (bp)	6,149	23,655	17,720	15,041

New *Ca*. Liberibacter Taxa Uncovered by Phylogenetic, DNA–DNA Hybridization, and Average Nucleotide Identity Analyses

A phylogenetic analysis was first conducted with *Ca*. Liberibacter 16S rRNA gene sequences that were derived from both 16S rRNA amplicon sequencing and metagenomic sequencing. The *Ca*. Liberibacter species from *T. walkeri* (P1–28) formed a clade together within other *Ca*. L. psyllaurous taxa with 92% bootstrap support (**Figure 4**). The *Ca*. Liberibacter species from *R. capsici* (P1–16) forms a distinct lineage apart from other *Ca*. Liberibacter species (**Figure 4**). This latter *Ca*. Liberibacter taxa shares a more recent common ancestor with *Ca*. L. americanus compared to other *Ca*. Liberibacter species (**Figure 4**). Only the 16S rRNA sequence of *Ca*. Liberibacter from *M. gladiata* (P1–9) was obtained through 16S rRNA amplicon sequencing and this sequence appears to be more closely related *Ca*. L. asiaticus (**Figure 4** and **Supplementary Table 5**). The sequence divergence between the 16S PCR-derived sequence and the metagenomic-derived 16S sequence for both P1–16 and P1–28 was present, however, bootstrap support was very high (100%) and nucleotide differences were very small (as the scale on the figure indicates 0.006 nucleotide substitutions per site). This sequence divergence between PCR and metagenomic 16S sequences may be attributed to sequencing error or nucleotide substitutions due to multiple 16S rRNA operons per Liberibacter genome and/or co-occurring strains in pooled psyllid samples.

Since the latter 16S rRNA phylogenetic analysis was constrained in only using a 402 nt sequence region, which was amplified by 16S amplicon sequencing, a more robust phylogenetic analysis was subsequently conducted. The second phylogenetic analysis consists of a 27,922 amino acid alignment of 102 orthologous proteins. From this analysis the *Ca*. Liberibacter species from *R. capsici* (P1–16) forms a distinct clade apart from the other *Ca*. Liberibacter species based on the high amount of amino acid changes per site (**Figure 5**). The *Ca*. Liberibacter taxa isolated from *T. walkeri* (P1–28) and *S. umbelliferum* significantly clustered within *Ca*. L. psyllaurous (also known as *Ca*. L. solanacearum) with 100% bootstrap support (**Figure 5**).

To further determine if the *Ca*. Liberibacter species from *R. capsici* (P1–16) is a distinct *Ca*. Liberibacter species compared to known *Ca*. Liberibacter reference genomes we conducted both DDH and ANI analyses. Pairwise DDH estimates for all reference Liberibacter species genomes and *Ca*. L. capsica ranged from 18.9 to 31.1% (**Supplementary Table 9**). These values are well below the 79% cutoff commonly applied to members of the same subspecies and the 70% cutoff applied to members of the same species. Pairwise ANI estimates for all reference *Ca*. Liberibacter species genomes and *Ca*. L. capsica ranged from 69.72 to 84.49% (**Supplementary Table 10**). These values are well below the 95% cutoff commonly applied to members of the same species for ANI analyses (Goris et al., 2007). Collectively, these results provide further support that *Ca*. L. capsica (P1–16) is a distinct *Ca*. Liberibacter species.

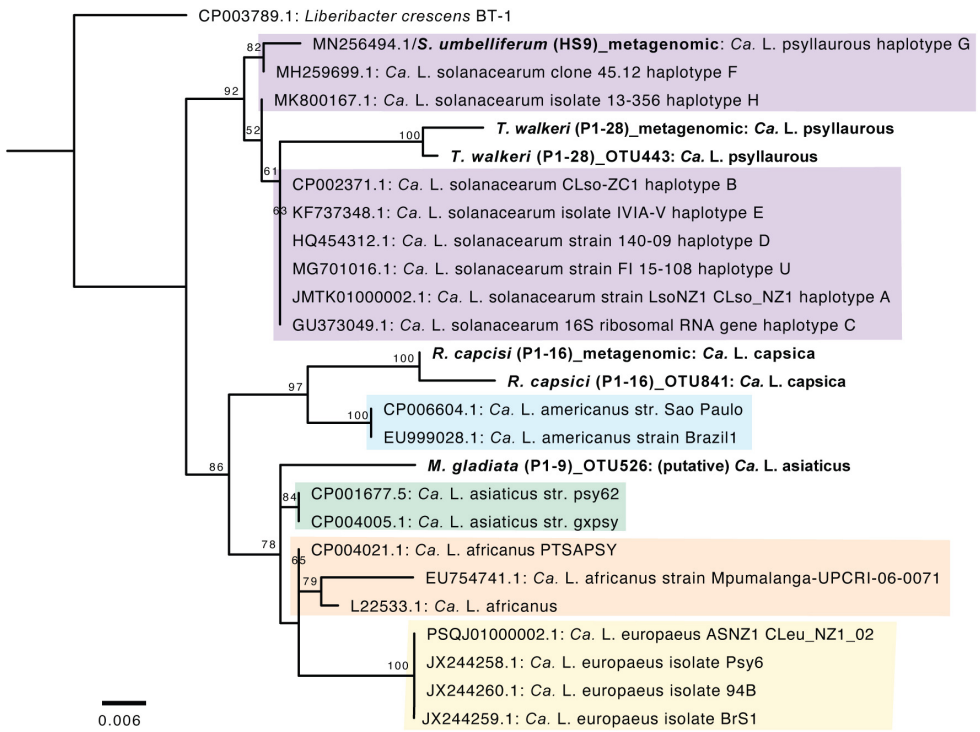

FIGURE 4 | Phylogenetic relationships of *Ca*. Liberibacter species based on a 402-nt 16S rRNA region using RAxML with 100 bootstraps. The branch labels in bold are 16S rRNA sequences obtained here from 16S rRNA amplicon sequencing (indicated with OTU numbers) and metagenomic sequencing (indicated as metagenomic). The tree was rooted with the outgroup *Liberibacter crescens* BT-1. Only branch support at 50% or above is shown. Scale bar indicates nucleotide changes per site.

Candidatus Liberibacter Taxa Is Detected in Additional Psyllid Specimens of *Trichocherms Walkeri*

The purpose of the *Ca*. Liberibacter screening was to (1) determine if the *Ca*. Liberibacter infection is prevalent in the psyllid species that were identified with *Ca*. Liberibacter OTUs from 16S rRNA gene amplicon sequencing, and (2) if the *Ca*. Liberibacter infection occurs in psyllid species that share the same plant host genus as *T. walkeri* (*Rhamnus*); samples screened were based on sample availability, see "Materials and Methods" and **Supplementary Table 4**. Therefore, all DNA extracts from these latter psyllid specimens were screened with the primer set LG774F/LG1463R, which universally amplifies ∼0.7 kb of *Ca*. Liberibacter 16S rRNA fragments (see "Materials and Methods"). Only *T. walkeri* samples (N = 9, **Supplementary Table 4**) produced a positive PCR band using this primer set, and therefore were cloned and Sanger sequenced one PCR clone from each sample for BLAST analysis.

Based on NCBI BLAST results, the best BLAST hit (E-value = 0) from the nine *T. walkeri* samples was the taxon *Ca*. L. psyllaurous with >97% sequence identity (**Supplementary Table 11**). Although all the *T. walkeri* samples matched *Ca*. L. psyllaurous with high sequence identity, there was small nucleotide differences between sample sequences, which may be attributed to the multiple 16S rRNA operon copies within a single *Ca*. Liberibacter genome and/or strain differences within or among psyllid individuals (**Supplementary Table 11**). These screening results, in terms of identity (*Ca*. L. psyllaurous) and sequence variation, are consistent with 16S rRNA amplicon sequencing and metagenomic sequencing from the *T. walkeri* (P1–28) sample, and in turn, this may indicate that *Ca*. Liberibacter psyllaurous is highly prevalent in some *T. walkeri* populations.

DISCUSSION

Our study provides the most taxonomically and geographically diverse dataset of psyllid endosymbiont associations to date, covering 44 divergent taxa across five families. Our results suggest that psyllids house minimal bacterial communities, in agreement with more regionally focused studies of psyllid microbiomes and the microbiomes of other hemipterans (Thao et al., 2000a; Jing et al., 2014; Overholt et al., 2015; Morrow et al., 2017, 2020; Nakabachi et al., 2020a). Similar to the findings of Morrow et al. (2017), we found that bacteria in the class *Enterobacteriaceae* are particularly prevalent in psyllid microbiomes (**Figure 1** and **Supplementary Table 5**). We also found that most sequences recovered during microbiome profiling closely match NCBI GenBank sequences of other insect endosymbionts (**Supplementary Table 5**). This result indicates that the majority of microbial sequences detected in our study are those of actual psyllid endosymbionts rather than transient

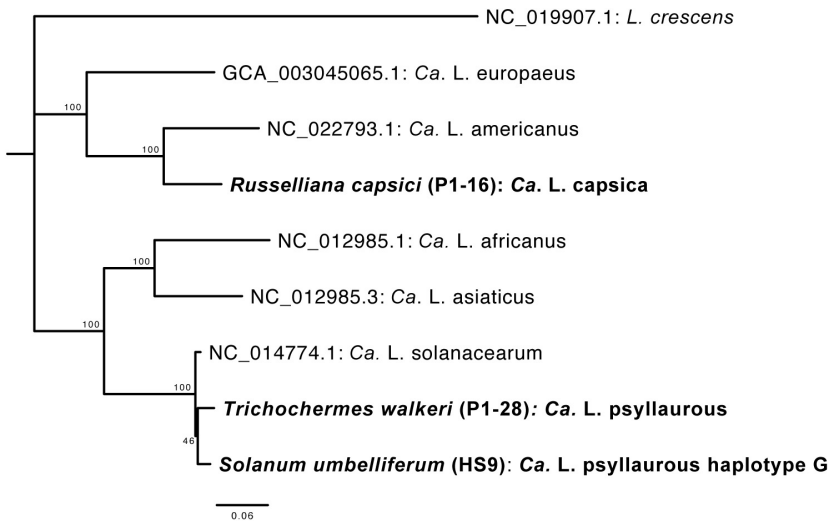

FIGURE 5 | Phylogenetic relationships of *Ca*. Liberibacter species based on a 27,922 amino acid alignment of 102 orthologous genes using RAxML with 100 bootstraps. Orthologs from the *Ca*. Liberibacter taxa were obtained from three draft metagenomes sequenced here and are shown in bold with their psyllid host names indicated. The tree was rooted with the outgroup *Liberibacter crescens*. Scale bar indicates amino acid changes per site.

associates or contaminants from the environment. Using the genomic data generated through microbiome profiling, we also uncovered putative long-term endosymbiont associations in the psyllid families Triozidae and Psyllidae based on signatures of long-term endosymbiont evolution. Moreover, we identified three psyllid species that are potential hosts for *Ca*. Liberibacter taxa, as well as a new "*Candidatus*" Liberibacter species from the psyllid *R. capsici*, for which we propose the name "*Candidatus*" Liberibacter capsica after the psyllid host it was isolated from.

Long-term insect endosymbionts are generally characterized by possessing higher evolutionary rates, lower GC content, and co-cladogenesis patterns with their insect host (Heddi et al., 1998; Nováková et al., 2009). Sap-feeding insects that belong to Hemiptera within the suborder Auchenorrhyncha epitomize very ancient and complex co-occurring endosymbiont associations (Koga et al., 2013). In these latter cases, at least two endosymbionts are obligate for auchenorrhynchan host survival, and losses of some of these long-term endosymbionts occur, and are replaced with a more recent endosymbiont association (Koga et al., 2013). Based on genome content of long-term psyllid symbiont genomes at least three endosymbiont taxa are expected to be long-term endosymbiont associates of psyllids, but these symbiont taxa are not closely related to one another and belong to divergent psyllid lineages (Sloan and Moran, 2012; Nakabachi et al., 2020a,b). Here, we identify two clades (defined here as clade 1 and 2) in *Enterobacteriaceae* that appear to be congruent with two families of psyllids, Triozidae and Psyllidae, respectively (**Figure 3**). The GC content of clade 1 and 2 is an average of 42 and 45% GC, respectively, which is in between the average range of known obligate and long-term insect endosymbiont sequences (∼41–49%) examined in this study, which primarily belong to Gammaproteobacteria (**Figure 2**).

Bacterial sequences within clade 1 and 2 had the same best BLAST hit ∼90% sequence identity (within the top three best BLAST hits for two psyllid species) to an already characterized symbiont in Triozidae ("Secondary endosymbiont of *Trioza magnoliae*") and Psyllidae ("Y-symbiont of *Anomoneura mori*"), respectively (**Supplementary Table 5** and **Figure 3**). Interestingly, the "Y-symbiont of *Anomoneura mori*" was previously characterized to be localized inside the bacteriome (i.e., specialized insect organ to house endosymbionts) of *A. mori* within the syncytium of the bacteriome with *Carsonella* being localized within the bacteriocytes in the bacteriome (Fukatsu and Nikoh, 1998). Other long-term obligate endosymbionts of insects including *Profftella* have very similar localization patterns in bacteriomes (Nakabachi et al., 2013). Surprisingly, we did not find a related symbiont to the "Secondary endosymbiont of *Trioza magnoliae*" in *T. magnoliae* from our sample as it possessed very high levels of *Wolbachia* contigs, similar to what Morrow et al. (2017) observed for this psyllid species in addition to *Diaphorina citri* in their study. In turn, we conducted a post hoc analysis of *T. magnoliae* and found that this *Enterobacteriaceae* endosymbiont was present in our dataset before we filtered out OTUs with low contig coverage, and these sequences had a best BLAST hit with 99% sequence identity with 100% coverage to the "Secondary endosymbiont of *Trioza magnoliae*." During our post hoc analysis of filtered microbiome reads we also recovered one other psyllid species within Triozidae (*Trioza erytreae*) that had a best BLAST hit to the "Secondary endosymbiont of *Trioza magnoliae*" with ∼90% sequence identity. Analogously, when we searched for filtered microbiome sequences within Psyllidae, sequences from *Cacopsylla saliceti* gave a best BLAST hit to the "Y-symbiont of *Anomoneura mori*" with ∼97% sequence identity. In turn, our dataset is very conservative in regard to the presence of symbiont taxa in specific psyllid species. Therefore, if symbionts within clades 1 and 2 have a congruent relationship with psyllid lineages within Triozidae and Psyllidae, respectively, the remaining

psyllid species in these lineages where we did not detect these latter long-term symbionts could have either lost their long-term symbiont or alternatively our sampling effort was not sensitive enough to detect the presence of these symbionts. Understanding putative long-term endosymbiont associations will require more screening of Triozidae and Psyllidae with targeted primers, as well as fluorescence in situ hybridization studies to identify symbiont locations in bacteriomes.

Previous phylogenetic studies on psyllid symbiont taxa have established that numerous facultative symbionts have been horizontally transmitted recently in psyllid lineages (Thao et al., 2000a; Hall et al., 2016; Morrow et al., 2017). Here we identified similar patterns of rampant horizontal transmission in *Enterobacteriaceae* and *Wolbachia* among all psyllid families analyzed here (**Figure 3** and **Supplementary Figure 2**). This was especially the case for OTUs that occurred in more than one psyllid species including the widespread *Wolbachia* lineage (OTU1) (**Supplementary Figure 2**). For example, *Wolbachia* OTU1 is present in 19 divergent psyllid species spanning across five psyllid families (**Supplementary Figure 1**). These latter results indicate that a recent divergence of the *Wolbachia* OTU1 lineage has occurred (as an OTU consists of 16S rRNA sequences with 97% sequence identity or higher), and this *Wolbachia* lineage was acquired multiple times in divergent psyllid taxa (**Supplementary Figure 2**). Very similar findings of recent endosymbiont divergence and horizontal transmission of *Ca*. Hamiltonella defensa, *Ca*. Regiella insecticola, and *Ca*. Serratia symbiotica have also been observed among highly divergent insect species (Russell et al., 2003; Moran et al., 2005).

The most well-known facultative symbionts of psyllids that are of economic concern are those in the genus *Ca*. Liberibacter because many are associated with disease in psyllid plant hosts (Wang et al., 2017; Mauck et al., 2019). In plants, *Ca*. Liberibacter taxa infect phloem vascular tissue and several *Ca*. Liberibacter taxa have emerged as serious threats to food production in the last 100 years (Wang et al., 2017). Interestingly, some *Ca*. Liberibacter taxa, such as *Ca*. L. psyllaurous may actually benefit the psyllid host by suppressing plant defenses that are directed toward the psyllid (Casteel et al., 2012). *Ca*. Liberibacter primarily is an unculturable bacterium which belongs to the Alphaproteobacteria class of bacteria in the phylum Proteobacteria (Bové, 2006). Currently, eight species of *Ca*. Liberibacter have been identified around the world, mostly because of emergence as disease causing agents in crops, and these include *Ca*. L. psyllaurous, *Ca*. L. asiaticus, *Ca*. L. africanus, *Ca*. L. americanus, *Ca*. L. europaeus, *Ca*. L. brunswickensis, *Ca*. L. ctenarytainae, and *L. crescens* (Mauck et al., 2019). Based on comprehensive phylogenetic analyses, DDH, ANI and BLAST analyses here, we discovered a new *Ca*. Liberibacter species. The closest relative of this latter new species is *Ca*. L. americanus (**Supplementary Tables 5, 9, 10** and **Figures 4**, **5**). This new *Ca*. Liberibacter species, *Ca*. L. capsica, is harbored in *R. capsici*, which was collected from Brazil (**Supplementary Table 1**). *R. capsici* has been reported from three localities in Argentina and Brazil so far, including this study, and it is known as a pest of peppers (*Capsicum annuum*) (Burckhardt et al., 2012).

Although it is not known if *R. capsici* is a vector for *Ca*. L. capsica, this psyllid species is an emerging pest of concern and has strong potential to invade new areas based on its crop host range (Burckhardt et al., 2012; Syfert et al., 2017). If *Ca*. L. capsica is plant-infecting, pepper and other solanaceous crop plants fed upon by the putative vector may be susceptible to infection. This host's range is similar to that of *Ca*. L. psyllaurous, which is transmitted primarily by the potato psyllid, *Bactericera cockerelli*, and infects crops (tomato, potato, and pepper) and native plants in the genus *Solanum* (Hansen et al., 2008; Munyaneza et al., 2009; Thinakaran et al., 2015a,b). However, our phylogenetic analysis, DDH, and ANI analyses indicate that *Ca*. L. psyllaurous is not closely related to *Ca*. L. capsica (**Supplementary Tables 5, 9, 10** and **Figures 4**, **5**). Instead, the closest relative to *Ca*. L. capsica, based on our phylogenetic, DDH, ANI, and BLAST analyses is *Ca*. L. americanus (**Supplementary Tables 5, 9, 10** and **Figures 4**, **5**), which is also found in Brazil. *Ca*. L. americanus is only known to naturally infect plants in the genus *Citrus* (family Rutaceae) and is transmitted by *Diaphorina citri* (Teixeira et al., 2005). However, *Ca*. L. americanus can be transmitted from citrus to a solanaceous host, *Nicotiana tabacum* cv. Xanthi, in the laboratory using the parasitic plant *Cuscuta* (Francischini et al., 2007).

We also detected additional *Ca*. Liberibacter taxa in microbiomes of the psyllid species *T. walkeri* (family Triozidae) and *M. gladiata* (family Carsidaridae). Subsequent phylogenetic analyses of the *Ca*. Liberibacter species from *T. walkeri* suggest that this *Ca*. Liberibacter taxon is nested within *Ca*. L. psyllaurous (**Supplementary Tables 5, 11** and **Figures 4**, **5**). The psyllid species *T. walkeri* specializes on the woody shrub, *Rhamnus cathartica* (family Rhamnaceae) (McLean, 1998) and specimens for the present study, including the nine additional samples that were positive for *Ca*. L. psyllaurous, were collected in the United Kingdom (**Supplementary Tables 1, 4**). The species *Ca*. L. psyllaurous is known to establish facultative infections in psyllids within the *Bactericera* and *Trioza* genera and has recently been detected in two *Craspedolepta* species (family Aphalaridae) collected in the United Kingdom (Sumner-Kalkun et al., 2020). *Ca.* L. psyllaurous has not been previously recorded in association with *T. walkeri* or other psyllids that feed primarily on woody shrubs or trees. Interestingly, *Ca*. L. psyllaurous has the widest known host plant range of any *Ca.* Liberibacter species to date, however, it is only known to infect herbaceous hosts in the Solanaceae, Apiaceae, and Urticaceae (Nelson et al., 2011; Hajri et al., 2017; Haapalainen et al., 2018). If *T. walkeri* is a vector for the new variant of *Ca*. L. psyllaurous detected in this study, it may be able to transmit this pathogen to *Rhamnus* hosts, where it could subsequently establish local or systemic infections.

Candidatus Liberibacter sequences were also detected from the psyllid microbiome of *M. gladiata*, which was collected from Taiwan (**Supplementary Table 1**). Unfortunately, the DNA from our specimen was of insufficient quantity to produce a high-quality draft metagenomic assembly of this *Ca.* Liberibacter taxon for phylogenetic analyses using shared orthologs. Nevertheless, the 16S rRNA sequence that we obtained shares 98% sequence similarity to *Ca*. L. asiaticus based on BLAST and 16S rRNA analyses indicates that this taxon is most likely *Ca*. L. asiaticus

or a lineage that diverged only very recently from *Ca*. L. asiaticus. *Candidatus* L. asiaticus is one of the main causal agents of the devastating citrus disease, Huanglongbing (HLB) (Bové, 2006). Only two other psyllids, *D. citri* and *Cacopsylla citrisuga*, are known to harbor *Ca*. L. asiaticus and they both feed primarily on citrus trees (Sapindales: Rutaceae) (Cen et al., 2012). In contrast, *M. gladiata* feeds primarily on *Ficus* species, including cultivated figs (*Ficus carica*) (Rung, 2016). *Ficus* may seem like an unlikely host for *Ca*. L. asiaticus, but it has been recorded as an alternative host for the vector, *Diaphorina citri*, in Florida (where HLB is now endemic), with evidence that it may also support *D. citri* reproduction (Thomas and De León, 2011). Use of *Ficus* by *D. citri* has not been explored extensively outside of this one study, but several other recent reports document use of various alternative hosts by *D. citri* adults, likely as a source of water (Zhang et al., 2019; George et al., 2020). These ecological studies of *D. citri* host use suggest there are pathways for rare *Ca*. L. asiaticus horizontal transmission to new psyllid hosts under the right circumstances. In this case, since *M. gladiata* is a pest of cultivated *Ficus* species, our detection of a putative *Ca*. L. asiaticus taxon in specimens of this psyllid raises the possibility that a variant of this pathogen could emerge as a new disease-causing agent in figs.

In summary, we documented evidence of new putative long-term psyllid symbiont associations in the Triozidae and Psyllidae, as well as more recent horizontal acquisitions of symbionts belonging to *Enterobacteriaceae* and *Wolbachia*. Additionally, we identified a novel species of *Ca*. Liberibacter associated with an emerging psyllid pest, detected a new association between *Ca*. L. psyllaurous and a psyllid that feeds on woody plants, and detected a potential new association between a *Ca*. L. asiaticus related taxon and a psyllid pest of figs. When examined in the context of psyllid host ecology, host range, and distribution, these findings suggest that expanded microbiome profiling of psyllids has great potential for revealing potential risk of new pathogen development and regulatory concerns. Future studies are needed to further understand the importance of these new psyllid-symbiont relationships of ecological and agricultural importance.

DATA AVAILABILITY STATEMENT

Raw 16S rRNA amplicon and metagenomic sequencing data are available at NCBI under SRA BioProject IDs PRJNA612536/PRJNA744186. Partial 16S rRNA sequences from the additional *Trichochermes walkeri* samples are deposited to NCBI Genbank with accession numbers OK047422-OK047430.

AUTHOR CONTRIBUTIONS

AH helped to design the study, conducted the data and bioinformatic analyses, and helped write the manuscript. YK conducted the data and phylogenetic analyses and helped write the manuscript. VM conducted the bioinformatic analyses of 16S rRNA amplicons, metagenomic assemblies, annotation, and phylogenetic analyses, and helped write the manuscript. KM helped to design the study and helped write the manuscript. DP collected, extracted, and identified all psyllid samples for this study, conducted the psyllid phylogenetic analyses, and helped write the manuscript. PS constructed 16S rRNA libraries, collected the herbarium specimen included in metagenomic sequencing, and performed DNA extractions on this specimen. All authors contributed to the article and approved the submitted version.

FUNDING

AH's research was supported by funding from the National Institute of Food and Agriculture (NIFA), United States Department of Agriculture (USDA) (Award number: 2019-70016-29066), the Department of Entomology at the University of California, Riverside (UCR), and the UCR Regents Faculty Development Award. Also, AH and KM's research was supported by UCR's Center for Infectious Disease Vector Research.

ACKNOWLEDGMENTS

We are grateful to the following for assistance in collecting specimens: Daniel Burckhardt, Philip Butterill, Kevin Johnson, John Noyes, and Dick Shaw. We would also like to thank Claire Davis for her help with psyllid DNA extractions and PCRs. We would also like to thank YK's committee members (Quinn McFrederick and Caroline Roper) for previous comments on an earlier draft.

SUPPLEMENTARY MATERIAL

The Supplementary Material for this article can be found online at: https://www.frontiersin.org/articles/10.3389/fmicb.2021.739763/full#supplementary-material

REFERENCES

Andrews, S. (2010). *FastQC: A Quality Control Tool for High Throughput Sequence Data*. Available online at: http://www.bioinformatics.babraham.ac.uk/projects/fastqc/ (accessed July 10, 2019).

Baumann, P. (2005). Biology bacteriocyte-associated endosymbionts of plant sap-sucking insects. *Annu. Rev. Microbiol.* 59, 155–189. doi: 10.1146/annurev.micro.59.030804.121041

Bolger, A. M., Lohse, M., and Usadel, B. (2014). Trimmomatic: a flexible trimmer for Illumina sequence data. *Bioinformatics* 30, 2114–2120. doi: 10.1093/bioinformatics/btu170

Bové, J. M. (2006). Huanglongbing: a destructive, newly-emerging, century-old disease of citrus. *J. Plant Pathol.* 88, 7–37. Available online at: http://www.sipav.org/main/jpp/index.php/jpp/article/view/828/615

Buchner, P. (1965). *Endosymbiosis of Animals With Plant Microorganisms*. New York: Interscience Publishers.

Burckhardt, D., Ouvrard, D., and Percy, D. M. (2021). An updated classification of the jumping plant-lice (Hemiptera: Psylloidea) integrating molecular and morphological evidence. *EJT* 736, 137–182. doi: 10.5852/ejt.2021.736.1257

Burckhardt, D., Queiroz, D. L., Rezende, M. Q., Castro de Queiroz, E., and Bouvet, J. P. (2012). The capsicum psyllid, Russelliana capsici (Hemiptera, Psylloidea), a pest on Capsicum annuum (Solanaceae) in Argentina and Brazil. *Mitt. Schweiz. Entomol. Ges.* 85, 71–78.

Bushnell, B. (2014). *BBMap: A Fast, Accurate, Splice-Aware Aligner*. Berkeley, CA: Lawrence Berkeley National Lab.(LBNL).

Capella-Gutiérrez, S., Silla-Martínez, J. M., and Gabaldón, T. (2009). trimAl: a tool for automated alignment trimming in large-scale phylogenetic analyses. *Bioinformatics* 25, 1972–1973. doi: 10.1093/bioinformatics/btp348

Caporaso, J. G., Lauber, C. L., Walters, W. A., Berg-Lyons, D., Huntley, J., Fierer, N., et al. (2012). Ultra-high-throughput microbial community analysis on the Illumina HiSeq and MiSeq platforms. *ISME J.* 6, 1621–1624. doi: 10.1038/ismej.2012.8

Casteel, C. L., and Hansen, A. K. (2014). Evaluating insect-microbiomes at the plant-insect interface. *J. Chem. Ecol.* 40, 836–847.

Casteel, C. L., Hansen, A. K., Walling, L. L., and Paine, T. D. (2012). Manipulation of plant defense responses by the tomato psyllid (*Bactericerca cockerelli*) and its associated endosymbiont *Candidatus* Liberibacter psyllaurous. *PLoS One* 7:e35191. doi: 10.1371/journal.pone.0035191

Cen, Y., Zhang, L., Xia, Y., Guo, J., Deng, X., Zhou, W., et al. (2012). Detection of '*Candidatus* Liberibacter asiaticus' in *Cacopsylla (Psylla) citrisuga* (Hemiptera: Psyllidae). *Florida Entomol.* 95, 304–311.

Douglas, A. E. (2009). The microbial dimension in insect nutritional ecology. *Functional Ecol.* 23, 38–47. doi: 10.1111/j.1365-2435.2008.01442.x

Emms, D. M., and Kelly, S. (2015). OrthoFinder: solving fundamental biases in whole genome comparisons dramatically improves orthogroup inference accuracy. *Genome Biol.* 16:157. doi: 10.1186/s13059-015-0721-2

Feldhaar, H. (2011). Bacterial symbionts as mediators of ecologically important traits of insect hosts. *Ecol. Entomol.* 36, 533–543. doi: 10.1111/j.1365-2311.2011.01318.x

Francischini, F. J. B., Oliveira, K. D. S., Astúa-Monge, G., Novelli, A., Lorenzino, R., Matiolli, C., et al. (2007). First report on the transmission of "*Candidatus* Liberibacter americanus" from citrus to *Nicotiana tabacum* cv. Xanthi. *Plant Dis.* 91, 631–631. doi: 10.1094/PDIS-91-5-0631B

Fukatsu, T., and Nikoh, N. (1998). Two intracellular symbiotic bacteria from the mulberry psyllid *Anomoneura mori* (insecta, homoptera). 64, 3599–3606. doi: 10.1128/AEM.64.10.3599-3606.1998

George, J., Kanissery, R., Ammar, E.-D., Cabral, I., Markle, L. T., Patt, J. M., et al. (2020). Feeding behavior of asian citrus psyllid [*Diaphorina citri* (Hemiptera: Liviidae)] nymphs and adults on common weeds occurring in cultivated citrus described using electrical penetration graph recordings. *Insects* 11:48. doi: 10.3390/insects11010048

Goris, J., Konstantinidis, K. T., Klappenbach, J. A., Coenye, T., Vandamme, P., and Tiedje, J. M. (2007). DNA-DNA hybridization values and their relationship to whole-genome sequence similarities. *Int. J. Syst. Evol. Microbiol.* 57, 81–91. doi: 10.1099/ijs.0.64483-0

Haapalainen, M., Wang, J., Latvala, S., Lehtonen, M. T., Pirhonen, M., and Nissinen, A. I. (2018). Genetic variation of "*Candidatus* Liberibacter solanacearum" haplotype C and identification of a novel haplotype from trioza urticae and stinging nettle. *Phytopathology* 108, 925–934. doi: 10.1094/PHYTO-12-17-0410-R

Hajri, A., Loiseau, M., Cousseau-Suhard, P., Renaudin, I., and Gentit, P. (2017). Genetic characterization of "*Candidatus* Liberibacter solanacearum" haplotypes associated with apiaceous crops in france. *Plant Dis.* 101, 1383–1390. doi: 10.1094/PDIS-11-16-1686-RE

Hall, A. A. G., Morrow, J. L., Fromont, C., Steinbauer, M. J., Taylor, G. S., Johnson, S. N., et al. (2016). Codivergence of the primary bacterial endosymbiont of psyllids versus host switches and replacement of their secondary bacterial endosymbionts. *Environ. Microbiol.* 18, 2591–2603. doi: 10.1111/1462-2920.13351

Hansen, A., Trumble, J., Stouthamer, R., and Paine, T. (2008). A new huanglongbing species,"*Candidatus* Liberibacter psyllaurous," found to infect tomato and potato, is vectored by the psyllid *Bactericera cockerelli* (Sulc). *Appl. Environ. Microbiol.* 74, 5862–5865.

Hansen, A. K., and Moran, N. A. (2014). The impact of microbial symbionts on host plant utilization by herbivorous insects. *Mol. Ecol.* 23, 1473–1496. doi: 10.1111/mec.12421

Heddi, A., Charles, H., Khatchadourian, C., Bonnot, G., and Nardon, P. (1998). Molecular characterization of the principal symbiotic bacteria of the weevil *Sitophilus oryzae*: a peculiar G + C content of an endocytobiotic DNA. *J. Mol. Evol.* 47, 52–61. doi: 10.1007/pl00006362

Jing, X., Wong, A. C.-N., Chaston, J. M., Colvin, J., McKenzie, C. L., and Douglas, A. E. (2014). The bacterial communities in plant phloem-sap-feeding insects. *Mol. Ecol.* 23, 1433–1444. doi: 10.1111/mec.12637

Katoh, K., and Standley, D.M. (2013). MAFFT multiple sequence alignment software version 7: improvements in performance and usability. *Mol. Biol. Evol.* 30, 772–780. doi: 10.1093/molbev/mst010

Koga, R., Bennett, G. M., Cryan, J. R., and Moran, N. A. (2013). Evolutionary replacement of obligate symbionts in an ancient and diverse insect lineage. *Environ. Microbiol.* 15, 2073–2081. doi: 10.1111/1462-2920.12121

Kozich, J. J., Westcott, S. L., Baxter, N. T., Highlander, S. K., and Schloss, P. D. (2013). Development of a dual-index sequencing strategy and curation pipeline for analyzing amplicon sequence data on the MiSeq Illumina sequencing platform. *Appl. Environ. Microbiol.* 79, 5112–5120. doi: 10.1128/AEM.01043-13

Lambert, J. D., and Moran, N. A. (1998). Deleterious mutations destabilize ribosomal RNA in endosymbiotic bacteria. *Proc. Natl. Acad. Sci. U.S.A.* 95, 4458–4462. doi: 10.1073/pnas.95.8.4458

Li, D., Liu, C.-M., Luo, R., Sadakane, K., and Lam, T.-W. (2015). MEGAHIT: an ultra-fast single-node solution for large and complex metagenomics assembly via succinct de Bruijn graph. *Bioinformatics* 31, 1674–1676. doi: 10.1093/bioinformatics/btv033

Maddison, W., and Maddison, D. (2018). *Mesquite: A Modular System for Evolutionary Analysis. Version 3.51*.

Mauck, K. E., Sun, P., Meduri, V. R., and Hansen, A. K. (2019). New *Ca.* Liberibacter psyllaurous haplotype resurrected from a 49-year-old specimen of *Solanum umbelliferum*: a native host of the psyllid vector. *Sci. Rep.* 9, 1–13. doi: 10.1038/s41598-019-45975-6

McFrederick, Q. S., and Rehan, S. M. (2016). Characterization of pollen and bacterial community composition in brood provisions of a small carpenter bee. *Mol. Ecol.* 25, 2302–2311. doi: 10.1111/mec.13608

McLean, I. F. G. (1998). "The population ecology of *Trichochermes walkeri*," in *Insect Populations In theory and in practice: 19th Symposium of the Royal Entomological Society 10–11 September 1997 at the University of Newcastle*, eds J. P. Dempster and I. F. G. McLean (Dordrecht: Springer Netherlands), 341–366. doi: 10.1007/978-94-011-4914-3_15

Meier-Kolthoff, J. P., Auch, A. F., Klenk, H.-P., and Göker, M. (2013). Genome sequence-based species delimitation with confidence intervals and improved distance functions. *BMC Bioinform.* 14:60. doi: 10.1186/1471-2105-14-60

Moran, N. A. (2007). Symbiosis as an adaptive process and source of phenotypic complexity. *Proc. Natl. Acad. Sci. U.S.A.* 104, 8627–8633. doi: 10.1073/pnas.0611659104

Moran, N. A., and Bennett, G. M. (2014). The tiniest tiny genomes. *Annu. Rev. Microbiol.* 68, 195–215. doi: 10.1146/annurev-micro-091213-112901

Moran, N. A., Russell, J. A., Koga, R., and Fukatsu, T. (2005). Evolutionary relationships of three new species of *Enterobacteriaceae* living as symbionts of aphids and other insects. *Appl. Environ. Microbiol.* 71, 3302–3310. doi: 10.1128/AEM.71.6.3302-3310.2005

Morris, J., Shiller, J., Mann, R., Smith, G., Yen, A., and Rodoni, B. (2017). Novel "*Candidatus* Liberibacter" species identified in the Australian eggplant psyllid, *Acizzia solanicola*. *Microb. Biotechnol.* 10, 833–844. doi: 10.1111/1751-7915.12707

Morrow, J. L., Hall, A. A. G., and Riegler, M. (2017). Symbionts in waiting: the dynamics of incipient endosymbiont complementation and replacement in minimal bacterial communities of psyllids. *Microbiome* 5:58. doi: 10.1186/s40168-017-0276-4

Morrow, J. L., Om, N., Beattie, G. A. C., Chambers, G. A., Donovan, N. J., Liefting, L. W., et al. (2020). Characterization of the bacterial communities of psyllids

associated with Rutaceae in Bhutan by high throughput sequencing. *BMC Microbiol.* 20:1895. doi: 10.1186/s12866-020-01895-4

Munyaneza, J. E., Sengoda, V. G., Crosslin, J. M., Garzón-Tiznado, J. A., and Cardenas-Valenzuela, O. G. (2009). First report of "*Candidatus* Liberibacter solanacearum" in Tomato Plants in México. *Plant Dis.* 93, 1076–1076. doi: 10.1094/PDIS-93-10-1076A

Eren, A. M., Esen, ÖC., Quince, C., Vineis, J. H., Morrison, H. G., Sogin, M. L., et al. (2015). Anvi'o: an advanced analysis and visualization platform for 'omics data. *PeerJ* 3:e1319. doi: 10.7717/peerj.1319

Nachappa, P., Levy, J., Pierson, E., and Tamborindeguy, C. (2011). Diversity of endosymbionts in the potato psyllid, *Bactericera cockerelli* (Hemiptera: Triozidae), vector of zebra chip disease of potato. *Curr. Microbiol.* 62, 1510–1520. doi: 10.1007/s00284-011-9885-5

Nadarasah, G., and Stavrinides, J. (2011). Insects as alternative hosts for phytopathogenic bacteria. *FEMS Microbiol. Rev.* 35, 555–575. doi: 10.1111/j.1574-6976.2011.00264.x

Nakabachi, A., Malenovský, I., Gjonov, I., and Hirose, Y. (2020a). 16S rRNA sequencing detected *Profftella, Liberibacter, Wolbachia,* and *Diplorickettsia* from relatives of the Asian citrus psyllid. *Microbial. Ecol.* 80, 410–422. doi: 10.1007/s00248-020-01491-z

Nakabachi, A., Piel, J., Malenovský, I., and Hirose, Y. (2020b). Comparative genomics underlines multiple roles of *Profftella*, an obligate symbiont of psyllids: providing toxins, vitamins, and carotenoids. *Geno. Biol. Evolu.* 12, 1975–1987. doi: 10.1093/gbe/evaa175

Nakabachi, A., Ueoka, R., Oshima, K., Teta, R., Mangoni, A., Gurgui, M., et al. (2013). Defensive bacteriome symbiont with a drastically reduced genome. *Curr. Biol.* 23, 1478–1484. doi: 10.1016/j.cub.2013.06.027

Nelson, W. R., Fisher, T. W., and Munyaneza, J. E. (2011). Haplotypes of "*Candidatus* Liberibacter solanacearum" suggest long-standing separation. *Eur. J. Plant Pathol.* 130, 5–12. doi: 10.1007/s10658-010-9737-3

Nováková, E., Hypša, V., and Moran, N. A. (2009). *Arsenophonus*, an emerging clade of intracellular symbionts with a broad host distribution. *BMC Microbiol.* 9:1–14. doi: 10.1186/1471-2180-9-143

Oliver, K. M., Degnan, P. H., Burke, G. R., and Moran, N. A. (2010). Facultative symbionts in aphids and the horizontal transfer of ecologically important traits. *Annu. Rev. Entomol.* 55, 247–266. doi: 10.1146/annurev-ento-112408-085305

Overholt, W. A., Diaz, R., Rosskopf, E., Green, S. J., and Overholt, W. A. (2015). Deep Characterization of the Microbiomes of *Calophya* spp. (Hemiptera: Calophyidae) gall-inducing psyllids reveals the absence of plant pathogenic bacteria and three dominant endosymbionts. *PLoS One* 10:e0132248. doi: 10.1371/journal.pone.0132248

Paradis, E., Claude, J., and Strimmer, K. (2004). APE: analyses of phylogenetics and evolution in R language. *Bioinformatics* 20, 289–290.

Percy, D. M., Crampton-Platt, A., Sveinsson, S., Lemmon, A. R., Lemmon, E. M., Ouvrard, D., et al. (2018). Resolving the psyllid tree of life: phylogenomic analyses of the superfamily Psylloidea (Hemiptera). *Syst. Entomol.* 43, 762–776. doi: 10.1111/syen.12302

R Core Team (2021). *R: A Language and Environment for Statistical Computing*. Vienna: R Foundation for Statistical Computing.

Raddadi, N., Gonella, E., Camerota, C., Pizzinat, A., Tedeschi, R., Crotti, E., et al. (2011). '*Candidatus* Liberibacter europaeus' sp. nov. that is associated with and transmitted by the psyllid *Cacopsylla pyri* apparently behaves as an endophyte rather than a pathogen. *Environ. Microbiol.* 13, 414–426.

Rambaut, A. (2018). Available online at: http://tree.bio.ed.ac.uk/software/figtree/, viewed (accessed September 9, 2021)

Rodriguez, R. L. M., and Konstantinidis, K. T. (2016). The enveomics collection: a toolbox for specialized analyses of microbial genomes and metagenomes. *PeerJ* 4:e1900v1. doi: 10.7287/peerj.preprints.1900v1

Rung, A. (2016). A new pest of ficus in California: *Macrohomotoma gladiata* Kuwayama, 1908 (Hemiptera: Psylloidea: Homotomidae), new to North America. *CheckList* 12, 1–5. doi: 10.15560/12.3.1882

Russell, J. A., Latorre, A., Sabater-Muñoz, B., Moya, A., and Moran, N. A. (2003). Side-stepping secondary symbionts: widespread horizontal transfer across and beyond the Aphidoidea. *Mol. Ecol.* 12, 1061–1075. doi: 10.1046/j.1365-294x.2003.01780.x

Schloss, P. D., Westcott, S. L., Ryabin, T., Hall, J. R., Hartmann, M., Hollister, E. B., et al. (2009). Introducing mothur: open-source, platform-independent, community-supported software for describing and comparing microbial communities. *Appl. Environ. Microbiol.* 75, 7537–7541. doi: 10.1128/aem.01541-09

Seemann, T. (2014). Prokka: rapid prokaryotic genome annotation. *Bioinformatics* 30, 2068–2069. doi: 10.1093/bioinformatics/btu153

Sloan, D. B., and Moran, N. A. (2012). Genome reduction and co-evolution between the primary and secondary bacterial symbionts of psyllids. *Mol. Biol. Evolu.* 29, 3781–3792. doi: 10.1093/molbev/mss180

Spaulding, A. W., and von Dohlen, C. D. (2001). Psyllid endosymbionts exhibit patterns of co-speciation with hosts and destabilizing substitutions in ribosomal RNA. *Insect Mol. Biol.* 10, 57–67. doi: 10.1093/oxfordjournals.molbev.a025878

Stackebrandt, E., and Goebel, B. M. (1994). Taxonomic note: a place for DNA-DNA reassociation and 16S rRNA sequence analysis in the present species definition in bacteriology. *Int. J. Syst. Evol. Microbiol.* 44, 846–849. doi: 10.1099/00207713-44-4-846

Stamatakis, A. (2014). RAxML version 8: a tool for phylogenetic analysis and post-analysis of large phylogenies. *Bioinformatics* 30, 1312–1313. doi: 10.1093/bioinformatics/btu033

Sudakaran, S., Kost, C., and Kaltenpoth, M. (2017). Symbiont acquisition and replacement as a source of ecological innovation. *Trends Microbiol.* 25, 375–390.

Sumner-Kalkun, J. C., Highet, F., Arnsdorf, Y. M., Back, E., Carnegie, M., Madden, S., et al. (2020). '*Candidatus* Liberibacter solanacearum'distribution and diversity in Scotland and the characterisation of novel haplotypes from *Craspedolepta* spp.(Psyllidae: Aphalaridae). *Sci. Rep.* 10, 1–11. doi: 10.1038/s41598-020-73382-9

Syfert, M. M., Serbina, L., Burckhardt, D., Knapp, S., and Percy, D. M. (2017). Emerging new crop pests: ecological modelling and analysis of the South American potato psyllid *Russelliana solanicola* (Hemiptera: Psylloidea) and its wild relatives. *PLoS One* 12:e0167764. doi: 10.1371/journal.pone.0167764

Teixeira, D., do, C., Saillard, C., Eveillard, S., Danet, J. L., Costa, P. I., et al. (2005). "*Candidatus* Liberibacter americanus", associated with citrus huanglongbing (greening disease) in São Paulo State. *Brazil. Int. J. Syst. Evol. Microbiol.* 55, 1857–1862. doi: 10.1099/ijs.0.63677-0

Thao, M. L., Clark, M. A., Baumann, L., Brennan, E. B., Moran, N. A., and Baumann, P. (2000a). Secondary endosymbionts of psyllids have been acquired multiple times. *Curr. Microbiol.* 41, 300–304. doi: 10.1007/s002840010138

Thao, M. L., Moran, N. A., Abbot, P., Brennan, E. B., Burckhardt, D. H., and Baumann, P. (2000b). Cospeciation of psyllids and their primary prokaryotic endosymbionts. *Appl. Environ. Microbiol.* 66, 2898–2905. doi: 10.1128/AEM.66.7.2898-2905.2000

Thinakaran, J., Pierson, E., Kunta, M., Munyaneza, J. E., Rush, C. M., and Henne, D. C. (2015a). Silverleaf nightshade (*Solanum elaeagnifolium*), a reservoir host for '*Candidatus* Liberibacter solanacearum', the putative causal agent of zebra chip disease of potato. *Plant Dis.* 99, 910–915. doi: 10.1094/PDIS-12-14-1254-RE

Thinakaran, J., Pierson, E., Longnecker, M., Tamborindeguy, C., Munyaneza, J., Rush, C., et al. (2015b). Settling and ovipositional behavior of *Bactericera cockerelli* (Hemiptera: Triozidae) on solanaceous hosts under field and laboratory conditions. *J. Econ. Entomol.* 108, 904–916. doi: 10.1093/jee/tov058

Thomas, D. B., and De León, J. H. (2011). Is the old world fig, *Ficus carica* L.(Moraceae), an alternative host for the asian citrus psyllid, *Diaphorina citri* (Kuwayama)(Homoptera: Psyllidae)? *Florida Entomol.* 94, 1081–1083. doi: 10.1653/024.094.0455

Thompson, S., Jorgensen, N., Bulman, S., and Smith, G. (2017). "A novel Candidatus Liberibacter species associated with Ctenarytaina fuchsiae, the New Zealand native fuchsia psyllid," in *Proceedings of the Science Protecting Plant Health 2017, 27 Sept. 2017,* Brisbane, QLD.

Walters, W., Hyde, E. R., Berg-Lyons, D., Ackermann, G., Humphrey, G., Parada, A., et al. (2016). Improved bacterial 16S rRNA gene (V4 and V4-5) and fungal internal transcribed spacer marker gene primers for microbial community surveys. *Msystems* 1, e00009–e00015.

Wang, N., Pierson, E. A., Setubal, J. C., Xu, J., Levy, J. G., Zhang, Y., et al. (2017). The *Candidatus* Liberibacter–host interface: insights into pathogenesis mechanisms and disease control. *Ann. Rev. Phytopathol.* 55, 451–482.

Wickham, H. (2016). *ggplot2: Elegant Graphics for Data Analysis*. New York: Springer-Verlag.

Zhang, R., He, S., Wu, W., Huang, Y., Zhu, C., Xiao, F., et al. (2019). Survival and lifespan of *Diaphorina citri* on non-host plants at various temperatures. *Crop Protection* 124:104841.

Conflict of Interest: The authors declare that the research was conducted in the absence of any commercial or financial relationships that could be construed as a potential conflict of interest.

Publisher's Note: All claims expressed in this article are solely those of the authors and do not necessarily represent those of their affiliated organizations, or those of the publisher, the editors and the reviewers. Any product that may be evaluated in this article, or claim that may be made by its manufacturer, is not guaranteed or endorsed by the publisher.

frontiers in Microbiology

ORIGINAL RESEARCH
published: 13 October 2021
doi: 10.3389/fmicb.2021.754245

A Novel *Microviridae* Phage (CLasMV1) From "*Candidatus* Liberibacter asiaticus"

Ling Zhang[1], Ziyi Li[1], Minli Bao[2], Tao Li[1], Fang Fang[1], Yongqin Zheng[1], Yaoxin Liu[3], Meirong Xu[1], Jianchi Chen[4], Xiaoling Deng[1] and Zheng Zheng[1]**

[1] Guangdong Province Key Laboratory of Microbial Signals and Disease Control, South China Agricultural University, Guangzhou, China, [2] China-United States Citrus Huanglongbing Joint Laboratory, National Navel Orange Engineering Research Center, Gannan Normal University, Ganzhou, China, [3] Horticulture Research Institute, Guangxi Academy of Agricultural Sciences, Nanning, China, [4] United States Department of Agriculture, San Joaquin Valley Agricultural Sciences Center, Agricultural Research Service, Parlier, CA, United States

OPEN ACCESS

Edited by:
Xuefeng Wang,
Citrus Research Institute, Chinese Academy of Agricultural Sciences (CAAS), China

Reviewed by:
Wenxing Xu,
Huazhong Agricultural University, China
Shujian Zhang,
New Mexico Consortium, United States

***Correspondence:**
Xiaoling Deng
xldeng@scau.edu.cn
Zheng Zheng
zzheng@scau.edu.cn

Specialty section:
This article was submitted to Microbe and Virus Interactions with Plants, a section of the journal Frontiers in Microbiology

Received: 06 August 2021
Accepted: 07 September 2021
Published: 13 October 2021

Citation:
Zhang L, Li Z, Bao M, Li T, Fang F, Zheng Y, Liu Y, Xu M, Chen J, Deng X and Zheng Z (2021) A Novel Microviridae Phage (CLasMV1) From "Candidatus Liberibacter asiaticus". Front. Microbiol. 12:754245. doi: 10.3389/fmicb.2021.754245

"*Candidatus* Liberibacter asiaticus" (CLas) is an unculturable phloem-limited α-proteobacterium associated with citrus Huanglongbing (HLB; yellow shoot disease). HLB is currently threatening citrus production worldwide. Understanding the CLas biology is critical for HLB management. In this study, a novel single-stranded DNA (ssDNA) phage, CLasMV1, was identified in a CLas strain GDHZ11 from Guangdong Province of China through a metagenomic analysis. The CLasMV1 phage had a circular genome of 8,869 bp with eight open reading frames (ORFs). While six ORFs remain uncharacterized, ORF6 encoded a replication initiation protein (RIP), and ORF8 encoded a major capsid protein (MCP). Based on BLASTp search against GenBank database, amino acid sequences of both MCP and RIP shared similarities (coverage > 50% and identity > 25%) to those of phages in *Microviridae*, an ssDNA phage family. Phylogenetic analysis revealed that CLasMV1 MCP and RIP sequences were clustered with genes from CLas and "*Ca*. L. solanacearum" (CLso) genomes and formed a unique phylogenetic lineage, designated as a new subfamily *Libervirinae*, distinct to other members in *Microviridae* family. No complete integration form but partial sequence (∼1.9 kb) of CLasMV1 was found in the chromosome of strain GDHZ11. Read-mapping analyses on additional 15 HiSeq data sets of CLas strains showed that eight strains harbored complete CLasMV1 sequence with variations in single-nucleotide polymorphisms (SNPs) and small sequence insertions/deletions (In/Dels). PCR tests using CLasMV1-specific primer sets detected CLasMV1 in 577 out of 1,006 CLas strains (57%) from southern China. This is the first report of *Microviridae* phage associated with CLas, which expands our understanding of phage diversity in CLas and facilitates current research in HLB.

Keywords: "*Candidatus* Liberibacter asiaticus," *Microviridae*, phage, genomic characterization, prevalence, evolution

INTRODUCTION

"*Candidatus* Liberibacter asiaticus" (CLas) is an unculturable phloem-limited α-proteobacterium associated with citrus Huanglongbing (HLB; also known as yellow shoot disease), a highly destructive disease in citrus production worldwide. Knowledge about CLas biology was limited due to the inability to culture it *in vitro*. However, recent development in high-throughput sequencing technology has opened a new venue for research in CLas (Duan et al., 2009; Zheng et al., 2014b). Among the new discoveries are CLas phages, i.e., viruses infecting CLas (Zhang et al., 2011; Zheng et al., 2018; Dominguez-Mirazo et al., 2019). Analyses of these phage genomes have significantly enriched the biological information of CLas.

Typically, a phage particle is composed of a protein capsid and a circular DNA genome (Adams, 1959). Since CLas titers are generally low, observations on phages particles using electron microscopy are challenging (Zhang et al., 2011). However, with the aid of high-throughput sequencing technology, the circular phage DNA genome could be detected (Zhang et al., 2011; Zheng et al., 2018). Based on the presence of circular plasmid form genomic DNA, three types of phages/prophages (Type 1, Type 2, and Type 3) have been described (Zhang et al., 2011; Zheng et al., 2018). Type 1 prophage (represented by SC1) was reported to be involved in the lytic cycle of forming phage particles; Type 2 prophage (represented by SC2) was found to be involved in the lysogenic conversion of CLas pathogenesis (Fleites et al., 2014; Jain et al., 2015); and Type 3 prophage (represented by prophage P-JXGC-3) carried a restriction-modification system (R-M system) (Zheng et al., 2018). Variants within a phage type have been reported in CLas strains from Pakistan (Cui et al., 2020). It is in general believed that more CLas phages remain to be discovered.

Most characterized phages possessed double-stranded DNA (dsDNA) genome as three known phage types in CLas (Zhang et al., 2011; Zheng et al., 2018). However, recent metagenomic studies demonstrate that phages with single-stranded DNA (ssDNA) genomes, especially for those in the family of *Microviridae*, are more common in many bacteria (Desnues et al., 2008; Tucker et al., 2010; Labonté and Suttle, 2013; Székely and Breitbart, 2016). *Microviridae* phages had a 4.4∼6.1 kb circular ssDNA genome enclosed within small icosahedral capsid (∼30 nm) (Székely and Breitbart, 2016). The phage replicates using a rolling-circle mechanism associated with a circular dsDNA, named as replicative form or RF that can be detected by standard DNA research techniques.

All *Microviridae* phages encoded two relatively conserved proteins, a capsid protein and a replication initiator protein (Cherwa and Fane, 2011). Currently, *Microviridae* is mainly classified into two subfamilies, *Bullavirinae* and *Gokushovirinae*, and an unclassified group (Cherwa and Fane, 2011; Krupovic et al., 2016). *Bullavirinae* contain 11 genes with genome size from 5.4 to 6 kb, typified by the bacteriophage phiX174 (Sanger et al., 1977). *Gokushovirinae* have genome ranging from 4.4 to 4.9 kb including nine genes and are specialized to infect intracellular parasites such as phage SpV4 infecting *Spiroplasma citri*, the pathogen of citrus stubborn disease (Saglio et al., 1973).

Here, we reported a novel *Microviridae* phage, CLasMV1, discovered through a metagenomic analysis of CLas strain GDHZ11 from China. CLasMV1 had a circular genome with eight open reading frames (ORFs): one encoded a unique major capsid protein (MCP), one encoded a replication initiation protein (RIP), and the encoding status of the other ORFs remained unknown. Phylogenetic analysis revealed that CLasMV1 represent a newly recognized lineage, designated as subfamily *Libervirinae*, along with *Bullavirinae* and *Gokushovirinae* under *Microviridae* family. A partial CLasMV1 sequence was found in CLas strain GDHZ11 chromosome. Population diversity and biological significance of CLasMV1 in CLas were further analyzed and discussed.

MATERIALS AND METHODS

Source of *Candidatus* Liberibacter asiaticus Strains

Citrus leaves with typical HLB symptoms from seven citrus cultivars were collected from nine provinces in China between March 2016 and November 2019 (**Table 1**). DNA was extracted from each sample following protocols published previously (Zheng et al., 2014b). Briefly, plant total DNA was extracted by using E. Z. N. A. HP Plant DNA Kit (OMEGA Bio-Tek Co., Guangdong, China). The presence of CLas in DNA sample was confirmed by TaqMan Real-time PCR with primer-probe set (RNRf/RNRp/RNRr) (Zheng et al., 2016) or CLas4G/HLBp/HLBr (Bao et al., 2020).

Illumina Sequencing and Assembly

CLas strain GDHZ11, originally collected from an HLB-affected citrus tree (*Citrus reticulata* Blanco cv. Shatangju) located in Huizhou City of Guangdong Province, was enriched by the dodder-mediated CLas enrichment system developed previously (Li et al., 2021). Total DNA of CLas-enriched dodder was extracted and used for genome sequencing. Sequencing data of strain GDHZ11 were initially used for analyses of CLas-associated novel sequences. For further analyses, 11 additional CLas DNA samples from Guangdong and Yunnan provinces were selected and used for whole-genome sequencing (**Table 2**).

All genome sequencing was performed with Illumina HiSeq platform (Illumina Inc., San Diego, CA, United States) after PCR-free library construction. For dodder-enriched CLas samples, the HiSeq data were filtered with whole-genome sequence of *Cuscuta australis* (NQVE00000000.1) and *Cuscuta campestris* (OOIL00000000.1) using Bowtie2 software (Langmead and Salzberg, 2012). For citrus-CLas samples, the HiSeq data were filtered with the genome sequences of *Citrus sinensis* (AJPS00000000.1), *Citrus clementina* (AMZM00000000.1), *C. sinensis* mitochondrion (NC_037463.1), and *C. sinensis* chloroplast genome (DQ864733.1) by using Bowtie2 software. All mapped reads were removed, and only the unmapped reads were retained for further assembly.

De novo assembly was performed by CLC Genomic Workbench v9.5 (QIAGEN Bioinformatics, Aarhus, Denmark) with default setting. The ordering of CLas contigs was performed

TABLE 1 | A summary of "*Candidatus* Liberibacter asiaticus" (CLas) sample collection in China and CLasMV1 related information.

No.	Geographical origin	No. of samples			Copy number of CLasMV1 per CLas cell (No. of samples)*				
		CLas	CLasMV1	Frequency	<1	1	>1	Range	Average
1	Guangdong	248	169	68%	8	6	155	0.35∼285	15.6
2	Guangxi	272	203	75%	18	15	170	0.54∼1,178	67.5
3	Jiangxi	69	51	74%	2	4	45	0.68∼206	26.4
4	Hunan	81	63	78%	1	4	58	0.82∼420	82.3
5	Fujian	45	38	84%	1	1	36	0.86∼37	6.1
6	Yunnan	125	19	15%	7	1	11	0.75∼40	4.5
7	Hainan	49	8	16%	1	1	6	0.28∼19	4.4
8	Guizhou	60	19	32%	0	0	19	4∼867	245.1
9	Zhejiang	57	7	12%	0	0	7	3∼12	4.7
	Total	1,006	577	57%	38	32	507	0.35∼1,178	50.7

**Copy number (R) of CLasMV1 per CLas cell is calculated based on the ΔCt method, i.e., $R = 2^{-\Delta Ct}$, ΔCt = Ct (CLasMV1-1F/CLasMV1-1R) - Ct (CLas-4G/HLBr) + 1.585.*

TABLE 2 | General information of CLasMV1 phage strains from China.

No.	Strain name	Source plant	Geographical origin (city, province)	Tissue type	Total size (bp)	Accession number	GC%
1	GDHZ11	*Citrus reticulata* Blanco cv. Shatangju	Huizhou, Guangdong	Dodder	8,869	CP045566.1	36.8
2	A4	*C. reticulata* Blanco cv. Shatangju	Guangzhou, Guangdong	Midribs	8,869	MN890136	36.8
3	GDCZ2	*C. reticulata* Blanco cv. Tankan	Chaozhou, Guangdong	Fruit pith	8,696	MN890137	36.9
4	GDDQ6	*C. reticulata* Blanco cv. Gongkan	Deqing, Guangdong	Fruit pith	8,869	MN890138	36.8
5	GDDQ7	*C. reticulata* Blanco cv. Gongkan	Deqing, Guangdong	Fruit pith	8,690	MN890139	36.9
6	GDQY1	*C. reticulata* Blanco cv. Shatangju	Qingyuan, Guangdong	Midribs	8,696	MN890140	36.9
7	GDXH1	*C. reticulata* Blanco cv. Chachiensis	Xinhui, Guangdong	Fruit pith	8,851	MN890141	36.8
8	YNJS5	*C. reticulata* Blanco cv. Maogukan	Jianshui, Yunnan	Fruit pith	8,885	MN890142	36.7
9	YNJS47	*C. sinensis*	Jianshui, Yunnan	Midribs	8,869	MN890143	36.8

by using all *de novo* assembly contigs to BLAST against CLas strain A4 genome (CP010804.2) through standalone BLAST software (word_size = 28, *e*-value = 1e-5) (Camacho et al., 2009). For prophage region, the reference-guided assembly was performed by using three phage sequences (SC1, SC2, and P-JXGC-3) as reference. The draft CLas genome sequence was generated from the combination of *de novo* assembly and reference-guide assembly.

Identification and Validation of the *Candidatus* Liberibacter asiaticus-Associated Novel Sequence

To identify the novel CLas-associated sequence, all *de novo* assembly contigs from GDHZ11 HiSeq data were used to BLASTn (word_size = 28, *e*-value = 1e-5) against 25 available CLas genomes and three phage sequences (SC1, SC2, and P-JXGC-3) (**Supplementary Table 1**). Contigs with partial match (>500 bp of non-matched sequence) were retrieved from the blast result and used for contig extension. The reads (150 bp for each) from two ends of candidate novel CLas contig were collected and used as query to BLASTn against *de novo* contigs of GDHZ11 by using Standalone BLAST software (word size = 16, *e*-value = 10) (Camacho et al., 2009). Contigs with > 95% identity were selected and used for contig extension. A circular sequence would be found through contig overlapping extensions that connected the 3′ end of a contig to the 5′ end of the same contig. The overlapped regions were further confirmed with standard PCR-Sanger's sequencing method. Primers were designed with Primer 3 server (Untergasser et al., 2012; **Supplementary Table 2**). The expected PCR amplicon were sequenced by Sanger's sequencing after cloning with *pEASY-T1* plasmid (TransGen Biotech, Beijing, China). Amplicon sequences were assembled using SeqMan software.[1]

Sequence circularity was further evaluated by an *in silico* "Reads Mapping Test" approach described previously (Zheng et al., 2018). Briefly, the first 4,000 bp at the 5′ end of circular sequence was cut and attached to the 3′ end to generate a new circular sequence. For comparison, a 4,000-bp sequence randomly selected from the chromosomal region of CLas GDHZ11 genome was cut and added to the end of the circular sequence (without the first 4,000 bp) that generated another sequence to serve as the reference. Both two sequences were used as reference for read-mapping with GDHZ11 HiSeq reads. A continuous read coverage (no gap) of the connection region suggested sequence circularity (**Supplementary Figure 1**).

Gene Annotation and Phylogenetic Analysis

Annotation of sequence was performed on RAST server (Aziz et al., 2008). All predicted ORFs were further analyzed through BLASTx against the non-redundant protein sequences in

[1]http://www.dnastar.com

National Center for Biotechnology Information (NCBI) GenBank database (version 235.0) and the NCBI conserved domain database (CDD, v3.17). The homologous genes between phage and CLas were identified by using each phage ORFs as query to BLASTn against CLas genome sequences (**Supplementary Table 1**). All predicted protein sequences were further used to BLAST against the Viruses database (taxid:10239) and the Plasmids database (taxid:36549) in NCBI GenBank database (version 235.0) through NCBI web Quick BLASTp with default setting (expect threshold = 10 and word size = 6).

MCP and RIP sequences from representative ssDNA phages under *Microviridae* family and top BLAST hits toward the MCP and RIP genes of candidate phage were selected for phylogenetic analyses (**Supplementary Table 1**). The complete amino acid sequences of MCP and RIP were aligned by MEGA6 using default setting (Tamura et al., 2013). Phylogenetic trees were constructed using MEGA6 with maximum-likelihood method and bootstrap value of 500 (Tamura et al., 2013).

Identification and Comparison of CLasMV1 From Different *Candidatus* Liberibacter asiaticus Strains

As described later, CLasMV1 was the phage identified in CLas strain GDHZ11 in this study. In addition to 12 CLas HiSeq data sequenced in this study, four additional HiSeq/MiSeq data (A4, HHCA, FL17, and SGCA5) from our previous studies (Zheng et al., 2014a,b, 2015, 2017) were also selected for identification of phage through read-mapping approach (**Table 2**). Briefly, the HiSeq data were directly mapped to candidate phage sequence through CLC Genomic Workbench v9.5 (QIAGEN Bioinformatics, Aarhus, Denmark) with default setting. The presence of candidate phage was directly extracted from the mapping result when the fraction of reference covered over 80. Whole-genome comparison of phages from different CLas samples was performed with standalone BLAST software (word_size = 28, *e*-value = 1e-5) (Camacho et al., 2009). Sequence variants, including SNPs and In/Dels, were directly identified from BLAST result.

For CLas DNA samples collected from nine provinces in southern China, the presence of CLasMV1 phage was identified by CLasMV1-specific real-time PCR as described below. In addition to CLasMV1, the first *Microviridae* phage was identified in CLas strain GDHZ11, and others identified by phage were named by adding the sample name after an underscore following the phage name. For example, CLasMV1_GDDQ6 denoted phage CLasMV1 strain GDDQ6 (from CLas sample GDDQ6).

Development of CLasMV1-Specific Real-Time PCR

All phage sequences obtained in this study were aligned with MEGA6 to identify the phage conserved region (Tamura et al., 2013). The phage-specific primer sets (CLasMV1-1F/CLasMV1-1R and CLasMV1-2F/CLasMV1-2R) were designed based on the unique and conserved region of phage sequence using Primer 3 server (Untergasser et al., 2012; **Supplementary Table 2**). The specificity of primers was evaluated by using the primer sequence to blast against with NCBI nucleotide database through NCBI web BLASTn (expect threshold = 10 and word size = 16). In addition, the specificity of primers was also verified with real-time PCR by using a GDHZ11 DNA sample (CLasMV1-positive) and CLas-free DNA samples extracted from healthy citrus samples and dodder tendrils.

The SYBR Green Real-time PCR assays were performed in CFX Connect Real-Time System (Bio-Rad, Hercules, CA, United States). The reaction mixture contained 1 μl of DNA template (∼25 ng), 0.5 μl of each forward and reverse primer (10 μM), and 10 μl of iQ^{TM} SYBR® Green Supermix (Bio-Rad) in a final volume of 20 μl with the following procedure: 95°C for 3 min, followed by 40 cycles at 95°C for 10 s and 60°C for 30 s. Fluorescence signal was captured at the end of each 60°C step, followed by a melting point analysis.

Evaluation of CLasMV1 Copy Number

For CLas samples sequenced with Illumina platform, the copy number of CLasMV1 was evaluated by comparison of the average nucleotide coverage (ANC) of CLasMV1 sequence and CLas chromosome through read-mapping. Briefly, the HiSeq data were directly mapped to CLas strain A4 chromosomal region (CP010804.2, from nucleotide position of 1 to 1,191,644) and CLasMV1 sequence (CP045566.1) by CLC Genomic Workbench v9.5 (QIAGEN Bioinformatics, Aarhus, Denmark) with default setting. The ANC of CLas chromosomal region and CLasMV1 phage sequence was calculated with the following equation: ANC = total bases of all aligned reads/the length of the consensus sequence. The copy number of CLasMV1 was indicated as the copy number of CLasMV1 per CLas cell, i.e., the copy number of CLasMV1 = the ANC of CLasMV1 sequence/the ANC of CLas chromosomal region.

For other CLas samples not sequenced, the copy number of CLasMV1 was evaluated by relative quantitative real-time PCR with the CLasMV1-specific primer set and CLas-specific primer set. The density of CLasMV1 was indicated as the copy number of CLasMV1 per CLas cell with the ΔCt method (Wittwer et al., 2001), i.e., $R = 2^{-\Delta Ct}$, ΔCt = Ct (CLasMV1-1F/CLasMV1-1R) - Ct (primer set targeted single copy gene). The Ct value generated by primer set targeted single copy gene was converted from the Ct value generated by primer set CLas4G/HLBr targeted three copies of 16S rRNA gene with the following equation: Ct (primer set targeted single copy gene) = Ct (CLas4G/HLBr) + X, where X is 1.585.

RESULTS

Detection of CLasMV1

The HiSeq platform yielded a total of 67,133,182 short reads (150 bp) derived from GDHZ11 DNA sample. A total of 900 contigs (> 1 kb) were generated from *de novo* assembly. Twenty-eight contigs had 100% length coverage and > 98% identity to the referenced CLas genome sequences (**Supplementary Table 3**). One contig (Contig_3 with 7,324 bp) showed 59% length coverage and 99% identity (**Supplementary Table 3**). Contig extension of Contig_3 sequence showed that the 3′ end

of Contig_3 was connected to 5′ end of Contig_63 (1,379 bp), while the 3′ end of Contig_63 was connected back to the 5′ end of Contig_3, forming an 8,869-bp circular DNA molecule (**Figure 1**). Read-mapping test further confirmed the circularity of Contig_3–Contig_63 sequence (**Supplementary Figure 1**). In addition, the full length of Contig_3–Contig_63 sequence was also confirmed by PCR and Sanger sequencing (**Supplementary Figure 2** and **Supplementary Table 2**).

RAST annotation of the circular Contig_3–Contig_63 sequence detected eight ORFs (**Figure 1** and **Table 3**). BLASTp search using amino acid sequences of each ORF against NCBI Plasmid (taxid:36549) and Viruses database (taxid:10239) showed that ORF6 encoded a RIP and ORF8 encoded an MCP in *Microviridae*, an ssDNA phage family (**Figure 2** and **Table 3**). The genetic nature of the other six ORFs remained as putative proteins. Based on HiSeq read-mapping, the ANC of Contig_3 was 305 × and that of Contig_63 was 342 × (**Supplementary Table 3**). These were in contrast to the ANC of ∼65 × of the CLas chromosome (**Supplementary Table 3**), leading to about five copies of the circular DNA per CLas cell calculated.

Considering the similarity of ORF6 (37%) and ORF8 (25%) to members of *Microviridae* (**Table 3**), the circular Contig_3–Contig_63 sequence could be taken as the RF of a not-yet reported ssDNA phage, designated as CLasMV1. CLasMV1 phage genome had a G + C content of 36.8%. The CLasMV1 sequence had been deposited in GenBank under the accession number of CP045566.1.

Phylogenetic Analysis of CLasMV1

Phylogenetic analyses of MCP and RIP sequences showed that CLasMV1 was distantly related to the known ssDNA phages from two subfamilies (*Gokushovirinae* and *Bullavirinae*) of *Microviridae* (**Figures 3**, **4**). Both two sequences were

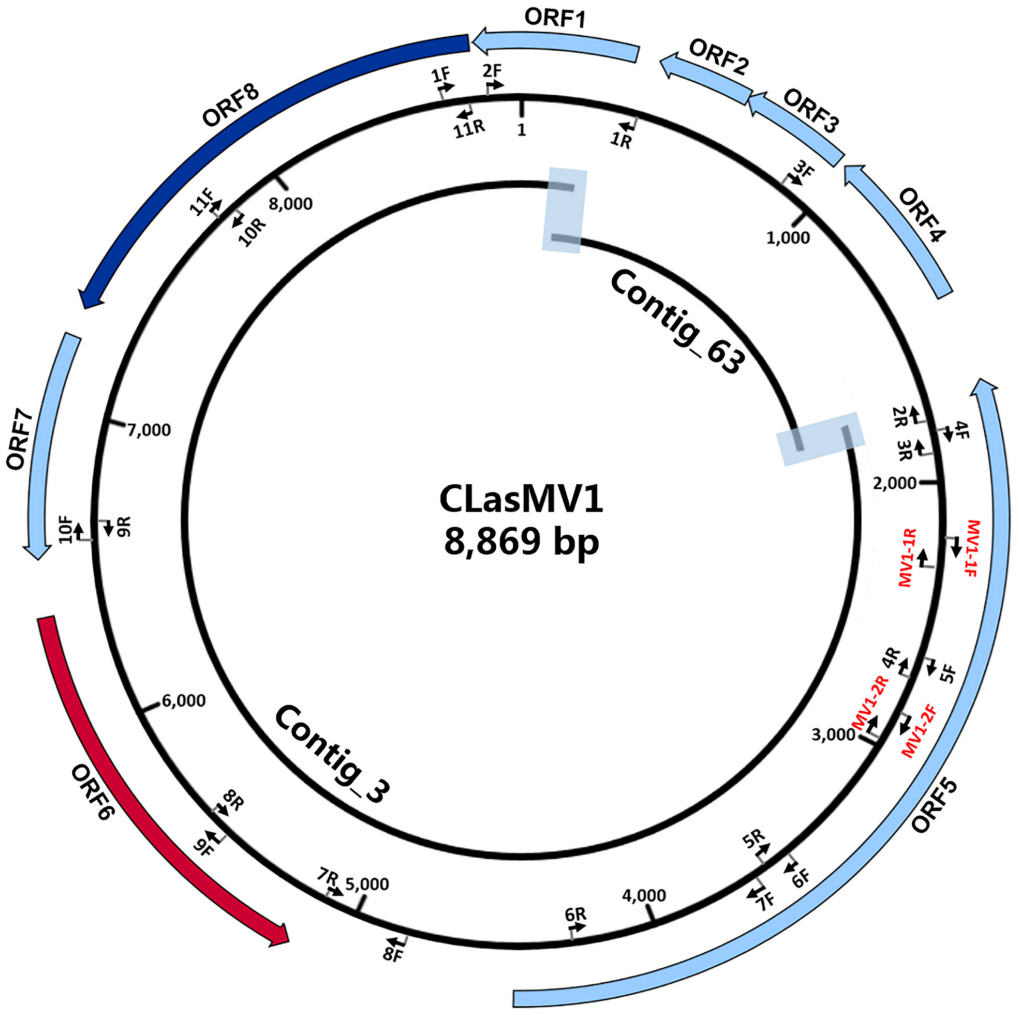

FIGURE 1 | Schematic representation of genome assembly of CLasMV1 phage. Outside ring: open reading frame (ORF) annotations. ORF6 (marked in red arrow) = replication initiation protein (RIP) gene; ORF8 (marked in blue arrow) = major capsid protein (MCP) gene. Middle ring: arrow pairs (nF–nR) are primer sets for gap closure and Sanger sequencing confirmations; arrow pairs in red (MV1-1F–MV1-1R and MV1-2F–MV1-2R) are CLasMV1 specific primer sets. All primers sequences are listed in **Supplementary Table 2**. Inside ring: Contig_3 and Contig_63 with overlapped regions highlighted.

TABLE 3 | General information of open reading frames (ORFs) in CLasMV1 genome.

Name	Locus_tag	Start	End	Nucleotide (bp)	Amino acid (aa)	BLASTp with NCBI conserved domain database		BLAST result (matched length in amino acid/similarity %)*		Annotation
						Conserved domain	Domain ID	CLas genome	Viruses + plasmids	
ORF1	GE519_gp01	351	8,735	486	161	NF	NF	WP_144299319 (161/100%)	NF	Hypothetical protein
ORF2	GE519_gp02	701	420	282	93	NF	NF	WP_015452912.1 (93/100%)	NF	Hypothetical protein
ORF3	GE519_gp03	1,024	698	327	108	NF	NF	WP_015452913.1 (102/100%)	NF	Hypothetical protein
ORF4	GE519_gp04	1,530	1,048	483	160	NF	NF	WP_015452914.1 (160/100%)	NF	Hypothetical protein
ORF5	GE519_gp05	4,451	1,797	2,655	884	NF	NF	WP_015452962.1 (109/99%)	NF	Hypothetical protein
ORF6	GE519_gp06	6,365	5,148	1,218	405	Replication initiation protein	PHA00330	WP_015452965.1 (405/100%)	ATW62975.1 (71/37%)	Replication initiation protein
ORF7	GE519_gp07	6,534	7,208	675	224	2OG-FeII_Oxy	cl21496	WP_015452962.1 (44/86%)	NF	Hypothetical protein
ORF8	GE519_gp08	8,725	7,298	1,428	475	NF	NF	WP_045490387.1 (447/99%)	QJB21054.1 (112/25%)	Major capsid protein

*NF, not found; NCBI, National Center for Biotechnology Information. *Only the best match was listed here.*

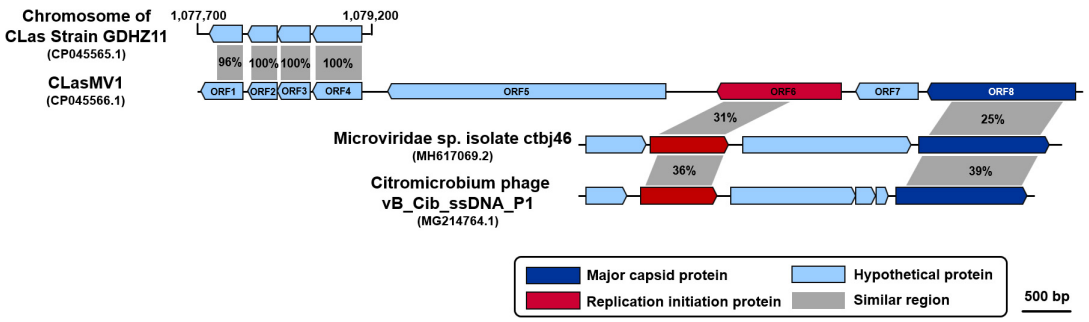

FIGURE 2 | Comparison of amino acid sequences among CLasMV1, homologs in "*Candidatus* Liberibacter asiaticus" (CLas) strain GDHZ11 chromosome, and representative *Microviridae* phages. Percentage similarities are marked within gray shadows.

clustered with homologous genes from CLas genome. Homologs of CLasMV1 MCP and RIP were also found in multiple genome sequences of "*Ca*. L. solanacearum" (CLso), a bacterium associated with potato zebra chip disease, but constituted a different phylogenetic cluster (**Figures 3**, **4**). The CLas cluster and CLso cluster formed a unique phylogenetic lineage, designated as a new subfamily *Libervirinae*, distinct to other members in *Microviridae* family (**Figures 3**, **4**).

Genomic Diversity of CLasMV1 Strains

With the HiSeq reads data of 15 CLas strains from China and the United States, eight showed the 100% coverage of CLasMV1 sequence, including six from Guangdong Province and two from Yunnan Province, but none from the United States (**Figure 5**). The genome size of the eight CLasMV1 strains ranged from 8,690 to 8,885 bp (**Table 2**). Sequence comparison of the CLasMV1 strains identified a total of 22 sequence variants, including 17 single-nucleotide polymorphisms (SNPs) and five Insertion/Deletions (In/Dels) (**Figure 6**). Two SNPs (nucleotide positions of 3,176 and 6,163) and two In/Dels (nucleotide positions of 168 and 6,831∼6,848) were located in the gene coding region (ORF1, 5, 6, and 7) reference to CLasMV1 genome (CP045566.1), and none of them caused the frame shifts (**Figure 6**). The 12-bp insertion at nucleotide position 168 of CLasMV1 genome was detected in the CLasMV1_GDDQ7 and CLasMV1_YNJS5 sequences and increased the corresponding protein by four amino acids in comparison with ORF1 of CLasMV1 (**Figure 6**). Conversely, an 18-bp deletion between nucleotide positions 6,831 and 6,848 of CLasMV1 was identified in CLasMV1_GDXH1 and CLasMV1_GDDQ7 sequence by reducing six amino acids of the corresponding protein as compared with the ORF7 of CLasMV1 (**Figure 6**). In addition, a 186-bp deletion between nucleotide positions 1,547 and 1,734, a non-coding region in

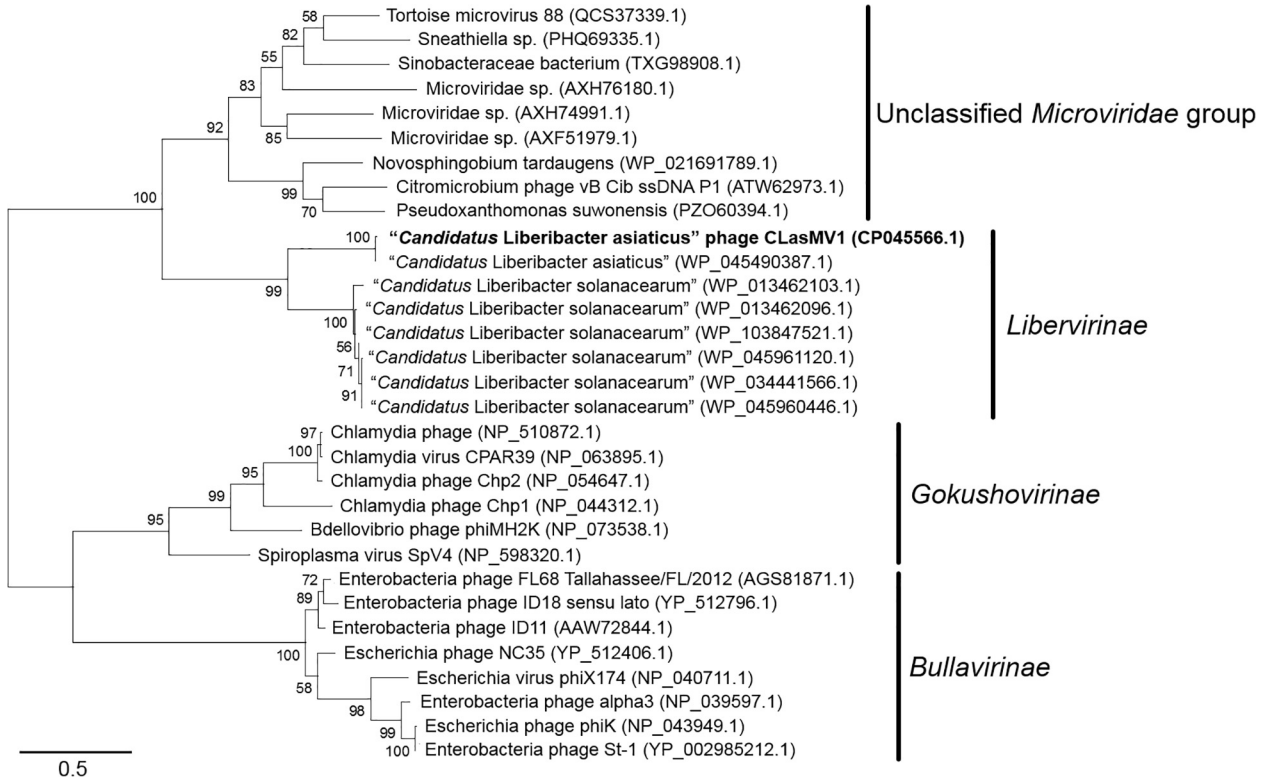

FIGURE 3 | Unrooted maximum-likelihood phylogenetic analyses of CLasMV1 phage based on the full-length major capsid protein (MCP) sequence. MCP sequences from representative members of *Microviridae* and top BLAST hits toward the replication initiation protein (RIP) of CLasMV1 phage are selected for phylogenetic analyses. Bootstrap value = 500. Note the proposed subfamily *Libervirinae*.

CLasMV1, was identified in the CLasMV1_GDQY1, GDCZ2, and GDDQ7 sequences.

The copy number of CLasMV1, as estimated by the ratio of ANC between CLasMV1 and CLas, varied among nine CLas strains (**Figure 5**). The multiple copies of CLasMV1 per CLas cell were observed in six CLas strains (strains GDHZ11, GDDQ6, GDDQ7, GDQY1, GDCZ2, and YNJS5) (**Figure 5**). A nearly single copy of CLasMV1 per CLas cell was detected in CLas strains GDXH1 and YNJS47 with the CLasMV1/CLas ratio of 1.02 and 1.03, respectively. In addition, a CLasMV1/CLas ratio of 0.70 was observed in CLas A4 strain.

Partial CLasMV1 Sequences in *Candidatus* Liberibacter asiaticus Chromosome

As shown in **Figure 5**, seven out of the 15 CLas strains (four from Yunnan Province, China, and three from the United States) did not harbor a complete CLasMV1 sequence. Instead, sections of CLasMV1 were detected in CLas genomes. Interestingly, BLASTn search with CLasMV1 as a query against the 25 representative whole-genome sequences of CLas deposit in GenBank database also showed partial sequence hits (**Figure 7**). The hit regions (represented by CLasMV1 positions) were summarized into three main sections: A, positions 1–1,752, (ORF1–4); B, positions 4,081–6,683 (ORF6, partial ORF5, and ORF7); and C, positions 7,332–8,734 (ORF8). Region A was shared by all CLas strains, while Regions B and C were only found in some CLas strains completely or partially (**Figure 7**). In addition to the blast result, the read-mapping test also confirmed the presence of homologous regions between CLas strain GDHZ11 chromosome and CLasMV1 genome (**Supplementary Figure 3**).

Frequency and Copy Number of CLasMV1 in *Candidatus* Liberibacter asiaticus Population in China

To further investigate the prevalence of CLasMV1, a total of 1,006 CLas strains samples were collected from southern China. The presence of CLasMV1 was detected by real-time PCR assay with CLasMV1-specific primer sets (**Supplementary Table 2**). PCR result showed that CLasMV1 was detected in 577 out of 1,006 CLas strains (577/1006, 57%) (**Table 1**). CLas population from nine provinces in China can be divided into two groups, the high-frequency group (>50%), including Guangdong (68%), Guangxi (75%), Jiangxi (74%), Hunan (78%), and Fujian (84%) provinces, and low-frequency group (<50%), including Yunnan (15%), Hainan (16%), Guizhou (32%), and Zhejiang (12%). The density of CLasMV1 varied among CLas strains, ranging from 0.35 to 1,178 copies per CLas cell with an average of 50.7 copies per CLas cell (**Table 1**). Of 577 CLas strains that harbored CLasMV1, 507 (507/577, 88%) contained multiple copies of CLasMV1 per

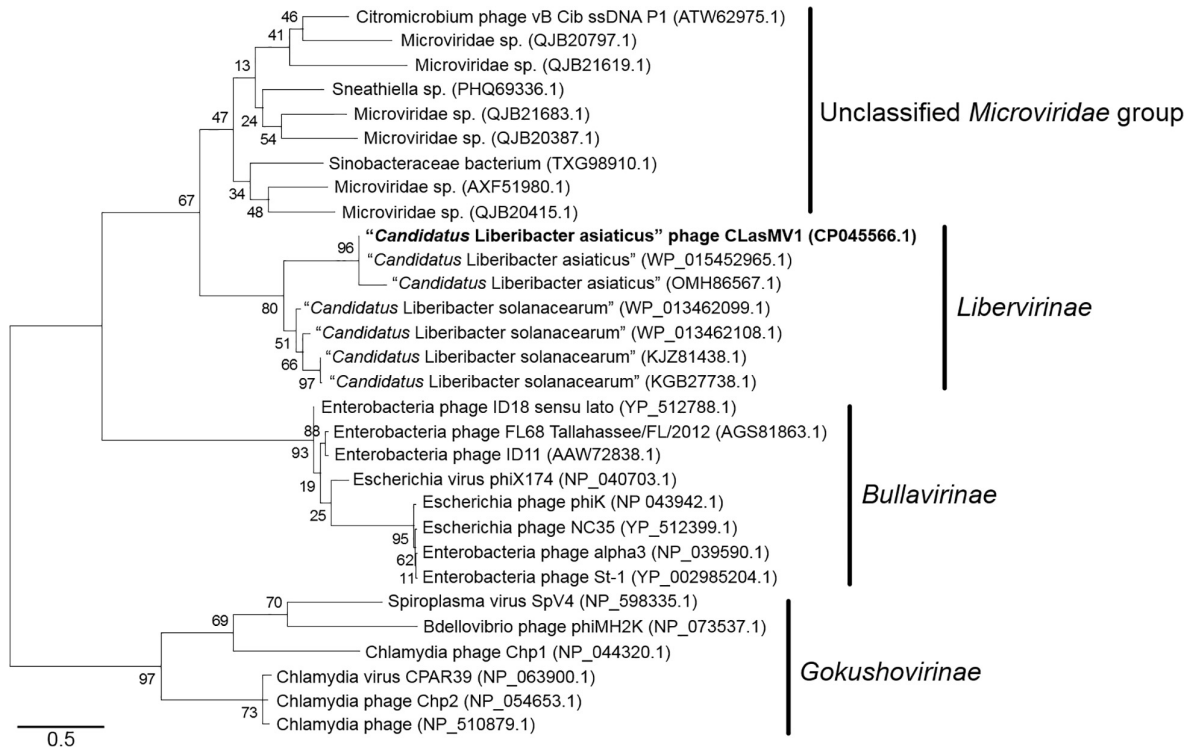

FIGURE 4 | Unrooted maximum-likelihood phylogenetic analyses of CLasMV1 phage based on the full-length replication initiation protein (RIP) sequence. RIP sequences from representative members of *Microviridae* and top BLAST hits toward the RIP of CLasMV1 phage are selected for phylogenetic analyses. Bootstrap value = 500. Note the proposed subfamily *Libervirinae*.

CLas cell, and 32 CLas samples (32/577, 6%) harbored nearly a single copy of CLasMV1 per CLas cell (**Table 1**). Conversely, less than one copy of CLasMV1 per CLas cell was only observed in 38 CLas samples.

DISCUSSION

The circular CLasMV1 phage genome was generated from an assembly of two contigs (Contig_3 and Contig_63) rather than directly from a single contig. Contig_63 (1,379 bp) was a repetitive sequence that presents in both CLasMV1 phage and CLas genome (**Figure 2**). The assembly of long repetitive sequence using only Illumina short reads (150 bp for each read in this study) remains challenging due to assembly collapse (Tørresen et al., 2019), which can explain the disconnection of Contig_3 and Contig_63 during *de novo* assembly process. In this study, Contig_63 was first identified as a phage sequence candidate through BLAST analysis. The "contig extension" on Contig_63 was critical to resolve the *de novo* assembly collapse. However, as sequencing technology advances, long-read sequencing technologies, such as Pacific Biosciences or Oxford Nanopore Technologies, can be employed to obtain a single contig phage sequence.

Evidence for the identification of CLasMV1 as a member in *Microviridae* family was mainly based on similarities of MCP and RIP to available GenBank database (**Figure 2**). Especially, the CLasMV1 RIP contained a conserved domain PHA0030 (**Table 3**), which only occurred in members of *Microviridae* family (Lu et al., 2020). The biological nature of CLasMV1 phage remains unknown. For further phage characterization, it will be beneficial to observe and obtain phage particles. In an attempt to bypass the CLas unculturable barrier, transmission electron microscopy (TEM) was used to examine CLas-infected plant samples, and phage particles were not observed (data not shown). In the SC1 and SC2 phage study, phage particles were observed by TEM (Zhang et al., 2011). However, no procedure for further isolation of CLas phage particles has been reported so far, an indication of technical challenge in CLas phage study. In this study, we demonstrated that mining sequence data via bioinformatics was highly effective and productive for CLas phage research.

While complete integration of CLasMV1 genome sequence in CLas chromosome was not found, some CLas strains contained homologous genes of RIP and MCP of CLasMV1 (**Figures 2**, **7**). It was noted that among these CLas strains, some contained both RIP and MCP genes, and some only contained one of the two genes. In addition, more strains contained RIP genes than MCP genes. All these suggested that the two genes were not integrated in CLas chromosome simultaneously, or if they did, the MCP gene was deleted in a faster rate than that of the RIP gene. It was also reported that the genome of an obligate intracellular pathogen, *Chlamydophila pneumoniae*, contained

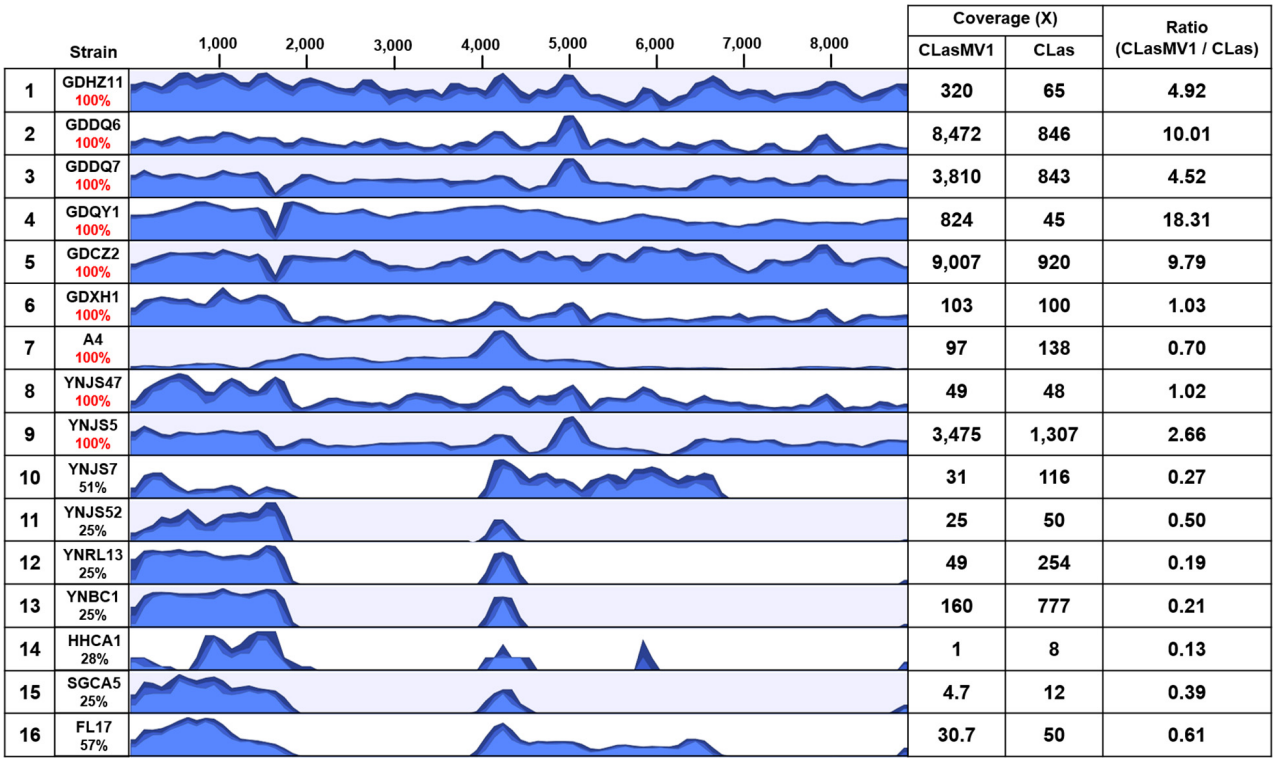

	Strain	Coverage (X) CLasMV1	Coverage (X) CLas	Ratio (CLasMV1 / CLas)
1	GDHZ11 100%	320	65	4.92
2	GDDQ6 100%	8,472	846	10.01
3	GDDQ7 100%	3,810	843	4.52
4	GDQY1 100%	824	45	18.31
5	GDCZ2 100%	9,007	920	9.79
6	GDXH1 100%	103	100	1.03
7	A4 100%	97	138	0.70
8	YNJS47 100%	49	48	1.02
9	YNJS5 100%	3,475	1,307	2.66
10	YNJS7 51%	31	116	0.27
11	YNJS52 25%	25	50	0.50
12	YNRL13 25%	49	254	0.19
13	YNBC1 25%	160	777	0.21
14	HHCA1 28%	1	8	0.13
15	SGCA5 25%	4.7	12	0.39
16	FL17 57%	30.7	50	0.61

FIGURE 5 | Results of read-mapping to CLasMV1 sequence (8,869 bp) with HiSeq data from 16 "*Candidatus* Liberibacter asiaticus" (CLas) strains. Row 1, reference CLas strain GDHZ11; Rows 2–13, CLas strains from China (2–7 from Guangdong Province and 8–13 from Yunnan Province). Row 14–16, CLas strains from the United States (14–15 from California and 16 from Florida). Percentages of CLasMV1 length covered are listed in column 2. The HiSeq data of CLas strains detected full length (100%) of CLasMV1 are highlighted in red in column 2. Column 3, read-mapping track. Blue graph represents read coverage in log scale. Column 4, average nucleotide coverages (ANCs) to CLasMV1 and CLas chromosome; and Column 5, ratio of ANCs inferring copy numbers of CLasMV1 in each CLas strain.

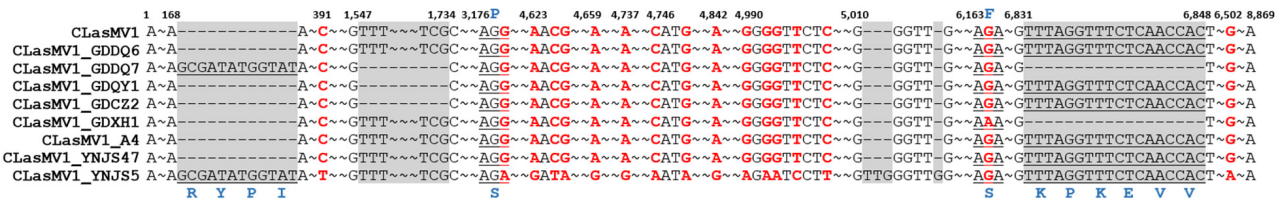

FIGURE 6 | A list of single-nucleotide polymorphisms (SNPs) and small insertions/deletions (In/Dels) in nine CLaMV1 strains from southern China. The numbers above the alignment graph are sequence position reference to CLasMV1 (CP045566.1). The SNPs are highlighted in red. The In/Dels are highlighted by gray shadow. The corresponding codon located in SNPs and In/Dels are underlined with amino acids in blue. "–" represents the nucleotide deletion. "∼" represents omitted identical nucleotides.

homologs of RIP and MCP genes of a *Chlamydia*-infecting phages in *Microviridae* (Rosenwald et al., 2014). Mechanisms of phage RIP and MCP gene integrations in bacterial chromosome and their biological functions remain an interesting subject for future research.

Homologs of CLasMV1 RIP and MCP gene were also found in the genome of CLso strains (**Figures 3**, **4**), evidence of horizontal gene transfer (HGT) among species of "*Ca.* Liberibacter" mediated through phages. The relatively high divergency between the RIP and MCP sequences (**Figures 3**, **4**) suggested that the HGT events occurred early, although we could not calibrate the exact timeline. There has been a longtime association between CLasMV1 and its ancestor phage with CLas and CLso. The proposal of subfamily *Libervirinae* was to reflect the current status of the phage evolution and divergency (**Figures 3**, **4**). However, it remains unclear if the RIP and MCP genes in CLso were chromosome-borne or phage-borne or both.

In contrast to the scattered distribution of RIP and MCP genes among CLas strains, a large region of CLasMV1 sequence, equivalent to Contig_63 (1,379 bp), which included ORF2, ORF3, ORF4, and the partial region of ORF1, was found in 26 CLas genomes from different countries (**Figure 7**). The bacterial genes are usually quickly deleted unless retained for

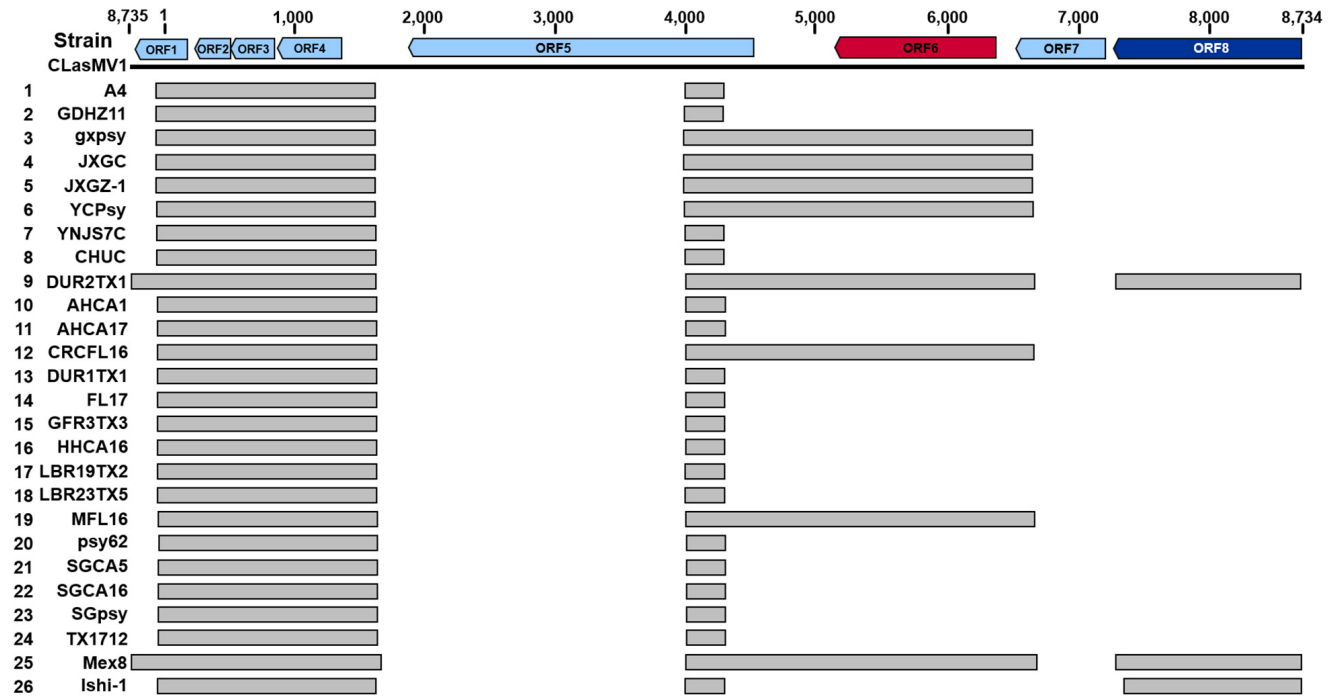

FIGURE 7 | BLASTn detection of CLasMV1 sequence in "*Candidatus* Liberibacter asiaticus" genomes available in GenBank database. The homologous sequences of CLasMV1 detected in CLas strain are marked by the gray box. Rows 1–8, from China; Rows 9–24, from the United States; Row 25, from Mexico; and Row 26, from Japan. GenBank accession numbers in the order are as follows: 1, CP010804.2; 2, CP045565.1; 3, CP004005.1; 4, CP019958.1; 5, VIQL00000000.1; 6, LIIM00000000.1; 7, QXDO00000000.1; 8, VTLV00000000.1; 9, VTLS00000000.1; 10, CP029348.1; 11, VNFL00000000.1; 12, VTLW00000000.1; 13, VTLT00000000.1; 14, JWHA00000000.1; 15, VTLR00000000.1; 16, VTLY00000000.1; 17, VTMA00000000.1; 18, VTMB00000000.1; 19, VTLX00000000.1; 20, CP001677.5; 21, LMTO00000000.1; 22, VTLZ00000000.1; 23, QFZJ00000000.1; 24, QEWL00000000.1; 25, VTLU00000000.1; and 26, AP014595.1. ORF6 in red encoding major capsid protein (MCP) and ORF8 in deep blue encoding replication initiation protein (RIP).

some specific purposes (Moran, 2002). It can be assumed that this sequence contains critical genes to the bacterium despite the unknown functions of the three ORFs. Alternatively, with the conservativeness of Contig_63 among CLas strains (**Figure 7**), it may have originated from CLas chromosome and was later acquired by CLasMV1. An extensive analysis showed that members of *Microviridae* were able to integrate genes of interest such as peptidase genes from external sources into their genomes (Roux et al., 2012).

Based on the survey of over 1,000 CLas strains collected in southern China, 57% contained CLasMV1 phage, indicating that the phage could likely have an important role in CLas biology. Despite the overall high sequence similarities, it was apparent that strains of CLasMV1 from different sources could vary in the form of SNPs or In/Dels (**Figure 6**). In addition to HGT, the accumulation of point mutation has been thought to be more important for the evolution of bacteriophage, especially for small ssDNA phages (Székely and Breitbart, 2016), mainly due to their limited genome size and high nucleotide mutation rate (Sanjuan et al., 2010). The diversity of CLasMV1-type phages, revealed by SNPs or In/Dels, indicated that the sequence mutation could be the major force for current evolution of CLasMV1-type phages, although the biological nature of these variations is currently unknown. However, they could set a baseline for future phage diversity study.

CONCLUSION

In conclusion, we identified a novel *Microviridae* phage, CLasMV1, with a small circular genome in CLas strain from China. The CLasMV1 encoded eight ORFs, including a phage replication initiation gene, a major capsid gene, and six hypothetical genes. Based on the phylogenetic analysis, CLasMV1 defined a new lineage, designated as subfamily *Libervirinae*, in *Microviridae* family. CLasMV1 was widely distributed with a high copy number in CLas population from southern China. Identification of homologous genes between CLasMV1 phage and CLas strains indicated that the gene transfer could play an important role in early evolution of CLasMV1 phage. The mutation-driven evolution was thought to be the major force diversifying the current CLasMV1-type phage population. The discovery of this novel *Microviridae* phage in CLas strain provided new insights into the biology, diversity, and evolution of *Microviridae* phage.

DATA AVAILABILITY STATEMENT

Genomes of CLasMV1-type phages has been deposited at DDBJ/ENA/GenBank under the accession number listed in **Table 2**.

AUTHOR CONTRIBUTIONS

LZ, JC, XD, and ZZ conceived and designed the experiments. LZ, ZL, MB, YL, TL, FF, YZ, MX, and ZZ collected the samples and performed the experiments. LZ, ZL, TL, MB, and ZZ contributed to the bioinformatics and statistical analyses. LZ and ZZ prepared the figures and tables and wrote the draft manuscript. JC, XD, and ZZ reviewed and revised the manuscript. All authors contributed to the article and approved the submitted version.

FUNDING

This study was supported by the National Natural Science Foundation of China (31901844), the Special fund for the National Key Research and Development Program of China (2018YFD0201500), and China Agriculture Research System of MOF and MARA. Mention of trade names or commercial products in this publication is solely for the purpose of providing specific information and does not imply recommendation or endorsement by the U.S. Department of Agriculture. The USDA is an equal-opportunity provider and employer.

SUPPLEMENTARY MATERIAL

The Supplementary Material for this article can be found online at: https://www.frontiersin.org/articles/10.3389/fmicb.2021.754245/full#supplementary-material

REFERENCES

Adams, M. H. (1959). *Bacteriophages*. New York, NY: Interscience Publishers.

Aziz, R. K., Bartels, D., Best, A. A., DeJongh, M., Disz, T., Edwards, R. A., et al. (2008). The RAST server: rapid annotations using subsystems technology. *BMC Genomics* 9:75. doi: 10.1186/1471-2164-9-75

Bao, M., Zheng, Z., Sun, X., Chen, J., and Deng, X. (2020). Enhancing PCR capacity to detect '*Candidatus Liberibacter* asiaticus' utilizing whole genome sequence information. *Plant Dis.* 104, 527–532. doi: 10.1094/PDIS-05-19-0931-RE

Camacho, C., Coulouris, G., Avagyan, V., Ma, N., Papadopoulos, J., Bealer, K., et al. (2009). BLAST+: architecture and applications. *BMC Bioinformatics* 10:421. doi: 10.1186/1471-2105-10-421

Cherwa, J. E., and Fane, B. A. (2011). *Microviridae: Microviruses and Gokushoviruses. eLS*. Chichester: John Wiley & Sons, Ltd.

Cui, X., Liu, K., Atta, S., Zeng, C., Zhou, C. Y., and Wang, X. (2020). Two unique prophages of "*Candidatus Liberibacter* asiaticus" strains from Pakistan. *Phytopathology* 111, 784–788. doi: 10.1094/PHYTO-10-20-0454-SC

Desnues, C., Rodriguez-Brito, B., Rayhawk, S., Kelley, S., Tran, T., Haynes, M., et al. (2008). Biodiversity and biogeography of phages in modern stromatolites and thrombolites. *Nature* 452, 340–343. doi: 10.1038/nature06735

Dominguez-Mirazo, M., Jin, R., and Weitz, J. S. (2019). Functional and comparative genomic analysis of integrated prophage-like sequences in "*Candidatus Liberibacter* asiaticus". *mSphere* 4, e409–e419. doi: 10.1128/mSphere.00409-19

Duan, Y., Zhou, L., Hall, D. G., Li, W., Doddapaneni, H., Lin, H., et al. (2009). Complete genome sequence of citrus huanglongbing bacterium, '*Candidatus Liberibacter* asiaticus' obtained through metagenomics. *Mol. Plant Microbe Interact.* 22, 1011–1020. doi: 10.1094/MPMI-22-8-1011

Fleites, L. A., Jain, M., Zhang, S., and Gabriel, D. W. (2014). "*Candidatus Liberibacter* asiaticus" prophage late genes may limit host range and culturability. *Appl. Environ. Microbiol.* 80, 6023–6030. doi: 10.1128/AEM.01958-14

Jain, M., Fleites, L., and Gabriel, D. W. (2015). Prophage encoded peroxidase in "*Candidatus Liberibacter* asiaticus" is a secreted effector that suppresses plant defenses. *Mol. Plant Microbe Interact.* 28, 1330–1337. doi: 10.1094/MPMI-07-15-0145-R

Krupovic, M., Dutilh, B. E., Adriaenssens, E. M., Wittmann, J., Vogensen, F. K., Sullivan, M. B., et al. (2016). Taxonomy of prokaryotic viruses: update from the ICTV bacterial and archaeal viruses subcommittee. *Arch. Virol.* 161, 1095–1099. doi: 10.1007/s00705-015-2728-0

Labonté, J. M., and Suttle, C. A. (2013). Previously unknown and highly divergent ssDNA viruses populate the oceans. *ISME J.* 7, 2169–2177. doi: 10.1038/ismej.2013.110

Langmead, B., and Salzberg, S. L. (2012). Fast gapped-read alignment with Bowtie 2. *Nat. Methods* 9, 357–359. doi: 10.1038/nmeth.1923

Li, T., Zhang, L., Deng, Y., Deng, X., and Zheng, Z. (2021). Establishment of a *Cuscuta* campestris–mediated enrichment system for genomic and transcriptomic analyses of "*Candidatus Liberibacter* asiaticus". *Microb. Biotechnol.* 14, 737–751. doi: 10.1111/1751-7915.13773

Lu, S., Wang, J., Chitsaz, F., Derbyshire, M. K., Geer, R. C., Gonzales, N. R., et al. (2020). CDD/SPARCLE: the conserved domain database in 2020. *Nucleic Acids Res.* 48, D265–D268. doi: 10.1093/nar/gkz991

Moran, N. A. (2002). Microbial minimalism: genome reduction in bacterial pathogens. *Cell* 108, 583–586. doi: 10.1016/s0092-8674(02)00665-7

Rosenwald, A. G., Murray, B., Toth, T., Madupu, R., Kyrillos, A., and Arora, G. (2014). Evidence for horizontal gene transfer between *Chlamydophila pneumoniae* and *Chlamydia phage*. *Bacteriophage* 4:e965076. doi: 10.4161/21597073.2014.965076

Roux, S., Krupovic, M., Poulet, A., Debroas, D., and Enault, F. (2012). Evolution and diversity of the microviridae viral family through a collection of 81 new complete genomes assembled from virome reads. *PLoS One* 7:e40418. doi: 10.1371/journal.pone.0040418

Saglio, P., Lhospital, M., Lafleche, D., Dupont, G., Bové, J. M., Tully, J. G., et al. (1973). Spiroplasma citri gen. and sp. n.: a mycoplasma-like organism associated with "stubborn" disease of citrus. *Int. J. Syst. Evol. Microbiol.* 23, 191–204. doi: 10.1099/00207713-23-3-191

Sanger, F., Air, G. M., Barrell, B. G., Brown, N. L., Coulson, A. R., Fiddes, J. C., et al. (1977). Nucleotide sequence of bacteriophage φX174 DNA. *Nature* 265, 687–695. doi: 10.1038/265687a0

Sanjuan, R., Nebot, M. R., Chirico, N., Mansky, L. M., and Belshaw, R. (2010). Viral mutation rates. *J. Virol.* 84, 9733–9748. doi: 10.1128/JVI.00694-10

Székely, A. J., and Breitbart, M. (2016). Single-stranded DNA phages: from early molecular biology tools to recent revolutions in environmental microbiology. *FEMS Microbiol. Lett.* 363:fnw027. doi: 10.1093/femsle/fnw027

Tamura, K., Stecher, G., Peterson, D., Filipski, A., and Kumar, S. (2013). MEGA6: molecular evolutionary genetics analysis version 6.0. *Mol. Biol. Evol.* 30, 2725–2729. doi: 10.1093/molbev/mst197

Tørresen, O. K., Star, B., Mier, P., Andrade-Navarro, M. A., Bateman, A., Jarnot, P., et al. (2019). Tandem repeats lead to sequence assembly errors and impose multi-level challenges for genome and protein databases. *Nucleic Acids Res.* 47, 10994–11006. doi: 10.1093/nar/gkz841

Tucker, K. P., Parsons, R., Symonds, E. M., and Breitbart, M. (2010). Diversity and distribution of single-stranded DNA phages in the North Atlantic Ocean. *ISME J.* 5, 822–830. doi: 10.1038/ismej.2010.188

Untergasser, A., Cutcutache, I., Koressaar, T., Ye, J., Faircloth, B. C., Remm, M., et al. (2012). Primer3 - new capabilities and interfaces. *Nucleic Acids Res.* 40:e115. doi: 10.1093/nar/gks596

Wittwer, C. T., Herrmann, M. G., Gundry, C. N., and Elenitoba-Johnson, K. S. (2001). Real-time multiplex PCR assays. *Methods* 25, 430–442. doi: 10.1006/meth.2001.1265

Zhang, S., Flores-Cruz, Z., Zhou, L., Kang, B. H., Fleites, L., Gooch, M. D., et al. (2011). "*Ca. Liberibacter* asiaticus" carries an excision plasmid prophage and a chromosomally integrated prophage that becomes lytic in plant infections. *Mol. Plant Microbe Interact.* 24, 458–468. doi: 10.1094/MPMI-11-10-0256

Zheng, Z., Bao, M., Wu, F., Van, H. C., Chen, J., and Deng, X. (2018). A type 3 prophage of '*Candidatus Liberibacter* asiaticus' carrying a restriction-modification system. *Phytopathology* 108, 454–461. doi: 10.1094/PHYTO-08-17-0282-R

Zheng, Z., Deng, X., and Chen, J. (2014b). Whole-genome sequence of "*Candidatus Liberibacter* asiaticus" from Guangdong, China. *Genome Announc.* 2, e273–e214. doi: 10.1128/genomeA.00273-14

Zheng, Z., Deng, X., and Chen, J. (2014a). Draft genome sequence of "*Candidatus Liberibacter* asiaticus" from California. *Genome Announc.* 2, e999–e914. doi: 10.1128/genomeA.00999-14

Zheng, Z., Sun, X., Deng, X., and Chen, J. (2015). Whole-genome sequence of "*Candidatus Liberibacter* asiaticus" from a huanglongbing-affected citrus tree in central Florida. *Genome Announc.* 3, e169–e115. doi: 10.1128/genomeA.00169-15

Zheng, Z., Wu, F., Kumagai, L. B., Polek, M., Deng, X., and Chen, J. (2017). Two '*Candidatus Liberibacter* asiaticus' strains recently found in California harbor different prophages. *Phytopathology* 107, 662–668. doi: 10.1094/PHYTO-10-16-0385-R

Zheng, Z., Xu, M., Bao, M., Wu, F., Chen, J., and Deng, X. (2016). Unusual five copies and dual forms of nrdB in "*Candidatus Liberibacter* asiaticus": biological implications and PCR detection application. *Sci. Rep.* 6:39020. doi: 10.1038/srep39020

Conflict of Interest: The authors declare that the research was conducted in the absence of any commercial or financial relationships that could be construed as a potential conflict of interest.

Publisher's Note: All claims expressed in this article are solely those of the authors and do not necessarily represent those of their affiliated organizations, or those of the publisher, the editors and the reviewers. Any product that may be evaluated in this article, or claim that may be made by its manufacturer, is not guaranteed or endorsed by the publisher.

frontiers in Microbiology

ORIGINAL RESEARCH
published: 21 February 2022
doi: 10.3389/fmicb.2021.797841

Overexpression of a "*Candidatus* Liberibacter Asiaticus" Effector Gene *CaLasSDE115* Contributes to Early Colonization in *Citrus sinensis*

*Meixia Du, Shuai Wang, Liting Dong, Rongrong Qu, Lin Zheng, Yongrui He, Shanchun Chen and Xiuping Zou**

National Citrus Engineering Research Center, Citrus Research Institute, Southwest University, Chongqing, China

OPEN ACCESS

Edited by:
Kranthi Kiran Mandadi, Texas A&M University, United States

Reviewed by:
Veronica Ancona, Texas A&M University-Kingsville, United States
Freddy Ibanez-Carrasco, Texas A&M AgriLife Research and Extension Center at Weslaco, United States

***Correspondence:**
Xiuping Zou
zouxiuping@cric.cn

Specialty section:
This article was submitted to Microbe and Virus Interactions with Plants, a section of the journal Frontiers in Microbiology

Received: *19 October 2021*
Accepted: *20 December 2021*
Published: *21 February 2022*

Citation:
Du M, Wang S, Dong L, Qu R, Zheng L, He Y, Chen S and Zou X (2022) Overexpression of a "Candidatus Liberibacter Asiaticus" Effector Gene CaLasSDE115 Contributes to Early Colonization in Citrus sinensis. Front. Microbiol. 12:797841. doi: 10.3389/fmicb.2021.797841

Huanglongbing (HLB), caused by "*Candidatus* liberibacter asiaticus" (*Ca*Las), is one of the most devastating diseases in citrus but its pathogenesis remains poorly understood. Here, we reported the role of the *Ca*LasSDE115 (CLIBASIA_05115) effector, encoded by *Ca*Las, during pathogen-host interactions. Bioinformatics analyses showed that *Ca*LasSDE115 was 100% conserved in all reported *Ca*Las strains but had sequence differences compared with orthologs from other "*Candidatus* liberibacter." Prediction of protein structures suggested that the crystal structure of *Ca*LasSDE115 was very close to that of the invasion-related protein B (IalB), a virulence factor from *Bartonella henselae*. Alkaline phosphatase (PhoA) assay in *E. coli* further confirmed that *Ca*LasSDE115 was a Sec-dependent secretory protein while subcellular localization analyses in tobacco showed that the mature protein of SDE115 (mSDE115), without its putative Sec-dependent signal peptide, was distributed in the cytoplasm and the nucleus. Expression levels of *CaLasSDE115* in *Ca*Las-infected Asian citrus psyllid (ACP) were much higher (~45-fold) than those in *Ca*Las-infected Wanjincheng oranges, with the expression in symptomatic leaves being significantly higher than that in asymptomatic ones. Additionally, the overexpression of *mSDE115* favored *Ca*Las proliferation during the early stages (2 months) of infection while promoting the development of symptoms. Hormone content and gene expression analysis of transgenic plants also suggested that overexpressing *mSDE115* modulated the transcriptional regulation of genes involved in systemic acquired resistance (SAR) response. Overall, our data indicated that *Ca*LasSDE115 effector contributed to the early colonization of citrus by the pathogen and worsened the occurrence of Huanglongbing symptoms, thereby providing a theoretical basis for further exploring the pathogenic mechanisms of Huanglongbing disease in citrus.

Keywords: Citrus Huanglongbing, *Candidatus* Liberibacter asiaticus, effector, LasSDE115, overexpression, SAR, early colonization

INTRODUCTION

Citrus Huanglongbing (HLB) is the most devastating disease which has harmed citrus trees in more than 50 countries and regions around the world, thereby causing serious economic losses to the citrus industry (Gottwald, 2010). Its causative agent is a phloem-limited α-*Proteobacterium* "*Candidatus* Liberibacter" (Jagoueix et al., 1994; Bové, 2006) for which three species namely "*Candidatus* Liberibacter asiaticus (*Ca*Las)," "*Candidatus* Liberibacter africanus" and "*Candidatus* Liberibacter americanus" are known to be associated with HLB in citrus (Teixeira et al., 2005; Wulff et al., 2014; Lin et al., 2015). However, to date, HLB pathogens have not been successfully cultured *in vitro*. Among these, *Ca*Las is the most prevalent one in citrus, with its insect vector being the Asian citrus psyllid (ACP) *Diaphorina citri* Kuwayama. *Ca*Las resides in sieve elements and spreads through the phloem transport system (Duan et al., 2009). HLB symptoms mainly include flush yellowing, leaf mottling, as well as inverted fruit coloring before eventually resulting in plant death (Bassanezi et al., 2009; Graham et al., 2013). Although there have been many successful cases of HLB management based on the "Three basic measures" (planting HLB-free nursery trees, timely clearing of any HLB-infected trees and controlling psyllid populations as much as possible), neither effective cures against the disease and nor HLB-resistant citrus cultivars have, so far, been identified (Wang et al., 2017).

Host-pathogen interactions are vital to understanding and controlling HLB disease. This interplay between hosts and pathogens involves a myriad of molecular interactions that play important roles both in a pathogen's ability to suppress or avoid a plant's immunity as well as in the host's ability to detect and remove the pathogen. First, the plant perceives pathogen-associated molecular patterns (PAMP) such as fungal chitin and bacterial flagellin through its immune receptors PRRs (pattern recognition receptors) to initiate PAMP-triggered immunity (PTI) that prevents pathogen invasion (Boller and Felix, 2009; Segonzac and Zipfel, 2011). To defeat the PTI responses, pathogens manipulate the host's cellular functions by secreting diverse effector proteins (Yuan et al., 2021) which are recognized by specialized receptors (usually the plant disease resistance proteins) and this further leads to the activation of the host's effector-triggered immunity (ETI) to prevent pathogen attack (Jones and Dangl, 2006; Haitao et al., 2015). However, a pathogen can also evolve its effectors to suppress the ETI (Nguyen et al., 2021). In *Ca*Las-citrus interactions, the effectors involved and their functions in pathogen virulence are poorly understood, partly due to the unculturability of the pathogen. Thus, exploring the role of *Ca*Las effectors could be key to understanding the pathogenicity mechanisms of *Ca*Las as well as for identifying citrus resistance genes which could eventually be exploited for developing new control methods and improving HLB resistance in citrus.

Many extracellular plant pathogens suppress plant immunity through the translocation of effector proteins using the type-III secretion system (T3SS) (Jones and Dangl, 2006; Toruno et al., 2016). However, since *Ca*Las does not possess a T3SS (Duan et al., 2009) but instead harbors a complete Sec-dependent secretion system (Duan et al., 2009), it is believed that *Ca*Las secrets Sec-dependent effectors (SDEs) including virulence factors into plant cells through this system (Pitino et al., 2016; Prasad et al., 2016; Pagliaccia et al., 2017). In other phloem-limited pathogens such as phytoplasma, several SDEs have been shown to be critical for pathogenicity (Saskia et al., 2008). Similarly, for *Ca*Las SDEs, 86 putative SDE proteins have been shown to have functional Sec-dependent secretion signal peptides (Prasad et al., 2016). Clark et al. (2018) reported that *Ca*Las SDE1 suppressed citrus immunity by inhibiting the activity of papain-like cysteine proteases (PLCPs). Pang et al. (2020) showed that SDE15 suppressed plant immunity by interacting with the citrus protein CsACD2, a homolog of *Arabidopsis* ACCELERATED CELL DEATH 2. In fact, overexpression of *SDE15* or *CsACD2* in Duncan grapefruit was found to suppress plant immunity and promote *Ca*Las growth. Furthermore, the authors indicated that SDE15-CsACD2 interactions repressed citrus PTI by affecting the expression of PTI marker genes such as *FRK1*, *GST1* and *WRKY22*. Other *Ca*Las SDEs were also reported to regulate plant immunity responses (Liu et al., 2019; Ying et al., 2019; Li et al., 2020). In addition, it has been shown that *Ca*Las also transported non-classically secreted proteins (ncSecPs) into host cells to regulate host immunity. In this context, Du et al. (2021) indicated that 10 ncSecPs had opposing effects on early plant defenses. For instance, SC2_gp095 effectors, encoded by *Ca*Las prophages, could suppress the development of host symptoms through the manipulation of plant H_2O_2-mediated defense signaling (Jain et al., 2015). Similarly, *Ca*Las SahA could degrade salicylic acid (SA) to suppress plant defenses (Li et al., 2017) while the peroxiredoxin effector LasBCP simultaneously inhibited localized as well as systemic innate immune responses through oxylipin-mediated defense signaling in plants (Jain et al., 2018, 2019).

In this study, we investigated the potential role of a putative virulence factor *Ca*LasSDE115 (CLIBASIA_05115) during *Ca*Las infections. Bioinformatics predictions indicated that *Ca*LasSDE115 was very close to that of a virulence factor IalB from *Bartonella henselae*, which is not only an invasion-associated locus B but is also involved in pathogen-host invasions (Vayssier-Taussat et al., 2010). The sec-dependent secretory characteristics of *Ca*LasSDE115 was also confirmed by bioinformatics analyses and phoA assays while its involvement in citrus' responses to *Ca*Las infections were investigated by overexpressing *mSDE115* in HLB-susceptible Wanjincheng oranges. Altogether, our data indicated that *Ca*LasSDE115 positively regulated early pathogenic colonization of citrus by modulating the transcriptional regulation of genes involved in SAR responses. The potential mechanisms of *Ca*LasSDE115 were eventually discussed in this study. Overall, it is expected that this study will help to

A

```
CaLasSDE115  MFLNVLKDFFVPRIRFLIVLMVSSVSAGYANASQPEPTLRNQFSRWSVY-VYPDLNKKLC  59
CaLafSDE115  MFLNILKGCFIFRVGLFIILMMSGISNVYAVVSHPIPTLRNQFSKWSVY-QYSDLNKTVC  59
CaLsoSDE115  MFLRILKNFFIFGRRFFVLLIITGMPVAYADSTNSNPVLRNEFIRWLVYYHSPDSNRKIC  60
CaLamSDE115  ----------------FALLFIIGKLNIIYAENRTTSVSWISNFGNWSVN-----RDKYFC  40
AgvIalB      ---------FVKKIATAFALVVGFA--GVAMAQAPSPTRIEQFKAWGAY-SYKSGNNTVC  48
RhuIalB      --------MFVKRIATACAMMLATV--SVATAQSPSPTRIEQFKAWGAY-SYKSGANTVC  49
                        :::       *          .:*  * .        . .*

CaLasSDE115  FSLSVPVTVEPLEGVRHGVNFFIISLKKEENSAYVSELVMDYPLDEEEMVSLEVKGKNAS  119
CaLafSDE115  FALSVPSVSEPLEGVKHGVNFLIVSLKKGHNDSYLPELVMDYPLDEETMISVEVIGKYSS  119
CaLsoSDE115  YTVTVPTFSEPEKGVKHGINFFMIGLKKETKDSYVSELVMDYPLDENTMVSIEVIGKNSS  120
CaLamSDE115  YAISSPIISKPSTNINHGNNYFIIASNPEKKGSYVLEAVMDYPLDKNKNISLQVKGKNSN  100
AgvIalB      YVLSVPTTKEPA-SVNHGDIFFIVSQRPGQNISYEPQAMMGYPLKAGSKVTVKIDAKS--  105
RhuIalB      YVLSVPTSKEPP-SVNHGDVFFIVSQRPGQNISYEPQVMVGYPLKAGSKVTVKIDAKS--  106
             : :: *   :*  .:.**  ::::. .    : :*  : ::.***.     ::::: .*

CaLasSDE115  GTIFKMKSYNNR-AAFEKRS--QDTVLIEEMKRGKELVVSAKSKRGTNTRYIYSLIGLSD  176
CaLafSDE115  GQIFKMKPRNNR-AIFEKRF--DDDILIQAMKSGRALSVSAKSKRGTNTHYTFSLEGLSD  176
CaLsoSDE115  GQIFTMHPHNNR-ATFQKES--DNEILIKEMKLGKEVIVSAKSKRGTNTRYVYSLSGLSD  177
CaLamSDE115  EKIFTMNFYNDHRTIFPPESDNDVDLLIKSMKMGKDLILKAKSKRGTDTEYVYSLNGLSK  160
AgvIalB      ---FTMFTKDSA-AWVEN--AAEEPALVAAMKSGKTMSVQAVSGRGTPTNYTYSLQGISD  159
RhuIalB      ---FSMFVKDSA-AWVEN--AAEEPQLVQAMKTGKTLTVQAVSGRGTQTNYAYSLQGISD  160
                *.*   :.  : .      :   *:  ** *: : :.* * *** *.* :** *:*.

CaLasSDE115  SLADIRKCN      185
CaLafSDE115  ALADVPKCQ      185
CaLsoSDE115  ALADLPKC-      185
CaLamSDE115  ALEDIGRC-      168
AgvIalB      AFKRIEKC-      167
RhuIalB      ALKRIEKC-      168
             ::   : :*
```

B

Abbreviation	Species	Identity	Accession
CaLafSDE115	*Candidatus* Liberibacter africanus	65%	WP_047264608.1
CaLsoSDE115	*Candidatus* Liberibacter solanacearum	58%	WP_034441745.1
CaLamSDE115	*Candidatus* Liberibacter americanus	41%	WP_007557400.1
RhuIalB	*Rhizobium undicola*	38%	WP_027487009.1
AgvIalB	*Agrobacterium vitis*	38%	WP_184299347.1

C

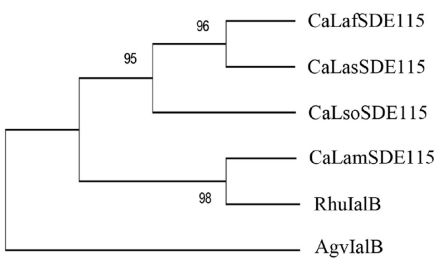

FIGURE 1 | Analysis of *Ca*LasSDE115 protein sequence. **(A,B)** Multiple sequence alignment of *Ca*LasSDE115 with selected homologs. **(C)** A phylogenetic tree containing *Ca*LasSDE115 and other selected homologs. The reliability of the tree was estimated using 1000 bootstrap replicates and the bootstrap values (%) are shown above branches. In **(A)**, "*", ":" and "." indicate a single completely conservative, highly and low similar among residues, respectively.

further reveal the pathogenic mechanisms of Huanglongbing disease in the future.

MATERIALS AND METHODS

Plant Materials, Asian Citrus Psyllids, Pathogens and Growth Conditions

Wanjincheng orange plants (*C. sinensis* Osbeck) as well as all the transgenic ones used in this study were plantged in a greenhouse, with a 16 h photoperiod of 45 μmol $m^{-2}s^{-1}$ illumination and a relative humidity of 60%, at the National Citrus Engineering Research Center, Chongqing, China. Citrus trees containing *Ca*Las were also maintained in the greenhouse. Healthy adult ACPs were reared on young leaf flush of *Ca*Las-infected or *Ca*Las-free sweet orange (*C. sinensis*) seedlings in incubators at a temperature of 25 ± 1°C and after 3-weeks of feeding, the insects were collected, frozen with liquid nitrogen and stored at -80°C. Using the primers Cs16S-F/16s-R (**Supplementary Table 1**), the

presence of the *Ca*Las pathogens in both plants and ACPs was confirmed by PCR.

Cloning and Analysis of *CaLasSDE115*

Using cDNA from *Ca*Las-infected Wanjincheng orange plants as a template, the gene encoding for *Ca*LasSDE115 (CLIBASIA_05115) was amplified with the primer pair T-SDE115-F/R (**Supplementary Table 1**). The PCR was performed in a final volume of 50 μL, containing 25 μL of Primer STAR Max Premix (TaKaRa, Ojin, Japan), 1.5 μL of each primer (10 $mM \cdot L^{-1}$), 19 μL of H_2O and 3 μL of cDNA (0.5×10^{-5} $ng \cdot L^{-1}$). The PCR conditions were as follows: pre-denaturation at 96°C for 5 min, followed by 35 amplification cycles (96°C for 30 s, 56°C for 30 s and 72°C for 30 s), before a final extension at 72°C for 3 min. The PCR product was T-cloned into the pGEM-Teasy vector (Promega, WI, United States). The sequence of *CaLasSDE115* was then determined by Sanger sequencing.

The signal peptide (SP) and transmembrane structure of *Ca*LasSDE115 were predicted using the signalP5.0 tool[1] and TMHMM Server (v.2.0)[2], respectively. The secondary as well as tertiary structures of its mature protein were analyzed using SOPMA[3], SWISS-MODEL [4] and Phyre[5] tools, respectively. Multiple sequence alignment of the *Ca*LasSDE115 protein with homologs from other selected species was also performed using ClustalW2 tool[6]. A phylogenetic tree was constructed based on the neighbor-joining method using MEGA7.0 software (Kumar et al., 2016).

Alkaline Phosphatase (PhoA) Assay

PhoA assays of *Ca*LasSDE115 were performed, in triplicate, as previously described (Liu et al., 2019). *CaLasSDE115*, *mSDE115* without the SP-coding sequence, as well as *SDE115sp* containing only the SP-coding sequences were separately inserted into *mphoA*-containing pET-mphoA (without the SP-coding sequence), to generate different in-frame gene fusions while PET-phoA (containing its SP-coding sequence) and PET-mphoA vectors were used as positive and negative controls, respectively. These different constructs were then transformed into *E. coli* BL21 cells which were incubated overnight at 37°C on LB medium supplemented with 90 μg/ml of BCIP (5-bromo-4-chloro-3-indolylphosphate) and 75 mM of Na_2HPO_4 in order to detect phoA activities. The blue transformants indicated that fusion proteins were secreted outside the cells.

Subcellular Localization Analysis in *Nicotiana benthamiana* Cells

The *mSDE115* sequence was cloned into pCAMBIA1300-35S-GFP to construct the fusion gene *mSDE115:GFP* prior to its transfer into *A. tumefaciens* EHA105. Agroinfiltration of *N. benthamiana* leaves was performed as described before (Liu et al., 2019) and 3 days post-inoculation, the localization of the fusion protein was determined using an FV3000 confocal microscope equipped with a UV light source (Olympus, Tokyo, Japan). A histone 2B (H2B) fusion with the red fluorescent protein (RFP) was used as a marker for the nucleus (Martin et al., 2009). This test was repeated twice.

Citrus Transformation

For citrus transformation, the *mSDE115* gene sequence was first cloned into a pLGN vector (Zou et al., 2017) to construct the *p35S:mSDE115* vector in which *mSDE115* expression was controlled by a 35S strong constitutive promoter. The vector was then introduced into an EHA105 strain.

Epicotyl segments from Wanjincheng orange seedlings were used for *A. tumefaciens*-mediated transformation, with the experiment performed as previously described (Peng et al., 2015). Transgenic shoots were then identified by GUS staining as well as PCR analysis before being micrografted onto Troyer citrange [*Poncirus trifoliata* (L.) Raf. × *C. sinensis* (L.) Osbeck] seedlings *in vitro*. The resulting plantlets were further grafted onto Troyer citrange seedlings in a greenhouse, and the expression levels of *mSDE115* gene in those transgenic plants were determined by RT-qPCR analysis.

Evaluation of Huanglongbing Tolerance in Transgenic Citrus

Evaluating the tolerance of transgenic plants to *Ca*Las was performed as previously described by Zou et al. (2017). Three to five plants per independent transgenic line, including wild type (WT) plants, were inoculated by *Ca*Las-infected Wanjincheng orange branches using the shoot top grafting method (Cifuentes-Arenas et al., 2019). All the inoculated plants were then maintained in a greenhouse and regularly checked for any sign of disease incidence.

The *Ca*Las bacterial populations (*Ca*Las cells μg^{-1} of citrus DNA) were determined as previously described (Zou et al., 2017). Every 2 months, three midrib sections from three different leaves per plant were randomly extracted and pooled into one sample from which DNA was isolated. The amount of *Ca*Las 16S rRNA genes and citrus 18S rRNA genes in the isolated DNA samples were subsequently detected by quantitative PCR (qPCR) using the Cs16S-f/Cs16S-r and Cs18S-f/Cs18S-r primers (**Supplementary Table 1**), respectively. The qPCR was performed in a final volume of 12 μL, containing 6 μL of the SYBRPRIME qPCR Kit (Bioground Biotech, Chongqing, China), 4.4 μL H_2O, 0.3 μL of each primer (10 $mM \cdot L^{-1}$) as well as 1 μL DNA(10 $ng \cdot \mu L^{-1}$)while the PCR protocol involved a pretreatment (95°C for 2 min) followed by 40 amplification cycles (each at 94°C for 10 s and 60°C for 60 s). Using the citrus 18S gene as the internal reference, the *Ca*Las bacterial populations were calculated as reported by Zou et al. (2017). In this case, the disease intensity in the transgenic lines was evaluated based on the bacterial populations of three to five plants compared with the WT control.

[1] http://www.cbs.dtu.dk/services/SignalP/

[2] http://www.cbs.dtu.dk/services/TMHMM/

[3] https://npsa-prabi.ibcp.fr/

[4] https://swissmodel.expasy.org/

[5] http://www.sbg.bio.ic.ac.uk/phyre2/

[6] https://www.ebi.ac.uk/Tools/msa/clustalo/

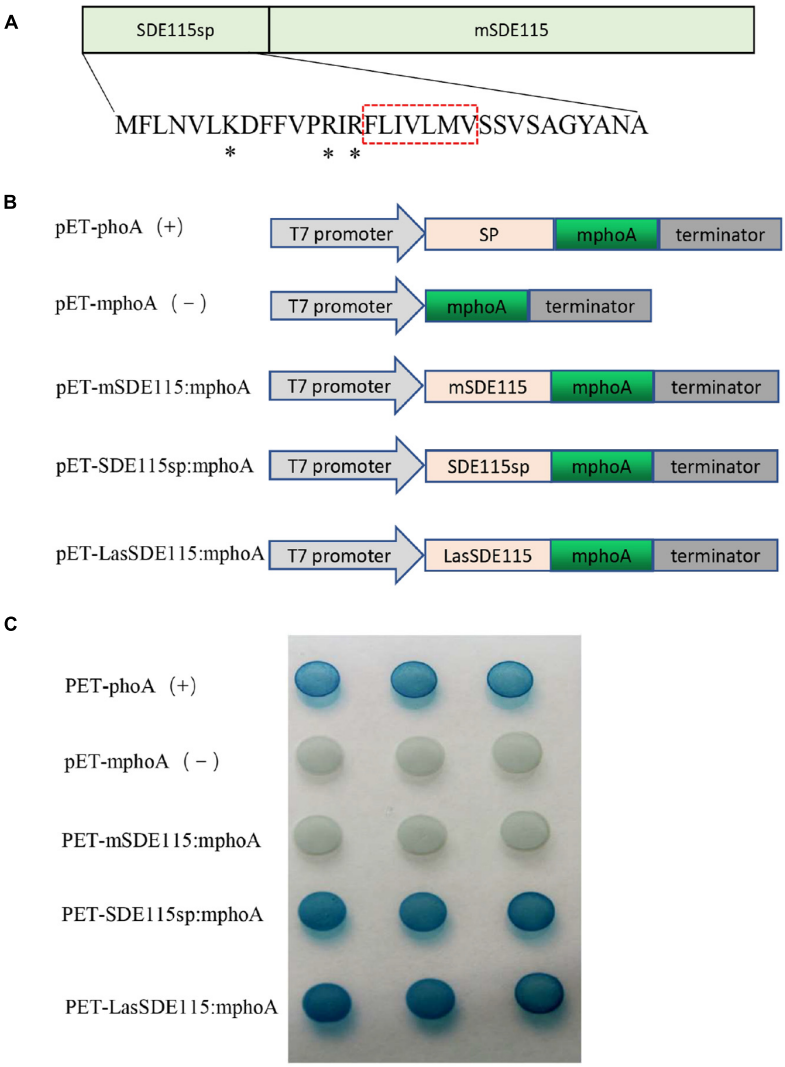

FIGURE 2 | *Ca*LasSDE115 is a Sec-dependent secretory protein. **(A)** Structure of the *Ca*LasSDE115 protein. Its signal peptide and mature protein were named SDE115sp and mSDE115, respectively. *indicated the positively charged amino acids lysine (K) and arginine (R) while the red box indicated the central hydrophobic core. **(B)** Schematic diagram of the prokaryotic expression cassettes for phoA assay. **(C)** PhoA assay for the secretion of *Ca*LasSDE115 in *E. coli* cells. The data showed that SDE115sp directed the extracellular translocation of mPhoA lacking its native SP and that of *Ca*LasSDE115:mphoA fusion.

RT-qPCR Analysis

Total RNA isolation from citrus tissues, including leaves, roots and midrib sections were performed using the EASYspin Plant RNA Extraction Kit according to the manufacturer's instructions (Aidlab, Beijing, China). In the case of ACPs, 30–40 *Ca*Las-infected insects were ground to a powder in liquid nitrogen before immediately extracting total RNA with TRIzol Reagent (Invitrogen, MA, United States). A 1 μg cDNA was then synthesized by reverse transcription (RT) using the PrimeScript ^{TM}RT Master Mix (TaKaRa, Ojin, Japan) prior to quantitative reverse transcription-polymerase chain reaction (QRT-PCR using the primers listed in **Supplementary Table 1**). Gene expression was detected using the SYBRPRIME qPCR Kit (Bioground Biotech, Chongqing, China). The PCR reactions were as follows: pre-denaturation (50°C for 60 s, 95°C for 120 s), followed by 40 cycles of amplification (each at 95°C for 5 s, 60°C for 15 s). The *Ca*Las DNA *gyrase subunit A* (*CaLasgyrA*, GenBank No. CP001677.5) gene was employed as an internal reference to investigate the expression of *CaLas05115* in *Ca*Las-infected plants and ACPs while the citrus *GAPDH* gene (Mafra et al., 2012) was used as an internal reference to evaluate gene expression in transgenic plants. All experiments were performed in triplicate. All the relative expression values were calculated by the Ct method ($2^{-\Delta\Delta Ct}$) (Livak and Schmittgen, 2001).

Measurement of Hormone Content

Fresh tissues (0.1 g) were collected from three fully mature leaves per line and ground to a fine powder in liquid nitrogen. The powder was then homogenized in 0.9 mL of phosphate saline buffer (PBS) of pH = 7.4, before being centrifuged at 800 rpm

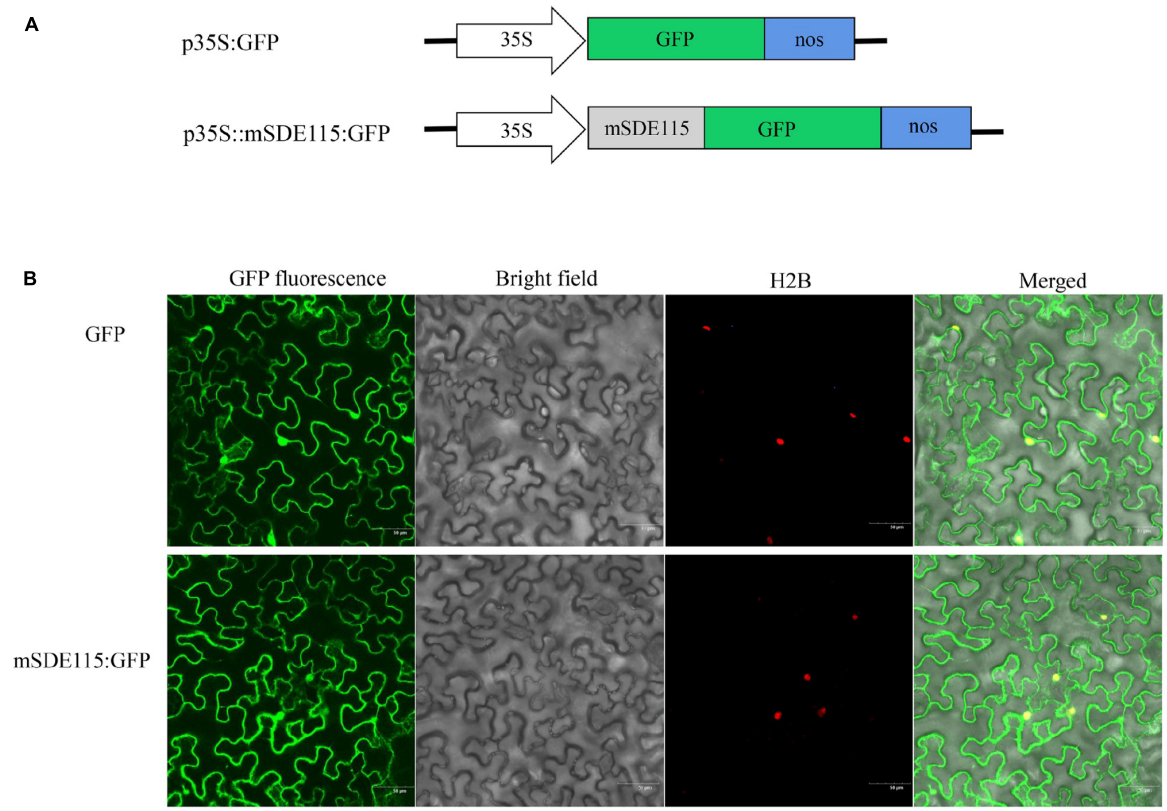

FIGURE 3 | Subcellular location of mSDE115 in tobacco epidermis cell. **(A)** Schematic diagram of the constructs used for agroinfiltration. A 35S, CaMV 35S promoter; NOS, the nopaline synthase terminator. **(B)** Subcellular localization of mSDE115:GFP fusion protein as observed by confocal microscopy. A histone 2B (H2B) fusion with the red fluorescent protein (RFP) was used as a marker for the nucleus (Martin et al., 2009).

for 10 min. The resulting supernatant was transferred to a new, enzyme-free tube and stored in -20°C until assayed.

The SA, methyl salicylate (MeSA) and jasmonic acid (JA) content in the supernatant was determined using plant enzyme-linked immunosorbent assay (ELISA) kits (Jiweibio, Shanghai, China) (Zou et al., 2021). Briefly, the supernatant was first diluted with a 5 × ELISA diluent buffer before adding 50 μL of the diluted supernatant to reaction wells, followed by 100 μl of the detection antibody (horseradish peroxidase-conjugated antibody). After incubating the mixture at 37°C for 1 h, the wells were washed five times with 350 μL of the washing buffer prior to a second incubation with 100 μL of 1 × TMB (3,3′, 5,5′-tetramethylbenzidine) solution at 37°C for 15 min. The reaction was eventually stopped by adding 50 μL of the stop solution. The OD of each well was then measured, at 450 nm, using a SpectraMax® M2 microplate reader (Molecular Devices Corporation, Menlo Park, CA, United States). The hormone content per gram of fresh weight leaf (μg/g) was calculated using Excel 365. All the assays were repeated three times.

Statistical Analyses

Statistical analyses of all data were conducted in Excel 365, using the Student's *t*-test to compare differences between the control and samples at 5% significance level.

RESULTS

Cloning and Sequence Analysis of *CaLasSDE115*

Based on the sequence of *CaLasSDE115* from *Ca*Las psy62 (Duan et al., 2009), a 558-bp long coding sequence was cloned from *Ca*Las-infected Wanjincheng oranges. This gene encoded 186 amino acid residues and was found to be 100% conserved in all *Ca*Las strains based on the complete genomes which are currently available (**Supplementary Figure 1**). Multiple alignments were performed by ClustalW2 using *Ca*LasSDE115 homologs from selected, different species (**Figures 1A,B**). The results showed that *Ca*LasSDE115 had a 41 to 65% similarity in amino acid sequence compared with the selected orthologs from other *Candidatus* Liberibacters. Phylogenetic analysis also showed that *Ca*LasSDE115 was closely related to the orthologs from "*Candidatus* Liberibacter africanus" and "*Candidatus* Liberibacter solanacearum" (**Figure 1C**). The prediction of tertiary structures further indicated that the crystal structure of *Ca*LasSDE115 was very close to that of the virulence factor IalB from *Bartonella henselae* (Vayssier-Taussat et al., 2010) despite only 15.6% of sequence identity between them (**Supplementary Figures 2**, **3**). In fact, the amino acid sequence of *Ca*LasSDE115 had a 38% identity to those of the IalB homologs

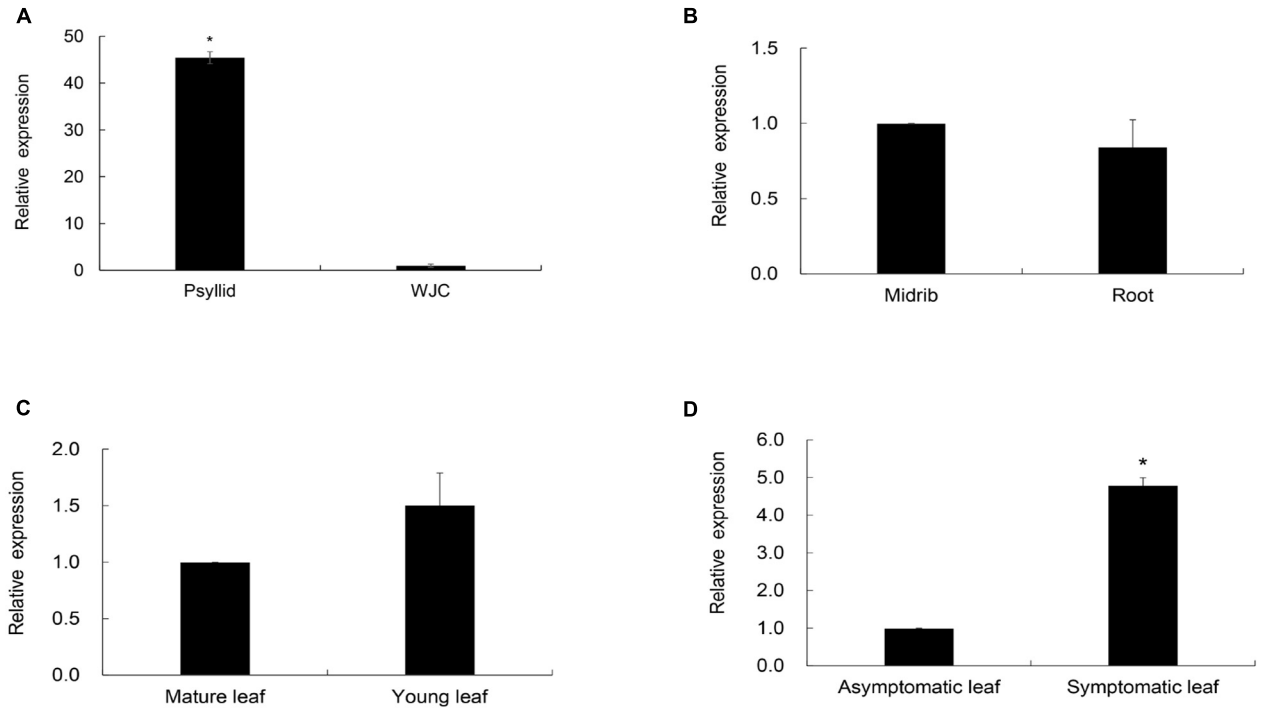

FIGURE 4 | Transcription levels of *CaLasSDE115* in Wanjincheng (WJC) orange and psyllids. Psyllid RNA was isolated from psyllid fed by *Ca*Las-infected sweet orange for 3 weeks, and citrus RNA was isolated from Wanjincheng orange tissues infected by *Ca*Las for 1 years. Using *CaLasgyrA* gene (GenBank No. CP001677.5) gene as internal reference, relative expressions in **(A)** psyllids, **(B)** root, **(C)** young leaf and **(D)** symptomatic leaf were determined compared to WJC orange, root, midrib, mature leaf and asymptomatic leaf, respectively. The Ct values of *CaLasSDE115* and *CaLasgyrA* are listed in **Supplementary Table 2**. Values are expressed as means ± standard deviation of three independent tests. *on top of the bars indicates a significant difference ($p < 0.05$, Student's *t*-test).

from *Rhizobium undicola* and *Agrobacterium vitis* (**Figure 1B**). These results suggested that *Ca*LasSDE115 was involved in *Ca*Las pathogenicity.

*Ca*LasSDE115 as a Sec-Dependent Presecretory Protein

SignalP5.0 predicted that *Ca*LasSDE115 was a Sec-dependent presecretory protein containing a putative signal peptide (namely SDE115sp) with a cleavage site between amino acids 32 and 33 (ANA-SQ; probability: 0.885) (**Figure 2A**). The SDE115sp had a hydrophobic core, flanked by three positively charged residues at the N-terminus and a less positively charged C terminus (**Figure 2A**), which had the characteristics of a Sec-dependent signal peptide (Tamar and Damon, 2018). Based on the TMHMM Server (v.2.0) analysis, no transmembrane domains were found in the mature *Ca*LasSDE115 protein. To determine the export of this protein via the Sec-dependent secretory system, an *E. coli* phoA assay was also used (**Figures 2B,C**). In this case, the data showed that bacteria containing fusions between mphoA (without its native SP) and either the native *Ca*LasSDE115 or only its signal peptide SDE115sp became blue overnight. On the other hand, bacteria containing only mphoA (without its native SP) or its fusion with the mature protein mSDE115 remained white. These results, along with the positive control containing the complete phoA (mphoA + its native SP), confirmed that *Ca*LasSDE115 was a typical Sec-dependent secretory protein and that the signal peptide, as predicted by SignalP5.0, was involved in directing extracellular secretion of proteins in bacteria.

Subcellular Localization of the *Ca*LasSDE115 Mature Protein in Tobacco Cells

Since the above results revealed that the *Ca*LasSDE115 mature protein crossed the bacterial outer membrane into the host cells via a Sec-dependent secretory system, the next step was to observe the subcellular localization of *Ca*LasSDE115 mature proteins in plants. For this purpose, the mSDE115 coding sequence was fused with the GFP reporter gene (**Figure 3A**). Transient expression tests in *N. benthamiana* leaves showed that the mSDE115:GFP fusion had similar cellular locations as those of the GFP protein alone, with fluorescence signals detected in the nucleus and cytoplasm (**Figure 3B**).

Transcription Characteristics of *CaLasSDE115* in Wanjincheng Oranges and Psyllids

To compare the expression levels of *CaLasSDE115* in citrus and insect hosts, RT-qPCR was performed on the total RNA extracted from *Ca*Las-infected Wanjincheng oranges and ACPs (CT values of Wanjincheng oranges and psyllids were listed

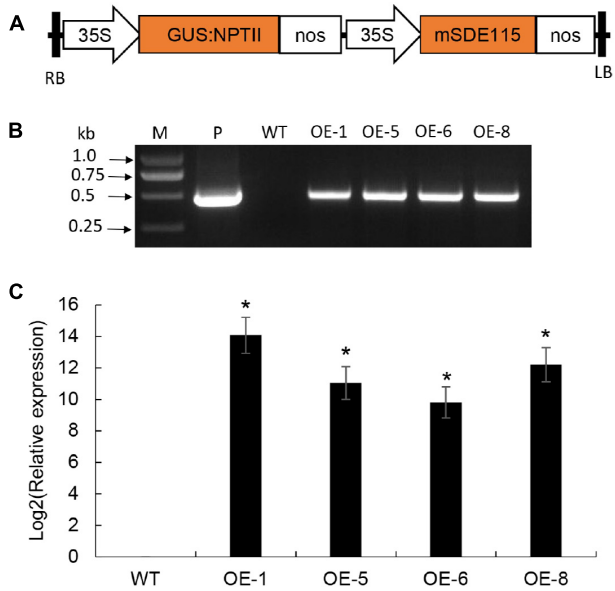

FIGURE 5 | Wanjincheng orange transgenic plants overexpressing *mSDE115*. **(A)** T-DNA structure of plant expression vector for the genetic transformation of citrus. A 35S, CaMV 35S promoter; GUS:NPTII, fusion of β-glucuronidase and neomycin phosphotransferase genes (for the screening of citrus transformants); *mSDE115*, the coding sequence of *Ca*LasSDE115 mature protein; NOS, the nopaline synthase terminator; LB, left border; RB, right border. **(B)** Identification of transgenic plants by PCR. M, DNA marker, P, *p35S:mSDE115* plasmid; WT, wildtype control; OE-#, transgenic plants. **(C)** Relative expression levels of *mSDE115* in transgenic plants. Relative expression of *mSDE115* in transgenic plans was normalized against its expression in wildtype control using the citrus *GAPDH* gene (Mafra et al., 2012) as internal reference. Values are expressed as means ± standard deviation of three independent tests. *on top of the bars indicates significant differences compared to WT control ($p < 0.05$, Student's *t*-test).

in **Supplementary Table 2**). The results showed that the expression level of *CaLasSDE115* in *Ca*Las-infected ACPs was significantly higher (∼45-fold) than that in *Ca*Las-infected Wanjincheng oranges (**Figure 4A** and **Supplementary Table 2**), hence indicating that *CaLasSDE115* could play a role in *Ca*Las infections by the Asian citrus psyllid. Moreover, the data showed that *CaLasSDE115* expression in symptomatic leaves was significantly higher than that in asymptomatic ones, thereby indicating that *CaLasSDE115* was involved in the development of symptoms in citrus. However, it was also found that the expression levels between midribs and roots, as well as between mature and young leaves were not significantly different (**Figures 4B–D** and **Supplementary Table 2**).

Generation of Transgenic Citrus Overexpressing *mSDE115*

To understand the functions of *Ca*LasSDE115 in *Ca*Las pathogenicity, the *mSDE115* gene, encoding for the mature protein SDE115, was used to construct the plant expression vector *p35S:mSDE115* in which *mSDE115* expression was controlled by a strong promoter 35S (**Figure 5A**). Four transgenic plants were identified by PCR (**Figure 5B**) and qRT-PCR analysis showed that all four had significant overexpression of *mSDE115* transcripts, when compared with the wildtype control (**Figure 5C**). After being planted in a greenhouse, those transgenic plants displayed no obvious differences in phenotypes compared with WT ones.

Overexpression of *mSDE115* Contributes to Early Colonization by *Ca*Las in Transgenic Plants

To determine the response of transgenic plants to *Ca*Las infections, three to five plants per transgenic line, including the wildtype control, were infected by grafting them with branches containing *Ca*Las. *Ca*Las growth in plant tissues was then detected using qPCR at two, four and 6 months after the infection (**Supplementary Table 3**), with the data showing that bacterial growth in the transgenic plants was faster than that in WT plants after 2 months of infection (**Figure 6A**). In this case, the OE-1, OE-6, and OE-8 lines had significantly higher titers of *Ca*Las compared with WT plants (**Figure 6A**). However, between two and 6 months after infection, *Ca*Las growth accelerated in WT plants compared with transgenic ones, such that the *Ca*Las titers in the latter, were no longer significantly different from those of WT plants at four to 6 months after inoculation (**Figure 6A**). After 6 months of infection, chlorosis or mottled yellow symptoms were first detected in the new leaves of transgenic plants while no visible symptoms appeared in the WT control (**Figure 6B**). Our data suggested that overexpression of *mSDE115* favored early colonization by *Ca*Las in citrus, which could promote the development of symptoms.

Effects of Overexpressing *mSDE115* on Systemic Acquired Resistance Response in Transgenic Plants

Plant SAR resistance plays important roles in citrus tolerance to HLB (Zou et al., 2021), with SA, MeSA, and JA being essential signals for plant SAR responses (Park et al., 2007; Zhu et al., 2014). To understand the effects of *mSDE115* overexpression on SAR response, we first determined changes in the levels of SA, MeSA, and JA for OE1, OE6, and OE8 transgenic plants which were more susceptible to *Ca*Las (**Figure 7A**). Compared with the WT control, SA and JA levels in all the transgenic lines were downregulated after overexpressing *mSDE115* while MeSA content was not affected by the overexpression. Furthermore, the expression of nine SAR-associated genes, including three *CsNPR3* genes (*CsNPR3-73* for Ciclev10017873m, *CsNPR3-15* for Ciclev10031115m, *CsNPR3-49* for Ciclev10031749m) and one *CsNPR4-08* (Ciclev10033908m) (Wang et al., 2016), and *CsPR1*, *CsPR2*, *CsPR5, CsWRKY45,* and *CsWRKY70* (Zou et al., 2021) in transgenic plants were investigated by qRT-PCR. The results showed that the expression levels of all the PR and WRKY genes were significantly lower in OE1, OE6 and OE8 transgenic lines compared with the control. *CsNPR3-15* and *CsNPR3-49* exhibited enhanced expression while the expression of *CsNPR3-73* and *CsNPR4-08* was reduced (**Figure 7B**). The response characteristics of citrus SAR modulated by *Ca*LasSDE115 was illustrated in **Figure 7C**.

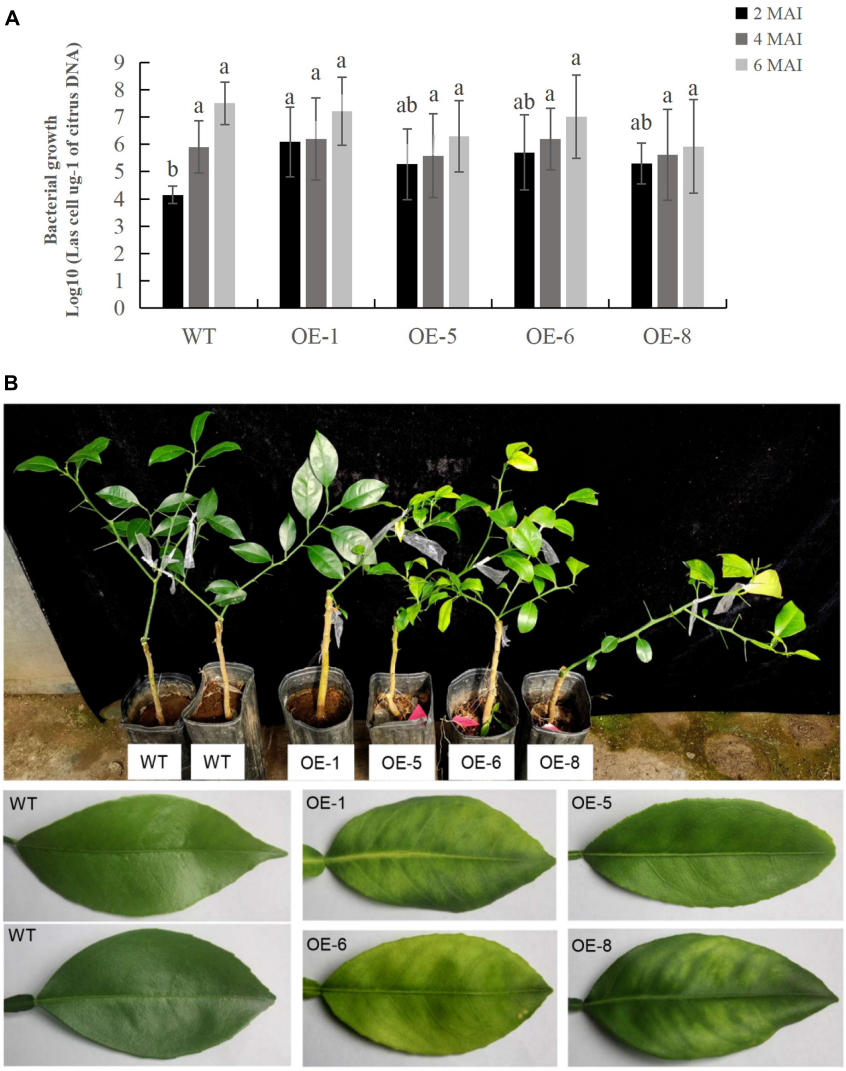

FIGURE 6 | Evaluation of Citrus Huanglongbing (HLB) resistance in transgenic plants grown in a greenhouse. **(A)** Quantitative analysis of *Ca*Las growth at 2, 4, and 6 months after infection (MAI). The bacterial populations (*Ca*Las cells μg^{-1} of citrus DNA) were determined using qPCR. Standard errors were calculated from three to five plants per line. Different letters on top of the bars indicates significant differences from the WT control ($p < 0.05$, Student's *t* test). **(B)** HLB symptoms in the transgenic plants and wild type (WT) controls after 6 MAI. WT, wild type; OE-#, transgenic plants.

DISCUSSION

Function prediction showed that *Ca*LasSDE115 was very close to that of IalB homologs from *Bartonella henselae*, *Rhizobium undicola,* and *Agrobacterium vitis*. *Bartonella* IalB (BaIalB) is a 19.9 kDa protein with a putative signal peptide (Deng et al., 2018) and similarly, *Ca*LasSDE115 is a 21.1 kDa protein with a signal peptide. In addition, BaIalB shares high homology with the Ail protein, a virulence marker of *Yersinia enterocolitica* that plays a major role in cell attachment and invasion (Deng et al., 2016). In this context, it has been shown that BaIalB is also a virulence factor for pathogen-erythrocyte invasion as the transformation of *E. coli* with *BaIalB* from *Bartonella bacilliformis* conferred the ability to invade erythrocytes while the deletion of this gene from both *B. birtlesii* and *B. tribocorum* reduced erythrocyte infection (Vayssier-Taussat et al., 2010; Deng et al., 2016). *Ca*Las and *Bartonella henselae* are also both considered to be intracellular parasitic bacteria. In terms of functions, the expression of *CaLasSDE115* was higher in young leaves of *Ca*Las-infected WT plants compared with mature ones (**Figure 4C**), with young leaves generally considered to be the site where most new infections occur (Martinelli et al., 2013). Our evaluation of resistance confirmed that the overexpression of *CaLasSDE115* in transgenic plants triggered *Ca*Las growth mainly during the initial months, hence suggesting that, in the same way as IalB, *Ca*LasSDE115 could contribute to early colonization of citrus by *Ca*Las.

Despite the above similarities between *Ca*LasSDE115 and IalB, it should be noted that the latter's location in bacteria

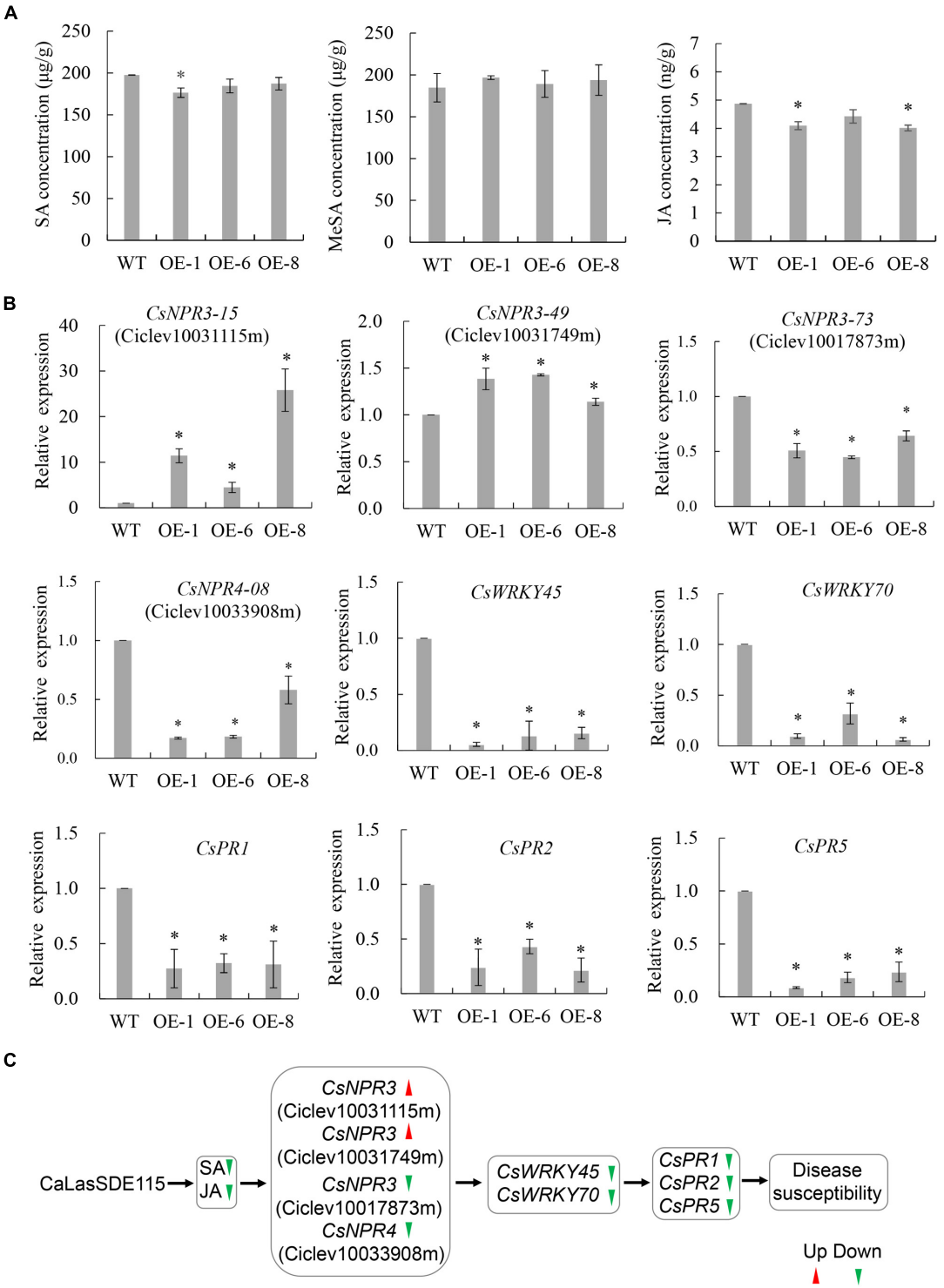

FIGURE 7 | SAR characteristics of transgenic plants overexpressing *mSDE115*. **(A)** Characteristics of SA, MeSA, and JA contents in transgenic plants compared to WT control. **(B)** Expression characteristics of SAR-associated genes in transgenic plants. Compared to WT control, relative expressions were determined using *GAPDH* gene (Mafra et al., 2012) as internal reference. **(C)** Illustration of the transcriptional regulation of SAR response modulated by *Ca*LasSDE115 effector in citrus. Red and green arrowheads indicate up-regulated and down-regulated, respectively. Values are expressed as means ± standard deviation of three independent tests. *on top of the bars indicates a significant difference ($p < 0.05$, *T*-test). WT, wild type; OE-#, transgenic plants.

cell membrane remains unclear. For example, IalB from *B. bacilliformis* is an inner membrane protein, but that from *B. henselae* is an outer membrane protein (Coleman and Minnick, 2001; Chenoweth et al., 2004; Vayssier-Taussat et al., 2010; Saenz et al., 2017). Our data showed that *Ca*LasSDE115 was secreted outside bacterial cells through a Sec-dependent secretion system. Prediction analysis of transmembrane domains revealed that the mature *Ca*LasSDE115 protein was not a membrane protein. All the data suggested that the mature *Ca*LasSDE115 protein could cross the bacterial cell membrane into the host cells to regulate host immune response. Subcellular localization analysis in tobacco implied that the *Ca*LasSDE115 mature protein functioned possibly in the nucleus and cytoplasm of the plants. However, it has yet to be determined whether *Ca*LasSDE115 adhered to extracellular surfaces of *Ca*Las cells by binding to some bacterial membrane proteins or whether it was secreted into host cells.

The expression of virulence factors at different stages of the infection process is determined by continuous changes within the host's environment (Chowdhury et al., 1996). *Ca*Las is a plant pathogen transmitted by the Asian citrus psyllid and during transmission, it differentially expresses genes which are critical for its survival and/or pathogenicity in either host. This was reported by Yan et al. (2013) who compared the expression levels of 381 *Ca*Las genes in plants and psyllids. In this case, the authors noted that 182 genes were up-regulated in plants when compared with psyllids while, at the same time, only 16 genes were up-regulated in the latter, with the majority of these 16 genes being predicted to be involved in cell motility (Yan et al., 2013). In this study, it was shown that the expression levels of *CaLasSDE115* were significantly higher in psyllids compared with those in plants. In the same way in which *Bartonella* species enter mammalian erythrocytes (Deng et al., 2018), *Ca*Las cells enter a psyllid's body by crossing the gut epithelium before subsequently moving to other internal organs and tissues (Carmo-Sousa et al., 2020). Thus, it is suggested that *CaLasSDE115* could also be involved in *Ca*Las's entry and intracellular movement in the Asian citrus psyllid.

Pathogen effectors have vital roles in maintaining the virulence of bacteria and symptoms of HLB. For instance, transient expression of *CaLas5315* in tobacco can induce callose deposition (Pitino et al., 2016), while overexpressing *CLIBASIA_03915* and *CLIBASIA_04250* SDEs in *Nicotiana benthamiana* caused phloem necrosis in the senescent leaves (Li et al., 2020). Since the higher expression level of *CaLasSDE115* in symptomatic leaves indicated that this effector could be contributing to the symptoms of HLB, the functions of *CaLasSDE115* in symptom development was determined via the overexpression of the gene in HLB-susceptible Wanjincheng oranges. In this case, the results showed that *CaLasSDE115* overexpression worsened the development of HLB symptoms in transgenic plants after *Ca*Las infection.

Our data indicated that *Ca*LasSDE115 was a virulence effector which participated in the regulation of the citrus SAR defense, with many reports even showing that *Ca*Las triggered citrus susceptibility by suppressing the host's SAR response (Martinelli et al., 2013; Zou et al., 2019). *Ca*Las resides in the sieve elements and spreads systemically within plants through the phloem transport system (Folimonova and Achor, 2010). At the same time, SA, JA and MeSA also transfer SAR signals through this system to regulate the plant's defense (Van Bel and Gaupels, 2004; Park et al., 2007). As a result, strong interactions occur between these signals and *Ca*Las, leading to the possibility that *Ca*Las could regulate SA, JA and MeSA-mediated defense response through its effectors in citrus. For example, Li et al. (2017) indicated that *Ca*Las suppressed plant defenses by expressing a SahA to degrade the host's SA. Similarly, Clark et al. (2018) showed that the *Ca*Las effector SDE1 targeted citrus PLCPs proteases that were involved in SA-induced defense. It was shown that phytopathogen secreted effectors to directly bind NPR1, the master regulator of SA signaling, to inhibit the expression of downstream genes for dampening plant immunity (Chen et al., 2017; Han and Kahmann, 2019; Li et al., 2019). In this study, the overexpression of *mSDE115* reduced SA and JA levels but also significantly decreased the expression of *CsPR1*, *CsPR2*, *CsPR5,* Cs*WRKY45,* and Cs*WRKY70* in transgenic plants. PR2 is a SAR marker and the expression levels of *CsPR2*, *CsPR5*, *WRKY45,* and *WRKY70* have been correlated with tolerance to HLB in citrus (Zou et al., 2019). These data indicated that mSDE115 could modulate some regulators of SA signaling to negatively regulate plant defense (**Figure 7C**). In addition, *PR1*, *PR2*, *PR5, WRKY45,* and *WRKY70* have also been reported as being downstream of NPR-mediated signaling (Martinelli et al., 2013; Dutt et al., 2015; Ali et al., 2018). NPR4 is a required part of the basal defense against pathogens and, hence could be involved in the interactions between the pathogens and the SA- or JA-dependent signaling pathways (Liu et al., 2005). Furthermore, at low or basal concentration of SA, NPR3 and NPR4 serve as negative regulators to suppress defense genes, but once the SA concentration is elevated, NPR1-dependent gene expression is activated to defeat pathogen attack (Ding et al., 2018; Ding and Ding, 2020). Meanwhile, the suppression of NPR3 and NPR4 on defense genes is derepressed by increased SA, which further enhanced NPR1-dependent gene expression (Ding et al., 2018; Ding and Ding, 2020). *CsNPR3* and *CsNPR4* genes displayed different expression levels (two had increased expression and the other two had decreased expression) in the transgenic plants, thereby suggesting that they played different functions in *Ca*LasSDE115-mediated defense responses. Our previous study confirmed that the overexpression of the *NPR1*-like homology (named as *CsNPR3-49* here) from HLB-tolerant "Jackson" grapefruit (*Citrus paradisi Macf.*) enhanced resistance of Wanjincheng oranges to HLB (Peng et al., 2021). Interestingly, the current data showed that the expression of this gene was also increased by *mSDE115* overexpression. Likewise, overexpressing *AtNPR1* from *Arabidopsis* conferred enhanced resistance to HLB in citrus (Dutt et al., 2015). Thus, in future studies, it would be meaningful to acquire a deeper understanding of the functions of these *CsNPR3* and *CsNPR4* genes in response to *Ca*Las infection.

Our study indicated that the *Ca*LasSDE115 effector was an invasion-associated locus B of "*Candidatus* liberibacter asiaticus" and it participated in the early bacterial colonization of citrus. It also regulated citrus resistance to HLB through modulating

the transcriptional regulation of SAR-related genes (**Figure 7C**). However, the potential molecular mechanism of this effector during interactions between the pathogen and the host remains to be verified, especially to determine whether the *Ca*LasSDE115 effector targeted specific host proteins or genes and this could form the basis of future studies.

DATA AVAILABILITY STATEMENT

The original contributions presented in the study are included in the article/**Supplementary Material**, further inquiries can be directed to the corresponding author.

AUTHOR CONTRIBUTIONS

MD and XZ designedthe experiments, analyzed the data, wrote, and revised the manuscript. MD, SW, RQ, LD, LZ, YH, and SC performed the experiments. XZ supervised the research. All authors read and approved the final version of the manuscript.

FUNDING

This work was supported by the National Natural Science Foundation of China (31972393), the Key-Area Research and Development Program of Guangdong Province (2018B020202009), Science and Technology Major Project of Guangxi (Gui Ke AA18118046-6) and the Earmarked Fund for China Agriculture Research System (CARS-27).

ACKNOWLEDGMENTS

We thank Weimin Li (Biotechnology Research Institute, Chinese Academy of Agricultural Sciences, Beijing, China) for providing pET-mphoA and pET-phoA plasmids and Shuo Duan (Gannan Normal University, China) for providing ACPs.

SUPPLEMENTARY MATERIAL

The Supplementary Material for this article can be found online at: https://www.frontiersin.org/articles/10.3389/fmicb.2021.797841/full#supplementary-material

REFERENCES

Ali, S., Ganai, B. A., Kamili, A. N., Bhat, A. A., Mir, Z. A., Bhat, J. A., et al. (2018). Pathogenesis-related proteins and peptides as promising tools for engineering plants with multiple stress tolerance. *Microbiol. Res.* 212-213, 29–37. doi: 10.1016/j.micres.2018.04.008

Bassanezi, R. B., Montesino, L. H., and Stuchi, E. S. (2009). Effects of huanglongbing on fruit quality of sweet orange cultivars in Brazil. *Eur. J. Plant Pathol.* 125, 565–572. doi: 10.3389/fpls.2021.641457

Boller, T., and Felix, G. (2009). A renaissance of elicitors: perception of microbe-associated molecular patterns and danger signals by pattern-recognition receptors. *Annu. Rev Plant Biol.* 60, 379–406. doi: 10.1146/annurev.arplant

Bové, J. M. (2006). Huanglongbing: a destructive, newly emerging, century-old disease of citrus. *J. Plant Pathol.* 88, 7–37. doi: 10.1371/journal.pone.0111032

Carmo-Sousa, M., Cortés, M. T. B., and Lopes, J. R. S. (2020). Understanding psyllid transmission of *candidatus* liberibacter as a basis for managing huanglongbing. *Trop. Plant Pathol.* 45, 572–585. doi: 10.1007/s00248-016-0733-9

Chen, H., Chen, J., Li, M., Chang, M., Xu, K., Shang, Z., et al. (2017). A bacterial type III effector targets the master regulator of salicylic acid signaling, NPR1, to subvert plant immunity. *Cell Host Microbe* 22, 777–788. doi: 10.1016/j.chom

Chenoweth, M. R., Greene, C. E., Krause, D. C., and Gherardini, F. C. (2004). Predominant outer membrane antigens of *bartonella henselae*. *Infect. Immuni.* 72, 3097–3105. doi: 10.1128/IAI.72.6.3097-3105

Chowdhury, R., Sahu, G. K., and Das, J. (1996). Stress response in pathogenic bacteria. *J. Biosci.* 21, 149–160. doi: 10.1007/BF02703105

Cifuentes-Arenas, J. C., Beattie, G. A. C., and Lopes, S. A. (2019). *Murraya paniculata* and *swinglea glutinosa* as short-term transient hosts of ' *candidatus* liberibacter asiaticus' and implications for the spread of huanglongbing. *Phytopathology* 109, 2064–2073. doi: 10.1094/PHYTO-06-19-0216-R

Clark, K., Franco, J. Y., Schwizer, S., Pang, Z. Q., Hawara, E., Liebrand, T. W. H., et al. (2018). An effector from the huanglongbing-associated pathogen targets citrus proteases. *Nat. Commun.* 9:1718. doi: 10.1038/s41467-018-04140-9

Coleman, S. A., and Minnick, M. F. (2001). Establishing a direct role for the *bartonella bacilliformis* invasion-associated locus b (ialb) protein in human erythrocyte parasitism. *Infect. Immun.* 69, 4373–4381. doi: 10.1128/IAI.69.7.4373-4381.2001

Deng, H., Pang, Q., Xia, H., Le Rhun, D., Naour, E. L., Yang, C., et al. (2016). Identification and functional analysis of invasion associated locus b (ialb) in bartonella species. *Microb. Pathog.* 98, 171–177. doi: 10.1016/j.micpath.2016.05.007

Deng, H., Pang, Q., Zhao, B., and Vayssier-Taussat, M. (2018). Molecular mechanisms of *Bartonella* and mammalian erythrocyte interactions: a review. *Front. Cell. Infect. Microbiol.* 8:431. doi: 10.3389/fcimb.2018.00431

Ding, P., and Ding, Y. (2020). Stories of salicylic acid: a plant defense hormone. *Trends Plant Sci.* 25, 549–565. doi: 10.1016/j.tplants.2020.01.004

Ding, Y., Sun, T., Ao, K., Peng, Y., Zhang, Y., Li, X., et al. (2018). Opposite roles of salicylic acid receptors NPR1 and NPR3/NPR4 in transcriptional regulation of plant immunity. *Cell* 173, 1–14. doi: 10.1016/j.cell.2018.03.044

Du, P., Zhang, C., Zou, X., Zhu, Z., Yan, H., Wuriyanghan, H., et al. (2021). '*Candidatus* Liberibacter asiaticus' secretes nonclassically cecreted proteins that suppress host hypersensitive cell death and induce expression of plant pathogenesis-related proteins. *Appl. Environ. Microbiol.* 87:e00019-21. doi: 10.1128/AEM.00019-21

Duan, Y., Zhou, L., Hall, D. G., Li, W., Doddapaneni, H., Lin, H., et al. (2009). Complete genome sequence of citrus huanglongbing bacterium, '*candidatus* liberibacter asiaticus' obtained through metagenomics. *Mol. Plant Microbe Interact.* 22, 1011–1020. doi: 10.1094/MPMI-22-8-1011

Dutt, M., Barthe, G., Irey, M., and Grosser, J. (2015). Transgenic citrus expressing an *Arabidopsis NPR1* gene exhibit enhanced resistance against huanglongbing (HLB; Citrus Greening). *PLoS One* 10:e0137134. doi: 10.1371/journal.pone.0137134

Folimonova, S. Y., and Achor, D. S. (2010). Early events of citrus greening (Huanglongbing) disease development at the ultrastructural level. *Phytopathology* 100, 949–958. doi: 10.1094/PHYTO-100-9-0949

Gottwald, T. R. (2010). Current epidemiological understanding of citrus huanglongbing. *Annu. Rev. Phytopathol.* 48, 119–139. doi: 10.1146/annurev-phyto-073009-114418

Graham, J. H., Johnson, E. G., Gottwald, T. R., and Irey, M. S. (2013). Pre-symptomatic fibrous root decline in citrus trees caused by huanglongbing and potential interaction with *phytophthora* spp. *Plant Dis.* 97, 1195–1199. doi: 10.1094/PDIS-01-13-0024-RE

Haitao, C., Kenichi, T., and Jane, E. P. (2015). Effector-triggered immunity: from pathogen perception to robust defense. *Annu. Rev. Plant Biol.* 66, 487–511. doi: 10.1146/annurev-arplant-050213-040012

Han, X., and Kahmann, R. (2019). Manipulation of phytohormone pathways by effectors of filamentous plant pathogens. *Front. Plant Sci.* 10:822. doi: 10.3389/fpls.2019.00822

Jagoueix, S., Bove, J., and Garnier, M. (1994). The phloem-limited bacterium of greening disease of citrus is a member of the α subdivision of the *proteobacteria*. *Int. J. Syst. Bacteriol.* 44, 379–386. doi: 10.1099/00207713-44-3-379

Jain, M., Fleites, L. A., and Gabriel, D. W. (2015). Prophage-encoded peroxidase in '*candidatus* liberibacter asiaticus' is a secreted effector that suppresses plant defenses. *Mol. Plant Microbe Interact.* 28, 1330–1337. doi: 10.1094/MPMI-07-15-0145-R

Jain, M., Munoz-Bodnar, A., and Gabriel, D. W. (2019). '*Candidatus* liberibacter asiaticus' peroxiredoxin (LasBCP) suppresses oxylipin-mediated defense signaling in citrus. *J. Plant Physiol.* 236, 61–65. doi: 10.1016/j.jplph.2019.03.001

Jain, M., Munoz-Bodnar, A., Zhang, S., and Gabriel, D. W. (2018). A secreted '*candidatus* liberibacter asiaticus' peroxiredoxin simultaneously suppresses both localized and systemic innate immune responses in planta. *Mol. Plant Microbe Interact.* 31, 1312–1322. doi: 10.1094/MPMI-03-18-0068-R

Jones, J. D. G., and Dangl, J. L. (2006). The plant immune system. *Nature* 444, 323–329. doi: 10.1038/nature05286

Kumar, S., Stecher, G., and Tamura, K. (2016). Mega7: molecular evolutionary genetics analysis version 7.0 for bigger datasets. *Mol. Biol. Evol.* 33, 1870–1874. doi: 10.1093/molbev/msw054

Li, H., Ying, X., Shang, L., Redfern, B., Kypraios, N., Xie, X., et al. (2020). Heterologous expression of clibasia_03915/clibasia_04250 by *tobacco mosaic virus* resulted in phloem necrosis in the senescent leaves of *nicotiana benthamiana*. *Int. J. Mol. Sci.* 21:1414. doi: 10.3390/ijms21041414

Li, J., Pang, Z., Trivedi, P., Zhou, X., Ying, X., Jia, H., et al. (2017). '*Candidatus* liberibacter asiaticus' encodes a functional salicylic acid (SA) hydroxylase that degrades SA to suppress plant defenses. *Mol. Plant Microbe Interact.* 30, 620–630. doi: 10.1094/MPMI-12-16-0257-R

Li, Q., Chen, Y., Wang, J., Zou, F., Jia, Y. L., Shen, D. Y., et al. (2019). A *phytophthora capsici* virulence effector associates with NPR1 and suppresses plant immune responses. *Phytopathol. Res.* 1:6. doi: 10.1186/s42483-019-0013-y

Lin, H., Pietersen, G., Han, C., Read, D. A., Lou, B., Gupta, G., et al. (2015). Complete genome sequence of '*candidatus* liberibacter africanus, ' a bacterium associated with citrus huanglongbing. *Genome Announc.* 3:e00733-15. doi: 10.1128/genomeA.00733-15

Liu, G., Holub, E. B., Alonso, J. M., Ecker, J. R., and Fobert, P. R. (2005). An *Arabidopsis NPR1-like* gene. *NPR4*, is required for disease resistance. *Plant J.* 41, 304–318. doi: 10.1111/j.1365-313X.2004.02296.x

Liu, X., Fan, Y., Zhang, C., Dai, M., Wang, X., and Li, W. (2019). Nuclear import of a secreted '*candidatus* liberibacter asiaticus' protein is temperature dependent and contributes to pathogenicity in *nicotiana benthamiana*. *Front. Microbiol.* 10:1684. doi: 10.3389/fmicb.2019.01684

Livak, K. J., and Schmittgen, T. D. (2001). Analysis of relative gene expression data using real-time quantitative pcr and the $2^{-\Delta\ \Delta\ CT}$ method. *Methods* 25, 402–408. doi: 10.1006/meth.2001.1262

Mafra, V., Kubo, K. S., Alves-Ferreira, M., Ribeiro-Alves, M., Stuart, R. M., Boava, L. P., et al. (2012). Reference genes for accurate transcript normalization in citrus genotypes under different experimental conditions. *PLoS One* 7:e31263. doi: 10.1371/journal.pone.0031263

Martin, K., Kopperud, K., Chakrabarty, R., Banerjee, R., Brooks, R., and Goodin, M. M. (2009). Transient expression in Nicotiana benthamiana fluorescent marker lines provides enhanced definition of protein localization, movement and interactions in planta. *Plant J.* 59, 150–162. doi: 10.1111/j.1365-313X.2009.03850.x

Martinelli, F., Reagan, R. L., Uratsu, S. L., Phu, M. L., Albrecht, U., Zhao, W., et al. (2013). Gene regulatory networks elucidating huanglongbing disease mechanisms. *PLoS One* 8:e74256. doi: 10.1371/journal.pone.0074256

Nguyen, Q. M., Iswanto, A., Son, G. H., and Sang, H. K. (2021). Recent advances in effector-triggered immunity in plants: new pieces in the puzzle create a different paradigm. *Int. J. Mol. Sci.* 22:4709. doi: 10.3390/ijms22094709

Pagliaccia, D., Shi, J. X., Pang, Z. Q., Hawara, E., Clark, K., Thapa, S. P., et al. (2017). A pathogen secreted protein as a detection marker for citrus huanglongbing. *Front. Microbiol.* 8:2041. doi: 10.3389/fmicb.2017.02041

Pang, Z., Zhang, L., Coaker, G. L., Ma, W., and Wang, N. (2020). Citrus CsACD2 is a target of *candidatus* liberibacter asiaticus in huanglongbing disease. *Plant Physiol.* 184, 792–805. doi: 10.1104/pp.20.00348

Park, S. W., Kaimoyo, E., Kumar, D., Mosher, S., and Klessig, D. F. (2007). Methyl salicylate is a critical mobile signal for plant systemic acquired resistance. *Science* 318, 113–116. doi: 10.1126/science.1147113

Peng, A., Xu, L., He, Y., Lei, T., Yao, L., Chen, S., et al. (2015). Efficient production of marker-free transgenic 'Tarocco' blood orange (*Citrus sinensis Osbeck*) with enhanced resistance to citrus canker using a Cre/*loxP* site-recombination system. *Plant Cell Tissue Organ Cult.* 123, 1–13. doi: 10.1007/s11240-015-0799-y

Peng, A., Zou, X., He, Y., Chen, S., Liu, X., Zhang, J., et al. (2021). Overexpressing a *NPR1-like* gene from citrus paradisi enhanced huanglongbing resistance in *C. sinensis*. *Plant Cell Rep.* 40, 529–541. doi: 10.1007/s00299-020-02648-3

Pitino, M., Armstrong, C. M., Cano, L. M., and Duan, Y. (2016). Transient expression of *candidatus* liberibacter asiaticus effector induces cell death in *Nicotiana benthamiana*. *Front. Plant Sci.* 7:982. doi: 10.3389/fpls.2016.00982

Prasad, S., Xu, J., Zhang, Y., and Wang, N. (2016). SDE-translocon dependent extracytoplasmic proteins of *candidatus* liberibacter asiaticus. *Front. Microbiol.* 7:1989. doi: 10.3389/fmicb.2016.01989

Saenz, H., Engel, P., Stoeckli, M., Lanz, C., Raddatz, G., Vayssier-Taussat, M., et al. (2017). Genomic analysis of bartonella identifies type IV secretion systems as host adaptability factors. *Nat. Genet.* 39, 1469–1476. doi: 10.1038/ng.2007.38

Saskia, A. H., Kenro, O. S., Ammar, E. D., Shigeyuki, K., Heather, N., and Kingdom, S. N. (2008). Phytoplasmas: bacteria that manipulate plants and insects. *Mol. Plant Pathol.* 9, 403–423. doi: 10.1111/j.1364-3703.2008.00472.x

Segonzac, C., and Zipfel, C. (2011). Activation of plant pattern-recognition receptors by bacteria. *Curr. Opin. Microbiol.* 14, 54–61. doi: 10.1016/j.mib.2010.12.005

Tamar, C. S., and Damon, H. (2018). The way is the goal: how seca transports proteins across the cytoplasmic membrane in bacteria. *Fems Microbiol. Lett.* 365:fny093. doi: 10.1093/femsle/fny093

Teixeira, D. C., Saillard, C., Eveillard, S., Danet, J. L., Ayres, A. J., and Bové, J. M. (2005). A new liberibacter species, *candidatus* liberibacter americanus sp. nov. is associated with citrus huanglongbing (greening disease) in São Paulo State, Brazil. *Int. J. Syst. Evol. Microbiol.* 55, 1857–1862. doi: 10.1099/ijs.0.63677-0

Toruno, T. Y., Stergiopoulos, I., and Coaker, G. (2016). Plant-pathogen effectors: cellular probes interfering with plant defenses in spatial and temporal manners. *Annu. Rev. Phytopathol.* 54, 419–441. doi: 10.1146/annurev-phyto-080615-100204

Van Bel, A. J., and Gaupels, F. (2004). Pathogen-induced resistance and alarm signals in the phloem. *Mol. Plant Pathol.* 5, 495–504. doi: 10.1111/j.1364-3703.2004.00243.x

Vayssier-Taussat, M., Rhun, D. L., Deng, H. K., Biville, F., Cescau, S., Danchin, A., et al. (2010). The trw type iv secretion system of *bartonella* mediates host-specific adhesion to erythrocytes. *PLoS Pathog.* 6:e1000946. doi: 10.1371/journal.ppat.1000946

Wang, N., Pierson, E. A., Setubal, J. C., Xu, J., Levy, J. G., Zhang, Y., et al. (2017). The *candidatus* liberibacter-host interface: insights into pathogenesis mechanisms and disease control. *Annu. Rev. Phytopathol.* 55, 451–482. doi: 10.1146/annurev-phyto-080516-035513

Wang, Y., Zhou, L., Yu, X., Stover, E., Luo, F., and Duan, Y. (2016). Transcriptome profiling of huanglongbing (HLB) tolerant and susceptible citrus plants reveals the role of basal resistance in HLB tolerance. *Front. Plant Sci.* 7:933. doi: 10.3389/fpls.2016.00933

Wulff, N. A., Zhang, S., Setubal, J. C., Almeida, N. F., Martins, E. C., Harakava, R., et al. (2014). The complete genome sequence of '*candidatus* liberibacter americanus', associated with citrus huanglongbing. *Mol. Plant Microbe Interact.* 27, 163–176. doi: 10.1094/MPMI-09-13-0292-R

Yan, Q., Sreedharan, A., Wei, S., Wang, J., Pelz-Stelinski, K., Folimonova, S., et al. (2013). Global gene expression changes in *candidatus* liberibacter asiaticus during the transmission in distinct hosts between plant and insect. *Mol. Plant Pathol.* 14, 391–404. doi: 10.1111/mpp.12015

Ying, X., Wan, M., Hu, L., Zhang, J., Li, H., and Lv, D. (2019). Identification of the virulence factors of *candidatus* liberibacter asiaticus via heterologous expression in *nicotiana benthamiana* using *tobacco mosaic virus*. *Int. J. Mol. Sci.* 20:5575. doi: 10.3390/ijms20225575

Yuan, M. H., Ngou, B. P. M., Ding, P., and Xin, X. F. (2021). PTI-ETI crosstalk: an integrative view of plant immunity. *Curr. Opin. Plant Biol.* 62:102030. doi: 10.1016/j.pbi.2021.102030

Zhu, F., Xi, D. H., Yuan, S., Xu, F., Zhang, D. W., and Lin, H. H. (2014). Salicylic acid and jasmonic acid are essential for systemic resistance against tobacco mosaic virus in *nicotiana benthamiana*. *Mol. Plant Microbe Interact.* 27, 567–577. doi: 10.1094/MPMI-11-13-0349-R

Zou, X., Bai, X., Wen, Q., Xie, Z., Wu, L., Peng, A., et al. (2019). Comparative analysis of tolerant and susceptible citrus reveals the role of methyl salicylate signaling in the response to huanglongbing. *J. Plant Growth Regul.* 38, 1516–1528. doi: 10.1007/s00344-019-09953-6

Zou, X., Jiang, X., Xu, L., Lei, T., Peng, A., He, Y., et al. (2017). Transgenic citrus expressing synthesized *cecropin* B genes in the phloem exhibits decreased susceptibility to huanglongbing. *Plant Mol. Biol.* 93, 341–353. doi: 10.1007/s11103-016-0565-5

Zou, X., Zhao, K., Liu, Y., Du, M., Zheng, L., Wang, S., et al. (2021). Overexpression of salicylic acid carboxyl methyltransferase (*CsSAMT1*) enhances tolerance to huanglongbing disease in wanjincheng orange (*Citrus sinensis* (L.) Osbeck). *Int. J. Mol. Sci.* 22:2803. doi: 10.3390/ijms22062803

Conflict of Interest: The authors declare that the research was conducted in the absence of any commercial or financial relationships that could be construed as a potential conflict of interest.

Publisher's Note: All claims expressed in this article are solely those of the authors and do not necessarily represent those of their affiliated organizations, or those of the publisher, the editors and the reviewers. Any product that may be evaluated in this article, or claim that may be made by its manufacturer, is not guaranteed or endorsed by the publisher.

frontiers in Microbiology

ORIGINAL RESEARCH
published: 03 March 2022
doi: 10.3389/fmicb.2022.799819

Integrated Analysis of the miRNAome and Transcriptome Reveals miRNA–mRNA Regulatory Networks in *Catharanthus roseus* Through *Cuscuta campestris*-Mediated Infection With "*Candidatus* Liberibacter asiaticus"

Chunhua Zeng‡, Haodi Wu†‡, Mengji Cao, Changyong Zhou, Xuefeng Wang and Shimin Fu**

National Citrus Engineering Research Center, Citrus Research Institute, Southwest University/Chinese Academy of Agricultural Sciences, Chongqing, China

Citrus Huanglongbing (HLB) is the most devastating disease of citrus caused by the Gram-negative phloem-limited bacterium "*Candidatus* Liberibacter asiaticus" (CLas). It can be transmitted by the Asian citrus psyllid "*Diaphorina citri*," by grafting, and by the holoparasitic dodder. In this study, the non-natural host periwinkle (*Catharanthus roseus*) was infected via dodder (*Cuscuta campestris*) from CLas-infected citrus plants, and the asymptomatic leaves (AS) were subjected to transcriptomic and small-RNA profiling. The results were analyzed together with a transcriptome dataset from the NCBI repository that included leaves for which symptoms had just occurred (S) and yellowing leaves (Y). There were 3,675 differentially expressed genes (DEGs) identified in AS, and 6,390 more DEGs in S and further 2109 DEGs in Y. These DEGs were commonly enriched in photosystem, chloroplast, membrane, oxidation-reduction process, metal/zinc ion binding on GO. A total of 14,974 DEGs and 336 DE miRNAs (30 conserved and 301 novel) were identified. Through weighted gene co-expression network and nested network analyses, two critical nested miRNA–mRNA regulatory networks were identified with four conserved miRNAs. The primary miR164-NAC1 network is potentially involved in plant defense responses against CLas from the early infection stage to symptom development. The secondary network revealed the regulation of secondary metabolism and nutrient homeostasis through miR828-MYB94/miR1134-HSF4 and miR827-ATG8 regulatory networks, respectively. The findings discovered new potential mechanisms in periwinkle–CLas interactions, and its confirmation can be done in citrus–CLas system later on. The advantages of periwinkle plants in facilitating the quick establishment and greater multiplication of CLas, and shortening latency for disease symptom development make it a great surrogate for further studies, which could expedite our understanding of CLas pathogenesis.

Keywords: huanglongbing, periwinkle, miRNA–mRNA regulatory network, "*Candidatus* Liberibacter asiaticus" (CLas), defense response

OPEN ACCESS

Edited by:
Marco Scortichini, Council for Agricultural and Economics Research (CREA), Italy

Reviewed by:
Jun-Min Li, Ningbo University, China
Susheel Kumar Sharma, ICAR Research Complex for NEH Region, India

****Correspondence:***
Xuefeng Wang
wangxuefeng@cric.cn
Shimin Fu
minniefu2017@cric.cn

†Present address:
Haodi Wu, Fruit Specialty Promotion Station of Sanmen, Taizhou, China

‡These authors share first authorship

Specialty section:
This article was submitted to Microbe and Virus Interactions with Plants, a section of the journal Frontiers in Microbiology

Received: *22 October 2021*
Accepted: *27 January 2022*
Published: *03 March 2022*

Citation:
Zeng C, Wu H, Cao M, Zhou C, Wang X and Fu S (2022) Integrated Analysis of the miRNAome and Transcriptome Reveals miRNA–mRNA Regulatory Networks in Catharanthus roseus Through Cuscuta campestris-Mediated Infection With "Candidatus Liberibacter asiaticus". Front. Microbiol. 13:799819. doi: 10.3389/fmicb.2022.799819

INTRODUCTION

Citrus Huanglongbing (HLB) is one of the most destructive globally distributed citrus diseases and is responsible for tremendous economic losses to citrus industries worldwide (Wang, 2019). HLB is associated with three species of phloem-limited Gram-negative α-Proteobacteria, namely *Candidatus* Liberibacter asiaticus (CLas), *Candidatus* L. americanus (CLam), and *Candidatus* L. africanus (CLaf) (Bové, 2006). CLas is the most widely distributed and is vectored by the Asian citrus psyllid, *Diaphorina citri*. HLB affects almost all commercial citrus and citrus relatives within the family Rutaceae, including the ornamental jasmine (*Murraya paniculata*) (Zhou et al., 2007). Disease symptoms include blotchy mottle, yellow shoots, zinc deficiency, stunting, and twig dieback of citrus plants, as well as the dramatic decrease of fibrous root mass (Johnson et al., 2014; Wu et al., 2018).

Dodder is a holoparasitic plant with a simplified morphology consisting of a stem and haustorium (Sun et al., 2018). Its importance was emphasized with its application as an experimental tool to widen the host range of viruses (Hosford, Jr., 1967) and phytoplasmas (Kamińska and Korbin, 1999) so that they could be studied in a more amenable host. In addition to natural transmission by *D. citri*, CLas also can be transmitted by graft inoculation within the same host genus and via at least three species of dodder (*Cuscuta campestris, Cuscuta pentagona,* and *Cuscuta indecora*) from citrus to non-natural host plants, including periwinkle (*Catharanthus roseus*) (Garnier and Bové, 1983; Hartung et al., 2010), tomato (*Solanum lycopersicum*) (Duan et al., 2008), and tobacco (*Nicotiana xanthi* and *Nicotiana benthamiana*) (Francischini et al., 2007; Pitino et al., 2018). All three non-natural host plants develop HLB-like symptoms, particularly periwinkle, in which CLas colonizes at a higher concentration than in the other two. Therefore, periwinkle has been used as a surrogate for studying phylogenetic and taxonomic characteristics (Teixeira et al., 2008), distribution patterns (Ya et al., 2018), new detection method evaluation (Ding et al., 2017; Gottwald et al., 2020), genomic DNA enrichment and pathogenic effector screening of CLas (Zhang et al., 2011b; Jain et al., 2015), and therapeutic compound/molecule screening for HLB control (Zhang et al., 2010; Zhang et al., 2011a).

Although CLas has been studied for a century, no curable way is available so far. CLas has not been cultured *in vitro*, therefore Koch's postulates have not been completed and little is known about its pathogenesis through traditional molecular and genetic analyses (Wang et al., 2017). With the application of high-throughput sequencing (HTS) approaches, a large number of transcriptomic studies and a few small-RNA studies have been conducted on different citrus varieties in response to CLas. However, there has been only one transcriptomic profiling study where periwinkle was infected by CLas (Liu et al., 2019), and no combined transcriptomic and small-RNA studies have been reported. Therefore, we simultaneously analyzed the transcriptome and miRNAome of CLas-affected periwinkle in this study. The characterized miRNA-mediated networks could provide valuable information for better understanding the molecular regulatory mechanism of periwinkle in response to CLas infection.

MATERIALS AND METHODS

Plant Materials and Treatments

Candidatus Liberibacter asiaticus Inoculation on Periwinkle Through Dodder Bridge Transmission

The CLas strain was originally collected from a virus-free HLB-infected "Guanximiyou" pomelo plant from Ganzhou, Jiangxi Province, China. The CLas-infected budwoods were grafted onto two-year-old sweet orange seedlings (*Citrus sinensis*), and its presence was verified by PCR with the primer pair OI1/OI2c (Jagoueix et al., 1996).

Dodder (*C. campestris*) was placed on two-year-old healthy periwinkle plants (*C. roseus*) after germination from the seeds to obtain more tendrils, and then some of the tendrils were transferred to another healthy periwinkle. After approximately 1 week, the dodder successfully formed haustoria and parasitized the periwinkle, and its tendrils were manually connected to CLas-infected citrus plants (Li et al., 2021). One week after connection, the dodder bridge was completely established (**Figure 1A**). Healthy periwinkle plants (H2) were also connected to healthy citrus plants through healthy dodder (**Figure 1B**), and healthy periwinkle plants (H1) not parasitized with dodder (**Figure 1C**) were set as controls. As dodder is a stressor for host plants and is capable of mediating the trafficking of mobile mRNA, small-RNAs, and proteins between hosts and parasitic plants, it likely plays important roles in coordinating plant growth, development, and adaptation to stressors (Liu et al., 2020). All plants were maintained in the greenhouse at the Citrus Research Institute in Chongqing, China. Temperatures were maintained between 25 and 30°C, and supplemental lighting was provided. The potting mix contained turf soil, sand, and rice husks (1:1:1). Chemical fertilizers with a macronutrient content of 12:12:12 (NPK) were used twice per month, and rapeseed dregs were added to supply microelements.

Candidatus Liberibacter asiaticus Detection and RNA Collection

The presence of CLas on dodder (about 40 days of dodder bridge assembly) and periwinkles (approximately 3 months of dodder bridge assembly) was verified by PCR with the primer pair OI1/OI2c (Jagoueix et al., 1996) (**Supplementary Figure 1**). Three newly flushed, fully expanded, and asymptomatic periwinkle leaves (AS) from infected plants (n = 3, **Figure 1A**), non-infected plants parasitized with dodder (n = 3, **Figure 1B**), and non-infected plants not parasitized with dodder (n = 3, **Figure 1C**) were sampled. Total RNA was extracted with TRIzol reagent (Invitrogen, United States) according to standard procedure, and residual DNA was removed with DNAseI (Takara, Shiga, Japan). The quantity and quality of the total RNA were determined with a NanoDrop ND-1000 and Agilent 2100 Bioanalyzer (Thermo Fisher Scientific, MA, United States), respectively. The nine RNA extracts, which included three biological replicates for each treatment, were sent to BGI

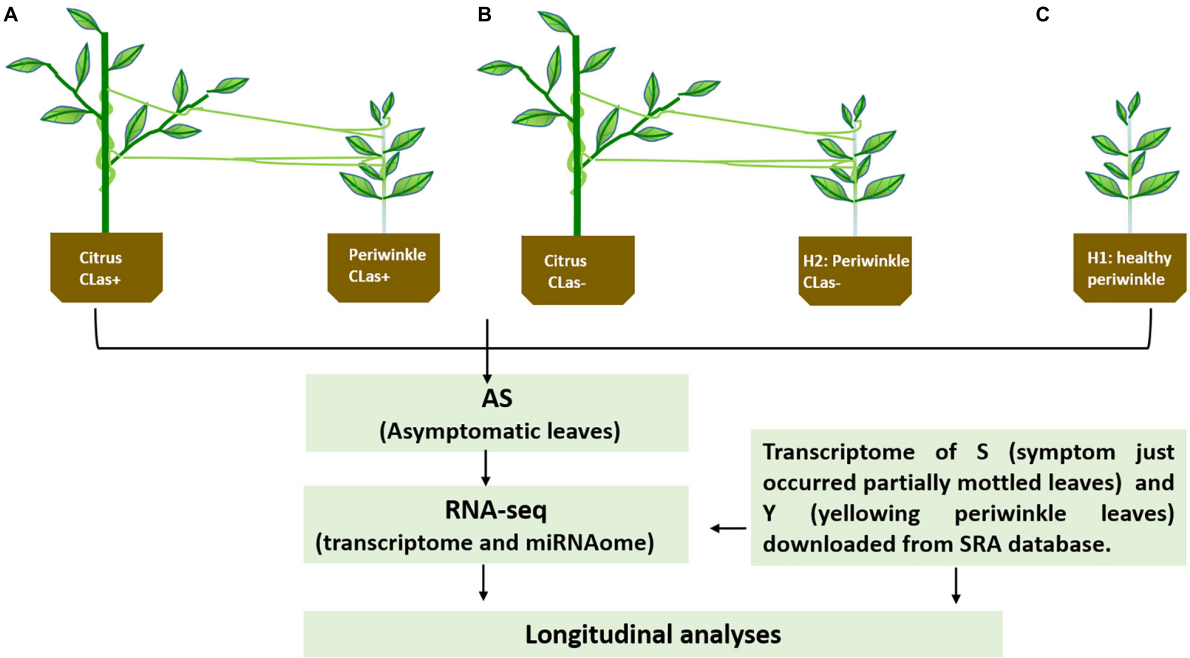

FIGURE 1 | (A,B) Schematics for the experimental setup and downstream analyses. CLas+ and CLas- represent *Candidatus Liberibacter* asiaticus positive and negative, respectively, by PCR test; H1, healthy periwinkle not parasitic with healthy dodder as control; H2, healthy periwinkle parasitic with healthy dodder as control.

(Shenzhen, China) for both transcriptome and small-RNA library construction and sequencing.

RNA Library Construction and Sequencing

Five micrograms of total RNA were used for transcriptome library preparation with a TruSeq RNA sample preparation kit (Illumina, San Diego, CA, United States) following the manufacturer's protocol. The small-RNA libraries were constructed with a TruSeq Small-RNA Library Prep Kit according to the manufacturer's instructions (Illumina, San Diego, CA, United States). The obtained cDNA libraries were directly sequenced on a BGISEQ-500 platform (BGI-Shenzhen, China) with paired-end 150 bp and single-end 50 bp reads for mRNA and small-RNA, respectively.

Bioinformatics Analyses

For transcriptomic profiling, the raw reads were adapter-trimmed and quality-filtered with Trimmomatic (Bolger et al., 2014). The clean reads were mapped to the reference genome of *C. roseus* (She et al., 2019) using CLC Genomics Workbench 20.0.4 (Qiagen, Hilden, Germany) with the default parameters. The expression of transcripts was qualified with the reads per kilobase per million mapped reads (RPKM) method (Mortazavi et al., 2008), and differentially expressed genes (DEGs) were filtered by $|\log2(FC)| \geq 0$, P-value < 0.05, and false discovery rate (FDR) < 0.1. The functions of the DEGs were enriched in Gene ontology (GO) database, and mapping to *C. roseus* with MapMan 4.0 and the mapping files of *C. roseus* were annotated with the PlaBi database by Mercator4 V3.0 (Schwacke et al., 2019). The transcriptomic dataset with nine periwinkle samples infected with CLas by grafting was downloaded from the NCBI database and processed as above (Liu et al., 2019). It contained three groups, with three replicates for each group, and included early symptoms on partially mottled leaves (S), yellow periwinkle leaves (Y), and healthy periwinkle leaves (H).

For the small-RNA datasets, reads shorter than 18 nt or longer than 32 nt were removed using Trimmomatic (Bolger et al., 2014) and then filtered for rRNA, tRNA, snoRNA, snRNA, repeat sequences, and other ncRNAs using Pfam v.14.0 with the default parameters (Kalvari et al., 2021). The remaining reads were mapped to known miRNAs from the miRBase database to identify conserved miRNAs (Kozomara and Griffiths-Jones, 2014) and further analyzed to identify novel miRNAs using miRPREFer v. 0.24 with the default parameters (Lei and Sun, 2014). The identified conserved and novel miRNAs were compared against *C. roseus* mRNA transcript coding sequences with psRNATarget v.2.0 (Dai et al., 2018). The differential expression of miRNAs was analyzed using DEseq2 with a cutoff value of $P < 0.05$ (Love et al., 2014). The annotated mRNA targets were identified using Blast2Go (Götz et al., 2008).

Nested Network Analysis of Differentially Expressed Genes and miRNAs

Genes with an expression value (RPKM) < 1 from all expressed genes were filtered out, and the remaining genes were used to infer a weighted gene co-expression network analysis WGCNA (signed network) using an online tool[1] with the default parameters. An appropriate soft power = 1 was automatically

[1]http://www.ehbio.com/Cloud_Platform/front/#/

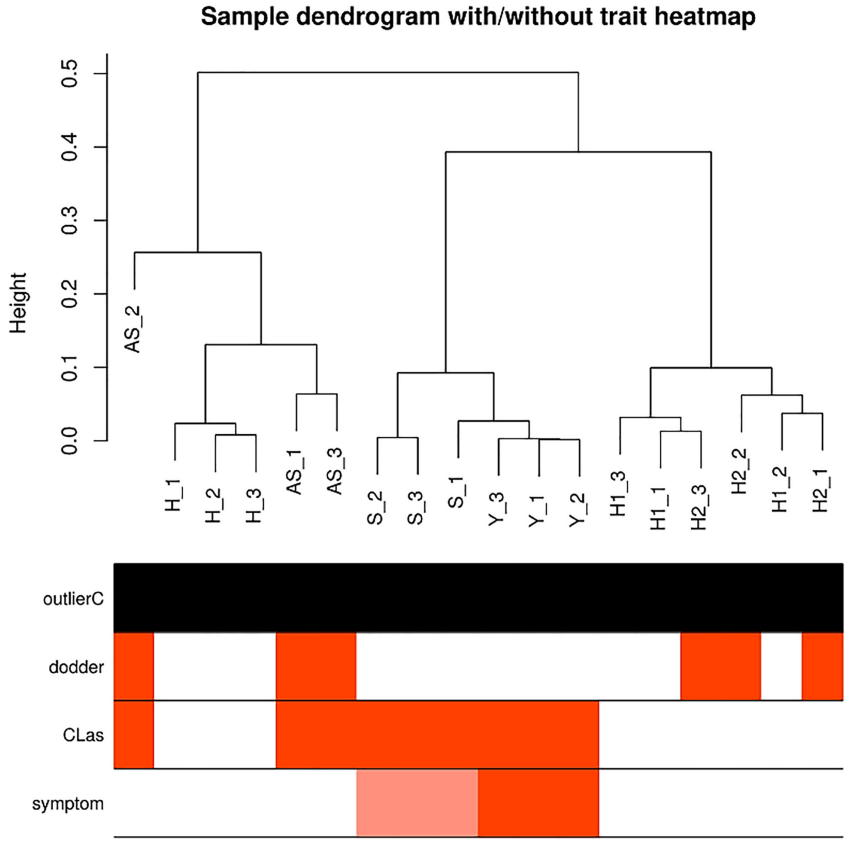

FIGURE 2 | Sample correlations evaluated with dendrogram. Red bars in each row indicate samples in relation to factors, including dodder, CLas and symptom. None is detected as outlier samples. H1, healthy periwinkle not parasitic with healthy dodder as control; H2, healthy periwinkle parasitic with healthy dodder as control; AS, asymptomatic periwinkle infected with CLas by dodder-mediated transmission. H, healthy periwinkle leaves; S, symptom just occurred partially mottled leaves; Y, yellow periwinkle leaves.

selected to make the scale-free topology index greater than 0.8. The WGCNA algorithm was used to construct gene modules and evaluate the connectivity of genes in a module. In our study, CLas infection and dodder parasitism were considered the two traits among different sample groups, and then the module eigengene (ME) value was calculated and used to test the association with different traits. After the MEs with the highest relationship to the CLas infection trait were determined, $|\text{geneModuleMembership}| > 0.8$ and $|\text{geneTraitCorrelation}| > 0.2$ were used as the cutoff values for gene member selection in each module. Overlapping components of the DEGs and miRNA-target in the CLas infection groups versus the control group were selected from MEs to construct the nested network using Cytoscape v3.8.2 (Kohl et al., 2011).

Validation of Differentially Expressed Genes, miRNAs, and Their Target Genes in *Catharanthus roseus*

For expression analysis, real-time quantitative PCR (RT-qPCR) (Fu et al., 2016) and stem-loop RT-qPCR (Kramer, 2011) were applied for DEGs and miRNA, respectively, with the same set of samples used for RNA-seq. The expression of both the DEGs and miRNAs was normalized with the U6 small nuclear ribonucleic acid (snRNA) gene. The primers used in this study are listed in **Supplementary Table 1**. The first strand was synthesized using the PrimeScript RT reagent kit with a gDNA Eraser (Takara, Shiga, Japan) for both mRNA and miRNA according to the manufacturer's protocol. The RT-qPCR was conducted on a qTower3G platform (Analytikjena, Jena, Germany) with GoTaq qPCR Master Mix (Promega, China) for mRNA and miRNA. All experiments were performed with three biological replicates and three technical replicates. Specificity of primers was determined with melting curves. The $2^{-\Delta\Delta Ct}$ method was applied for relative quantification, with the U6 small nuclear ribonucleic acid (snRNA) gene as an internal reference (Livak and Schmittgen, 2001). Expression fold change was further used to analyze the differences between the treatment group and control group.

RESULTS

Overview of Transcriptome and miRNAome Profiling

For transcriptomic profiling, 40–47 million clean reads were obtained from each plant with/without CLas infection, and

approximately 56–60% (average of three biological replicates) of reads were successfully mapped to the *C. roseus* genome (**Supplementary Table 2**). For the small-RNA datasets, 20–26 million clean reads were obtained, and approximately 65–82% (average of three biological replicates) of reads were successfully aligned to the *C. roseus* genome (**Supplementary Table 2**).

Identification of Differentially Expressed Genes and Differentially Expressed miRNAs and Functional Analyses

Sample correlations were evaluated for eighteen samples (**Figure 2**), and the DEGs for four comparisons were determined (**Table 1**). Healthy periwinkle H1 and H2 were clustered together, and the number of DEGs was approximately the same in the asymptomatic samples AS/H1 and AS/H2, indicating that dodder parasitism makes no significant effect on periwinkle in the process of CLas transmission. Although symptomatic samples S were slightly varied from Y, both were still closely clustered and away from asymptomatic samples AS. The number of DEGs was doubled in the S/H and Y/H compared to AS/H1(AS/H2). The results indicated that more genes and corresponding pathways were perturbed as symptom development.

There were 3,657 DEGs were commonly regulated in AS/H1 and AS/H2. They were enriched in oxidation-reduction process, protein phosphorylation and photosynthesis on the biological process (BP) level, in integral component of membrane, plasma membrane, chloroplast (envelop and thylakoid membrane) on the cellular component (CC) level, in ATP binding, metal ion binding and protein serine/threonine kinase activity on molecular function (MF) level (**Supplementary Figure 2**). There were 6,390 more DEGs were identified in S/H than in AS/H1(AS/H2). These DEGs were enriched in oxidation-reduction process, protein phosphorylation, and translation on the BP level, in integral component of membrane, nucleus/plasma membrane/cytoplasm, chloroplast/mitochondrion on the CC level, in ATP binding, zinc ion binding, protein serine/threonine kinase activity/nucleotide binding on the MF level (**Supplementary Figure 3**). As the further development of symptoms, 2,109 more DEGs were identified in Y/H than in S/H and they were enriched in oxidation-reduction process, photosynthesis and related pathways on the BP level, in integral component of membrane, chloroplast/cytoplasm/mitochondrion, and golgi apparatus on the CC level (**Supplementary Figure 4**). There were 1,867 DEGs that were commonly regulated and 14,974 DEGs that were overall regulated among the four comparisons (**Figure 3**), and they were also enriched on the three levels of GO (**Supplementary Figures 5**, **6**). These DEGs were also assigned to different pathways in MapMan (**Supplementary Table 3**). Generally, photosynthesis-, secondary metabolism-, and cell wall organization-related pathways were down-regulated, while cellular respiration, carbohydrate metabolism, RNA biosynthesis, protein modification, protein homeostasis, vesicle trafficking, and external stimuli response were up-regulated in AS (**Supplementary Figure 7A**). As symptoms developed in S and Y, it appeared that the up-regulation level of the DEGs was reduced compared to AS (**Supplementary Figure 7B**), particularly the DEGs related to external stimuli response, which changed from up-regulated to down-regulated (**Supplementary Table 3**).

In total, 336 (30 conserved and 301 novel) differentially expressed (DE) miRNAs (**Table 1**) were identified that potentially targeted 2144 *C. roseus* mRNAs, in which 720 were differentially expressed in the transcriptome profiling (**Table 1**). These DEG targets were mostly enriched in RNA biosynthesis, vesicle trafficking, and solute transport, followed by photosynthesis, carbohydrate metabolism, phytohormone action, protein biosynthesis, and protein homeostasis (**Supplementary Table 4**).

miRNA–mRNA Network Analyses

Through WGCNA analysis of 18 transcriptomic expression profiles, three modules were determined, and MEbrown was most highly related to CLas infection, followed by MEblue (**Supplementary Figure 8A**). Hub genes were also determined for each module (**Supplementary Figure 8B**). By application of threshold cutoff values of $|\text{geneModuleMembership}| > 0.8$ and $|\text{geneTraitCorrelation}| > 0.2$, 187 and 383 DEGs were selected from MEbrown and MEblue, respectively (**Supplementary Table 5**) and integrated with the DE miRNA and their differentially expressed targets to construct nested networks in Cytoscape v3.8.2.

The primary network was constructed with DEGs from MEbrown containing six miRNAs (one conserved and five novel) and 154 DEGs (**Supplementary Table 6** and **Supplementary Figure 9**). Within the network, genes in photosynthesis, carbohydrate metabolism, coenzyme metabolism, redox homeostasis, and secondary metabolism were overwhelmingly down-regulated. Three up-regulated novel miRNAs (novel-m1620-5p, novel-m0655-5p, and novel-m0381-5p) targeted a down-regulated chlorophyll *a/b*-binding protein 5 of photosystem I, and a down-regulated novel-m0431-5p targeted a down-regulated chlorophyll a-b binding protein CP29.1. Another induced novel miRNA (novel-m0499-3p) was predicated to target induced nucleoredoxin involved in redox homeostasis. The known miR164-x was repressed and targeted a highly induced transcription factor (TF) NAC1/ANAC022/anac021 (CRO_T007448) (**Figure 4** and **Supplementary Table 6**), which served as the core node connecting a bunch of significantly expressed TFs, including highly expressed HD-ZIP I/II and NAC, and down-expressed bHLH, C2H2, and TCP (**Supplementary Table 6**), functioning in transcriptional regulation. Genes in protein biosynthesis/homeostasis/modification and nutrient uptake/transport were differentially expressed (**Supplementary Table 6**).

The secondary network was constructed with DEGs from MEblue containing four miRNAs (three conserved and one novel) and 316 DEGs (**Supplementary Table 7** and **Supplementary Figure 10**). Within this network, genes in photosynthesis were generally down-regulated. Many genes in solute transport were differentially expressed. miR827 was Pi deficiency-inducible, and its expression was highly induced. It was predicted to target a down-expressed TF, BALDIBIS/BIB (CRO_T003413) in positive regulation of transcription. A novel miRNA (novel-m0275-5p) was repressed and predicted to

TABLE 1 | Number of regulated genes and miRNAs in periwinkle infected with "*Candidatus* Liberibacter asiaticus."

Sample	Number of DEGs					Number of DE miRNA							DEG/total targets
	Up	Down	Co-	S^+	Y^+	Up	Down	Total	Co-	Known	Novel	Total	
AS/H1	2,696	2,301				88	66	154					
AS/H2	2,558	2,577	3,657			58	209	267	85	30	301	336	
S/H	3,791	6,324		6,390									
Y/H	4,091	7,017	4,895		2,109								720/2144

DEGs, differentially expressed genes; DE miRNA, differentially expressed miRNA; H1, healthy periwinkle not parasitic with healthy dodder as control; H2, healthy periwinkle parasitic with healthy dodder as control; AS, asymptomatic periwinkle infected with CLas by dodder-mediated transmission; H, healthy periwinkle leaves; S, symptom just occurred partially mottled leaves; Y, yellow periwinkle leaves; S^+, more DEGs identified in S samples; Y^+, more DEGs identified in Y samples; co-, commonly regulated DEGs or DE miRNA.

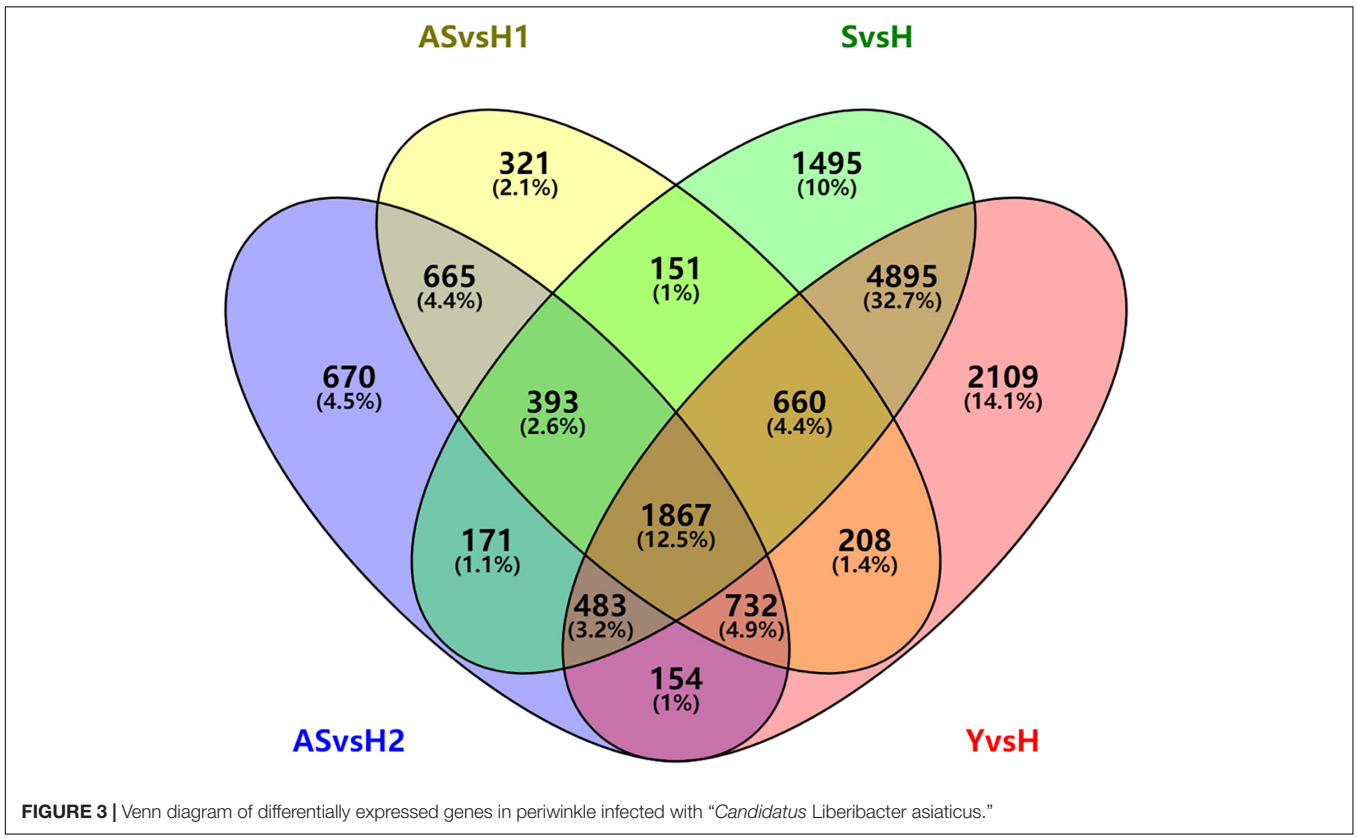

FIGURE 3 | Venn diagram of differentially expressed genes in periwinkle infected with "*Candidatus* Liberibacter asiaticus."

target an overexpressed ZIP5 transporter (CRO_T005117). A gene-encoding ubiquitin-conjugating E2 protein (PHO2) in phosphate assimilation was slightly up-regulated, while phosphate transporters (PHT2 and PHT4) were down-regulated (**Figure 5A**). Redox homeostasis, brassinosteroid and gibberellin phytohormone, and protein modification and homeostasis were disturbed, and genes in ubiquitin-proteasome system, phosphorylation, and S-glutathionylation were particularly up-regulated. Notably, a gene encoding ubiquitin-fold protein (ATG8) involved in autophagy was induced in the symptomatic samples (**Supplementary Table 7**). The expression of miR828-x was repressed and targeted the down-expressed MYB94 (CRO_T026098), which formed a network with an overexpressed HSF4 (CRO_T018303) and LCY-b (CRO_T009445, lycopene beta cyclase) involved in the terpenoid pathway (**Figure 5B**). Meanwhile, HSF4 was targeted by the down-expressed miR1134-y. The expression of both effector-triggered immunity co-regulator PAD4 and programmed cell death metacaspase-like regulator MCP2 was induced (**Supplementary Table 7**).

Validation of mRNA and miRNA Expression by RT-qPCR

The expression level of 25 DEGs, 19 of which were the targets of 20 DE miRNAs, was assayed by RT-qPCR. These genes were found to be involved in different biological processes encoding NAC1, ZIP1, ZIP5, light harvesting complex (LHCA6, LHCB4.1), phloem protein (PP2-A13, PP-B15), autophagy-related protein (ATG8), E3 ubiquitin-protein ligase, LecRK-VII.1, MuDR transposase, remorin protein, indole-3-acetic acid

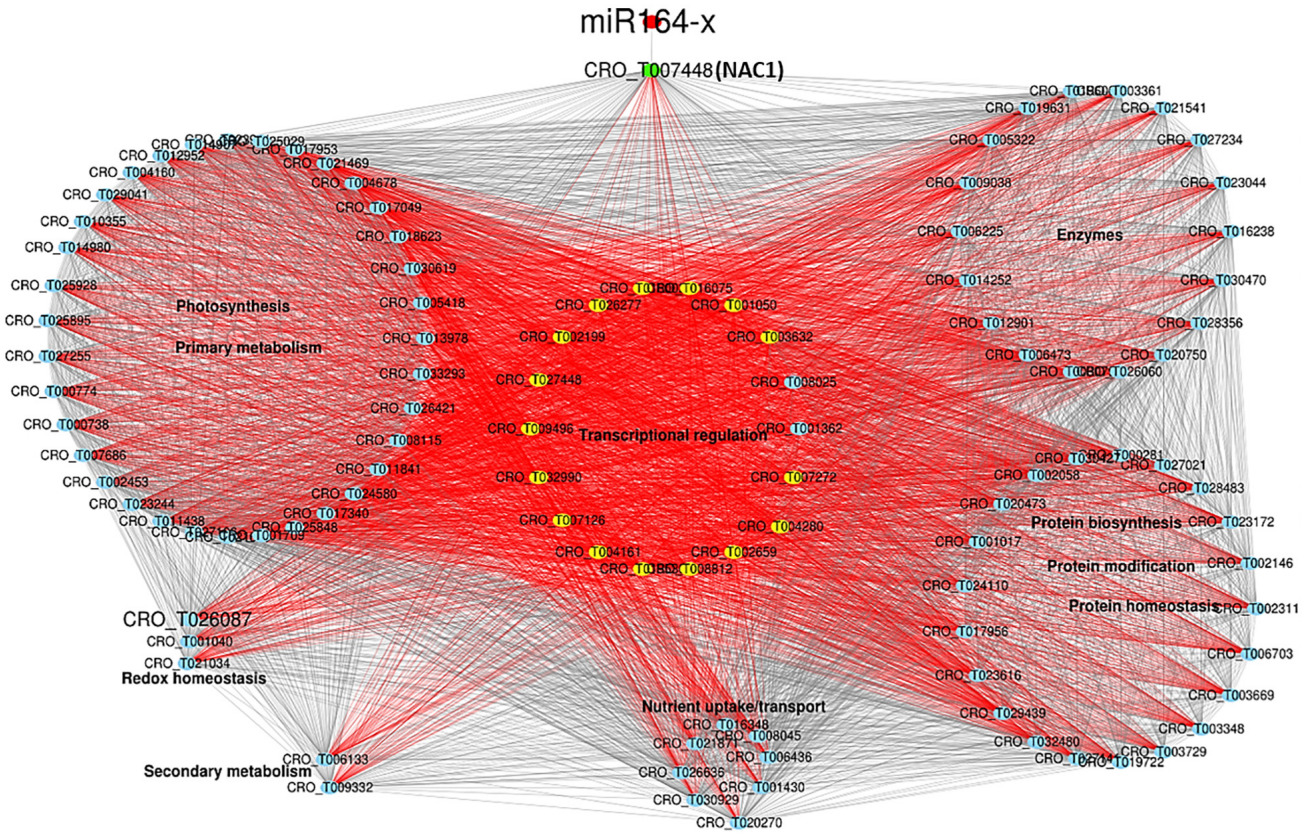

FIGURE 4 | miR164-NAC1 regulatory network highly related to CLas infection. The red nodes are miRNA. The green and yellow nodes are transcription factors (TFs). The blue nodes are genes. Red lines indicate connections to TFs.

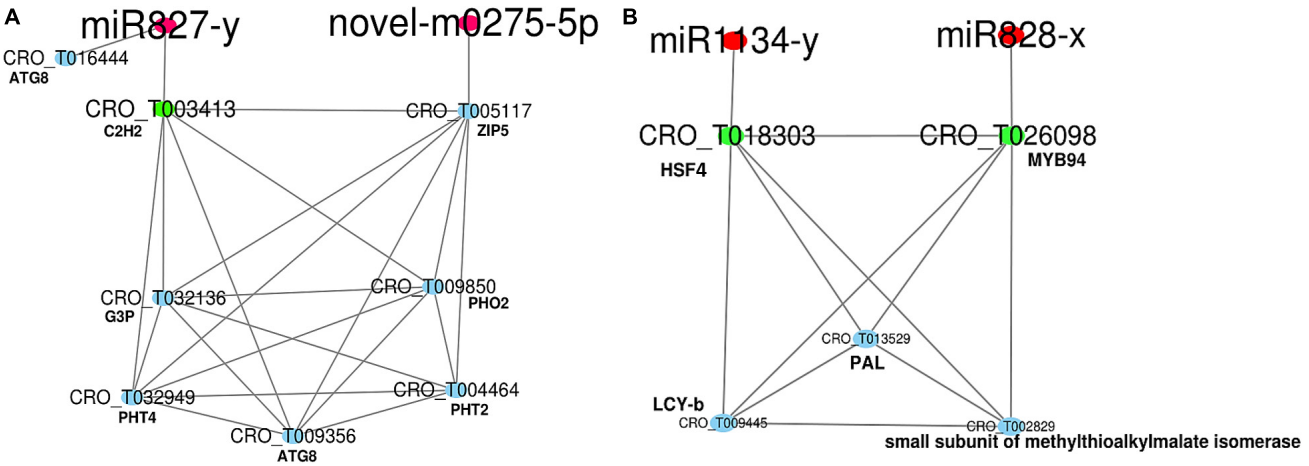

FIGURE 5 | The network of miRNA in the regulation of nutrient and secondary metabolism. The red nodes are miRNAs. The green nodes are transcription factors (TFs). The blue nodes are genes. **(A)** and **(B)** The nutrient and secondary related regulatory networks, respectively. The red nodes are miRNAs. The green nodes are TFs. The blue nodes are genes.

inducible, CIPK10, osmotin 34, curculin-like (mannose-binding) lectin, and gibberellin 2-oxidase. The expression of eight DE miRNAs with two conserved miRNAs (miR164-x and miR828-x) was verified by stem-loop RT-qPCR. Spearman's rho values of 0.9 for mRNA and 0.68 for miRNA (**Figure 6**) confirmed the reliability of the transcriptomic and small-RNA profiling data. The expression levels of the DEGs and DE miRNAs between the RNA-seq and RT-qPCR are detailed in **Supplementary Figure 11**.

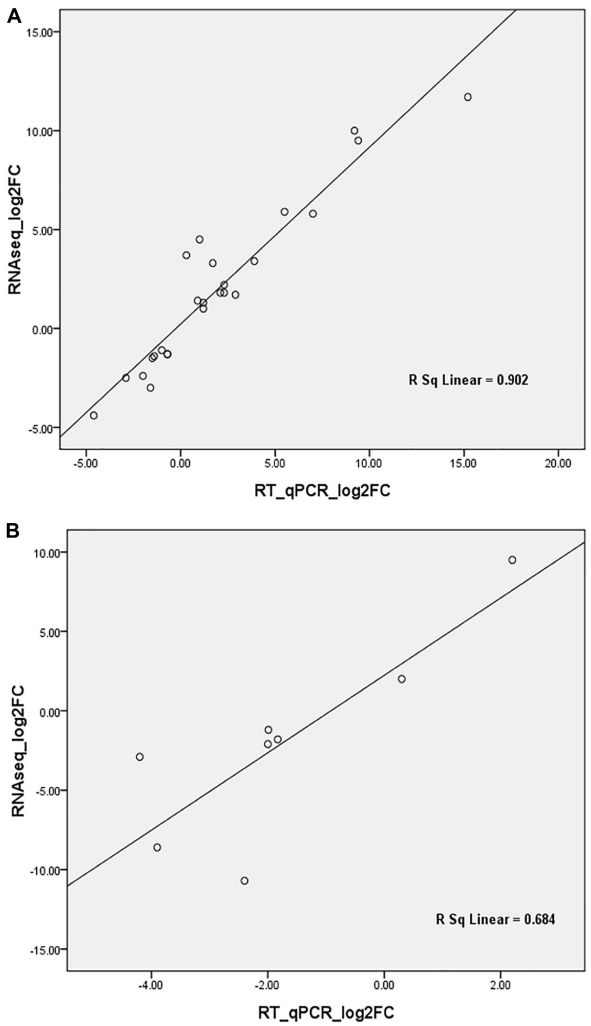

FIGURE 6 | Correlation analyses of differential gene expression by RT-qPCR and RNA-seq. **(A)** verification analyses for differentially expressed genes; **(B)** verification analyses for differentially expressed miRNAs. FC, Fold change.

DISCUSSION

The Invasion of *Candidatus* Liberibacter asiaticus and Symptom Development Affect Host Responses Rather Than Transmission Method

Although the 18 transcriptome profiles were collected from two independent experiments with periwinkle infected by CLas either by grafting or dodder bridge, the results showed that all datasets are comparable and dodder does not make significant effect on periwinkle responses during CLas transmission. What does greatly affect host responses is the invasion of CLas and the disease progress from asymptomatic to symptomatic. Prior to symptom occur, photosystem and chloroplast have already been perturbed. With symptom appearance, organelles nucleus, mitochondrion and golgi apparatus were gradually disturbed, but defense response related pathways were not significantly enriched.

The miR164-NAC1 Network Potentially Regulates Plant Defense Responses to *Candidatus* Liberibacter asiaticus

ORE1, an NAC TF, has been demonstrated to positively regulate age-induced cell death in *Arabidopsis* leaves and is negatively regulated by miR164 (Kim et al., 2009). Both miR164 and its target *NAC21/22* were activated, and *NAC21/22* negatively regulates wheat resistance to stripe-rust (Feng et al., 2014). The *Arabidopsis NAC4* promotes pathogen-induced cell death under negative regulation by miR164 (Lee et al., 2017). The miR164a-NAC60 module negatively regulates immunity in rice against the blast fungus *Magnaporthe oryzae* (Wang et al., 2018). The miR164-NAC100 regulatory system modulates cotton plant resistance against *Verticillium dahlia* (Hu et al., 2020). The conserved miR164-NAC regulatory pathway was identified for disease defense in *Populus* during leaf black spot fungus infection (Chen et al., 2021). Plants can sense signals from pathogens during their invasion and activate a complicated and fine-tune network in relation to phytohormones and reactive oxygen species (ROS). NAC TFs have been demonstrated to participate in plant–pathogen interactions as negative and positive regulators by connecting signaling pathways of PCD, plant hormones, and to regulate the resistance against pathogens (Bian et al., 2020). The differential expression of miR164 and NAC1 was identified and verified in AS samples, and further confirmed by (stem-loop) RT-qPCR in another independent set of diseased periwinkle leaves with early blotchy mottle symptom (**Supplementary Figure 12**). Therefore, the early activation of miR164-NCA1 regulatory network is potentially involved in periwinkle defense responses against CLas, but it couldn't prevent the multiplication of CLas and symptom development.

miRNA–mRNA Networks Regulate Secondary Metabolism and Nutrient Homeostasis

miR828 regulates lignin and H_2O_2 accumulation in sweet potato upon wounding to participate in defense by targeting *MYB* (Lin et al., 2012). miR828 is also involved in the regulation of trichome and cotton fiber development by targeting *MYB2* in *Arabidopsis* (Guan et al., 2014), as well as anthocyanin and flavonol accumulation by targeting *MYB114* in grape (Tirumalai et al., 2019). As the target of miR828, *MYB* modulate gene expression patterns in the flavonoid biosynthetic pathway (Samad et al., 2020). *MYB94* formed a network with *LCY-b* in terpenoid pathway and *HSF4* targeted by miR1134, which is involved in the terpenoid biosynthetic pathway by miRNA-based regulation (Fan et al., 2015; Samad et al., 2020). The expression of genes in the flavonoid and terpenoid biosynthetic pathways was altered in periwinkle in response to CLas infection (**Supplementary Tables 6**, **7**). Therefore, miR828-MYB94 and miR1134-HSF4 potentially function in the regulation of secondary metabolism in periwinkle against CLas.

miR827 is a phosphate (Pi) starvation-inducible miRNA. The miR827-NAL (nitrogen limitation adaption) and miR827-PHT (phosphate transporter 5) modules were found to maintain cellular Pi homeostasis in *Arabidopsis* and *Oryza sativa* (Lin et al., 2018), respectively. miR399, another Pi deficiency-inducible miRNA, was significantly induced in citrus by CLas infection, and HLB symptom severity was significantly reduced by Pi supplementation (Zhao et al., 2013). The expression of miR399 was induced in periwinkle but was not involved in the identified core network (not shown). Nutrient deficiency, particularly zinc deficiency, is commonly observed in citrus parasitized by CLas. ZIP5, functioning in zinc transportation, was up-regulated in periwinkle, strongly associated with the enrichment of DEGs in zinc ion binding in symptom just occurred samples (**Supplementary Figure 3**). Zn and Pi transport and homeostasis are recognized as highly co-regulated process and it has been demonstrated that Zn deficiency induced Pi accumulation in *Arabidopsis* (Khan et al., 2014). This result indicates that periwinkle experienced a nutrient imbalance, in particular Pi and Zn deficiency, which partially resulted from the blockage of the phloem system and root decline with the disease development under CLas stress (Johnson et al., 2014).

In addition to the Pi homeostasis regulation, miR827 acts as a negative regulator suppressing basal defense responses in *Arabidopsis,* favoring nematode parasitism through post-transcriptional gene silencing of its ubiquitin E3 ligase target gene (Hewezi et al., 2016). ATG8 is another target of miR827 that is involved in maintaining protein homeostasis through autophagy, which occurs in response to nutrient limitation and bacterial effectors (Üstün et al., 2018). In facilitating *Pseudomonas syringae* pv. tomato (*Pto*) DC3000 infection, effector HrpZ1 oligomerization targets the ATG4b-mediated cleavage of ATG8 to enhance autophagy, while HopF3 targets ATG8 to suppress autophagy (Lal et al., 2020). CLas encodes 166 sec-dependent presumable effectors, and 86 out of 166 were experimentally validated to contain a signal peptide with poorly understood mechanisms (Prasad et al., 2016). One effector was primarily identified to interact with citrus ATG8a (not shown), and the associated molecular mechanism is currently being researched by our laboratory. Thirty-five autophagy-related genes were identified in sweet orange (*C. sinensis*), and CsATG18a and CsATG18b were verified to enhance plant tolerance to abiotic stress (Fu et al., 2020). Effectors play vital roles in the pathogenesis of virulent plant pathogens by targeting host ATG proteins. The activation of the effector-triggered immunity pathway was observed in the current study, but autophagy-related machinery has not been reported either in citrus or in periwinkle by CLas infection, indicating that this could be a promising research focus for future studies.

Currently, the citrus-dodder–periwinkle transmission system has been well-established in our laboratory by optimizing growing conditions. Periwinkle plants can be infected by CLas within two weeks and show symptoms within one month. The early developed symptom on periwinkle resembles the typical blotchy mottle on citrus, then it gradually changes to yellowing (**Supplementary Figure 12**). Due to the ability of periwinkle to support the quick establishment and the higher colonization level of CLas, and greatly shortening the long latency for disease symptom development on citrus, periwinkle can be used as surrogate for CLas pathogenesis studies in the future.

CONCLUSION

Through concurrent analyses of the transcriptome and miRNAome of periwinkle in response to CLas infection, primary and secondary nested miRNA–mRNA networks were identified with four conserved miRNAs. The primary network miR164-NAC1 is potentially involved in plant defense responses against CLas from the early infection stage to symptom development. The secondary network revealed the potential regulation of secondary metabolism and nutrient homeostasis through miR828-MYB94/miR1134-HSF4 and miR827-ATG8 regulatory networks, respectively. By using periwinkle as a surrogate, the identified miRNAs-mRNA regulatory networks provide promising perspectives on host–CLas interactions.

DATA AVAILABILITY STATEMENT

The RNA-seq datasets supporting the manuscript are available in the SRA database under accession ID PRJNA723735.

AUTHOR CONTRIBUTIONS

SF performed the experiments, data analyses, and wrote the manuscript. HW and ChZ prepared the experimental plant settings and collected the data. MC did small RNA data analyses. CyZ and XW conceptualized the idea and revised the manuscript. All authors contributed to the article and approved the submitted version.

FUNDING

This project was supported by National Natural Science Foundation of China (31871925), Natural Science Foundation of Chongqing (cstc2020jcyj-msxmX1036), Natural Science Foundation of Southwest University (SWU120023), and 111 Project (B18044).

SUPPLEMENTARY MATERIAL

The Supplementary Material for this article can be found online at: https://www.frontiersin.org/articles/10.3389/fmicb.2022.799819/full#supplementary-material

REFERENCES

Bian, Z., Gao, H., and Wang, C. (2020). NAC transcription factors as positive or negative regulators during ongoing battle between pathogens and our food crops. *Int. J. Mol. Sci.* 22:81. doi: 10.3390/ijms22010081

Bolger, A. M., Lohse, M., and Usadel, B. (2014). Trimmomatic: a flexible trimmer for illumina sequence data. *Bioinformatics* 30, 2114–2120. doi: 10.1093/bioinformatics/btu170

Bové, J. M. (2006). Huanglongbing: a destructive, newly-emerging, century-old disease of citrus. *J. Plant Pathol.* 88, 7–37. doi: 10.1371/journal.pone.0111032

Chen, S., Wu, J., Zhang, Y., Zhao, Y., Xu, W., Li, Y., et al. (2021). Genome-wide analysis of coding and non-coding RNA reveals a conserved miR164-NAC-mRNA regulatory pathway for disease defense in populus. *Front. Genet.* 12:668940. doi: 10.3389/fgene.2021.668940

Dai, X., Zhuang, Z., and Zhao, P. X. (2018). psRNAtarget: a plant small RNA target analysis server (2017 release). *Nucl. Acids Res.* 46, W49–W54. doi: 10.1093/nar/gky316

Ding, F., Paul, C., Brlansky, R., and Hartung, J. S. (2017). Immune tissue print and immune capture-PCR for diagnosis and detection of 'Candidatus liberibacter asiaticus'. *Sci. Rep.* 7:46467. doi: 10.1038/srep46467

Duan, Y. P., Gottwald, T., Zhou, L. J., and Gabriel, D. W. (2008). First report of dodder transmission of 'Candidatus liberibacter asiaticus' to tomato (Lycopersicon esculentum). *Plant Dis.* 92:831 doi: 10.1094/PDIS-92-5-0831C

Fan, R., Li, Y., Li, C., and Zhang, Y. (2015). Differential microRNA analysis of glandular trichomes and young leaves in Xanthium strumarium L. reveals their putative roles in regulating terpenoid biosynthesis. *PLoS One* 10:e0139002. doi: 10.1371/journal.pone.0139002

Feng, H., Duan, X., Zhang, Q., Li, X., Wang, B., Huang, L., et al. (2014). The target gene of tae-miR164, a novel NAC transcription factor from the nam subfamily, negatively regulates resistance of wheat to stripe rust. *Mol. Plant Pathol.* 15, 284–296. doi: 10.1111/mpp.12089

Francischini, F. J. B., Oliveira, K. D. S., Astúa-Monge, G., Novelli, A., Lorenzino, R., Matiolli, C., et al. (2007). First report on the transmission of 'Candidatus liberibacter americanus' from citrus to *Nicotiana tabacum* cv. Xanthi. *Plant Dis.* 91:631. doi: 10.1094/pdis-91-5-0631b

Fu, S., Shao, J., Zhou, C., and Hartung, J. S. (2016). Transcriptome analysis of sweet orange trees infected with'Candidatus liberibacter asiaticus' and two strains of Citrus tristeza virus. *BMC Genomics* 17:349. doi: 10.1186/s12864-016-2663-9

Fu, X., Zhou, X., Xu, Y., Hui, Q., Chun, C., Ling, L., et al. (2020). Comprehensive analysis of autophagy-related genes in sweet orange (Citrus sinensis) highlights their roles in response to abiotic stresses. *Int. J. Mol. Sci.* 21:2699. doi: 10.3390/ijms21082699

Garnier, M., and Bové, J. M. (1983). Transmission of the organism associated with citrus greening disease from sweet orange to periwinkle by dodder. *Phytopathology* 73, 1358–1363.

Gottwald, T., Poole, G., McCollum, T., Hall, D., Hartung, J., Bai, J., et al. (2020). Canine olfactory detection of a vectored phytobacterial pathogen, liberibacter asiaticus, and integration with disease control. *Proc. Natl. Acad. Sci. U.S.A.* 117, 3492–3501. doi: 10.1073/pnas.1914296117

Götz, S., García-Gómez, J. M., Terol, J., Williams, T. D., Nagaraj, S. H., Nueda, M. J., et al. (2008). High-throughput functional annotation and data mining with the blast2go suite. *Nucl. Acids Res.* 36, 3420–3435. doi: 10.1093/nar/gkn176

Guan, X., Pang, M., Nah, G., Shi, X., Ye, W., Stelly, D. M., et al. (2014). miR828 and miR858 regulate homoeologous MYB2 gene functions in arabidopsis trichome and cotton fibre development. *Nat. Commun.* 5:3050. doi: 10.1038/ncomms4050

Hartung, J. S., Paul, C., Achor, D., and Brlansky, R. H. (2010). Colonization of dodder, Cuscuta indecora, by 'Candidatus liberibacter asiaticus' and 'Ca. L. Americanus'. *Phytopathology* 100, 756–762. doi: 10.1094/PHYTO-100-8-0756

Hewezi, T., Piya, S., Qi, M., Balasubramaniam, M., Rice, J. H., and Baum, T. J. (2016). Arabidopsis miR827 mediates post-transcriptional gene silencing of its ubiquitin E3 ligase target gene in the syncytium of the cyst nematode heterodera schachtii to enhance susceptibility. *Plant J.* 88, 179–192. doi: 10.1111/tpj.13238

Hosford, R. M. Jr. (1967). Transmission of plant viruses by dodder. *Bot. Rev.* 33, 387–406.

Hu, G., Lei, Y., Liu, J., Hao, M., Zhang, Z., Tang, Y., et al. (2020). The ghr-miR164 and GhNAC100 modulate cotton plant resistance against Verticillium dahlia. *Plant Sci.* 293:110438. doi: 10.1016/j.plantsci.2020.110438

Jagoueix, S., Bové, J. M., and Garnier, M. (1996). PCR detection of the two 'Candidatus liberobacter species' associated with greening disease of citrus. *Mol. Cell. Probes* 10, 43–50. doi: 10.1006/mcpr.1996.0006

Jain, M., Fleites, L. A., and Gabriel, D. W. (2015). Prophage-encoded peroxidase in 'Candidatus liberibacter asiaticus' is a secreted effector that suppresses plant defenses. *Mol. Plant Microbe Interact.* 28, 1330–1337. doi: 10.1094/MPMI-07-15-0145-R

Johnson, E., Wu, J., Bright, D., and Graham, J. (2014). Association of 'Candidatus liberibacter asiaticus' root infection, but not phloem plugging with root loss on Huanglongbing-affected trees prior to appearance of foliar symptoms. *Plant Pathol.* 63, 290–298.

Kalvari, I., Nawrocki, E. P., Ontiveros-Palacios, N., Argasinska, J., Lamkiewicz, K., Marz, M., et al. (2021). Rfam 14: expanded coverage of metagenomic, viral and microRNA families. *Nucl. Acids Res.* 49, D192–D200. doi: 10.1093/nar/gkaa1047

Kamińska, M., and Korbin, M. G. (1999). Graft and dodder transmission of phytoplasma affecting lily to experimental hosts. *Acta Physiol. Plant.* 21, 21–26.

Khan, G. A., Bouraine, S., Wege, S., Li, Y., de Carbonnel, M., Berthomieu, P., et al. (2014). Coordination between zinc and phosphate homeostasis involves the transcription factor phr1, the phosphate exporter pho1, and its homologue PHO, H3 in arabidopsis. *J. Exp. Bot.* 65, 871–884. doi: 10.1093/jxb/ert444

Kim, J. H., Woo, H. R., Kim, J., Lim, P. O., Lee, I. C., Choi, S. H., et al. (2009). Trifurcate feed-forward regulation of age-dependent cell death involving miR164 in arabidopsis. *Science* 323, 1053–1057. doi: 10.1126/science.1166386

Kohl, M., Wiese, S., and Warscheid, B. (2011). Cytoscape: software for visualization and analysis of biological networks. *Methods Mol. Biol.* 696, 291–303. doi: 10.1007/978-1-60761-987-1_18

Kozomara, A., and Griffiths-Jones, S. (2014). mirBase: annotating high confidence microRNAs using deep sequencing data. *Nucl. Acids Res.* 42, D68–D73. doi: 10.1093/nar/gkt1181

Kramer, M. F. (2011). Stem-loop RT-qPCR for miRNAs. *Curr. Protoc. Mol. Biol.* 15:10

Lal, N. K., Thanasuwat, B., Huang, P. J., Cavanaugh, K. A., Carter, A., Michelmore, R. W., et al. (2020). Phytopathogen effectors use multiple mechanisms to manipulate plant autophagy. *Cell Host Microbe* 28, 558–571.e6. 558-571.e556. doi: 10.1016/j.chom.2020.07.010

Lee, M. H., Jeon, H. S., Kim, H. G., and Park, O. K. (2017). An arabidopsis NAC transcription factor NAC4 promotes pathogen-induced cell death under negative regulation by microRNA164. *New Phytol.* 214, 343–360. doi: 10.1111/nph.14371

Lei, J., and Sun, Y. (2014). miR-prefer: an accurate, fast and easy-to-use plant miRNA prediction tool using small RNA-seq data. *Bioinformatics* 30, 2837–2839. doi: 10.1093/bioinformatics/btu380

Li, T., Zhang, L., Deng, Y., Deng, X., and Zheng, Z. (2021). Establishment of a Cuscuta campestris-mediated enrichment system for genomic and transcriptomic analyses of 'Candidatus liberibacter asiaticus'. *Microbial Biotechnol.* 14, 737–751. doi: 10.1111/1751-7915.13773

Lin, J. S., Lin, C. C., Lin, H. H., Chen, Y. C., and Jeng, S. T. (2012). miR828 regulates lignin and H2O2 accumulation in sweet potato on wounding. *New Phytol.* 196, 427–440. doi: 10.1111/j.1469-8137.2012.04277.x

Lin, W. Y., Lin, Y. Y., Chiang, S. F., Syu, C., Hsieh, L. C., and Chiou, T. J. (2018). Evolution of microRNA827 targeting in the plant kingdom. *New Phytol.* 217, 1712–1725. doi: 10.1111/nph.14938

Liu, N., Shen, G., Xu, Y., Liu, H., Zhang, J., Li, S., et al. (2020). Extensive inter-plant protein transfer between Cuscuta parasites and their host plants. *Mol. Plant* 13, 573–585. doi: 10.1016/j.molp.2019.12.002

Liu, X., Zheng, Y., Wang-Pruski, G., Gan, Y., Zhang, B., Hu, Q., et al. (2019). Transcriptome profiling of periwinkle infected with Huanglongbing ('Candidatus liberibacter asiaticus'). *Eur. J. Plant Pathol.* 153, 1573-8469

Livak, K. J., and Schmittgen, T. D. (2001). Analysis of relative gene expression data using real-time quantitative PCR and the 2- $\Delta\Delta$ct method. *Methods* 25, 402–408.

Love, M. I., Huber, W., and Anders, S. (2014). Moderated estimation of fold change and dispersion for RNA-seq data with Deseq2. *Genome Biol.* 15:550. doi: 10.1186/s13059-014-0550-8

Mortazavi, A., Williams, B. A., McCue, K., Schaeffer, L., and Wold, B. (2008). Mapping and quantifying mammalian transcriptomes by RNA-seq. *Nat. Methods* 5, 621–628. doi: 10.1038/nmeth.1226

Pitino, M., Allen, V., and Duan, Y. (2018). Las△5315 effector induces extreme starch accumulation and chlorosis as 'Ca. Liberibacter asiaticus' infection in Nicotiana benthamiana. *Front. Plant Sci.* 9:113. doi: 10.3389/fpls.2018.00113ODOI

Prasad, S., Xu, J., Zhang, Y., and Wang, N. (2016). Sec-translocon dependent extracytoplasmic proteins of 'Candidatus liberibacter asiaticus'. *Front. Microbiol.* 7:1989. doi: 10.3389/fmicb.2016.01989

Samad, A. F. A., Sajad, M., and Ismail, I. (2020). Emerging of microRNAs as key regulators in plant secondary metabolism. *Plant microRNAs* 20, 121–142. doi: 10.1007/978-3-030-35772-6_7

Schwacke, R., Ponce-Soto, G. Y., Krause, K., Bolger, A. M., Arsova, B., Hallab, A., et al. (2019). Mapman4: a refined protein classification and annotation framework applicable to multi-omics data analysis. *Mol. Plant* 12, 879–892. doi: 10.1016/j.molp.2019.01.003

She, J., Yan, H., Yang, J., Xu, W., and Su, Z. (2019). croFDG: catharanthus roseus functional genomics database. *Front. Genetics* 10:238. doi: 10.3389/fgene.2019.00238.NODOI

Sun, G., Xu, Y., Liu, H., Sun, T., Zhang, J., Hettenhausen, C., et al. (2018). Large-scale gene losses underlie the genome evolution of parasitic plant Cuscuta australis. *Nat. Commun.* 9:2683. doi: 10.1038/s41467-018-04721-8

Teixeira, D. C., Eveillard, S., Sirand-Pugnet, P., Wulff, A., Saillard, C., Ayres, A. J., et al. (2008). The tufB-secE-nusG-rplKAJL-rpoB gene cluster of the liberibacters: sequence comparisons, phylogeny and speciation. *Int. J. Syst. Evol. Microbiol.* 58, 1414–1421. doi: 10.1099/ijs.0.65641-0

Tirumalai, V., Swetha, C., Nair, A., Pandit, A., and Shivaprasad, P. V. (2019). miR828 and miR858 regulate VvMYB114 to promote anthocyanin and flavonol accumulation in grapes. *J. Exp. Bot.* 70, 4775–4792. doi: 10.1093/jxb/erz264

Üstün, S., Hafrén, A., Liu, Q., Marshall, R. S., Minina, E. A., Bozhkov, P. V., et al. (2018). Bacteria exploit autophagy for proteasome degradation and enhanced virulence in plants. *Plant Cell* 30, 668–685. doi: 10.1105/tpc.17.00815

Wang, N. (2019). The Citrus Huanglongbing crisis and potential solutions. *Mol. Plant* 12:607. doi: 10.1016/j.molp.2019.03.008

Wang, N., Pierson, E. A., Setubal, J. C., Xu, J., Levy, J. G., Zhang, Y., et al. (2017). The Candidatus liberibacter–host interface: insights into pathogenesis mechanisms and disease control. *Ann. Rev. Phytopathol.* 55, 451–482. doi: 10.1146/annurev-phyto-080516-035513

Wang, Z., Xia, Y., Lin, S., Wang, Y., Guo, B., Song, X., et al. (2018). Osa-miR164a targets OsNAC60 and negatively regulates rice immunity against the blast fungus Magnaporthe oryzae. *Plant J.* [Epub online ahead of print] doi: 10.1111/tpj.13972

Wu, J., Johnson, E., Gerberich, K., Bright, D., and Graham, J. (2018). Contrasting canopy and fibrous root damage on swingle citrumelo caused by 'Candidatus liberibacter asiaticus' and Phytophthora nicotianae. *Plant Pathol.* 67, 202–209. doi: 10.1111/ppa.12711

Ya, L., Xu, M.-R., Dai, Z.-H., and Deng, X.-l (2018). Distribution pattern and titer of 'Candidatus liberibacter asiaticus' in periwinkle (Catharanthus roseus). *J. Integr. Agric.* 17, 2501–2508. doi: 10.1016/s2095-3119(18)61918-5

Zhang, M., Duan, Y., Zhou, L., Turechek, W. W., Stover, E., and Powell, C. A. (2010). Screening molecules for control of Citrus Huanglongbing using an optimized regeneration system for 'Candidatus liberibacter asiaticus'-infected periwinkle (Catharanthus roseus) cuttings. *Phytopathology* 100, 239–245. doi: 10.1094/phyto-100-3-0239

Zhang, S., Flores-Cruz, Z., Zhou, L., Kang, B.-H., Fleites, L. A., Gooch, M. D., et al. (2011b). 'Ca. Liberibacter asiaticus' carries an excision plasmid prophage and a chromosomally integrated prophage that becomes lytic in plant infections. *Mole. Plant Microbe Interact.* 24, 458–468. doi: 10.1094/MPMI-11-10-0256

Zhang, M., Powell, C. A., Zhou, L., He, Z., Stover, E., and Duan, Y. (2011a). Chemical compounds effective against the Citrus Huanglongbing bacterium 'Candidatus liberibacter asiaticus' in planta. *Phytopathology* 101, 1097–1103. doi: 10.1094/phyto-09-10-0262

Zhao, H., Sun, R., Albrecht, U., Padmanabhan, C., Wang, A., Coffey, M. D., et al. (2013). Small RNA profiling reveals phosphorus deficiency as a contributing factor in symptom expression for Citrus Huanglongbing disease. *Mole. Plant* 6, 301–310. doi: 10.1093/mp/sst002

Zhou, L., Gabriel, D., Duan, Y., Halbert, S., and Dixon, W. (2007). First report of dodder transmission of Huanglongbing from naturally infected Murraya paniculata to citrus. *Plant Dis.* 91, 227–227. doi: 10.1094/PDIS-91-2-0227B

Conflict of Interest: The authors declare that the research was conducted in the absence of any commercial or financial relationships that could be construed as a potential conflict of interest.

Publisher's Note: All claims expressed in this article are solely those of the authors and do not necessarily represent those of their affiliated organizations, or those of the publisher, the editors and the reviewers. Any product that may be evaluated in this article, or claim that may be made by its manufacturer, is not guaranteed or endorsed by the publisher.

frontiers in Microbiology

REVIEW
published: 10 March 2022
doi: 10.3389/fmicb.2022.850588

An Overview of the Mechanisms Against "*Candidatus* Liberibacter asiaticus": Virulence Targets, Citrus Defenses, and Microbiome

Chuanyu Yang and Veronica Ancona**

Department of Agriculture, Agribusiness, and Environmental Sciences, Citrus Center, Texas A&M University-Kingsville, Weslaco, TX, United States

Citrus Huanglongbing (HLB) or citrus greening, is the most destructive disease for citrus worldwide. It is caused by the psyllid-transmitted, phloem-limited bacteria "*Candidatus* Liberibacter asiaticus" (*C*Las). To date, there are still no effective practical strategies for curing citrus HLB. Understanding the mechanisms against *C*Las can contribute to the development of effective approaches for combatting HLB. However, the unculturable nature of *C*Las has hindered elucidating mechanisms against *C*Las. In this review, we summarize the main aspects that contribute to the understanding about the mechanisms against *C*Las, including (1) *C*Las virulence targets, focusing on inhibition of virulence genes; (2) activation of citrus host defense genes and metabolites of HLB-tolerant citrus triggered by *C*Las, and by agents; and (3) we also review the role of citrus microbiome in combatting *C*Las. Finally, we discuss novel strategies to continue studying mechanisms against *C*Las and the relationship of above aspects.

Keywords: HLB, unculturable bacteria, CLas, citrus defenses, HLB-tolerance

OPEN ACCESS

Edited by:
Changyong Zhou,
Southwest University, China

Reviewed by:
Xuefeng Wang,
Citrus Research Institute, China
Orlando Borras-Hidalgo,
Qilu University of Technology, China

****Correspondence:***
Chuanyu Yang
chuanyu.yang@tamuk.edu
Veronica Ancona
veronica.ancona-contreras@tamuk.edu

Specialty section:
This article was submitted to Microbe and Virus Interactions With Plants, a section of the journal Frontiers in Microbiology

Received: *07 January 2022*
Accepted: *18 February 2022*
Published: *10 March 2022*

Citation:
Yang C and Ancona V (2022) An Overview of the Mechanisms Against "Candidatus Liberibacter asiaticus": Virulence Targets, Citrus Defenses, and Microbiome. Front. Microbiol. 13:850588. doi: 10.3389/fmicb.2022.850588

INTRODUCTION

Citrus Huanglongbing (HLB), or citrus greening, is the most destructive citrus disease worldwide. It is associated with three species of fastidious, phloem-restricted α-proteobacteria: "*Candidatus* Liberibacter asiaticus" (*C*Las), "*Candidatus* Liberibacter americanus"(*C*Lam), and "*Candidatus* Liberibacter africanus" (*C*Laf), which are transmitted by the psyllids *Diaphorina citri* or *Trioza erytreae* (Jagoueix et al., 1994; Bové, 2006; Gottwald, 2010). *C*Las is the most prevalent species found in commercial citrus production regions, including the United States, China, and Brazil (Jagoueix et al., 1994; Bové, 2006; Gottwald, 2010; Bassanezi et al., 2020; Zhou, 2020). HLB symptomology include yellowing of shoots, blotchy mottled leaves, corky veins, malformed and discolored fruits, premature fruit drop, root loss, and eventually tree death (Wang and Trivedi, 2013; Blaustein et al., 2018). Unfortunately, no commercial citrus varieties are resistant to HLB.

The HLB epidemic has affected all major citrus growing regions in the world (Hodges and Spreen, 2012; Kumagai et al., 2013; da Graça et al., 2015; Graham et al., 2020). In the United States, Florida has been the most affected citrus producing state. Since HLB arrival in 2005 (Bové, 2006), citrus production in Florida has decreased by 74% (Singerman and Rogers, 2020). Production losses due to HLB have resulted in the reduction of citrus

growers from 7,389 in 2002 to 2,775 in 2017, juice processing facilities from 41 in 2003/2004 to 14 in 2016/2017, and packinghouses from 79 to 26 during the same period (Singerman and Rogers, 2020). In China, HLB was first reported in Guangdong province nearly a century ago (Reinking, 1919). To date, HLB has occurred in 10 provinces in China, including Guangdong, Guangxi, Fujian, Zhejiang, Jiangxi, Hunan, Guizhou, Hainan, and Sichuan. Especially, citrus production in Guangdong, Guangxi, and Fujian have been affected by HLB for a long time (Zhou, 2020). In Brazil, HLB was first reported in São Paulo State in 2004 (Coletta-Filho et al., 2004). After the first HLB outbreak, the disease spread to the States of Minas Gerais, Paraná and Mato Grosso do Sul, causing reduction of citrus production (Bassanezi et al., 2020).

Currently, many strategies have been developed for HLB mitigation, including application of antimicrobials (Zhang et al., 2011a, 2012, 2014, 2021; Hu and Wang, 2016; Hu et al., 2018; Yang et al., 2018), thermotherapy (Hoffman et al., 2013; Fan et al., 2016; Yang et al., 2016b; Doud et al., 2017; Ghatrehsamani et al., 2019; Vincent et al., 2019), macro-and micronutrients (Spann and Schumann, 2009; Gottwald et al., 2012; Rouse et al., 2017; Mattos-Jr et al., 2020; Dong et al., 2021; Zhou et al., 2021), plant defense inducers (Canales et al., 2016; Li et al., 2016, 2019, 2021a; Hu et al., 2018; Wang, 2021), control of the insect vector (Grafton-Cardwell et al., 2013; Boina and Bloomquist, 2015; Cocuzza et al., 2017; Pierre et al., 2021), biocontrol (Trivedi et al., 2011; Hopkins and Wall, 2021; Nan et al., 2021; Poveda et al., 2021), and eradication of HLB symptomatic citrus trees (Bassanezi et al., 2013; Yuan et al., 2020). However, these strategies have shown limited success in field applications and effective HLB management remains a challenge. Three-pronged approach including control of the psyllid vector, aggressive removal of infected trees to reduce sources of the disease, and planting with HLB-free nursery stock, has proven successful in China and Brazil, and has resulted in drastic reductions in the proportion of symptomatic trees (Bové, 2006). While this approach was advocated early on in Florida's HLB outbreak, it was deemed to be too expensive by most producers, who instead decided to maintain symptomatic trees as long as they were bearing usable fruit (Hall and Gottwald, 2011). In addition, non-uniform distribution of *C*Las within citrus tree (Tatineni et al., 2008; Li et al., 2009) makes early detection of *C*Las very difficult, which is crucial for the management of citrus HLB. Thus, breeding for HLB disease-resistance may provide the most effective and sustainable solution to combat HLB (Bové, 2006).

In order to develop novel and effective strategies to suppress HLB, it is important to understand the virulence mechanisms employed by *C*Las to be able to elucidate potential targets against the pathogen. In this review, we describe the different virulence mechanisms of *C*Las and strategies used to identify virulence inhibitors. We also discuss the role of plant defenses in conferring HLB tolerance and the potential role of the citrus microbiome against *C*Las. We conclude with a discussion about the new pathways for studying this uncultured bacterial pathogen.

*C*LAS VIRULENCE TARGETS

Most insights of *C*Las virulence and biological processes are derived from the genome sequence of *C*Las (Duan et al., 2009), and other related Liberibacters (Coyle et al., 2018). Many putative virulence factors have been identified by utilizing surrogate models, and several strategies also have been developed for targeting these virulence genes associated with *C*Las pathogenicity and survival.

SECRETION SYSTEMS AND EFFECTORS

Systems capable of secreting bacterial proteins, called effectors, into host cells are among the most important virulence factors of bacterial pathogens. Protein effectors often suppress plant defenses or manipulate developmental processes within the host to benefit the pathogen (Jones and Dangl, 2006). *C*Las encodes type I secretion systems (T1SS), a complete general secretory pathway (Sec), and an autotransporter type V secretion system (T5SS), but lacks other secretion systems (Duan et al., 2009; Fagen et al., 2014; Wulff et al., 2014; Wang et al., 2017). The Sec machinery facilitates the majority of proteins transport across the cytoplasmic membrane and is essential for bacterial viability (Segers and Anné, 2011). The Sec apparatus also secretes important virulence factors in some plant-pathogenic bacteria. It has been reported that *C*Las has at least 86 proteins with functional Sec-dependent secretion signals (Prasad et al., 2016). Many of these proteins, also called Sec-delivered effectors (SDEs) are highly conserved in *C*Las genomes and exhibit differential expression patterns in the citrus host and the psyllid vector (Thapa et al., 2020). *C*Las Sec-delivered effector 1 (SDE1, CLIBASIA_05315), is conserved across *C*Las isolates with a typical Sec-dependent secretion signal (Pitino et al., 2016; Prasad et al., 2016; Pagliaccia et al., 2017). SDE1 is highly expressed in citrus relative to psyllid, indicating a plausible role in *C*Las colonization of citrus and HLB disease progression (Yan et al., 2013). SDE1 inhibits the enzymatic activity of citrus papain-like cysteine proteases (PLCPs), which regulate multiple processes in plants, including defense against microbial pathogens (Clark et al., 2018). Other studies also suggested that SDE1 contributes to *C*Las colonization and the development of leaf yellowing symptoms, possibly by promoting premature senescence in citrus (Pitino et al., 2016; Clark et al., 2020). Although, there is no evidence that targeting effectors would lead to *C*Las suppression, targeting the Sec system could inhibit protein translocation and have a significant effect on *C*Las virulence and survival. The SecA ATPase drives protein translocation when it is bound to the SecYEG complex (Economou and Wickner, 1994; Van den Berg et al., 2004). Based on characteristics of SecA, 20 small molecules against *C*Las were identified by molecular docking *in silico*, and five of these compounds were confirmed to have antimicrobial activity *in vitro* using *Agrobacterium tumefaciens* as culturable model (Akula et al., 2012). Using a similarity search methodology, 11 compounds were identified based on the five SecA inhibitors (Hu et al., 2016). Although these 11 compounds had poor

aqueous solubility, they were coupled in a micro-emulsion to assess their antimicrobial activities on eight bacteria phylogenetically related to *C*Las (*A. tumefaciens*, *Liberibacter crescens*, *Rhizobium etli*, *Bradyrhizobium japonicum*, *Mesorhizobium loti*, and *Sinorhizobium meliloti*). The inhibitions obtained from these compounds were similar to those described for streptomycin (Hu et al., 2016). Thus, the compounds targeting SecA, could also inhibit protein translocation in *C*Las and have a significant effect on HLB suppression.

TRANSCRIPTIONAL REGULATORS

The reduced genome of *C*Las has a small number of transcriptional regulators that if targeted by high affinity inhibitors could result in strong reduction of *C*Las fitness and survival (**Table 1**). For instance, the transcriptional regulator *PrbP* was identified and the genome of *C*Las and was shown to bind to specific promoter regions of *C*Las DNA as well as to interact with *RpoB*, the β subunit of RNA polymerase (Gardner et al., 2016). *In vitro* screening of chemical compounds that target this gene identified one compound, tolfenamic acid, that inhibited PrbP/RpoB interaction and *PrbP* DNA binding. Further evaluation showed that tolfenamic acid inhibited *in vitro* growth of *L. crescens*, affected viability of *C*Las in citrus leaf-soaking assays, and reduced *C*Las titers in infected seedlings causing the recovery of roots and canopy tissues (Gardner et al., 2016). The antimicrobial activity of Tolfenamic acid against *C*Las might be the result of targeting key regulatory components that inhibit multiple pathways for bacterial survival.

LdtR belongs to the MarR family transcription regulator and it has been linked to the regulation of more than 180 genes in *Liberibacter* species (Pagliai et al., 2017). In *S. meliloti*, mutation of *LdtR* resulted in morphological changes and reduced tolerance to osmotic stress. Small molecules including benzbromarone that targeted at *LdtR* were identified that caused a phenotype in *S. meliloti* and *L. crescens* similar with the insertional mutants (Pagliai et al., 2014). These small molecules were then assessed *via* a citrus shoot assay and shown to decrease the expression of *LdtR* and a gene regulated by *LdtR* potentially involved in cell wall biosynthesis. Therefore, application of small molecules that target *LdtR*, as a potential treatment option against citrus HLB.

As inhibition of transcriptional regulators provide an alternative method for mitigating *C*Las and HLB, a synthetic, high-throughput screening system to identify molecules that target *C*Las transcriptional regulators was developed (Barnett et al., 2019). This system used the closely related model bacterium, *S. meliloti*, as a heterologous host for expression of the *C*Las transcriptional activator, the activity of which was detected through expression of an enhanced green fluorescent protein (EGFP) gene fused to a target promoter. Around 120,000 compounds were screened by this system to target regulators including *LdtR*, *RpoH*, and *VisNR* and compounds that inhibited regulator activity were selected as candidate compound for combating HLB (Barnett et al., 2019). *C*Las sigma factor *RpoH* is most similar to *RpoH1* in *S. meliloti* (72% identity), which mediate response to various stressors, including heat, acid, hydrogen peroxide, stationary phase growth, and envelope disrupting agents (Mitsui et al., 2004; de Lucena et al., 2010; Barnett et al., 2012). *VisN* and *VisR*, members of the LuxR transcriptional factor family, negatively regulate the expression of the *C*Las pilin gene *flp3*, which is associated with bacterial adherence and psyllid colonization (Andrade and Wang, 2019). Thus, targeting transcriptional regulators is a potential strategy for reducing *C*Las fitness and HLB mitigation.

ROLE OF PROPHAGE IN *C*LAS SURVIVAL

A prophage, also considered as a temperate phage, can integrate into the circular bacterial DNA chromosome, continuing this lysogenic cycle for as long as host physiology remains stable. However, stresses such as heat, UV light, starvation, or chemicals like antibiotics, which cause DNA damage to bacterial cells,

TABLE 1 | Transcriptional regulators in uncultured bacteria *Candidatus* Liberibacter and inhibitors found in surrogate models for screening chemicals targeted the gene.

Transcriptional regulators	Function	Surrogate bacterial models	Inhibitors	References
LdtR	Controlling the expression of nearly 180 genes, distributed in processes such as cell motility, cell wall biogenesis, energy production, and transcription.	*Sinorhizobium meliloti*, and *Liberibacter crescens*	Benzbromarone, phloretin, hexestrol etc.	Pagliai et al., 2014; Barnett et al., 2019
PrbP	Regulating gene expression through interactions with the RNA polymerase β-subunit and a specific sequence on the promoter region	*Liberibacter crescens* and *Escherichia coli*	Tolfenamic acid	Gardner et al., 2016
VisNR	Regulate the expression of the pilin gene *flp3* involved in adhesion and psyllid colonization	*Sinorhizobium meliloti*	Bortezomib, Chemdiv C549-0604, and Chemdiv D244-0326 etc.	Sourjik et al., 2000; Andrade and Wang, 2019; Barnett et al., 2019
RpoH	Alternative sigma factor mediating stress responses including heat, acid, hydrogen peroxide, stationary phase growth, and envelope disrupting agents	*Sinorhizobium meliloti*	Rosiglitazone	Mitsui et al., 2004; de Lucena et al., 2010; Barnett et al., 2012, 2019

activate the "SOS" stress response inducing the excision of phage DNA from the host (Oppenheim et al., 2005). Three prophage regions have been identified in *C*Las and have been classified as SC1, SC2, and SC3, based on genomic data (Zhang et al., 2011b; Zheng et al., 2016, 2018). SC1 carries putative lytic cycle genes, as phage particles in the phloem of infected periwinkle have been observed by transmission electron microscopy, although phage particles have not been observed in citrus (Fleites et al., 2014). SC2 lacks lytic cycle genes and can be integrated in the *C*Las genome or replicate as an excision plasmid prophage (Zhang et al., 2011b). Study of Zhang (2011b) indicated that SC1 and SC2 also encode multiple virulence factors that might contribute to the pathogenicity of *C*Las. Two predicated peroxidases are encoded by SC1 and SC2, which might detoxify *C*Las against reactive oxygen species (ROS), including superoxide radicals, hydrogen peroxide, and hydroxyl radicals. SC1 and SC2 also encode two predicated adhesins, which might be useful in transmission by psyllid (Zhang et al., 2011b). SC3 is not capable of reproduction *via* the lytic cycle. A restriction-modification (R-M) system of SC3 was speculated to play a role against Type 1 prophage-phage invasion (Zheng et al., 2018). The involvement of SC3 in survive of *C*Las still needs to be investigated.

Study of Ding et al. (2018) demonstrated that the relative copy number of both prophage SC1 and SC2 increased in HLB-affected host plants (citrus and periwinkle), in response to heat and antibiotic (tetracycline) treatments. These results suggest a potential mechanism for the activity of heat treatment and antibiotics against HLB through induction of *C*Las prophages causes lysis of *C*Las bacteria, reducing *C*Las population and mitigating HLB symptoms in citrus trees (Ding et al., 2018). Therefore, understanding the factors that trigger the lytic cycle in *C*Las prophages can provide a potential control strategy of citrus HLB.

MECHANISMS OF HLB-TOLERANT CITRUS TO *C*LAS

Citrus Huanglongbing affects all commercial citrus varieties, citrus species, and relatives (Bové, 2006). Nevertheless, several citrus cultivars and relatives have shown tolerance to *C*Las, and many studies have deciphered the mechanism of these tolerance to HLB (**Table 2**). Here, we would discuss host defense genes and metabolites against *C*Las (**Figure 1**).

CITRUS DEFENSE GENES INVOLVED IN COMBATING *C*LAS

Multiple defense genes in HLB-tolerant citrus have been identified by multi-omics approaches (**Table 2**), although just the function of *Constitutive disease resistance* (*CDR*) and Non-expressor of *Pathogenesis Related genes 1* (*NPR1*) was confirmed in surrogate models or citrus.

Constitutive disease resistance genes belong to the plant aspartic proteinase (APs) gene family. *CDR1* was first identified and cloned in *Arabidopsis*. Its product has been implicated in disease resistance signaling (Xia et al., 2004). Overexpression of a rice (*Oryza sativa* L) *CDR 1* gene, led to constitutive activation of defense response and enhanced resistance in rice and *Arabidopsis* against bacterial and fungal pathogens (Prasad et al., 2009). Several studies have demonstrated that *CDR1* as potential candidate genes for HLB tolerance in *Poncirus* (Albrecht and Bowman, 2012; Du et al., 2015; Rawat et al., 2015). A study was undertaken to mine and characterize the *CDR* gene family in Citrus and *Poncirus* and to understand its association with HLB tolerance in *Poncirus*. It found that *PtCDR2* and *PtCDR8* were high abundance in *Poncirus* leaf transcriptomes. The expression of *PtCDR2* and *PtCDR8* genes responded to *C*Las infection differently in HLB-tolerant and susceptible genotypes (Rawat et al., 2017). The role of *PtCDR2* and *PtCDR8* in disease resistance was confirmed in *Arabidopsis* mutants that showed that transformation of *PtCDR2* and *PtCDR8* into *Arabidopsis cdr1* mutant induced *PR1* expression and recovered the hypersensitive response to *Pseudomonas syringae* pv. *tomato* strain DC3000 (Ying et al., 2020). Therefore, *PtCDR2* and *PtCDR8* play a key role in plant defense responses and serve as strong candidate genes for engineering citrus for HLB disease tolerance.

Non-expressor of *Pathogenesis Related genes 1* gene is a key regulator in the signal transduction pathway that leads to SAR response. The *NPR1* gene may act as a regulator of the transcription factor/s that controls *PR* gene expression (Kinkema et al., 2000) and mediates the salicylic acid (SA) induced expression of *PR* genes and SAR (Clarke et al., 1998). Plants over expressing *NPR1* display enhanced resistance to several pathogens (Cao et al., 1998). For instance, transcriptome profiling of HLB-tolerant "Jackson" (grapefruit hybrid) and HLB-susceptible "Marsh" grapefruit found that four *NPR1*-like genes were significantly upregulated in HLB tolerant citrus trees (Wang et al., 2016). Furthermore, transgenic sweet orange cultivars "Hamlin" and "Valencia" expressing an *A. thaliana npr1* gene under the control of a constitutive CaMV 35S promoter or a phloem specific *Arabidopsis* SUC2 (*AtSUC2*) promoter resulted in trees with normal phenotypes that exhibited enhanced resistance to HLB. Additionally, the transgenic trees exhibited reduced diseased severity and a few lines remained disease-free even after 36 months of planting in a high-disease pressure field site (Dutt et al., 2015). *AtNPR1* can enhance expression of transcription of genes encoding pathogen-associated molecular patterns (PAMPs), transcription factors, leucine-rich repeat receptor kinases (LRR-RKs), and putative ankyrin repeat-containing proteins, in *AtNPR1* transgenic line compared to the control plant (Qiu et al., 2020). These results suggested that *NPR1* positively regulates the innate defense mechanisms in citrus, contributing to enhance tolerance to citrus HLB.

ACTIVATION OF ANTIMICROBIAL METABOLITES

Plants have a number of unique defense mechanisms including physical barriers to pathogen invasion as well as a wide range

TABLE 2 | The mechanisms of Citrus Huanglongbing (HLB)-tolerant citrus elucidated by multi-omics approaches.

Citrus genotypes	Putative tolerance mechanisms of citrus to HLB	References
Poncirus trifoliata and *hybrids*	*Constitutive disease resistance 1* (*CDR1*) genes activate *PR1* expression	Folimonova et al., 2009; Albrecht and Bowman, 2011, 2012; Killiny and Hijaz, 2016; Killiny, 2017; Curtolo et al., 2020; Huang et al., 2021b
	Downregulation of gibberellin (GA) synthesis and the induction of cell wall strengthening	
	Poncirus trifoliata hybrids (US-942) have a stronger defense response, more efficient nutrient uptake and increased accumulation of secondary metabolites, flavonoids, phenolics, and volatile organic compounds (VOC).	
	Increased accumulation of phenylalanine, tyrosine, and tryptophan, and some sugars such as mannose, and α-D-mannopyranoside which are important in secondary metabolite biosynthesis and reduction of availability of essential sugars for *Candidatus* Liberibacter asiaticus (*C*Las) survival	
Ichang papeda (*Citrus ichangensis* "2586")	Carbohydrate metabolism, photosynthesis process, and amino acids are not activated during *C*Las infection, which may suppress HLB development	Wu et al., 2020
	Upregulation of genes involved in secondary metabolism, such as the isoprenoid and flavonoid biosynthesis pathways	
"Jackson" grapefruit (*Citrus paradisi* Macf)	Increased expression of *NPR1*-like genes and secondary metabolite pathways	Wang et al., 2016
Mexican lime (*Citrus aurantifolia*)	Increase expression of genes related to cell wall, secondary metabolism, transcription factors, signaling, and redox reactions	Arce-Leal et al., 2020
Rough lemon (*Citrus jambhiri*)	Upregulation of genes involved in maintaining or recovering of phloem transport activity and possible enhancement of stress tolerance	Fan et al., 2012
Kaffir lime (*Citrus hystrix*)	Upregulation of genes involved in cell wall metabolism and secondary metabolism	Zou et al., 2019
	Increased expression of peroxidases, Cu/Zn-SOD, and *POD4* genes	
Sydney hybrid (*Microcitrus virgata*)	Strong defense response upon *C*Las infection, more efficient nutrient uptake and increased accumulation of secondary metabolites, flavonoids, phenolics, and VOC	Huang et al., 2021a,b
Australian finger lime (*Microcitrus australiasica*)	Production of stable antimicrobial peptides, induction of defense responses such as salicylic acid (SA) biosynthesis, phenylpropanoid pathways, and defense genes	Huang et al., 2021a
Volkamer lemon (*Citrus Volkameriana*)	Upregulation of four glutathione-S-transferases proteins involved in radical ion detoxification	Martinelli et al., 2016
Lisbon lemon (*Citrus limon*)	Upregulation of genes involved in defense responses	Ramsey et al., 2020
Curry leaf [*Murraya koenigii* (L.) Spreng]	High level of phenolics and flavonoids with antimicrobial activity	Killiny et al., 2017; Hijaz et al., 2020
LB8-9 Sugar Belle {"Clementine" mandarin (*Citrus reticulata*) × "Minneola" tangelo [(*Citrus x Tangelo*), "Duncan" grapefruit (*Citrus paradisi*) × "Dancy" tangerine (*C. reticulata*)]}	Increased accumulation of phenolics, flavonoids, and VOCs with known antimicrobial activity such as aldehydes, monoterpenes, and sesquiterpenes	Killiny et al., 2017; Deng et al., 2021; Suh et al., 2021
	Increase accumulation of plant hormones responsible for plant growth and phloem regeneration	

of secondary metabolites and antimicrobial peptides (AMP). Secondary metabolites have long been suggested to interact with pathogen (Hartmann, 2008). Several studies have revealed a vast number of secondary metabolites with proven or putative functions in plant responses to pathogen microorganisms (Piasecka et al., 2015). In several HLB-tolerance citrus cultivars, the transcriptomic analysis reveals that most differentially expressed genes (DEGs) increase in secondary metabolites pathways from HLB-tolerant citrus including *Poncirus trifoliata* and its hybrids (Albrecht and Bowman, 2012), "Jackson" (grapefruit hybrid; Wang et al., 2016), Mexican lime (*Citrus aurantifolia*; Arce-Leal et al., 2020), and Kaffir lime (*Citrus hystrix*; Zou et al., 2019). The secondary metabolites are higher in HLB-affected tolerant citrus cultivars, indicating a strong relationship between HLB-tolerance and secondary metabolites accumulation (Rao et al., 2018). In addition, amino acids including phenylalanine, tyrosine, and tryptophan were accumulated on HLB-tolerant citrus relative *P. trifoliata* (Killiny and Hijaz, 2016), which are involved in synthesis of many secondary metabolites. Furthermore, several studies demonstrated that HLB-tolerant citrus including US-942 (*P. trifoliata*×*Citrus reticulata*), Curry leaf [*Murraya koenigii* (L.) Spreng], and LB8-9 Sugar Belle contained high level of secondary metabolites such as volatile organic compounds (VOC), phenolics, and flavonoids (Killiny et al., 2017; Hijaz et al., 2020; Deng et al., 2021; Huang et al., 2021b).

Volatile organic compounds play a key role in protecting plants under insect and pathogen attack. VOCs, including aldehydes, monoterpenes, sesquiterpenes, thymol, b-elemene, and (E)-b-caryophyllene, have antimicrobial activities against pathogens, and accumulate in HLB-tolerant LB8-9 Sugar Belle (Killiny, 2017; Deng et al., 2021). Phenolics are a group of secondary metabolites, which are produced *via* the shikimic acid pathway through the phenylpropanoid pathway (Lin et al., 2016). It has been demonstrated that the accumulation of phenolic compounds at the infection site could result in pathogen restriction and prevention of their spread to other plant's tissues (Nicholson and Hammerschmidt, 1992). Flavonoids are widely distributed in plants and they are synthesized in the cytosol through the phenylpropanoid pathway by a set of enzymes (Treutter, 2006; Petrussa et al., 2013). Flavonoids could exhibit their resistance to pathogens by inhibition and crosslinking of the microbial enzymes, chelation of metals necessary for enzyme activity, and formation of physical barrier (Treutter, 2006). The HLB-tolerant

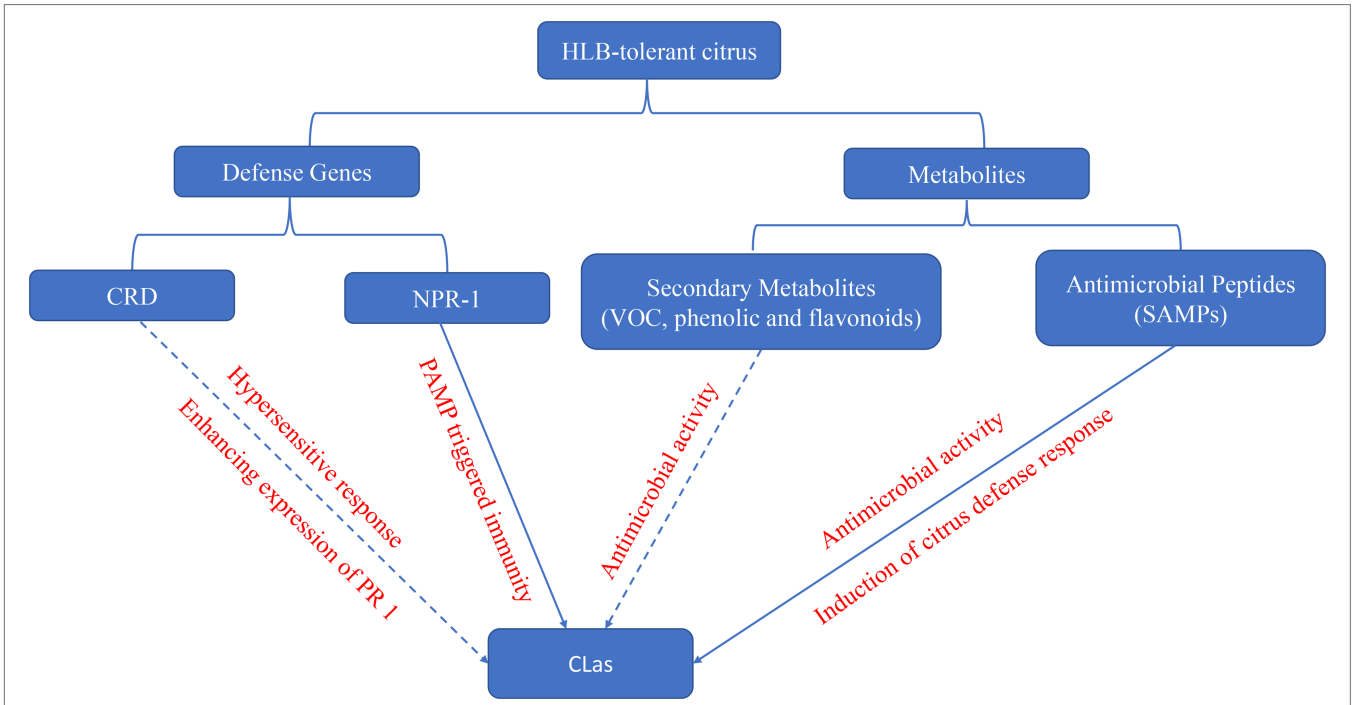

FIGURE 1 | The potential mechanism of defense genes and metabolites in HLB-tolerant citrus against *C*Las. Solid line indicates that the functions were confirmed in citrus, and dash line indicates that the function were just confirmed in other species.

Curry leaf [*M. koenigii* (L.) Spreng] and LB8-9 Sugar Belle contain high level of phenolics and flavonoids, which correlate with their enhanced tolerance to *C*Las (Killiny et al., 2017; Hijaz et al., 2020). Therefore, increased levels of VOCs, phenolics, and flavonoids in citrus may contribute to HLB tolerance.

Antimicrobial peptides stand out as one of the most prominent components of the plant immune system. These small and usually basic peptides are deployed as a generalist defense strategy that grants direct and durable resistance against plant pathogens. A recent study identified a novel class of heat stable antimicrobial peptides (SAMPs), from HLB-tolerant citrus Australian finger lime (*Microcitrus australiasica*). SAMPs not only effectively reduced *C*Las titer and disease symptoms in HLB-positive trees but also prevented and inhibited infections by induction of defense response genes such as *PR1* and *PR2*, an enzyme of SA biosynthesis, phenylpropanoid pathways, and phenylalanine ammonia-lyase 1(PAL; Huang et al., 2021a). Thus, HLB-tolerant citrus can also be a source of defense peptides against *C*Las.

HOST DEFENSE TRIGGERED BY AGENTS

Citrus defense mechanisms not only can be activated by pathogens, but also induced by agents such as chemical compounds, heat and nutrients. Systemic acquired resistance (SAR) can be useful to control of several plant diseases (Ryals et al., 1996; Sticher et al., 1997; Durrant and Dong, 2004). SAR involves in a specific defense signaling pathway that required SA and is associated with accumulation of pathogenesis-related proteins (PR). Several chemical compounds can activate SAR in plant. Four SAR activators including SA, oxalic acid, acibenzolar-S-methyl, and potassium phosphate, provided significant control of HLB by suppressing *C*Las titer and disease progress when applied by trunk injection (Hu et al., 2018). Furthermore, both SA and acibenzolar-S-methyl significantly induced expression of *PR-1* and *PR-2* genes, and oxalic acid and potassium phosphate resulted in significant induction of *PR-2* and *PR-15* gene expression, respectively (Hu et al., 2018). In addition, foliar spray application of several plant defense inducers [i.e., β-aminobutyric acid (BABA), 2,1,3-benzothiadiazole (BTH), 2,6-dichloroisonicotinic acid (INA), and ascorbic acid (AA)] were reported to suppress progress of HLB in the field. BTH and INA, which are functional analogs of SA, can induce plant defenses in citrus. The effect control of BABA on citrus HLB may be in SA-depend pathway. Furthermore, AA may alleviate HLB symptoms by interfering with biosynthesis of plant hormones (including salicylic acid and jasmonic acid; Li et al., 2016). Other plant hormones, such as brassinosteroids, can induce plant defenses against a wide range of pathogens including *C*Las. Foliar spray of brassinosteroid (24-epibrassinolide) in greenhouse and field experiments of HLB-affected citrus showed *C*Las titer was reduction after treatment under both conditions (Canales et al., 2016). Moreover, several chemical compounds have antimicrobial activities against *C*Las, and can also induce plant defense against the pathogen. Sulphonamide antibiotics such as sulfadimethoxine

sodium (SDX) and sulfathiazole sodium (STZ) have been proved to be effective against *C*Las (Zhang et al., 2014; Yang et al., 2016a). Transcriptomic analysis of citrus plants revealed that SDX can induce genes related to the metabolism of jasmonates, brassinosteroids, ROS, and secondary metabolites, which are beneficial for resistance against HLB (Yang et al., 2020b; **Table 3**).

Candidatus Liberibacter asiaticus is a heat-tolerant bacterium and can thrive under high temperature conditions extending to 35°C (Lopes et al., 2009). Many studies demonstrated that heat treatment (temperature ranged from 40 to 50°C) can eliminate or suppress *C*Las titer in HLB-affected citrus (Hoffman et al., 2013; Fan et al., 2016; Yang et al., 2016a,b). Moreover, the heat treatment also can enhance vigor of HLB-affected citrus and promote new flush (Hoffman et al., 2013; Yang et al., 2016b; Armstrong et al., 2021). Transcriptome analysis has shown that the gene expression profiles of HLB-affected trees post solar-heat treatment more closely modeled healthy trees than their gene profiles prior to treatment, with many genes involved in plant-bacterium interactions being upregulated post treatment, which may contribute to host defense against *C*Las (Doud et al., 2017). In addition, proteomics analysis indicated that a strong upregulation of chaperones including small (23.6, 18.5, and 17.9 kDa) heat shock proteins, a HSP70-like protein and a ribulose-1,5-bisphosphate carboxylase oxygenase (RuBisCO)-binding 60 kDa chaperonin, in response to heat treatment (40°C), which has been involved in reversing the effects of *C*Las infection in citrus plants (Nwugo et al., 2016; **Table 3**).

For several years, it has been reported that the application of enhanced nutritional products can extend the vigor of HLB-affected citrus and trigger citrus defense against *C*Las (Spann and Schumann, 2009; Shen et al., 2013; da Silva et al., 2020; Shahzad et al., 2020; Dong et al., 2021). Although nutrient treatments have no effect on reducing *C*Las titer and cannot enhance yield of HLB-affected citrus in the field (Gottwald et al., 2012; da Silva et al., 2020; Phuyal et al., 2020), the application of macro-and micronutrients have been adopted worldwide as they induce host defenses and help maintain production of HLB-affected trees. For instance, a field study in Florida showed application of phosphorus (P) oxyanion solutions to HLB-affected citrus mitigated disease symptom severity during a 3-year field trial (Zhao et al., 2013). It is known that phosphite has a direct action on plant defense mechanisms by the activation of the PAL activity and the biosynthesis of phytoalexins (Saindrenan and Guest, 1994), which may be involved in citrus defense induced by P. HLB-affected citrus display interveinal chlorotic leaves due to iron (Fe) deficiency caused by *C*Las (Masaoka et al., 2011) and foliar application of Fe^{2+} have shown to alleviate symptoms of HLB-affected citrus trees (Inoue et al., 2020). In other pathosystems, such as in rice-*Magnoporthe* interactions, rice plants growing at high Fe levels have enhanced resistance against the fungus. Although this has not been evaluated, application of Fe may induce host defense against *C*Las (Peris-Peris et al., 2017). Recent research indicates that elevated levels of manganese (Mn) promote better tree response to the effects of HLB increasing citrus tree lifespan (Morgan et al., 2016; Zambon et al., 2019). Sufficient Mn in the rhizosphere is critical for scavenging ROS (Alscher et al., 2002), which is known to be produced extensively in *C*Las-damaged cells (Ma et al., 2022). Although many nutrients can mitigate symptoms of HLB-affected trees, the mechanisms of how these nutrients trigger citrus defenses are still unclear and warrant investigation.

TABLE 3 | Chemicals and heat activate citrus defense response.

Agent types	Name	Mechanisms against *C*Las	References
Chemicals	Salicylic acid	Induction of expression of *PR-1* and *PR-2* genes	Hu et al., 2018
	Acibenzolar-S-methyl	Induction of expression of *PR-1* and *PR-2* genes	Hu et al., 2018
	Oxalic acid	Induction of *PR-2* gene expression	Hu et al., 2018
	Potassium phosphate	Induction of *PR-15* gene expression	Hu et al., 2018
	β-Aminobutyric acid	Involving in SA-depend pathway	Li et al., 2016
	2,1,3-Benzothiadiazole	Functional analogs of SA	Li et al., 2016
	2,6-Dichloroisonicotinic acid	Functional analogs of SA	Li et al., 2016
	Ascorbic acid	Interfering with biosynthesis of plant hormones and the signaling process	Li et al., 2016
	24-Epibrassinolide	Induction of some plant defense genes such as glutathione peroxidase, Jasmonate acid	Canales et al., 2016
	Sulfadimethoxine sodium	Induction of genes related to the metabolism of jasmonates, brassinosteroids, reactive oxygen species (ROS), and secondary metabolites	Yang et al., 2020b
Heat	Solar thermotherapy	Many genes involved in plant-bacterium interactions being upregulated post treatment, which may be contributed to host defense against *C*Las	Doud et al., 2017
	Heat treatment (40°C)	A strong upregulation of chaperones involved in reversing the effects of *C*Las infection in citrus plants	Nwugo et al., 2016

ROLE OF CITRUS MICROBIOME IN COMBATTING *C*LAS

The plant microbiome is an important contributor to plant health and defense against pathogens. Plant-associated microbiota

can suppress pathogens through direct competition, producing antimicrobial compounds or stimulating plant immunity to resist or tolerate pathogen infection (Saikkonen et al., 2004; Kaul et al., 2016; Brader et al., 2017). To date, a plethora of studies have focused on deciphering the role of the citrus microbiome with the goal of identifying members of the microbial community associated with HLB and *C*Las suppression. However, comparison of microbiomes from healthy and HLB-affected citrus have shown that *C*Las affects the microbial community structure and reduce the putative beneficial microbe associations within citrus leaves and roots (Trivedi et al., 2011; Zhang et al., 2017; Ginnan et al., 2020; Yan et al., 2021).

For example, *C*Las infection in mandarin leaves (*C. reticulata* cv. Shatangju) causes reduction of several beneficial bacteria genera including *Variovorax*, *Novosphingobium*, *Methylobacillus*, *Methylotenera*, and *Lysobacters*, which are known to be involved in promoting plant growth and antibiotic production (Yan et al., 2021). Study of Blaustein (2017)identified citrus-health-associated endophytes of leaves (such as *Methylpbacterium*, *Burkholderia*, and *Sphingomonas*) and roots (*Bradyrhizobiaceae*) based on increased relative abundances in healthy vs. HLB-diseased citrus trees. These potential beneficial microbes are known to be involved in competing with pathogens for nutrients, antagonize pathogens through antibiosis, assist the host with nutrient acquisition, and induce host defense responses (Compant et al., 2005; Madhaiyan et al., 2006; Enya et al., 2007; Lugtenberg and Kamilova, 2009; Verma et al., 2010; Innerebner et al., 2011; Ardanov et al., 2012). However, their reduction in HLB-affected citrus provides insights into the role of the microbial community into HLB progression.

Interestingly, inoculations of *Burkholderia* stains isolated from the rhizosphere of healthy citrus roots can induce the expression of genes involved in activation of citrus defenses and SA mediated induced systemic resistance (Zhang et al., 2017). Other studies have shown that *Bacillus* sp. can also induce host defense responses against *C*Las through enhancing expression of several transcription factors involved in disease resistance (Tang et al., 2018; Munir et al., 2020). Moreover, when the biocontrol agent *Xylella fastidiosa* strain EB92-1 was applied to HLB-affected citrus plants, the results indicated that it could reduce the incidence of HLB symptoms in mature trees through 18 months after inoculation and the incidence of severe symptoms up to 3 years (Hopkins and Wall, 2021). Although the mechanism of HLB suppression by *X. fastidiosa* EB92-1 and the other bacteria remain to be studied in depth, these studies show that beneficial bacteria can be used to suppress *C*Las and improve plant health by induction of plant defenses that confer broad-spectrum resistance against pathogens.

Manipulation of the citrus microbiome to enrich the populations of beneficial microbes in HLB-affected trees could aid in disease suppression. Actually, nutrients play a role in activating plant immunity system by altering the microbial community structure and the metabolism (Sugimoto et al., 2010; Shi et al., 2012; Huber and Jones, 2013). A recent study has reported that application of calcium, magnesium, and boron to the soil can alter microbial structure and communities in phyllosphere and rhizosphere of HLB-affected citrus and promoted beneficial microorganism (*Burkholderiaceae*, *Xanthomonas*, and *Stenotrophomonas*) enrichment, which may have contributed to the reduced HLB incidence, and *C*Las titers (Zhou et al., 2021).

Chemotherapy is another method that can shape the citrus microbiome. Antimicrobial activity of the effective antibiotics against *C*Las have been associated with shifts in endophytic microbial structure and communities in HLB-affected citrus after treatment (Zhang et al., 2014; Yang et al., 2015, 2020a; Li et al., 2019). Foliar application of penicillin and oxytetracycline to HLB-affected citrus, caused an increase in the relative abundance of beneficial bacterial species, including *Streptomyces avermitilis* and *Bradyrhizobium*, compared to those treated with water control (Yang et al., 2020a). Moreover, the relative abundance of the bacterial species associated with *C*Las survival, such as *Propionibacterium acnes* and *Synechocystis* sp. PCC 6803, was lower in penicillin and oxytetracycline treated plants compared to the control (Yang et al., 2020a). Other studies have shown that the endophytic microbiome was altered in HLB-affected scion treated with ampicillin, and 10 abundant operational taxonomic units (OTUs) from antibiotic producing *Stenotrophomonas* spp. were only detected in the ampicillin-treatment (Zhang et al., 2013). Study of Ascunce et al. (2019) also showed that Bacilli, involved in the elicitation of plant defenses against pests and pathogens, were relatively more abundant in petioles and roots from penicillin treated HLB-affected citrus. Moreover, it was also found that the endophytic microbiome was changed in HLB-affected citrus plants under heat and sulfonamide (sulfathiazole sodium–STZ, and sulfadimethoxine sodium—SDX) treatments (Yang et al., 2016a). Following antibiotic treatment with SDX and STZ, there was enhanced abundance of OTUs belonging to the families *Streptomycetaceae*, *Desulfobacteraceae*, *Chitinophagaceae*, and *Xanthomonadaceae*, which are beneficial for control of plant pathogens and promoting plant growth (Hell, 1997; Kim and Jung, 2007; Mhedbi-Hajri et al., 2011; Mendes et al., 2013). Therefore, the enrichment of beneficial bacteria in these antibiotic treatments, may be contributed to their antimicrobial activity against *C*Las.

It is clear that the citrus microbiome plays a key role in citrus health. Whether some bacteria have an effect in survival of *C*Las is still unclear. The enrichment of beneficial bacteria in healthy citrus or in response to effective chemical compounds, may be involved in combating *C*Las. However, more studies are needed to validate the role of beneficial bacteria in citrus, and identify antagonistic bacteria against *C*Las (Trivedi et al., 2011; Riera et al., 2017; Zhang et al., 2017). Therefore, isolation and identification of the enriched beneficial bacteria can provide more insight into the role of citrus microbiome in HLB mitigation.

NEW APPROACHES FOR STUDYING MECHANISMS AGAINST UNCULTURED BACTERIAL PATHOGENS

Despite the advances in uncovering virulence mechanisms of *C*Las, identification of genes conferring disease tolerance, discovering potential antagonistic bacteria, and identifying many

small molecules that inhibit *C*Las, we are still far from deploying sustainable solutions to the HLB epidemic.

Establishing *C*Las in culture can provide an extended vision in mechanism of agents against *C*Las. Although several reports of transient *C*Las cultures have been published, most of these attempts have only been able to maintain *C*Las in coculture (Davis et al., 2008; Parker et al., 2014; Fujiwara et al., 2018; Ha et al., 2019; Merfa et al., 2019). These studies partially fulfilled Koch's postulates and could potentially be used to unravel the complex relationships of *C*Las with other citrus endophytes; however, no follow-up research using these approaches to obtain a pure *C*Las culture has been published. Currently, the methods employed to study the mode of action of small molecules with antimicrobial activity have been elucidated *in vitro* using as culturable surrogate models such as *L. crescens* and *S. meliloti* (Pagliai et al., 2014; Barnett et al., 2019). However, all sequenced *C*Las strains have reduced genome size of about 1.2 Mb (Duan et al., 2009; Thapa et al., 2020), compared with the slightly larger 1.5 Mb of *L. crescens* BT-1 (Leonard et al., 2012), and the about 6.7 Mb genome of the phylogenetically related *S. meliloti* (Sugawara et al., 2013) which could cause differences in biosynthetic pathways, metabolic enzymes, and secretion systems. Therefore, novel approaches are needed to uncover how chemicals, nutrition, beneficial microorganisms or hosts, directly or indirectly affect *C*Las. One such approach is the recent development of a plant hairy root system that mimics the host environment and supports the growth of *C*Las (Irigoyen et al., 2020). This system was developed as a tool for high throughput screening of antimicrobials against *C*Las and *Candidatus* Liberibacter solanacearum (CLso), which is faster and more reliable compared to conventional compound screening approaches (Irigoyen et al., 2020). Thus, this system could also be used as a model to study the mode of action of antimicrobials against *C*Las inside the citrus host.

Uncovering the complex interactions of *C*Las and the host, is key to discover pathways that can be exploited for disease suppression. However, genome-wide transcriptome profiling of a phloem-restricted pathogen in planta is very difficult, since the bacterial mRNA constitutes a minor fraction of the total mRNA. Thus, most research has focused on gene expression of the citrus host, and smaller number of studies describe global gene expression profiles of the pathogen. To examine the expression profiles of *C*Las in the host, most studies rely on quantitative reverse transcription-polymerase chain reaction approaches which only address targeted genes. *In vivo* transcriptomic analyses are required to understand the active pathways in *C*Las. A recent study identified the regions in the citrus fruit pith with higher bacterial titers which was used to conduct RNA-seq analysis after rRNA removal (Fang et al., 2021). This study compared the gene expression profiles of the fruit pit vs. leaf midribs and found different gene expression profiles related to virulence genes; however, the resolution of the transcriptome profile was lower in midribs compared to fruit pit mainly due to the lower bacterial titers (Fang et al., 2021).

Because the main limitation of conducting transcriptomic profiles of *C*Las is bacterial titers, different enrichment approaches are being developed. A *C*Las enrichment system using dodder showed about 419-fold *C*Las titer increase in dodder system as compared to the corresponding citrus hosts, and the dual RNA-seq data indicated that similar *C*Las gene expression profiles in dodder and citrus samples, yet dodder samples generated a higher solution than those obtained in citrus host (Li et al., 2021b). Although the *C*Las-enrichment dodder system could be used as surrogate model for studying interaction of *C*Las and host, dodder defense system against *C*Las is very different from citrus. To overcome the limitation of surrogate systems, a bacterial cell enrichment procedure has been developed

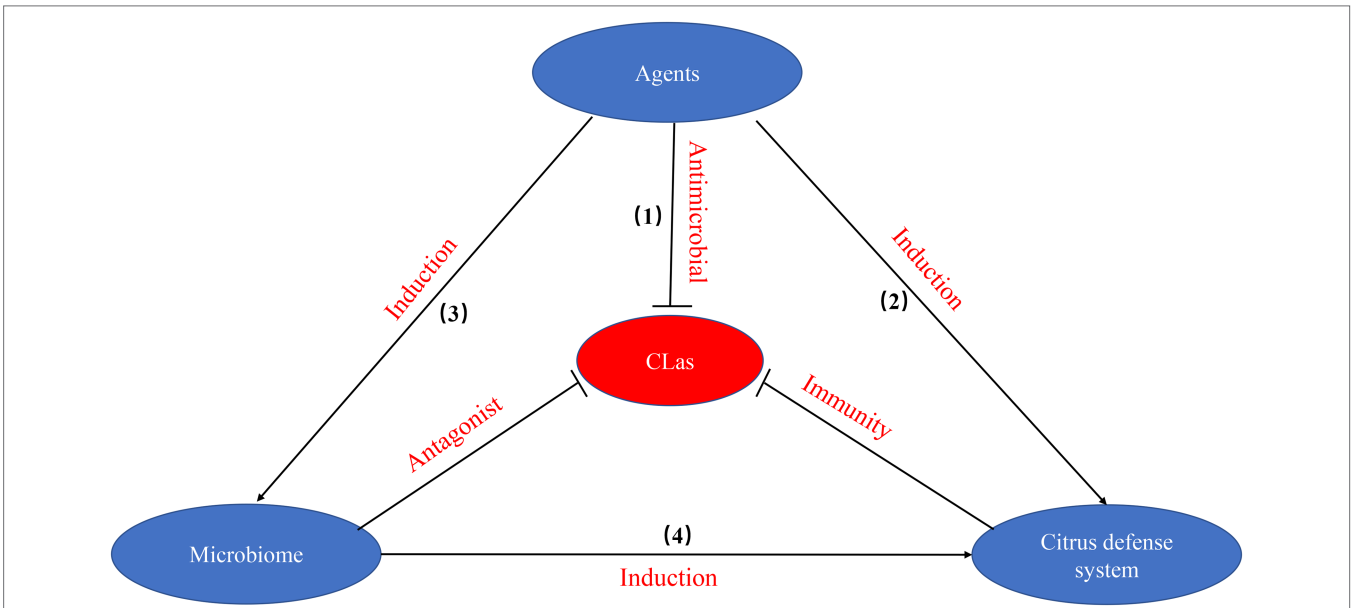

FIGURE 2 | The pathways involved in effective agents including chemicals, nutrition, and plant defense activators against CLas.

for transcriptome profiling of *C*Las in citrus in which bacteria is isolated from citrus samples prior to RNA extraction, reaching detectable expression to 84% of the *C*Las genome coverage (De Francesco et al., 2022). This *C*Las-enrichment method will be useful for mechanisms of *C*Las within the citrus host and for elucidating potential targets for *C*Las suppression.

CONCLUSION

The mechanisms to study phloem-limited and uncultured plant bacterial pathogens are a complicated process. The development of novel approaches to understand the virulence mechanisms of the pathogen, the mode of action of antimicrobial therapies, the interactions with host and other endophytic microbes will aid in the search of effective and sustainable methods to combat *C*Las and ultimately HLB.

Until we unravel the mechanistic black box in the interactions between citrus phloem and *C*Las, the combination of effective agents including chemicals, nutrition, and plant defense activators will continue to be the only path to combat HLB (**Figure 2**). To effectively combat HLB, multiple strategies need to be applied against *C*Las: (1) the use of antimicrobial agents that directly disturb the biological processes of *C*Las, thus affecting bacterial survival; (2) the use of chemical agents that suppress *C*Las by inducing citrus host defense systems; (3) modifying the environment by agents to promote the enrichment of beneficial bacteria to antagonize *C*Las; and (4) the enrichment of beneficial bacteria that trigger citrus defense system against *C*Las. These pathways may work separately or together to promote tree health, mitigate HLB and recover tree productivity. Therefore, the relationship of virulence targets, citrus defenses and microbiome plays a key role in elucidating mechanisms against *C*Las.

AUTHOR CONTRIBUTIONS

CY and VA contributed to writing and editing this manuscript. All authors read and approved the final version of the manuscript.

FUNDING

This study was supported by funds from the USDA-NIFA-SCRI (2019-70016-29096, 2018-70016-28198, and 2016-70016-24833) to VA.

REFERENCES

Akula, N., Trivedi, P., Han, F. Q., and Wang, N. (2012). Identification of small molecule inhibitors against SecA of *Candidatus* Liberibacter asiaticus by structure based design. *Eur. J. Med. Chem.* 54, 919–924. doi: 10.1016/j.ejmech.2012.05.035

Albrecht, U., and Bowman, K. D. (2011). Tolerance of the trifoliate citrus hybrid US-897 (*Citrus reticulata* Blanco× *Poncirus trifoliata* L. Raf.) to huanglongbing. *HortScience* 46, 16–22. doi: 10.21273/HORTSCI.46.1.16

Albrecht, U., and Bowman, K. D. (2012). Transcriptional response of susceptible and tolerant citrus to infection with *Candidatus* Liberibacter asiaticus. *Plant Sci.* 185–186, 118–130. doi: 10.1016/j.plantsci.2011.09.008

Alscher, R. G., Erturk, N., and Heath, L. S. (2002). Role of superoxide dismutases (SODs) in controlling oxidative stress in plants. *J. Exp. Bot.* 53, 1331–1341. doi: 10.1093/jexbot/53.372.1331

Andrade, M., and Wang, N. (2019). The tad pilus apparatus of '*Candidatus* Liberibacter asiaticus' and its regulation by VisNR. *Mol. Plant-Microbe Interact.* 32, 1175–1187. doi: 10.1094/MPMI-02-19-0052-R

Arce-Leal, Á. P., Bautista, R., Rodríguez-Negrete, E. A., Manzanilla-Ramírez, M. Á., Velázquez-Monreal, J. J., Santos-Cervantes, M. E., et al. (2020). Gene expression profile of Mexican lime (*Citrus aurantifolia*) trees in response to huanglongbing disease caused by *Candidatus* Liberibacter asiaticus. *Microorganisms* 8:528. doi: 10.3390/microorganisms8040528

Ardanov, P., Sessitsch, A., Häggman, H., Kozyrovska, N., and Pirttilä, A. M. (2012). Methylobacterium-induced endophyte community changes correspond with protection of plants against pathogen attack. *PLoS One* 7:e46802. doi: 10.1371/journal.pone.0046802

Armstrong, C. M., Doud, M. S., Luo, W., Raithore, S., Baldwin, E. A., Zhao, W., et al. (2021). Beneficial horticultural responses from the application of solar thermotherapy to mature huanglongbing-affected citrus trees. *Horticult. Plant J.* 7, 411–422. doi: 10.1016/j.hpj.2021.04.008

Ascunce, M. S., Shin, K., Huguet-Tapia, J. C., Poudel, R., Garrett, K. A., Van Bruggen, A. H., et al. (2019). Penicillin trunk injection affects bacterial community structure in citrus trees. *Microb. Ecol.* 78, 457–469. doi: 10.1007/s00248-018-1302-1

Barnett, M. J., Bittner, A. N., Toman, C. J., Oke, V., and Long, S. R. (2012). Dual RpoH sigma factors and transcriptional plasticity in a symbiotic bacterium. *J. Bacteriol.* 194, 4983–4994. doi: 10.1128/JB.00449-12

Barnett, M. J., Solow-Cordero, D. E., and Long, S. R. (2019). A high-throughput system to identify inhibitors of *Candidatus* Liberibacter asiaticus transcription regulators. *Proc. Natl. Acad. Sci. U. S. A.* 116, 18009–18014. doi: 10.1073/pnas.1905149116

Bassanezi, R., Belasque, J., and Montesino, L. (2013). Frequency of symptomatic trees removal in small citrus blocks on citrus huanglongbing epidemics. *Crop Prot.* 52, 72–77. doi: 10.1016/j.cropro.2013.05.012

Bassanezi, R. B., Lopes, S. A., De Miranda, M. P., Wulff, N. A., Volpe, H. X. L., and Ayres, A. J. (2020). Overview of citrus huanglongbing spread and management strategies in Brazil. *Trop. Plant Pathol.* 45, 251–264. doi: 10.1007/s40858-020-00343-y

Blaustein, R. A., Lorca, G. L., Meyer, J. L., Gonzalez, C. F., and Teplitski, M. (2017). Defining the core citrus leaf-and root-associated microbiota: Factors associated with community structure and implications for managing huanglongbing (citrus greening) disease. *Appl. Environ. Microbiol.* 83, e00210–00217. doi: 10.1128/AEM.00210-17

Blaustein, R. A., Lorca, G. L., and Teplitski, M. (2018). Challenges for managing *Candidatus* Liberibacter spp. (huanglongbing disease pathogen): current control measures and future directions. *Phytopathology* 108, 424–435. doi: 10.1094/PHYTO-07-17-0260-RVW

Boina, D. R., and Bloomquist, J. R. (2015). Chemical control of the Asian citrus psyllid and of huanglongbing disease in citrus. *Pest Manag. Sci.* 71, 808–823. doi: 10.1002/ps.3957

Bové, J. M. (2006). Huanglongbing: a destructive, newly-emerging, century-old disease of citrus. *J. Plant Pathol.* 88, 7–37. doi: 10.4454/jpp.v88i1.828

Brader, G., Compant, S., Vescio, K., Mitter, B., Trognitz, F., Ma, L.-J., et al. (2017). Ecology and genomic insights into plant-pathogenic and plant-nonpathogenic endophytes. *Annu. Rev. Phytopathol.* 55, 61–83. doi: 10.1146/annurev-phyto-080516-035641

Canales, E., Coll, Y., Hernández, I., Portieles, R., García, M. R., López, Y., et al. (2016). '*Candidatus* Liberibacter asiaticus', causal agent of citrus huanglongbing, is reduced by treatment with brassinosteroids. *PLoS One* 11:e0146223. doi: 10.1371/journal.pone.0146223

Cao, H., Li, X., and Dong, X. (1998). Generation of broad-spectrum disease resistance by overexpression of an essential regulatory gene in systemic acquired resistance. *Proc. Natl. Acad. Sci. U. S. A.* 95, 6531–6536. doi: 10.1073/pnas.95.11.6531

Clark, K., Franco, J. Y., Schwizer, S., Pang, Z., Hawara, E., Liebrand, T. W., et al. (2018). An effector from the huanglongbing-associated pathogen targets citrus proteases. *Nat. Commun.* 9, 1–11. doi: 10.1038/s41467-018-04140-9

Clark, K. J., Pang, Z., Trinh, J., Wang, N., and Ma, W. (2020). Sec-delivered effector 1 (SDE1) of '*Candidatus* Liberibacter asiaticus' promotes citrus huanglongbing. *Mol. Plant-Microbe Interact.* 33, 1394–1404. doi: 10.1094/MPMI-05-20-0123-R

Clarke, J. D., Liu, Y., Klessig, D. F., and Dong, X. (1998). Uncoupling PR gene expression from NPR1 and bacterial resistance: characterization of the dominant *Arabidopsis* cpr6-1 mutant. *Plant Cell* 10, 557–569. doi: 10.1105/tpc.10.4.557

Cocuzza, G. E. M., Alberto, U., Hernández-Suárez, E., Siverio, F., Di Silvestro, S., Tena, A., et al. (2017). A review on *Trioza erytreae* (African citrus psyllid), now in mainland Europe, and its potential risk as vector of huanglongbing (HLB) in citrus. *J. Pest. Sci.* 90, 1–17. doi: 10.1007/s10340-016-0804-1

Coletta-Filho, H., Targon, M., Takita, M., De Negri, J., Pompeu, J., Machado, M., et al. (2004). First report of the causal agent of huanglongbing ("*Candidatus* Liberibacter asiaticus") in Brazil. *Plant Dis.* 88:1382. doi: 10.1094/PDIS.2004.88.12.1382C

Compant, S., Reiter, B., Sessitsch, A., Nowak, J., Clément, C., and Barka, E. D. A. (2005). Endophytic colonization of *Vitis vinifera* L. by plant growth-promoting bacterium *Burkholderia* sp. strain PsJN. *Appl. Environ. Microbiol.* 71, 1685–1693. doi: 10.1128/AEM.71.4.1685-1693.2005

Coyle, J. F., Lorca, G. L., and Gonzalez, C. F. (2018). Understanding the physiology of *Liberibacter asiaticus*: an overview of the demonstrated molecular mechanisms. *J. Mol. Microbiol. Biotechnol.* 28, 116–127. doi: 10.1159/000492386

Curtolo, M., De Souza Pacheco, I., Boava, L. P., Takita, M. A., Granato, L. M., Galdeano, D. M., et al. (2020). Wide-ranging transcriptomic analysis of *Poncirus trifoliata*, *Citrus sunki*, *Citrus sinensis* and contrasting hybrids reveals HLB tolerance mechanisms. *Sci. Rep.* 10, 1–14. doi: 10.1038/s41598-020-77840-2

Da Graça, J., Kunta, M., Sétamou, M., Rascoe, J., Li, W., Nakhla, M., et al. (2015). Huanglongbing in Texas: report on the first detections in commercial citrus. *J. Citrus Pathol.* 2

Da Silva, J. R., De Alvarenga, F. V., Boaretto, R. M., Lopes, J. R. S., Quaggio, J. A., Coletta Filho, H. D., et al. (2020). Following the effects of micronutrient supply in HLB-infected trees: plant responses and '*Candidatus* Liberibacter asiaticus' acquisition by the Asian citrus psyllid. *Trop. Plant Pathol.* 45, 597–610. doi: 10.1007/s40858-020-00370-9

Davis, M. J., Mondal, S. N., Chen, H., Rogers, M. E., and Brlansky, R. H. (2008). Co-cultivation of '*Candidatus* Liberibacter asiaticus' with actinobacteria from citrus with huanglongbing. *Plant Dis.* 92, 1547–1550. doi: 10.1094/PDIS-92-11-1547

De Francesco, A., Lovelace, A. H., Shaw, D., Qiu, M., Wang, Y., Gurung, F., et al. (2022). Transcriptome profiling of '*Candidatus* Liberibacter asiaticus' in citrus and psyllids. *Phytopathology* 112, 116–130. doi: 10.1094/PHYTO-08-21-0327-FI

De Lucena, D. K., Pühler, A., and Weidner, S. (2010). The role of sigma factor RpoH1 in the pH stress response of *Sinorhizobium meliloti*. *BMC Microbiol.* 10, 1–17. doi: 10.1186/1471-2180-10-265

Deng, H., Zhang, Y., Reuss, L., Suh, J. H., Yu, Q., Liang, G., et al. (2021). Comparative leaf volatile profiles of two contrasting mandarin cultivars against *Candidatus* Liberibacter asiaticus infection illustrate huanglongbing tolerance mechanisms. *J. Agric. Food Chem.* 69, 10869–10884. doi: 10.1021/acs.jafc.1c02875

Ding, F., Allen, V., Luo, W., Zhang, S., and Duan, Y. (2018). Molecular mechanisms underlying heat or tetracycline treatments for citrus HLB control. *Hortic. Res.* 5, 1–11. doi: 10.1038/s41438-018-0038-x

Dong, Z., Srivastava, A. K., Liu, X., Riaz, M., Gao, Y., Liang, X., et al. (2021). Interactions between nutrient and huanglongbing pathogen in citrus: an overview and implications. *Sci. Hortic.* 290:110511. doi: 10.1016/j.scienta.2021.110511

Doud, M. M., Wang, Y., Hoffman, M. T., Latza, C. L., Luo, W., Armstrong, C. M., et al. (2017). Solar thermotherapy reduces the titer of *Candidatus* Liberibacter asiaticus and enhances canopy growth by altering gene expression profiles in HLB-affected citrus plants. *Hortic. Res.* 4, 1–9. doi: 10.1038/hortres.2017.54

Du, D., Rawat, N., Deng, Z., and Gmitter, F. G. (2015). Construction of citrus gene coexpression networks from microarray data using random matrix theory. *Hortic. Res.* 2, 1–8. doi: 10.1038/hortres.2015.26

Duan, Y., Zhou, L., Hall, D. G., Li, W., Doddapaneni, H., Lin, H., et al. (2009). Complete genome sequence of citrus huanglongbing bacterium, '*Candidatus* Liberibacter asiaticus' obtained through metagenomics. *Mol. Plant-Microbe Interact.* 22, 1011–1020. doi: 10.1094/MPMI-22-8-1011

Durrant, W. E., and Dong, X. (2004). Systemic acquired resistance. *Annu. Rev. Phytopathol.* 42, 185–209. doi: 10.1146/annurev.phyto.42.040803.140421

Dutt, M., Barthe, G., Irey, M., and Grosser, J. (2015). Transgenic citrus expressing an *Arabidopsis* NPR1 gene exhibit enhanced resistance against huanglongbing (HLB; citrus greening). *PLoS One* 10:e0137134. doi: 10.1371/journal.pone.0137134

Economou, A., and Wickner, W. (1994). SecA promotes preprotein translocation by undergoing ATP-driven cycles of membrane insertion and deinsertion. *Cell* 78, 835–843. doi: 10.1016/S0092-8674(94)90582-7

Enya, J., Shinohara, H., Yoshida, S., Tsukiboshi, T., Negishi, H., Suyama, K., et al. (2007). Culturable leaf-associated bacteria on tomato plants and their potential as biological control agents. *Microb. Ecol.* 53, 524–536. doi: 10.1007/s00248-006-9085-1

Fagen, J. R., Leonard, M. T., Mccullough, C. M., Edirisinghe, J. N., Henry, C. S., Davis, M. J., et al. (2014). Comparative genomics of cultured and uncultured strains suggests genes essential for free-living growth of *Liberibacter*. *PLoS One* 9:e84469. doi: 10.1371/journal.pone.0084469

Fan, J., Chen, C., Yu, Q., Khalaf, A., Achor, D. S., Brlansky, R. H., et al. (2012). Comparative transcriptional and anatomical analyses of tolerant rough lemon and susceptible sweet orange in response to '*Candidatus* Liberibacter asiaticus' infection. *Mol. Plant-Microbe Interact.* 25, 1396–1407. doi: 10.1094/MPMI-06-12-0150-R

Fan, G.-C., Xia, Y.-L., Lin, X.-J., Hu, H.-Q., Wang, X.-D., Ruan, C.-Q., et al. (2016). Evaluation of thermotherapy against huanglongbing (citrus greening) in the greenhouse. *J. Integr. Agric.* 15, 111–119. doi: 10.1016/S2095-3119(15)61085-1

Fang, F., Guo, H., Zhao, A., Li, T., Liao, H., Deng, X., et al. (2021). A significantly high abundance of "*Candidatus* Liberibacter asiaticus" in citrus fruit pith: *in planta* transcriptome and anatomical analyses. *Front. Microbiol.* 12:681251. doi: 10.3389/fmicb.2021.681251

Fleites, L. A., Jain, M., Zhang, S., and Gabriel, D. W. (2014). "*Candidatus* Liberibacter asiaticus" prophage late genes may limit host range and culturability. *Appl. Environ. Microbiol.* 80, 6023–6030. doi: 10.1128/AEM.01958-14

Folimonova, S. Y., Robertson, C. J., Garnsey, S. M., Gowda, S., and Dawson, W. O. (2009). Examination of the responses of different genotypes of citrus to huanglongbing (citrus greening) under different conditions. *Phytopathology* 99, 1346–1354. doi: 10.1094/PHYTO-99-12-1346

Fujiwara, K., Iwanami, T., and Fujikawa, T. (2018). Alterations of *Candidatus* Liberibacter asiaticus-associated microbiota decrease survival of Ca. L. asiaticus in in vitro assays. *Front. Microbiol.* 9:3089. doi: 10.3389/fmicb.2018.03089

Gardner, C. L., Pagliai, F. A., Pan, L., Bojilova, L., Torino, M. I., Lorca, G. L., et al. (2016). Drug repurposing: tolfenamic acid inactivates PrbP, a transcriptional accessory protein in *Liberibacter asiaticus*. *Front. Microbiol.* 7:1630. doi: 10.3389/fmicb.2016.01630

Ghatrehsamani, S., Czarnecka, E., Verner, F. L., Gurley, W. B., Ehsani, R., and Ampatzidis, Y. (2019). Evaluation of mobile heat treatment system for treating in-field HLB-affected trees by analyzing survival rate of surrogate bacteria. *Agronomy* 9:540. doi: 10.3390/agronomy9090540

Ginnan, N. A., Dang, T., Bodaghi, S., Ruegger, P. M., Mccollum, G., England, G., et al. (2020). Disease-induced microbial shifts in citrus indicate microbiome-derived responses to huanglongbing across the disease severity spectrum. *Phytobiomes J.* 4, 375–387. doi: 10.1094/PBIOMES-04-20-0027-R

Gottwald, T. R. (2010). Current epidemiological understanding of citrus huanglongbing. *Annu. Rev. Phytopathol.* 48, 119–139. doi: 10.1146/annurev-phyto-073009-114418

Gottwald, T., Graham, J., Irey, M., Mccollum, T., and Wood, B. W. (2012). Inconsequential effect of nutritional treatments on huanglongbing control, fruit quality, bacterial titer and disease progress. *Crop Prot.* 36, 73–82. doi: 10.1016/j.cropro.2012.01.004

Grafton-Cardwell, E. E., Stelinski, L. L., and Stansly, P. A. (2013). Biology and management of Asian citrus psyllid, vector of the huanglongbing pathogens. *Annu. Rev. Entomol.* 58, 413–432. doi: 10.1146/annurev-ento-120811-153542

Graham, J., Gottwald, T., and Setamou, M. (2020). Status of huanglongbing (HLB) outbreaks in Florida, California and Texas. *Trop. Plant Pathol.* 45, 265–278. doi: 10.1007/s40858-020-00335-y

Ha, P. T., He, R., Killiny, N., Brown, J. K., Omsland, A., Gang, D. R., et al. (2019). Host-free biofilm culture of "*Candidatus* Liberibacter asiaticus," the bacterium associated with huanglongbing. *Biofilms* 1:100005. doi: 10.1016/j.bioflm.2019.100005

Hall, D. G., and Gottwald, T. R. (2011). Pest management practices aimed at curtailing citrus huanglongbing disease. *Outlooks Pest Manag.* 22:189. doi: 10.1564/22aug11

Hartmann, T. (2008). The lost origin of chemical ecology in the late 19th century. *Proc. Natl. Acad. Sci. U. S. A.* 105, 4541–4546. doi: 10.1073/pnas.0709231105

Hell, R. (1997). Molecular physiology of plant sulfur metabolism. *Planta* 202, 138–148. doi: 10.1007/s004250050112

Hijaz, F., Al-Rimawi, F., Manthey, J. A., and Killiny, N. (2020). Phenolics, flavonoids and antioxidant capacities in citrus species with different degree of tolerance to huanglongbing. *Plant Signal. Behav.* 15:1752447. doi: 10.1080/15592324.2020.1752447

Hodges, A. W., and Spreen, T. H. (2012). "Economic impacts of citrus greening (HLB) in Florida, 2006/07-2010/11," in *Electronic Data Information Source (EDIS) FE903*. Gainseville, FL: University of Florida.

Hoffman, M. T., Doud, M. S., Williams, L., Zhang, M.-Q., Ding, F., Stover, E., et al. (2013). Heat treatment eliminates '*Candidatus* Liberibacter asiaticus' from infected citrus trees under controlled conditions. *Phytopathology* 103, 15–22. doi: 10.1094/PHYTO-06-12-0138-R

Hopkins, D., and Wall, K. (2021). Biological control of citrus huanglongbing with EB92-1, a benign strain of *Xylella fastidiosa*. *Plant Dis.* 105, 2914–2918. doi: 10.1094/PDIS-02-21-0362-RE

Hu, J., Akula, N., and Wang, N. (2016). Development of a microemulsion formulation for antimicrobial SecA inhibitors. *PLoS One* 11:e0150433. doi: 10.1371/journal.pone.0167792

Hu, J., Jiang, J., and Wang, N. (2018). Control of citrus huanglongbing via trunk injection of plant defense activators and antibiotics. *Phytopathology* 108, 186–195. doi: 10.1094/PHYTO-05-17-0175-R

Hu, J., and Wang, N. (2016). Evaluation of the spatiotemporal dynamics of oxytetracycline and its control effect against citrus huanglongbing via trunk injection. *Phytopathology* 106, 1495–1503. doi: 10.1094/PHYTO-02-16-0114-R

Huang, C.-Y., Araujo, K., Sánchez, J. N., Kund, G., Trumble, J., Roper, C., et al. (2021a). A stable antimicrobial peptide with dual functions of treating and preventing citrus huanglongbing. *Proc. Natl. Acad. Sci. U. S. A.* 118:e2019628118. doi: 10.1073/pnas.2019628118

Huang, C. Y., Niu, D., Kund, G., Jones, M., Albrecht, U., Nguyen, L., et al. (2021b). Identification of citrus immune regulators involved in defence against huanglongbing using a new functional screening system. *Plant Biotechnol. J.* 19, 757–766. doi: 10.1111/pbi.13502

Huber, D. M., and Jones, J. B. (2013). The role of magnesium in plant disease. *Plant Soil* 368, 73–85. doi: 10.1007/s11104-012-1476-0

Innerebner, G., Knief, C., and Vorholt, J. A. (2011). Protection of *Arabidopsis thaliana* against leaf-pathogenic *Pseudomonas syringae* by *Sphingomonas* strains in a controlled model system. *Appl. Environ. Microbiol.* 77, 3202–3210. doi: 10.1128/AEM.00133-11

Inoue, H., Yamashita-Muraki, S., Fujiwara, K., Honda, K., Ono, H., Nonaka, T., et al. (2020). Fe2+ ions alleviate the symptom of citrus greening disease. *Int. J. Mol. Sci.* 21:4033. doi: 10.3390/ijms21114033

Irigoyen, S., Ramasamy, M., Pant, S., Niraula, P., Bedre, R., Gurung, M., et al. (2020). Plant hairy roots enable high throughput identification of antimicrobials against *Candidatus* Liberibacter spp. *Nat. Commun.* 11, 1–14. doi: 10.1038/s41467-020-19631-x

Jagoueix, S., Bove, J.-M., and Garnier, M. (1994). The phloem-limited bacterium of greening disease of citrus is a member of the α subdivision of the Proteobacteria. *Int. J. Syst. Evol. Microbiol.* 44, 379–386. doi: 10.1099/00207713-44-3-379

Jones, J. D., and Dangl, J. L. (2006). The plant immune system. *Nature* 444, 323–329. doi: 10.1038/nature05286

Kaul, S., Sharma, T., and Dhar, M. K. (2016). "Omics" tools for better understanding the plant–endophyte interactions. *Front. Plant Sci.* 7:955. doi: 10.3389/fpls.2016.00955

Killiny, N. (2017). Metabolite signature of the phloem sap of fourteen citrus varieties with different degrees of tolerance to *Candidatus* Liberibacter asiaticus. *Physiol. Mol. Plant Pathol.* 97, 20–29. doi: 10.1016/j.pmpp.2016.11.004

Killiny, N., and Hijaz, F. (2016). Amino acids implicated in plant defense are higher in *Candidatus* Liberibacter asiaticus-tolerant citrus varieties. *Plant Signal. Behav.* 11:e1171449. doi: 10.1080/15592324.2016.1171449

Killiny, N., Valim, M. F., Jones, S. E., Omar, A. A., Hijaz, F., Gmitter, F. G., et al. (2017). Metabolically speaking: possible reasons behind the tolerance of 'Sugar Belle'mandarin hybrid to huanglongbing. *Plant Physiol. Biochem.* 116, 36–47. doi: 10.1016/j.plaphy.2017.05.001

Kim, M. K., and Jung, H.-Y. (2007). *Chitinophaga terrae* sp. nov., isolated from soil. *Int. J. Syst. Evol. Microbiol.* 57, 1721–1724. doi: 10.1099/ijs.0.64964-0

Kinkema, M., Fan, W., and Dong, X. (2000). Nuclear localization of NPR1 is required for activation of PR gene expression. *Plant Cell* 12, 2339–2350. doi: 10.1105/tpc.12.12.2339

Kumagai, L., Levesque, C., Blomquist, C., Madishetty, K., Guo, Y., Woods, P., et al. (2013). First report of *Candidatus* Liberibacter asiaticus associated with citrus huanglongbing in California. *Plant Dis.* 97:283. doi: 10.1094/PDIS-09-12-0845-PDN

Leonard, M. T., Fagen, J. R., Davis-Richardson, A. G., Davis, M. J., and Triplett, E. W. (2012). Complete genome sequence of *Liberibacter crescens* BT-1. *Stand. Genomic Sci.* 7, 271–283. doi: 10.4056/sigs.3326772

Li, J., Kolbasov, V. G., Pang, Z., Duan, S., Lee, D., Huang, Y., et al. (2021a). Evaluation of the control effect of SAR inducers against citrus huanglongbing applied by foliar spray, soil drench or trunk injection. *Phytopathol. Res.* 3, 1–15. doi: 10.1186/s42483-020-00079-2

Li, W., Levy, L., and Hartung, J. S. (2009). Quantitative distribution of '*Candidatus* Liberibacter asiaticus' in citrus plants with citrus huanglongbing. *Phytopathology* 99, 139–144. doi: 10.1094/PHYTO-99-2-0139

Li, J., Li, L., Pang, Z., Kolbasov, V. G., Ehsani, R., Carter, E. W., et al. (2019). Developing citrus huanglongbing (HLB) management strategies based on the severity of symptoms in HLB-endemic citrus-producing regions. *Phytopathology* 109, 582–592. doi: 10.1094/PHYTO-08-18-0287-R

Li, J., Trivedi, P., and Wang, N. (2016). Field evaluation of plant defense inducers for the control of citrus huanglongbing. *Phytopathology* 106, 37–46. doi: 10.1094/PHYTO-08-15-0196-R

Li, T., Zhang, L., Deng, Y., Deng, X., and Zheng, Z. (2021b). Establishment of a *Cuscuta campestris*-mediated enrichment system for genomic and transcriptomic analyses of '*Candidatus* Liberibacter asiaticus'. *Microb. Biotechnol.* 14, 737–751. doi: 10.1111/1751-7915.13773

Lin, D., Xiao, M., Zhao, J., Li, Z., Xing, B., Li, X., et al. (2016). An overview of plant phenolic compounds and their importance in human nutrition and management of type 2 diabetes. *Molecules* 21:1374. doi: 10.3390/molecules21101374

Lopes, S., Frare, G., Bertolini, E., Cambra, M., Fernandes, N., Ayres, A., et al. (2009). Liberibacters associated with citrus huanglongbing in Brazil: '*Candidatus* Liberibacter asiaticus' is heat tolerant, 'Ca. L. americanus' is heat sensitive. *Plant Dis.* 93, 257–262. doi: 10.1094/PDIS-93-3-0257

Lugtenberg, B., and Kamilova, F. (2009). Plant-growth-promoting rhizobacteria. *Annu. Rev. Microbiol.* 63, 541–556. doi: 10.1146/annurev.micro.62.081307.162918

Ma, W., Pang, Z., Huang, X., Xu, J., Pandey, S. S., Li, J., et al. (2022). Citrus huanglongbing is a pathogen-triggered immune disease that can be mitigated with antioxidants and gibberellin. *Nat. Commun.* 13, 1–13. doi: 10.1038/s41467-022-28189-9

Madhaiyan, M., Reddy, B. S., Anandham, R., Senthilkumar, M., Poonguzhali, S., Sundaram, S., et al. (2006). Plant growth–promoting methylobacterium induces defense responses in groundnut (*Arachis hypogaea* L.) compared with rot pathogens. *Curr. Microbiol.* 53, 270–276. doi: 10.1007/s00284-005-0452-9

Martinelli, F., Reagan, R. L., Dolan, D., Fileccia, V., and Dandekar, A. M. (2016). Proteomic analysis highlights the role of detoxification pathways in increased tolerance to huanglongbing disease. *BMC Plant Biol.* 16, 1–14. doi: 10.1186/s12870-016-0858-5

Masaoka, Y., Pustika, A., Subandiyah, S., Okada, A., Hanundin, E., Purwanto, B., et al. (2011). Lower concentrations of microelements in leaves of citrus infected with '*Candidatus* Liberibacter asiaticus'. *Jpn. Agr. Res. Q.* 45, 269–275. doi: 10.6090/jarq.45.269

Mattos-Jr, D., Kadyampakeni, D. M., Da Silva, J. R., Vashisth, T., and Boaretto, R. M. (2020). Reciprocal effects of huanglongbing infection and nutritional status of citrus trees: a review. *Trop. Plant Pathol.* 45, 586–596. doi: 10.1007/s40858-020-00389-y

Mendes, R., Garbeva, P., and Raaijmakers, J. M. (2013). The rhizosphere microbiome: significance of plant beneficial, plant pathogenic, and human

pathogenic microorganisms. *FEMS Microbiol. Rev.* 37, 634–663. doi: 10.1111/1574-6976.12028

Merfa, M. V., Pérez-López, E., Naranjo, E., Jain, M., Gabriel, D. W., and De La Fuente, L. (2019). Progress and obstacles in culturing '*Candidatus* Liberibacter asiaticus', the bacterium associated with huanglongbing. *Phytopathology* 109, 1092–1101. doi: 10.1094/PHYTO-02-19-0051-RVW

Mhedbi-Hajri, N., Jacques, M.-A., and Koebnik, R. (2011). Adhesion mechanisms of plant-pathogenic Xanthomonadaceae. *Adv. Exp. Med. Biol.* 715, 71–89. doi: 10.1007/978-94-007-0940-9_5

Mitsui, H., Sato, T., Sato, Y., Ito, N., and Minamisawa, K. (2004). Sinorhizobium meliloti RpoH 1 is required for effective nitrogen-fixing symbiosis with alfalfa. *Mol. Gen. Genomics.* 271, 416–425. doi: 10.1007/s00438-004-0992-x

Morgan, K. T., Rouse, R. E., and Ebel, R. C. (2016). Foliar applications of essential nutrients on growth and yield of 'Valencia'sweet orange infected with huanglongbing. *HortScience* 51, 1482–1493. doi: 10.21273/HORTSCI11026-16

Munir, S., Li, Y., He, P., He, P., Ahmed, A., Wu, Y., et al. (2020). Unraveling the metabolite signature of citrus showing defense response towards *Candidatus* Liberibacter asiaticus after application of endophyte *Bacillus subtilis* L1-21. *Microbiol. Res.* 234:126425. doi: 10.1016/j.micres.2020.126425

Nan, J., Zhang, S., and Jiang, L. (2021). Antibacterial potential of *Bacillus amyloliquefaciens* GJ1 against citrus huanglongbing. *Plants* 10:261. doi: 10.3390/plants10020261

Nicholson, R. L., and Hammerschmidt, R. (1992). Phenolic compounds and their role in disease resistance. *Annu. Rev. Phytopathol.* 30, 369–389. doi: 10.1146/annurev.py.30.090192.002101

Nwugo, C. C., Doud, M. S., Duan, Y.-P., and Lin, H. (2016). Proteomics analysis reveals novel host molecular mechanisms associated with thermotherapy of 'Ca. Liberibacter asiaticus'-infected citrus plants. *BMC Plant Biol.* 16, 1–15. doi: 10.1186/s12870-016-0942-x

Oppenheim, A. B., Kobiler, O., Stavans, J., Court, D. L., and Adhya, S. (2005). Switches in bacteriophage lambda development. *Annu. Rev. Genet.* 39, 409–429. doi: 10.1146/annurev.genet.39.073003.113656

Pagliaccia, D., Shi, J., Pang, Z., Hawara, E., Clark, K., Thapa, S. P., et al. (2017). A pathogen secreted protein as a detection marker for citrus huanglongbing. *Front. Microbiol.* 8:2041. doi: 10.3389/fmicb.2017.02041

Pagliai, F. A., Coyle, J. F., Kapoor, S., Gonzalez, C. F., and Lorca, G. L. (2017). LdtR is a master regulator of gene expression in *Liberibacter asiaticus*. *Microb. Biotechnol.* 10, 896–909. doi: 10.1111/1751-7915.12728

Pagliai, F. A., Gardner, C. L., Bojilova, L., Sarnegrim, A., Tamayo, C., Potts, A. H., et al. (2014). The transcriptional activator LdtR from '*Candidatus* Liberibacter asiaticus' mediates osmotic stress tolerance. *PLoS Pathog.* 10:e1004101. doi: 10.1371/journal.ppat.1004101

Parker, J. K., Wisotsky, S. R., Johnson, E. G., Hijaz, F. M., Killiny, N., Hilf, M. E., et al. (2014). Viability of '*Candidatus* Liberibacter asiaticus' prolonged by addition of citrus juice to culture medium. *Phytopathology* 104, 15–26. doi: 10.1094/PHYTO-05-13-0119-R

Peris-Peris, C., Serra-Cardona, A., Sánchez-Sanuy, F., Campo, S., Ariño, J., and San Segundo, B. (2017). Two NRAMP6 isoforms function as iron and manganese transporters and contribute to disease resistance in rice. *Mol. Plant-Microbe Interact.* 30, 385–398. doi: 10.1094/MPMI-01-17-0005-R

Petrussa, E., Braidot, E., Zancani, M., Peresson, C., Bertolini, A., Patui, S., et al. (2013). Plant flavonoids—biosynthesis, transport and involvement in stress responses. *Int. J. Mol. Sci.* 14, 14950–14973. doi: 10.3390/ijms140714950

Phuyal, D., Nogueira, T. A. R., Jani, A. D., Kadyampakeni, D. M., Morgan, K. T., and Ferrarezi, R. S. (2020). 'Ray Ruby'grapefruit affected by huanglongbing II. Planting density, soil, and foliar nutrient management. *HortScience* 55, 1420–1432. doi: 10.21273/HORTSCI15255-20

Piasecka, A., Jedrzejczak-Rey, N., and Bednarek, P. (2015). Secondary metabolites in plant innate immunity: conserved function of divergent chemicals. *New Phytol.* 206, 948–964. doi: 10.1111/nph.13325

Pierre, M. O., Salvatierra-Miranda, J., Rivera, M. J., Etxeberria, E., Gonzalez, P., and Vincent, C. I. (2021). White and red-dyed kaolin particle films reduce Asian citrus psyllid populations, delay huanglongbing infection, and increase citrus growth. *Crop Prot.* 150:105792. doi: 10.1016/j.cropro.2021.105792

Pitino, M., Armstrong, C. M., Cano, L. M., and Duan, Y. (2016). Transient expression of *Candidatus* Liberibacter asiaticus effector induces cell death in *Nicotiana benthamiana*. *Front. Plant Sci.* 7:982. doi: 10.3389/fpls.2016.00982

Poveda, J., Roeschlin, R. A., Marano, M. R., and Favaro, M. A. (2021). Microorganisms as biocontrol agents against bacterial citrus diseases. *Biol. Control* 158:104602. doi: 10.1016/j.biocontrol.2021.104602

Prasad, B. D., Creissen, G., Lamb, C., and Chattoo, B. B. (2009). Overexpression of rice (*Oryza sativa* L.) OsCDR1 leads to constitutive activation of defense responses in rice and *Arabidopsis*. *Mol. Plant-Microbe Interact.* 22, 1635–1644. doi: 10.1094/MPMI-22-12-1635

Prasad, S., Xu, J., Zhang, Y., and Wang, N. (2016). SEC-translocon dependent extracytoplasmic proteins of *Candidatus* Liberibacter asiaticus. *Front. Microbiol.* 7:1989. doi: 10.3389/fmicb.2016.01989

Qiu, W., Soares, J., Pang, Z., Huang, Y., Sun, Z., Wang, N., et al. (2020). Potential mechanisms of AtNPR1 mediated resistance against huanglongbing (HLB) in citrus. *Int. J. Mol. Sci.* 21:2009. doi: 10.3390/ijms21062009

Ramsey, J. S., Chin, E. L., Chavez, J. D., Saha, S., Mischuk, D., Mahoney, J., et al. (2020). Longitudinal transcriptomic, proteomic, and metabolomic analysis of citrus limon response to graft inoculation by *Candidatus* Liberibacter asiaticus. *J. Proteome Res.* 19, 2247–2263. doi: 10.1021/acs.jproteome.9b00802

Rao, M. J., Ding, F., Wang, N., Deng, X., and Xu, Q. (2018). Metabolic mechanisms of host species against citrus huanglongbing (greening disease). *Crit. Rev. Plant Sci.* 37, 496–511. doi: 10.1080/07352689.2018.1544843

Rawat, N., Kiran, S. P., Du, D., Gmitter, F. G., and Deng, Z. (2015). Comprehensive meta-analysis, co-expression, and miRNA nested network analysis identifies gene candidates in citrus against huanglongbing disease. *BMC Plant Biol.* 15, 1–21. doi: 10.1186/s12870-015-0568-4

Rawat, N., Kumar, B., Albrecht, U., Du, D., Huang, M., Yu, Q., et al. (2017). Genome resequencing and transcriptome profiling reveal structural diversity and expression patterns of constitutive disease resistance genes in huanglongbing-tolerant *Poncirus trifoliata* and its hybrids. *Hortic. Res.* 4, 1–8. doi: 10.1038/hortres.2017.64

Reinking, O. A. (1919). Diseases of economic plants in southern China. *Philipp. Agr.* 8, 109–134.

Riera, N., Handique, U., Zhang, Y., Dewdney, M. M., and Wang, N. (2017). Characterization of antimicrobial-producing beneficial bacteria isolated from huanglongbing escape citrus trees. *Front. Microbiol.* 8:2415. doi: 10.3389/fmicb.2017.02415

Rouse, R. E., Ozores-Hampton, M., Roka, F. M., and Roberts, P. (2017). Rehabilitation of huanglongbing-affected citrus trees using severe pruning and enhanced foliar nutritional treatments. *HortScience* 52, 972–978. doi: 10.21273/HORTSCI11105-16

Ryals, J. A., Neuenschwander, U. H., Willits, M. G., Molina, A., Steiner, H.-Y., and Hunt, M. D. (1996). Systemic acquired resistance. *Plant Cell* 8, 1809–1819. doi: 10.1105/tpc.8.10.1809

Saikkonen, K., Wäli, P., Helander, M., and Faeth, S. H. (2004). Evolution of endophyte–plant symbioses. *Trends Plant Sci.* 9, 275–280. doi: 10.1016/j.tplants.2004.04.005

Saindrenan, P., and Guest, D. I. (1994). "Involvement of phytoalexins in the response of phosphonate-treated plants to infection by Phytophthora species." in *Handbook of Phytoalexin Metabolism and Action*. eds. M., Daniel and R. P., Purkayasthsa (New York: CRC Press), 375–390.

Segers, K., and Anné, J. (2011). Traffic jam at the bacterial sec translocase: targeting the SecA nanomotor by small-molecule inhibitors. *Chem. Biol.* 18, 685–698. doi: 10.1016/j.chembiol.2011.04.007

Shahzad, F., Chun, C., Schumann, A., and Vashisth, T. (2020). Nutrient uptake in huanglongbing-affected sweet orange: transcriptomic and physiological analysis. *J. Am. Soc. Hortic. Sci.* 145, 349–362. doi: 10.21273/JASHS04929-20

Shen, W., Cevallos-Cevallos, J. M., Nunes Da Rocha, U., Arevalo, H. A., Stansly, P. A., Roberts, P. D., et al. (2013). Relation between plant nutrition, hormones, insecticide applications, bacterial endophytes, and *Candidatus* Liberibacter Ct values in citrus trees infected with huanglongbing. *Eur. J. Plant Pathol.* 137, 727–742. doi: 10.1007/s10658-013-0283-7

Shi, X., Li, B., Qin, G., and Tian, S. (2012). Mechanism of antifungal action of borate against *Colletotrichum gloeosporioides* related to mitochondrial degradation in spores. *Postharvest Biol. Technol.* 67, 138–143. doi: 10.1016/j.postharvbio.2012.01.003

Singerman, A., and Rogers, M. E. (2020). The economic challenges of dealing with citrus greening: the case of Florida. *J. Integr. Pest Manag.* 11:3. doi: 10.1093/jipm/pmz037

Sourjik, V., Muschler, P., Scharf, B., and Schmitt, R. D. (2000). VisN and VisR are global regulators of chemotaxis, flagellar, and motility genes in Sinorhizobium (Rhizobium) meliloti. *J. Bacteriol.* 182, 782–788. doi: 10.1128/JB.182.3.782-788.2000

Spann, T. M., and Schumann, A. W. (2009). The role of plant nutrients in disease development with emphasis on citrus and huanglongbing. *Proc. Fla. State Hort. Soc.* 122, 169–171.

Sticher, L., Mauch-Mani, B., and Métraux, J. P. (1997). Systemic acquired resistance. *Annu. Rev. Phytopathol.* 35, 235–270. doi: 10.1146/annurev.phyto.35.1.235

Sugawara, M., Epstein, B., Badgley, B. D., Unno, T., Xu, L., Reese, J., et al. (2013). Comparative genomics of the core and accessory genomes of 48 *Sinorhizobium* strains comprising five genospecies. *Genome Biol.* 14, R17–R20. doi: 10.1186/gb-2013-14-2-r17

Sugimoto, T., Watanabe, K., Yoshida, S., Aino, M., Furiki, M., Shiono, M., et al. (2010). Field application of calcium to reduce Phytophthora stem rot of soybean, and calcium distribution in plants. *Plant Dis.* 94, 812–819. doi: 10.1094/PDIS-94-7-0812

Suh, J. H., Tang, X., Zhang, Y., Gmitter, F. G., and Wang, Y. (2021). Metabolomic analysis provides new insight into tolerance of huanglongbing in citrus. *Front. Plant Sci.* 12:710598. doi: 10.3389/fpls.2021.710598

Tang, J., Ding, Y., Nan, J., Yang, X., Sun, L., Zhao, X., et al. (2018). Transcriptome sequencing and ITRAQ reveal the detoxification mechanism of *Bacillus* GJ1, a potential biocontrol agent for huanglongbing. *PLoS One* 13:e0200427. doi: 10.1371/journal.pone.0200427

Tatineni, S., Sagaram, U. S., Gowda, S., Robertson, C. J., Dawson, W. O., Iwanami, T., et al. (2008). In planta distribution of '*Candidatus* Liberibacter asiaticus' as revealed by polymerase chain reaction (PCR) and real-time PCR. *Phytopathology* 98, 592–599. doi: 10.1094/PHYTO-98-5-0592

Thapa, S. P., De Francesco, A., Trinh, J., Gurung, F. B., Pang, Z., Vidalakis, G., et al. (2020). Genome-wide analyses of *Liberibacter* species provides insights into evolution, phylogenetic relationships, and virulence factors. *Mol. Plant Pathol.* 21, 716–731. doi: 10.1111/mpp.12925

Treutter, D. (2006). Significance of flavonoids in plant resistance: a review. *Environ. Chem. Lett.* 4, 147–157. doi: 10.1007/s10311-006-0068-8

Trivedi, P., Spann, T., and Wang, N. (2011). Isolation and characterization of beneficial bacteria associated with citrus roots in Florida. *Microb. Ecol.* 62, 324–336. doi: 10.1007/s00248-011-9822-y

Van Den Berg, B., Clemons, W. M., Collinson, I., Modis, Y., Hartmann, E., Harrison, S. C., et al. (2004). X-ray structure of a protein-conducting channel. *Nature* 427, 36–44. doi: 10.1038/nature02218

Verma, J., Yadav, J., Tiwari, K., Lavakush, S., and Singh, V. (2010). Impact of plant growth promoting rhizobacteria on crop production. *Int. J. Agric. Res.* 5, 954–983. doi: 10.3923/ijar.2010.954.983

Vincent, C., Pierre, M., Li, J., and Wang, N. (2019). Implications of heat treatment and systemic delivery of foliar-applied oxytetracycline on citrus physiological management and therapy delivery. *Front. Plant Sci.* 10:41. doi: 10.3389/fpls.2019.00041

Wang, N. (2021). A promising plant defense peptide against citrus huanglongbing disease. *Proc. Natl. Acad. Sci. U. S. A.* 118:e2026483118. doi: 10.1073/pnas.2026483118

Wang, N., Pierson, E. A., Setubal, J. C., Xu, J., Levy, J. G., Zhang, Y., et al. (2017). The *Candidatus* Liberibacter–host interface: insights into pathogenesis mechanisms and disease control. *Annu. Rev. Phytopathol.* 55, 451–482. doi: 10.1146/annurev-phyto-080516-035513

Wang, N., and Trivedi, P. (2013). Citrus huanglongbing: a newly relevant disease presents unprecedented challenges. *Phytopathology* 103, 652–665. doi: 10.1094/PHYTO-12-12-0331-RVW

Wang, Y., Zhou, L., Yu, X., Stover, E., Luo, F., and Duan, Y. (2016). Transcriptome profiling of huanglongbing (HLB) tolerant and susceptible citrus plants reveals the role of basal resistance in HLB tolerance. *Front. Plant Sci.* 7:933. doi: 10.3389/fpls.2016.00933

Wu, H., Hu, Y., Fu, S., Zhou, C., and Wang, X. (2020). Coordination of multiple regulation pathways contributes to the tolerance of a wild citrus species (*Citrus ichangensis* '2586') against huanglongbing. *Physiol. Mol. Plant Pathol.* 109:101457. doi: 10.1016/j.pmpp.2019.101457

Wulff, N. A., Zhang, S., Setubal, J. C., Almeida, N. F., Martins, E. C., Harakava, R., et al. (2014). The complete genome sequence of '*Candidatus* Liberibacter americanus', associated with citrus huanglongbing. *Mol. Plant-Microbe Interact.* 27, 163–176. doi: 10.1094/MPMI-09-13-0292-R

Xia, Y., Suzuki, H., Borevitz, J., Blount, J., Guo, Z., Patel, K., et al. (2004). An extracellular aspartic protease functions in *Arabidopsis* disease resistance signaling. *EMBO J.* 23, 980–988. doi: 10.1038/sj.emboj.7600086

Yan, Q., Sreedharan, A., Wei, S., Wang, J., Pelz-Stelinski, K., Folimonova, S., et al. (2013). Global gene expression changes in *Candidatus* Liberibacter asiaticus during the transmission in distinct hosts between plant and insect. *Mol. Plant Pathol.* 14, 391–404. doi: 10.1111/mpp.12015

Yan, H., Zhou, B., Jiang, B., Lv, Y., Moniruzzaman, M., Zhong, G., et al. (2021). Comparative analysis of bacterial and fungal endophytes responses to *Candidatus* Liberibacter asiaticus infection in leaf midribs of *Citrus reticulata* cv. Shatangju. *Physiol. Mol. Plant Pathol.* 113:101590. doi: 10.1016/j.pmpp.2020.101590

Yang, C., Hu, H., Wu, Y., Lin, X., Fan, G., Duan, Y., et al. (2020a). Metagenomic analysis reveals the mechanism for the observed increase in antibacterial activity of penicillin against uncultured bacteria *Candidatus* Liberibacter asiaticus relative to oxytetracycline in planta. *Antibiotics* 9:874. doi: 10.3390/antibiotics9120874

Yang, C., Powell, C. A., Duan, Y., Ancona, V., Huang, J., and Zhang, M. (2020b). Transcriptomic analysis reveals root metabolic alteration and induction of huanglongbing resistance by sulphonamide antibiotics in huanglongbing-affected citrus plants. *Plant Pathol.* 69, 733–743. doi: 10.1111/ppa.13154

Yang, C., Powell, C. A., Duan, Y., Shatters, R., Fang, J., and Zhang, M. (2016a). Deciphering the bacterial microbiome in huanglongbing-affected citrus treated with thermotherapy and sulfonamide antibiotics. *PLoS One* 11:e0155472. doi: 10.1371/journal.pone.0155472

Yang, C., Powell, C. A., Duan, Y., Shatters, R. G., Lin, Y., and Zhang, M. (2016b). Mitigating citrus huanglongbing via effective application of antimicrobial compounds and thermotherapy. *Crop Prot.* 84, 150–158. doi: 10.1016/j.cropro.2016.03.013

Yang, C., Powell, C. A., Duan, Y., Shatters, R., and Zhang, M. (2015). Antimicrobial nanoemulsion formulation with improved penetration of foliar spray through citrus leaf cuticles to control citrus huanglongbing. *PloS one* 10:e0133826. doi: 10.1371/journal.pone.0133826

Yang, C., Zhong, Y., Powell, C. A., Doud, M. S., Duan, Y., Huang, Y., et al. (2018). Antimicrobial compounds effective against *Candidatus* Liberibacter asiaticus discovered via graft-based assay in citrus. *Sci. Rep.* 8, 1–11. doi: 10.1038/s41598-018-35461-w

Ying, X., Redfern, B., Gmitter, F. G., and Deng, Z. (2020). Heterologous expression of the constitutive disease resistance 2 and 8 genes from *Poncirus trifoliata* restored the hypersensitive response and resistance of *Arabidopsis* cdr1 mutant to bacterial pathogen *Pseudomonas syringae*. *Plants* 9:821. doi: 10.3390/plants9070821

Yuan, X., Chen, C., Bassanezi, R., Wu, F., Feng, Z., Shi, D., et al. (2020). Region-wide comprehensive implementation of roguing infected trees, tree replacement, and insecticide applications successfully controls citrus HLB. *Phytopathology* 111, 1361–1368. doi: 10.1094/PHYTO-09-20-0436-R

Zambon, F. T., Kadyampakeni, D. M., and Grosser, J. W. (2019). Ground application of overdoses of manganese have a therapeutic effect on sweet orange trees infected with *Candidatus* Liberibacter asiaticus. *HortScience* 54, 1077–1086. doi: 10.21273/HORTSCI13635-18

Zhang, S., Flores-Cruz, Z., Zhou, L., Kang, B.-H., Fleites, L. A., Gooch, M. D., et al. (2011b). 'Ca. Liberibacter asiaticus' carries an excision plasmid prophage and a chromosomally integrated prophage that becomes lytic in plant infections. *Mol. Plant-Microbe Interact.* 24, 458–468. doi: 10.1094/MPMI-11-10-0256

Zhang, M., Guo, Y., Powell, C. A., Doud, M. S., Yang, C., and Duan, Y. (2014). Effective antibiotics against '*Candidatus* Liberibacter asiaticus' in HLB-affected citrus plants identified via the graft-based evaluation. *PLoS One* 9:e111032. doi: 10.1371/journal.pone.0116056

Zhang, M., Karuppaiya, P., Zheng, D., Sun, X., Bai, J., Ferrarezi, R. S., et al. (2021). Field evaluation of chemotherapy on HLB-affected citrus trees with emphasis on fruit yield and quality. *Front. Plant Sci.* 12:611287. doi: 10.3389/fpls.2021.611287

Zhang, M., Powell, C. A., Benyon, L. S., Zhou, H., and Duan, Y. (2013). Deciphering the bacterial microbiome of citrus plants in response to '*Candidatus* Liberibacter asiaticus'-infection and antibiotic treatments. *PLoS One* 8:e76331. doi: 10.1371/journal.pone.0085170

Zhang, M., Powell, C. A., Guo, Y., Doud, M. S., and Duan, Y. (2012). A graft-based chemotherapy method for screening effective molecules and

rescuing huanglongbing-affected citrus plants. *Phytopathology* 102, 567–574. doi: 10.1094/PHYTO-09-11-0265

Zhang, M., Powell, C. A., Zhou, L., He, Z., Stover, E., and Duan, Y. (2011a). Chemical compounds effective against the citrus huanglongbing bacterium '*Candidatus* Liberibacter asiaticus' in planta. *Phytopathology* 101, 1097–1103. doi: 10.1094/PHYTO-09-10-0262

Zhang, Y., Xu, J., Riera, N., Jin, T., Li, J., and Wang, N. (2017). Huanglongbing impairs the rhizosphere-to-rhizoplane enrichment process of the citrus root-associated microbiome. *Microbiome* 5, 1–17. doi: 10.1186/s40168-017-0304-4

Zhao, H., Sun, R., Albrecht, U., Padmanabhan, C., Wang, A., Coffey, M. D., et al. (2013). Small RNA profiling reveals phosphorus deficiency as a contributing factor in symptom expression for citrus huanglongbing disease. *Mol. Plant* 6, 301–310. doi: 10.1093/mp/sst002

Zheng, Z., Bao, M., Wu, F., Chen, J., and Deng, X. (2016). Predominance of single prophage carrying a CRISPR/cas system in "*Candidatus* Liberibacter asiaticus" strains in southern China. *PLoS One* 11:e0146422. doi: 10.1371/journal.pone.0169138

Zheng, Z., Bao, M., Wu, F., Van Horn, C., Chen, J., and Deng, X. (2018). A type 3 prophage of '*Candidatus* Liberibacter asiaticus' carrying a restriction-modification system. *Phytopathology* 108, 454–461. doi: 10.1094/PHYTO-08-17-0282-R

Zhou, C. (2020). The status of citrus huanglongbing in China. *Trop. Plant Pathol.* 45, 279–284. doi: 10.1007/s40858-020-00363-8

Zhou, Y., Tang, Y., Hu, C., Zhan, T., Zhang, S., Cai, M., et al. (2021). Soil applied Ca, Mg and B altered phyllosphere and rhizosphere bacterial microbiome and reduced huanglongbing incidence in gannan navel orange. *Sci. Total Environ.* 791:148046. doi: 10.1016/j.scitotenv.2021.148046

Zou, X., Bai, X., Wen, Q., Xie, Z., Wu, L., Peng, A., et al. (2019). Comparative analysis of tolerant and susceptible citrus reveals the role of methyl salicylate signaling in the response to huanglongbing. *J. Plant Growth Regul.* 38, 1516–1528. doi: 10.1007/s00344-019-09953-6

Conflict of Interest: The authors declare that the research was conducted in the absence of any commercial or financial relationships that could be construed as a potential conflict of interest.

Publisher's Note: All claims expressed in this article are solely those of the authors and do not necessarily represent those of their affiliated organizations, or those of the publisher, the editors and the reviewers. Any product that may be evaluated in this article, or claim that may be made by its manufacturer, is not guaranteed or endorsed by the publisher.

frontiers | Frontiers in Microbiology

ORIGINAL RESEARCH
published: 27 July 2022
doi: 10.3389/fmicb.2022.857493

Identification and Characterization of Potato Zebra Chip Resistance Among Wild *Solanum* Species

Victoria Mora[1†], *Manikandan Ramasamy*[1†], *Mona B. Damaj*[1], *Sonia Irigoyen*[1], *Veronica Ancona*[2], *Carlos A. Avila*[1,3], *Maria Isabel Vales*[3], *Freddy Ibanez*[1,4] *and Kranthi K. Mandadi*[1,5,6*]

[1] Texas A&M AgriLife Research and Extension Center, Weslaco, TX, United States, [2] Department of Agriculture, Agribusiness, and Environmental Sciences, Texas A&M University-Kingsville, Weslaco, TX, United States, [3] Department of Horticultural Sciences, Texas A&M University, College Station, TX, United States, [4] Department of Entomology, Texas A&M University, College Station, TX, United States, [5] Department of Plant Pathology & Microbiology, Texas A&M University, College Station, TX, United States, [6] Institute for Advancing Health Through Agriculture, Texas A&M AgriLife, College Station, TX, United States

OPEN ACCESS

Edited by:
Xiangming Xu,
National Institute of Agricultural Botany (NIAB), United Kingdom

Reviewed by:
Assunta Bertaccini,
University of Bologna, Italy
Maria Julissa Ek-Ramos,
Autonomous University of Nuevo León, Mexico
Xuefeng Wang,
Chinese Academy of Agricultural Sciences (CAAS), China

***Correspondence:**
Kranthi K. Mandadi
kkmandadi@tamu.edu

[†] *These authors have contributed equally to this work*

Specialty section:
This article was submitted to Microbe and Virus Interactions with Plants, a section of the journal Frontiers in Microbiology

Received: *18 January 2022*
Accepted: *16 June 2022*
Published: *27 July 2022*

Citation:
Mora V, Ramasamy M, Damaj MB, Irigoyen S, Ancona V, Avila CA, Vales MI, Ibanez F and Mandadi KK (2022) Identification and Characterization of Potato Zebra Chip Resistance Among Wild Solanum Species. Front. Microbiol. 13:857493. doi: 10.3389/fmicb.2022.857493

Potato zebra chip (ZC) disease, associated with the uncultured phloem-limited bacterium, *Candidatus* Liberibacter solanacearum (*C*Lso), is transmitted by the potato psyllid *Bactericera cockerelli*. Potato ZC disease poses a significant threat to potato production worldwide. Current management practices mainly rely on the control of the psyllid to limit the spread of *C*Lso. The present study investigated new sources of ZC resistance among wild *Solanum* species. A taxonomically diverse collection of tuber-bearing *Solanum* species was screened; one ZC-resistant accession and three ZC-tolerant accessions were identified among the 52 screened accessions. Further characterization of the resistant accession showed that the resistance was primarily associated with antibiosis effects due to differences in leaf trichome density and morphology of the wild accession, which could limit the psyllid feeding and oviposition. This germplasm offers a good resource for further understanding ZC and psyllid resistance mechanisms, contributing to potato breeding efforts to develop ZC resistance cultivars. Alternatively, it could be used as a potential trap crop to manage psyllid and control ZC disease.

Keywords: *Candidatus* Liberibacter solanacearum, Fastidious bacteria, *Bactericera cockerelli*, zebra chip (ZC), wild accessions, resistant traits, antibiosis

INTRODUCTION

Potato (*Solanum tuberosum* L.) is cultivated in over 160 countries and is rated as the fourth most important staple food crop after wheat, corn, and rice. It is a rich source of carbohydrates and provides other essential nutrients, such as dietary fiber, vitamins, minerals, protein, and antioxidants (Dahal et al., 2019). Based on its global consumption, nutritional benefits, tonnage production, and cash value, the global production was estimated at ∼395 metric tons in 2019. Its importance in the United States was at 3.94 billion (Faostat, 2020; USDA, 2020). However, increasing the incidence of biotic (diseases and pests) as well as abiotic (drought, heat, and salinity) stresses limit potato production (Savary et al., 2019).

Since its identification in 1994 in Mexico and in 2000 in the United States, the zebra chip (ZC) disease of potato has spread into several commercial potato-growing regions of Central America, Australia, New Zealand, Northern Africa, and the Middle East (Munyaneza et al., 2007, 2009a, 2010; Tahzima et al., 2014; Mawassi et al., 2018; Mora et al., 2021) and recently in Spain (Portal, 2017). ZC disease could result in potato yield losses of up to 94% (Greenway, 2014). The disease is associated with the uncultured phloem-limited bacterium *Candidatus* Liberibacter solanacearum (*C*Lso) and vectored by the potato psyllid *Bactericera cockerelli* Šulc (Hemiptera: Triozidae) (Munyaneza, 2012; Nwugo et al., 2017; Mora et al., 2021). Typical foliar symptoms of ZC-affected plants include purplish discoloration/chlorosis of young leaves, upward rolling of top leaves, presence of axillary buds, presence of aerial tubers, wilting, stunted growth, and ultimately plant death. ZC symptoms in tubers are associated with the synthesis and accumulation of phenolic compounds, reducing sugars and defense enzymes (Navarre et al., 2009; Wallis et al., 2012), giving chips a bitter taste and a dark brown striped, zebra-like appearance when fried (Munyaneza, 2012), ultimately causing the entire tubers to become unmarketable (Mora et al., 2021). If left uncontrolled, ZC disease can become one of the potato's economically significant diseases.

Current ZC management strategies rely on controlling the psyllid vector, involving insecticides (Guenthner et al., 2012; Greenway, 2014; Greenway and Rondon, 2018) and the possibility of increased insecticide resistance. Recently, resistance to neonicotinoid-based insecticides has been reported in Texas potato psyllids, which threatens future control of this insect (Prager et al., 2013; Szczepaniec et al., 2019). The primary mode of acquisition and spreading of *C*Lso is by psyllids feeding on *C*Lso-infected plants and then on healthy plants transferring *C*Lso (Munyaneza et al., 2009b; Buchman et al., 2011). Hence, identifying novel genetic resistance and tolerance to *C*Lso or the psyllid can be valuable components of ZC's integrated pest/diseases management. Previous studies have reported variations in the psyllid preference for the wild potato species, namely, *Solanum bulbocastanum*, *Solanum habrochaites,* and *Solanum Verrucosum,* and the breeding clones, namely, *Solanum berthaultii* and *Solanum tuberosum* (Butler et al., 2011; Cooper and Bamberg, 2014, 2016; Diaz-Montano et al., 2014; Levy and Tamborindeguy, 2014). Variations in the tolerance response to *C*Lso have also been noted among various *Solanum* breeding clones (Prager et al., 2013; Rashidi et al., 2017; Vigue, 2018; Fife et al., 2020; Vigue et al., 2020).

A 2015 taxonomic and genetic study established a *Solanum* section *Petota* panel of tuber-bearing relatives of cultivated potatoes, representing a genetic resource of broadly diverse germplasm of highly regarded agronomic traits and tuber size (Hawkes, 1990; Spooner and Castillo, 1997; Hardigan et al., 2015). In this study, screening and identification of new ZC-resistant and -tolerant germplasm in the *Solanum* sect. *Petota* panels were performed. The ZC resistance of one accession (*S. berthaultii*) could be attributed to modifications in leaf trichome shape and density, affecting potato psyllid fecundity and survival.

MATERIALS AND METHODS

Plant Materials, Propagation, and Maintenance

Plant material consisted of 52 wild potato accessions grown from true potato seeds obtained from the U.S. National Plant Germplasm System (NPGS) in Wisconsin, USA. The introductions belong to the *Solanum* sect. *Petota* diversity panel (**Supplementary Table 1**). This panel represents the germplasm of tuber-bearing *Solanum* species exhibiting morphological variations (**Supplementary Figure 1**) (Hardigan et al., 2015). *Solanum tuberosum* L. var. Atlantic (chip processing market class) was used as a susceptible control in all experiments and was initially propagated from certified disease-free seed tubers. For *in vitro* germination and propagation, the *Solanum* botanical seeds were pretreated with 10% (w/v) gibberellic acid (GA3) overnight in a 1.5 ml microcentrifuge tube to break dormancy and enhance seed germination. Furthermore, seeds were surface sterilized in 70% (v/v) ethanol for 3 min and then with 10% (v/v) bleach and 2% (v/v) Tween® 20 (Sigma-Aldrich, St. Louis, MO, USA) for 10 min, followed by rinsing four times with sterile water. Sterilized seeds were placed on a sterile wetted Whatman™ paper inside a sterile 100 × 25 mm Petri dish and kept at 22°C in the dark for 1 week. Germinated seeds were grown on Murashige and Skoog (Murashige and Skoog, 1962) solid media supplemented with pre-made MS vitamins (Caisson Labs, North Logan, Utah, USA), 2% sucrose (w/v), and 2 g/L of Gelrite™ (Research Products International, Mt. Prospect, IL, USA), pH 5.8. When plants were 4 weeks old (about 8 cm tall), micropropagation was done using internode cutting as explants; sub-culturing every 4 weeks was necessary to increase plant material for each wild potato accession for screening against ZC. All explants were maintained in a temperature-controlled growth chamber at 22°C under 14-h light/10-h dark photoperiod.

Psyllid Maintenance

Potato psyllid (*Bactericera cockerelli* Šulc.) colonies consisted of *C*Lso-free (*C*Lso$^-$) and *C*Lso-positive (*C*Lso$^+$) haplotype B, which were obtained and reared for several generations at Texas A&M AgriLife Research and Extension Center in Weslaco in 60 × 60 × 60 cm nylon mesh cages (Bugdorm, BioQuip Products Rancho Dominguez, CA, USA). Psyllid colonies were reared and maintained on potato plants (Atlantic) and periodically diagnosed for the presence of *C*Lso (>90% *C*Lso$^+$) and the absence of *C*Lso (*C*Lso$^-$) by polymerase chain reaction (PCR) using genomic DNA isolated from adult psyllids (Sengoda et al., 2014) and primers specific to the 16s rDNA of *C*Lso (OA2-F and OI2c-R) (**Supplementary Table 2**) (French-Monar et al., 2010). PCR conditions were given as follows: one denaturing cycle at 95°C for 30 s; 35 cycles each at 95°C for 30 s, 68°C for 30 s, and 68°C for 2 min; and a final extension cycle at 68°C for 5 min. PCR amplicons were separated by electrophoresis on a 1.0% (w/v) agarose gel stained with ethidium bromide (0.5 μg/ml).

Screening of Wild *Solanum* Sect. *Petota* Accessions for ZC Resistance

For primary screening, 52 wild potato accessions were grown in a professional growth mix (Berger BM6 All-Purpose mix,

pH 5.4–6.2) in 2.84-l pots at 22°C under 14-h light/10-h dark photoperiod and 50% relative humidity in controlled growth chambers. No choice feeding was performed on 4-week-old plants by inoculating each plant with 20 *C*Lso$^+$ psyllids enclosed into two separate organza drawstring bags (10 psyllids/bag), which were tied to the second and third fully expanded leaves (**Supplementary Figure 2B**), with four replicates of inoculated plants per accession. The bags and psyllids were removed from plants 1 week after placement. Phenotypic evaluations of foliar ZC disease symptoms were done at 14, 21, and 28 days post-inoculation (dpis) in an environment-controlled growth chamber. Foliar symptoms were evaluated and rated based on a scale of 1–3, where 1 = being resistant (no symptoms), 2 = moderately susceptible (some symptoms), and 3 = highly susceptible (severe symptoms and morbidity) (**Supplementary Figures 2C**, **3**). Chip frying and ZC scoring were performed as described in other studies (Henne et al., 2010; Harrison et al., 2019).

A second screening of the ZC resistant and moderately susceptible accessions chosen from the primary screening and a screening of the single seed lines from true potato seeds were done using 1-month-old plants. To increase quantity, all plants were vegetatively propagated by tissue culture and were planted in modified enclosed transparent 32 oz. plastic cups. No choice feeding was performed by releasing five *C*Lso$^+$ psyllids (presence of *C*Lso was confirmed by PCR diagnostics) into each enclosed cup containing two plants in a professional growth mix Berger BM6 All-Purpose mix, pH 5.4–6.2, with two cups per accession. *C*Lso$^-$ psyllid (absence of *C*Lso was confirmed by PCR diagnostics) challenged and non-challenged plants were used as negative controls (**Supplementary Figure 2A**). Phenotypic evaluations of inoculated plants consisted of assessing foliar symptoms of ZC at 14, 21, and 28 dpi. At 7 dpi, the soil was drenched with Admire Pro (Bayer Crop Science, Germany) to kill all psyllids in enclosed cups and prevent further plant damage. Leaf tissue was collected at 21 and 28 dpi, with 3–4 leaves from the top, middle, and bottom of each plant, cut into pieces with a single edge blade, and pooled to produce four replicates before freezing in liquid nitrogen (VWR Reinforced 2 ml Bead Mill Tubes, Radnor, PA, USA). Tissues were lyophilized before genomic DNA extraction for PCR and quantitative PCR (qPCR) analyses.

Molecular Diagnostics for *C*Lso Detection and Quantification

Genomic DNA was extracted from leaf tissue using a modified protocol as previously published (Edwards et al., 1991). For the detection of *C*Lso in tissues collected from wild potato accessions and Atlantic control, conventional PCR was performed on a ProFlex™ PCR System (Applied Biosystems, Life Technologies, Carlsbad, CA) in a total reaction volume of 20 μl, using 150 ng of DNA, 0.5 μM of each target-specific primer, 10 μl of AccuStart Tough Mix (Quantabio, Beverly, MA, USA), 0.5 μl of 50× loading dye, and 6.6 μl of nuclease-free water (Ambion, Life Technologies, Austin, TX, USA). For initial conventional (gel) PCR analysis, a primer pair, OI2C-F and OA2-R, was used to specifically amplify *C*Lso 16S rDNA (Levy et al., 2011). The potato *Ribosomal Protein L2(RPL2)*-specific primers RPL2-F and RPL2-R were used to amplify an endogenous reference gene (**Supplementary Table 2**) (Avila et al., 2012). PCR conditions were given as follows: one denaturing cycle at 95°C for 30 s; 28 cycles each at 95°C for 30 s, 50°C for 30 s, and 68°C for 2 min; and a final extension cycle at 68°C for 5 min. PCR amplicons were separated by electrophoresis on a 1.0% (w/v) agarose gel stained with ethidium bromide (0.5 μg/ml).

The *C*Lso relative titer was quantified in tissues collected from wild potato accessions and Atlantic control using quantitative PCR (qPCR) in a CFX384™ Real-Time System (Bio-Rad Laboratories, Inc., Hercules, CA, USA) in a total reaction of 10 μl, using 50 ng of DNA, 0.4 μM of each target-specific primer, and 5 μl of i*Taq*™ Universal SYBR Green Supermix (Bio-Rad Laboratories, Inc., Hercules, CA, USA). Three biological replicates were used with two technical replicates. Lso-F and HLB-R primers (**Supplementary Table 2**) were used to specifically amplify *C*Lso 16S rDNA, while Sotu-RPL2-F and Sotu-RPL2-R primers (**Supplementary Table 2**) were used for the amplification of an endogenous reference gene, *RPL2* (Levy et al., 2011; Irigoyen et al., 2020). PCR conditions were given as follows: one denaturing cycle at 95°C for 3 min; 40 two-step cycles each at 95°C for 15 s and at 55°C for 30 s; and a final melting curve of 65–95°C for 55 s. The results were analyzed and recorded as C_T (threshold cycle) values, which were normalized against the C_T values of the potato *RPL2* (**Supplementary Table 2**) for quantification using the comparative C_T method ($2_T^{-\Delta\Delta C}$) (Zuñiga et al., 2020). The Student's *t*-test was used to determine statistically significant ($p \leq 0.05$ or 0.01) differences between the controls and treatments.

Host Selection and Olfactometer Assays

The olfactory host-preference assays of *B. cockerelli* adults (*C*Lso$^-$), reared and maintained on Atlantic potato plants, were conducted using 2-month-old *Sb*-PI310927 and Atlantic plants and a Y-tube olfactometer (35 cm long × 2.5 cm diameter). Twenty *B. cockerelli* adults per set of plants ($n = 10$ sets of plants, *Sb*-PI310927 and Atlantic plants) were collected into plastic vials for 16 h before initiating the behavioral assays to promote insect host choice. The Y-tube was connected to a 2-port Humidified Air Delivery system (ARS, Gainesville, FL, USA). The air was filtered through an activated carbon filter (16 cm, ARS). Airflow of each arm (bifurcated at a 45 angle) was set up at a constant rate of 10 L/min, leading into two separated sealed cylindrical glass chambers (15 cm diameter, 35 cm high) that contained individual plants, *Sb*-PI310927 or Atlantic, as odor sources. The Y-tube was placed at a 30° angle from the surface and adult psyllids were released at the end of the tube. To examine the insect olfactory behavior, observations were recorded by counting the number of psyllids at each arm's terminal end (set threshold = 4 cm) every 15 min for a 60-min period. All others were considered as a non-responding group. All measurements were conducted between 2 and 4 p.m. Central Standard Time (CST) at ambient temperature (21°C) and under constant light (∼250 μmol/m^2 s).

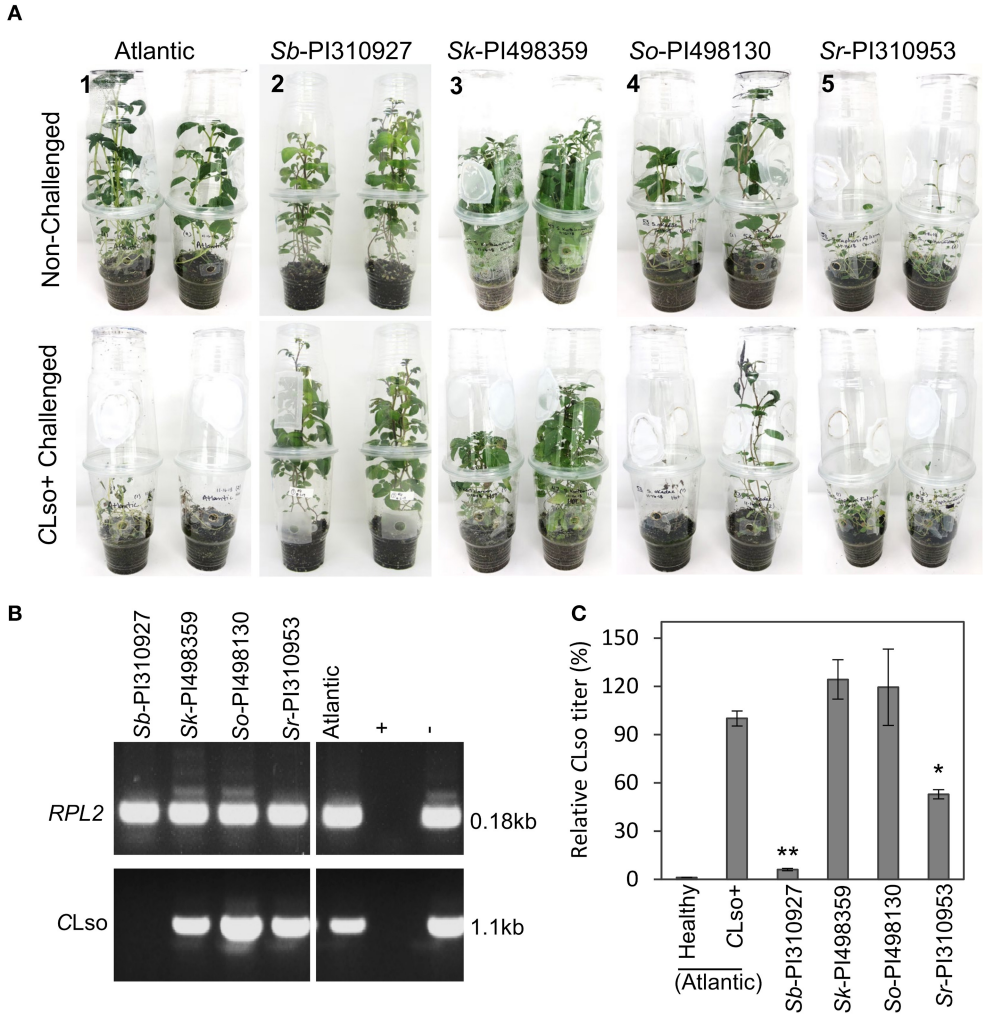

FIGURE 1 | Phenotypic evaluation and *C*Lso quantification of ZC resistant and tolerant wild *Solanum* accessions. A no-choice psyllid feeding assay was performed by releasing five *C*Lso^{+} psyllids on two plants (1-month-old) in a professional growth mix per enclosed cup in an environment-controlled growth chamber. (**A**) The top panel shows representative photos of non-challenged accessions, and the bottom panel representative photos of *C*Lso^{+} challenged accessions at 28 dpi [1, Atlantic control, severity index (SI) = 3. 2; *S. berthaultii PI310927*, SI = 1; 3, *S. kurtzianum* PI498359, SI = 2; 4, *S. okadae* PI498130, SI = 2. 5; and *S. raphanifolium* PI310953, SI = 2). (**B**) Detection of *C*Lso by PCR amplification of *C*Lso 16s rDNA in leaf tissues of the resistant accession (*Sb*-PI310927) and the three tolerant accessions (*Sk*-PI498359, *So*-PI498130, and *Sr*-PI310953) at 28 days post-inoculation (dpi). The potato *RPL2* endogenous gene was used as the PCR control. (**C**) Relative quantification of *C*Lso titers of the accessions at 28 dpi by qPCR. Relative *C*Lso titers were calculated from three biological replicates; error bars represent the mean *C*Lso titer ± standard error of the mean. The *p*-values were calculated by Student's *t*-test relative to the infected control. *, **$P \leq 0.05$ and 0.01, respectively.

Survival and Oviposition of *B. cockerelli* on *Sb*-PI310927 and Atlantic Plants

The survival of *B. cockerelli* adults (*C*Lso^{-}) on 2-month-old *Sb*-PI310927 and Atlantic plants (n = 10 plants; 10 psyllids/plant) was evaluated to record the surviving insects every day for 7 days. To examine the oviposition of *B. cockerelli* on *Sb*-PI310927 and Atlantic plants, a non-choice assay was performed on insect-proof mesh cages (30 × 30 × 30 cm). Before the assay was initiated, couples (female and male psyllids) were allowed to mate for 4 h in a 1.7-ml tube and subsequently transferred onto plants (n = 10 plants; 10 psyllids/plant). After 7 days, adult psyllids were removed, and the total number of eggs was recorded.

Trichome Evaluation of *Sb*-PI310927

One-month-old *in vitro* culture plants of ZC-resistant single seed line 10 of *Sb*-PI310927 accession and Atlantic control were hardened for 1 month in the growth mix. Three 2-mm diameter disks were excised from one leaflet of the second and third fully expanded leaves from two plants of each of *Sb*-PI310927-resistant line 10 and Atlantic control, using a 2-mm sampling tool (Electron Microscopy Sciences, Hatfield, PA, USA), and observed at 60× on an Olympus BX51 stereomicroscope (Olympus Corporation, Tokyo, Japan). Leaflet disks were evaluated for leaf trichome shape and density based on two biological samplings and 12 technical replications. Trichome density was calculated as

the number of trichomes per mm^2 leaf area on both the adaxial and abaxial leaflet surfaces.

Data Analysis and Statistics

The data analysis, statistics, and graphs were displayed as described in the figure legends using the Microsoft Excel software (version 2009). The Student's *t*-test was used to determine statistically significant ($p \leq 0.05$, 0.01, or 0.001) differences in *C*Lso titer and oviposition between control and treatment. The Chi-square (χ^2) test was used to compare the number of potato psyllids responding to plant odor sources using a Y-tube olfactometer. The survival of potato psyllids was estimated using the Kaplan–Meier survival analysis using the RStudio environment (Allaire, 2011).

RESULTS

ZC Resistance Exists Among the Wild *Solanum* Sect. *Petota* Collection

Primary screening of 52 wild potato accessions was performed from the *Solanum* sect. *Petota* collection (**Supplementary Table 1**) to identify potential lines with resistance and tolerance to *C*Lso or the psyllid. Multiple *in vitro* propagated plants of each accession were hardened in pots for 2 months, followed by exposure to *C*Lso$^+$ psyllids. Foliar symptoms of ZC were then observed every 7 days for up to 4 weeks (**Supplemental Figure 2A, B**) and rated based on a scale of 1–3, where 1 = being resistant (no symptoms), 2 = moderately susceptible (some symptoms), and 3 = highly susceptible (severe symptoms and morbidity) (**Supplementary Figure 2C**). Several of the 52 accessions were susceptible and moderately susceptible, showing some upward leaf rolling, chlorosis, and plant stunting, but they grew new leaves at 21–28 dpi. Interestingly, one diploid accession *Solanum berthaultii* Hawkes (*Sb*-PI310927), sourced initially from Bolivia, seemed resistant with no visible ZC symptoms. The nine accessions (one resistant and eight moderately susceptible) were selected, and the challenges with *C*Lso$^+$ psyllids were repeated using 1-month-old plants grown in terrariums (enclosed cups). In addition to phenotypic observation for ZC symptoms, the relative *C*Lso titers were estimated at 28 dpi when *C*Lso could be sufficiently detected. The single resistant accession, *Sb*-PI310927, reproducibly showed no visible symptoms and continued to grow after 28 dpi with a severity index of 1, compared with the susceptible Atlantic control that displayed severe symptoms and died at 28 dpi (severity index 3). Three accessions, namely, *Sk*-PI498359, *So*-PI498130, and *Sr*-PI310953, again showed reproducible ZC symptoms with a severity index scale of 2 (**Figure 1A**). The remaining five accessions displayed variable symptoms and died at 28 dpi, with a severity index of 3. In this experiment, both conventional and quantitative PCR confirmed the presence or absence of *C*Lso (**Figures 1B,C**). The resistant accession *Sb*-PI310927 and the three moderately susceptible accessions (i.e., *Sk*-PI498359, *So*-PI498130, and *Sr*-PI310953) displayed *C*Lso titers of 6.05% and 52.44–119.36%, respectively, relative to that of the Atlantic control (set to 100%) (**Figure 1C**).

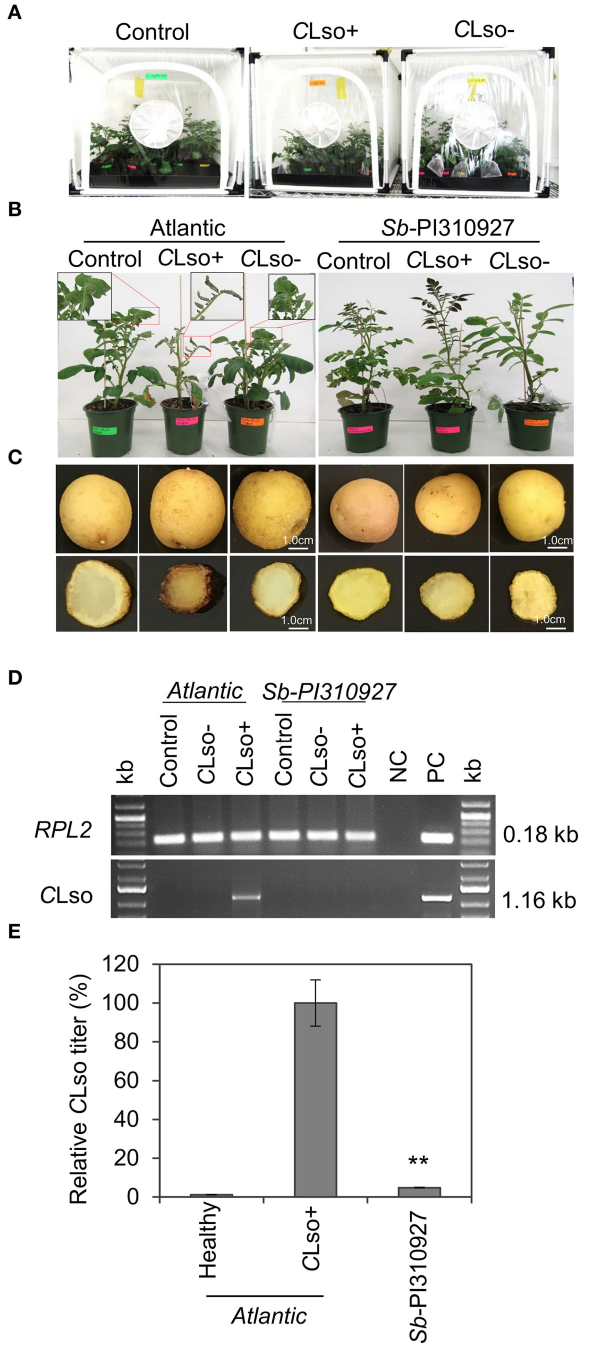

FIGURE 2 | ZC resistance trait evaluation of the *Solanum berthaultii* accession PI310927. (**A**) Two-month-old *Sb*-PI310927 accession and Atlantic control plants in pots were randomized and challenged with *C*Lso$^+$ and *C*Lso$^-$ psyllids inside cages under greenhouse conditions. (**B, C**) The above-ground phenotype of 4-week-old *Sb*-PI310927 accession and Atlantic plants and their corresponding tuber and fried chip phenotypes. (**D**) Detection of *C*Lso by PCR amplification of *C*Lso 16s rDNA in leaf tissues of *Sb*-PI310927 accession and Atlantic at 28 dpi. The potato *RPL2* endogenous gene was used as the PCR control (NC, negative control; PC, positive control). (**E**) Relative quantification of *C*Lso titer of *Sb*-PI310927 accession and Atlantic control plants at 28 dpi by qPCR. Relative *C*Lso titers were calculated from three biological replicates; error bars represent ± standard error of the mean. The *p*-values were calculated by Student's *t*-test relative to the infected control. $^{**}P \leq 0.01$.

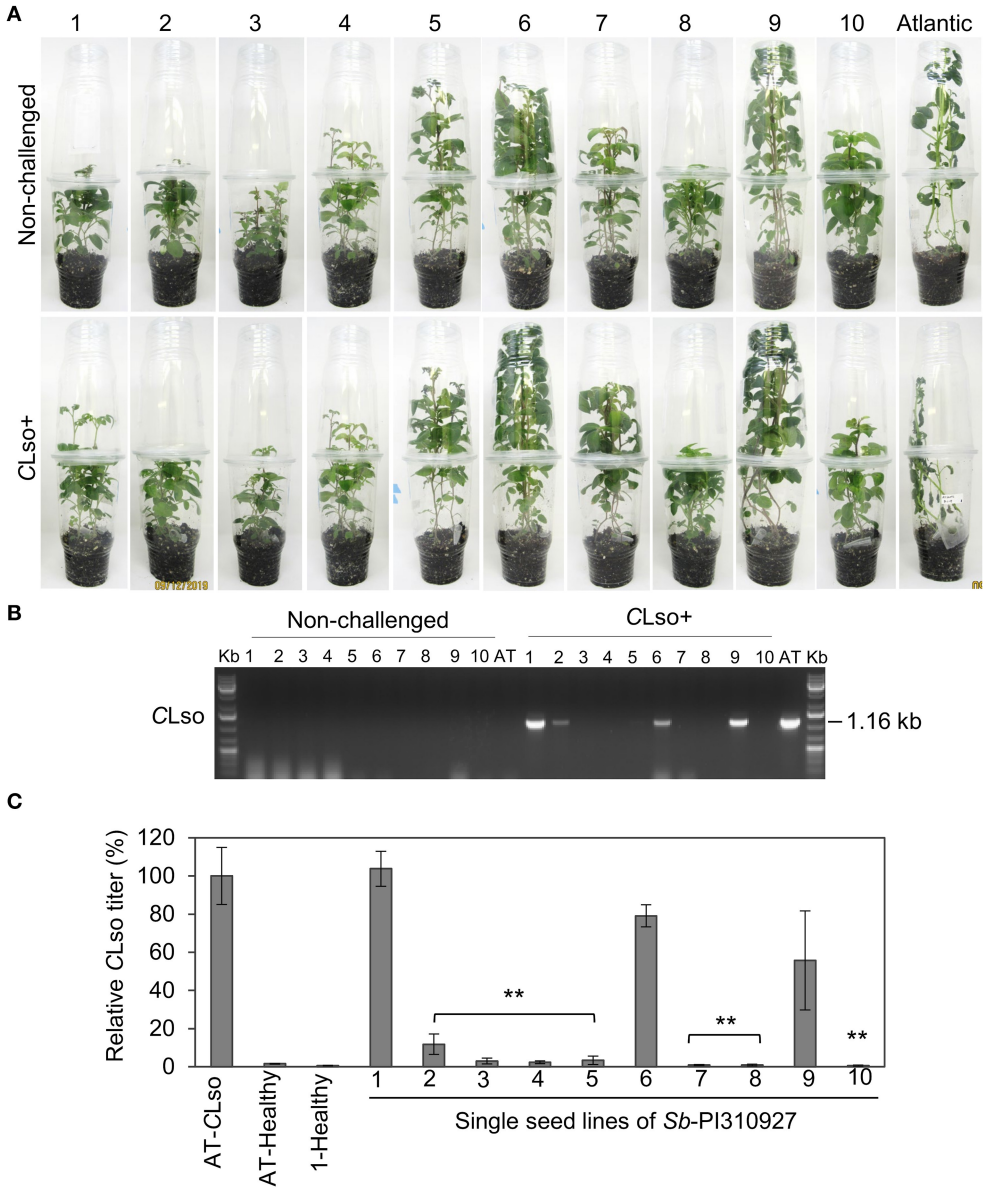

FIGURE 3 | ZC resistance trait evaluation of single seed lines of *Solanum berthaultii* accession PI310927. (**A**) Photos of representative lines 1–10 of *Sb*-PI310927 and Atlantic controls following challenge with *C*Lso^{+} psyllids at 28 dpi. (**B**) Detection of *C*Lso by PCR amplification of *C*Lso 16s rDNA in leaf tissues of 10 single seed lines of *Sb*-PI310927 accession and Atlantic (AT) control plants challenged with *C*Lso^{+} psyllids or no psyllids at 28 dpi. Controls included a positive control, *C*Lso-infected Atlantic, a negative control, healthy Atlantic (H), and water (W). (**C**) Relative quantification of *C*Lso titers of the single seed lines and Atlantic (AT) at 28 dpi by qPCR. Relative *C*Lso titers were calculated from three biological replicates; error bars represent ± standard error of the mean. The *p*-values were calculated by Student's *t*-test relative to the infected control. $^{**}P \leq 0.01$.

Further comparative studies were carried on with the resistant (*Sb*-PI310927) and highly susceptible control (Atlantic) plants.

Sb-PI310927 Is ZC Resistant

The ZC resistance trait of *Sb*-PI310927 was confirmed by repeating the ZC challenges, using 2-month-old plants under greenhouse conditions, and evaluating the ZC tuber symptoms. Typically, *C*Lso-psyllid feeding for the brief period of the challenge (∼7 days) causes the inoculated lower leaves to wilt, while the newly emerging (upper) non-inoculated leaves remain asymptomatic. In contrast, *C*Lso+ psyllids induce symptoms associated with ZC on new upper non-inoculated leaves ranging from leaf wilting, upward curling, and chlorosis/necrosis. They can also lead to severe stunting of the plants (**Supplementary Figure 4**). *Sb*-PI310927 plants consistently showed no visual ZC foliar symptoms with a severity index of 1 when challenged with *C*Lso^{+} or *C*Lso^{-} psyllids. However, the susceptible Atlantic variety displayed

typical ZC foliar symptoms with a severity index of 3 when infected with *C*Lso$^+$ psyllids at 28 dpi (**Figure 2B**). Freshly cut tubers and fried chips of *C*Lso-infected *Sb*-PI310927 accession showed no brown discoloration, whereas Atlantic displayed characteristic ZC tuber symptoms (**Figure 2C**). Furthermore, molecular diagnostic analyses by qPCR and conventional PCR indicated that *Sb*-PI310927 had a very low relative *C*Lso titer of 4.87% compared with Atlantic plants (*C*Lso titer set to 100%) (**Figures 2D,E**).

Segregation of ZC Resistance Among True Seed Progeny of *Sb-PI310927*

All screening was conducted using *in vitro* micro-propagated plants from a true seed sourced from the USDA-ARS germplasm bank. As with most wild germplasm collections, *Sb*-PI310927 true seeds could be heterozygous and pooled from multiple plants during germplasm maintenance, thus having the potential for segregating alleles (Bamberg and Del Rio, 2020). To determine if there would be any segregation of the ZC-resistant trait of *Sb*-PI310927 among true seed progeny and to recover a stable resistant line for further studies, 10 true botanical seeds of *Sb*-PI310927 were germinated and multiplied individually by micropropagation. The ZC resistance trait of the 10 single seed lines was then evaluated following no-choice challenges with *C*Lso$^+$, *C*Lso$^-$, or no psyllids under growth chamber conditions (**Figure 3A**). At 21 dpi, the susceptible Atlantic control showed characteristic ZC symptoms with high titers of *C*Lso transmission, whereas almost all *Sb*-PI310927 lines did not show any ZC symptoms. However, conventional PCR revealed that only ∼50% of *Sb*-PI310927 single seed lines were negative for *C*Lso (**Figure 3B**). Further confirmation by quantitative PCR showed that six *Sb*-PI310927 single seed lines (#3, 4, 5, 7, 8, and 10) were *C*Lso$^-$ or had undetectable levels of *C*Lso. Three lines (#2, 6, and 9) showed low to moderate levels of *C*Lso compared with Atlantic control (*C*Lso titer set to 100%). We also noted some segregation in plant height among the 10 lines, which can be observed even among unchallenged (healthy) plants. Together, these results suggest some degree of segregating alleles among the true seed pools of these wild accessions possible for multiple traits (Bamberg and Del Rio, 2020).

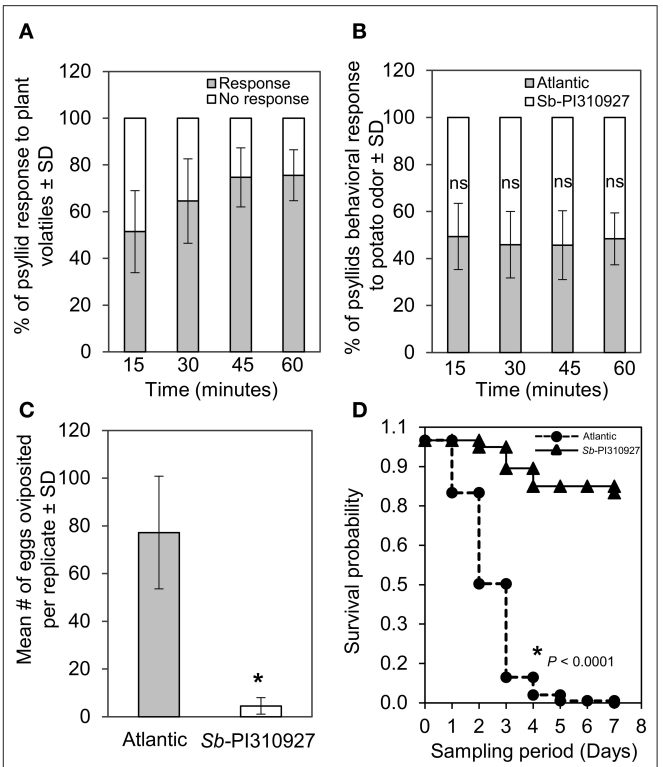

FIGURE 4 | Olfactometer, oviposition, and survival evaluations of *Bactericera cockerelli* adults on *Solanum berthaultii* PI310927. (**A**) Olfactometer (Y-tube) behavioral response of potato psyllid adults to plant volatiles under stable conditions observed every 15 min for a maximum of 60 min. Bar graphs represent the overall mean percentages of adults choosing either odor source ± standard deviation ($n = 10$). (**B**) Potato psyllid's behavioral response to *Sb*-PI310927 and susceptible Atlantic (control). Bar graphs represent the mean percentages of adults ± standard deviation ($n = 10$). (**C**) Female psyllids oviposition at day 7 in no-choice assays using whole plants. Bar graphs represent the mean number of oviposited eggs per replicate ± standard deviation ($n = 10$); the *p*-value was calculated by Student's *t*-test relative to the Atlantic control, $^*P \leq 0.0001$. (**D**) Survival analysis of potato psyllid adults ($n = 10$) for 7 days showed significant psyllids mortality after exposure to *Sb*-PI310927 when compared with Atlantic plants. The *p*-value was calculated by the Kaplan–Meier analysis, $P < 0.0001$. SD, standard deviation; ns, no significance.

Host Preference, Fecundity, and Survival of the Psyllids on Sb-PI310927

The following two possible mechanisms explain the ZC resistance trait of *Sb*-PI310927: (i) resistance to the psyllid either by antixenosis or antibiosis effects and (ii) immune gene-mediated resistance to the bacteria or the insect. Although not mutually exclusive, we first explored if there were antixenosis or antibiosis effects. For this, we evaluated whether there was a host preference between *Sb*-PI310927 line#10 and Atlantic plants equidistantly placed in an olfactometer-based choice assay ($n = 10$ plants; 20 psyllids/plant). Of the total psyllids analyzed in the experiment (20 psyllids × 10 plants = 200 psyllids), the majority (76%) of them responded within 60 min after the assay was initiated, i.e., reached a 4-cm set threshold distance in the arms toward the plant odor sources (**Figure 4A**). However, no significant differences in host-selection were found between *Sb*-PI310927 and Atlantic odor sources at the sampling points tested (**Figure 4B**; 15 min: $\chi^2 = 0.053$, $df = 1$, $P = 0.82$; 30 min: $\chi^2 = 0.644$, $df = 1$, $P = 0.42$; 45 min: $\chi^2 = 0.65$, $df = 1$, $P = 0.42$; and 60 min: $\chi^2 = 0.118$, $df = 1$, $P = 0.73$).

As there were no differences in host preference, we next evaluated if there were any adverse effects on oviposition, hatching, and survival of psyllids using no-choice assays with 2-month-old *Sb*-PI310927 line#10 and Atlantic plants ($n = 10$ plants; 10 psyllids/plant). The results showed a significant reduction ($F = 113.68$, $df = 1$, $P < 0.001$) in the number of oviposited eggs after 7 days on *Sb*-PI310927 when compared with Atlantic plants (**Figure 4C**). The few oviposited eggs on *Sb*-PI310927 were also defective in hatching. Furthermore,

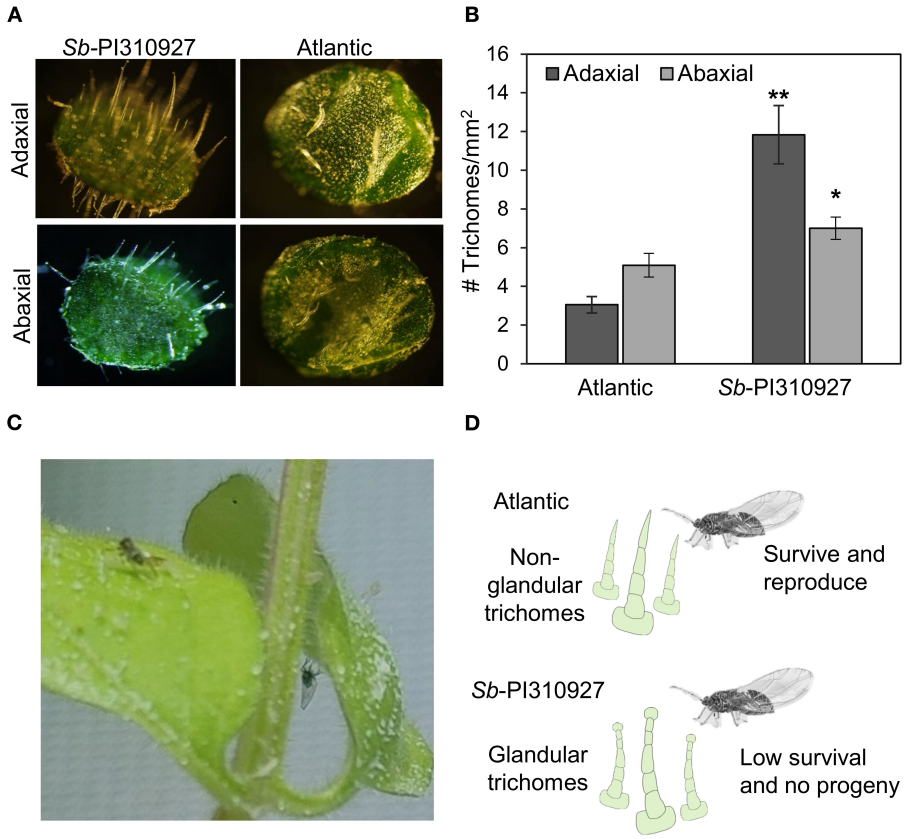

FIGURE 5 | Evaluation of leaf trichomes on *Solanum berthaultii* PI310927 and Atlantic. (**A**) Microscopic evaluation of shape and density of trichomes on the abaxial and adaxial surfaces of leaves of *Sb*-PI310927 line 10 and Atlantic controls. (**B**) Estimation of trichome density on the adaxial and abaxial leaf surfaces of *Sb*-PI310927 and Atlantic controls. Errors bars represent the mean number of trichomes per mm^2 ± standard error of the mean ($n = 12$). The *p*-values were calculated by Student's *t*-test relative to the Atlantic control. * $P \leq 0.01$; ** $P \leq 0.001$. (**C**) Dead psyllids on abaxial and adaxial leaf surfaces of *Sb*-PI310927 plants using non-choice assays. (**D**) Proposed mechanism of negative effects of *Sb*-PI310927 on potato psyllid.

survival analysis showed that adult psyllids on *Sb*-PI310927 had a significantly (Kaplan Meier analysis, $P < 0.0001$) lowered probability of survival beyond day 3 when compared with Atlantic plants (**Figure 4D**).

Leaf Trichome Density and Morphological Differences of *Sb-PI310927*

Lastly, in our experiments, we observed that the leaves of *S. berthaultii* were "sticky," and the movement of psyllids appeared to be impaired (**Figure 5C**). Hence, under a microscope, we examined the adaxial and abaxial surfaces of 1-month-old Sb-PI310927 line #10. *Sb*-PI310927 leaves had a more significant number of trichomes, and they appear longer than those of Atlantic leaves (**Figures 5A,B**). The number of trichomes was significantly ($P < 0.01$) higher in *Sb*-PI310927 than in Atlantic leaves on both the adaxial and abaxial surfaces (**Figures 5A,B**). It is possible that the observed reduced fecundity and survival of psyllids effects on *Sb*-PI310927 could be associated with the increased trichome density and the presence of glandular trichomes (**Figures 5C,D**).

DISCUSSION

Zebra chip, a devastating potato disease worldwide, is complex due to its association with the phloem-limited and uncultured CLso and the potato psyllid vector. Using chemical measures has helped control the psyllid population, but it is associated with high costs and positive selection for insecticide resistance (Szczepaniec et al., 2019). In the present study, new sources of ZC resistance were identified among a wild collection of tuber-bearing *Solanum* spp. (*Solanum* sect. *Petota*) (Hardigan et al., 2015). This panel is a taxonomically well-characterized and diverse collection to mine for valuable traits (Hardigan et al., 2015).

Following the screening, phenotypic evaluations, and quantitation of CLso titers of 52 accessions infected with CLso carrying psyllids, we identified one ZC-resistant accession, *S. berthaultii* PI310927, and three ZC moderately tolerant accessions, namely, *Solanum kurtzianum* PI498359, *Solanum okadae* PI498130, and *Solanum raphanifolium* PI310953. Phenotypically, although the three ZC-tolerant wild *Solanum* accessions (*S. kurtzianum* PI498359, *S. okadae* PI498130, and *S.*

raphanifolium PI310953) showed some ZC foliar symptoms at 28 dpi, they were able to tolerate and survive *C*Lso. In contrast, the susceptible Atlantic control plants showed severe symptoms, wilting, and eventual death. There are some commonalities among the three tolerant and one resistant accessions. They were all sourced from countries that are relatively closer to the South American continent (Hardigan et al., 2015). The four species are diploids and belong to the same species, clade 4, as described by Spooner and Castillo (1997). Several of these accessions were also previously reported to be tolerant to other potato pests, including green peach aphid, potato aphid, Colorado potato beetle, potato flea beetle, and potato leafhopper (Flanders et al., 1992).

The *S. berthaultii* PI310927 is a highly promising candidate among the ZC-resistant lines. Characterization of resistance among the *S. berthaultii* PI310927 true seeds showed a low-to-moderate level of transmission of *C*Lso among true seed progeny, indicating the presence of heterozygosity or allelic variation among the true seed progeny, which is expected from wild germplasm where traits and alleles are not fixed. Potato breeding efforts with hybrids that incorporated *S. berthaultii* as one of the parents reported variable levels of tolerance to *C*Lso, likely caused due to the heterogeneity of the progeny (Butler et al., 2011; Prager et al., 2013; Rashidi et al., 2017). Our results suggest that natural allelic variations present among the true seed progenies of wild germplasm can impact trait phenotypes and underscore the need to evaluate multiple seed progeny independently propagated.

Importantly, we were able to recover several true seed lines of *S. berthaultii* PI310927 (#3, 4, 5,7, 8, and 10) that showed no ZC symptoms and detectable *C*Lso, when compared with the Atlantic control (100%) (**Figures 3B,C**). Further characterization of the resistant single seed line #10 showed no differences in psyllid preference to odor sources of *Sb*-PI310927 and Atlantic plants (**Figures 4A,B**). However, we found greater leaf trichome density that may cause the negative impacts observed on psyllid fecundity and survival (**Figures 4C,D**, **5A–D**). Previous studies on other wild potato relatives and hybrids suggested similar effects of the glandular trichomes against several potato pests (Tingey and Gibson, 1978; Tingey and Laubengayer, 1981; Yencho and Tingey, 1994; Malakar and Tingey, 2000; Butler et al., 2011; Diaz-Montano et al., 2014; Rubio-Covarrubias et al., 2017). Additionally, specific secondary metabolites produced by glandular trichomes were reported to influence host selection (Prager et al., 2018). Further investigation into potential chemical signatures or metabolites synthesized by the *S. berthaultii* PI310927 glandular trichomes may bring new insights into the mechanisms of the observed ZC and psyllid resistance.

CONCLUSION

In this study, screening 52 tuber-bearing wild *Solanum* species resulted in identifying a ZC resistant and several tolerant accessions. The resistant *S. berthaultii* accession has dense glandular leaf trichomes. This foliar structural modification could be responsible for much of the observed ZC resistance. We suggest the *S. berthaultii* as a promising source for ZC/psyllid resistance that can be further studied to understand insect resistance mechanisms and incorporated into the potato production system as a trap crop for psyllid or breeding new potato cultivars.

DATA AVAILABILITY STATEMENT

The original contributions presented in the study are included in the article/**Supplementary Material**, further inquiries can be directed to the corresponding author/s.

AUTHOR CONTRIBUTIONS

KM conceived the project and supervised the study. KM, FI, CA, VA, and MV designed the experiments and interpreted the results. VM, MR, MD, and SI conducted the experiments, analyzed the data, and prepared the manuscript. All authors contributed to the editing and review of the manuscript.

FUNDING

This study was supported in part by funds from Texas A&M AgriLife Research Insect-Vectored Disease Seed Grant (124185-96210) and the Texas A&M AgriLife Institute for Advancing Health Through Agriculture, USDA-NIFA (HATCH 1023984) to KM and USDA-NIFA (2019-03814) to MIV. We thank Jesse Schartner and John Bamberg (U.S. Potato Genebank, NRSP-6, Sturgeon Bay, WI) for providing the *Solanum* accessions. We also thank the technical assistance of Denise Rossi, Ashley Jacques, Briana Jacques, and Renesh Bedre (Texas A&M AgriLife Research).

SUPPLEMENTARY MATERIAL

The Supplementary Material for this article can be found online at: https://www.frontiersin.org/articles/10.3389/fmicb.2022.857493/full#supplementary-material

Supplementary Figure 1 | Morphological diversity among the tuber-bearing *Solanum* section *Petota* species.

Supplementary Figure 2 | Phenotypic evaluation of zebra chip (ZC) disease symptoms in wild *Solanum* section *Petota* accessions. Screening of accessions was done using a no-choice feeding assay and *Candidatus* Liberibacter solanacearum-carrying psyllids in the soil in modified cups (**A**) and pots (**B**) inside cages. (**C**) ZC severity index (SI) scale (1, resistant; 2, moderately susceptible; 3, highly susceptible).

Supplementary Figure 3 | Preliminary screening of *Solanum* section *Petota* accessions for resistance or tolerance to zebra chip disease, with a no-choice feeding assay with *Candidatus* Liberibacter solanacearum-carrying psyllids. Morphological differences in ZC symptoms of 28-day-old *Solanum* sect. *Petota* accessions.

Supplementary Figure 4 | The phenotypes of 4-week-old Atlantic and *Sb*-PI310927 accession zebra chip disease, with a no-choice feeding assay with *Candidatus* Liberibacter solanacearum-carrying psyllids. Morphological differences in ZC symptoms (leaf curling and wilting) of Atlantic (28-day-old) (**A**) and *Sb*-PI310927 (**B**) are shown. A closeup of ZC symptoms is shown in the inset box.

Supplementary Table 1 | List of the *Solanum* species and accessions screened for zebra chip resistance.

Supplementary Table 2 | List of primers used in this study.

REFERENCES

Allaire, J. J. (2011). "RStudio: Integrated development environment for R," in *The R User Conference* (Coventry: University of Warwick). Available online at: https://www.r-project.org/conferences/useR-2011/abstracts/180111-allairejj.pdf

Avila, C. A., Arévalo-Soliz, L. M., Jia, L., Navarre, D. A., Chen, Z., Howe, G. A., et al. (2012). Loss of function of fatty acid desaturase 7 in tomato enhances basal aphid resistance in a salicylate-dependent manner. *Plant Physiol.* 158, 2028–2041. doi: 10.1104/pp.111.191262

Bamberg, J., and Del Rio, A. (2020). Assessing under-estimation of genetic diversity within wild potato (*Solanum*) species populations. *Am. J. Pot. Res.* 97, 547–553. doi: 10.1007/s12230-020-09802-3

Buchman, J. L., Heilman, B. E., and Munyaneza, J. E. (2011). Effects of liberibacter-infective *Bactericera cockerelli* (Hemiptera: Triozidae) density on zebra chip potato disease incidence, potato yield, and tuber processing quality. *J. Econ. Entom.* 104, 1783–1792. doi: 10.1603/EC11146

Butler, C. D., Gonzalez, B., Manjunath, K. L., Lee, R. F., Novy, R. G., Miller, J. C., et al. (2011). Behavioral responses of adult potato psyllid, *Bactericera cockerelli* (Hemiptera: Triozidae), to potato germplasm and transmission of *Candidatus* Liberibacter psyllaurous. *J. Crop Protect.* 30, 1233–1238. doi: 10.1016/j.cropro.2011.05.006

Cooper, W. R., and Bamberg, J. B. (2014). Variation in *Bactericera cockerelli* (Hemiptera: Triozidae) oviposition, survival, and development on *Solanum bulbocastanum* germplasm. *Am. J. Pot. Res.* 91, 532–537. doi: 10.1007/s12230-014-9384-x

Cooper, W. R., and Bamberg, J. B. (2016). Variation in susceptibility to potato psyllid, *Bactericera cockerelli* (Hemiptera: Triozidae), among *Solanum verrucosum* germplasm accessions. *Am. J. Pot. Res.* 93, 386–391. doi: 10.1007/s12230-016-9512-x

Dahal, K., Li, X.-Q., Tai, H., Creelman, A., and Bizimungu, B. (2019). Improving potato stress tolerance and tuber yield under a climate change scenario–a current overview. *Front. Plant Sci.* 10, 563. doi: 10.3389/fpls.2019.00563

Diaz-Montano, J., Vindiola, B. G., Drew, N., Novy, R. G., Miller, J. C., and Trumble, J. T. (2014). Resistance of selected potato genotypes to the potato psyllid (Hemiptera: Triozidae). *Am. J. Pot. Res.* 91, 363–367. doi: 10.1007/s12230-013-9356-6

Edwards, K., Johnstone, C., and Thompson, C. (1991). A simple and rapid method for the preparation of plant genomic DNA for PCR analysis. *Nucleic Acids Res.* 19, 1349. doi: 10.1093/nar/19.6.1349

Faostat, F. (2020). FAOSTAT [Online]. Available online at: http://www.fao.org/faostat/en/#data/QC (accessed May 04, 2020).

Fife, A. N., Cruzado, K., Rashed, A., Novy, R. G., and Wenninger, E. J. (2020). Potato psyllid (Hemiptera: Triozidae) behavior on three potato genotypes with tolerance to '*Candidatus* Liberibacter solanacearum'. *J. Insect Sci.* 20, 15. doi: 10.1093/jisesa/ieaa020

Flanders, K. L., Hawkes, J. G., Radcliffe, E. B., and Lauer, F. I. (1992). Insect resistance in potatoes: sources, evolutionary relationships, morphological and chemical defenses, and ecogeographical associations. *Euphytica* 61, 83–111. doi: 10.1007/BF00026800

French-Monar, R., Patton Iii, A., Douglas, J., Abad, J., Schuster, G., Wallace, R., et al. (2010). First report of "*Candidatus* Liberibacter solanacearum" on field tomatoes in The United States. *Plant Dis.* 94, 481–481. doi: 10.1094/PDIS-94-4-0481A

Greenway, G. (2014). Economic impact of zebra chip control costs on grower returns in seven US states. *Am. J. Potato Res.* 91, 714–719. doi: 10.1007/s12230-014-9404-x

Greenway, G. A., and Rondon, S. (2018). Economic impacts of zebra chip in Idaho, Oregon, and Washington. *Am. J. Pot. Res.* 95, 362–367. doi: 10.1007/s12230-018-9636-2

Guenthner, J., Goolsby, J., and Greenway, G. (2012). Use and cost of insecticides to control potato psyllids and zebra chip on potatoes. *Southwestern Entomol.* 37, 263–270, 268. doi: 10.3958/059.037.0302

Hardigan, M. A., Bamberg, J., Buell, C. R., and Douches, D. S. (2015). Taxonomy and genetic differentiation among wild and cultivated germplasm of *Solanum* sect. *Petota*. *Plant Genome* 8, 1–16. doi: 10.3835/plantgenome2014.06.0025

Harrison, K., Tamborindeguy, C., Scheuring, D. C., Herrera, A. M., Silva, A., Badillo-Vargas, I. E., et al. (2019). Differences in Zebra Chip severity between '*Candidatus* Liberibacter solanacearum' haplotypes in Texas. *Am. J. Pot. Res.* 96, 86–93. doi: 10.1007/s12230-018-9692-7

Hawkes, J. G. (1990). *The Potato: Evolution, Biodiversity and Genetic Resources*. Belhaven Press.

Henne, D., Workneh, F., Wen, A., Price, J., Pasche, J., Gudmestad, N., et al. (2010). Characterization and epidemiological significance of potato plants grown from seed tubers affected by zebra chip disease. *Plant Dis.* 94, 659–665. doi: 10.1094/PDIS-94-6-0659

Irigoyen, S., Ramasamy, M., Pant, S., Niraula, P., Bedre, R., Gurung, M., et al. (2020). Plant hairy roots enable high throughput identification of antimicrobials against *Candidatus* Liberibacter spp. *Nature Comm.* 11, 1–14. doi: 10.1038/s41467-020-19631-x

Levy, J., Ravindran, A., Gross, D., Tamborindeguy, C., and Pierson, E. (2011). Translocation of *Candidatus* Liberibacter solanacearum, the zebra chip pathogen, in potato and tomato. *Phytopathology* 101, 1285–1291. doi: 10.1094/PHYTO-04-11-0121

Levy, J., and Tamborindeguy, C. (2014). *Solanum habrochaites*, a potential source of resistance against *Bactericera cockerelli* (Hemiptera: Triozidae) and "*Candidatus* Liberibacter solanacearum". *J. Econ. Entom.* 107, 1187–1193. doi: 10.1603/EC13295

Malakar, R., and Tingey, W. M. (2000). Glandular trichomes of *Solanum berthaultii* and its hybrids with potato deter oviposition and impair growth of potato tuber moth. *Entomol. Exp. Appl.* 94, 249–257. doi: 10.1046/j.1570-7458.2000.00627.x

Mawassi, M., Dror, O., Bar-Joseph, M., Piasezky, A., Sjölund, J., Levitzky, N., et al. (2018). '*Candidatus* Liberibacter solanacearum' is tightly associated with carrot yellows symptoms in Israel and transmitted by the prevalent psyllid vector *Bactericera trigonica*. *Phytopathology* 108, 1056–1066. doi: 10.1094/PHYTO-10-17-0348-R

Mora, V., Ramasamy, M., Damaj, M. B., Irigoyen, S., Ancona, V., Ibanez, F., et al. (2021). Potato zebra chip: an overview of the disease, control strategies and prospects. *Front. Microbiol.* 12:700663. doi: 10.3389/fmicb.2021.700663

Munyaneza, J., Crosslin, J., and Upton, J. (2007). Association of Bactericera cockerelli (Homoptera: Psyllidae) with "zebra chip," a new potato disease in southwestern United States and Mexico. *J. Econ. Entom.* 100, 656–663. doi: 10.1603/0022-0493(2007)100[656:AOBCHP]2.0.CO;2

Munyaneza, J., Fisher, T., Sengoda, V., Garczynski, S., Nissinen, A., and Lemmetty, A. (2010). First report of "*Candidatus* Liberibacter solanacearum" associated with psyllid-affected carrots in Europe. *Plant Disease* 94, 639. doi: 10.1094/PDIS-94-5-0639A

Munyaneza, J., Sengoda, V., Crosslin, J., Garzon-Tiznado, J., and Cardenas-Valenzuela, O. (2009a). First report of "*Candidatus* Liberibacter solanacearum" in tomato plants in Mexico. *Plant Dis.* 93, 1076–1076. doi: 10.1094/PDIS-93-10-1076A

Munyaneza, J. E. (2012). Zebra chip disease of potato: biology, epidemiology, and management. *Am. J. Potato Res.* 89, 329–350. doi: 10.1007/s12230-012-9262-3

Munyaneza, J. E., Crosslin, J. M., and Buchman, J. L. (2009b). Seasonal occurrence and abundance of the potato psyllid, *Bactericera cockerelli*, in south central Washington. *Am. J. Pot. Res.* 86, 513. doi: 10.1007/s12230-009-9108-9

Murashige, T., and Skoog, F. (1962). A revised medium for rapid growth and bio assays with tobacco tissue cultures. *Physiol. Plant.* 15, 473–497. doi: 10.1111/j.1399-3054.1962.tb08052.x

Navarre, D. A., Shakya, R., Holden, J., and Crosslin, J. M. (2009). LC-MS analysis of phenolic compounds in tubers showing zebra chip symptoms. *Am. J. Pot. Res* 86, 88–95. doi: 10.1007/s12230-008-9060-0

Nwugo, C. C., Sengoda, V. G., Tian, L., and Lin, H. (2017). Characterization of physiological and molecular processes associated with potato response to zebra chip disease. *Hortic. Res.* 4, 1–9. doi: 10.1038/hortres.2017.69

Portal, U. P. H. I. (2017). *Pest Alert: Zebra Chip Disease of Potato*. Available online at: https://planthealthportal.defra.gov.uk/pests-and-diseases/high-profile-pests-and-diseases/zebra-chip-disease-of-potato/

Prager, S., Wallis, C., Jones, M., Novy, R., and Trumble, J. (2018). Examining the potential role of foliar chemistry in imparting potato germplasm tolerance to potato psyllid, green peach aphid, and zebra chip disease. *J. Econ. Entom.* 111, 327–336. doi: 10.1093/jee/tox255

Prager, S. M., Vindiola, B., Kund, G. S., Byrne, F. J., and Trumble, J. T. (2013). Considerations for the use of neonicotinoid pesticides in management of *Bactericera cockerelli* (Šulk)(Hemiptera: Triozidae). *Journal of Crop Protection* 54, 84–91. doi: 10.1016/j.cropro.2013.08.001

Rashidi, M., Novy, R. G., Wallis, C. M., and Rashed, A. (2017). Characterization of host plant resistance to zebra chip disease from species-derived potato genotypes and the identification of new sources of zebra chip resistance. *PLOS ONE* 12, e0183283. doi: 10.1371/journal.pone.0183283

Rubio-Covarrubias, O., Cadena-Hinojosa, M., Prager, S., Wallis, C., and Trumble, J. (2017). Characterization of the tolerance against zebra chip disease in tubers of advanced potato lines from Mexico. *Am. J. Potato Res.* 94, 342–356. doi: 10.1007/s12230-017-9570-8

Savary, S., Willocquet, L., Pethybridge, S. J., Esker, P., Mcroberts, N., and Nelson, A. (2019). The global burden of pathogens and pests on major food crops. *Nat. Ecol. Evol* 3, 430–439. doi: 10.1038/s41559-018-0793-y

Sengoda, V. G., Cooper, W. R., Swisher, K. D., Henne, D. C., and Munyaneza, J. E. (2014). Latent period and transmission of "*Candidatus* Liberibacter solanacearum" by the potato psyllid *Bactericera cockerelli* (Hemiptera: Triozidae). *PLoS ONE* 9, e93475. doi: 10.1371/journal.pone.0093475

Spooner, D. M., and Castillo, R. (1997). Reexamination of series relationships of South American wild potatoes (Solanaceae: *Solanum* sect. Petota): evidence from chloroplast DNA restriction site variation. *Am. J. Bot.* 84, 671–685. doi: 10.2307/2445904

Szczepaniec, A., Varela, K. A., Kiani, M., Paetzold, L., and Rush, C. M. (2019). Incidence of resistance to neonicotinoid insecticides in *Bactericera cockerelli* across Southwest US. *Crop Protect.* 116, 188–195. doi: 10.1016/j.cropro.2018.11.001

Tahzima, R., Maes, M., Achbani, E., Swisher, K., Munyaneza, J., and De Jonghe, K. (2014). First report of '*Candidatus* Liberibacter solanacearum' on carrot in Africa. *Plant Dis.* 98, 1426. doi: 10.1094/PDIS-05-14-0509-PDN

Tingey, W. M., and Gibson, R. W. (1978). Feeding and mobility of the potato leafhopper impaired by glandular trichomes of *Solanum berthaultii* and *S. polyadenium*. *J. Econ. Entom.* 71, 856–858. doi: 10.1093/jee/71.6.856

Tingey, W. M., and Laubengayer, J. E. (1981). Defense against the green peach aphid and potato leafhopper by glandular trichomes of *Solanum berthaultii*. *J. Econ. Entom.* 74, 721–725. doi: 10.1093/jee/74.6.721

USDA (2020). Potatoes 2019 Summary [Online]. Available online at: https://www.nass.usda.gov›reports›pots0919 (accessed July 02, 2020).

Vigue, S. J. (2018). *Identification of Zebra Chip Tolerant Diploid and Tetraploid Potato Genotypes with Good Processing Quality*. College Station, TX: Texas A&M University.

Vigue, S. J., Scheuring, D. C., Koym, J. W., Rush, C. M., Workneh, F., Tamborindeguy, C., et al. (2020). Identification of tetraploid potato clones with good processing quality among genotypes with reduced zebra chip disease symptomatology. *Am. J. Pot. Res.* 97, 565–579. doi: 10.1007/s12230-020-09804-1

Wallis, C. M., Chen, J., and Civerolo, E. L. (2012). Zebra chip-diseased potato tubers are characterized by increased levels of host phenolics, amino acids, and defense-related proteins. *Physiol. Mol. Plant Pathol.* 78, 66–72. doi: 10.1016/j.pmpp.2012.02.001

Yencho, G. C., and Tingey, W. M. (1994). Glandular trichomes of *Solanum berthaultii* alter host preference of the Colorado potato beetle, *Leptinotarsa decemlineata*. *Entomol. Exp. Appl.* 70, 217–225. doi: 10.1111/j.1570-7458.1994.tb00750.x

Zuñiga, C., Peacock, B., Liang, B., Mccollum, G., Irigoyen, S. C., Tec-Campos, D., et al. (2020). Linking metabolic phenotypes to pathogenic traits among "*Candidatus* Liberibacter asiaticus" and its hosts. *NPJ Syst. Biol. Appl.* 6, 1–12. doi: 10.1038/s41540-020-00142-w

Conflict of Interest: The authors declare that the research was conducted in the absence of any commercial or financial relationships that could be construed as a potential conflict of interest.

The reviewer XW is currently organizing a Research Topic with the author KM.

Publisher's Note: All claims expressed in this article are solely those of the authors and do not necessarily represent those of their affiliated organizations, or those of the publisher, the editors and the reviewers. Any product that may be evaluated in this article, or claim that may be made by its manufacturer, is not guaranteed or endorsed by the publisher.

Advantages of publishing in Frontiers

OPEN ACCESS
Articles are free to read for greatest visibility and readership

FAST PUBLICATION
Around 90 days from submission to decision

HIGH QUALITY PEER-REVIEW
Rigorous, collaborative, and constructive peer-review

TRANSPARENT PEER-REVIEW
Editors and reviewers acknowledged by name on published articles

Frontiers
Avenue du Tribunal-Fédéral 34
1005 Lausanne | Switzerland

Visit us: www.frontiersin.org
Contact us: frontiersin.org/about/contact

REPRODUCIBILITY OF RESEARCH
Support open data and methods to enhance research reproducibility

DIGITAL PUBLISHING
Articles designed for optimal readership across devices

FOLLOW US
@frontiersin

IMPACT METRICS
Advanced article metrics track visibility across digital media

EXTENSIVE PROMOTION
Marketing and promotion of impactful research

LOOP RESEARCH NETWORK
Our network increases your article's readership